FUSULINID AND CONODONT BIOSTRATIGRAPHY OF THE UPPER PENNSYLVANIAN–CISURALIAN RIEPE SPRING LIMESTONE, SPRUCE MOUNTAIN RIDGE, ELKO COUNTY, NEVADA, U.S.A.

by

MICHAEL TAYLOR READ

DISSERTATION

Submitted in partial fulfillment of the requirements
for the degree of Doctor of Philosophy at
The University of Texas at Arlington
December 2018

Arlington, Texas

Supervising Committee:

Merlynd K. Nestell, Supervising Professor
Galina P. Nestell
James E. Barrick
Andrew Hunt
John S. Wickham

ABSTRACT

Fusulinid and conodont biostratigraphy of the Upper Pennsylvanian–Cisuralian Riepe Spring Limestone, Spruce Mountain Ridge, Elko County, Nevada, U.S.A.

Michael Taylor Read, Ph.D.

The University of Texas at Arlington, 2018

Supervising Professor: Merlynd K. Nestell

The Upper Pennsylvanian-Cisuralian (lower Permian) mixed carbonate-siliciclastic strata exposed at Spruce Mountain Ridge, Elko County, Nevada, record the shallow-marine microfauna and oscillating depositional history of the Ferguson Trough during the final glacial interval of the late Paleozoic ice age. The 420 m thick North Spruce Mountain Ridge (NSMR) section includes the uppermost part of the Ely Limestone, the Riepe Spring Limestone, and the base of the Rib Hill Formation. A discontinuous Pennsylvanian-Permian transition is preserved within the approximately 390 m thick Riepe Spring Limestone along the west side of Spruce Mountain Ridge, where an erosional disconformity separates upper Gzhelian (Upper Pennsylvanian) strata of the middle informal member of the Riepe Spring Limestone from Asselian(?)-Sakmarian (lower Cisuralian) deposits of the upper informal member of the Riepe Spring Limestone. Age control of the

system-bounding erosional vacuity and/or hiatus is determined from the integration of co-occurring fusulinid and conodont faunas. Six fusulinid assemblage zones are recognized in the uppermost part of the Ely Limestone and the overlying Riepe Spring Limestone at Spruce Mountain Ridge. Upper Pennsylvanian zones include the *Eowaeringella-Triticites* Group I assemblage zone, *Triticites* Group II-*Dunbarinella* assemblage zone, and the *Triticites* Group IV assemblage zone. Cisuralian zones include the *Schwagerina wellsensis* assemblage zone, *Eoparafusulina linearis* assemblage zone, and the "advanced" *Schwagerina* assemblage zone. Descriptions of 38 fusulinid species identified from loaned Smithsonian thin sections and recently collected material are provided. Additionally, eight species of Late Pennsylvanian conodonts such as *Idiognathodus* and *Streptognathodus* (i.e., idiognathodids) and 12 species of Cisuralian *Sweetognathus* and *Neostreptognathodus* (i.e., sweetognathids) are described from the sparse conodont faunas recovered from the Riepe Spring Limestone.

ACKNOWLEDGEMENTS

First and foremost, I thank my research advisors, Drs. Merlynd and Galina Nestell, without whom this endeavor would not have been possible. Throughout my doctoral research, the Nestells generously offered their support through funding, encouragement, academic wisdom, and endless literary loans. It has been an absolute pleasure learning from and working with such thoughtful and knowledgeable scientists. I also thank Dr. Jim Barrick, Dr. Andrew Hunt, Dr. John Wickham, and the late Dr. Bruce Wardlaw for insightful discussions and taking the time to serve on my graduate committee.

Thank you to Jenny Rashall, Zach Sutton, Ryan Collins, Andrew Plymale, Mark Huntsberry, Emma Gaines, and Mark Khan for assistance with sample collection and preparation. Special thanks to Jennifer Jett and Dr. Brian Huber at the Smithsonian National Museum of Natural History for arranging the fusulinid specimen loan that was so crucial to this research.

I also thank those who provided constructive suggestions during the peer review process of the two published articles contained herein, including Dr. Jim Barrick, Dr. Jeffrey Over, Dr. Charles Henderson, Dr. Scott Ritter, Dr. Greg Wahlman, Dr. Yi-Chun Zhang, Dr. Vladimir Davydov, and Dr. Mike Kaminski.

The Geological Society of America, the Dallas Paleontological Society, and the University of Texas at Arlington provided funding through grants and scholarships that are gratefully acknowledged.

Finally, I thank the University of Texas at Arlington Department of Earth and Environmental Sciences for providing me with the opportunity and the means to grow as both a researcher and an educator.

DEDICATION

I dedicate this dissertation

to my father and mother, for the ceaseless love and support;

to my friends, for the good times;

and to Jenny Rashall, for everything.

In memory of

Lawrence Read (1937-2015), Kenneth Crosby (1958-2016),

and Dr. Bruce Wardlaw (1947-2016)

TABLE OF CONTENTS

LIST OF FIGURES

CHAPTER 1

CHAPTER 2

CHAPTER 3

CHAPTER 5

CHAPTER 6

CHAPTER 7

CHAPTER 8

LIST OF PLATES

CHAPTER 4

LIST OF TABLES

CHAPTER 5

CHAPTER 8

APPENDIX A

CHAPTER 1: INTRODUCTION AND BACKGROUND

Introduction

This study describes the lithostratigraphy and integrated fusulinid and conodont biostratigraphy of the uppermost part of the Ely Limestone and the overlying Riepe Spring Limestone Formations following Hope's (1972) Section 1 near Spruce Mountain, Elko County, Nevada. The 420 m thick, west-to-east stratigraphic section comprises mixed and alternating carbonate-siliciclastic strata exposed on the west side of Spruce Mountain Ridge. The biostratigraphy of the Riepe Spring Limestone is the primary focus of this study and this unit consists of nearly 13,000 km^2 of exposed Upper Pennsylvanian and Cisuralian (lower Permian) strata in eastern Nevada and western Utah (Steele, 1960). The exposure of the Riepe Spring Limestone at Spruce Mountain Ridge (after Hope, 1972) is approximately 390 m thick and is divided herein into three informal "lower, middle, and upper" members separated from one another by thick beds of quartzose conglomerate.

The microfaunal assemblages recovered from the Riepe Spring Limestone at Spruce Mountain Ridge indicate that the formation is Kasimovian (Upper Pennsylvanian)-Artinskian (middle Cisuralian), whereas most other studies of the Riepe Spring Limestone in the general area have described lower Cisuralian, carbonate-dominated strata disconformably overlying Pennsylvanian deposits. The conodont biostratigraphy of these strictly Cisuralian exposures of the Riepe Spring Limestone near Moorman Ranch, Nevada, and the Burbank Hills area of western Utah were described

by Ritter (1986, 1987), but the geology of the Spruce Mountain quadrangle has not been thoroughly studied since the investigations of Hope (1972), Clark (1974), and Marcantel (1975). Neither fusulinids nor conodonts from the Riepe Spring Limestone in the Spruce Mountain area have ever been formally described.

In addition to constraining the age of the NSMR measured section, the microfaunal assemblages of the Riepe Spring Limestone provide evidence for several discrete yet significant disconformities throughout the section. During the Late Pennsylvanian and early Cisuralian, the continental margin of western Pangea was a region in which fluctuating sedimentation trends were controlled by the effects of regional or local tectonism and glacioeustatic sea-level oscillations related to peak Gondwanan glaciation during the late Paleozoic ice age (Trexler et al., 2004; Stevens and Stone, 2007; Rygel et al., 2008; Wahlman and Tasker, 2013). As a result, a number of other nearly coeval, potentially correlative unconformities have been described from Carboniferous and Permian strata of southeast California and West Texas, and certainly more remain unreported. Without the distinct faunal juxtapositions resulting from these discontinuities, the duration of the associated erosional vacuities or hiatuses at Spruce Mountain Ridge would be indeterminate.

Primary Objectives of this Study

i. Perform a detailed lithostratigraphic study of the mixed carbonate-siliciclastic strata of the uppermost part of the Ely Limestone and the Riepe Spring Limestone along Section 1 of Hope (1972) at Spruce Mountain Ridge (USGS map GQ-942). This study includes analyses of dominant microfacies to aid in the interpretation of depositional settings.

ii. Describe the Late Pennsylvanian and Wolfcampian (early to middle Cisuralian) fusulinid succession at Spruce Mountain Ridge. Fusulinids provide critical regional age control for interconnected shelf and marginal basin deposits. Biostratigraphic correlations with West Texas, New Mexico, and Midcontinent North America (e.g., Iowa, Kansas) are inferred. Several new forms and the occurrences of genera previously unreported from Nevada are discussed.

iii. Discuss the occurrences of two large and uncommon schubertellid fusulinid genera, including a newly described genus, *Douglassites* Read and Nestell, 2018, and the predominantly Paleo-Tethyan genus *Biwaella* Morikawa and Isomi, 1960.

iv. Describe the Kasimovian (Late Pennsylvanian) through Artinskian conodont succession preserved at Spruce Mountain Ridge. The observed assemblage is compared with more continuous, contemporaneous faunas from other Basin and Range localities and West Texas, New Mexico, Midcontinent North America, and the southern Ural Mountains of Russia

and Kazakhstan. Integrating conodont and fusulinid data offers greater precision by incorporating both regional and global biostratigraphic indices.

v. Discuss potential phylogenetic discrepancies within Cisuralian sweetognathid conodont lineages. Newly described taxa from Spruce Mountain Ridge may be attributed to instances of near-homeomorphy or undocumented first occurrences within the Sweetognathidae (e.g., *Sweetognathus* Clark, 1972 and *Neostreptognathodus* Clark, 1972).

Locality Description: Spruce Mountain Ridge, Elko County, Nevada

The herein described section is regarded as the "North Spruce Mountain Ridge" (NSMR) section to distinguish it from two additional measured sections of Hope (1972) located farther to the south, closer to Spruce Mountain. Spruce Mountain Ridge is located in northeast Nevada, 66 km west of the Nevada-Utah border and approximately 57 km south of Wells, Nevada, in the central Western Cordillera. The north-south trending ridge is located centrally within the Chase Spring quadrangle of Elko County, Nevada. The North Spruce Mountain Ridge section is located 16 km north of Spruce Mountain and 15 km east-northeast of the junction of Great Basin Highway and Spruce Mountain Road (Fig. 1.1).

Adjacent mountain ranges include the Ruby Mountains, a range within a chain of metamorphic core complexes stretching across the North American Basin and Range province, the East Humboldt Range, and the Pequop Mountains,

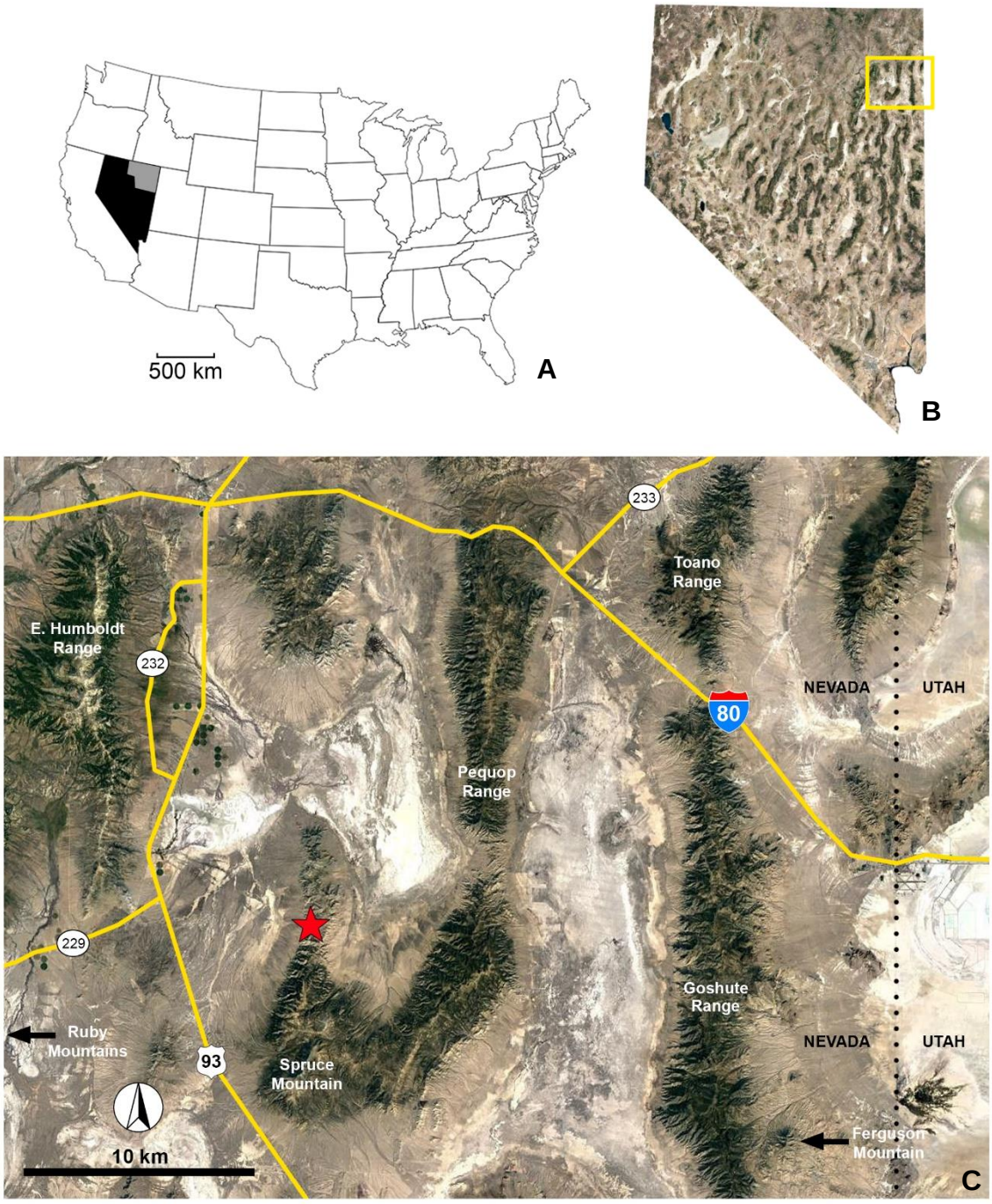

Figure 1.1 – A) Location of Elko County (gray), Nevada (black), U.S.A.; **B)** Satellite image of Nevada, U.S.A. Enclosed region shows the Spruce Mountain area near the NV-UT border; **C)** Enlarged view of the yellow enclosed region of Fig. 2.1B. The North Spruce Mountain Ridge section (NSMR) is denoted by the red star (modified from Google Earth, 2014).

which flank Spruce Mountain to the west, northwest, and east-to-northeast, respectively (Fig. 1.1). The position of the NSMR measured section is illustrated in Figure 1.2. The strata of the uppermost part of the Ely Limestone and the overlying Pennsylvanian-Permian Riepe Spring Limestone of the NSMR section dip uniformly 43-47^{o} east throughout. The northward-striking bedding planes, particularly of the lower and middle informal members of the Riepe Spring Limestone, can be seen in the darker, banded exposures in Figure 1.2. Beyond the western base of the section, the Lower to Middle Pennsylvanian deposits of the Ely Limestone are covered by Quaternary basin-fill (lacustrine and alluvial fan deposits) (Hope, 1972). The Ely Limestone overlies the Mississippian Diamond Peak Formation and Chainman Shale, which are exposed along the western side of the ridge southwest of the NSMR section. Farther south and closer to Spruce Mountain, the Carboniferous and Permian units of the area are juxtaposed against Silurian-Devonian dolomite and the Ordovician Eureka Quartzite by high-angle faults (Hope, 1972).

North American Basin and Range Province

The North American Basin and Range province is a distinctive taphrogenic region encompassing an area of approximately 300,000 km^2 from southern Oregon to central Mexico, between the Sierra Nevada range to the west and the Colorado Plateau to the east. The province is nearly centered on

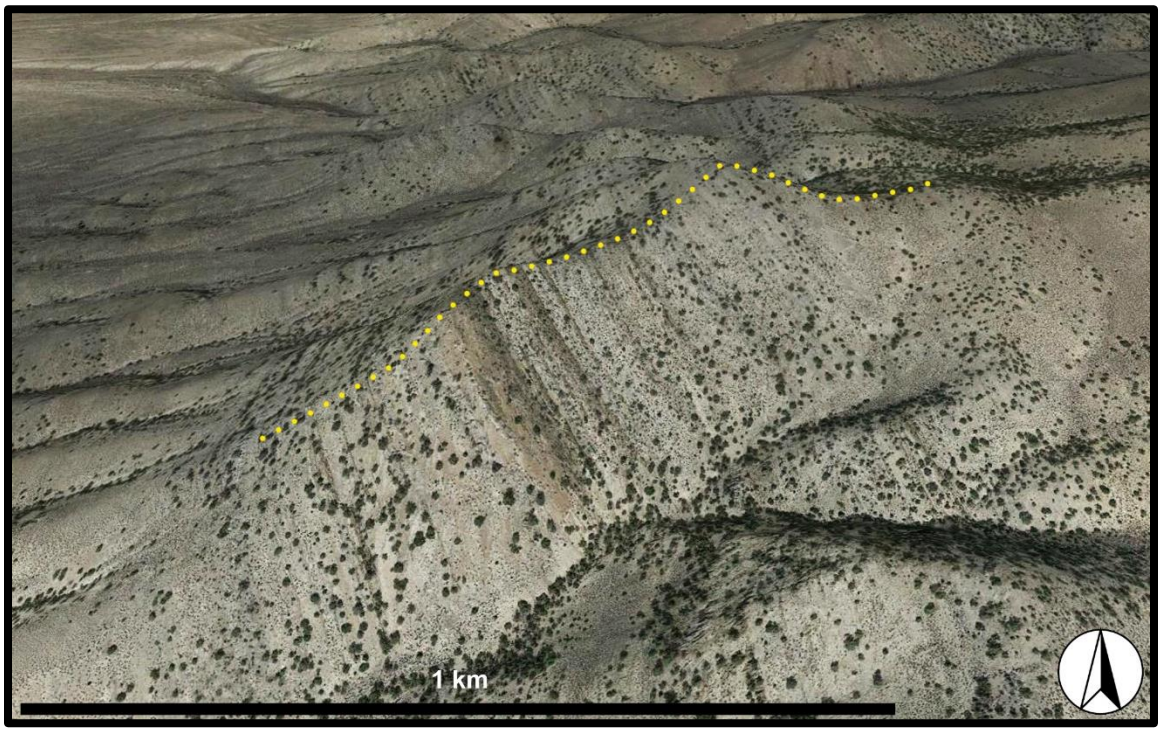

Figure 1.2 – Yellow dotted line illustrates the path of the NSMR measured section along the west side of Spruce Mountain Ridge (modified from Google Earth, 2013).

Nevada, altogether dominating the state's topography, and is composed of numerous north-south trending, high-angle normal fault-bounded mountain ranges and adjacent flat, filled valleys (Fig. 1.3). The process by which this alternating "Basin and Range" topography formed involved the large-scale extension of the western United States, beginning with the onset of rapid lithospheric extension during the early Miocene (approximately 17.5 Ma) (Thompson and Burke, 1974; Thatcher et al., 1999; Dickinson, 2006). Dickinson (2002) has suggested that additional geodynamic mechanisms contributing to the repetitive structure of the province include Late Paleocene to Miocene slab rollback along the cratonal margin and Eocene transrotational tectonism in the Pacific Northwest. The earliest extension within the province likely began as the culmination of regional tectonism, over-thickening of the weakened lithosphere, reduced convergence along the subducting margin of western North America, and subsequent gravitational collapse (Parsons, 1995). Large-scale extension occurred in several stages, with potentially as many as twelve discrete episodes. The longest, sustained extensional period occurred during the Middle Miocene (Parsons, 1995; Dickinson, 2002).

Further Neogene extension of the region led to a significant thinning of the structurally compromised lithosphere, which relieved pressure on the underlying asthenosphere. Subsequent upwelling of the asthenosphere created a provincial-scale thermal dome which continued to stretch the

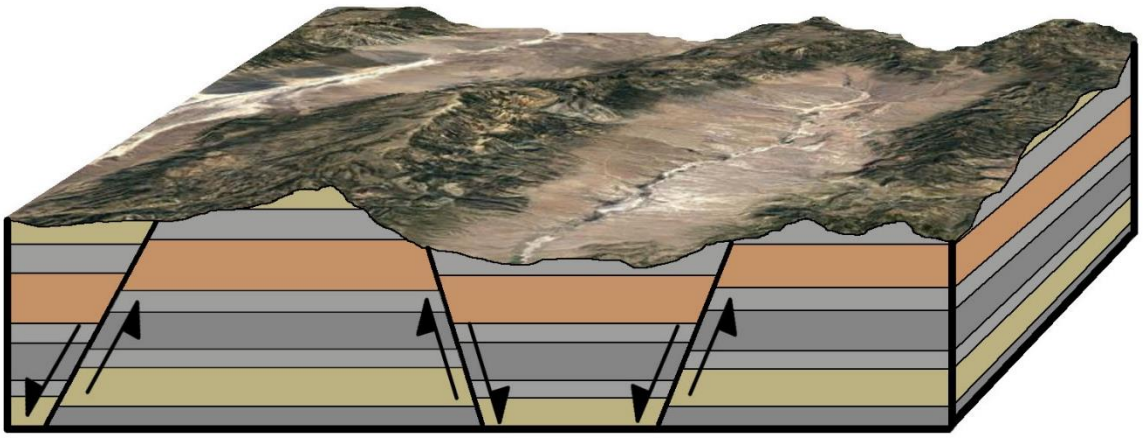

Figure 1.3 – Simplified cross-section illustrating the north-south, high-angle normal faulting produced during the Cenozoic lithospheric extension of the North American Basin and Range province (modified from Google Earth, 2014).

lithosphere. The thinned upper lithosphere began to fracture as the result of the tensional stress, and numerous north-south oriented normal faults began to propagate throughout the region. Large fault blocks were displaced downward along the steeply dipping fault planes, creating the basins of the horst and graben complexes that are characteristic of the region. Since the beginning of the province's extension, it has been estimated that the lithosphere has extended 100-300% in the most extreme instances, and less than 10% in areas of only minor extension (Parsons, 1995). Modern, basin-wide earthquakes, basaltic volcanism, and low-angle faulting indicate that the Basin and Range province is still active and extension may be ongoing (Johnson and Loy, 1992; Parsons, 1995; Thatcher et al., 1999).

Upper Pennsylvanian and Cisuralian Paleogeography

Antler orogenic belt

The Antler orogeny was the most physiographically significant tectonic event to occur in the development of the western margin of Laurentia during the late Paleozoic. Despite the scale and significance of the Antler mobile belt, the timing of initiation and duration of the orogen still lack precise age control and have been the subject of debate since the Antler's formal description by (Roberts, 1949; Ketner, 2013). Although geochronologic age values remain unknown, researchers of the Western Cordillera agree that development of the Antler belt began during the Late Devonian and

orogenesis persisted through the Early Mississippian (Merriam and Anderson, 1942; Roberts et al., 1958; Silberling and Roberts, 1962; Stewart and Poole, 1974; Evans and Theodore, 1978; Stewart, 1980; Speed and Sleep, 1982; Murphy et al., 1984; Levy and Christie-Blick, 1989; Jansma and Speed, 1995; Dickinson, 2006; Cashman et al., 2011; Ketner, 2012, 2013).

During its tenancy, the Antler orogenic belt extended southwest-northeast from eastern California through much of present-day Nevada and into southern Idaho and was responsible for a considerable hiatus in Devonian-Mississippian carbonate sedimentation as terrigenous material shed from the orogen filled the Antler foreland (Silberling and Roberts, 1962). Although the Antler belt's considerable effects on late Paleozoic sedimentation trends of the Western Cordillera are indisputable, there are two competing hypotheses regarding the tectonic nature of the Antler orogeny. The first and most widely accepted hypothesis for the formation of the Antler belt involves plate convergence and the obduction of oceanic lithosphere in regional overthrust subduction complexes, resulting in the emplacement of the Roberts Mountains allocthon (Burchfiel and Davis, 1972; Jansma and Speed, 1995; Dickinson, 2006). Within this broad, generally accepted hypothesis, there have been opposing sides as well: one in support of east-dipping subduction and one favoring west-dipping subduction (Ketner, 2012). Among the previous studies, eastward subduction/obduction seems to be the prevailing hypothesis. In this scenario, the Roberts Mountain thrust

was responsible for the emplacement of western, lower and middle Paleozoic chert, shale, argillite, greenstone, and quartzite units (allochthon) over coeval carbonate strata to the east (autochthon) (Evans and Theodore, 1978).

Ketner (2012) argued that the disagreement on the matter of the direction of subduction/obduction suggested that both variants of the earlier hypothesis may be incorrect. The second, more recent hypothesis of Ketner (2012, 2013) posits that there was no tectonic emplacement of an allochthon during the Antler orogeny, and the extensive highlands were a result of strike-slip faulting. Ketner (2012) cited multiple lines of evidence from extensive regional field mapping in support of a zone of left-lateral strike-slip faulting that is apparently unrelated to the Roberts Mountains "allochthon," which Ketner claimed to be autochthonous. Ketner (2012) compared structural and sedimentological evidence with that from a study of the San Andreas Fault by Crowell (1974) as further support of the claim. In addition to the recently proposed strike-slip origins of the Antler orogeny, Ketner (2012) also proposed a linkage between the onset of fault rupture/uplift and the Frasnian (Late Devonian) Alamo bolide impact event that occurred in the shallow marine setting of eastern Nevada.

Butte Basin (post-Antler foreland)

Following the termination of Antler orogenesis, Early to Middle Mississippian through Lopingian (late Permian) mixed carbonate-siliciclastic

sedimentation related to the "Antler overlap sequence" began in the post-Antler foreland (Wardlaw et al., 1995; Dickinson, 2006). The decline in regional tectonism and increased subsidence to the east of the Antler highlands resulted in the development of several late Paleozoic marginal basins, including the Butte Basin, Wood River Basin, Oquirrh Basin, Cassia Basin, and Paradox Basin (Stevens, 1965; Wardlaw et al., 1995) (Figs. 1.4 and 1.5). During Late Pennsylvanian time (Kasimovian-Gzhelian), the Butte Basin occupied much of present-day northeastern Nevada and western Utah in the northern part of the remnant Antler foreland (the early "Strathearn Basin" of Trexler et al., 2004).

The Butte Basin represented a shallower, partially confined successor to the Early to Middle Pennsylvanian Ely Basin of Wardlaw et al. (1995). The Butte Basin was bounded to the west by the remnant Antler belt, to the north by the Northeast Nevada high, and to the south by the partially emergent, so-called "Ely Platform" (Steele, 1960; Marcantel, 1975; Larson and Langenheim, 1979; Wardlaw et al., 1995). Strata of the Butte Basin are separated from those of the underlying Ely Basin by a regional unconformity known as the "C6" unconformity and from the overlying Cisuralian age Ferguson Trough by the "P1" unconformity with an apparently locally variable upper boundary from Asselian to Sakmarian age (Wardlaw et al., 1995; Trexler et al., 2004).

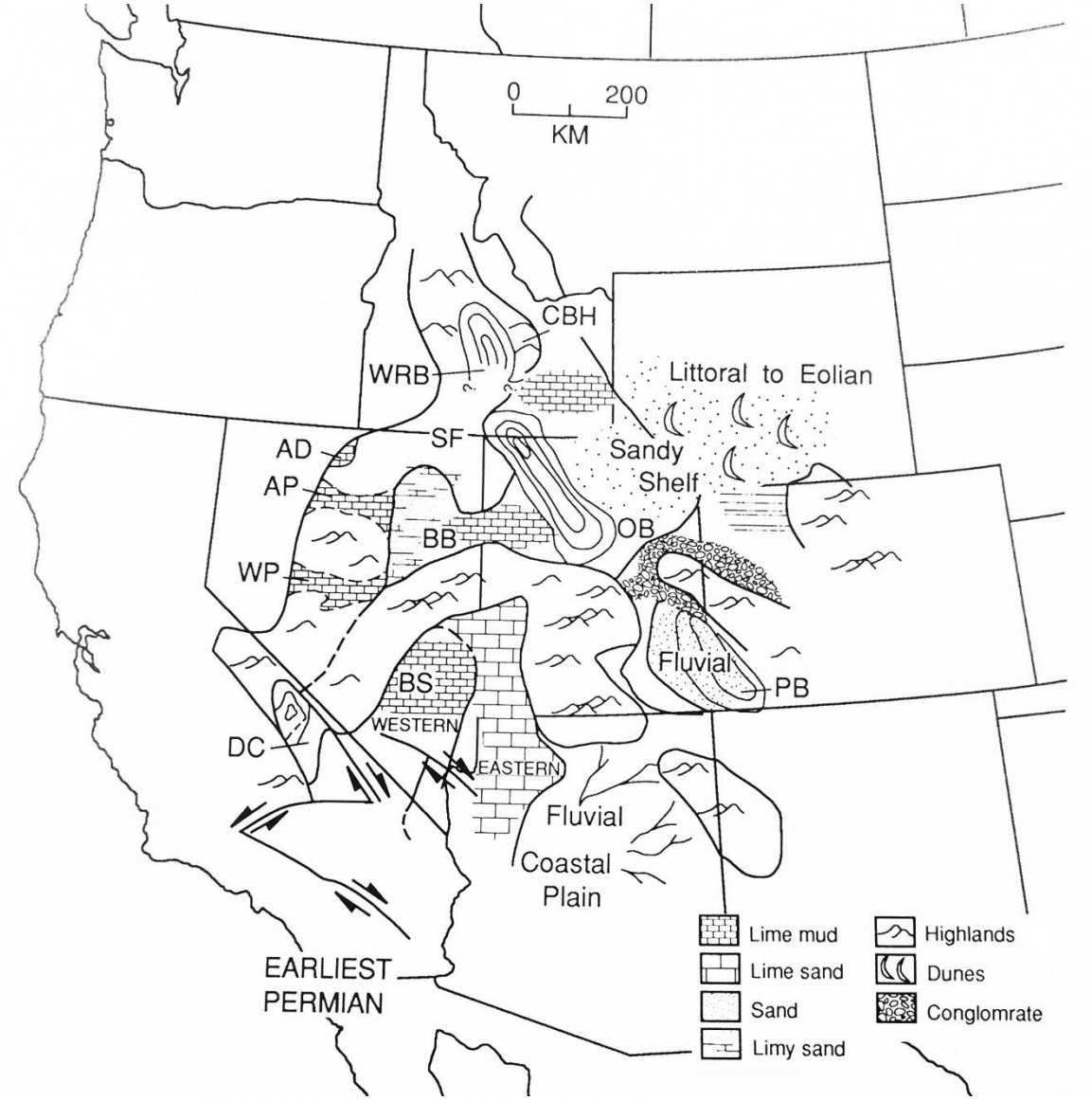

Figure 1.4 – Paleogeographic map of the western United States during the Asselian (earliest Permian). AD – Adam Peak Limestone; AP – Antler Peak; BB – Butte Basin; BS – Bird Spring Basin; CBH – Copper Basin Highland; DS – Darwin Canyon Basin; OB – Oquirrh Basin; PB – Paradox Basin; SF – Sunflower Basin; WP – Wildcat Peak Formation; WRB – Wood River Basin (from Wardlaw et al., 1995).

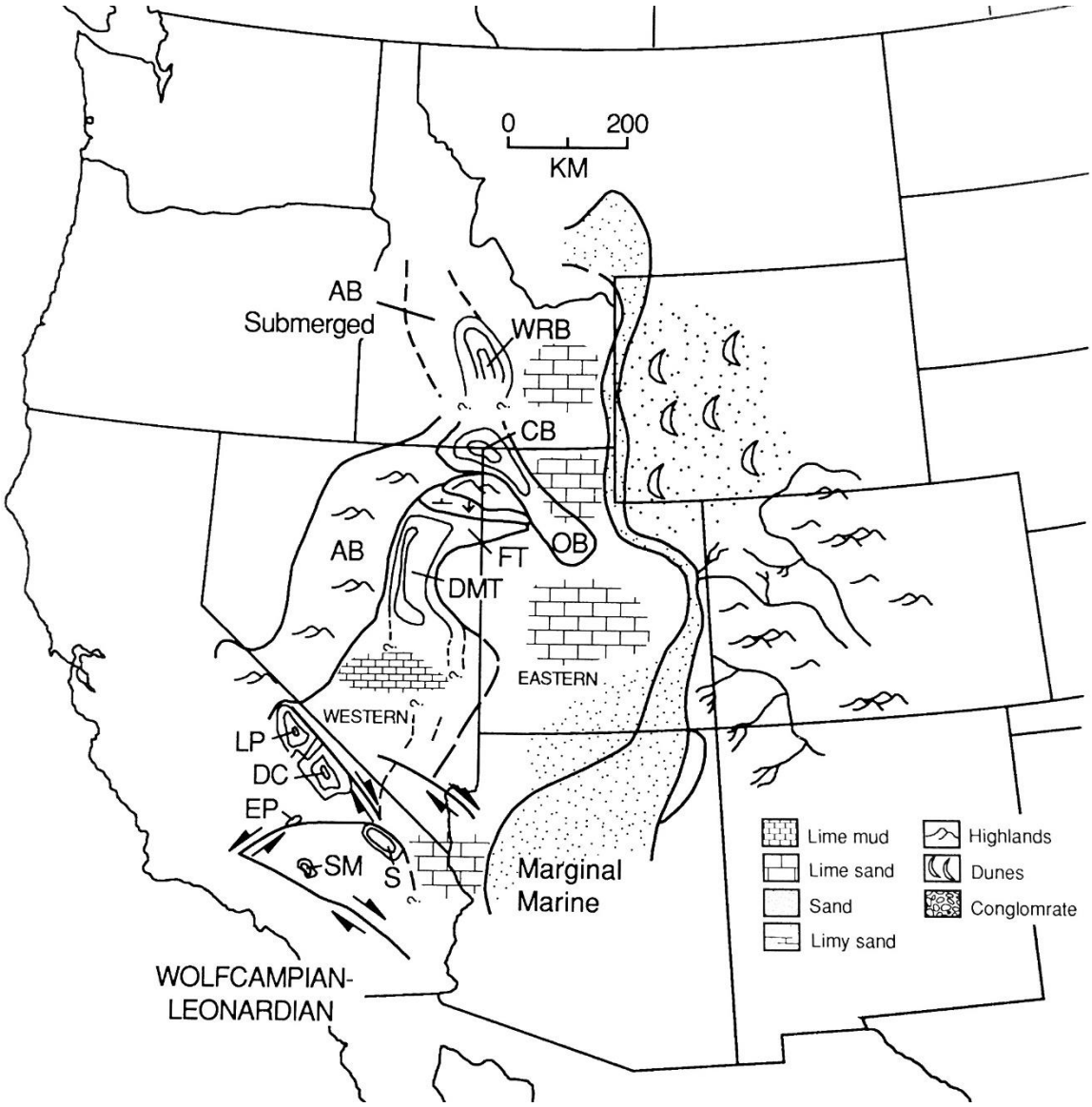

Figure 1.5 – Paleogeographic map of the western United States during the Sakmarian-late Artinskian. AB – Antler Belt; CB – Cassia Basin; DC – Darwin Canyon Basin; DMT – Dry Mountain Trough; EP – El Paso Mountains; FT – Ferguson Trough; LP – Lone Pine Basin; OB – Oquirrh Basin; S – Soda Mountains; SM – Shadow Mountains; WRB – Wood River Basin (from Wardlaw et al., 1995).

Ferguson Trough (post-Antler foreland)

The Ferguson Trough was a shallow, west-east trending depression of Cisuralian age following the Late Pennsylvanian Butte Basin. The Ferguson Trough, along with the coeval Dry Mountain Trough to the west, belonged to a regional complex of narrow, structural basins and platforms near the Oquirrh Basin in the post-Antler foreland (Wardlaw et al., 1995) (Fig. 1.5). The Ferguson Trough was bounded by the remnant Antler highlands to the west, the Northeast Nevada high/Oquirrh-Uinta uplift to the north and northeast, and the Deep Creek-Tintic uplift to the south (Stevens, 1979).

The mixed carbonate-siliciclastic deposits of the Ferguson and Dry Mountain Troughs are upper Asselian/lower Sakmarian to middle Leonardian. These Cisuralian deposits were strongly influenced by both local tectonism and glacioeustatic fluctuations related to the third and final glacial interval of the late Paleozoic ice age (see Chapter 3). However, exposures of the Ferguson Mountain Formation at Ferguson Mountain seem to preserve a more continuous fusulinid succession than that of Spruce Mountain Ridge, potentially reflecting a portion of the trough that was not as strongly influenced by the effects of local uplift and exposure. The preservation of Gzhelian-Asselian strata at this locality was discussed by Marcantel (1975) and Wardlaw et al. (1995) and is preliminarily confirmed by the author's assessment of Ferguson Mountain fusulinid material from the Smithsonian's Douglass-Henbest collection.

Upper Pennsylvanian and Cisuralian (lower Permian)

Chronostratigraphy

The Upper Pennsylvanian and Cisuralian (lower Permian) Series of the upper Paleozoic are defined by an internationally ratified sequence of chronostratigraphic stages, as well as a number of regional subdivisions from chronostratigraphic schemes employed around the world (e.g., Russia, Western Europe, China, and North America). The various regional schemes are often independent of the internationally recognized time scale, occasionally making it difficult for workers to globally correlate strata, fossils, or events that have previously been discussed solely in terms of a regional framework elsewhere. Internationally, the Upper Pennsylvanian Series consists of the Kasimovian and Gzhelian Stages (oldest to youngest), and the lower Permian Cisuralian Series consists of the Asselian, Sakmarian, Artinskian, and Kungurian Stages (oldest to youngest). The following is a brief synopsis of approximate correlations between the time scale outlined by the International Commission on Stratigraphy and regional North American chronostratigraphic schemes of the Upper Pennsylvanian and Cisuralian (some of which may even be considered "sub-regional" within North America) (Fig. 1.6). Geochronologic ages are from Cohen et al. (2013; updated) and Ramezani and Bowring (2017).

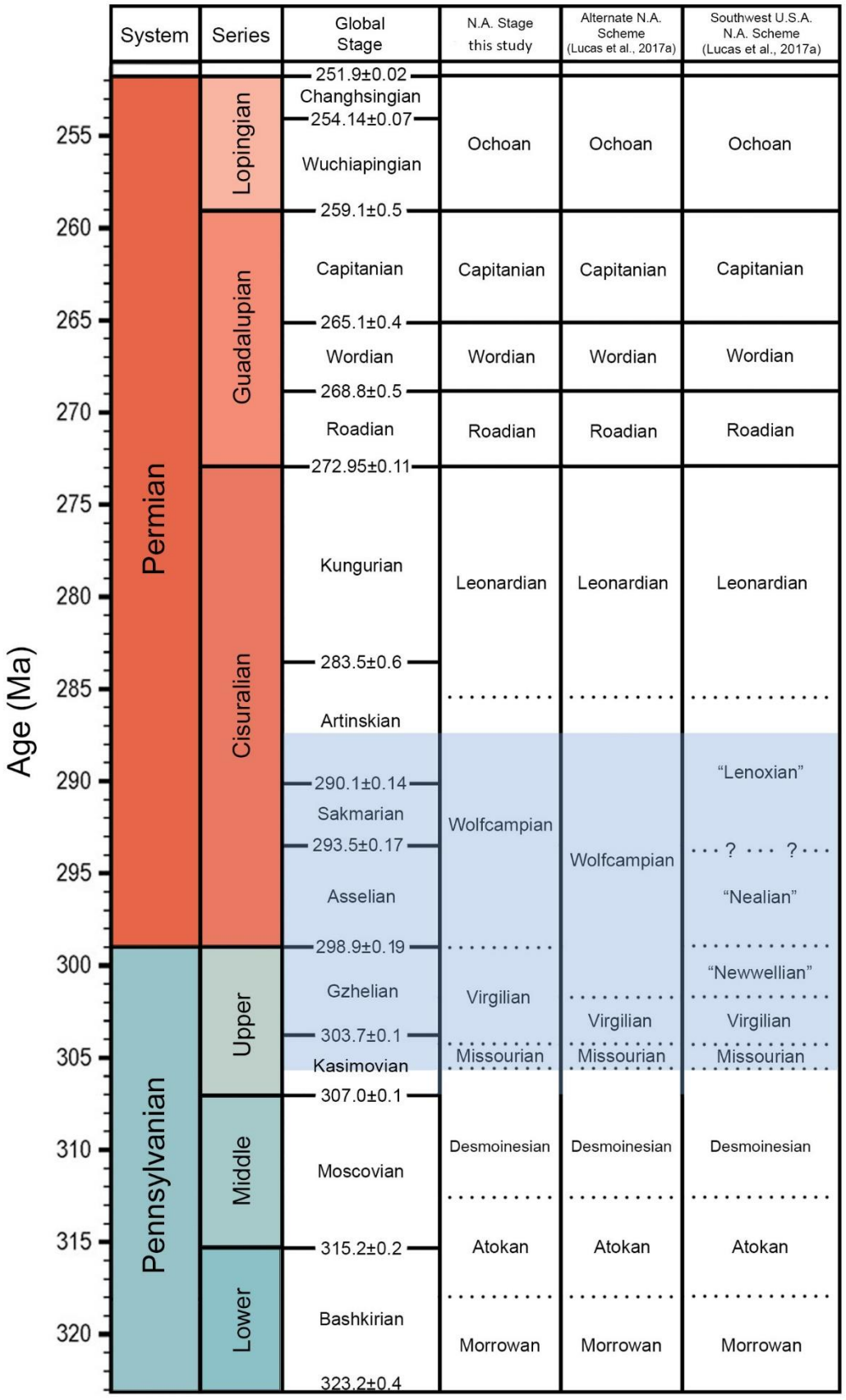
System
Series
Global Stage
N.A. Stage this study
Alternate N.A. Scheme (Lucas et al., 2017a)
Southwest U.S.A. N.A. Scheme (Lucas et al., 2017a)
Age (Ma)
255
260
265
270
275
280
285
290
295
300
305
310
315
320
Permian
Pennsylvanian
Lopingian
Guadalupian
Cisuralian
Upper
Middle
Lower
251.9±0.02
Changhsingian
254.14±0.07
Wuchiapingian
259.1±0.5
Capitanian
265.1±0.4
Wordian
268.8±0.5
Roadian
272.95±0.11
Kungurian
283.5±0.6
Artinskian
290.1±0.14
Sakmarian
293.5±0.17
Asselian
298.9±0.19
Gzhelian
303.7±0.1
Kasimovian
307.0±0.1
Moscovian
315.2±0.2
Bashkirian
323.2±0.4
Ochoan
Capitanian
Wordian
Roadian
Leonardian
Wolfcampian
Virgilian
Missourian
Desmoinesian
Atokan
Morrowan
Ochoan
Capitanian
Wordian
Roadian
Leonardian
Wolfcampian
Virgilian
Missourian
Desmoinesian
Atokan
Morrowan
Ochoan
Capitanian
Wordian
Roadian
Leonardian
"Lenoxian"
? ? ?
"Nealian"
"Newwellian"
Virgilian
Missourian
Desmoinesian
Atokan
Morrowan

Upper Pennsylvanian Series – Kasimovian Stage (International)

The Kasimovian Stage (307.0±0.1 to 303.7±0.1 Ma), named after the Russian city of Kasimov, denotes the international transition from the Middle to the Upper Pennsylvanian Series. The base of the Kasimovian Stage coincides with the base of the Tethyan *Protriticites pseudomontiparus* Zone (Davydov et al., 2012). The lowest Kasimovian is associated with a eustatic lowstand and subsequent globally distributed unconformities (Davydov et al., 2004). The Kasimovian currently lacks a ratified GSSP, but proposed stratotype candidates are in the southern Ural Mountains, the southwest United States, and South China. In North America, the Kasimovian is subdivided into eight conodont biozones (oldest to youngest): *Swadelina neoshoensis* Zone, *Sw. nodocarinata* Zone, *Idiognathodus turbatus* Zone, *I. cancellosus* Zone, *I. confragus* Zone, *Streptognathodus gracilis* Zone, *I. eudoraensis* Zone, and the *S. zethus* Zone (Davydov et al., 2012).

Upper Pennsylvanian Series – Gzhelian Stage (International)

The Gzhelian Stage (303.7±0.1 to 298.9±0.15 Ma) represents the youngest international subdivision of the Pennsylvanian System. The

← **Figure 1.6** – Pennsylvanian and Permian timescale with global stages and differing chronostratigraphic schemes used in North America. Geochronologic ages are from Cohen et al. (2013; updated). The blue-shaded area illustrates the chronostratigraphic interval associated with the NSMR section. Dotted lines represent approximate levels of North American regional stages boundaries lacking geochronologic ages.

Gzhelian, like the Kasimovian, derives its names from a Russian town, Gzhel, near the type locality of the stage and approximately 50 km west-southwest of Moscow. The base of the Gzhelian is defined by the FAD (first appearance datum) of the conodont species *Idiognathodus simulator* (Ellison, 1941) *sensu stricto*, which was described from the Heebner Shale of the Oread cyclothem of the North American Midcontinent. A detailed discussion of the greater "*I. simulator* group" and the morphological distinctions among the group's constituents was presented by Hogancamp et al. (2016) to refine the biozonation of the earliest Gzhelian. Proposed GSSP candidates for the base of the Gzhelian are in the southern Urals and South China. Davydov et al. (2012) subdivided the Gzhelian Stage in North America into seven conodont biozones (oldest to youngest): *Idiognathodus simulator s. s.* Zone, *Streptognathodus vitali* Zone, *S. virgilicus* Zone, *S. bellus* Zone, *S. flexuosus* Zone, *S. farmeri* Zone, and the *S. binodosus* Zone. The upper boundary of the Gzhelian Stage marks the base of the Permian System.

Upper Pennsylvanian Series – Missourian Stage (North America)

The North American regional Missourian Stage is within the Kasimovian Stage of the international chronostratigraphic timescale. The base of the Missourian Stage is defined at the base of the Midcontinent Exline cyclothem by the FAD of *Idiognathodus eccentricus* (Ellison, 1941) (Heckel et al., 2002). The FAD of the fusulinid genus *Eowaeringella* Skinner

and Wilde, 1967 is nearly coincident with the Desmoinesian-Missourian boundary, and it is often used as an auxiliary marker in North America. The Missourian records the rise and subsequent dominance of the prolific schwagerinid walled fusulinids, beginning with the genus *Triticites* Girty, 1904. Barrick et al. (2013b) subdivided the Missourian Stage of the North American Midcontinent into six conodont biozones (oldest to youngest): *Idiognathodus eccentricus* Zone, *I. turbatus* Zone, *I. cancellosus* Zone, *I. confragus* Zone, *Streptognathodus gracilis* Zone, and the *I. eudoraensis* Zone (formerly included within the concept of *I. simulator*). The Missourian Midcontinent stratigraphic succession consists of 13 cyclothems (Barrick et al., 2013b).

Upper Pennsylvanian Series – Virgilian Stage (North America)

By most accounts, the Virgilian Stage represents the uppermost stage of the North American Pennsylvanian System. The base of the Virgilian has been emended several times within the Midcontinent region of North America, but the Missourian-Virgilian boundary is currently denoted by the FAD of *Streptognathodus zethus* Chernykh and Reshetkova, 1987, which occurs in the lower part of the Cass cyclothem in Kansas (Barrick et al., 2013b). The upper boundary of the Virgilian has been the subject of debate for decades among biostratigraphers of different regional affinities and faunal specialties in the United States. The source of the discrepancy is the

diachroneity between the base of the North American Wolfcampian Stage and the internationally recognized (for the most part) base of the Permian System. American fusulinid workers have long-included schwagerinid faunas (e.g., *Triticites* and *Schwagerina* Möller, 1877) that are older than those recovered from the base of the type Wolfcampian in the Glass Mountains of West Texas in their definitions of the Wolfcampian (following Thompson, 1954) (Lucas et al., 2017a). Solutions attempting to remedy the problem have introduced several independent approaches, including a proposed extension of the Virgilian and restriction of the base of the Wolfcampian to the base of the Permian by Baars et al., (1994a, b), the introduction of the uppermost Pennsylvanian "Bursumian" Substage by Ross and Ross (1994), and the more recent proposal of the "Newwellian" Substage (described below) by Wilde (2002). Barrick et al. (2013b) subdivided the Virgilian (sharing an upper boundary with the base of the Permian) into eight conodont biozones (oldest to youngest): *Streptognathodus zethus* Zone, *Idiognathodus simulator* Zone, *S. vitali* Zone, *S. virgilicus s. s.* Zone, *S. bellus* Zone, *S. flexuosus* Zone, *S. farmeri* Zone, and the *S. binodosus* Zone. The same Carboniferous-Permian boundary interpretation of the Virgilian and Wolfcampian Stages is employed in this study.

Upper Pennsylvanian Series – "Newwellian" Substage (SW North America)

The introduction of the "Newwellian" Substage was one of the solutions attempting to further divide the Pennsylvanian-Permian concept of the Wolfcampian into more useful chronostratigraphic intervals, at least in the American southwest. The substage was named after New Well Peak, located in the Big Hatchet Mountains of southwest New Mexico, where Wilde (2002) established the concept of the "Newwellian" based on fusulinids. The "Newwellian" was recently refined by Lucas et al. (2017a), who defined the base of the substage (and, therefore, the base of their Wolfcampian) as the lowest occurrence (LO) of "primitive" forms of the fusulinid genus *Schwagerina*, which the authors referred to as *Thompsonites* Bensh, 1987. The upper boundary of the "Newwellian" was placed at the LO of *Pseudoschwagerina* Dunbar and Skinner, 1936, which nearly coincides with the base of the Permian System.

Cisuralian Series (lower Permian) – Asselian Stage (International)

The Cisuralian Series consists of four stages, of which the Asselian Stage is the oldest (298.9±0.15 to 293.5±0.17 Ma). The Asselian Stage was named after the Assel River of the southern Ural Mountains, and its base (the base of the Permian) is globally defined by the FAD of *Streptognathodus isolatus* Chernykh et al., 1997, a distinctive, nodular species, and the FAD of

the conodont species *Sweetognathus expansus* (Perlmutter, 1975) follows closely. Additional auxiliary markers for the base of the Permian include the FAD of *Streptognathodus invaginatus* Reshetkova and Chernykh, 1986 and *S. nodulinearis* Chernykh and Reshetkova, 1987 (Davydov et al., 1998) The GSSP of the Asselian is at the Aidaralash Creek section in northern Kazakhstan. Henderson (2016) proposed eight globally recognized Asselian conodont biozones (seven in the article, but this division was prior to the establishment of the current, revised and shortened concept of the Sakmarian Stage) (oldest to youngest): *S*treptognathodus *isolatus* Zone, *S. glenisteri* Zone, *S. cristellaris* Zone, *S. sigmoidalis* Zone, *S. constrictus* Zone, *S. fusus* Zone, *S. postfusus* Zone, and the *Sweetognathus* '*merrilli*' Zone.

Cisuralian Series (lower Permian) – Sakmarian Stage (International)

The Sakmarian Stage (293.5±0.17 to 290.1±0.26 Ma) is the second oldest stage (and shortest in duration) of the Cisuralian Series. Named after the Sakmar River of the southern Urals, the base of the Sakmarian has recently been redefined by the voting members of the Subcommission on Permian Stratigraphy as the FAD of *Mesogondolella monstra* Chernykh, 2005, with the FAD of *Sweetognathus binodosus* Chernykh, 2005 serving as the secondary marker. Although gondollelid conodonts are conspicuously absent from the Sakmarian interval of the NSMR section, there are a fair amount of sweetognathid conodonts present, in addition to rather abundant

fusulinids, and the assemblage still provides good biostratigraphic control. A GSSP for the Sakmarian is currently being established, with the tentative stratotype assignment located along the Usolka River, south of Krasnousolsk, in the Republic of Bashkortostan, Russia. Henderson (2016) proposed two conodont biozones for the recently truncated Sakmarian Stage (oldest to youngest): *Sweetognathus binodosus* Zone, and the *Sw. anceps* Zone.

Cisuralian Series (lower Permian) – Artinskian Stage (International)

The Artinskian Stage (290.1±0.26 to 283.5.1±0.6 Ma) is the third and penultimate stage of the Cisuralian Series. The Artinskian Stage was named after the Russian town of Arti (formerly known as Artinsk), also located in the southern Ural Mountains. The base of the Artinskian has long been associated with the FAD of *Sweetognathus* '*whitei*' (or *Sw.* aff. *whitei*) (Rhodes, 1963), and the primary GSSP candidate is located at the Dal'ny Tulkas section in the southern Urals of Russia (Chuvashov et al., 2013). Henderson (2016) proposed three conodont biozones for the Artinskian Stage (oldest to youngest): *Sw.* '*whitei*' Zone, *Sw. clarki* Zone, and the *Neostreptognathodus pequopensis* Zone. A discussion of the discrepancy between the types of *Sw. whitei* and the forms regarded as *Sw.* '*whitei*' is provided in the systematic description of the latter taxon in Chapter 8. The boundary of the Wolfcampian and Leonardian is within the upper part of the Artinskian Stage.

Cisuralian Series (lower Permian) – Kungurian Stage (International)

The Kungurian Stage (283.5.1±0.6 to 272.95±0.11 Ma) is the last and longest stage of the Cisuralian Series. Named after the city of Kungur, near Perm, Russia (the namesake of the Permian System), the Kungurian is succeeded by the Roadian Stage, the oldest stage of the Guadalupian Series (middle Permian). The base of the Kungurian is defined by the FAD of *Neostreptognathodus pnevi* Kozur and Movshovitsch in Movshovitsch et al., 1979, with *N. exsculptus* Igo, 1981 as the secondary marker. The primary GSSP candidate is located along the Yuryuzan River near the town of Mechetlino, Republic of Bashkortostan, Russia (Chuvashov and Chernykh, 2011). Henderson (2016) proposed four conodont biozones for the Kungurian Stage (oldest to youngest): *Neostreptognathodus pnevi* Zone, *N. clinei* Zone, *N. prayi-N. sulcoplicatus* Zone, and the *Mesogondolella lamberti* Zone. The Kungurian comprises the great majority of the North American Leonardian Stage, with which it shares an upper boundary (Fig. 1.6).

Cisuralian Series (lower Permian) – Wolfcampian Stage (North American)

The Wolfcampian Stage was originally described by Adams et al., (1939) as a "series" based on lower Permian strata exposed in the Glass Mountains of West Texas, but was later regarded by most authors as a

"stage." The type Wolfcampian has a disconformable base overlying Pennsylvanian strata, whereas equivalent successions elsewhere in the Permian Basin and New Mexico preserve a similar "type" Wolfcampian fusulinid fauna, but with a conformable, older fossil assemblage beneath it. The strata containing the older fusulinid assemblage represent the "Bursumian," or "Newwellian," Substage of the Wolfcampian. Regardless of the nomenclature used for this older interval (e.g., "Bursumian," "Newwellian," lower Wolfcampian, Virgilian), strata of this age unequivocally belong to the Upper Pennsylvanian Series based on conodonts.

The Permian portion of the Wolfcampian was subdivided into two substages, the lower "Nealian" Substage (originally "stage") and the upper "Lenoxian" Substage (originally "stage") (Ross and Ross, 1987a, b). These Cisuralian substages of the Wolfcampian do not directly correspond to the internationally recognized stages of the Permian and are based on fusulinid occurrences rather than conodonts.

Fusulinids: Background and General Morphology

Foraminifera of the superorder Fusulinoida (fusulinids or fusulinaceans) have been a cornerstone of biostratigraphy for nearly 200 years, during which time these large (primarily), benthic protists have proven themselves as invaluable guide fossils for the Pennsylvanian and Permian. Although the earliest, peripheral constituents of the group arose during the

latest Mississippian, the fusulinid lineages of such renowned biostratigraphic utility are only known from the lowest part of the Pennsylvanian (Bashkirian) through the Guadalupian (Thompson, 1948). Following the often-overlooked end-Guadalupian mass extinction event, fusulinids persisted with markedly diminished size and numbers, and low diversity into the latest Permian before ultimately succumbing, like many other groups, to "The Great Dying."

During the geologically fleeting history of the Fusulinoida, the group proliferated into six orders with nearly 30 distinct families whose constituents may be found in shallow-marine deposits on all continents except Australia and Antarctica (Rauser-Chernousova et al., 1996). In addition to being near-globally abundant in carbonate-dominated strata (and occasionally in sandstone or shale), fusulinids derive their paleontological usefulness from their short taxon ranges and their readily interpreted phylogenetic relationships (Thompson, 1948). Douglass (1977) subdivided the full extent of the Pennsylvanian and Permian into nine generic assemblage biozones, including (in ascending order): the Zone of *Millerella*, Zone of *Profusulinella*, Zone of *Fusulinella*, Zone of *Beedeina*, Zone of *Triticites*, Zone of *Pseudoschwagerina*, Zone of *Parafusulina–Neoschwagerina*, Zone of *Polydiexodina–Yabeina*, and the Zone of *Lepidolina–Palaeofusulina*.

The planispirally coiled shells, or tests, of fusulinids consist of dense microgranular calcite and range greatly in size, from a fraction of a

millimeter to nearly 14 cm in length (Douglass, 1977). Within any given lineage of fusulinids, there is a general trend towards an increase in test size throughout progressive steps in evolutionary development (Douglass, 1977). Outwardly, many fusulinids bear a superficial resemblance to one another, but the septate internal structure of the organisms is highly complex and no two organisms are alike, often exhibiting significant intraspecific variability within populations (Thompson, 1948). Fusulinids are observed and described primarily from axial thin sections (oriented perpendicular to the direction of coiling and through the initial chamber), but equatorial sections may be illustrated as well (parallel to the direction of coiling; "sagittal" section) (Fig. 1.7). Tangential sections of the outer volutions of the test are seldom illustrated but may reveal diagnostic features. The following list provides brief definitions of key morphological terms.

i. **Proloculus** (or proloculum; plural proloculi) – The initial chamber of the test. Proloculi tend to be spherical or slightly subspherical but may be nearly cubic in rare instances. The proloculus is typically thin-walled and has a single circular aperture (Thompson, 1948). The proloculi of some species demonstrate dimorphism of asexual and sexual generations (e.g., megalospheric and microspheric) (Douglass, 1977).

ii. **Spirotheca** – The skeletal "spiral wall" of the test. Growth of the spirotheca occurs through the addition of progressively larger

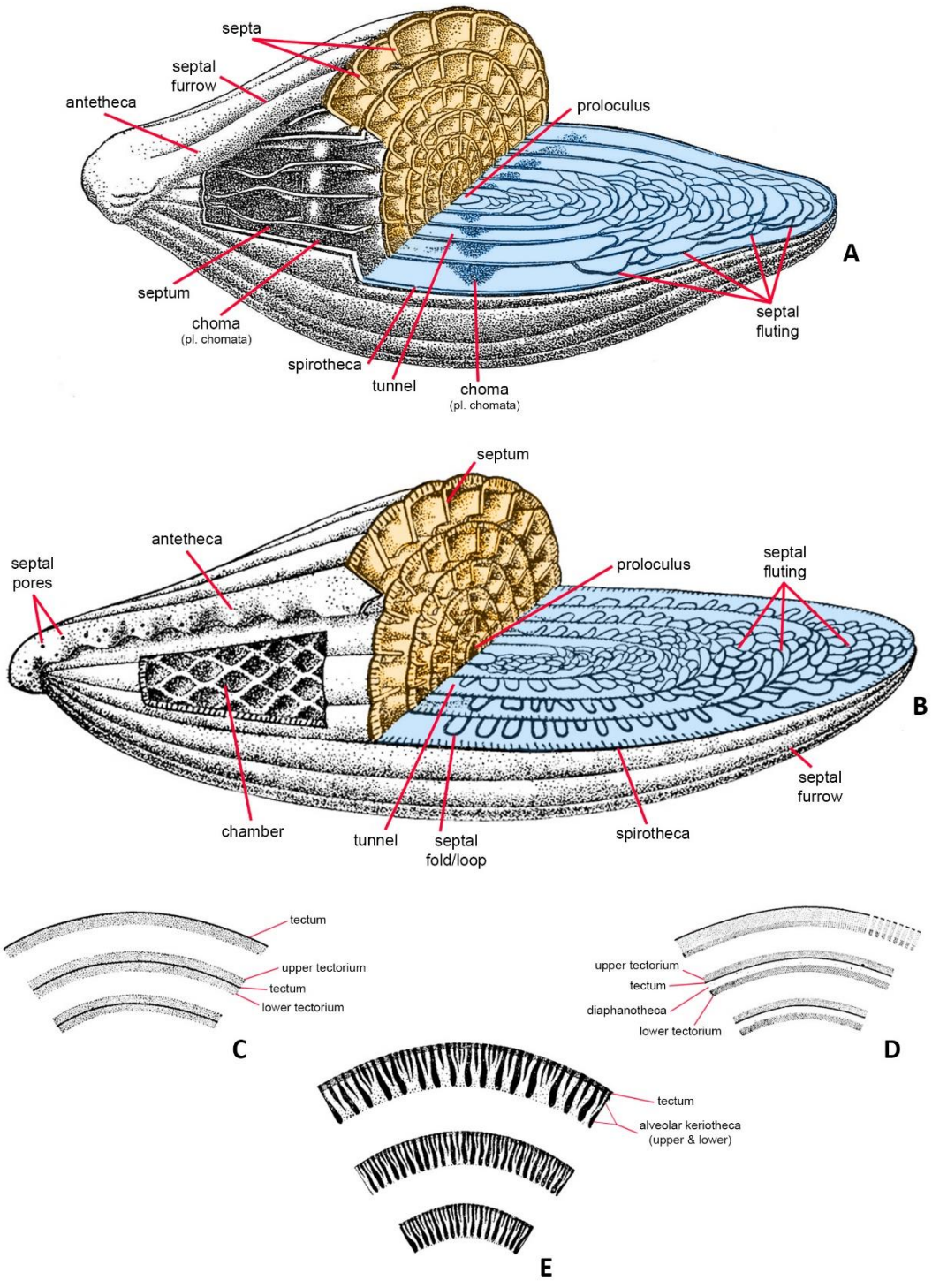
septa
septal furrow
antetheca
proloculus
septum
choma
(pl. chomata)
spirotheca
tunnel
choma
(pl. chomata)
septal fluting
A
septum
antetheca
septal pores
proloculus
septal fluting
B
chamber
tunnel
septal fold/loop
spirotheca
septal furrow
tectum
upper tectorium
tectum
lower tectorium
C
upper tectorium
tectum
diaphanotheca
lower tectorium
D
tectum
alveolar keriotheca
(upper & lower)
E

iii. volutions. Successive volutions are partitioned by septa, which may be planar or intensely crenulated ("fluted"). The terminal septum of the test (which changed as volutions were added) is known as the antetheca. The initial, primary wall is composed of a simple, dense layer known as tectum (Douglass, 1977). Several distinct spirothecal types are known among the fusulinids. These wall structures are primarily divided into three taxonomically useful groups: 1) profusulinellid; 2) fusulinellid; and 3) schwagerinid (Figs. 1.7C–1.7E). An additional, highly advanced variant of the schwagerinid wall structure, known as "verbeekinid," is not illustrated.

iv. **Chomata** (singular choma) – Dense mounds of secondary calcite deposited on either side of the "tunnel," a resorbed interruption of the septa that follows the equatorial midplane of the test and generally widens throughout growth. Some groups of fusulinids (particularly Permian forms) do not possess chomata adjacent to the tunnel, making it difficult to observe the tunnel axial sections (Douglass, 1977).

← **Figure 1.7** – General morphological features of fusulinids. **A)** Labeled cross-section of a fusulinid test exhibiting a fusulinellid wall structure (orange = equatorial; blue = axial); **B)** Labeled cross-section of a fusulinid test exhibiting a schwagerinid wall structure; **C)** Labeled cross-section of spirotheca exhibiting a profusulinellid wall structure (three volutions illustrated); **D)** Labeled cross-section of spirotheca exhibiting a fusulinellid wall structure (three volutions illustrated); **E)** Labeled cross-section of spirotheca exhibiting a schwagerinid wall structure (three volutions illustrated) (modified from Rauser-Chernousova and Fursenko, 1959).

v. **Axial filling** – Additional deposits of secondary calcite, typically densest in the inner volutions, polar extremities, and along or near the axis of coiling (Douglass, 1977). The nature of the axial filling is often characteristic of a given species.

Conodonts: Background, Histologic Groups, and General Morphology

Conodonts, or more accurately, "conodont elements," are the phosphatic, tooth-like structures of small, extinct, lamprey-like organisms (i.e., chordates, although some would vehemently argue against this claim). Since the earliest descriptions of Silurian and Devonian conodont elements from Russia by Christian Heinrich Pander ("Heinz Christian Pander") in 1856, generations of micropaleontologists have been intrigued by the diversity, utility, and visual allure of these "fascinating little whatzits" (Sweet, 1985; Sweet, 1988).

The organisms broadly referred to as "conodont animals" include three histologic groups which differ in the growth and tissue layering of their elements; these are the protoconodonts, paraconodonts, and euconodonts (Bengtson, 1976; Sweet and Donoghue, 2001). The earliest forms, the protoconodonts, first appeared in the fossil record during the early Cambrian (Bengtson, 1983). Some conodont workers believe that these primitive forms, which were among the first organisms to produce biomineralized skeletal components, are related to chaetognaths rather than the "true" conodonts (=

euconodonts) (Szaniawski, 1980, 1982; Kasatkina and Buryi, 1996a, 1996b, 1997, 1999; Szaniawski, 2002; Murdock et al., 2013). Although the affinities of the protoconodonts remain unknown, some workers have suggested that the younger two groups, the paraconodonts and euconodonts, may be related to one another, but not to the protoconodonts (Sweet and Donoghue, 2001; Murdock et al., 2013). Historically, few authors have argued for a direct relationship between the three groups (see Bengtson, 1976; Müller and Nogami, 1971, 1972; Szaniawski, 1987).

The evolutionary origin of the group known as the paraconodonts (middle Cambrian-Devonian) is a closely related subject of debate among early Paleozoic conodont workers. Although the relationship between protoconodonts and paraconodonts is questionable, a paraconodont-to-euconodont lineage is generally accepted by most authors (Bengtson, 1976, 1982; Szaniawski and Bengtson, 1993; Sweet and Donoghue, 2001; Valentine, 2004; Murdock et al., 2013). A recent study by Terrill et al. (2018) suggested that further study of soft tissue (keratin) residues from paraconodonts and early euconodonts could provide additional evidence of a direct relationship between the two groups.

The ozarkodinid conodonts of the present study belong to the euconodonts. If the euconodonts are in fact a monophyletic group, they evidently arose from an ancestral stock of paraconodonts during the late Cambrian (Szaniawski and Bengtson, 1993). Terrill et al. (2018) suggested

that there is a possibility of cyclostome affinity among this youngest and most "complex" group. Euconodonts proliferated and diversified immensely throughout the mid-Paleozoic, with numbers declining into the late Paleozoic, and were among the few survivors of the Permian-Triassic extinction event (Clark, 1972, 1983). Unfortunately for the euconodonts, even after outlasting the greatest mass extinction of the Phanerozoic, the group suffered the fate of extinction during the latest Triassic (Clark, 1983).

Much of the controversy surrounding the zoological affinities of conodonts (herein referring only to euconodonts) is due to a lack of hard fossil evidence (in the literal sense) beyond the anterior elements. Although there are specimens which exhibit impressions of the soft-bodied organisms, they are few in number (around 20), only represent a handful of species, and, according to some workers (see Turner et al., 2010) do not provide enough evidence of a chordate affinity to resolve the ongoing debate (Barrick, 2012). Because of the unfortunate preservational circumstances, micropaleontologists typically only study what can be dissolved out of bulk rock samples: the oropharyngeal array of delicate, biogenic apatite (calcium phosphate) elements. Conodont elements grew continuously throughout the organisms' lives by the outward appositional growth of laminae (Sweet and Donoghue, 2001). A typical conodont animal of the order Ozarkodinida Dzik, 1976 possessed eight discrete types of elements (15 total elements) within its feeding "apparatus" (Purnell and Donoghue, 1998). A generalized

arrangement of the various elements within the ozarkodinid apparatus is illustrated in Figure 1.8. The following list provides brief definitions and orientations of the various skeletal elements present within the apparatus of ozarkodinid conodonts. The anatomical nomenclature used is that proposed by Purnell et al. (2000).

i. **S elements** – the S elements of the ozarkodinid apparatus typically consist of six bilaterally-paired bipennate elements (S_1-S_4) and one axial alate element S_0. The S_0 element occupied a medial position along the axis of symmetry and has a caudal process of moderate length. The short lateral (sinistral and dextral) processes curve ventrally away from the rostral junction with the base of the cusp. The paired S_1-S_4 elements (eight elements) have long, low, and straight caudal processes with numerous fine, comb-like denticles.

ii. **M elements** – the ozarkodinid apparatus has two bilaterally paired breviform digyrate M elements. The M elements occupied distal sinistral and dextral positions within the apparatus and would have been separated by the entire suite of S elements. The lateral processes form a u-shape and are asymmetrical, with the longer process located on the dorsal side.

iii. **P_2 elements** – the P_2 elements, or rostral pectiniform elements, consist of a pair of narrow, angulate elements, which opposed each other cusp-to-cusp along the animal's line of symmetry. The P_2

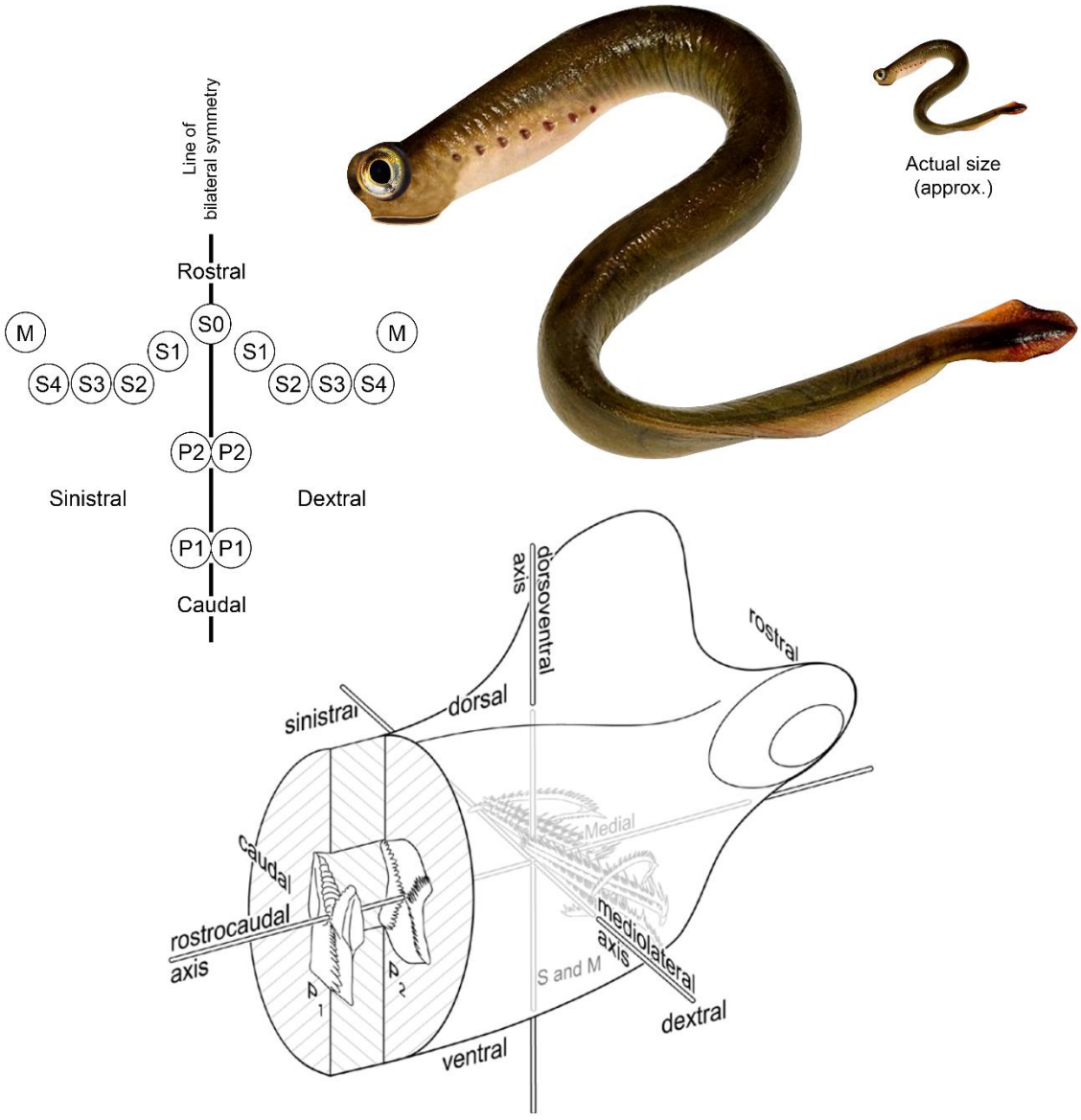

Figure 1.8 – General morphological and anatomical features of ozarkodinid conodonts. **A)** Dorsoventrally oriented diagram of the arrangement of S, M, and P elements within a typical ozarkodinid apparatus; **B)** Author's rendering of the conodont animal; **C)** Anatomical orientation of S, M, and P elements within the head of an ozarkodinid conodont animal (from Purnell et al., 2000).

iv. elements are strongly denticulate and slightly arcuate. The cusp is centrally located above the basal pit.

v. **P_1 elements** – the paired P_1 elements, located caudally to the P_2 elements, are the diagnostic piece of the apparatus for most conodonts. The two P_1 elements opposed each other platform-to platform, with the blades positioned ventrally. The conodonts illustrated in the present study are carminiscaphate P_1 elements. The nature of the carina and the platform are highly variable among different families and genera of the Ozarkodinida. The blade is often highly and regularly denticulate, and the platform may be ridged, nodular, troughed, denticulate, or some combination of these traits.

CHAPTER 2: SUMMARY OF PREVIOUS WORK

Description of Stratigraphic Units

Ely Limestone

The Ely Limestone Formation was originally described by Lawson (1906) as a thick-bedded, sporadically cherty limestone unit in the "Robinson" (Ruth) mining district of White Pine County, east-central Nevada (Steele, 1960). The original lower boundary at the type section of the Ely Limestone was placed above the Devonian Chainman Shale, and the upper boundary was placed at the base of the Cisuralian "Arcturus Limestone" (Steele, 1960). Spencer (1917) described an approximately 2,000 to 2,500 m thick section of the Ely Limestone in the Egan Range of White Pine County as a massive, gray to blueish, sporadically fossiliferous, cherty limestone.

Steele (1960) called for significant restriction of the Ely Limestone at the type section in the Ruth mining district because of a locally occurring Upper Pennsylvanian disconformity. The upper portion of the Ely Limestone (above the disconformity), which Steele described as "middle Wolfcampian," was then renamed as the Riepe Spring Limestone. The base of the restricted Ely Limestone of Steele (1960) is Atokan-Desmoinesian (Middle Pennsylvanian). Steele (1960) proposed a continuous reference section between Illipah Creek and Moorman Ranch, Nevada, because of the stratigraphic discontinuity at the type section. Hope (1972) described the upper part of the Ely Limestone as a thinly bedded limestone directly

overlain by the Upper Pennsylvanian conglomerate and limestone beds of the lower informal member of the Riepe Spring Limestone.

Riepe Spring Limestone

The Riepe Spring Limestone was originally described by Steele (1960) as a predominantly massive, coral-rich, fusulinid-bearing unit. Prior to the restriction and reassignment by Steele (1960), the Riepe Spring Limestone was included in the Ely Limestone (Spencer, 1917; Pennebaker, 1932). The type section of the Riepe Spring Limestone is near the north end of Ward Mountain, southeast of Moorman Ranch, White Pine County, Nevada (39°10'33.75"N, 114°55'59.80"W). Steele (1960) described the formation as a medium gray, bioclastic, medium- to thick-bedded limestone with a basal fusulinid coquina. According to Steele (1960), abundant colonial corals compose nearly 10% of the type section of the Riepe Spring Limestone. Steele (1960) also assigned outcrops in the Carbon Ridge area, the Ruth mining district, and the Confusion Range of western Utah to the Riepe Spring Limestone as well. Barosh (1964) provided detailed lithostratigraphic descriptions of Riepe Spring Limestone outcroppings in the Egan Range, the central and southern Butte Mountains, the White Pine Range, Dry Mountain, the Schell Creek Range, the Confusion Range, and the Needle Range. Barosh (1964) also identified three members within the Riepe Spring Limestone, regarded as the “lower,” “coralline,” and “upper” parts, which

differ from the three informal members identified and described in this study (see Chapter 3). Later descriptions were included in the Cisuralian conodont studies of Clark and Behnken (1971), Clark (1974), Behnken (1975a), and Ritter (1987).

At Spruce Mountain Ridge, Hope (1972) placed the Pennsylvanian-Permian Riepe Spring Limestone atop the uppermost part of the Ely Limestone. Approximately 140 m of highly conglomeratic Riepe Spring strata in Section 1 of Hope (1972) were originally considered undetermined Pennsylvanian-Permian (Fig. 2.1). This study provides necessary age control for the previously unassigned interval. Coeval, carbonate-dominated units in the region include parts of the Buckskin Mountain Formation, Carbon Ridge Formation, Ferguson Mountain Formation, and the Garden Valley Formation (Douglass, 1974; Marcantel, 1975; Wardlaw et al., 2015).

Rib Hill Formation

The Rib Hill Formation was formally described by Pennebaker in 1932 as an independent unit previously considered part of the "Arcturus Limestone." The type section for the Rib Hill Formation is located in the Ruth mining district, where the sandstone and limestone unit overlies the Ely Limestone and is situated beneath the "Arcturus Limestone." Steele (1960) revised the lower boundary, placing the Rib Hill atop the newly described Riepe Spring Limestone. The initial description of the Rib Hill Formation

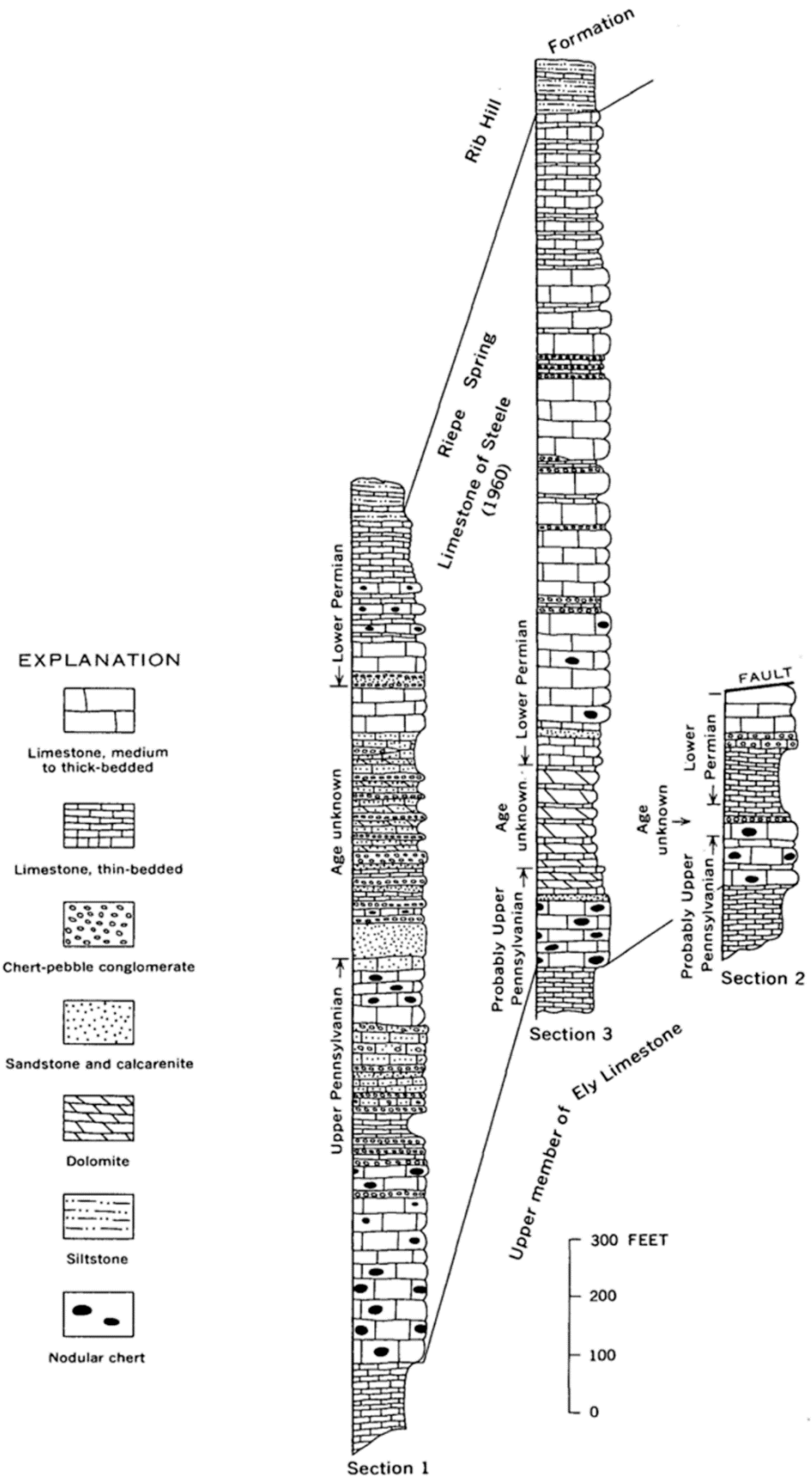
EXPLANATION
Limestone, medium to thick-bedded
Limestone, thin-bedded
Chert-pebble conglomerate
Sandstone and calcarenite
Dolomite
Siltstone
Nodular chert
Rib Hill Formation
Riepe Spring Limestone of Steele (1960)
Upper member of Ely Limestone
Lower Permian
Age unknown
Upper Pennsylvanian
Probably Upper Pennsylvanian
FAULT
300 FEET
200
100
0
Section 1
Section 2
Section 3

described the primary lithology as light gray to yellowish-gray, fine- to medium-grained, platy- to thick-bedded quartz sandstone (Pennebaker, 1932; Steele, 1960). The sandstone weathers yellowish-buff to brownish-red in color.

The Rib Hill Formation was later renamed by Steele (1960) as the Riepetown Sandstone, after the village of Riepetown, Nevada. The name of the formation was changed because the designation "Rib Hill" already belonged to a Precambrian quartzite unit from Wisconsin. However, this study uses the senior nomenclature of the Rib Hill Formation to avoid confusion with the underlying Riepe Spring Limestone. Steele (1960) also described the presence of the Rib Hill Formation near Moorman Ranch, Nevada. The Moorman Ranch section of the Rib Hill Formation is approximately 365 m thick and, like the NSMR section, lies above the Riepe Spring Limestone and below the Leonardian (upper Cisuralian) Pequop Formation (Steele, 1960).

The Rib Hill Formation at Moorman Ranch, Nevada was also discussed in the biofacies-refinement of Ritter (1987) as more than 300 m of thinly-bedded fine sandstone and siltstone with sparsely interbedded massive limestone beds. The exposure of the Rib Hill Formation at Moorman Ranch has less than 10% carbonate material throughout, whereas

← **Figure 2.1** – Stratigraphic columns of the three measured sections illustrated on USGS Map GQ-942 (Spruce Mountain Quadrangle). Section 1 corresponds with the NSMR section (in part) (from Hope, 1972).

the Burbank Hills section is dominated by carbonate lithofacies (Ritter, 1987). Three primary lithologies are recognized within the Rib Hill Formation at Moorman Ranch, Nevada. These lithofacies include thin-bedded, very fine sandstone and siltstone, skeletal wackestone to grainstone, and massively-bedded, crinoidal packstone to grainstone (Ritter, 1987). The depositional environment of the Moorman Ranch locality when the Rib Hill Formation was deposited is interpreted as a shallow ramp setting in the eastern portion of the Dry Mountain Trough. The Moorman Ranch exposure of the Rib Hill Formation is interrupted infrequently by turbidite deposits, and the massively-bedded crinoidal lithofacies may be attributed to turbidity currents destroying crinoid colonies (Ritter, 1987).

Missourian (Upper Pennsylvanian) – Wolfcampian (lower Permian) Fusulinid Biostratigraphy

Fusulinids provide biostratigraphers with rapidly evolving, easily observed foraminiferal lineages and serve as precise regional markers for Pennsylvanian and Permian strata. Fusulinid zones and species ranges have been established across the western, southwestern, and Midcontinent regions of the United States. The Late Pennsylvanian (Missourian-Virgilian) fusulinid faunas of North America are dominated by the genus *Triticites*, which first appeared in the earliest Missourian and marks the first occurrence of a schwagerinid wall structure. Studies of Missourian and

Virgilian fusulinids faunas in North America have been conducted in Arizona (Sabins and Ross, 1963; Ross and Tyrrell, 1965), California (Douglass, 1974; Stevens et al., 2001; Stevens and Stone, 2007), British Columbia (Thompson, 1965), Kansas and adjacent Midcontinent localities (Dunbar and Condra, 1927; Sanderson et al., 2001; Wahlman, 2013), Idaho (Bostwick, 1955; Thompson et al., 1958), Nevada (Verville et al., 1956; Rich, 1961; Slade, 1961; Cassity and Langenheim, 1966; Douglass, 1974; Langenheim et al., 1977), New Mexico (Thompson, 1942; Lucas et al., 2000, Wilde, 2006), Texas (White, 1932; Bostwick, 1962; Ross, 1965; Kauffman and Roth, 1966), and Utah (Thompson et al., 1950; Douglass, 1974).

Although *Triticites* is found in Permian strata, the lower part of the Wolfcampian records a major fusulinid faunal transition with the appearance and subsequent dominance of the genera *Pseudoschwagerina* Dunbar and Skinner, 1936 and *Schwagerina* throughout the remainder of the Wolfcampian. The same distinct, complete faunal turnover is associated with the Pennsylvanian-Permian disconformity within the NSMR section. The upper Virgilian (= "Newwellian" or latest Pennsylvanian) fusulinid succession of the middle informal member of the Riepe Spring Limestone is dominated by highly inflated species of *Triticites*, but also includes several small specimens of *Pseudofusulinella* Thompson, 1951 along with a single form of *Pseudofusulina* Dunbar and Skinner, 1931, which has the irregular septa characteristic of basal forms of the genus. Unfortunately for the few

active fusulinid taxonomists, several latest Pennsylvanian schwagerinids occasionally regarded as *Schwagerina* by some authors would be better characterized as *Pseudofusulina*, and vice versa. The distinction between the genera, as succinctly clarified by Wilde (2006), is the presence of highly irregular rugosity in the spirotheca in forms belonging to *Pseudofusulina*. Although overlap between "primitive" forms of *Schwagerina* and "advanced" *Triticites* are known from Pennsylvanian-Permian boundary deposits, no *Triticites* have been recovered directly above the NSMR unconformity, and the Wolfcampian fusulinid succession is composed primarily of large *Schwagerina* with regular septa and dense secondary deposits. Species of *Pseudoschwagerina* are also present above the NSMR unconformity but are generally poorly preserved due to their extreme test inflation and the delicate nature of the spirotheca.

Previous studies of Wolfcampian fusulinid faunas include localities in Arizona (Thompson, 1954; Sabins and Ross, 1963; Ross and Tyrrell, 1965), California (Thompson et al., 1946; Thompson, 1954; Skinner and Wilde, 1965b; Douglass, 1974; Magginetti et al.,1988; Stevens et al., 2001; Stevens and Stone, 2007; Stevens and Stone, 2009a, 2009b), Alaska (Skinner and Wilde, 1966; Petocz, 1970), British Columbia (Thompson, 1965), Kansas (Thompson, 1954; Wahlman, 2013), Idaho (Bostwick, 1955; Thompson et al., 1958), Nevada (Thompson, 1954; Cassity and Langenheim, 1966; Rich, 1961; Slade, 1961; Hoare, 1963; Douglass, 1974; Stevens, 1979), New

Mexico (Thompson, 1954; Skinner and Wilde, 1965a; Steiner and Williams, 1968; Myers, 1988; Ross and Ross, 1994; Wilde, 2006), Oklahoma (Thompson, 1954), Texas (White, 1932; Dunbar and Skinner, 1937; Thompson, 1954; Ross, 1963; Williams, 1963, 1966; Ross, 1967; Ross and Ross, 2003), Utah (Thompson, 1954; Douglass, 1974; Stevens, 1979), and Wyoming (Verville, 1957).

Upper Pennsylvanian and Cisuralian (lower Permian) Conodont Biostratigraphy

Upper Pennsylvanian and Cisuralian conodont faunas and their associated biozones were described extensively from numerous international localities. The most notable studies have described assemblages from western and Midcontinent North America, South China, Bolivia, Japan, the Canadian Arctic, and the southern Ural Mountains.

Most investigations of Kasimovian and Gzhelian (Late Pennsylvanian) conodonts have focused nearly exclusively on the genera *Idiognathodus* and *Streptognathodus*. The two genera are prolific and ubiquitous in Pennsylvanian marine strata, with a composite range from the Bashkirian (lowest Pennsylvanian) into the Sakmarian (lower-middle Cisuralian). The conodont biostratigraphy of the Upper Pennsylvanian has been described from Russia (Barskov and Alekseev, 1975; Barskov et al., 1984; Alekseev and Goreva, 2006; Goreva and Alekseev, 2010), Donets

Basin (Ukraine) (Shchegolev and Kozitskaya, 1984), Novaya Zemlya (an Arctic archipelago) (Sabolev and Nakrem, 1996), the southern Ural Mountains (Chernykh et al., 1997; Chernykh and Ritter, 1997; Chernykh, 2005, 2006; Chernykh et al., 2006; Heckel et al., 2006), the North American Midcontinent (Baesemann, 1973; Ritter, 1995; Barrick and Heckel, 2000; Boardman et al., 2009; Barrick et al., 2013b), California (Stevens et al., 2001), New Mexico (Barrick et al., 2013a; Lucas et al., 2017b) and South China (Ding and Wan, 1990; Wang and Qi, 2002, 2003).

Several researchers have taken a more combinatory approach to the conodont biostratigraphy of the Upper Pennsylvanian and have correlated biozones with stratigraphic cycles. These North American sequence biostratigraphic studies have described faunas from southern Vancouver Island (Katvala and Henderson, 2002) and the Paradox Basin of Utah (Ritter et al., 2002). Various other taxonomic and phylogenetic studies of Late Pennsylvanian conodonts include (from earliest to most recent) works of: Gunnell (1931, 1933); Ellison (1941); Rhodes (1952); von Bitter (1972); Merrill (1973); Perlmutter (1975); Merrill and Powell (1980); and Ritter (1994).

In addition to the rapid change observed within the American fusulinid faunas of the earliest Permian, conodonts underwent a nearly synchronous and likewise dramatic transition as well. The conodont faunal turnover associated with the Late Pennsylvanian and Cisuralian is

expressed by the widespread ecological replacement of *Streptognathodus* with *Sweetognathus* in shallow marine deposits. *Sweetognathus* and *Streptognathodus* briefly share the lower Cisuralian in the North American Midcontinent (Kozur, 1975; Bando et al., 1980; Ritter, 1986), California (Stevens et al., 2001), British Columbia (Orchard, 1984), the Sverdrup Basin (Henderson, 1989), and Bolivia (Riglos Suárez et al., 1987; Henderson et al., 2009), but there is no observed overlap among the genera in the NSMR section. The *Sweetognathus* lineage arose from *Diplognathodus* Kozur and Merrill, 1975 in the earliest Permian (Asselian) with the appearance of the diminutive, pustulose, adenticulate to subtly nodose *Sweetognathus expansus*. The pustulose nature of the carina remains the singular diagnostic characteristic of the genus throughout its range into the late Cisuralian. The evolution and distribution patterns of the *Sweetognathus* stock have been described extensively in both journal publications (Cheng-yuan et al., 1987; Mei and Henderson, 2001; Mei et al., 2002; Davydov et al., 2005) and newsletter correspondence (Chernykh, 2012; Henderson et al., 2012; Chernykh et al., 2013; Vuolo et al., 2014).

Investigations of Cisuralian conodont biozonation have focused primarily on the partial range lineage biozones of the last occurring (youngest) species of *Streptognathodus* (e.g., *S. fusus* Chernykh and Reshetkova, 1987, *S. barskovi* (Kozur, 1976)), *Sweetognathus*, and *Neostreptognathodus*. In addition to the comprehensive zonation scheme of

Henderson (2016), conodont zonation of the Cisuralian has been established in the Urals (Barskov et al., 1984; Isakova, 1989, 1998; Akhmetshina, 1990; Reshetkova and Chernykh, 1986; Chernykh and Reshetkova, 1988; Kozur, 1995; Chernykh and Ritter, 1997), the Great Basin region of North America (Clark and Behnken, 1971; Behnken, 1975a; Clark et al. 1979; Wardlaw and Collinson, 1979, 1986; Ritter, 1986), the North American Midcontinent (Wind, 1973; Ritter, 1995), Japan (Igo, 1981), New Mexico (Barrick et al., 2013b), British Columbia (Orchard, 1984), the Sverdrup Basin (Beauchamp and Henderson, 1994), South China (Ueno et al., 2002), and Thailand (Burrett et al., 2015). Global "provincial zones" have been established as well, including an Equatorial Warm Water Province, a peri-Gondwana Province, and a North Cool Water Province (Mei et al., 2001). A southwest North American sequence-biostratigraphic framework has also been erected utilizing Artinskian conodonts and parasequence sets from the Midland Basin of West Texas (Holterhoff et al., 2013).

Conodont Biostratigraphy of the Riepe Spring Limestone

The earliest conodont studies of the Riepe Spring Limestone began nearly a decade after the formation's formal description with Clark and Behnken (1971) near Moorman Ranch, Nevada. At the time of publication, and for some time to come, conodont workers were not yet able to differentiate upper Gzhelian from lower Cisuralian strata using only

conodont zones. Consequently, fusulinid and ammonoid biozones provided the most detailed indices for the Carboniferous-Permian boundary during biostratigraphic studies in the 1970's. Additional investigations of the Riepe Spring Limestone conodont succession at Moorman Ranch were conducted over the next two decades by the same few workers (Clark, 1974; Behnken, 1975b; Ritter, 1986; Ritter, 1987).

Ritter (1986) recognized the phylogenetic importance of the "post-Early Permian crisis" *Sweetognathus* stock and issued a taxonomic revision of the genus. Near extinction events or, in the case of the early Cisuralian, faunal turnovers and the ensuing radiative speciation offer critical insight into understanding the often-complex pathways within evolutionary lineages (Ritter, 1986). The study also classified the Cisuralian sweetognathids as Type I, Type II, Type III, and Type IV based on carinal morphology. A new carinal configuration is described in this study (Chapter 8) for specimens recovered from the upper informal member of the Riepe Spring Limestone displaying characteristics of both the Type III and Type IV groups (Read and Nestell, in press). Ritter (1987) provided refinement of the *Mesogondolella bisselli-Sweetognathus whitei* assemblage zone of the Riepe Spring Limestone at Burbank Hills, Utah, and other equivalent units in Nevada, Kansas, and Texas. Following the work of Ritter (1986, 1987), there was little research interest in conodonts of the Riepe Spring Limestone until Wardlaw et al. (1998) proposed new

composite reference sections for the Carboniferous-Permian boundary in northeast Nevada. Further investigations were never carried out, and the assigned ages of both sections were based on preliminary, unpublished conodont identifications.

CHAPTER 3 – INTRODUCTORY REMARKS

The following chapter provides a lithostratigraphic and depositional overview of the full exposure of Riepe Spring Limestone at Spruce Mountain Ridge. The stratigraphic sections described in each subsequent chapter coincide, either in whole or in part, with the measured section presented herein in Chapter 3.

CHAPTER 3: LITHOSTRATIGRAPHY AND MICROFACIES ANALYSIS OF THE RIEPE SPRING LIMESTONE, SPRUCE MOUNTAIN RIDGE, ELKO COUNTY, NEVADA

Abstract: A recently measured section of the Riepe Spring Limestone at Spruce Mountain Ridge, Elko County, Nevada, presents a stratigraphic record of the coastal evolution and shallow shoreline-to-open marine depositional history of a part of the post-Antler foreland. The 420 m thick "North Spruce Mountain Ridge" (NSMR) section consists of highly variable, mixed carbonate and siliciclastic Upper Pennsylvanian-Cisuralian (lower Permian) strata. The study was initiated in an attempt to document the Pennsylvanian Permian boundary. The NSMR section, which follows Section 1 of Hope (1972), was remeasured and sampled for stratigraphic revision of the Hope's Section 1 with an accompanying biostratigraphic study of the fusulinid and conodont assemblages. As a result, a new lithostratigraphic interpretation of the Riepe Spring Limestone at Spruce Mountain Ridge, herein consisting of three lithologically distinguishable members, is presented. The so-called lower, middle, and upper informal members of the formation are composed of thick, alternating units of limestone, calcareous sandstone, and quartzose conglomerate. Four discrete types of conglomerate macrofacies are discussed, expanding upon the original descriptions ("Types 1 and 2") of Marcantel (1975). In addition to the minor revision of the conglomeratic facies, petrographic analyses and depositional interpretations of rocks are provided in a discussion of primary carbonate-siliciclastic microfacies. Ten microfacies are described and illustrated, including: calcareous siltstone, fine to medium calcareous sandstone, bioclastic

sandstone, replacement dolomite, nodular fusulinid biomicrite, echinoderm-foraminifer biomicrite, quartzose biomicrite, echinoderm-*Tubiphytes* poorly-washed biosparite, poorly-washed pelsparite, and crinoid-brachiopod-bryozoan biosparudite.

Introduction

The lithologically heterogenous deposits of the Riepe Spring Limestone reflect rapid and numerous fluctuations in depositional setting. Throughout the North Spruce Mountain Ridge (NSMR) section, bedding units continuously alternate from shallow marine deposits of variably quartzose limestone to coarse, detrital beach and bar deposits. These drastic shifts in lithofacies are directly related to glacioeustatic fluctuations during the late Paleozoic ice age (LPIA) and the apparent tectonic instability of the western cratonal margin following the Devonian-Mississippian Antler orogeny.

The deposition of much, if not all, of the Riepe Spring Limestone was coincident with glacial stage III of the LPIA (Fig. 3.1). During this third and final glacial episode, changes in global ice volume produced estimated sea-level oscillations of 60 to 120 m (Rygel et al., 2008). The widespread coastal emergence associated with this dramatic sea-level fall is well-represented along the west coast of Pangea by several previously described, nearly coeval unconformities (Stevens and Stone, 2007; Wahlman and Tasker, 2013). In addition to pronounced glacioeustatic influence, the sedimentological

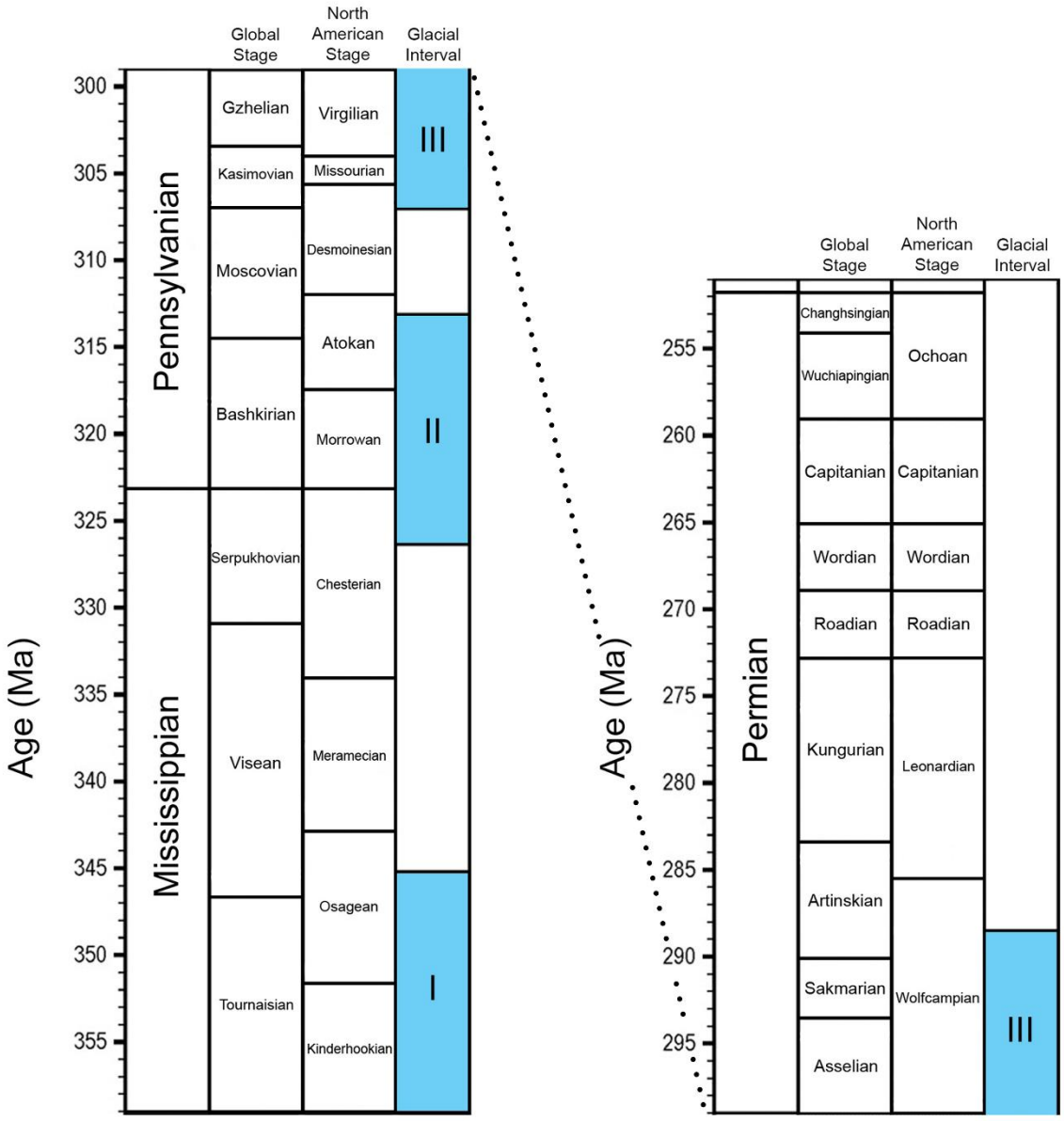

Figure 3.1 – Late Paleozoic timescale illustrating international and North American regional chronostratigraphic stages with corresponding Gondwanan glacial intervals (blue) of the late Paleozoic ice age (modified from Rygel et al., 2008).

composition of the Butte Basin (Late Pennsylvanian) and Ferguson Trough (Cisuralian) region was controlled in part by episodic regional tectonism (Yochelson and Fraser, 1973). Until the early 1990's, the west coast of Pangea was considered largely inactive during much of the Pennsylvanian and lower Permian, before post-Antler orogenesis resumed with the onset of the Permian-Triassic Sonoma orogeny (Dickinson, 1977; Stewart, 1980). Beginning with the work of Gallegos et al. (1991), Snyder et al. (1991), and Trexler et al. (1991), the hypothesis of prolonged quiescence along the cratonal margin began to receive scrutiny and was subsequently dismissed by most researchers of upper Paleozoic strata in central and eastern Nevada. More recent evidence for localized episodes of Carboniferous and Permian tectonism following the conclusion of Antler orogenesis has been presented from localities across central and eastern Nevada (Sweet et al., 2001; Sweet and Snyder, 2003; Trexler et al., 2003, 2004).

Location and Methods

The junction of Great Basin Highway (U.S. Route 93) and Spruce Mountain Road is located 57 km south of Wells, Nevada, on the east side of the highway (Fig. 3.2A). The unpaved Spruce Mountain Road stretches eastward for seven kilometers before its splits to the north and south to parallel the western base of the ridge. The base of the hill below the measured section is located approximately 14 km northeast (aerial

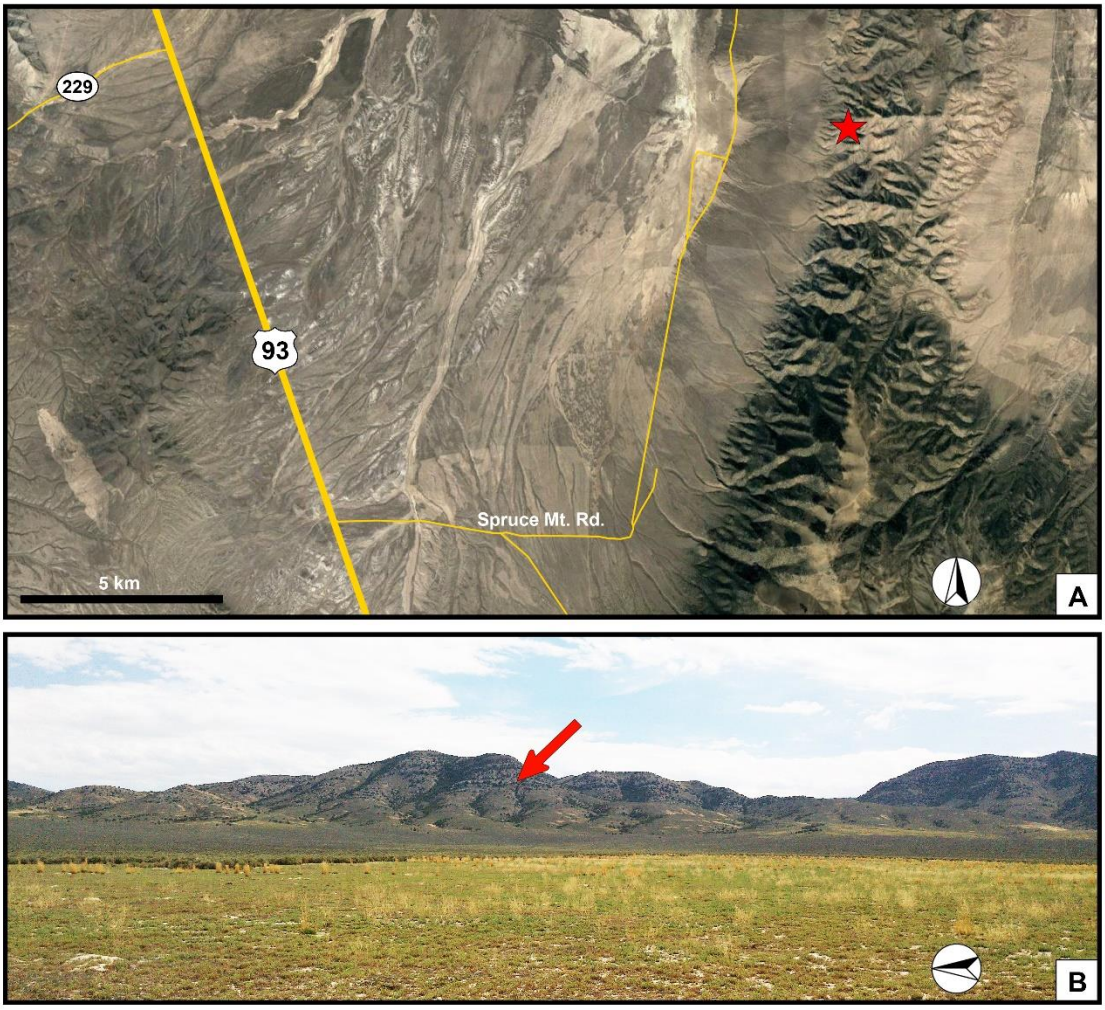

Figure 3.2 – A) Aerial map of Spruce Mountain Ridge (along the right side of the figure), east of Great Basin Highway (U.S. Route 93). The NSMR measured section (red star) is approximately 14 km northeast of the highway junction with Spruce Mountain Road (modified from Google Earth, 2014); **B)** Eastward view of the lower part of the NSMR section. The photograph was taken along northbound Spruce Mountain Road. The red arrow denotes the base of the section in the uppermost part of the Ely Limestone.

measurement) of the highway junction and is accessible only by foot or four-wheel drive vehicle (Fig. 3.2B). The greater north-south ridge is composed of a series of smaller, low, west-east trending hills extending from Spruce Mountain for approximately 25 km. Except for minor fault blocks of Silurian brecciated dolomite and undifferentiated Mesozoic-Cenozoic "iron-stained quartz breccia" to the south (in the western foothills of Spruce Mountain), the entirety of Spruce Mountain Ridge is Mississippian through Permian in age (Hope, 1972).

The NSMR measured section is located along one of the west-east hills of Spruce Mountain Ridge and directly corresponds to Section 1, the northernmost section of three measured sections described by Hope (1972) (40°40'47.08"N, 114°49'35.04"W). The base of the NSMR section is within the uppermost part of the Ely Limestone, which extends downward over 400 m westward beyond the base of the measured section before it is obscured by alluvial basin-fill. The uppermost interval of the NSMR section includes the gradational lithostratigraphic transition from the Upper Pennsylvanian-Cisuralian Riepe Spring Limestone to the Cisuralian Rib Hill Formation.

The NSMR section is a single, continuous interval and is relatively undeformed, although minor west-east trending folding and faulting occurs to the north and south respectively (Fig. 3.3). The section was measured with a 1.5 m Jacob's staff equipped with an inclinometer and an eyepiece. Strike and dip measurements were taken with a conventional Brunton pocket transit at

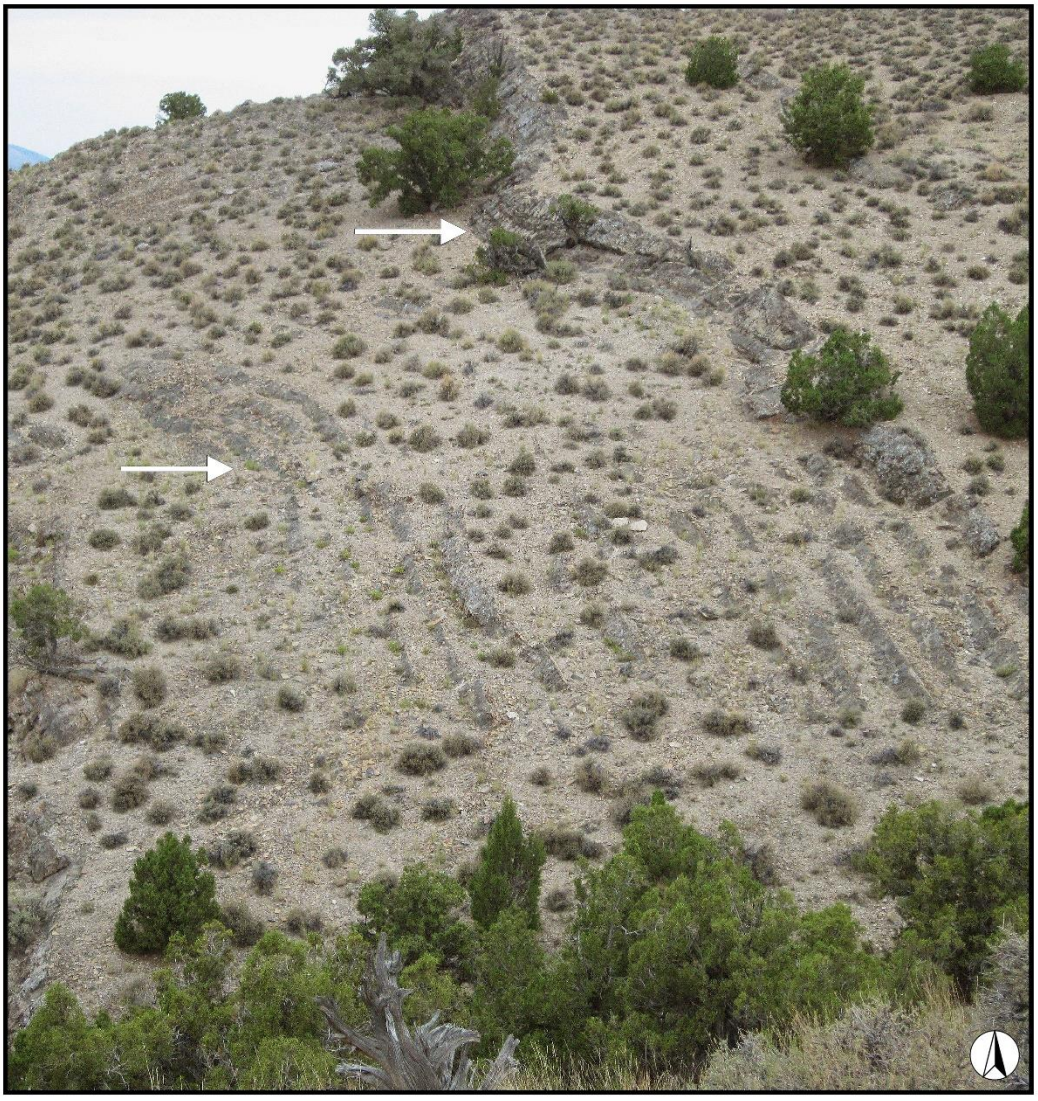

Figure 3.3 – Minor folds (white arrows) in the upper part of the Ely Limestone, located one hill to the north of the NSMR section. The illustrated interval is stratigraphically lower than the base of the measured section and is Desmoinesian (Middle Pennsylvanian).

regular intervals to insure accuracy. Samples were taken from each bedding unit of the section for the study of fusulinids, conodonts, and microfacies. Lithostratigraphic descriptions use a combinatory approach to discussing various lithofacies, including both "universal" geological terminology (i.e., calcareous sandstone, chert pebble conglomerate) for siliciclastic-dominated units, and Dunham (1962) classification terms for strictly carbonate units (i.e., wackestone, packstone). Descriptions of carbonate microfacies in thin sections follow the classification scheme of Folk (1959, 1962). Thin sections for the petrographic study were prepared by the M.T. Read at the thin section laboratory in the Department of Earth and Environmental Sciences at the University of Texas at Arlington. A SciScan digital slide scanner was used for microfacies photomicrographs.

Lithostratigraphy

The NSMR section is 420 m in total thickness and includes three formations: the uppermost part of the Ely Limestone, Riepe Spring Limestone, and lowest part of the Rib Hill Formation. The lithostratigraphy of the Riepe Spring Limestone near Spruce Mountain, the primary concern of this chapter, has not been studied in detail since the early to mid-1970's. To date, the most comprehensive petrological investigation of the Spruce Mountain area was presented by Marcantel (1973) as part of his doctoral dissertation, with a follow-up AAPG publication (see Marcantel, 1975). Prior

to Marcantel (1975), the quadrangle was mapped and briefly described by Hope (1972) (see USGS GQ-942). Marcantel (1975) expressed doubt regarding the genetic relationship between the Riepe Spring Limestone of the Ely-Moorman Ranch area and Hope's (1972) Riepe Spring Limestone of Spruce Mountain Ridge. Rather than referring to the strata exposed in the Spruce Mountain quadrangle as the Riepe Spring Limestone, Marcantel (1975) reservedly regarded the succession as the "Riepe Spring" Formation. Marcantel (1975) suggested that the formation is perhaps more closely related to the Strathearn Formation or that it may be genetically distinct, and therefore warrant the assignment of a new name. However, because the Strathearn Formation was not examined in this study and the GQ-942 map is still given priority for the Spruce Mountain area, Hope's (1972) stratigraphic nomenclature is used herein. Figure 3.4 illustrates a partial, modified version of the GQ-942 map area surrounding Section 1 of Hope (1972). The distinctions noted by Marcantel (1975) do have some merit, as the Riepe Spring Limestone of Spruce Mountain Ridge differs notably from most other interpretations of the formation by spanning the Carboniferous-Permian boundary. Most known exposures of the Riepe Spring Limestone are strictly lower to middle Cisuralian successions which disconformably overlay Middle Pennsylvanian (upper Moscovian) strata.

During the present study, the necessity for several stratigraphic revisions became evident. First, the lithostratigraphic contact between the

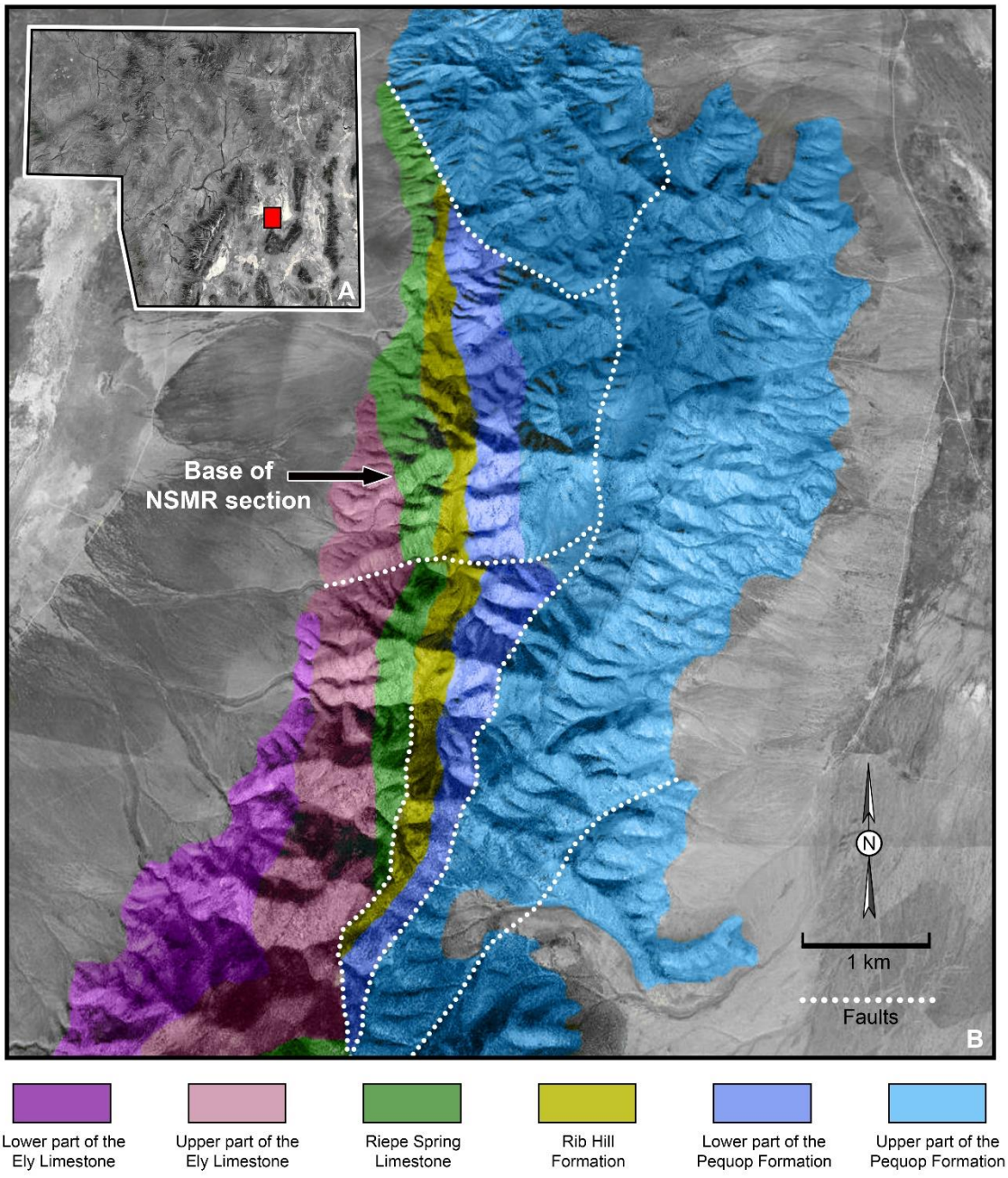

Figure 3.4 – A) Aerial map of Elko County, northeast Nevada, with the location of Spruce Mountain Ridge (red rectangle) (modified from Google Earth, 2014); **B)** Colorized aerial map illustrating the Pennsylvanian-Permian lithostratigraphic formations exposed along the north-central part of Spruce Mountain Ridge (after Hope, 1972; modified from Google Earth, 2014).

Ely Limestone and the Riepe Spring Limestone in the Spruce Mountain area is somewhat difficult to interpret due to the brevity of Hope's (1972) description. Marcantel (1975) suggested that a thin chert pebble orthoconglomerate denotes the base of the Riepe Spring Limestone at other localities, so herein the Ely-Riepe Spring contact is placed at the base of the lowest conglomerate on the west side of the hill (Fig. 3.5A). Hope (1972) described the conglomeratic beds as characteristic of the Riepe Spring Limestone. Following the initial occurrence of the conglomeratic lithofacies, varied conglomerate units compose an appreciable portion of the section referred to as Riepe Spring Limestone, accounting for 16% of the formation's total thickness. There are four recognized types of chert and quartzite pebble conglomerate present in the NSMR section, two of which were previously described by Marcantel (1975). These detrital "macrofacies" are discussed in detail under the heading *Macrofacies, Microfacies, and Depositional Settings*. The Riepe Spring Limestone of Spruce Mountain Ridge is subdivided into three distinctive parts, herein regarded as the lower, middle, and upper informal members (Fig. 3.5B). The present study is the first account of subdividing the Riepe Spring Limestone and individual descriptions of the three members follow.

Finally, in previous studies of the section there has been a discrepancy regarding the placement of the upper contact between the Riepe Spring Limestone and the overlying Rib Hill Formation. The placement of the base

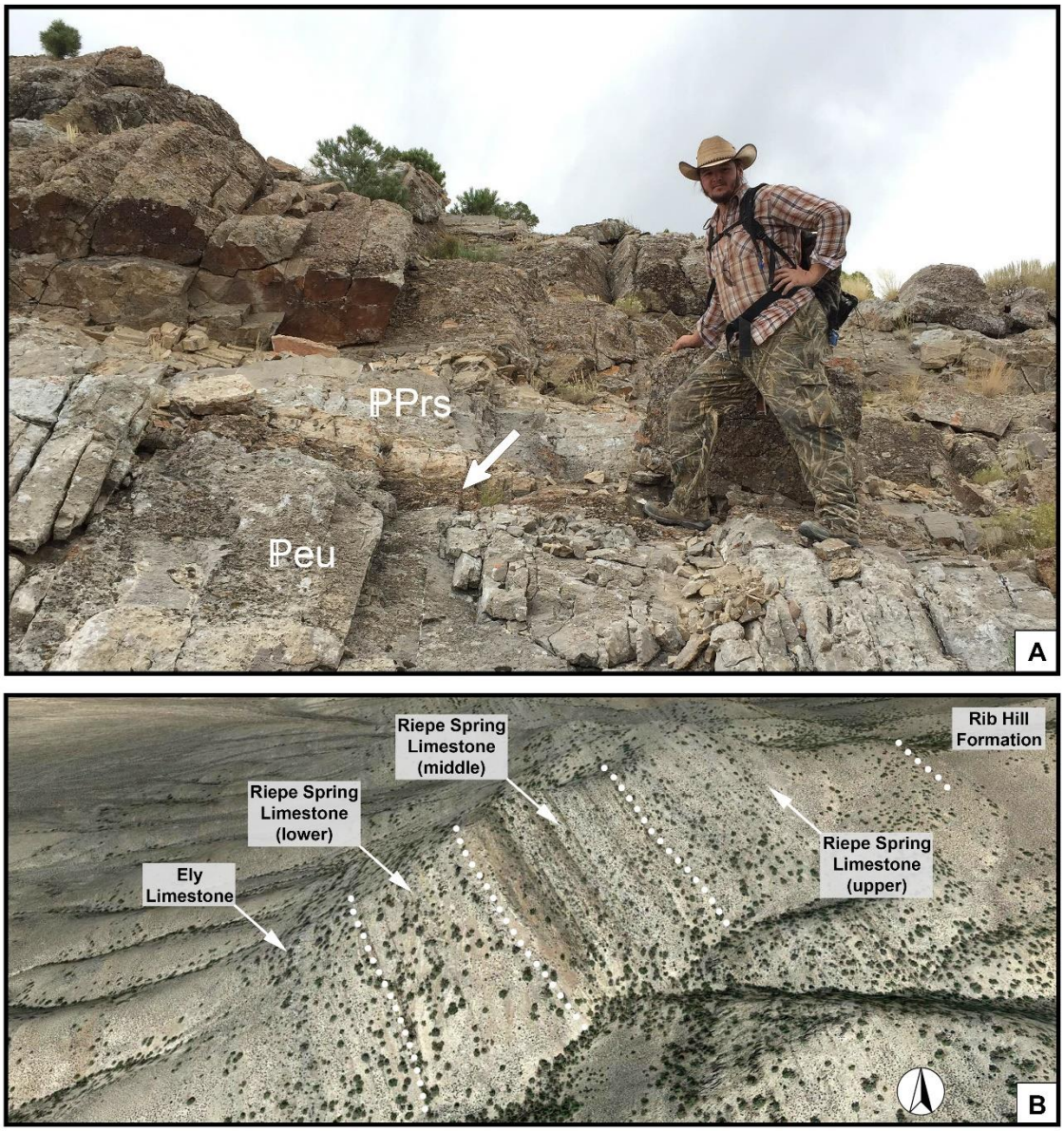

Figure 3.5 – A) Uppermost part of the Ely Limestone and the base of the lower member of the Riepe Spring Limestone (white arrow); **B)** Northward view of the NSMR section illustrating the herein revised division of Upper Pennsylvanian-Cisuralian stratigraphic units (Modified from Google Earth, 2013).

of the Rib Hill Formation by Hope (1972) is in agreement with its positioning in the present study, but personal correspondence between Hope and Douglass seems to place the boundary at a lower stratigraphic level along the east slope of the hill. These letters and notes from the Smithsonian's Douglass-Henbest collection were penned in 1969 when Douglass and Nestell collected Hope's Section 1 for fusulinid biostratigraphy, predating the publication of Hope (1972). The original section notes of Hope and Douglass were never located, but it seems that Hope must have revised the position of the Riepe Spring-Rib Hill contact after Douglass and Nestell collected their fusulinid material (1969, 1970), but before publication of the USGS GQ-942 map. Although there are units of thinly-bedded calcareous sandstone on the east slope and in the east saddle, there is still fossiliferous limestone exposed until the horizon marked as the base of the Rib Hill Formation on the stratigraphic column (Fig. 3.6). Beyond the contact there is only platy sandstone talus of the Rib Hill Formation (Fig. 3.7). This lithologic transition is sufficient enough to support Hope's (1972) final decision on the placement of the Riepe Spring-Rib Hill contact. The stratigraphic positions of Hope's (1972) Section 1, Marcantel's (1975) section in the southern Pequop Mountains, and the NSMR section are shown in Figure 3.8.

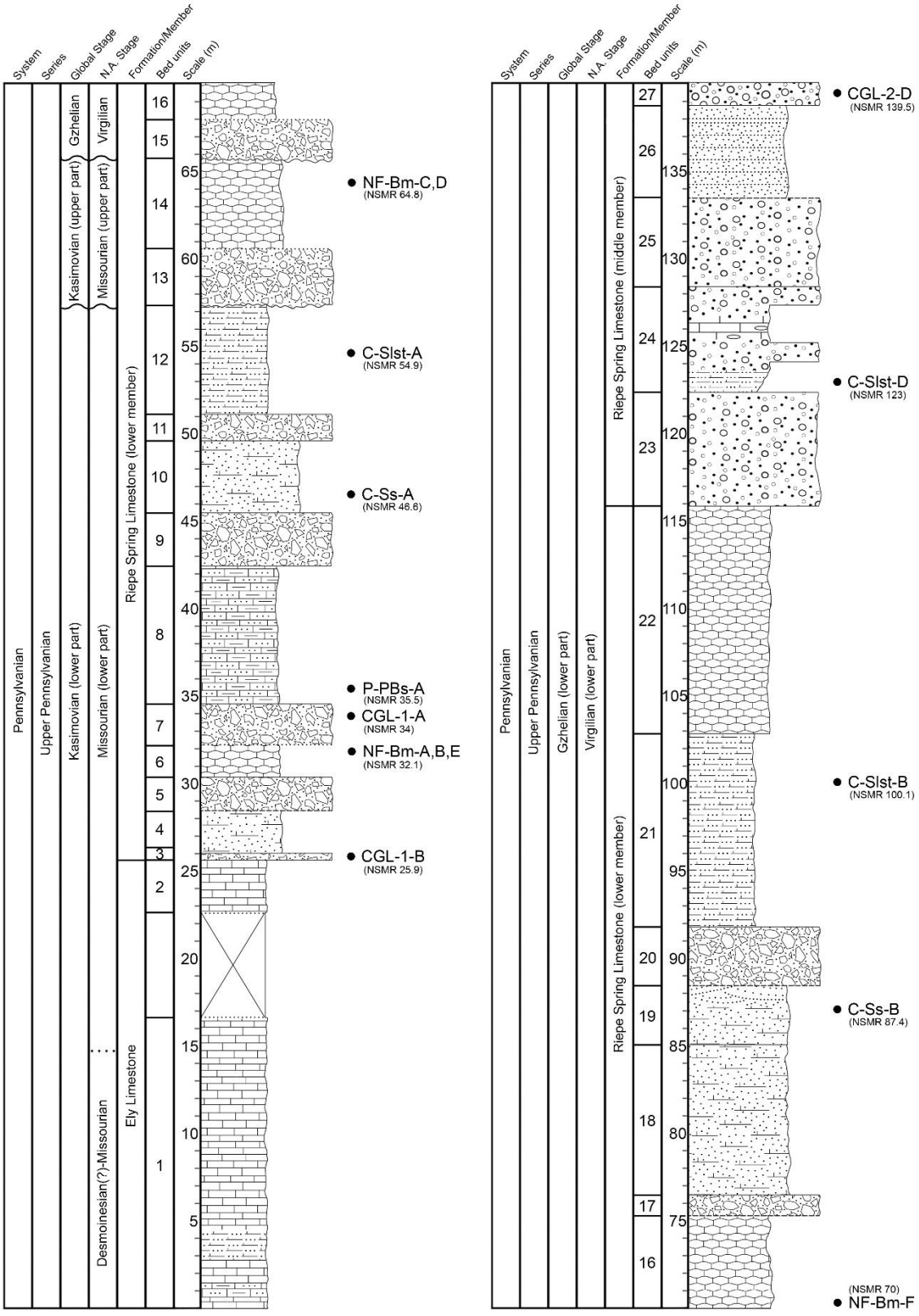
System
Series
Global Stage
N.A. Stage
Formation/Member
Bed units
Scale (m)
Pennsylvanian
Upper Pennsylvanian
Kasimovian (lower part)
Kasimovian (upper part)
Gzhelian
Desmoinesian(?)-Missourian
Missourian (lower part)
Missourian (upper part)
Virgilian
Ely Limestone
Riepe Spring Limestone (lower member)
Riepe Spring Limestone (middle member)
NF-Bm-C,D (NSMR 64.8)
C-Slst-A (NSMR 54.9)
C-Ss-A (NSMR 46.6)
P-PBs-A (NSMR 35.5)
CGL-1-A (NSMR 34)
NF-Bm-A,B,E (NSMR 32.1)
CGL-1-B (NSMR 25.9)
CGL-2-D (NSMR 139.5)
C-Slst-D (NSMR 123)
C-Slst-B (NSMR 100.1)
C-Ss-B (NSMR 87.4)
(NSMR 70)
NF-Bm-F

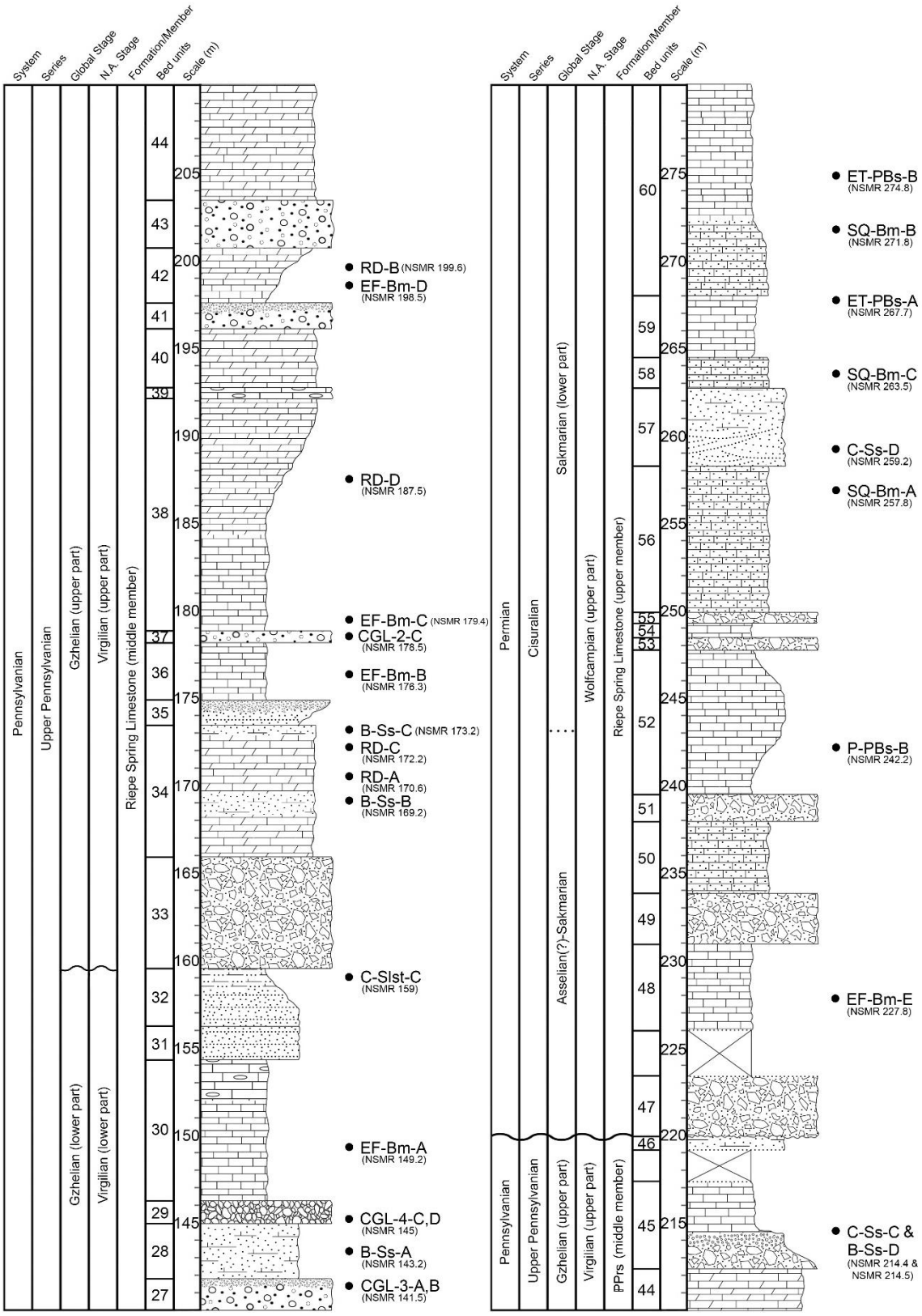
System
Series
Global Stage
N.A. Stage
Formation/Member
Bed units
Scale (m)
Pennsylvanian
Upper Pennsylvanian
Gzhelian (upper part)
Gzhelian (lower part)
Virgilian (upper part)
Virgilian (lower part)
Riepe Spring Limestone (middle member)
RD-B (NSMR 199.6)
EF-Bm-D (NSMR 198.5)
RD-D (NSMR 187.5)
EF-Bm-C (NSMR 179.4)
CGL-2-C (NSMR 178.5)
EF-Bm-B (NSMR 176.3)
B-Ss-C (NSMR 173.2)
RD-C (NSMR 172.2)
RD-A (NSMR 170.6)
B-Ss-B (NSMR 169.2)
C-Slst-C (NSMR 159)
EF-Bm-A (NSMR 149.2)
CGL-4-C,D (NSMR 145)
B-Ss-A (NSMR 143.2)
CGL-3-A,B (NSMR 141.5)
Permian
Cisuralian
Asselian(?)-Sakmarian
Sakmarian (lower part)
Wolfcampian (upper part)
Virgilian (upper part)
Riepe Spring Limestone (upper member)
ℙPrs (middle member)
ET-PBs-B (NSMR 274.8)
SQ-Bm-B (NSMR 271.8)
ET-PBs-A (NSMR 267.7)
SQ-Bm-C (NSMR 263.5)
C-Ss-D (NSMR 259.2)
SQ-Bm-A (NSMR 257.8)
P-PBs-B (NSMR 242.2)
EF-Bm-E (NSMR 227.8)
C-Ss-C & B-Ss-D (NSMR 214.4 & NSMR 214.5)

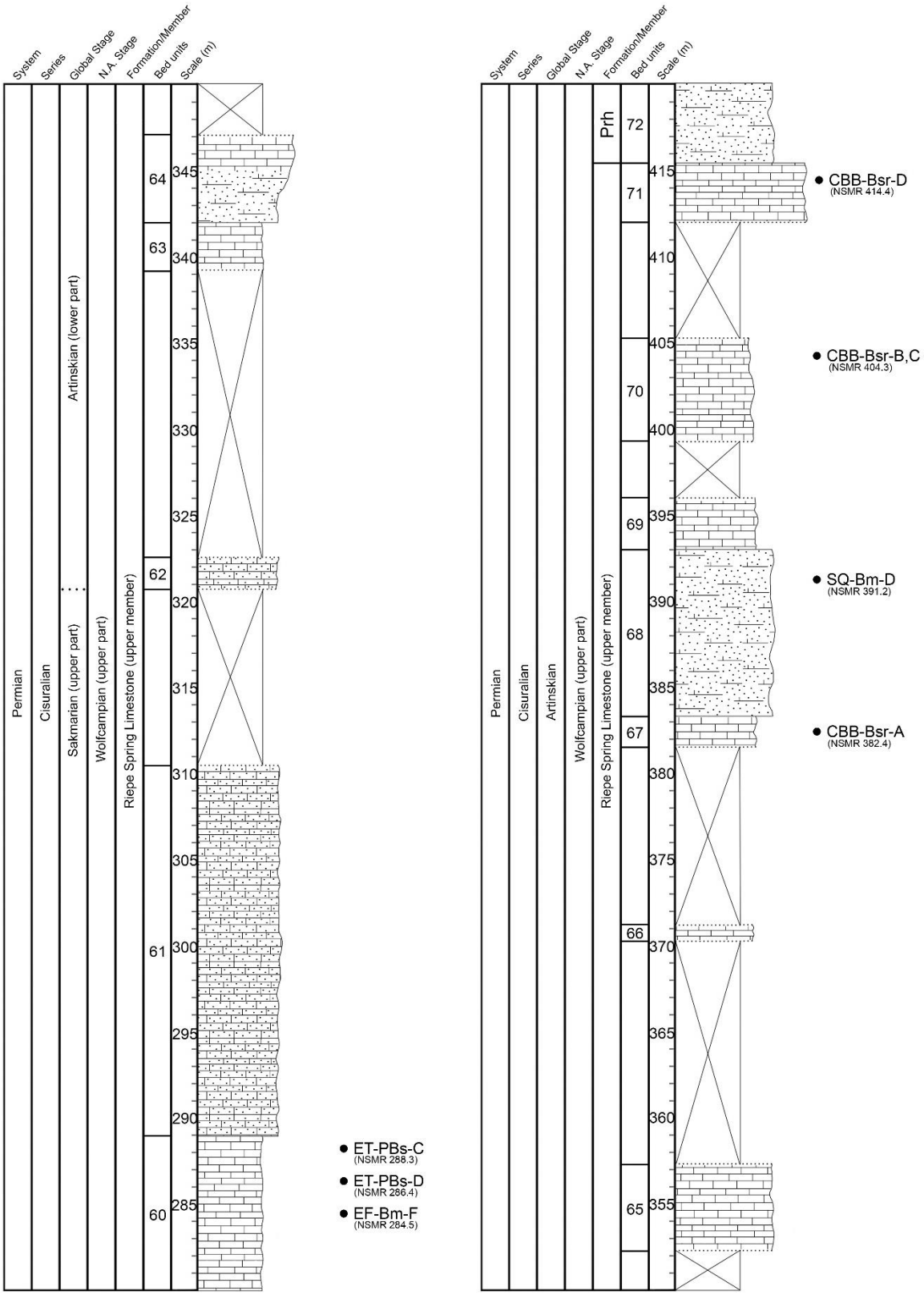
System
Series
Global Stage
N.A. Stage
Formation/Member
Bed units
Scale (m)
Permian
Cisuralian
Artinskian (lower part)
Sakmarian (upper part)
Wolfcampian (upper part)
Riepe Spring Limestone (upper member)
64
63
62
61
60
345
340
335
330
325
320
315
310
305
300
295
290
285
ET-PBs-C
(NSMR 288.3)
ET-PBs-D
(NSMR 286.4)
EF-Bm-F
(NSMR 284.5)
Prh
72
71
70
69
68
67
66
65
415
410
405
400
395
390
385
380
375
370
365
360
355
CBB-Bsr-D
(NSMR 414.4)
CBB-Bsr-B,C
(NSMR 404.3)
SQ-Bm-D
(NSMR 391.2)
CBB-Bsr-A
(NSMR 382.4)

Lithologic Key

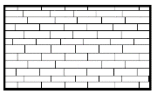
Limestone

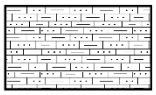
Silty limestone

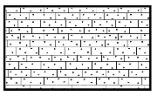
Sandy limestone

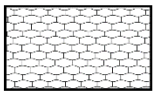
Nodular limestone

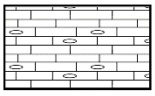
Chert pebble limestone

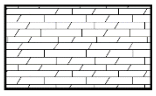
Replacement dolomite

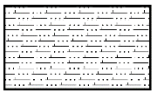
Calcareous siltstone

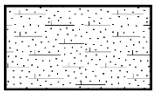
Calcareous sandstone

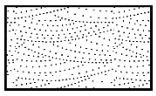
Cross-stratified sandstone

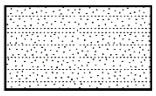
Siliceous sandstone

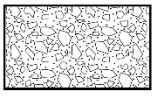
Type I conglomerate

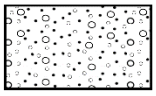
Type II conglomerate

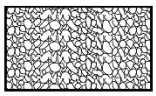
Type III conglomerate

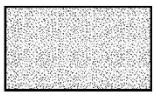
Type IV conglomerate

Type I conglomerate: CGL-1

Type II conglomerate: CGL-2

Type III conglomerate: CGL-3

Type IV conglomerate: CGL-4

Calcareous siltstone: C-Slst

Calcareous sandstone: C-Ss

Bioclastic sandstone: B-Ss

Replacement dolomite: RD

Nodular fusulinid biomicrite: NF-Bm

Echinoderm-foraminifera biomicrite: EF-Bm

Silty to sandy (quartzose) biomicrite: SSQ-Bm

Echinoderm-*Tubiphytes* poorly-washed biosparite: ET-PBs

Peloidal poorly-washed biosparite: P-PBs

Crinoid-brachipod-bryozoan biosparudite: CBB-Bsr

Uppermost part of the Ely Limestone

From the alluvial basin-fill to the contact with the Riepe Spring Limestone, the exposure of the Ely Limestone along the far west side of the ridge measures ~495 m in thickness. Only the uppermost part of the Ely Limestone was included in the study because much of the exposed, lower strata lack fusulinid-bearing beds. Nevertheless, conodont elements were recovered from several deep-water limestone samples taken several hundred meters below the included uppermost part of the Ely Limestone. The fusulinid assemblage includes *Beedeina weintzi* Verville, Thompson, and Lokke, 1956, *Bartramella bartrami* Verville, Thompson, and Lokke, 1956, and *Fusulinella alta* Verville, Thompson, and Lokke, 1956, indicating that this lower, excluded portion of the Ely Limestone is middle to upper Moscovian.

The lowest part of the NSMR section (units 1, 2) includes the uppermost 25.7 m of the Ely Limestone (lower Kasimovian) (Fig. 3.6). The measured section begins at the base of a thick wall of medium gray, brachiopod and crinoid-rich wackestone-packstone with sparse trilobites, brown, resistant lenses/nodules, and yellow-brown to red silty layers that range from thin, anastomosing stringers to approximately two meters thick (Figs. 3.6, 3.9). Above the wall is an approximately six-meter-thick slope that

← **Figure 3.6** – Multiple page figure includes a lithologic key and stratigraphic columns of the NSMR measured section. Letter codes along the right side of each column denote the position of corresponding illustrated microfacies samples.

Figure 3.7 – Platy, calcareous sandstone talus characteristic of the poorly exposed lower part of the Rib Hill Formation. The photograph was taken just above the lithostratigraphic contact with the upper member of the Riepe Spring Limestone.

is heavily obscured by talus from stratigraphically higher beds. It is difficult to gain a sense of the lithology associated with this interval because no remnants of bedded units were observed. The covered interval may represent a weakly cemented, fine-grained lithofacies, but there is no evidence of shale or poorly consolidated mudstone from any portion of the NSMR section. The uppermost bed of the Ely Limestone (unit 2; Fig. 3.6), which can be seen just below the first conglomerate in the lower portion of Figure 3.5A, is composed of light to medium gray algal wackestone.

Riepe Spring Limestone – lower informal member

The lower informal member of the NSMR Riepe Spring Limestone is Kasimovian-Gzhelian (Upper Pennsylvanian) based on conodonts and fusulinids and measures approximately 91 m in total thickness, though this value is likely inconsistent to the north and south of the section (along the ridge) due to lateral thickening and thinning of conglomerate units. At first glance, the lower informal member of the Riepe Spring Limestone superficially resembles the uppermost part of the Ely Limestone. The critical distinctions between the two formations are the presence of conglomeratic units and the more terrigenous composition of the limestone units in the lower informal member of the Riepe Spring Limestone. The lithological composition of the lower member is nodular wackestone to packstone (30%), conglomerate (22%), calcareous sandstone (20%), calcareous siltstone (19%),

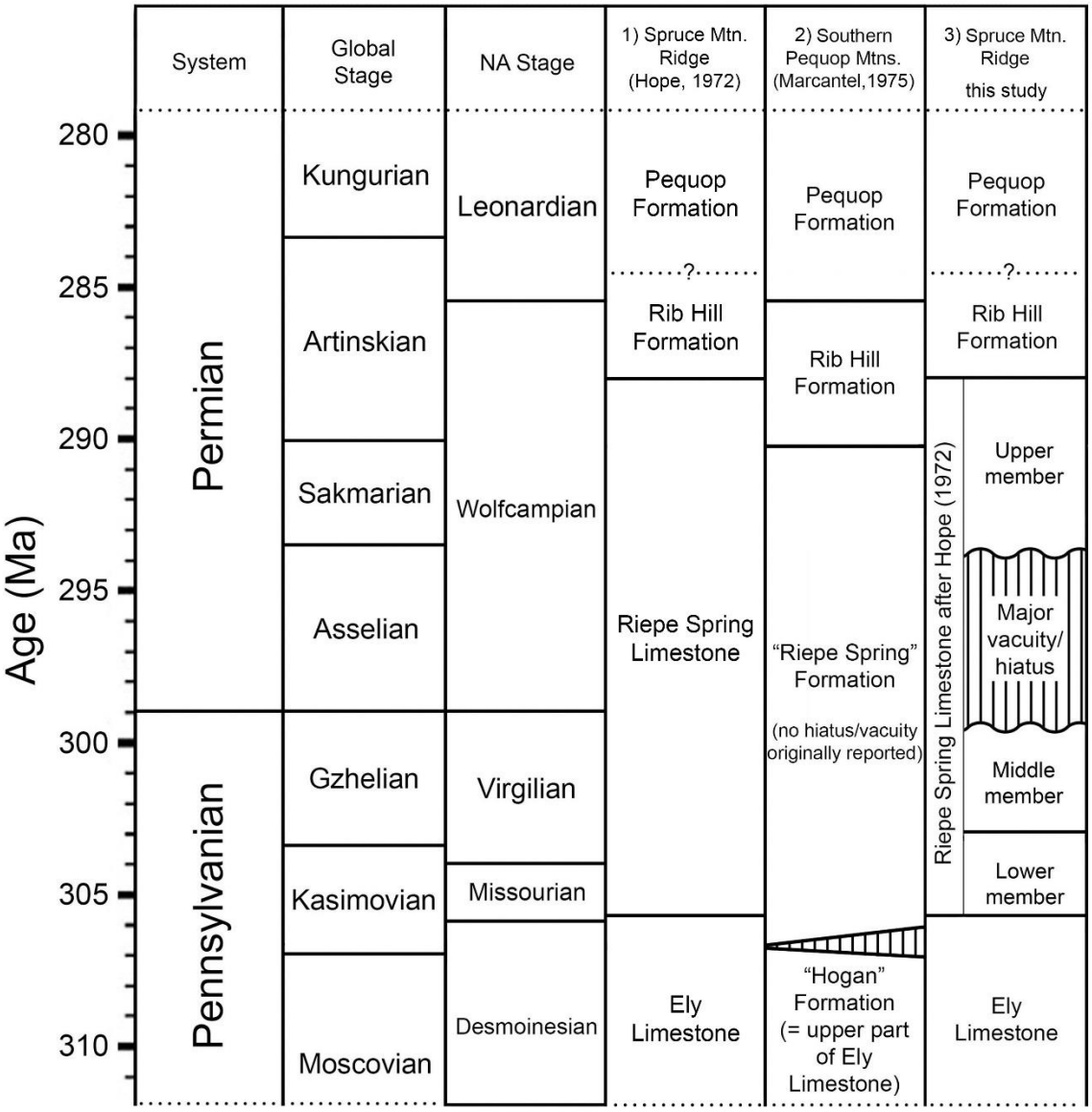

Figure 3.8 – Stratigraphic correlation and lithostratigraphic divisions of Hope's (1972) Section 1, Marcantel's (1975) section in the southern Pequop Mountains, and the North Spruce Mountain Ridge section.

and silty mudstone to wackestone (9%). Fusulinids are present sporadically throughout the lower informal member and occur most abundantly in the lower nodular wackestone-packstone lithofacies of units 6, 14, and 16 (Fig. 3.6).

The lowest conglomerate of the Riepe Spring Limestone is 0.6 m thick at its thickest point along the western face of the hill. The contact with the underlying Ely Limestone is sharp, but there is no evidence of significant incision into the lower algal limestone unit above. The nine conglomerate beds of the lower informal member belong to the volumetrically significant Type 1 (CGL-1) group of chert and quartzite pebble conglomerates and are often between one-half meter and three meters thick. Several of the thicker Type 1 conglomerate units have strongly scoured bases and incised channels with relief of a meter or more (Marcantel, 1975) (Figs. 3.6, 3.10).

The limestone units of the lower informal member are typically thick- to very thick-bedded and markedly siliciclastic, albeit fine-grained. The recurring presence of nodular limestone, a product of non-seam pressure solution, and deformed fusulinids in the upper part of unit 21 suggest that parts of the lower informal member of the Riepe Spring Limestone were subjected to significant overburden stress (Wanless, 1979). The uppermost bed of the lower informal member forms a very thick wall of nodular wackestone (with occasional chert gravel near the top) directly beneath the "boulder field" of the middle informal member.

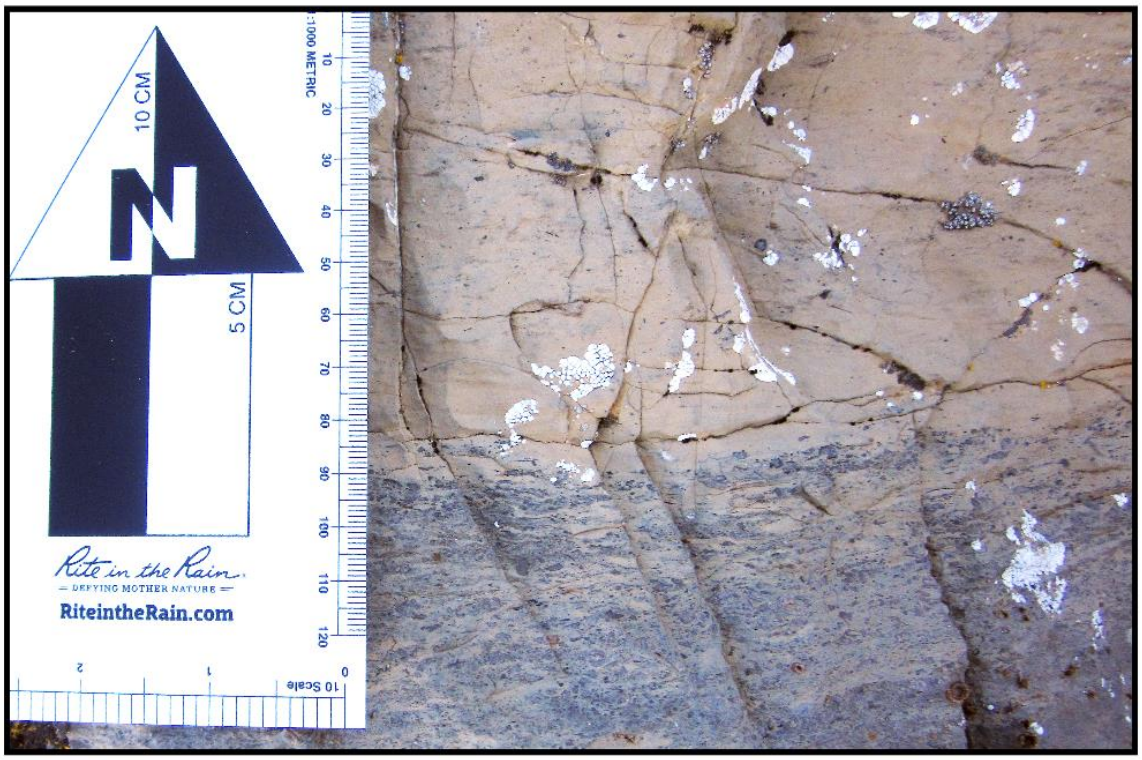

Figure 3.9 – Gradational transition from gray, fossiliferous, nearly nodular wackestone to a thin layer of tan, interbedded calcareous siltstone (unit 1; upper part of the Ely Limestone) (right side of scale bar in mm).

Riepe Spring Limestone – middle informal member

The middle informal member of the Riepe Spring Limestone is of Gzhelian age and measures approximately 104 m in thickness (Fig. 3.6). Of the three newly described members, the middle informal member has the highest volume of conglomeratic units (29% of the member) and the greatest diversity in conglomerate petrology. The base of the middle informal member is denoted by an unmistakable, appropriately named "boulder field" by the author (Fig. 3.11A). The darker, overwhelmingly siliciclastic strata of the lower part of the middle informal member form the distinctive false peak of the hill and this interval is easily seen in an aerial photograph of the section (Fig. 3.11B). The lithological composition of the middle member is conglomerate (29%), wackestone to packstone (24%), dolomitized wackestone to grainstone (23%), siliceous sandstone (10%), calcareous sandstone (9%), and wackestone with chert pebbles (5%).

The conglomeratic talus of the "boulder field" forms an uneven slope beneath the platy, siliceous sandstone of unit 26 (Fig. 3.6). The large, resistant blocks of conglomerate must have fractured and collapsed following the weathering and erosion of less resistant, thinly-interbedded limestone units. The sediments of the false peak grade from coarse sand to gravel, but appear to have a common provenance. Beyond the false peak, the middle informal member of the Riepe Spring Limestone is characterized by alternating intervals of light gray, carbonate-rich strata and brown to

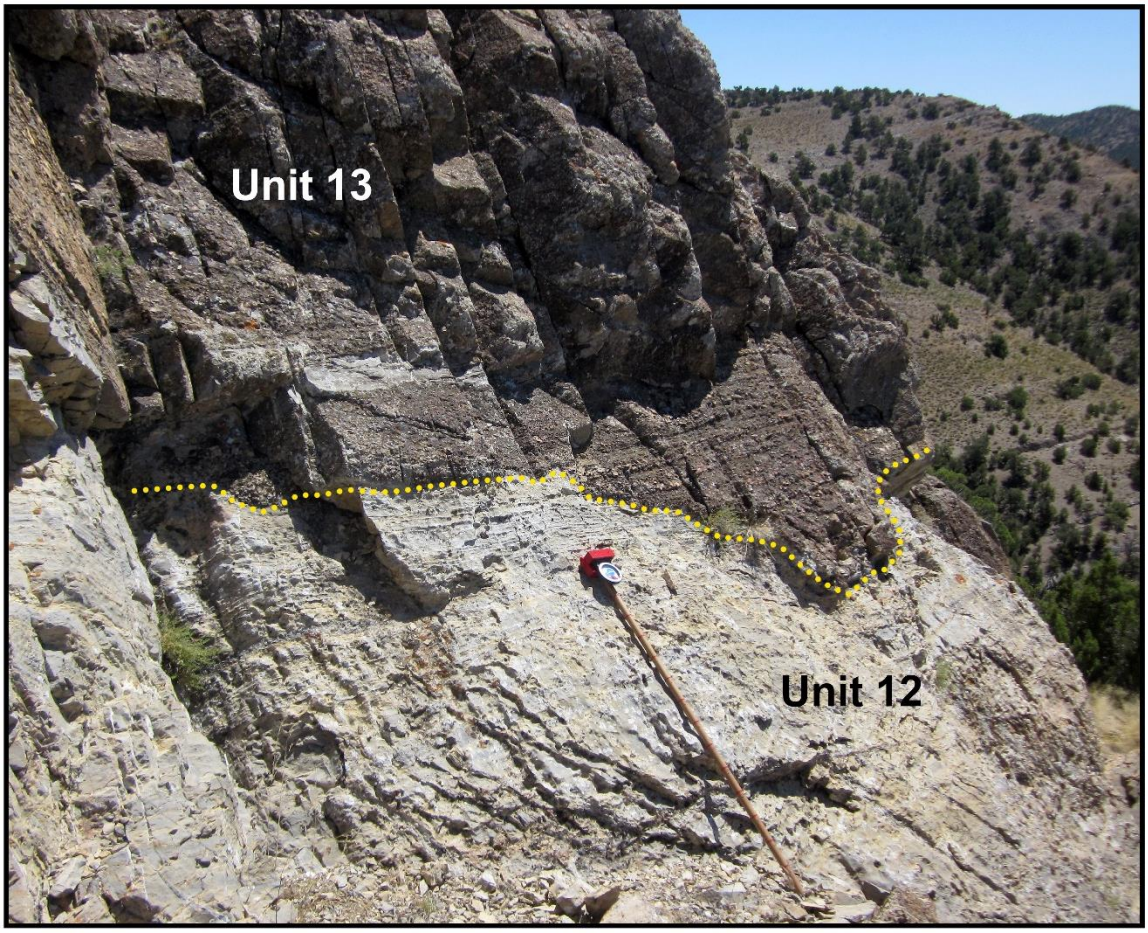

Figure 3.10 – Incised channel (yellow dotted line) of very thick-bedded Type 1 conglomerate of unit 13 (CGL-1) into the underlying calcareous siltstone of unit 12. Jacob's staff = 1.5 m.

reddish-brown conglomeratic units. The light-colored carbonate units are nearly equal parts limestone and replacement dolomite.

Riepe Spring Limestone – upper informal member

The upper informal member of the NSMR Riepe Spring Limestone sits directly atop a major disconformity, representing a Gzhelian-Sakmarian hiatus. Although the disconformity is discrete and was not identified in previous studies, the transition from the middle to the upper informal members of the Riepe Spring is denoted by two microsignatures: 1) a distinctive microfacies shift from light-colored, dolomitic, marginal marine and upper shoreface sediments to darker, muddy, open shelf deposits; 2) a complete microfaunal turnover in which there is no overlap between the fusulinid and conodont assemblages of the middle and upper members. In outcrop, the transition is marked by a slight color change in the limestone from light-medium to darker gray weathering beds and an overall reduction in the volume of conglomerate. The fusulinids of the middle and upper informal members, which are slightly altered, exhibit color variation as well, changing from a light pink-buff color to yellow-orange across the boundary. The base of the upper informal member is denoted by a very thick Type 1 conglomerate with a scoured base (unit 47) (Fig. 3.12).

The upper informal member of the Riepe Spring Limestone is Sakmarian-Artinskian (lower to middle Cisuralian) and is by far the thickest

Figure 3.11 – A) The distinctive, talus-strewn slope of the "boulder field," which denotes the base of the middle member of the Riepe Spring Limestone; **(B)** White arrow denotes the location of the "boulder field" within the NSMR section (modified from Google Earth, 2013).

of the three informal members, measuring approximately 195 m thick. The lithological composition of the upper informal member is fossiliferous wackestone to grainstone (31%), silty to sandy quartzose limestone (20%), calcareous sandstone (9%), and conglomerate (5%). The remaining 35% of the upper informal member is obscured by talus. The lower 68 m of the upper informal member compose the highest (topographically) western interval of the section up to the crest of the hill (Fig. 3.13A). Eastward beyond the crest, the section follows the east slope of the ridge downhill towards a saddle before gently rising to the next hilltop in the Rib Hill Formation (Fig. 3.13B).

Limestone units of the lower part of the upper informal member are among the most fossiliferous units of the Riepe Spring Limestone (Fig. 3.14). The topographically highest wackestone to packstone beds of the section, located just west of the crest of the hill, have the highest fusulinid yields of the entire Riepe Spring Limestone (Fig. 3.15A, B). Although conodont elements are difficult to recover from much of the Riepe Spring Limestone, the limestone beds of the lower part of the upper informal member reliably produced low to moderate yields. The eastern dip-slope interval is difficult to sample and there are several completely covered thick intervals of the section. Fortunately, fusulinids and conodont elements were still recovered from thin limestone and sandstone intervals along the slope and saddle, providing good biostratigraphic control throughout the uppermost ~125 m of the Riepe Spring Limestone. The Riepe Spring Limestone terminates at the

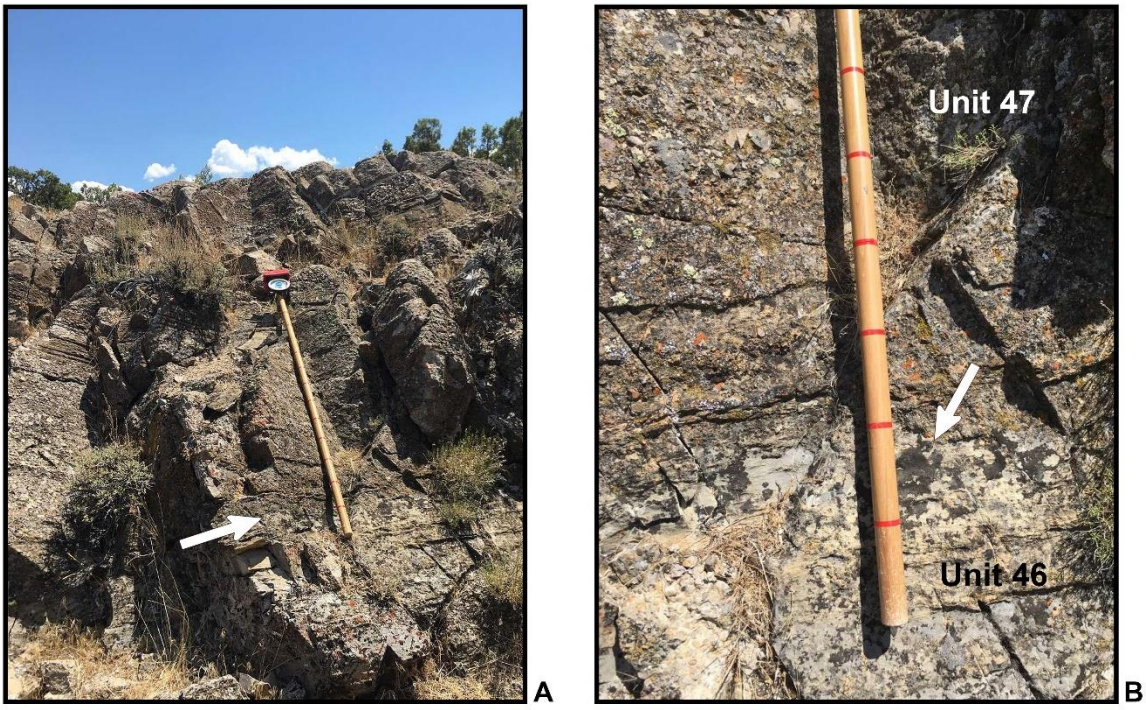

Figure 3.12 – A) Basal conglomerate of the upper member of the Riepe Spring Limestone associated with the Pennsylvanian-Permian disconformity. White arrow denotes erosional contact of the Type 1 conglomerate and the underlying calcareous sandstone (units 46 and 47). Jacob's staff = 1.5 m.; **B)** Close-up photograph of the basal scour between units 46 and 47.

initial expanse of platy, calcareous sandstone talus interpreted as the base of the Rib Hill Formation.

Macrofacies, Microfacies, and Depositional Settings

The depositional history of the Riepe Spring Limestone of Spruce Mountain Ridge is complex and variable. The three members comprise Kasimovian to Artinskian strata and record multiple sea-level changes along with an enigmatic history of shifting local paleoelevation. In order to establish a more comprehensive understanding of the depositional history of these strata, it is necessary to describe the carbonate and siliciclastic petrology and petrography of the NSMR section. The generalized lithofacies discussed in the previous *Lithostratigraphy* heading are described in detail with reference to inferred depositional paleoenvironments. Four conglomeratic macrofacies and 10 primary microfacies are described. The microfacies consist of three dominantly siliciclastic types (calcareous siltstone, fine to medium calcareous sandstone, and bioclastic sandstone) and seven carbonate-dominated types (replacement dolomite, nodular fusulinid biomicrite, echinoderm-foraminifer biomicrite, quartzose biomicrite, echinoderm-*Tubiphytes* poorly-washed biosparite, poorly-washed pelsparite, and crinoid-brachiopod-bryozoan biosparudite). Although other microfacies were observed in the petrographic study, only microfacies which occurred at least twice within the measured section are included among the following

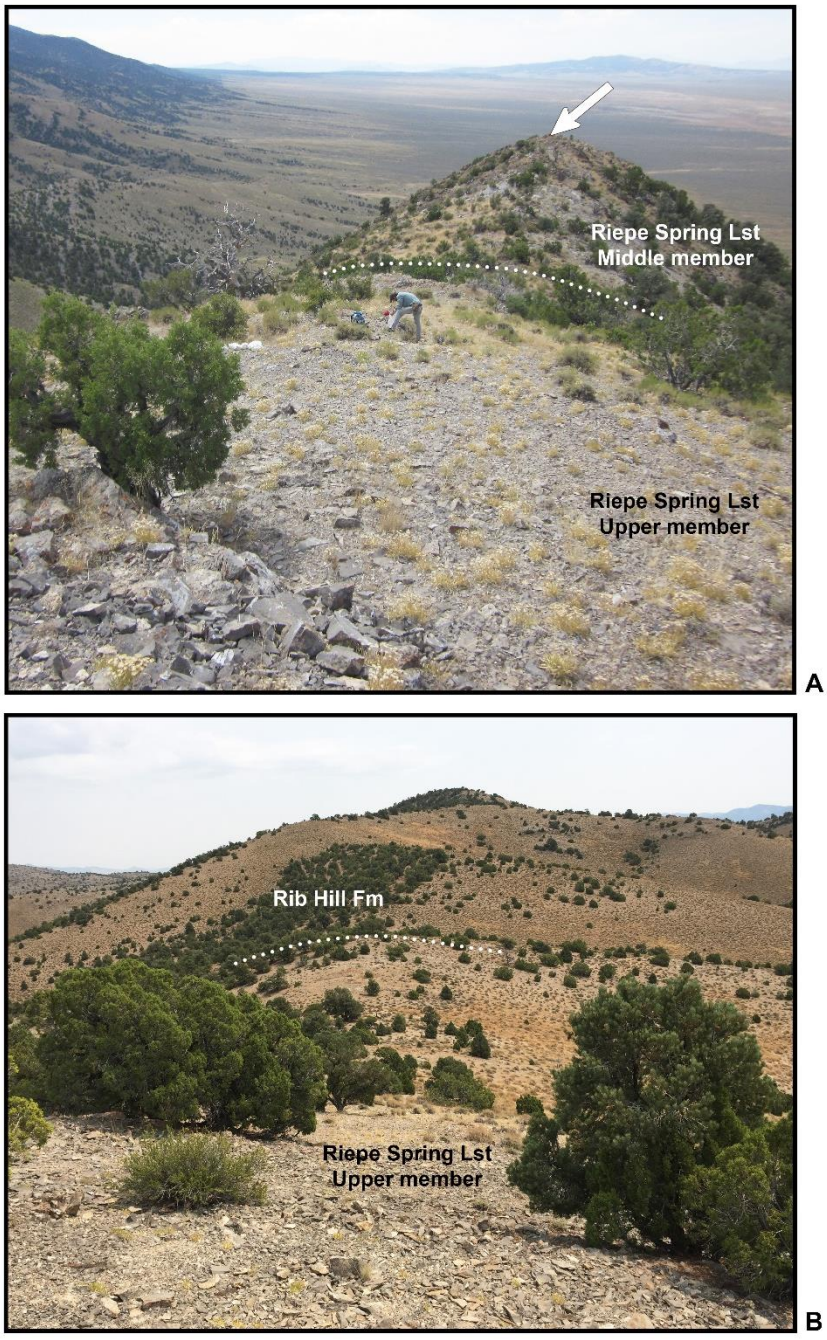

Figure 3.13 – A) West-southwest view of the section from just below the crest of the "hill." White dotted line denotes the level of the contact between the middle and upper members of the Riepe Spring Limestone. White arrow denotes the position of the top of the "false peak" conglomerate (unit 27); **B)** Eastward view of the NSMR section from just east of the crest of the ridge. Note the poor exposure and thick, talus-obscured intervals of the dip-slope. White dotted line denotes the approximate level of the contact between the upper member of the Riepe Spring Limestone and the Rib Hill Formation.

descriptions. Figure 3.16 illustrates a composite Late Pennsylvanian-Cisuralian depositional model depicting the generalized arrangement of inferred paleoenvironments associated with each of the macrofacies and microfacies discussed.

Type 1 Conglomerate of Marcantel (1975) (CGL-1)

The Type 1 conglomerate of Marcantel (1975) (CGL-1) is considered the defining lithological criterion of the Riepe Spring Limestone at Spruce Mountain Ridge (Hope, 1972; Marcantel, 1975). CGL-1 occurs throughout much of the NSMR section as thick to very thick, highly resistant, tan to brown weathering beds, but can also be thinly interbedded with C-Ss or SSQ-Bm units (Fig. 3.17A). CGL-1 is a texturally immature paraconglomerate composed of unsorted, subangular to angular polymictic chert and quartzite granules, pebbles, and cobbles within a sandy, quartzose matrix bound by calcareous or siliceous cement (Fig. 3.17B). Most of the chert and quartzite clasts are varying hues of gray or brown. Although Marcantel (1975) observed occasional intraclasts of Ely Limestone in samples of his previously described Type 1, none are present in the samples collected from NSMR Type 1 units. Crinoid columnals and other skeletal grains make up only a very minor component. The CGL-1 is the oldest exposed conglomerate of the four types discussed and is consistently the most texturally immature. Marcantel (1975) suggested that the logical provenances of the diverse chert and quartzite

Figure 3.14 – Highly fractured, fossiliferous wackestone to packstone from the lower part of the upper member of the Riepe Spring Limestone (unit 52). Unit 52 is primarily associated with the EF-Bm microfacies but is sparsely interbedded with the P-PBs microfacies. Jacob's staff = 1.5 m.

Figure 3.15 – A) Outcropping of massive, fossiliferous wackestone to packstone associated with the EF-Bm and ET-PBs microfacies. Dr. Bruce Wardlaw is shown at the upper right corner (unit 60); **B)** Crest-forming limestone (highest topographic point in the section). Jacob's staff = 1.5 m.

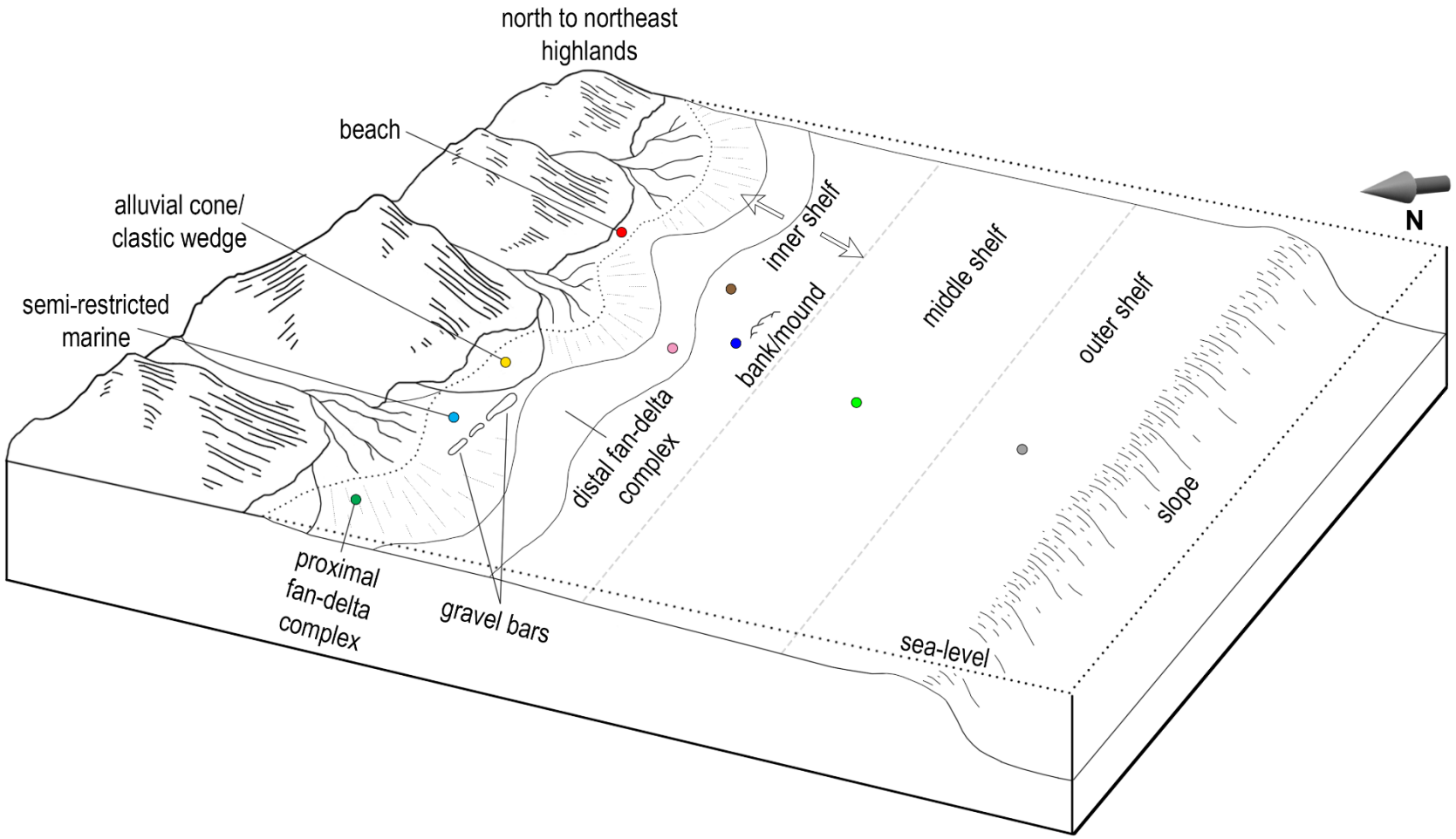

Figure 3.16 – Composite illustration of Late Pennsylvanian-Cisuralian depositional settings along the northern coast of the Ferguson Trough. Paleoenvironments are inferred from the dominant microfacies of the Riepe Spring Limestone.

clasts were chert-rich exposures of the Ely Limestone, the Mississippian-Lower Pennsylvanian Diamond Peak Formation, and Ordovician age rocks of the remnant Antler belt to the west. Strata of the former two formations would have been exposed to the north of the Spruce Mountain Ridge area by Late Pennsylvanian-Cisuralian episodes of local uplift (Yochelson and Fraser, 1973; Marcantel, 1975). The CGL-1 macrofacies is the most visibly erosive type of conglomerate occurring within the Riepe Spring Limestone.

In addition to illustrating examples of his Types 1 and 2 macrofacies, Marcantel (1975) provided basic depositional models for these prominent macrofacies outcropping throughout the Spruce Mountain Ridge area. The Type 1 conglomerate was interpreted by Marcantel (1975) as “clastic wedge" deposits shed into a marginal marine paleoenvironment from the recently exposed highlands to the north. The author agrees with this interpretation and suggests a coastal, distal alluvial cone setting. The sorting and angularity of CGL-1 detritus indicate that very little marine reworking occurred following the deposition of the terrigenous material (Marcantel, 1975).

Types II, III, and IV Conglomerate (CGL-2, 3, 4)

Although there are noticeable differences between the types II, III, and IV conglomerate, particularly in grain size, these three submature to mature types are discussed under the same subheading due to overall similarities in

A

B

2 cm

C

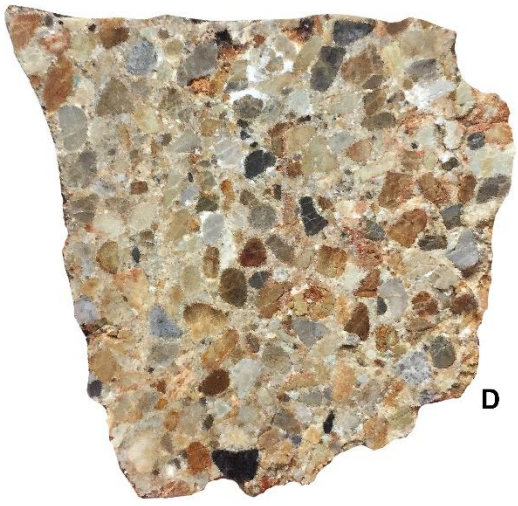

D

2 cm

grain composition, textural maturity, and matrix/cement mineralogy. The types II, III, and IV conglomerate lithofacies only occur within the middle informal member of the Riepe Spring Limestone, where they cumulatively supplant the Type 1 conglomerate and compose 29% of the member (~8% of the Riepe Spring Limestone). All three conglomerate types outcrop as tan to reddish-brown, highly resistant, medium to very thick-bedded units. The gravel-sized clasts are primarily chert, but quartzite and occasional fine-grained sandstone clasts are also present. Chert gravel exhibits an impressive array of colors, including gray, tan, brown, dark red, brown-yellow, black, and several shades of brilliant green. Nearly all gravel-sized grains present in the types II, III, and IV conglomerate are well-rounded but may exhibit characteristic differences in the degree of sphericity. No fossil grains were observed in any sample of types II, III, and IV conglomerate. An integral distinction between the Type 1 and types II, III, and IV lithofacies is the binding cement. Although the matrix composition of all four conglomerate types is quartz sand of varying grain size and textural maturity, the binding

← **Figure 3.17 – A)** Outcropping of interbedded layers of calcareous sandstone and Type 1 conglomerate from the lower member of the Riepe Spring Limestone (unit 7); **B)** Cut and clear-coated hand sample of Type 1 conglomerate from the base of the Riepe Spring Limestone. The fabric is unsorted with variably angular chert and quartzite clasts (unit 3); **C)** Outcropping of highly resistant type II conglomerate illustrating the well-sorted gravel clasts bound together with a matrix of fine quartz sand and siliceous cement (unit 37) (scale bar in mm); **D)** Cut and clear-coated hand sample of type II conglomerate. Note the textural maturity and color variation of the detrital chert, quartzite, and sandstone clasts (lower part of unit 27).

cement of types II, III, and IV is entirely siliceous. Type III is the only fully grain-supported conglomerate of the four. Photographs of each conglomerate type in outcrop and hand sample are presented in Figures 3.17 and 3.18.

The varied conglomeratic units of the middle informal member of the Riepe Spring Limestone are evidently closely related regarding both provenance and depositional setting. Therefore, types II, III, and IV are considered proximal or distal representatives of very similar lithofacies within a recurring beach paleoenvironment. Types II, III, and IV conglomerate are interpreted as a suite of foreshore to backshore lithofacies. Type II is similar to the Type 2 conglomerate of Marcantel (1975) but lacks calcareous material (both bioclasts and cement). The type II conglomerate was likely deposited along a highly energetic, biologically inhospitable shoreline as coarse, upper foreshore sand and gravel. Types III and IV are interpreted as extremely minor transgressive or regressive subsets of this type II lithofacies. However, these slight shifts in conglomeratic texture may also be indicative of changes in the gradient of the beach. The type III conglomerate is nearly a coarse-grained chert and quartzite sandstone and may have been deposited in a more seaward position than type II, representing a middle to lower foreshore (swash zone) setting in which intense wave agitation sorted, rounded, and winnowed the quartzose shoreline sediments. The type IV conglomerate, which only occurs at one distinctive horizon (unit 29), is essentially a “puddingstone” in which the

A

B

2 cm

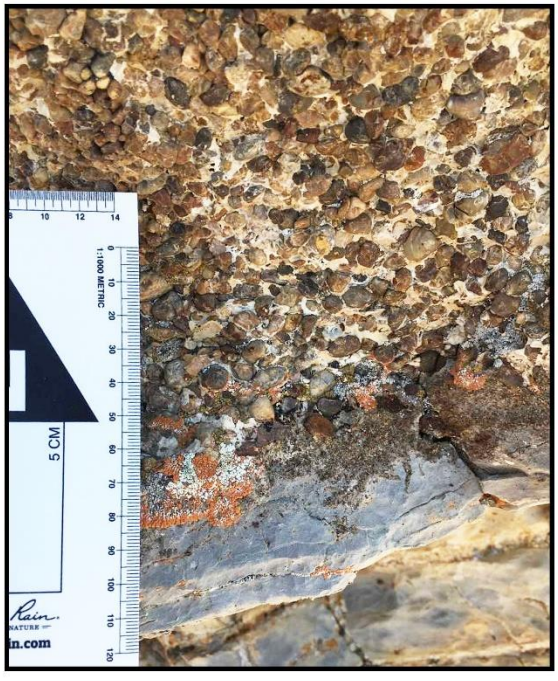

C

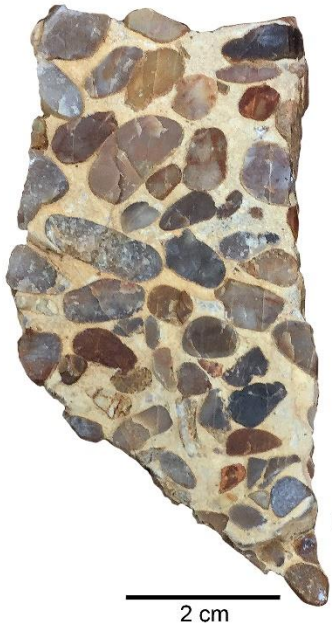

D

2 cm

oblate, gravel-sized clasts resemble those of modern shingle beaches. These matrix-supported sediments are interpreted as sandy, backshore berm deposits.

Calcareous Siltstone (C-Slst)

The calcareous siltstone (C-Slst) microfacies occurs as a volumetrically moderate component of the lower informal member and a minor component of the middle informal member of the Riepe Spring Limestone. Unit 21 is the thickest exposure of C-Slst in the NSMR section, measuring approximately 11 m thick, and is also an important fusulinid-bearing unit which is discussed in more detail in Chapter 4. Bedding units vary from massive and very thick-bedded to platy, thin beds. Thick beds weather tan to medium gray, whereas thin, platy beds typically weather tan to light brown. Tan-colored silt-rich sediments may occur as stringers within major limestone units. The composition of NSMR calcareous siltstone samples varies from nearly pure terrigenous, siliciclastic silt (with carbonate cement) to silt with

← **Figure 3.18 – A)** Outcropping of graded type II-type III conglomerate deposits. These centimeter-scale fining upward intervals represent minor shoreline fluctuations in a beach setting (top of unit 27) (standard Estwing hammer for scale); **B)** Fresh sample of type III conglomerate composed of coarse sand and granules of chert with very little matrix and siliceous cement (top of unit 27); **C)** The single outcropping of type IV conglomerate overlying a bed of partially dolomitized bioclastic calcareous sandstone (units 28, 29) (scale bar in mm); **D)** Small hand sample of type IV conglomerate ("pudding stone"). Note the oblate shape of most chert grains, which are strongly matrix-supported (fine quartz sand). Cementing agents are siliceous. The impressive likeness to the state of Nevada occurred naturally (unit 29).

an appreciable amount of quartz sand (Figs. 3.19C and 3.19D respectively). The cement is rarely dolomitic. Fossil grains are generally sparse in the C-Slst microfacies, but fusulinids, palaeotextularids, ostracods, mollusk fragments, and evidence of bioturbation are present. Thin sections show sparse, irregularly shaped patches of selectively dolomitized material, which may indicate the replacement of calcareous cement in burrowed sediments (Gingras et al., 2004). The more fragile fossil constituents (i.e., fusulinids) are often deformed, showing signs of compaction with obliterated tests or pressure solution grain truncation (both sutured and non-sutured seams). Minor microstylolite swarms are also present in C-Slst samples that show signs of compaction. Photomicrographs of C-Slst thin sections are presented in Figure 3.19.

The C-Slst microfacies, like many terrestrially influenced mixed carbonate-siliciclastic sediments, is a broad and nondescript category not likely attributed to a single depositional setting. Although there are several potential paleoenvironments represented among the C-Slst samples collected, deposition was undoubtedly confined to a low energy marine setting. Most C-Slst samples have at least a small proportion of subangular to angular quartz sand within the silt matrix. Mixed-grain siltstone is the subcategory of the C-Slst that may contain bioclasts and may have been deposited in a low energy, normal marine paleoenvironment with sources of bimodal terrigenous material. Where fusulinids are present, it is inferred that a shelf setting,

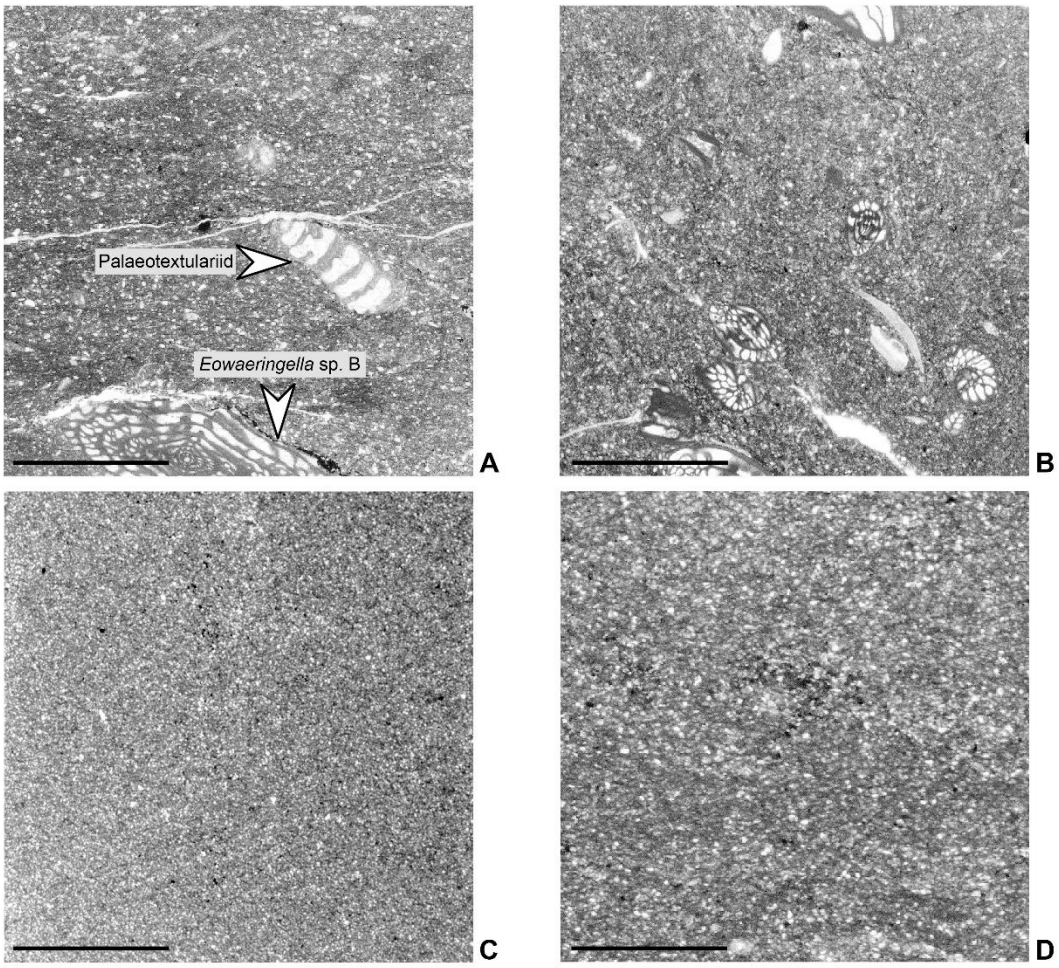

Figure 3.19 – A) Calcareous siltstone composed of terrigenous silt and fine sand with a minor amount of carbonate mud. Fractures are filled with secondary calcite. Sparse microstylolites are present, indicating chemical compaction (unit 12); **B)** Calcareous siltstone with small *Triticites* and miscellaneous shell fragments (unit 21); **C)** Pure calcareous siltstone composed primarily of terrigenous silt with carbonate mud (top of unit 32); **D)** Sandy calcareous siltstone with dark carbonate mud (lower part of unit 24). All scale bars = 2 mm.

farther removed from potential euryhaline paleoenvironments is likely (Yancey and Stevens, 1981; Stevens and Stone, 2007). Pure siltstone, like the sample collected from the top of unit 32, with a reduced amount of sand-sized grains and a lack of bioclasts may have been deposited in a semi-restricted lagoonal setting or possibly a brackish, paralic, marginal marine setting (Marcantel, 1975).

Fine to Medium Calcareous Sandstone (C-Ss)

The calcareous sandstone (C-Ss) microfacies is a volumetrically significant component occurring throughout the Riepe Spring Limestone, composing at least a moderate proportion of its three members. The C-Ss microfacies occurs as platy, thin beds to very thick beds and is commonly associated with small-scale sedimentary structures. Thick beds weather medium gray and may be differentially etched, accentuating the structures within the sand units (Fig. 3.20A). Centimeter-scale hummocks and laminae within thick-bedded sand units are occasionally present. Thin beds weather tan to brown and are typically more massive. The C-Ss microfacies is composed of texturally immature sandstone units, each with carbonate mud matrix significantly outweighing the volume of calcite cement. C-Ss samples are moderately to well sorted associations of subrounded to angular grains of quartz, chert (minor), and occasional accessory feldspar. Sparse, highly abraded crinoid fragments may be present and are easily recognizable due to

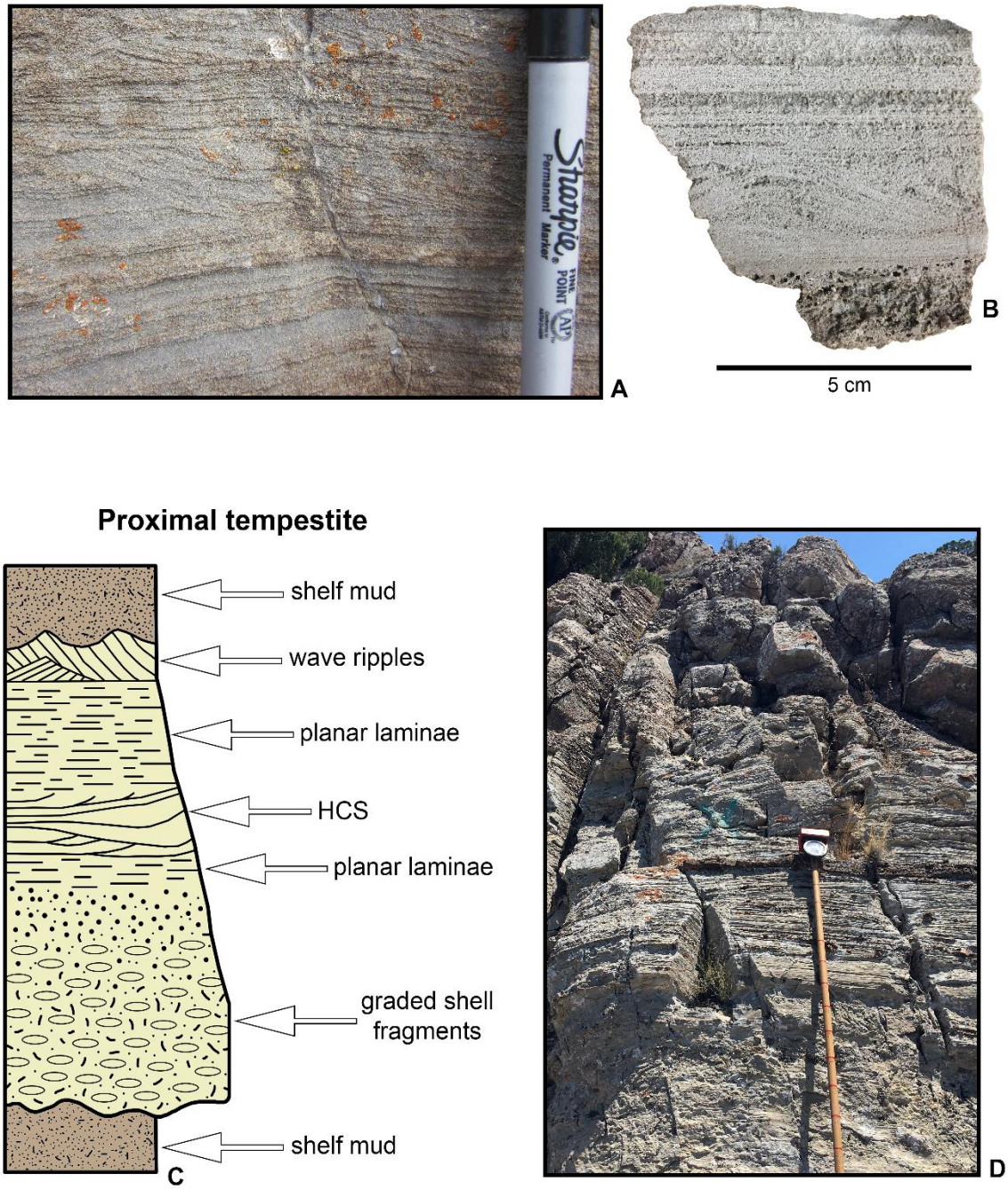

Figure 3.20 – **A)** Naturally etched outcropping of calcareous sandstone with characteristic wave-formed laminae and hummocky cross-stratification (lower part of unit 57); **B)** Acid etched hand sample of calcareous sandstone with a shelly, basal lag deposit (digested tests of *Schwagerina*). The sample is interpreted as a small, proximal tempestite deposit (lower part of unit 57); **C)** Generalized columnar section of a sandy, proximal tempestite (HCS = hummocky cross-stratification) (redrawn from Einsele, 2000); **D)** Outcropping of laminated and sparsely hummocky, fine-grained calcareous sandstone (unit 19). Jacob's staff = 1.5 m.

the overgrowth of syntaxial cements. Less mature samples often contain a higher percentage of chert grains. The C-Ss microfacies often occurs between foreshore conglomerate units in the lower and middle informal members but is also associated with the open marine crinoid-brachiopod-bryozoan biosparudite (CBB-Bsr) microfacies in the uppermost part of the Riepe Spring Limestone. The entirety of the Rib Hill Formation at Spruce Mountain Ridge belongs to the C-Ss microfacies group (Marcantel, 1975). Photomicrographs of C-Ss thin sections are presented in Figure 3.21.

Like the aforementioned C-Slst microfacies, the C-Ss microfacies is difficult to assign to a single depositional setting due to its rather unremarkable fabric. Several potential depositional settings are provided for C-Ss variants. Muddy, fine- to very fine-grained sandstone units with subangular to angular quartz grains and sparse marine fossil fragments were likely deposited in a shoreface paleoenvironment with a nearby source of terrigenous detritus. This setting may be associated with fan-delta complex deposits, like those described from parts of the Cisuralian Garden Valley Formation in east-central Nevada (Wardlaw et al., 2015). Although the fabric differs, medium to rarely coarse-grained C-Ss units, which can occur as low channel fills with shell fragments, laminae, and occasional hummocky cross-stratification, must have been deposited in an upper shoreface setting as well. Figure 3.20B illustrates an acid etched sample collected from unit 57 that is interpreted as part of a proximal tempestite deposited along the

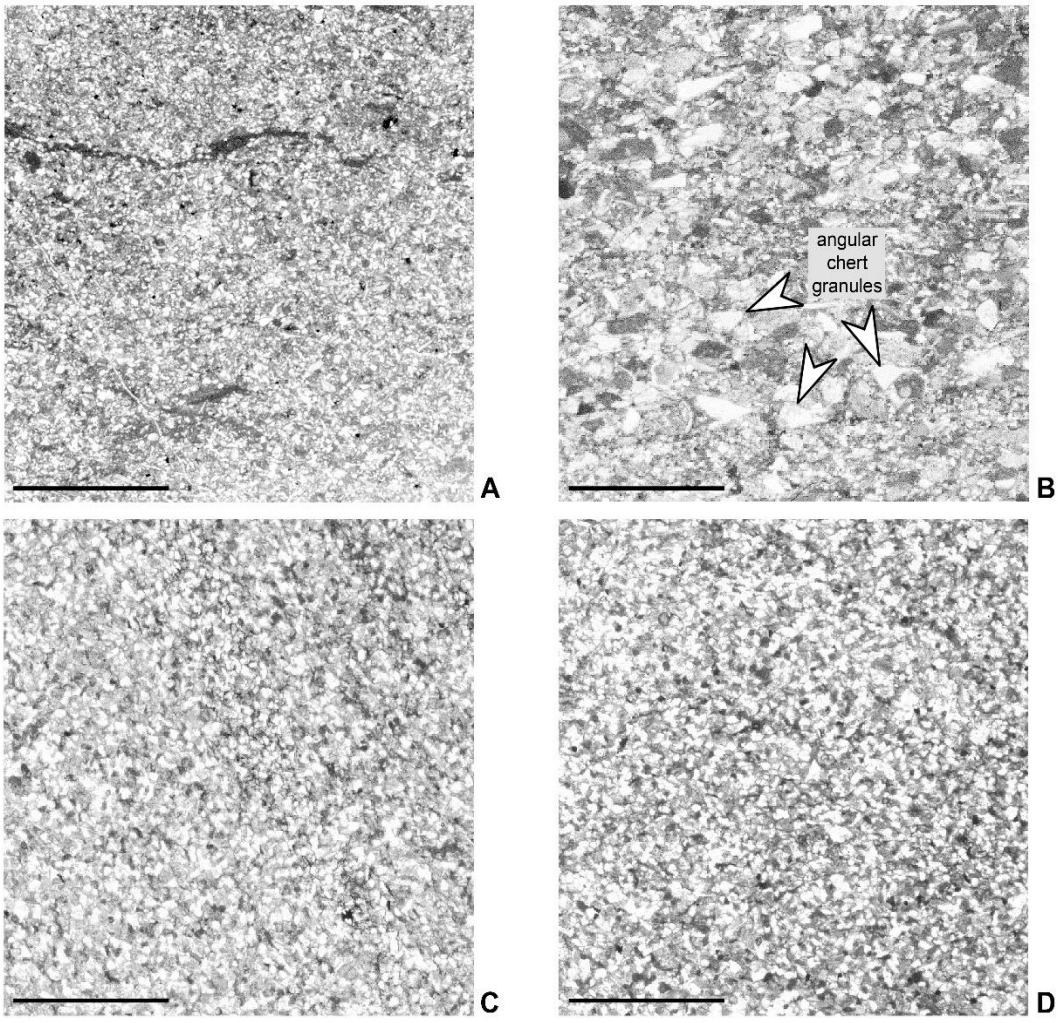

Figure 3.21 – A) Fine-grained calcareous sandstone composed of subangular quartz sand with a minor amount of terrigenous silt and dark carbonate mud (unit 10); **B)** Coarse-grained, weakly laminated calcareous sandstone composed of subangular to angular quartz grains with angular chert sand/granules in a carbonate mud matrix (unit 19); **C)** Medium-grained calcareous sandstone composed of subrounded to subangular quartz grains in a carbonate mud matrix (unit 45, as type III conglomerate grades into overlying wackestone); **D)** Medium-grained calcareous sandstone associated with proximal tempestite and rip channel deposits (unit 57). All scale bars = 2 mm.

innermost shelf during a brief regressive phase, as the unit is bounded above and below by deeper water quartzose limestone beds. The strongly etched lowest portion of the hand sample was a fusulinid shell lag deposit and is considered the base of an individual storm event deposit. Figure 3.20C illustrates an idealized columnar section of a proximal tempestite for comparison. The channelized nature of unit 57 suggests that at least the lower part of the unit may represent the establishment of a shoreline rip channel (Seilacher, 1982). Additional evidence of laminated to hummocky, wave-influenced sandstone was observed much lower in the section, at the top of unit 19, where angular chert clasts and coarse shell fragments compose the greater part of another small, potential tempestite deposit. Like the cross-stratified intervals in unit 57, the hummocks of unit 19 are centimeter-scale features within an overall finer-grained, strongly laminated sand unit (Fig. 3.20D).

Bioclastic Sandstone (B-Ss)

The bioclastic sandstone (B-Ss) microfacies occurs intermittently throughout the middle and upper informal members of the Riepe Spring Limestone. Except for the high volume of skeletal grains, there is little difference between the C-Ss and B-Ss microfacies. The ratio of terrigenous material to carbonate matrix in collected samples of B-Ss is nearly identical to that of the C-Ss, and the degree of rounding and sorting in the B-Ss falls

within the range of the C-Ss as well. The B-Ss microfacies occurs as thin intervals within limestone units or independently as thick-bedded units that weather light gray to light tan. The dominant fossil grains of the B-Ss include crinoids, fusulinids, productid brachiopods, mollusks, and bryozoans (from most to least common). Most bioclasts show some degree of abrasion or fragmentation. Photomicrographs of B-Ss thin sections are presented in Figure 3.22.

Based on the petrographic similarities between the C-Ss and B-Ss microfacies, it is plausible that these microfacies are associated with very similar shoreface settings (see *Fine to Medium Calcareous Sandstone* subheading). However, the regular presence of bioclasts as a major grain component suggests that the B-Ss microfacies may have been deposited in a more medial shoreface position at slightly greater depth along the inner shelf. Fusulinids are present in most samples of the B-Ss microfacies, suggesting that water depth must have been within the range of ~10-50 m (potentially up to 70 m) (Cushman, 1921, 1933; Stevens and Stone, 2007).

One particularly interesting sample of B-Ss from unit 28 (lower part of the middle informal member) exhibits alternating laminae of quartz sand and roughly imbricate fusulinid tests (*Triticites*), indicating brief periods of gentle wave agitation or bottom currents. The small to moderately-sized specimens of Gzhelian age *Triticites* in this sample are completely dolomitized, making it difficult to confidently assign a species-level designation. The replacement

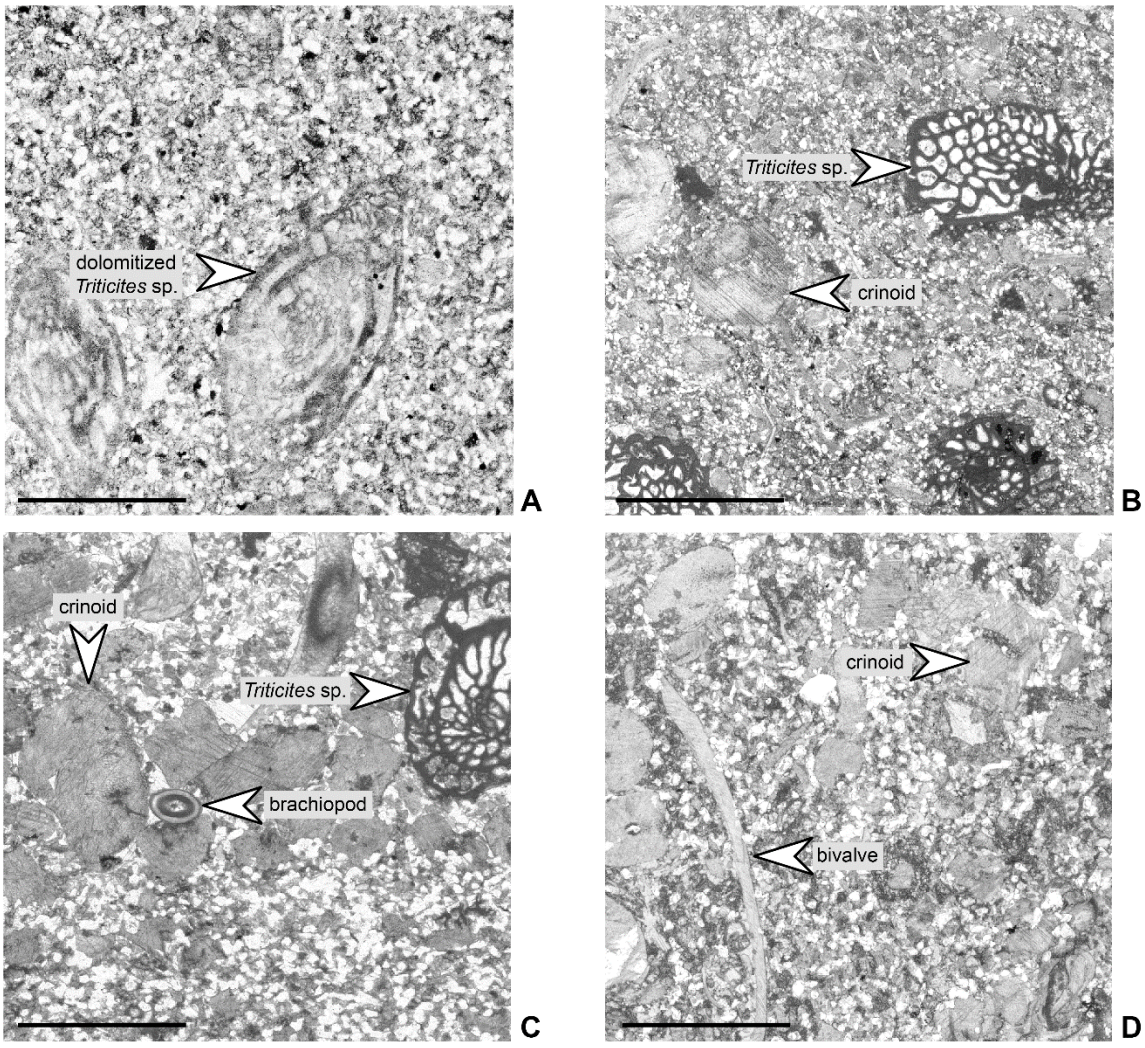

Figure 3.22 – A) Partially dolomitized, bioclastic calcareous sandstone with *Triticites* "ghost" tests. The sample is composed of subrounded to subangular quartz sand, terrigenous silt, and carbonate mud (unit 28); **B)** Weakly dolomitized, fine-grained, bioclastic calcareous sandstone with highly abraded *Triticites* and crinoid fragments (lower sandy interval of unit 34); **C)** Weakly dolomitized, highly bioclastic calcareous sandstone with medium-grained terrigenous quartz, abraded crinoid fragments, fusulinids, and brachiopods (top of unit 34); **D)** Medium-grained, bioclastic calcareous sandstone with abraded crinoid and bivalve fragments (unit 45; associated with sample C-Ss-C (Fig. 3.20C)). All scale bars = 2 mm.

of the tests is biostratigraphically unfortunate, but it is telling from a depositional perspective. Incorporating the indications of paleocurrent, prevalence of replacement dolomitization, and knowledge of fusulinid depth preference, it seems likely that unit 28 was deposited in a shallow, normal marine, nearshore setting. Again, potentially associated with sandy, inner shelf fan deposits. The fusulinid-bearing B-Ss unit was then subaerially exposed during an ensuing episode of sea-level fall. Type IV conglomerate sits atop unit 28, providing further evidence for rapid coastal emergence (Fig. 3.18C).

Replacement Dolomite (RD)

The replacement dolomite (RD) microfacies constitutes one of the dominant carbonate lithologies of the middle informal member of the Riepe Spring Limestone and is primarily confined to the upper part of this interval. The RD weathers very light- to light-gray and occurs in thick-bedded units often associated with mature chert gravel conglomerate. Each RD sample collected is interpreted as secondary or replacement dolomite (rather than penecontemporaneous) due to the presence of "ghost" fossil fragments (Figs. 3.23C, D). Replacement of the original limestone units may be complete or partial. One partially altered sample contains fossil grains (crinoid fragments) that were dolomitized only along the margins. Although it is difficult to observe in the photomicrograph, Figure 3.23A illustrates a crinoid

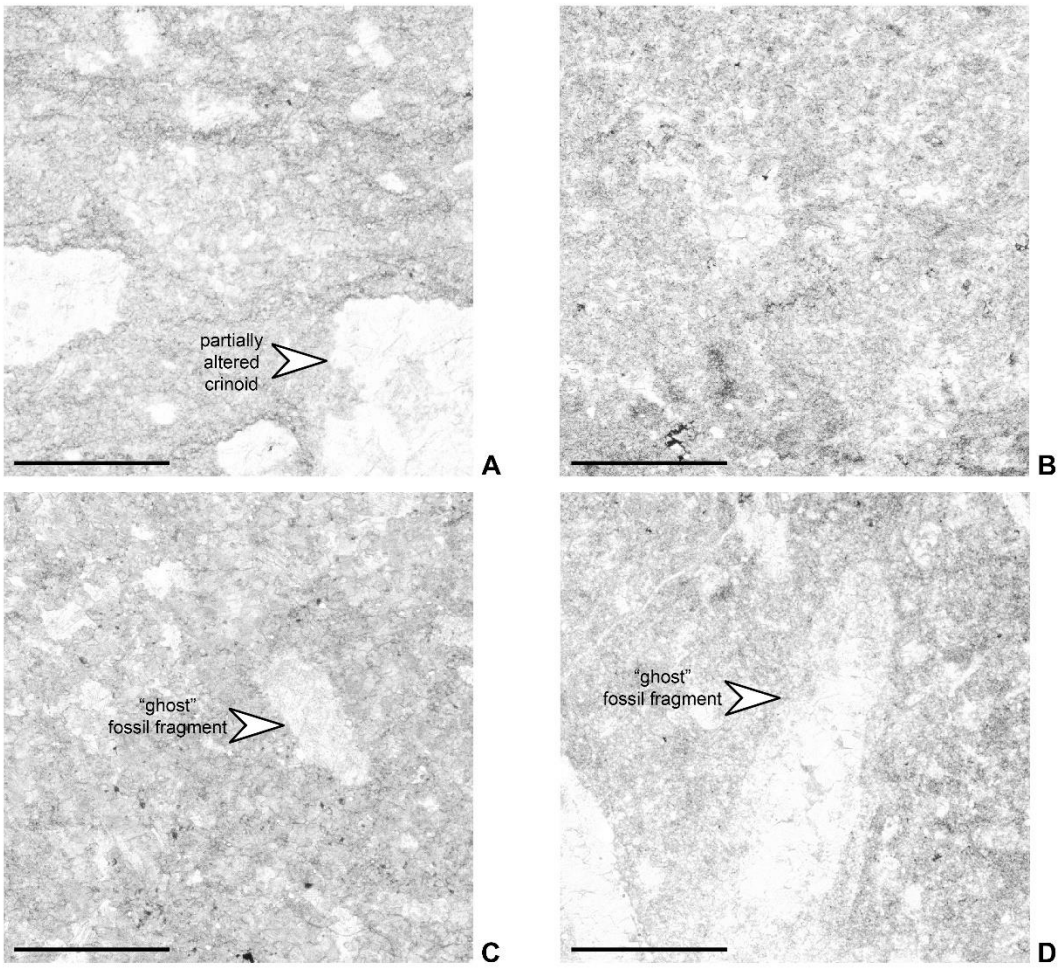

Figure 3.23 – A) Anhedral, microcrystalline replacement dolomite with mostly unaltered crinoid fragments (unit 34; above the sand from sample B-Ss-B(Fig. 3.21B)); **B)** Replacement dolomite with larger crystals exhibiting a partial "planar-s" fabric (unit 42); **C)** Microcrystalline replacement dolomite with cryptic, completely altered "ghost" fossil fragments (unit 34); **D)** Microcrystalline replacement dolomite with completely altered "ghost" fossil fragments (upper part of unit 38). All scale bars = 2 mm.

columnal with a rind of very finely crystalline dolomite which has only replaced the exterior of the grain (outer rim and adjacent to the lumen). Although a percentage of original calcite may remain in sparse samples as matrix, cement, or bioclasts, the degree of dolomitzation is greater than ~50% in all samples. Photomicrographs of RD thin sections are presented in Figure 3.23.

There is little textural variability among the RD samples collected, except for minor differences in coarseness. The fabric is inequigranular (mosaic) and the texture is typically fine-grained (<100 µm and often <50 µm), nonplanar, and consists of tightly packed anhedral crystals. One sample is notably more coarsely crystalline than others and exhibits a partial "planar-s" (subhedral) texture, although more than 50% of the groundmass is anhedral (Flügel, 2010; Fig. 3.23B). The largest individual crystals in the sample measure >600 µm.

Since the introduction of the so-called "dolomite question" by Fairbridge (1957), several mechanisms and models for dolomite formation have been proposed along with a number of depositional scenarios, most involving the post-burial influx of Mg-enriched pore fluids (meteoric or marine) or less frequently subaerial exposure. Flügel (2010) compiled and presented nine dolomitization models proposed by various authors. Based on the association of the RD microfacies with shoreline conglomeratic units, the falling sea-level mode is a likely explanation for the samples of the present

study (Magaritz and Peryt, 1994; Purser et al., 1994; Flügel, 2010). The extremely fine-grained nature of the RD and consistent presence of marine "ghost" fossils indicate that the original biomicritic limestone, which now constitutes the RD facies was deposited in a marine setting rather than peritidal or sabkha conditions. No evaporitic or stromatolitic textures, nor signs of microkarsting have been observed in any of the RD samples collected. The juxtaposition with the bounding conglomerate units suggests that the muddy, shallow-marine, potentially semi-restricted lagoonal paleoenvironment transitioned to shoreline upon sea-level fall, but the pervasiveness of the replacement makes it difficult to further asses the depositional paleoenvironment. Cathodoluminescence analysis could prove useful for a study of the diagenetic history of the RD microfacies, but this analysis is beyond the scope of the present study.

Nodular Fusulinid Biomicrite (NF-Bm)

The nodular fusulinid biomicrite (NF-Bm) microfacies is undoubtedly one of the most biostratigraphically important lithologies of the lower informal member of the Riepe Spring Limestone, as it consistently yields high volumes of well-preserved latest Kasimovian age specimens of *Triticites* and *Pseudofusulinella*. In addition to fusulinids, the NF-Bm microfacies preserves echinoderm fragments, globivalvulinids, palaeotextularids, encrusting foraminifers, productid brachiopods, and ostracods. The NF-Bm

microfacies occurs in three units (6, 14, 16) over an interval of approximately 45 m (Fig. 3.6). Each NF-Bm unit is bounded by Type 1 conglomerate beds, two of which are associated with mid-Kasimovian and upper Kasimovian-lower Gzhelian erosional disconformities (units 13 and 15, respectively). The NF-Bm occurs as thick to very thick-bedded units that weather tan to medium gray. Fresh surfaces, either cut or etched, exhibit two intermingled lithofacies within a single small sample: 1) fusulinid-rich biomicrite; and 2) terrigenous clay, silt, and sand. The amalgamation of fossiliferous limestone and terrigenous siliciclastic material produces a striking, nearly conglomeratic appearance in acid etched samples (Fig. 3.24E). Further acid digestion of the NF-Bm leaves nothing but a thin, extremely delicate framework of resistant siliciclastic mudstone to siltstone. The biomicritic component of the NF-Bm is very similar to the echinoderm-foraminifer biomicrite (CF-Bm) microfacies in units 6 and 16, but more like the silty to sandy (quartzose) biomicrite (SSQ-Bm) microfacies in unit 14. Photomicrographs of NF-Bm thin sections are presented in Figure 3.24.

Most limestone units with pervasively nodular fabrics are the result of physical and chemical compaction (pressure solution) due to overburden or tectonic stress (Wanless, 1979; Flügel, 2010; James and Jones, 2016). The most common indication of compaction and pressure solution in the NF-Bm microfacies of the Riepe Spring Limestone is the presence of non-sutured solution seams and swarms of microstylolites. These choked seams of fine-

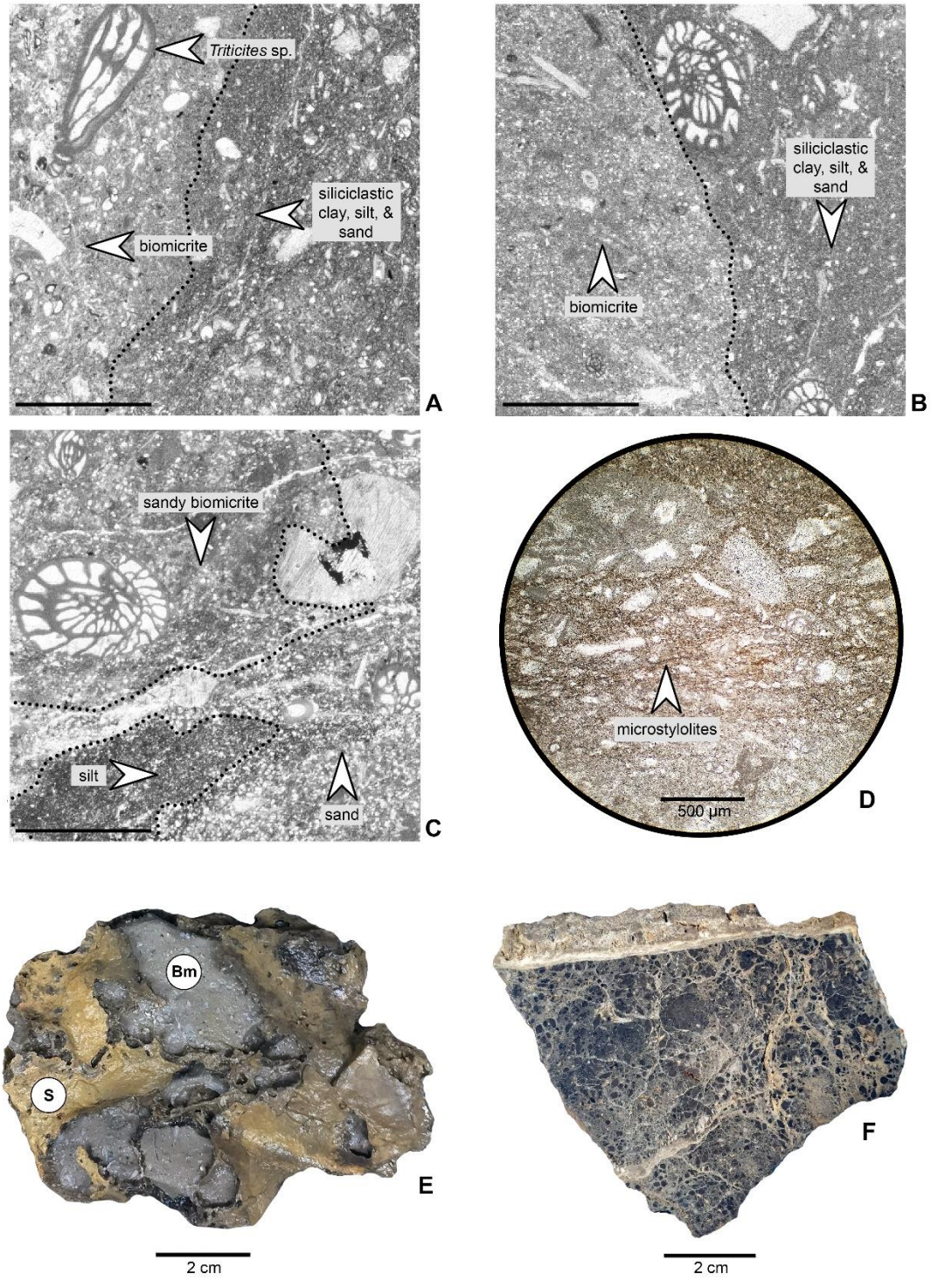
Triticites sp.
siliciclastic clay, silt, & sand
biomicrite
A
siliciclastic clay, silt, & sand
biomicrite
B
sandy biomicrite
silt
sand
C
microstylolites
500 µm
D
Bm
S
E
2 cm
F
2 cm

grained sediment and masses of countless, layered sutures act as conduits for fluid migration in the selective dissolution process and as slip surfaces in the relief of stress (Wanless, 1979).

Although nodular limestone is often associated with deep-water lithofacies, Dvořák (1972) provided evidence for the shallow-water formation of nodular limestone in the early stages of a regressive phase. Based on the presence of well-preserved fusulinid faunas in each unit, the NF-Bm microfacies is likely a similar occurrence of shallow-water nodular limestone. The strong association with Type 1 conglomerate units also suggests that NSMR NF-Bm units were not deposited in the basinal or slope settings typical of nodular limestone. Instead, it is proposed herein that the units of NF-Bm microfacies were deposited below fair-weather wave base, but at a depth less than 50-70 m, during periods of brief sea-level rise between lowstand tracts in which the bounding conglomeratic units were deposited.

← **Figure 3.24 – A)** Nodular fusulinid biomicrite with *Triticites* and small shell fragments. Black dotted line divides the two distinct sub-microfacies; biomicrite to the left (lighter) and terrigenous clay, silt, and sand to the right (darker) (unit 6); **B)** Nodular fusulinid biomicrite, again divided by the black dotted line. Note the truncation of the *Triticites* test by chemical compaction (unit 6); **C)** Coarser-grained nodular fusulinid biomicrite with crinoid and brachiopod fragments. The siliciclastic component is more strongly divided than the previous two samples (unit 14); **D)** Photomicrograph of a sample of nodular fusulinid biomicrite illustrating small swarms of microstylolites in the fine-grained terrigenous component (unit 14); **E)** Acid etched hand sample of nodular fusulinid biomicrite illustrating the differing properties of the two sub-facies. Bm = biomicrite; S = fine-grained terrigenous material (unit 6); **F)** Cut and clear-coated hand sample of friable nodular fusulinid limestone with *Pseudofusulinella* (unit 16). All scale bars = 2 mm unless otherwise noted.

Echinoderm-Foraminifer Biomicrite (EF-Bm)

The echinoderm-foraminifer biomicrite (EF-Bm) microfacies is one of the most commonly occurring lithologies throughout the uppermost part of the Ely Limestone and the Riepe Spring Limestone and constitutes a sizeable portion of the limestone exposed in the NSMR section. The EF-Bm microfacies occurs as moderately resistant, thick to very thick-bedded units that weather light-medium to dark gray. Most samples are classified as wackestone under the Dunham (1962) scheme, but packstone units are also present. Several packstone units with deformed or obliterated bioclasts are interpreted as diagenetic packstone formed by the compaction of depositional wackestone (Choquette and James, 1987) (Fig. 3.25F). EF-Bm units are often strewn with small fractures (micron to centimeter scale) and secondarily precipitated calcite (Figs. 3.25C, D, F). Primary bioclasts of the EF-Bm include sand to granule-sized fragments of echinoderms (echinoids and crinoids), fusulinids, palaeotextulariids (e.g., *Climacammina* Brady, 1873), globivalvulinids, endothyrids (*Bradyina* von Möller, 1878, *Bradyinelloides* Mamet and Pinard, 1992), tetrataxids (*Tetrataxis* Ehrenberg, 1854), nodosariids (*Nodosellinoides* Mamet and Pinard, 1992), encrusting foraminifers, and ostracods. The matrix is medium gray-brown to dark brown carbonate mud with a small percentage of terrigenous silt and fine sand.

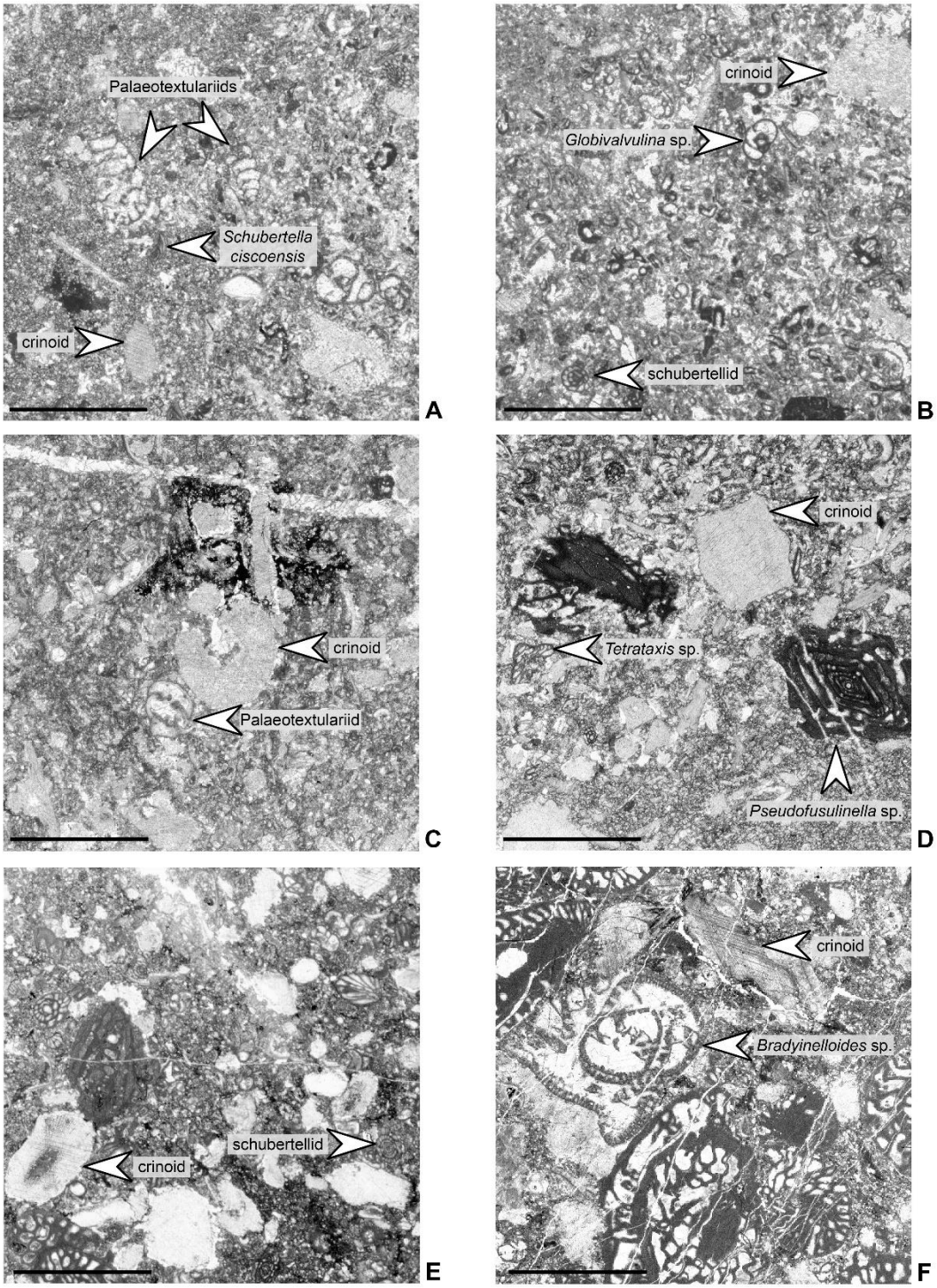
Palaeotextulariids
Schubertella ciscoensis
crinoid
A
crinoid
Globivalvulina sp.
schubertellid
B
crinoid
Palaeotextulariid
C
crinoid
Tetrataxis sp.
Pseudofusulinella sp.
D
schubertellid
crinoid
E
crinoid
Bradyinelloides sp.
F

Evidence of burrowing may be present in undeformed samples. Photomicrographs of EF-Bm thin sections are presented in Figure 3.25.

The volume of carbonate mud, paucity of terrigenous material, and preponderance of both large and small foraminifers indicate that the EF-Bm microfacies was deposited in a low to moderate energy, open marine paleoenvironment, likely in a mid-shelf position removed from the siliciclastic influence of inner shelf fans. Most EF-Bm samples preserve fusulinids and are therefore interpreted to have been deposited in water less than 50-70 m deep. Stevens (1971) suggested that *Bradyina* and palaeotextulariids often preferred depths greater than 20 m, further narrowing the depositional range of the CF-Bm microfacies. In contrast, others have asserted that the representatives of the family Bradyinidae Reitlinger, 1950 favored extremely shallow, energetic settings at water depths less than five meters (see Gallagher and Somerville, 2003), but depths this shallow are widely considered unfavorable for most mature fusulinids.

← **Figure 3.25 – A)** Echinoderm-foraminifer biomicrite with rounded echinoderm fragments, globivalvulinids, palaeotextularids, and small fusulinids (schubertellids) (unit 30); **B)** Echinoderm-foraminifer biomicrite with crinoid fragments, globivalvulinids, schubertellids, and small encrusting foraminifera (unit 36); **C)** Slightly quartzose echinoderm-foraminifer biomicrite with palaeotextularids and crinoid fragments (unit 38); **D)** Highly bioclastic echinoderm-foraminifer biomicrite (nearly a "packstone") with both whole crinoid elements and fragments, fusulinids (*Triticites* and *Pseudofusulinella*), and sparse *Tetrataxis* (unit 42); **E)** Slightly quartzose echinoderm-foraminifer biomicrite with crinoid fragments, *Schwagerina*, and abundant schubertellids (including *Biwaella americana* Skinner and Wilde, 1965) (unit 48); **F)** Packed echinoderm-foraminifer biomicrite deformed by compaction (unit 60). All scale bars = 2 mm.

Silty to Sandy (quartzose) Biomicrite (SSQ-Bm)

The "quartzose" limestone (SSQ-Bm) microfacies is a major component of the Cisuralian age upper informal member of the Riepe Spring Limestone. The SSQ-Bm is exposed as thick to very thick beds that weather medium gray to tan-brown with occasional pink hues. SSQ-Bm units outcrop in close proximity stratigraphically above and below calcareous sandstone, Type 1 conglomerate, and less siliciclastic limestone (wackestone to packstone) units. The primary fossil constituents of the SSQ-Bm microfacies include abraded crinoid columnals and fragments, fusulinids, bryozoans, brachiopods, and mollusks. Samples of the SSQ-Bm microfacies resemble a coalescence of the previously described B-Ss and EF-Bm microfacies. The critical difference between these microfacies is the ratio of terrigenous material to carbonate mud. Although the three microfacies may appear superficially alike in outcrop, petrographic inspection of B-Ss and CF-Bm samples demonstrates that these textures are strongly inclined to a dominant sediment type (siliciclastic vs. carbonate), whereas the SSQ-Bm is a more proportionate admixture of siliciclastic and carbonate material. Photomicrographs of SSQ-Bm thin sections are presented in Figure 3.26.

The gradational overlap between the B-Ss, CF-Bm, and SSQ-Bm microfacies suggests that the latter represents a transitional coupling of the former two. That said, the SSQ-Bm microfacies is likely to have been deposited in a shallow-marine paleoenvironment with low to moderate

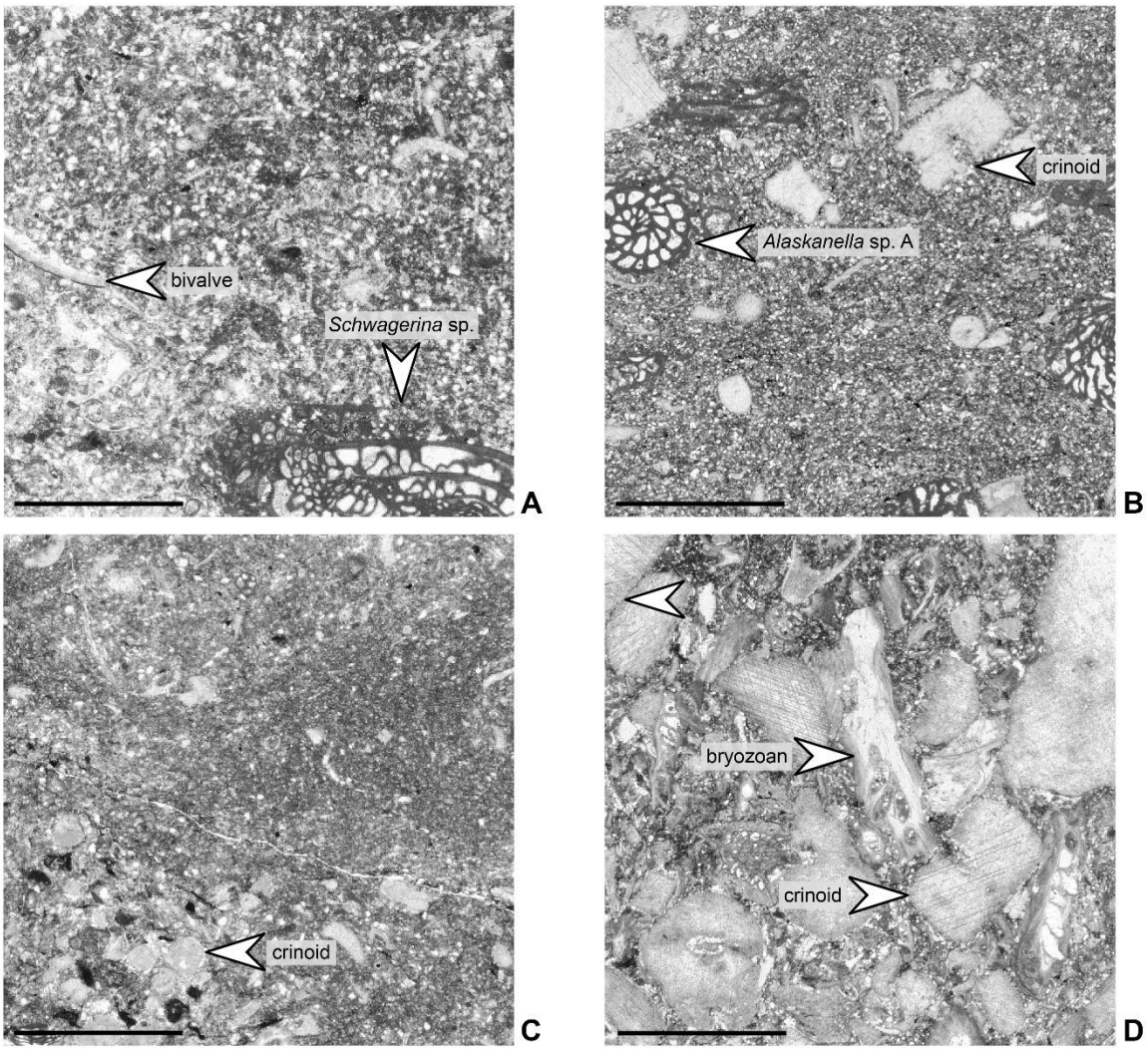

Figure 3.26 – A) Highly quartzose biomicrite with coarse, terrigenous sand, mollusk fragments, and *Schwagerina* (unit 56); **B)** Fine-grained quartzose biomicrite with abraded crinoid columnals and partially deformed fusulinid tests (lower part of unit 60); **C)** Fine-grained quartzose biomicrite with tightly-packed, crinoid and miscellaneous shell fragments (unit 58); **D)** Packed quartzose biomicrite with crinoid fragments and bryozoans (fistuliporoid and fenestrate) (interbedded SQ-Bm within unit 68). All scale bars = 2 mm.

turbidity, likely near fair-weather wave base. The depositional setting must have been close enough to shore to provide a sizeable volume of terrigenous silt and fine- to medium-grained quartz sand, but sufficiently deep enough to allow for the accumulation of carbonate mud without continuous winnowing. Therefore, a lower shoreface position is plausible, possibly along the distal edge of inner shelf fan lobes.

Echinoderm-Tubiphytes Poorly-Washed Biosparite (ET-PBs)

One of the most recognizable and fossiliferous microfacies of the upper informal member of the Riepe Spring Limestone is the echinoderm-*Tubiphytes* poorly-washed biosparite (ET-PBs). The ET-PBs microfacies only occurs within an approximately 25 m interval of the Cisuralian part of the section where it is interbedded with less fossiliferous, medium- to thick-bedded limestone units. Primary bioclasts of the ET-PBs include abraded or rounded echinoderm fragments, *Tubiphytes* Maslov, 1956, fusulinids (*Schwagerina*, *Schubertella*, and *Pseudoschwagerina*), small foraminifers, *Bradyinelloides*, palaeotextulariids, globivalvulinids, mollusks, cryptostomate bryozoans, and brachiopods. Cerioid rugose corals (*Kleopatrina*? McCutcheon and Wilson, 1963) occur intermittently through the upper part of the ET-PBs interval. Carbonate mud and sparry calcite cement are present in subequal proportions. Although *Tubiphytes* are a major grain component, they are not

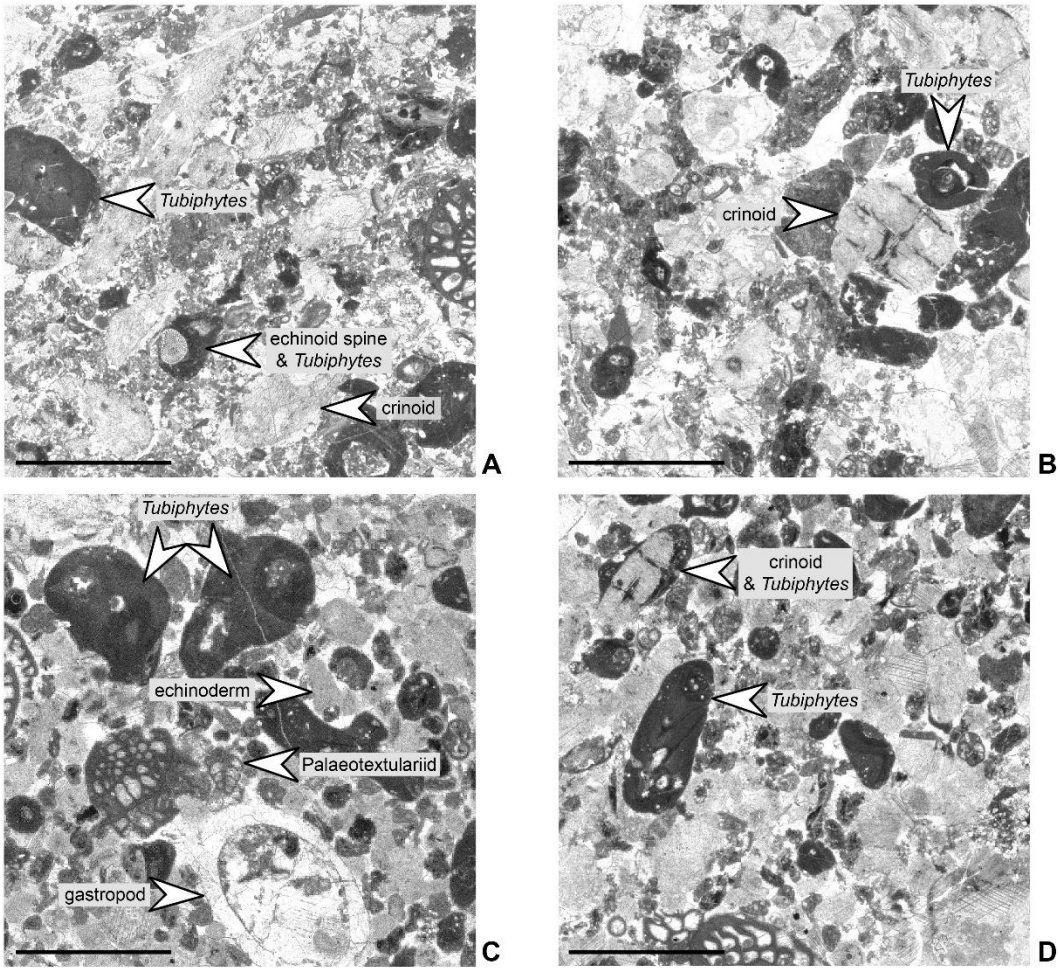

Figure 3.27 – A) Echinoderm-*Tubiphytes* poorly-washed biosparite with the notable presence of carbonate mud. Note the encrustation of *Tubiphytes* on echinoid fragments (unit 59); **B)** Echinoderm-*Tubiphytes* poorly-washed biosparite with crinoid pluricolumnals (articulated), sparry calcite cement, and sparse carbonate mud (middle part of unit 60); **C)** Echinoderm-*Tubiphytes* poorly-washed biosparite with less carbonate mud matrix than the previous two samples. Bioclasts include rounded echinoderm fragments, mollusks, *Schwagerina*, and palaeotextularids. Echinoderm fragments are infiltrated with carbonate mud, causing them to appear darker. The larger specimens of *Tubiphytes* clearly show central canals and partially enveloping growth bands (Riding and Guo, 1992) (upper part of unit 60); **D)** Echinoderm-*Tubiphytes* poorly-washed biosparite with fusulinids and small foraminifera. Note the *Tubiphytes* encrustation on a crinoid columnal at top left (upper part of unit 60). All scale bars = 2 mm.

large or pervasive enough to act as true binding agents. Photomicrographs of ET-PBs thin sections are in Figure 3.27.

Tubiphytes-rich packstone to boundstone lithofacies are often associated with a variety of reefal and shoal settings, including sponge patch reefs, microbialite mounds, fistuliporoid banks, back reef shoals, shelf margin (fore reef) shoal flanks, and sand shoals (Asquith and Drake, 1985; Igawa, 2003; Kossovaya et al., 2013; Wahlman and Tasker, 2013). The presence of spar cement and rounded skeletal grains indicates that some degree of winnowing by current or wave action occurred, but it was evidently not energetic enough to completely "wash" the microfacies of carbonate mud. A mound or bank setting seems plausible and is supported by the stratigraphic proximity with both open shelf and sparsely coralline lithofacies.

Poorly-Washed Pelsparite (P-Ps)

The poorly-washed pelsparite microfacies (P-Ps) is a markedly uncommon limestone fabric in the NSMR section. The two presented photomicrographs are of stratigraphically disparate samples collected from the lower and upper informal members of the Riepe Spring Limestone (Fig. 3.28A, B). The P-Ps microfacies is characterized by the presence of mottled, often irregular, rounded to subangular micritic grains. Based on the poor sorting and apparent heterogeneity, these grains are interpreted as mud peloids ("lithic peloids") of nonbiogenic origin. Mud peloids typically occur as

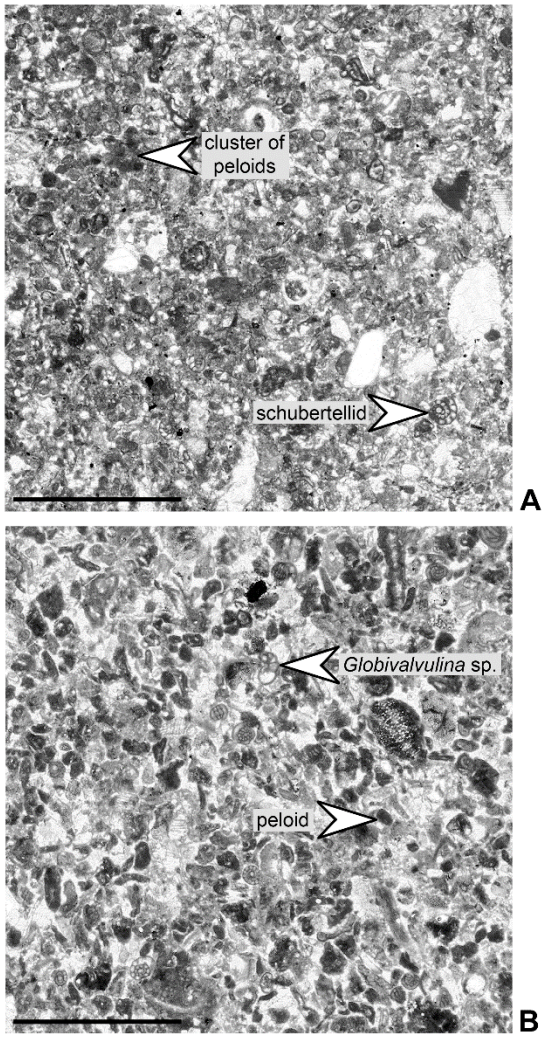

Figure 3.28 – A) Peloidal poorly-washed biosparite composed of crinoid fragments, brachiopod fragments, schubertellids, globivalvulinids, encrusting foraminifera, irregular mud peloids, and sparse, sand-sized chert grains (thin interval in silty limestone of unit 8); **B)** Higher energy peloidal poorly-washed biosparite that has been partially "washed," allowing for the precipitation of sparry calcite cement. Bioclasts include echinoderm fragments, schubertellids, and globivalvulinids (unit 52). All scale bars = 2mm.

small intraclasts (<2 mm) of reworked, poorly consolidated carbonate mud (Flügel, 2010). Bioclasts of the P-Ps include small fusulinids (schubertellids), globivalvulinids, encrusting foraminifers, echinoderm fragments, brachiopod fragments, and grains of possible algal or cyanobacterial affinity. As the name of the microfacies implies, carbonate mud and sparry calcite cement are present in subequal quantities.

The presence of sparry calcite cement and small, poorly sorted micritic peloid intraclasts indicates that some degree of winnowing occurred, although it is apparent from the two P-Ps photomicrographs that the sediments of Figure 3.28B may have been deposited in a somewhat more energetic paleoenvironment than those of Figure 3.28A. There is also a minor amount of terrigenous silt in the latter sample, as it is associated with a unit composed primarily of silty wackestone (unit 8). Unfortunately, there is nothing particularly revealing or exceptional about the P-Ps microfacies. The moderate level of wave agitation, presence of fusulinids, and paucity of terrestrial material suggests a lower shoreface setting, perhaps in an inner mid-shelf position.

Crinoid-Brachiopod-Bryozoan Biosparudite (CBB-Bsr)

The crinoid-brachiopod-bryozoan biosparudite (CBB-Bsr) microfacies is yet another uncommon microfacies among the strata of the Riepe Spring Limestone, only occurring in the Artinskian part of the uppermost limestone

beds of the upper informal member of the formation. The CBB-Bsr outcrops in the saddle and far eastern part of the section as thick to very thick beds of medium to dark gray encrinite. The three illustrated CBB-Bsr samples from the upper informal member are composed of >75% crinoid material, with minor components of brachiopod fragments, bryozoans, and fusulinids. CBB-Bsr units were an invaluable source of conodont elements (*Sweetognathus* Clark, 1972 and *Mesogondolella* Kozur, 1989) from the uppermost part of the NSMR section. Bioclasts of the CBB-Bsr are bound with syntaxial overgrowth cement, sparry calcite cement, and a minor amount of dark carbonate mud. Many crinoid fragments of unit 70 are partially and selectively silicified, with finely crystalline silica occasionally crossing grain boundaries, but the intergranular cement remains calcareous. Photomicrographs of CBB-Bsr thin sections are presented in Figure 3.29.

Although the CBB-Bsr is classified herein as a type of biosparite, this categorization may be somewhat misleading regarding the diagenetic history of the microfacies. The CBB-Bsr is yet another example of physical and chemical compaction resulting in the alteration of a carbonate fabric. Evidence of compaction includes long grain contacts, concavo-convex grain contacts, sutured grain contacts, and obliterated fusulinid tests. The presence of remnant micrite in narrow interstices suggests that the original, depositional microfacies of the CBB-Bsr may have been matrix-supported, and therefore classified as a biomicrudite. It is difficult to accurately assess

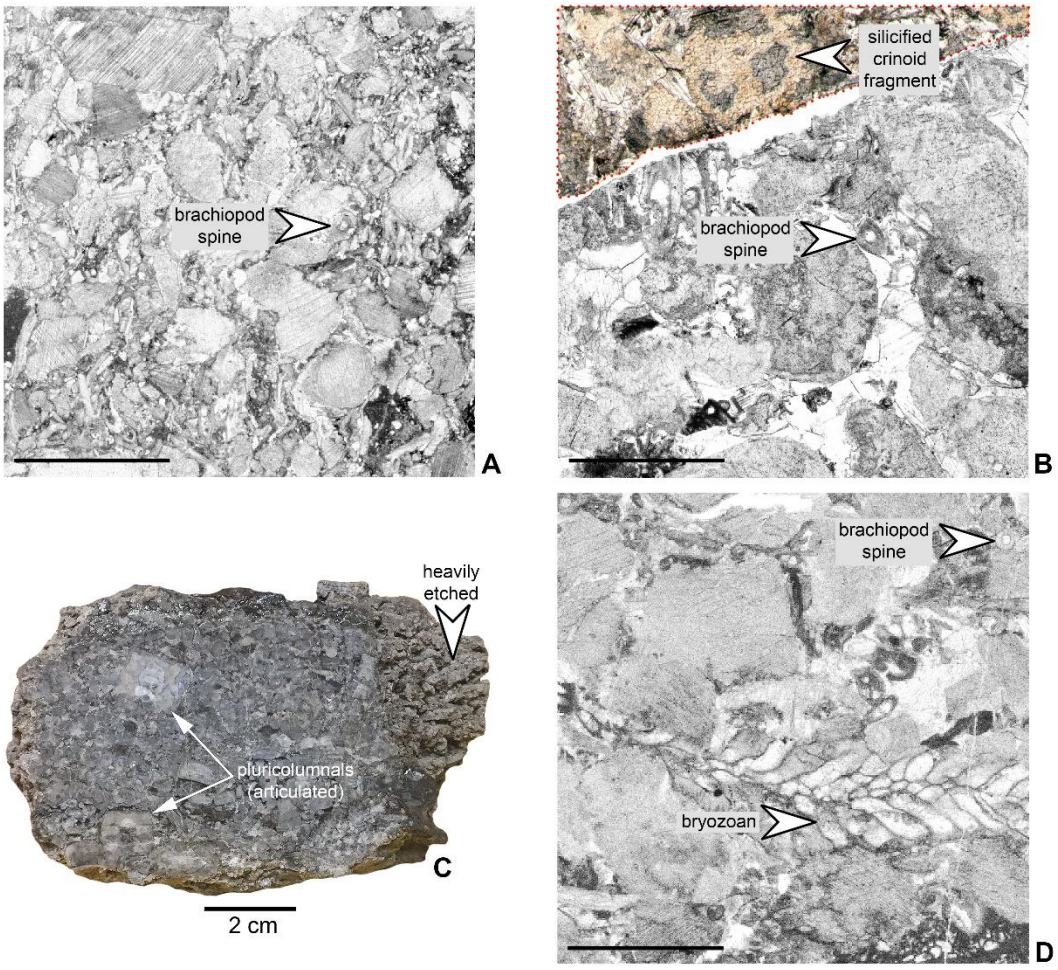

Figure 3.29 – A) Crinoid-brachiopod-bryozoan biosparudite with evidence of compaction along grain contacts. Although the sample is grain-supported, a minor amount of dark carbonate mud remains (unit 67); **B)** Coarse-grained crinoid-brachiopod-bryozoan biosparudite. The upper portion (outlined in red dotted line) is in original color to illustrate the yellow, silicified fabric (unit 70); **C)** Cut and clear-coated hand sample of crinoid-brachiopod-bryozoan biosparudite. Not the resistant, partially silicified crinoid columnals in the etched portion on the right side (unit 70); **D)** Coarse-grained crinoid-brachiopod-bryozoan biosparudite with evidence of compaction along grain contacts. Sample contains completely crushed specimens of *Schwagerina* and trepostomate(?) bryozoans (unit 71). All scale bars = 2 mm unless otherwise noted.

the depositional history of the CBB-Bsr microfacies with such complete destruction of the original fabric. Interpretive uncertainty is compounded when considering the vastly different paleoenvironments associated with encrinite deposits; from shallow, open shelf sediments to deep, toe of slope turbidites (Flügel, 2010). Therefore, two potential depositional scenarios are presented to explain the origins of the cryptic CBB-Bsr microfacies. First, accumulations of crinoid debris are known to form in a variety of muddy shelf settings. The occurrence of both *Schwagerina* and the "deep-water" conodont genus *Mesogondolella* suggests an outer shelf position near the maximum water depth tolerated by fusulinids. Second, the hash-like encrinite deposits may represent shelf margin sediments that were mobilized and transported by slope processes (i.e., turbidity currents). However, the bedding units lack the graded internal structure that is suggestive of turbidite affinity. Regardless of the interpretation, the CBB-Bsr microfacies seems to represent one of the deeper-water lithologies from the Riepe Spring Limestone.

Conclusions

The Upper Pennsylvanian-Cisuralian (lower Permian) strata of the Riepe Spring Limestone of the Spruce Mountain Ridge area were deposited along the margins of two successive shallow-marine basins in the post-Antler foreland (Wardlaw et al., 1995). These western cratonal margin deposits are attributed to alternating shoreline, shoreface, and open shelf sedimentation

trends in the Ely Basin and the Ferguson Trough during the final stage (stage III) of the late Paleozoic ice age (LPIA) (Rygel et al., 2008). Due to the ephemeral nature of these depositional settings, sediments of the Riepe Spring Limestone vary from extremely coarse, chert-rich detritus, to terrigenous sand and silt, to nearly pure autochthonous carbonates in rapid succession.

In this lithostratigraphic study of the North Spruce Mountain Ridge (NSMR) section, four distinctive chert pebble conglomerate lithofacies (macrofacies) and 10 siliciclastic and carbonate microfacies are described to provide a depositional framework for the Riepe Spring Limestone. The Types I-IV conglomeratic lithofacies are petrological variants composed of genetically related terrigenous sediments shed from northern, local highlands into a coastal setting (Yochelson and Fraser, 1973; Marcantel, 1975). The Diamond Peak Formation in northeast Nevada is commonly considered the source of this Upper Pennsylvanian-Cisuralian chert and quartzite detritus in north-central and northeast Nevada (Barosh, 1964; Yochelson and Fraser, 1973; Marcantel, 1975; Wardlaw et al., 2015). Depositional settings of the four conglomerate types are interpreted as (proximal to distal): marginal marine clastic wedge/alluvial cone (Type I), backshore berm (beach) (Type IV), upper foreshore (beach) (Type II), and middle to lower foreshore/swash zone (beach) (Type III).

Siliciclastic and carbonate microfacies from the Riepe Spring Limestone present a much broader, characteristically marine suite of depositional settings. The proportion of siliciclastic to carbonate material, paleoecology of fossil constituents, and wave energy indicators served as the primary indices for paleoenvironmental interpretation. Sedimentary structures were used when observed. The assemblage of illustrated microfacies forms a composite depositional area extending from near shoreline to an outer shelf, or potentially even slope position. Inferred paleoenvironments include (proximal to distal): proximal fan-delta complex (upper shoreface with evidence of tempestites and potential rip channel deposits), semi-restricted lagoon (with a terrigenous sediment source and benthic foraminifers), medial to distal fan-delta complex (mid-shoreface with mixed sand/mud), lower shoreface, mid-shelf (open marine), back reef, and outer shelf to slope.

CHAPTER 4 – INTRODUCTORY REMARKS

This article discusses the early Missourian-late Wolfcampian fusulinid succession from the uppermost part of the Ely Limestone and the full exposure of the Riepe Spring Limestone at Spruce Mountain Ridge, Elko County, Nevada. Six fusulinid assemblage zones are recognized. The stratigraphic section presented herein directly coincides with the full columnar section illustrated in Chapter 3, Figure 3.6.

CHAPTER 4: FUSULINID BIOSTRATIGRAPHY OF THE RIEPE SPRING LIMESTONE, SPRUCE MOUNTAIN RIDGE, ELKO COUNTY, NEVADA

Abstract: The lower Missourian (Upper Pennsylvanian) to upper Wolfcampian (lower Permian) Riepe Spring Limestone at Spruce Mountain Ridge, Elko County, northeast Nevada, consists of approximately 390 m of marginal and shallow marine deposits. These mixed carbonate-siliciclastic strata are biostratigraphically constrained by a fusulinid assemblage comprising six assemblage zones: *Eowaeringella-Triticites* Group I assemblage zone; *Triticites* Group II-*Dunbarinella* assemblage zone; *Triticites* Group IV assemblage zone; *Schwagerina wellsensis* assemblage zone; *Eoparafusulina linearis* assemblage zone; "advanced" *Schwagerina* assemblage zone. Fusulinid collections include recently recovered specimens and loaned material from the Smithsonian National Museum of Natural History's Douglass-Henbest collection. Descriptions of 38 species are provided, including two species of *Eowaeringella*, three species of *Pseudofusulinella*, one species of *Schubertella*, three species of *Alaskanella*, two species of *Cuniculinella*, one species of *Dunbarinella*, one species of *Eoparafusulina*, one species of *Pseudofusulina*, two species of *Pseudoschwagerina*, seven species of *Schwagerina*, 14 species of *Triticites*, and one new monotypic genus, Gen. n. A. Discontinuities in the fusulinid assemblage indicate that deposition of the Spruce Mountain Ridge succession was interrupted by at least four significant mid-Missourian, upper Missourian-lower Virgilian, mid-Virgilian, and Virgilian-Wolfcampian erosional disconformities. Biostratigraphically useful conodont genera (e.g.,

Idiognathodus, *Streptognathodus*, *Sweetognathus*) were incorporated in the study when recovered elements was available.

Introduction

This article discusses the early Missourian through late Wolfcampian fusulinid assemblage of the uppermost part of the Ely Limestone and the overlying Riepe Spring Limestone at Spruce Mountain Ridge, Elko County, northeastern Nevada. The material described was collected from a west-to-east trending measured section along the west side of Spruce Mountain Ridge corresponding to Section 1 of Hope's (1972) geologic map of the Spruce Mountain quadrangle (USGS GQ-942). Section 1 was the northernmost of Hope's three measured sections in the Spruce Mountain Ridge area and is referred to as the North Spruce Mountain Ridge (NSMR) section. Spruce Mountain Ridge extends directly north of Spruce Mountain and approximately 15 km east of the junction of US Route 93 (Great Basin Highway) and Route 229 (Fig. 4.1). The section is accessible by driving east and then north along Spruce Mountain Road before traveling an additional 2 km east (off-road) to the western base of the ridge.

Hope (1972) originally assigned this exposure of limestone and calcareous sandstone to the Riepe Spring Limestone based on preliminary fusulinid data and stratigraphic position, but a true genetic affinity with the type section of the Riepe Spring Limestone in the Ely area remains somewhat

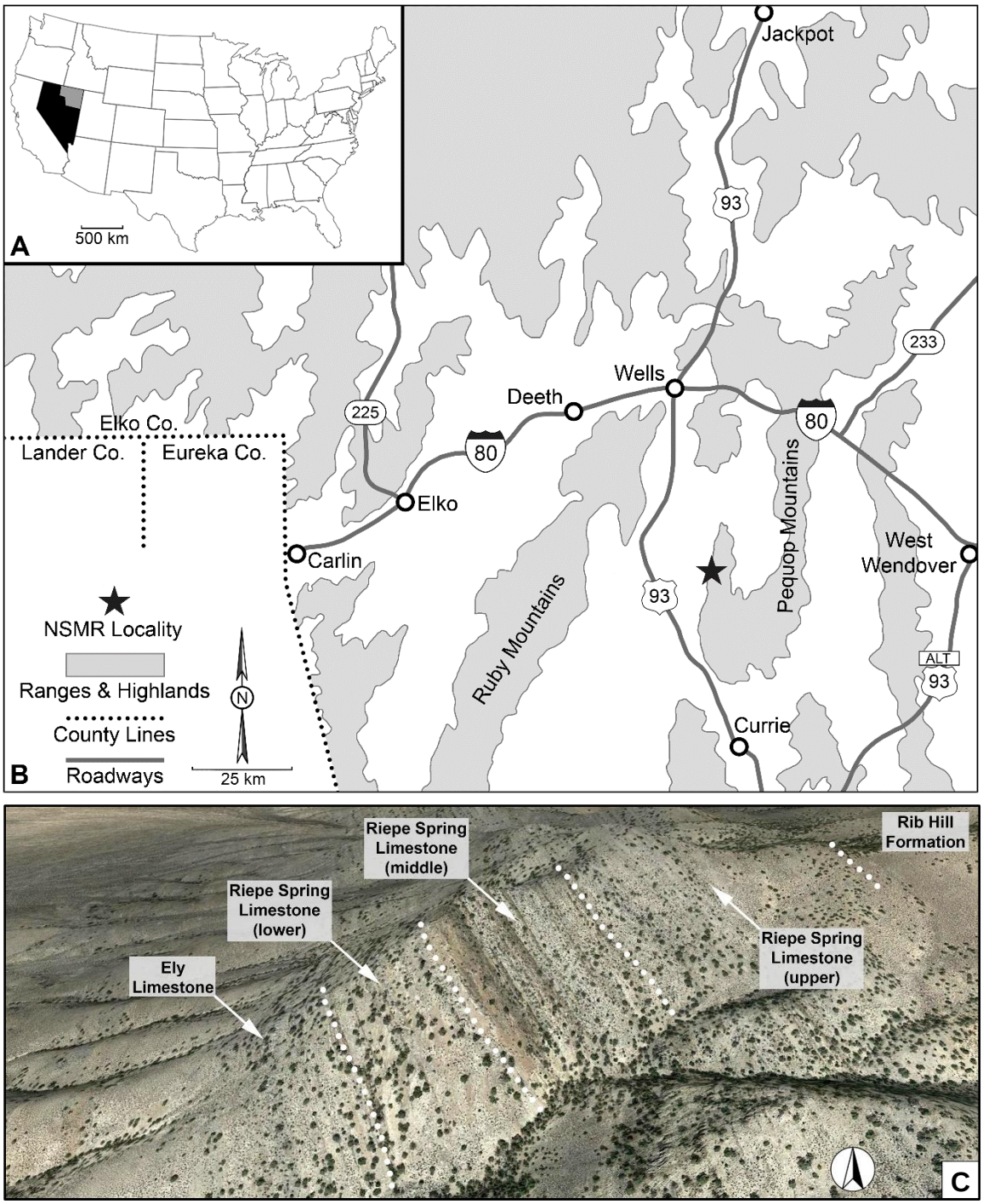

Figure 4.1 – A) Elko County (gray), Nevada (black), U.S.A.; **B)** Map of Elko County, Nevada, with general topography. Black star denotes the location of the NSMR section; C) Aerial view of the NSMR section along the west side of Spruce Mountain Ridge. The white dotted lines are plotted along contacts of lithostratigraphic units.

questionable. Nevertheless, all previous discussions of the Upper Pennsylvanian and Wolfcampian strata in the Spruce Mountain Ridge and southern Pequop Mountains areas refer to the exposure as the Riepe Spring Limestone. Continued usage of the name Riepe Spring Limestone is encouraged until it can be conclusively demonstrated that the exposure at Spruce Mountain Ridge is more closely related to another formation or deserving of a unique designation. Marcantel (1975) suggested a genetic relationship with the Strathearn Formation of similar age whose type section is located in Elko County, but more data collection and studies of additional sections are required before such an equivalence can be proven. To date, the stratigraphic position of the Riepe Spring Limestone at Spruce Mountain Ridge has lacked stage-level chronostratigraphic resolution beyond the general framework provided by Marcantel (1975, p. 2081, fig. 2). Hope's (1972) initial report on Section 1 (NSMR section herein) described approximately 140 m of section as undifferentiated Pennsylvanian-Permian strata. The integration of recently collected fusulinids and previously unpublished material on loan from the Smithsonian's Douglass-Henbest collection has greatly improved upon the efforts of previous studies in eastern Nevada, helping to identify two disconformable stage boundaries and eliminating the uncertainty surrounding the Pennsylvanian-Permian boundary interval.

The purpose of this study is to expand upon the limited knowledge of the Upper Pennsylvanian to upper Wolfcampian fusulinid succession in northeast Nevada. The work of Slade (1961) at Ferguson Mountain currently stands as the principal documentation of Missourian through Leonardian fusulinid faunas from Elko County. Douglass (1974) summarized all previously described fusulinid distributions throughout the greater Basin and Range province, but more recent revision of global and regional Pennsylvanian and Permian boundary intervals necessitates a reevaluation of Nevadan biostratigraphy. Stratigraphic correlations of the Riepe Spring Limestone with extensively studied strata of southeast California, southwest New Mexico, West Texas, north-central Texas, and the Midcontinent are inferred herein. Fusulinids with known affinities to each of the above regions are found within the Spruce Mountain Ridge succession, and several additional, poorly understood taxa, such as *Alaskanella* Skinner and Wilde, 1966 and *Biwaella* Morikawa and Isomi, 1960, are reported from Nevada for the first time.

Materials and Methods

All samples were collected from the uppermost part of the Ely Limestone and the overlying Riepe Spring Limestone of Hope's (1972) Section 1 and USGS Map GQ-942. Samples were collected by R.C. Douglass (USGS), M.K. Nestell, and R. Margerum in 1969 and 1970, and were recollected by

M.T. Read, M.K. Nestell, and B.R. Wardlaw (USGS) in 2014. Fusulinid collections include approximately 150 thin sections prepared by the author and 1,279 thin sections on loan from the Smithsonian National Museum of Natural History's Douglass-Henbest collection. Copies of R.C. Douglass' field notes were provided by the Department of Paleobiology at the Smithsonian and were greatly beneficial in many instances of assigning the Douglass-Henbest specimens a stratigraphic position within the new NSMR section.

Measured specimen parameters of axial sections include length/half length, width/half width, form ratio, number of volutions, diameter of proloculus, height of volutions, thickness of spirotheca, and tunnel angle (in individuals with chomata). Measurements pertaining to equatorial sections are not provided (i.e., septal count). Most parameters were measured using a compound light microscope equipped with a "toolmaker microscope" base and Mitutoyo digimatic micrometer heads. Tunnel angles were measured from photomicrographs using ImageJ image analysis software.

Chronostratigraphic Nomenclature

The purpose of this section is to clearly define the usage of Pennsylvanian and Permian chronostratigraphic units to avoid potential confusion or misinterpretation. Attention is directed to the various concepts in use for the North American Wolfcampian Stage. The chronostratigraphic scheme used herein follows the recommendation initially proposed by Baars

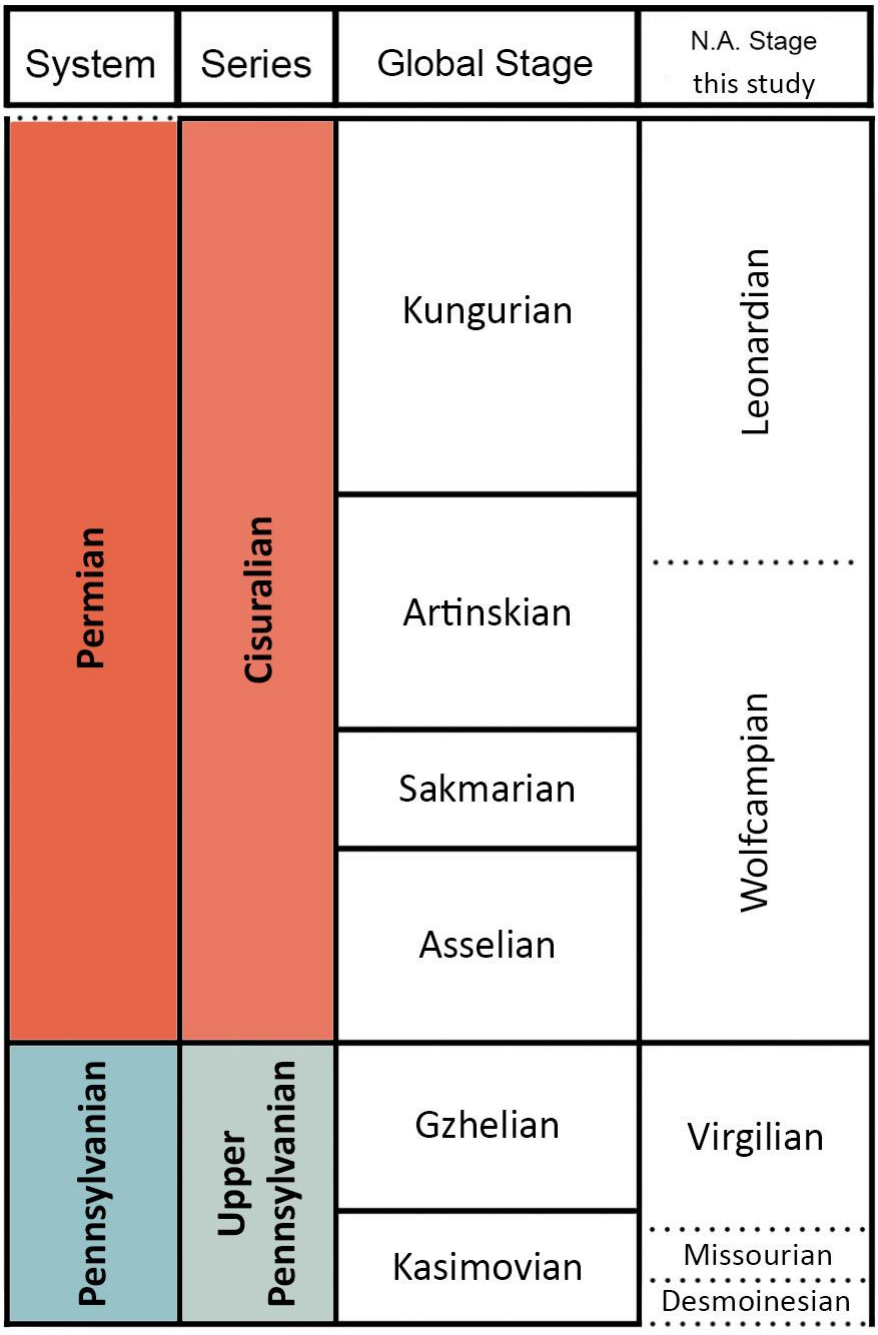

Figure 4.2 – Timescale of the Upper Pennsylvanian and Cisuralian (lower Permian) depicting global stages and the relative positions of the North American regional stages used in this study.

et al. (1994a, b), in which the Virgilian-Wolfcampian boundary is coincident with the base of the Permian System. Figure 4.2 demonstrates that the Wolfcampian Stage is strictly Permian within this concept and is approximately equivalent to the lower half of the Cisuralian Series. Regionally recognized substages of the Virgilian and Wolfcampian (i.e., "Newwellian/Bursumian, Nealian, and Lenoxian") are not applied, but are discussed in a correlative capacity when necessary.

Fusulinid Biostratigraphy and Correlation

The NSMR section includes the uppermost part of the Ely Limestone and the overlying Riepe Spring Limestone and comprises lower Missourian (Upper Pennsylvanian) through upper Wolfcampian (lower Permian) strata. Three informal members of the Riepe Spring Limestone are recognized herein and are delineated by two major lithofacies transitions. The age control is based on integrated fusulinid and conodont assemblages. Six fusulinid assemblage zones are recognized within the NSMR section. The limits of the six assemblage zones, stratigraphic levels of fusulinid species occurrences, and descriptions of the accompanying lithofacies are plotted on the columnar section illustrated in Figure 4.3. Inferred stratigraphic correlations of the Riepe Spring Limestone with the North American Midcontinent and southwestern/western United States are illustrated in Figures 4.4 and 4.5.

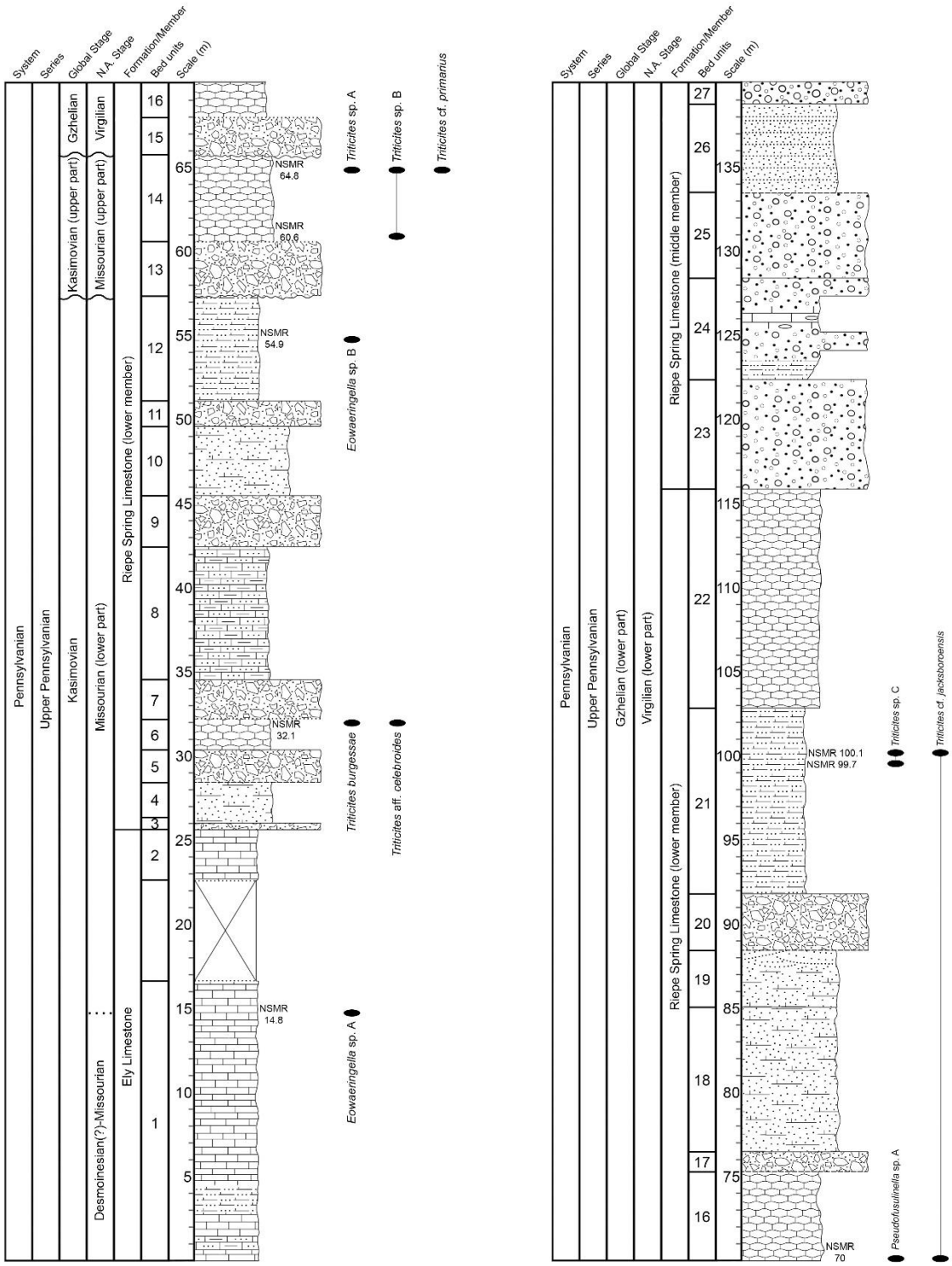
System
Series
Global Stage
N.A. Stage
Formation/Member
Bed units
Scale (m)
Pennsylvanian
Upper Pennsylvanian
Kasimovian
Gzhelian
Kasimovian (upper part)
Gzhelian
Desmoinesian(?)-Missourian
Missourian
Missourian (lower part)
Virgilian
Missourian (upper part)
Virgilian
Ely Limestone
Riepe Spring Limestone (lower member)
1
2
3
4
5
6
7
8
9
10
11
12
13
14
15
16
5
10
15
20
25
30
35
40
45
50
55
60
65
NSMR 14.8
NSMR 32.1
NSMR 54.9
NSMR 60.6
NSMR 64.8
Eowaeringella sp. A
Triticites burgessae
Triticites aff. celebroides
Eowaeringella sp. B
Triticites sp. A
Triticites sp. B
Triticites cf. primarius
System
Series
Global Stage
N.A. Stage
Formation/Member
Bed units
Scale (m)
Pennsylvanian
Upper Pennsylvanian
Gzhelian (lower part)
Virgilian (lower part)
Riepe Spring Limestone (lower member)
Riepe Spring Limestone (middle member)
16
17
18
19
20
21
22
23
24
25
26
27
75
80
85
90
95
100
105
110
115
120
125
130
135
NSMR 70
NSMR 100.1
NSMR 99.7
Pseudofusulinella sp. A
Triticites sp. C
Triticites cf. jacksboroensis

System
Series
Global Stage
N.A. Stage
Formation/Member
Bed units
Scale (m)
Pennsylvanian
Upper Pennsylvanian
Gzhelian (lower part)
Virgilian (upper part)
Riepe Spring Limestone (middle member)
NSMR 150.4
NSMR 149.2
f24122
NSMR 178
NSMR 167.5
f24126
Schubertella ciscoensis
Triticites creekensis
Triticites cf. inflatus
Triticites cf. cellamagnus
Dunbarinella kauffmani
Pseudofusulinella cf. nitida
Triticites bensonensis
Triticites cullomensis
Permian
Cisuralian
Asselian(?)-Sakmarian
Sakmarian (lower part)
Wolfcampian (upper part)
Riepe Spring Limestone (upper member)
PPrs (middle member)
NSMR 227.8
NSMR 215.8
f24136
f24135
f24134
f24133
f24131
f24130
Triticites pinguis
Biwaella americana
Schwagerina sp. A
Pseudoschwagerina robusta
Alaskanella sp. A
Schwagerina neolata
Triticites cf. californicus
Cuniculinella sp. A
Schwagerina wellsensis
Pseudofusulinella sp. B
Cuniculinella sp. A
Pseudofusulina mediotenebraseus
Schwagerina sp. B

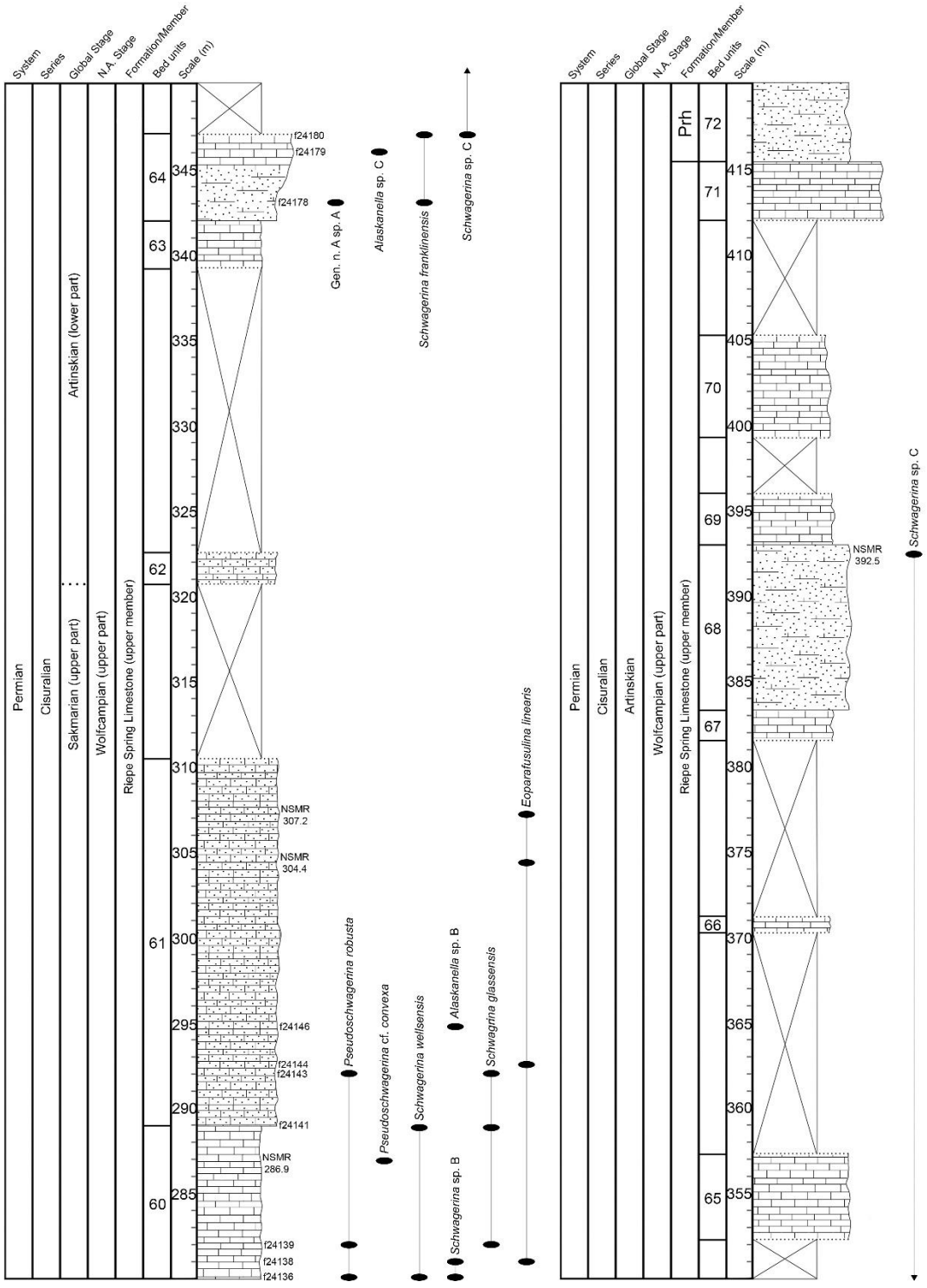
System
Series
Global Stage
N.A. Stage
Formation/Member
Bed units
Scale (m)
Permian
Cisuralian
Artinskian (lower part)
Sakmarian (upper part)
Wolfcampian (upper part)
Riepe Spring Limestone (upper member)
64
63
62
61
60
345
340
335
330
325
320
315
310
305
300
295
290
285
f24180
f24179
f24178
NSMR 307.2
NSMR 304.4
f24146
f24144
f24143
f24141
NSMR 286.9
f24139
f24138
f24136
Gen. n. A sp. A
Alaskanella sp. C
Schwagerina franklinensis
Schwagerina sp. C
Pseudoschwagerina robusta
Pseudoschwagerina cf. convexa
Schwagerina wellsensis
Alaskanella sp. B
Schwagerina sp. B
Schwagrina glassensis
Eoparafusulina lineanis
Artinskian
Prh
72
71
70
69
68
67
66
65
415
410
405
400
395
390
385
380
375
370
365
360
355
NSMR 392.5
Schwagerina sp. C

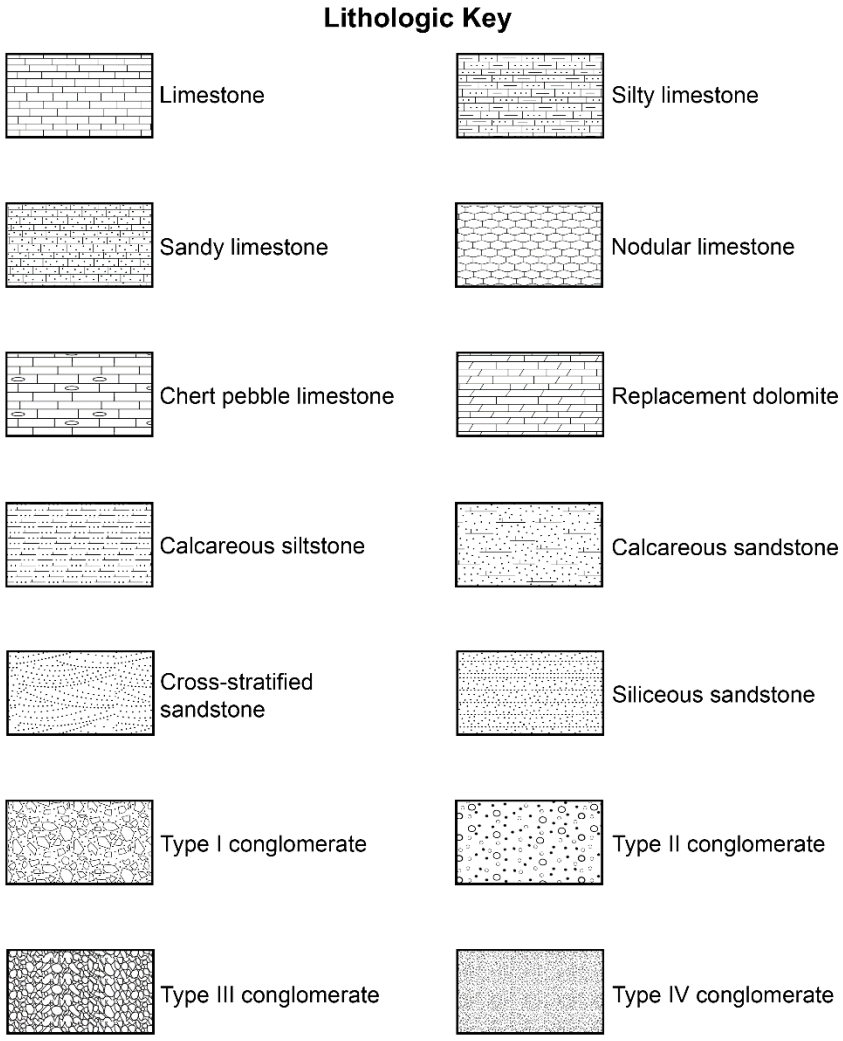

← **Figure 4.3** – Multiple page figure includes a lithologic key and stratigraphic columns of the NSMR measured section with fusulinid occurrences. NSMR numbers along the right side of the columns indicate the collection numbers of samples.

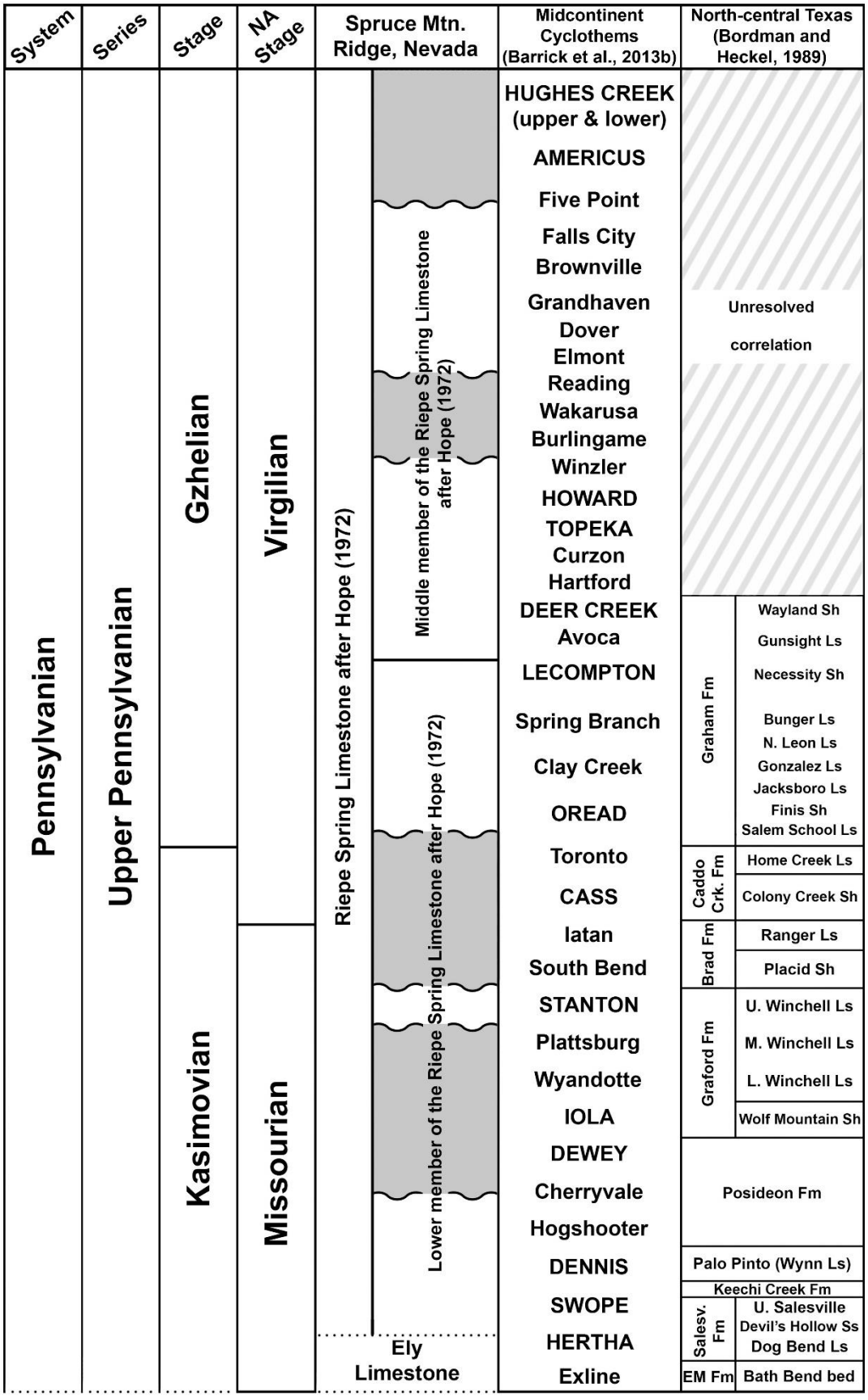
System
Series
Stage
NA Stage
Spruce Mtn. Ridge, Nevada
Midcontinent Cyclothems (Barrick et al., 2013b)
North-central Texas (Bordman and Heckel, 1989)
Pennsylvanian
Upper Pennsylvanian
Gzhelian
Kasimovian
Virgilian
Missourian
Riepe Spring Limestone after Hope (1972)
Middle member of the Riepe Spring Limestone after Hope (1972)
Lower member of the Riepe Spring Limestone after Hope (1972)
Ely Limestone
HUGHES CREEK (upper & lower)
AMERICUS
Five Point
Falls City
Brownville
Grandhaven
Dover
Elmont
Reading
Wakarusa
Burlingame
Winzler
HOWARD
TOPEKA
Curzon
Hartford
DEER CREEK
Avoca
LECOMPTON
Spring Branch
Clay Creek
OREAD
Toronto
CASS
Iatan
South Bend
STANTON
Plattsburg
Wyandotte
IOLA
DEWEY
Cherryvale
Hogshooter
DENNIS
SWOPE
HERTHA
Exline
Unresolved correlation
Graham Fm
Wayland Sh
Gunsight Ls
Necessity Sh
Bunger Ls
N. Leon Ls
Gonzalez Ls
Jacksboro Ls
Finis Sh
Salem School Ls
Caddo Crk. Fm
Home Creek Ls
Colony Creek Sh
Brad Fm
Ranger Ls
Placid Sh
Graford Fm
U. Winchell Ls
M. Winchell Ls
L. Winchell Ls
Wolf Mountain Sh
Posideon Fm
Palo Pinto (Wynn Ls)
Keechi Creek Fm
Salesv. Fm
U. Salesville
Devil's Hollow Ss
Dog Bend Ls
EM Fm
Bath Bend bed

← **Figure 4.4** – Inferred stratigraphic correlation of the Upper Pennsylvanian lower and middle members of the Riepe Spring Limestone at Spruce Mountain Ridge with Midcontinent cyclothems and cyclic deposits of north-central Texas. All caps = major cyclothem; sentence case = minor cyclothem (Barrick et al, 2013b; Boardman and Heckel, 1989).

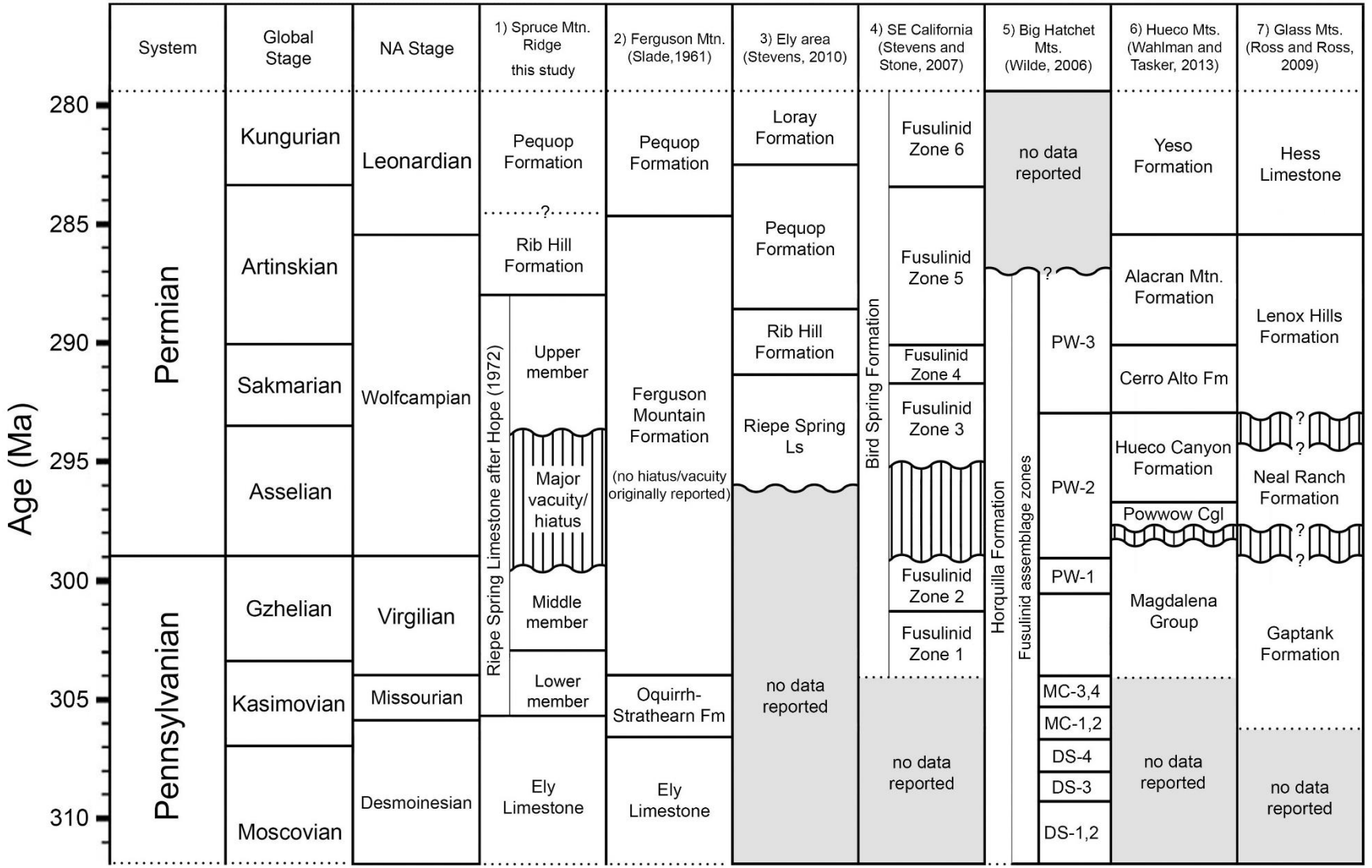
System
Global Stage
NA Stage
1) Spruce Mtn. Ridge this study
2) Ferguson Mtn. (Slade,1961)
3) Ely area (Stevens, 2010)
4) SE California (Stevens and Stone, 2007)
5) Big Hatchet Mts. (Wilde, 2006)
6) Hueco Mts. (Wahlman and Tasker, 2013)
7) Glass Mts. (Ross and Ross, 2009)
Age (Ma)
280
285
290
295
300
305
310
Permian
Pennsylvanian
Kungurian
Artinskian
Sakmarian
Asselian
Gzhelian
Kasimovian
Moscovian
Leonardian
Wolfcampian
Virgilian
Missourian
Desmoinesian
Pequop Formation
?
Rib Hill Formation
Riepe Spring Limestone after Hope (1972)
Upper member
Major vacuity/ hiatus
Middle member
Lower member
Ely Limestone
Pequop Formation
Ferguson Mountain Formation
(no hiatus/vacuity originally reported)
Oquirrh-Strathearn Fm
Ely Limestone
Loray Formation
Pequop Formation
Rib Hill Formation
Riepe Spring Ls
no data reported
Bird Spring Formation
Fusulinid Zone 6
Fusulinid Zone 5
Fusulinid Zone 4
Fusulinid Zone 3
Fusulinid Zone 2
Fusulinid Zone 1
no data reported
no data reported
Horquilla Formation
Fusulinid assemblage zones
?
PW-3
PW-2
PW-1
MC-3,4
MC-1,2
DS-4
DS-3
DS-1,2
Yeso Formation
Alacran Mtn. Formation
Cerro Alto Fm
Hueco Canyon Formation
Powwow Cgl
Magdalena Group
no data reported
Hess Limestone
Lenox Hills Formation
?
?
Neal Ranch Formation
?
?
Gaptank Formation
no data reported

← **Figure 4.5** – Inferred stratigraphic correlation of upper Paleozoic strata at Spruce Mountain Ridge with important equivalent units from the southwestern and western United States (Slade, 1961; Wilde, 2006; Stevens and Stone, 2007; Ross and Ross, 2009; Stevens, 2010; Wahlman and Tasker, 2013).

Desmoinesian Stage

The base of the NSMR measured section is on the western slope of Spruce Mountain Ridge (40°40'47.08"N, 114°49'35.04"W) and lies within the uppermost part of the Ely Limestone, just above the Desmoinesian-Missourian boundary. Unfortunately, the stratigraphic proximity to the boundary interval was unknown when the section was initially measured and described. No Middle Pennsylvanian fusulinids were observed in the recent collections, but several late Desmoinesian fusulinids were recovered by R.C. Douglass and M.K. Nestell only a short, albeit unmeasured distance below the first fusulinid occurrence of this study. Because the exact level of the Douglass material is unknown and the lowest 14 m of the section are devoid of any diagnostic fossils, this interval is considered to be "undifferentiated Desmoinesian-Missourian." A similar stratigraphic gap separating the latest occurrences of *Beedeina* from the first appearance of Missourian fusulinids is well-documented in the North American Midcontinent region (Wahlman, 2013). In Kansas, the Desmoinesian-Missourian boundary is placed within this fusulinid-barren interval at the base of the Exline cyclothem (Heckel et al., 2002; Wahlman, 2013).

Desmoinesian fusulinids from North Spruce Mountain Ridge include *Beedeina* cf. *weintzi* Verville, Thompson, and Lokke, 1956, *Bartramella bartrami* Verville, Thompson, and Lokke, 1956, and *Fusulinella alta* Verville, Thompson, and Lokke, 1956, all of which were originally described from the

Ely Limestone of the Cherry Creek Range, south of Spruce Mountain Ridge. Verville et al. (1956) proposed an inferred correlation of their Cherry Creek section with middle Desmoinesian successions in Iowa, but later work by Ross (1969), Wilde (2006), and Wahlman (2013) suggested that "advanced" forms of *Beedeina*, such as *B.* cf. *weintzi*, and the Zone of *Bartramella* are indicative of upper Desmoinesian strata. This study does not present a zonal scheme for the upper part of the Desmoinesian as these strata were not included in the measured section.

Missourian Stage

The Missourian fusulinid succession of the North American Basin and Range province is poorly documented and has not received much revision or new contributions since the mid-1960's. The handful of studies focused on Missourian fusulinid biostratigraphy were conducted by few researchers working on the Bird Spring Formation of California and Nevada, and the Oquirrh Formation of Utah (see Thompson et al., 1950; Rich, 1961; Cassity and Langenheim, 1966). Much of our knowledge regarding Missourian fusulinids came from studies of the Permian Basin, north-central Texas, and the cyclic deposits of the Midcontinent region. Wahlman (2013) compiled many of these data and presented a comprehensive Middle Pennsylvanian-lower Cisuralian fusulinid biozonation for the northern Midcontinent to north-central Texas. Consequently, many of the correlations inferred herein

for the Missourian part of the NSMR section are made with respect to well-documented Midcontinent localities offering high resolution fusulinid and conodont control without major tectonostratigraphic concerns. The most notable difference between the Missourian fusulinid succession of the Midcontinent and that of Spruce Mountain Ridge is the absence of *Kansanella* among the Riepe Spring Limestone collections. It is unclear whether the lack of *Kansanella* is a result of missing stratigraphic section or facies control, but Slade (1961) reported *K.* cf. *plicatula* and *K.* (*Iowanella*) cf. *winterensis* from the Missourian-Virgilian boundary interval at nearby Ferguson Mountain.

Eowaeringella–Triticites Group I Assemblage Zone

The known Missourian portion of the NSMR section measures 51 m in thickness and includes the uppermost part of the Ely Limestone and part of the lower informal member of the Riepe Spring Limestone. The relatively thin Missourian interval is truncated by at least two significant erosional disconformities, the higher of which spans the Missourian-Virgilian boundary. The oldest fusulinids recovered from the recent collections belong to the early Missourian genus *Eowaeringella* Skinner and Wilde, 1967 and were collected 14.8 m above the base of the section in the uppermost part of the Ely Limestone (unit 1; Fig. 4.3).

Eowaeringella is a critical marker taxon for constraining the relative age of the Ely-Riepe Spring contact (25.7 m above the base), as this genus has limited stratigraphic range and is considered one of the most useful indicators of lower Missourian strata in North America. In the northern Midcontinent, the Zone of *Eowaeringella* is restricted to the lowermost Missourian, preceding the earliest forms of *Triticites*, whereas the southern Midcontinent and Permian Basin regions provide evidence of a brief overlap in the stratigraphic ranges of the two taxa (Wahlman, 2013). In the Big Hatchet Mountains of southwest New Mexico there are at least two forms of *Eowaeringella* occurring as high as the lower-middle Missourian part of the Horquilla Formation at Big Hatchet Peak (Wilde, 2006). At Spruce Mountain Ridge, the appearance of *Eowaeringella* sp. A at 14.8 m denotes the base of the *Eowaeringella-Triticites* Group I assemblage zone, the lowest recognized fusulinid biozone of the NSMR section.

The lowest recovered fusulinids from the lower informal member of the Riepe Spring Limestone occur 32.4 m above the base of the section in the first nodular limestone of the formation (unit 6; Fig. 4.3), and include *Triticites burgessae* Burma, 1942 and *T.* aff. *celebroides* Ross, 1965. Both *Triticites burgessae* and *T. celebroides* are among the earliest forms of *Triticites*, which are characterized by their generally small size and thin, weakly keriothecal spirotheca. *Triticites burgessae* has been reported from the upper part of the Cherryvale cyclothem in the northern Midcontinent, the Bird Spring

Formation at Arrow Canyon, Nevada, and the Gaptank Formation of the Glass Mountains, West Texas (Thompson, 1957; Ross, 1965; Cassity and Langenheim, 1966). *Triticites burgessae* co-occurs with type *T. celebroides* at the latter locality. Additional reports of *Triticites celebroides* include occurrences in the Sol Mete Member of the Wild Cow Formation (Sol Mete Member) in central New Mexico and the Wynn Limestone Member of the Palo Pinto Formation in north-central Texas (Myers, 1988; Nestell, 1989). The observed assemblage indicates that units 6-8 of the Riepe Spring Limestone are approximately correlative with the lower-middle part of the Kansas City Group in the Midcontinent, the *T. celebroides* assemblage zone of the Gaptank Formation, and the Wynn Limestone in north-central Texas.

Triticites burgessae and *T.* aff. *celebroides* occupy a medial position in the lowest Missourian *Eowaeringella-Triticites* Group I assemblage zone at Spruce Mountain Ridge. Following the occurrence of these early forms of *Triticites* in unit 6, the overlying 22.8 m of section are highly conglomeratic and devoid of fusulinids. *Eowaeringella* sp. B occurs 54.9 m above the base of the section in the middle of unit 12, marking the highest occurrence of the genus in the section. The presence of *Eowaeringella* nearly 23 m higher than the lowest occurrence of *Triticites* is potentially significant and provides further insight into the upper extent of the genus' range in the western United States. Only *E. stricta* Wilde (2006) and *Eowaeringella* sp. A Wilde

(2006) from Big Hatchet Peak are known to range higher into the Missourian than *Eowaeringella* sp. B.

Unit 12 and the last occurrence of *Eowaeringella* are directly overlain by a lower-middle Missourian-upper Missourian erosional disconformity at the base of unit 13, where a thick conglomerate has markedly incised the underlying calcareous siltstone (Fig. 4.6). The upper limit of the erosional vacuity is inferred from the integration of fusulinid and conodont occurrences in the nodular limestone of unit 14, where *Triticites* sp. A, *Triticites* sp. B, and *Triticites* cf. *primarius* Merchant and Keroher, 1939 occur 64.8 m above the base of the section. *Triticites* sp. B bears a general resemblance to the elliptical Missourian-Virgilian boundary species *T. oryziformis* Newell, 1934, suggesting that the new morphotype is a transitional *Triticites* Group I-Group II form of late Missourian age. *Triticites* sp. A and *T.* cf. *primarius* are more typical late ("advanced") morphotypes of *Triticites* Group I, with subtly inflated tests and thicker spirotheca than the earlier, thin-walled, subcylindrical forms of the group (e.g., *T. ohioensis* Thompson, 1936).

Triticites primarius is a short-ranging marker taxon that is only associated with upper Missourian strata equivalent in age to the Stanton and South Bend cyclothems (Nail, 1996, unpublished dissertation). Previous reports of *T. primarius* include occurrences in the Placid Shale and Winchell Limestone in north-central Texas, and the Stanton Limestone, Rock Lake Shale, and South Bend Limestone (= middle to upper Lansing Group) in

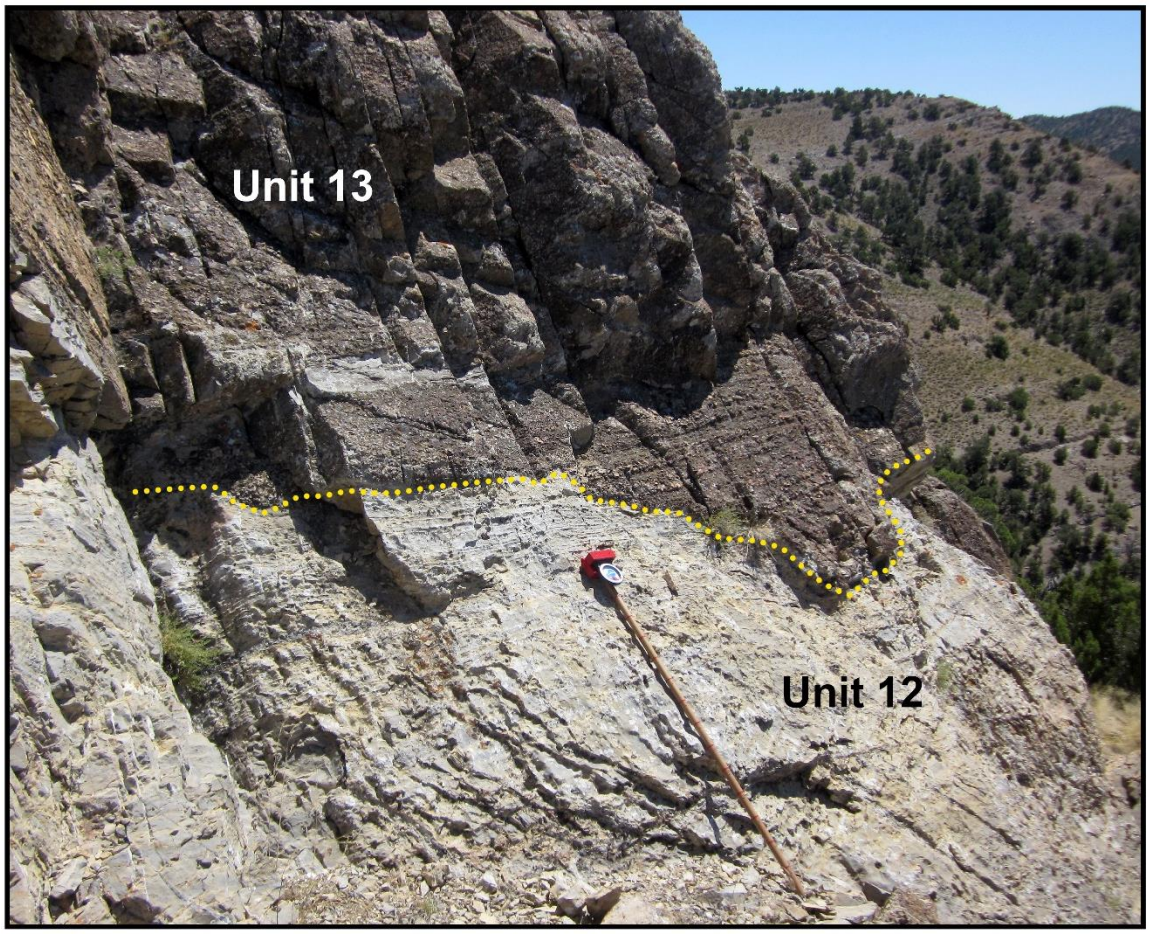

Figure 4.6 – Quartzose conglomerate (dark brown) of unit 13 incising (yellow dotted line) the underlying calcareous siltstone of unit 12. Jacob's staff = 1.5 m. The erosional surface is associated with a lower-middle Missourian-upper Missourian disconformity.

Kansas, suggesting a correlation of the uppermost preserved part of the *Eowaeringella-Triticites* Group I assemblage zone (units 13-14) with the Stanton and South Bend cyclothems (Thompson, 1957; Nail, 1991, unpublished thesis; Nail, 1996, unpublished dissertation). These upper Missourian units of the Riepe Spring Limestone are of biostratigraphic significance to the present study, but the interval is thin and terminates abruptly following unit 14 due to a Missourian-Virgilian boundary spanning disconformity. The associated erosional surface is recognized at the base of a 3.3 m thick conglomerate (unit 15) where the underlying nodular limestone is visibly truncated.

Virgilian Stage

The disconformable base of the Virgilian at Spruce Mountain Ridge is 65.8 m above the base of the section in the lower informal member of the Riepe Spring Limestone (unit 15). Although a continuous Missourian-Virgilian transition interval is not preserved at Spruce Mountain Ridge, the occurrence of conodonts belonging to the *Idiognathodus simulator* group in unit 16 indicates that the erosional base of the underlying conglomerate serves as an acceptable approximation for the base of the Gzhelian.

Triticites Group II–Dunbarinella Assemblage Zone

The fusulinid fauna of the lower part of the Virgilian is characterized by the appearance and subsequent dominance of *Triticites* Group II. Wilde (1976) defined *Triticites* Group II as those forms of *Triticites* which are distinctly larger and more inflated than the earlier subcylindrical to narrowly fusiform *Triticites* of Missourian age. Lucas et al. (2017b) appropriately referred to these diagnostic early to middle Virgilian forms as "intermediate *Triticites*."

The oldest Virgilian fusulinids occur 70 m above the base of the section in the lower informal member of the Riepe Spring Limestone and include abundant *Pseudofusulinella* sp. C with very sparse occurrences of *Triticites* cf. *jacksboroensis* Kauffman and Roth, 1966. The overwhelming number of *Pseudofusulinella* are not particularly useful for placement of the Missourian-Virgilian boundary, but the occurrence of *T*. cf. *jacksboroensis* denotes the first appearance of an unequivocally Virgilian morphotype of *Triticites* in the section. Only one well-oriented specimen of *T*. cf. *jacksboroensis* was found in unit 16, but the superficial and quantitative similarities with the type specimens are convincing enough to allow for the tentative assignment. Kauffman and Roth (1966) described *T*. *jacksboroensis* from the Jacksboro Limestone Member of the Graham Formation in north-central Texas, where the known stratigraphic range of the species spans from the type occurrence upward to the top of the Wayland Shale (Wahlman, 2013). This north-central Texas succession is equivalent to strata of the

Oread cyclothem through the Deer Creek cyclothem in the Midcontinent region (Boardman and Heckel, 1989). The presence of basal Gzhelian conodonts provides further constraint of unit 16, indicating that the lowest part of the *Triticites* Group II-*Dunbarinella* assemblage zone is correlative with strata assigned to the *Idiognathodus simulator* Zone.

Unit 16 is followed by nearly 17 m of regressive sandstone and conglomerate devoid of fusulinids and conodonts. *Triticites* cf. *jacksboroensis* occurs again in greater numbers 100.1 m above the base of the section in a calcareous siltstone (unit 21; Fig. 4.3), along with the small yet stoutly constructed *Triticites* sp. C. The presence of *T.* cf. *jacksboroensis* both below and above the terrigenously influenced interval (units 17-20) suggests that the conglomerate beds are not associated with erosional disconformities and deposition was relatively continuous. The remainder of the lower informal member of the Riepe Spring Limestone is considered lower to lower-middle Virgilian but lacks fusulinids and conodonts. Biostratigraphic control is provided by bounding fusulinid-bearing units. The dark, thick conglomerate and siliceous sandstone of units 23-27 compose the topographically highest part of the hill's western slope and separate the lower from the upper informal member of the Riepe Spring Limestone. From the eastward viewer's perspective, this portion of the section appears as the crest of the hill, but the dark bluffs are only a false peak followed by a shallow saddle.

The lowest occurring fusulinids from the middle informal member of the Riepe Spring Limestone were found 149.2 m above the base of the section in the first thick limestone bed above the conglomeratic false peak (unit 30; Fig. 4.3). Forms recovered from unit 30 include *Dunbarinella kauffmani* Wilde, 2006, *Schubertella ciscoensis* Kauffman and Roth, 1966, and *Triticites cullomensis* Dunbar and Condra, 1927. This fusulinid assemblage is characteristic of the lower-middle to middle Virgilian *Triticites beedei-Dunbarinella ervinensis* Zone of Wahlman (2013) in the Midcontinent and Wilde's (2006) VC-2 Zone (lower-middle Virgilian) of the Permian Basin of Texas and southwest New Mexico. In Kansas and north-central Texas the *Triticites beedei-Dunbarinella ervinensis* Zone occupies the lower two-thirds of the *Streptognathodus virgilicus* s.s. Zone (conodont zone) and includes all strata between the base of the Deer Creek Limestone (KS)/Gunsight Limestone (TX) and the top of the Soldier Creek Shale (KS)/Crystal Falls Limestone (TX) (Barrick et al., 2013b; Wahlman, 2013).

Triticites bensonensis Ross and Tyrrell, 1965 occurs 1.2 m higher than the previous sample, at 150.4 m above the base of the section. Reported occurrences of this small, highly inflated taxon are somewhat uncommon, but the form bears a distinct resemblance to coeval species of *Triticites* Group II from the Graham and Thrifty Formations in north-central Texas (Ross and Tyrrell, 1965). Ross and Tyrrell originally described *T. bensonensis* from the lower informal member of the Earp Formation (lower-middle Virgilian) in the

Whetstone Mountains of Arizona, where it occurs with *T. whetstonensis* Ross and Tyrrell, 1965 and an unnamed species of *Dunbarinella*. Additional reports of *T. bensonensis* include occurrences in the Pine Shadow Member of the Wild Cow Formation in the Manzano Mountains of New Mexico and the Virgilian part of the Bird Spring Formation in southeast California ("Fusulinid Zone 1") (Myers, 1988; Stevens and Stone, 2007). Although the fauna of the lower part of the middle informal member of the Riepe Spring Limestone has decent correlative potential, the associated fusulinid assemblage zones and conodont range zones are unfortunately rather long. Consequently, the inferred correlations for this part of the section do not demonstrate the level of resolution of previously discussed stratigraphic relationships, but the observed assemblage, particularly the presence of *Dunbarinella*, indicates that the lower part of the middle informal member of the Riepe Spring Limestone is middle Virgilian.

Triticites Group IV Assemblage Zone

Triticites Group IV of Wilde (1976) is composed of large, thick-walled, highly inflated morphotypes of late Virgilian to Wolfcampian age. Wilde (2006) and Lucas et al. (2017b) referred to the collective suite of ventricose *Triticites* as Group III, but this is perhaps a misnomer attributable to a typo. Wilde (2006) referred to *Triticites* Group III in both the Virgilian and "Newwellian" (= upper part of the Virgilian) portions of the study and made

no mention of the characteristically Late Pennsylvanian to earliest Permian *Triticites* Group IV (see Wilde, 2006, p. 12). It is unclear whether this was an omission or a mislabeling. Whatever the cause, Wilde (1976) clearly defined Group IV as highly inflated (ventricose) forms of *Triticites* with large proloculi and thick, coarsely alveolar spirotheca. Group III forms are likewise large and among the youngest species of *Triticites* as well, but they are never referred to as ventricose in the original definition.

A faunal replacement of Group II *Triticites* with the much larger Group IV taxa occurs between the collections of unit 30 and samples recovered from unit 34. The lowest occurring Group IV taxon, *T. creekensis* Thompson, 1954, was found 167.5 m above the base of the NSMR section (unit 34). *Dunbarinella*, although present in unit 30, is absent from unit 34 and the rest of the measured section. In the middle informal member of the Riepe Spring Limestone this faunal replacement is obvious and occurs over a relatively short, conglomeratic interval (17 m), suggesting that the middle Virgilian-upper Virgilian transition may be discontinuous. In the Big Hatchet Mountains, the stratigraphic range of *Dunbarinella* (VC-1 and VC-2 Zones of Wilde, 1990) is separated from that of *T. creekensis* (PW-1 Zone of Wilde, 1990) by nearly the full thickness of the VC-3 Zone of Wilde (1990), some 40 to 100 m. The VC-3 fauna of the Big Hatchet Mountains is composed of moderately large and inflated forms of *Triticites* (i.e., *T. sacramentoensis* Needham, 1937). No such forms were recovered from the markedly

siliciclastic 17 m interval separating units 30 and 34 of the NSMR section, thereby suggesting that the apparent hiatus is approximately equivalent to the upper middle Virgilian VC-3 Zone of the Horquilla Formation. The suspected erosional surface is located at the base of a 6.3 m thick conglomerate 159.6 m above the base of the section (unit 33; Fig. 4.3).

Triticites creekensis, which appears to have two co-occurring morphotypes in unit 34, is widely distributed throughout the western and southwestern United States. Previous reports include upper Virgilian occurrences in the lower part of the Pueblo Formation in north-central Texas, the Horquilla and Bursum Formations of southwest New Mexico, the Earp Formation of southeast Arizona, the Bird Spring Formation of Clark County, Nevada, and the lower part of the Ferguson Mountain Formation of Elko County, Nevada (Thompson, 1954; Rich, 1961; Slade, 1961; Sabins and Ross, 1963; Cassity and Langenheim, 1966; Wilde, 2006). However, based on the tentative placement of the Pennsylvanian-Permian boundary in north-central Texas near the base of the Stockwether Limestone, the Pueblo Formation occurrence is perhaps among the youngest reported occurrences of *T. creekensis* (Wahlman, 2013; Wardlaw and Nestell, 2014).

Following the occurrence of *T. creekensis* in unit 34, the rest of the middle informal member of the Riepe Spring Limestone is likewise considered upper Virgilian. Units 36 through 45 of the NSMR section contain sporadic occurrences of Group IV *Triticites* where the limestone units are not

completely dolomitized. Additional characteristically late Virgilian forms recovered from the upper part of the middle informal member include occurrences of *T.* cf. *inflatus* White, 1932 at 178 m (unit 36), *T. cellamagnus* Thompson and Bissell, 1954 at ~200 m (unit 42), and *T. pinguis* Dunbar and Skinner, 1937 and *Pseudofusulina mediotenebraeus* Wilde, 2006 at 215.8 m above the base of the section (unit 45). Each of the given forms occurs in the "Newwellian" PW-1 Zone of the Big Hatchets, supporting a correlation of the upper part of the middle informal member with the uppermost Virgilian part of the Horquilla Formation in southwest New Mexico.

Wolfcampian Stage

Four meters above the occurrence of *Triticites pinguis* and *Pseudofusulina mediotenebraeus*, at the top of unit 46, the uppermost Virgilian part of the Riepe Spring Limestone is erosionally truncated by a 3.5 m thick conglomerate (unit 47; Fig. 4.3) and disconformably overlain by Wolfcampian strata. This discontinuous Virgilian-Wolfcampian boundary is characterized by coincidental shifts in lithostratigraphic and biostratigraphic signatures at the contact of the middle and upper members of the Riepe Spring Limestone. The transition from prevailing dolomite and calcareous sandstone to dark limestone is accompanied by a complete faunal replacement among both fusulinids and conodonts. No Late Pennsylvanian genera of either group were present above the basal conglomerate separating

the middle and upper members of the Riepe Spring Limestone. A similar faunal juxtaposition was described from the Bird Spring Formation of southeast California by Stevens and Stone (2007), in which a single, potentially reworked, unnamed specimen of *Triticites* (*Triticites* sp. 1) was found in Permian strata. This dichotomy is in stark contrast to several more continuous Pennsylvanian-Permian successions in Nevada, such as the Bird Spring Formation near Lee Canyon as reported by Rich (1961) and the Ferguson Mountain Formation reported by Slade (1961), both of which demonstrate overlap between either *Triticites* or *Leptotriticites* and "primitive" forms of *Schwagerina.* However, because the primary signal for the base of the Permian System is the FAD of the conodont *Streptognathodus isolatus* Chernykh, Ritter, and Wardlaw, 1997, it remains unclear whether the above successions preserve continuous records of a Pennsylvanian-Permian boundary. Regardless of boundary placement, the previously described fusulinid assemblages of Lee Canyon and Ferguson Mountain suggest that if disconformities are present within these sections, the duration of any potential hiatus must have been considerably shorter than that of the NSMR disconformity.

Schwagerina wellsensis Assemblage Zone

The oldest Wolfcampian fusulinids recovered from the upper informal member of the Riepe Spring Limestone were found 227.8 m above the base of

the section (~21 m above the major disconformity) in a thick transgressive limestone (unit 48; Fig. 4.3) which produced perhaps the most intriguing fauna of the entire succession. The assemblage of unit 48 includes two new forms of the poorly understood genus *Cuniculinella* Skinner and Wilde, 1965b, the exceptionally uncommon *Biwaella americana* Skinner and Wilde, 1965a, myriad globose schubertellids (*Grovesella*? Davydov and Arefifard, 2007), and forms closely resembling *Schwagerina wellsensis* Thompson, 1954. Although the first categorical occurrence of *S. wellsensis* is higher in the NSMR section at 272 m above the base, the lower portion of the upper informal member, from 219.8 to 281 m, herein constitutes the *S. wellsensis* assemblage zone.

Cuniculinella sp. A was found in both the present collection and in the loaned material from the Douglass-Henbest collection, whereas the more uncommon *Cuniculinella*? sp. B was only observed in the Douglass-Henbest slides. Thompson and Wheeler (1946) first reported the occurrence of *Cuniculinella* from Zone F of the McCloud Limestone in northern California, and the authors erroneously regarded the first specimens as *Parafusulina*? *calx* and *Parafusulina*? *turgida* based on the presence of cuniculi in the outer volutions. Topotype material of these forms was included in a comprehensive fusulinid study of the McCloud Limestone performed by Skinner and Wilde (1965b). The authors recognized that Thompson and Wheeler's two questionable taxa were sufficiently different from true Leonardian

Parafusulina Dunbar and Skinner, 1931 and assigned them (and ten additional species) to the newly erected *Cuniculinella*. Attempts of accurate correlation with the McCloud Limestone are difficult because of the formation's structural complexities and local discontinuity, but Skinner and Wilde's (1965b) concurrent fusulinid zonation of 23 partial exposures of the McCloud Limestone indicates that faunal Zone F is middle to upper Wolfcampian. In a study of the Keeler Basin of east-central California, Stevens et al. (2001) tentatively suggested that McCloud Zone F is likely Sakmarian. Magginetti et al. (1988) described additional occurrences of *Cuniculinella* from nearly equivalent Wolfcampian parts of the Owens Valley Group of the Darwin Canyon area and the Conglomerate Mesa area in east-central California. Stevens and Stone (2009a) expanded upon the work of Magginetti et al. (1988), describing three additional species of *Cuniculinella* from unit 7 of the Owens Valley Group and suggesting that the strata are lower to middle Artinskian. The two mid-Wolfcampian forms of *Cuniculinella* described herein are tentatively considered early Sakmarian based on the presence of *Sweetognathus binodosus* Chernykh, 2005 ~15 m higher (unit 52), but a latest Asselian assignment cannot be ruled out as no conodonts were recovered in association with the fusulinids from unit 48. Although unit 52 contains Sakmarian conodonts, these are the lowest occurring Permian conodonts from the NSMR section and the major disconformity makes it

impossible to determine the FO of *Sw. binodosus* for more accurate placement of the Asselian-Sakmarian boundary.

Eight specimens of *Biwaella americana* were recovered from unit 48 as well; two from the Douglass-Henbest collection and six from the author's collection. *Biwaella americana* has previously only been formally reported from one other locality in the western and southwestern United States. Skinner and Wilde (1965a) originally described *B. americana* from the upper part of Zeller's (1958) bed 155 in the upper Wolfcampian PW-3 Zone of the Horquilla Formation. Although the present specimens are considered to be latest Asselian to early Sakmarian, Davydov (2014) interpreted the New Mexican forms as Artinskian. The Riepe Spring Limestone forms of *Biwaella* may be slightly older than those of the Big Hatchets, but the rarity of the genus in North America and global morphological conservatism throughout its range (Gzhelian-Cisuralian) make it difficult to be certain. Nevertheless, an approximate correlation of the lower part of the upper informal member of the Riepe Spring Limestone with McCloud Zone F (and potentially the upper part of Zone E) and the uppermost part of the Horquilla Formation is inferred (Fig. 4.5).

Following unit 48, the overlying ~44 meters of strata are composed primarily of quartzose limestone, conglomerate, and finely cross-bedded calcareous sandstone. Unsurprisingly, the terrigenously diluted strata of this part of the section are lacking in well-preserved fusulinids. Where fusulinids

were occasionally recovered many of the tests are highly abraded, often missing the outermost volutions. Most fusulinids from this interval are relatively small, nondescript, and difficult to properly identify. Several decently preserved specimens from the Douglass-Henbest collection recovered from ~254 m above the base of the section are regarded herein as *Schwagerina* sp. A. Above the interval of poor recovery, the first Nevadan specimens of the genus *Alaskanella* Skinner and Wilde, 1966 recognized as such and *Schwagerina wellsensis* occur 272 m above the base of the section. *Alaskanella* sp. A occurs in the lower, quartzose limestone portion of unit 60, ~19 m below the crest of the hill, where the form is incredibly abundant and constitutes the dominant taxon for a thin interval in the lower part of the unit. Nestell and Blome (2015) reported the occurrence of *Alaskanella* aff. *laudoni* Skinner and Wilde, 1966 from Hereford tectonic inliers of the Baker Terrane in northeast Oregon and concluded that the associated portion of the mélange is upper Sakmarian to lower Artinskian. The suggested age of the Oregon material agrees with the additional biostratigraphic control provided by the sweetognathid conodont assemblage from the same interval as *Alaskanella* sp. A in the NSMR section. *Schwagerina wellsensis* was described by Thompson (1954) from a nearby locality of unnamed "Wolfcampian rocks" approximately one mile southwest of Wells, Nevada, to the north of Spruce Mountain Ridge. Thompson (1954) suggested that the strata from which *S. wellsensis* was recovered were likely equivalent to part

of the Cerro Alto Formation (middle part of the Hueco Group) and the Lenox Hills Formation of West Texas, a claim that is in strong agreement with the author's inferred correlation of the upper informal member of the Riepe Spring Limestone.

Schwagerina neolata Thompson, 1954 occurs approximately two meters higher in the NSMR section (274 m above the base; unit 60; Fig. 4.3) in association with the Echinoderm-*Tubiphytes* poorly-washed biosparite microfacies (ET-PBs) (see Chapter 3). Thompson (1954) described *S. neolata* from the Cerro Alto Formation of the Hueco Mountains in West Texas, where it was one of only two forms observed (the other being *S. eolata* Thompson, 1954). The Cerro Alto Formation, formerly the middle part of the Hueco Formation, has been interpreted as correlative with part of the Lenox Hills Formation in the Glass Mountains and is considered by most to be Sakmarian (Wardlaw, et al., 2004; Fedorowski et al., 2007; Ross and Ross, 2009; Stevens and Stone, 2009; Mack et al., 2013). Ross (1963) and Magginetti et al. (1988) illustrated potentially slightly younger forms that very closely resemble Thompson's type specimens of *S. neolata* from upper Wolfcampian strata of the Lenox Hills Formation and the Owens Valley Group (respectively), but the authors each assigned these forms to *S. diversiformis* Dunbar and Skinner, 1937 (see *Systematic Paleontology*). Ross and Ross (2003) redescribed several of the specimens from the Glass Mountains and split them from the original concept of *S. diversiformis*,

instead reassigning them to *S. lenoxhillsensis* Ross and Ross, 2003. Although the authors agree with Ross and Ross (2003) that these forms do not belong to *S. diversiformis*, the specimen YPM 20639 of Ross (1963) is nearly identical to one of Thompson's paratypes of *S. neolata* (T-238-5), and Ross' form is regarded herein as such.

Eoparafusulina linearis Assemblage Zone

Eoparafusulina linearis (Dunbar and Skinner, 1937) first occurs at 281 m and continues upward to 307.2 m above the base of the NSMR section, over the crest of the hill and into the topographically higher portion of the dip-slope (Fig. 4.3). The appearance of *E. linearis* denotes the transition from the *Schwagerina wellsensis* assemblage zone to that of the *E. linearis* assemblage zone. *Eoparafusulina linearis* is among the most characteristic and widely distributed late Wolfcampian fusulinid species in western and southwestern United States. Dunbar and Skinner (19737) originally described *E. linearis* from the "Hueco Formation" at Victorio Canyon and the Lenox Hills Formation where it constitutes a major assemblage zone (Wilde, 1962). Ross (1962) reported a younger occurrence of *E. linearis* in the lower part of the Leonard Formation. Outside of West Texas *E. linearis* has been found in the Bird Spring Formation of southeast California and Arrow Canyon, Nevada, the Carbon Ridge Formation of east-central Nevada, the Pequop Formation of Ferguson Mountain and the Pequop Mountains, Nevada, the type section of

the Rib Hill Formation, and the Garden Valley Formation of the Diamond Mountains, Nevada (Steele, 1960; Robinson, 1961; Slade, 1961; Bissell, 1962; Stevens et al., 1979; Davydov et al., 1997; Stevens and Stone, 2009). Although *E. linearis* has an apparent Wolfcampian-Leonardian range, and therefore could be found in Artinskian strata, the species is generally considered indicative of Sakmarian deposits. In the upper informal member of the Riepe Spring Limestone at Spruce Mountain Ridge *E. linearis* occurs in the same interval as *Sweetognathus binodosus* and *Sweetognathus anceps* Chernykh, 2005, placing the *E. linearis* assemblage zone within the upper part of the Sakmarian. Other forms associated with the *E. linearis* assemblage zone include *Schwagerina glassensis* Ross and Ross, 2003, *Pseudoschwagerina robusta* (Meek, 1864), and *P.* cf. *convexa* Thompson, 1954. *Schwagerina glassensis* and *P. robusta* also occur together with *E. linearis* in sequence LH-2 of the Lenox Hills Formation (Ross and Ross, 2003), further reinforcing the strong correlation potential of the upper informal member of the Riepe Spring Limestone with classical "Lenoxian" (= upper Wolfcampian) strata. The presence of *P.* cf. *convexa*, which occurs one sequence higher than the *E. linearis* assemblage zone in the Glass and Hueco Mountains, is mildly perplexing, but a potential explanation for the Riepe Spring Limestone occurrence is provided under the *Systematic Paleontology* heading.

"Advanced" Schwagerina Assemblage Zone

The "advanced" *Schwagerina* assemblage zone succeeds the *E. linearis* assemblage zone as the uppermost fusulinid assemblage zone of the Riepe Spring Limestone, spanning from 307.2 m above the base of the section up to the Riepe Spring-Rib Hill contact at 415.2 m (Fig. 4.3). The Douglass-Henbest collection material contains several specimens of a highly advanced, potentially transitional morphotype of *E. linearis* from higher than 307.2 m, but the exact level of recovery is unknown, and the forms are therefore placed within the "advanced" *Schwagerina* assemblage zone. Unfortunately, many of the fusulinids occurring within this assemblage zone are poorly preserved and difficult to properly identify at the species level because of associations with intensely compacted crinoidal limestone and corrasive calcareous sandstone lithofacies. Although only two species of *Schwagerina* are fully described from the "advanced" *Schwagerina* assemblage zone (i.e., *Schwagerina franklinensis* Dunbar and Skinner, 1937 and *Schwagerina* sp. C), most of the damaged forms observed belong to the group of highly elongate *Schwagerina* that were transitional to the earliest forms of Leonardian age *Parafusulina*. Several examples of unnamed taxa from the Douglass-Henbest collection are illustrated but remain undescribed because only a few varied specimens were collected. "Advanced" morphotypes of *Schwagerina* are characterized by their intensely and steeply folded septa and incipient cuniculi in the outermost volutions (Jordan, 1971, unpublished dissertation). Previously described late Wolfcampian forms belonging to this

group include, but are not limited to, *S. menziesi* Williams, 1963, *S. jenkinsi* Thorsteinsson, 1960, *S. moffiti* Petocz, 1970, and *S. mankomenensis* Petocz, 1970. Other, potentially related forms are known from Artinskian deposits of the southern Urals (e.g., *Parafusulina*? *lutugini* (Schellwien, 1908)).

Schwagerina franklinensis is one of the more recognizable fusulinids from the "advanced" *Schwagerina* assemblage zone and occurs ~343 and ~347 m above the base of the NSMR section. Ross (1959) reported the occurrence of *S. franklinensis* from the uppermost part of the Lenox Hills Formation and the lower part of the Leonard Formation in the Glass Mountains. Two Nevadan specimens of *S. franklinensis* have been illustrated by Slade (1961) from a Wolfcampian-Leonardian boundary succession in the lower part of the Pequop Formation at Ferguson Mountain, Nevada. Slade (1961) considered both specimens Leonardian, but Stevens et al. (1979) reassigned the lower specimen of the two (recovered from Slade's unit 91) to the uppermost Wolfcampian (Slade, 1961, fig. 2). Williams (1966) noted that *S. franklinensis* is restricted to the upper Wolfcampian-lower Leonardian Alacran Mountain Formation (upper part of the Hueco Group) in the Hueco Mountains. Although it is apparent that *S. franklinensis* spans the Wolfcampian-Leonardian boundary elsewhere, the uppermost part of the Riepe Spring Limestone is dominated by the late Wolfcampian (Artinskian) conodont *Sweetognathus* aff. *whitei* (Rhodes, 1963) and no early Leonardian fusulinids (i.e., *S. crassitectoria* Dunbar and Skinner, 1937) nor conodonts were

recovered with *S. franklinensis*. Therefore, the uppermost part of the Riepe Spring Limestone at Spruce Mountain Ridge is considered to be uppermost Wolfcampian, with the Wolfcampian-Leonardian boundary in the overlying, unfossiliferous Rib Hill Formation. Additional fusulinids in association with the "advanced" *Schwagerina* assemblage zone include *Schwagerina* sp. C, *Alaskanella* sp. C, and Gen. n. A sp. A. More work concerning the latter two taxa should be completed before their correlation potential (if any) and taxonomic affinities are better understood.

Conclusions

The lower Missourian to upper Wolfcampian fusulinid succession of the Riepe Spring Limestone at Spruce Mountain Ridge, Elko County, Nevada includes representatives of cosmopolitan North American faunas in addition to several poorly understood genera previously unreported from Nevada. These uncommon forms include *Biwaella americana*, three new species of *Alaskanella*, and two new species of the McCloudian genus *Cuniculinella.* The Riepe Spring Limestone succession consists of six assemblage zones, including (stratigraphically lowest to highest): *Eowaeringella-Triticites* Group I assemblage zone (lower to lower-middle Missourian); *Triticites* Group II-*Dunbarinella* assemblage zone (lower to middle Virgilian); *Triticites* Group IV assemblage zone (upper Virgilian); *Schwagerina wellsensis* assemblage zone (upper Wolfcampian); *Eoparafusulina linearis* assemblage zone (upper

Wolfcampian); "advanced" *Schwagerina* assemblage zone (upper Wolfcampian). Erosional disconformities bound three of these assemblage zones.

Some inferred correlations can be made for the lower and middle members of the Riepe Spring Limestone at Spruce Mountain Ridge with equivalent Missourian and Virgilian deposits of California, southwest New Mexico, West Texas, north-central Texas, and Kansas. These include strata assigned to the Bird Spring Formation, Horquilla Formation, Gaptank Formation, and cyclic deposits of the Brazos River Valley and the North American Midcontinent region, respectively. The Upper Pennsylvanian strata of the Riepe Spring Limestone are disconformably overlain by upper Wolfcampian deposits similar in age to the upper part of the McCloud Limestone in California, the uppermost part of the Horquilla Formation, and the Lenox Hills, Cerro Alto, and Alacran Mountain Formations of the Glass and Hueco Mountains in West Texas.

Systematic Paleontology

Note: taxonomic assignments in open nomenclature under this subheading follow the recommended qualifiers and methods outlined by Bengston (1988). Systematics in the scheme of Rauser-Chernousova et al. (1996).

Superorder FUSULINOIDA Fursenko 1958; emend. Rauser-Chernousova et al. 1996

Order FUSULINIDA Fursenko 1958

Family FUSULINELLIDAE Staff and Wedekind 1910

Genus ***Eowaeringella*** Skinner and Wilde 1967

***Eowaeringella* sp. A**

Plate 1, figures 1–3

Description: A species of *Eowaeringella* with a small, faintly inflated fusiform test ranging in length from 3.84 to 4.57 mm (most values estimated from half length) with an average length of 4.27 mm among the six specimens measured. Test diameters range from 1.48 to 1.87 mm (some values estimated from half width). Mature specimens have seven to eight volutions. Form ratios among NSMR specimens show little variability, ranging from 2.41 to 2.59 and averaging 2.52. The axis of coiling is irregular and slightly curved, and the lateral slopes are slightly concave to asymmetrical and wavy. The proloculus is small and spherical with an average outside diameter of 0.112 mm. The test expands uniformly throughout growth and the heights of the first through seventh volutions average 0.036, 0.049, 0.077, 0.097, 0.125, 0.156, and 0.178 mm.

The thin, tripartite spirotheca is composed of a tectum, diaphanotheca, and lower tectorium. Wall thicknesses for the proloculus through the seventh volution average 0.011, 0.013, 0.019, 0.025, 0.026, 0.029, 0.036, and 0.035 mm. Septa are planar but occasionally show minor fluting near the poles. Chomata are well-developed, steep to overhanging on the tunnel side, and tapered poleward. The tunnel is extremely narrow and slightly askew to the equatorial plane. Measurements of this species are provided in Appendix A, Table 4.1.

Remarks: *Eowaeringella* sp. A is very similar to several previously illustrated forms of the genus from Texas, New Mexico, and the Canadian Arctic. Unfortunately, the most similar forms were likewise discussed in open nomenclature. The new specimens resemble *Eowaeringella* sp. A illustrated by Wilde (2006) from the Big Hatchets, but the NSMR forms are slightly larger. All other measured characters are very similar. NSMR forms of *Eowaeringella* sp. A also look quite similar to *Eowaeringella* sp. A and *Eowaeringella* sp. C described by Rui and Nassichuk (1994) from the Nansen Formation of northern Ellesmere Island in the Canadian Arctic, but the authors did not provide measurements of their specimens.

Although there is an undeniably close similarity among most forms of the genus, Riepe Spring Limestone specimens of *Eowaeringella* sp. A differ

slightly from most other previously described forms, primarily in their combination of test size, form ratio, and proloculus diameter.

Occurrence: 14.8 m above the base of the section (unit 1); level - lower part of the Missourian Stage (lower-middle part of the Kasimovian Stage).

***Eowaeringella* sp. B**

Plate 2, figures 1–6

Description: A species of *Eowaeringella* with a slender, elongate fusiform test that attains eight to nine volutions at maturity. Test lengths range from 5.13 to 6.00 mm (estimated from half length values), averaging 5.58 mm. Test diameters were difficult to determine accurately due to poor preservation resulting from pervasive swarms of microstylolites, but estimates from half widths of two specimens provide an average diameter of 1.85 mm. The form ratios, although only calculated from these two partial specimens, are estimated at 3.05 and 3.14. Diameters from the two additional measured specimens were not acquired. The axis of coiling is nearly straight in the innermost volutions but is curved and irregular in the outer volutions. The lateral slopes may be gently concave or highly irregular and strongly curved. The proloculus is small, spherical, and shows little variation in diameter, averaging 0.099 among the four measured specimens.

The spirotheca is extremely thin and is composed of a tectum, diaphanotheca, and lower tectorium. Wall thicknesses for the proloculus through the seventh volution average 0.012, 0.009, 0.015, 0.014, 0.019, 0.022, 0.026, and 0.029 mm. The septa may be planar or moderately fluted. Chomata are massive, ranging from tabular to steep and overhanging, often exceeding three-quarters the height of each volution. The tunnel is narrow and may be nearly straight to distinctly irregular in its path. Measurements of this species are provided in Appendix A, Table 4.2.

Remarks: The measurements of *Eowaeringella* sp. B, like *Eowaeringella* sp. A, do not strongly agree with any previously described species of the genus. *Eowaeringella* sp. B is larger and much more elongate than *Eowaeringella* sp. A. *Eowaeringella* sp. B closely resembles *Eowaeringella* sp. B of Rui and Nassichuk (1994), but it is impossible to make anything beyond a superficial comparison of the two without measurements of the latter.

Occurrence: 54.9 m above the base of the section (unit 12); level - lower to lower-middle part of the Missourian Stage (lower-middle to middle part of the Kasimovian Stage).

Genus ***Pseudofusulinella*** Thompson 1951

Pseudofusulinella* cf. *nitida Skinner and Wilde 1965b

Plate 4, figure 4

Pseudofusulinella nitida SKINNER and WILDE 1965b, p. 30-31, pl. 9, figs. 23-29.

Description: A species of *Pseudofusulinella* that is somewhat large for this genus, with an obese (extremely inflated) fusiform test that reaches eight volutions among the two specimens collected. The mature specimens measure 4.94 mm (estimated from half length) and 4.98 mm in length. The test diameters measure 2.49 (estimated from half width) and 2.28 mm respectively. Poles are narrow and sharply rounded. Lateral slopes are strongly concave, dipping steeply towards the polar regions from the highly inflated medial portion of the test. The proloculus is spherical and of moderate size, with outside diameters of the Riepe Spring Limestone specimens measuring 0.121 and 0.116 mm respectively.

The spirotheca is composed of a thin tectum, dense upper and lower tectoria, and a colorless diaphanotheca. Septa are strongly and tightly fluted throughout the length of the test. The chomata are very large, often nearly connecting the top and bottom of volutions. Chomata vary from massive and nearly tabular to broadly overhanging with outer margins that taper at a low angle toward the poles. Secondary deposits often connect the high, dense

chomata with the spirotheca of the following volutions. The tunnel is straight, narrow, and very well-defined.

Remarks: *Pseudofusulinella* cf. *nitida* is one of the more equatorially inflated ("obese") forms of this long-ranging genus. The specimens collected from Nevada closely resemble the type specimens of Skinner and Wilde (1965b) from the Upper Pennsylvanian part of the McCloud Limestone in northern California. The uncertainty in the present assignment is a result of sparse material, as only two well-oriented specimens were recovered from the Riepe Spring Limestone. Fortunately, the preservation of both specimens is good enough for accurate measurements. The primary differences between the type specimens and the two NSMR specimens are the straighter tunnel, slightly greater size (in both length and width), and larger proloculus of the latter.

Occurrence: 178 m above the base of the section (unit 45); level - upper part of the Virgilian Stage (upper part of the Gzhelian Stage).

Pseudofusulinella sp. A

Plate 3, figure 5

Description: A small to moderately sized and delicately constructed species of *Pseudofusulinella* with an elongate, faintly obese fusiform test of seven to eight volutions. Test lengths of mature specimens range from 3.84 to 4.81 mm, averaging 4.44 mm. Diameters range from 1.38 to 1.98 mm (the latter value estimated from half width), averaging 1.65 mm. The average form ratio from five measured specimens is 2.74. The axis of coiling is straight to gently curved, with maximum irregularity occurring near the polar regions. Poles are sharply to bluntly pointed. Lateral slopes are concave adjacent to the margins of the tunnel but straighten poleward. Axial filling is light, but dense secondary deposits are present on nearly all septa when observed in an equatorial view. The proloculus is spherical and small to moderate in size, with an average outside diameter of 0.103 mm.

The spirotheca is very thin, only gradually thickening throughout growth, and does not show much variance in thickness beyond the fourth or fifth volution. The spirotheca is composed of a tectum, very thin upper and lower tectoria, and a pronounced diaphanotheca. Septal fluting is weak and nearly planar in the innermost volutions but intensifies beyond the fourth volution. Fluting is restricted to the axial portion of the test. Chomata are remarkably symmetrical in most pairs and quite large, often nearly reaching the succeeding volution. Secondary deposits may bridge the space between chomata and the overlying spirotheca. Chomata vary from tabular, to mushroom-shaped, to steeply overhanging within individual specimens. The

tunnel is narrow, very well-defined, and shows little variability among the measured specimens. Measurements of this species are provided in Appendix A, Table 4.3.

Remarks: *Pseudofusulinella* sp. A bears a strong resemblance to the forms Slade (1961) described as *P. utahensis* Thompson, 1954 from the supposed Missourian-Virgilian boundary interval at Ferguson Mountain, Nevada. The stratigraphic level of the Ferguson Mountain forms is in general agreement with that of *Pseudofusulinella* sp. A and the forms have nearly identical measurements. The only exception is a slightly larger average proloculus size among the NSMR forms. Slade's assignment is problematic though, as Thompson (1954) and Thompson et al. (1958) considered *P. utahensis* a Wolfcampian form in the Wasatch Mountains and the Sublett Range. Closer inspection of photomicrographs and measurements of the type specimens of *P. utahensis* reveals that the test is slightly more obese than the early Virgilian forms from Ferguson Mountain and Spruce Mountain Ridge. The diachroneity and subtle differences in morphology suggest that Slade's Ferguson Mountain forms do not belong to *P. utahensis*, but instead may be conspecific with the herein reported *Pseudofusulinella* sp. A.

Occurrence: 70 m above the base of the section (unit 16); level- lower part of the Virgilian Stage (lowest part of the Gzhelian Stage).

***Pseudofusulinella* sp. B**

Plate 5, figures 1, 2

Description: A very small species of *Pseudofusulinella* with a short, inflated fusiform test that has seven to nine volutions at maturity. Test lengths range from 2.69 to 3.57 mm, averaging 3.03 mm. Diameters range from 1.51 to 1.85 mm, averaging 1.65 mm and producing an average form ratio of 1.84. Poor preservation of the tests has prevented accurate description of the polar regions; however, observation of the fifth or sixth volutions of the measured specimens shows that the poles become more sharply pointed with growth. The lateral slopes are concave (typical of the genus) and the axis of coiling is somewhat irregular. The proloculus is small and spherical, averaging 0.096 mm in outside diameter.

The thin spirotheca is composed of a tectum, upper and lower tectoria, and diaphanotheca. Septa are moderately fluted throughout, but several specimens demonstrate nearly planar septa in the outer volutions. The chomata are large and irregular in axial profile, varying between mound-like, tabular, and overhanging. Sparse secondary deposits are present on the peaks and outer slopes of chomata. The tunnel is well-defined and nearly straight in early volutions but becomes irregular in outer volutions, sometimes alternating in a side-to-side manner from one volution to the next.

Remarks: Unfortunately, the specimens of *Pseudofusulinella* sp. B described herein are few in number and poorly preserved. The orientation of specimens in both the recent collections and Douglass-Henbest material is less than ideal for confident and proper identification. Although the illustrated specimens bear some resemblance to Late Pennsylvanian forms described from the McCloud Limestone (see Skinner and Wilde, 1965b) and the specimens of *Pseudofusulinella occidentalis* (Thompson and Wheeler, 1946) illustrated by Slade (1961) from Ferguson Mountain, the author is hesitant to assign a species designation to only a handful of heavily corraded individuals.

Occurrence: 215.8 m above the base of the section (unit 45); level - upper part of the Virgilian Stage (upper part of the Gzhelian Stage).

Order SCHUBERTELLIDA Skinner 1931

Family SCHUBERTELLIDAE Skinner 1931

Genus ***Schubertella*** Staff and Wedekind 1910

Schubertella ciscoensis Kauffman and Roth 1966

Plate 3, figures 11–13

Schubertella ciscoensis KAUFFMAN and ROTH 1966, p. 6-7, 9, pl. 1, figs. 5-14; WILDE 2006, p. 54, pl. 51, figs. 15-24, pl. 109, figs. 1-8, pl. 110, figs. 1, 2.

Description: A minute species with an elongate fusiform test that has four volutions at maturity. Test lengths among NSMR specimens range from 0.59 to 1.26 mm, averaging 0.97 mm. Diameters range from 0.29 to 0.47 mm, averaging 0.38 mm and producing an average form ratio of 2.52, although this character seems to be highly variable among species of *Schubertella*. Poles are sharply rounded and lateral slopes are gently convex. The proloculus is exceptionally small, averaging 0.033 mm in outside diameter. The first volution is coiled at a right angle to the fusiform axis of coiling in the outer volutions (i.e., endothyroid juvenarium).

The spirotheca is nondescript and is composed of a very thin tectum with a fine, lighter colored lower tectorium beneath. There is no septal fluting and the septa are nearly planar, only dipping very slightly throughout the length of the test. Chomata are absent in the innermost volutions, but are well-defined hemispherical mounds in outer volutions. Measurements of this species are provided in Appendix A, Table 4.4.

Remarks: The diminutive, Virgilian age *Schubertella ciscoensis* and its Wolfcampian descendant, *S. kingi* Dunbar and Skinner, 1937, are often difficult to distinguish from one another. Wilde (2006) noted that *S. ciscoensis*

typically has a smaller proloculus, more pointed poles, and a wider tunnel. However, he also observed that there is often significant overlap between the two species when regarding these differences and suggested that the use of associated *Triticites* or *Schwagerina* assemblages is the most straightforward approach to correct identification. The recovered Riepe Spring Limestone specimens of *S. ciscoensis* were obtained from an interval that also produced critical early to middle Virgilian (early Gzhelian) marker species, such as *T. cullomensis* and *T. bensonensis*.

Occurrence: 149.2 and 150.4 m above the base of the section (unit 30); level - middle part of the Virgilian Stage (lower to middle part of the Gzhelian Stage).

Order SCHWAGERINIDA Solovieva in Epshteyn et al. 1985

Family PSEUDOFUSULINIDAE Dutkevich 1934; emend. Miklukho-Maclay 1959

Genus **Genus n. A**

Genus n. A sp. A

Plate 14, figures 1–4

Description: A curious species with an elongate fusiform test of moderate size that attains seven to eight volutions at maturity. Test lengths range from 5.73 to 7.17 mm, averaging 6.45 mm. Test diameters range from 2.16 to 2.65 mm, averaging 2.44 mm. The average form ratio among NSMR specimens is 2.65. Form ratio steadily increases throughout growth as the polar regions greatly elongate in the outer volutions. Test expands evenly throughout growth. The axis of coiling is straight to very slightly curved and the lateral slopes are nearly straight to gently concave. Poles are bluntly to somewhat sharply pointed. Axial filling is light, but dense secondary deposits are present along the chomata. Heights of the first through seventh volutions average 0.037, 0.058, 0.080, 0.143, 0.189, 0.236, and 0.247 mm. The proloculus is spherical to subspherical and of moderate size, averaging 0.171 mm in outside diameter.

The spirotheca is weakly keriothecal and thin. Wall thicknesses from the proloculus through the seventh volution average 0.018, 0.015, 0.021, 0.034, 0.046, 0.053, and 0.063 mm. Septal fluting is strong throughout the test and appears similar to the style observed in species of *Leptotriticites*. Chomata are massive and vary from tabular to slightly overhanging and are pronounced even in the outermost volutions. Measurements of this species are provided in Appendix A, Table 4.5.

Remarks: The new monotypic genus bears a strong resemblance to late Virgilian and early Wolfcampian forms of the genera *Triticites* and *Leptotriticites*. In fact, R.C. Douglass preliminarily, and with apparent reservation, referred to the forms as "*Triticites*?" in notations on the margins of thin sections from the Smithsonian's Douglass-Henbest collection. The specimens are moderately well-preserved, show no obvious evidence of reworking, and co-occur with *Alaskanella* sp. C in an interval that is dominated by "advanced," elongate forms of *Schwagerina* and the Artinskian (late Wolfcampian) conodont *Sweetognathus* aff. *whitei*.

The new forms are considerably younger than the youngest species of *Triticites* and must represent an extraordinary case of homeomorphy. Similarities in test morphology, particularly the strength of the chomata and the finely keriothecal nature of the spirotheca, suggest that Gen. n. A sp. A is closely related to the new forms of *Alaskanella* discussed below. To the author's knowledge, there are no previous reports of Gen. n. A and the new taxon is apparently endemic.

Occurrence: ~343 m above the base of the section (unit 64); level - upper part of the Wolfcampian Stage (lower part of the Artinskian Stage).

Genus ***Alaskanella*** Skinner and Wilde 1966

Alaskanella sp. A

Plate 8, figures 1–4

Description: A distinct species with an elongate subcylindrical to slightly elliptical test that attains seven to eight volutions at maturity. Test lengths (several estimated from half length) of mature specimens range from 5.03 to 8.79 mm, averaging an estimated 6.08 mm. The test diameters of *Alaskanella* sp. A were difficult to obtain because of poor preservation, but several measured widths range from 1.10 to 2.21 mm. The average form ratio of 3.23 is also an estimated value calculated from three of the seven measured specimens. The earliest volutions have a much lower form ratio and are ovate to globular in shape. Outer volutions are more loosely coiled than those of the interior. The axis of coiling may be straight to slightly curved and the lateral slopes vary accordingly. Poles are bluntly rounded. Secondary deposits are light along the axis of coiling, but dense secondary filling is present on the chomata of all measured specimens. Heights of the first through sixth volution average 0.051, 0.071, 0.09, 0.129, 0.141, and 0.177 mm. The proloculus is spherical to subspherical and highly variable in size, with outside diameters among the seven measured specimens ranging from 0.149 to 0.260 mm and averaging 0.186 mm.

The spirotheca is thin and is composed of a thin, dark tectum and very fine keriotheca. Wall thicknesses from the proloculus through the sixth

volution average 0.02, 0.018, 0.022, 0.03, 0.04, 0.056, and 0.069 mm. Septal fluting is confined to the axis of coiling where it is only moderate in intensity. Tangential sections demonstrate that the septa are primarily planar and that cuniculi are lacking. Very sparse septal pores appear to be present throughout the axial filling. The chomata are low but distinct and uniform, tapering towards the polar regions. Measurements of this species are provided in Appendix A, Table 4.6.

Remarks: These forms are assigned herein to the genus *Alaskanella* based on the strongly subcylindrical to elliptical test, well-developed chomata, and lack of cuniculi. *Alaskanella* has been regarded by some authors as a junior synonym of *Eoparafusulina* (Ross, 1967; Ross and Ross, 2003; Rauser-Chernousova et al., 1996; Ueno, 2006), but the latter exhibits cuniculi in the outer volutions and typically has weak chomata (if any) and pseudochomata. Although *Alaskanella* sp. A is the first representative of the genus from Nevada to be recognized as such, it may not be the first illustrated. Based on the fusulinid zonation of Stevens et al. (1979), it appears that previously reported forms regarded as "*Triticites* n. sp. a" and "*Triticites* n. sp. b" may belong to *Alaskanella*. Both forms in question occur within the upper Wolfcampian *Eoparafusulina linearis* Zone of Stevens et al. (1979). Although *Triticites* is known to occur in Wolfcampian rocks, the level of *E. linearis* is notably higher than the last occurrence of the last Pennsylvanian holdover

forms of *Triticites* or *Leptotriticites*. Additionally, Wolfcampian *Triticites* are fusiform and highly ventricose, whereas the described forms are subcylindrical.

Occurrence: 272.3 m above the base of the section (unit 60); level - upper part of the Wolfcampian Stage (middle to upper part of the Sakmarian Stage).

***Alaskanella* sp. B**

Pl. 10, figure 3

Description: A small and compact species with a short, subcylindrical test of five and one-half volutions. Unfortunately, only one specimen of *Alaskanella* sp. B was recovered from the upper informal member of the Riepe Spring Limestone. The lone specimen measures 3.47 mm in length and 1.15 mm in diameter with a form ratio of 3.02. The axis of coiling is straight and the lateral slopes are uniform and gently convex. Poles are bluntly rounded. Axial fillings are dense for such a small form and nearly fill the polar regions of the test. The test expands uniformly throughout growth and heights of the first through fifth full volutions measure 0.056, 0.070, 0.091, 0.152, and 0.176 mm. The proloculus is slightly subspherical and quite large compared to the small size of the test. Outside diameter measures 0.134 mm.

The spirotheca transitions from consistently thin in the inner three volutions to markedly thicker and coarsely keriothecal in the outer three volutions. Wall thicknesses from the proloculus through the outermost volution measure 0.012, 0.012, 0.012, 0.018, 0.035, 0.042, and 0.063 mm. Septal fluting is mild in the inner two volutions but increases in intensity throughout the outer portion of the test. Thick septal folds are present throughout the test and reach at least half the height of the associated volution. No septal pores are observed. Chomata are low, broad, and tapered towards the poles. Secondary deposits partially obscure several chomata.

Remarks: *Alaskanella* sp. B bears a resemblance to the form regarded as *Triticites* sp. B by Stevens et al. (1979), but because the article strictly discussed biozonation rather than taxonomy, no information was provided by the authors beyond a small photomicrograph. The lack of a full description makes it difficult to adequately compare the forms beyond noting their small size and general similarity in test morphology.

Occurrence: ~295 m above the base of the section (unit 61); level – upper part of the Wolfcampian Stage (upper part of the Sakmarian Stage).

***Alaskanella* sp. C**

Plate 15, figures 3–6

Description: A beautiful, "pill-shaped" fusulinid of moderate size with a robust subcylindrical test of seven to nine volutions. Mature specimens range in length from 8.05 to 10.67 mm, averaging 9.33 mm. Test diameters range from 2.18 to 2.79 mm, averaging 2.52 mm. The average form ratio of mature Riepe Spring Limestone specimens is 3.71. The test is tightly coiled and the axis is straight. Lateral slopes are straight to gently convex and the poles are bluntly rounded. In axial sections the middle portion of the test may be slightly depressed with respect to the height of the lateral slopes. Axial deposits of *Alaskanella* sp. C are slightly more pronounced than those of *Alaskanella* sp. A. The axial filling is perforated throughout by small septal pores. Dense secondary deposits are also present around the tunnel of most specimens, occasionally connecting opposing chomata across the top of a volution and creating an arch bridging the tunnel. The test expands very gradually and evenly throughout growth. The characteristic shape of the test begins to develop in the second volution following a globular first volution. Heights of the first through eighth volution average 0.043, 0.062, 0.079, 0.110, 0.160, 0.204, 0.262, and 0.275 mm. Like the previously described *Alaskanella* sp. A, the proloculus is spherical to subspherical and highly variable in size, ranging from 0.116 to 0.211 mm in outside diameter and averaging 0.157 mm.

The spirotheca is extremely thin and is composed of a thin, dark tectum and very fine keriotheca. Wall thicknesses from the proloculus through the eighth volution average 0.014, 0.014, 0.017, 0.021, 0.034, 0.044, 0.052, 0.062, and 0.059 mm. Septal fluting is moderate in intensity and occurs primarily along the axis of coiling, although small septal loops may be present adjacent to the tunnel in outer volutions. Fluting typically occurs along the lower part of individual septa, whereas the upper portion of the septum is plane. Sparse and irregular phrenothecae may be present in the outer volutions. Chomata are steep along the edge of the tunnel but taper towards the poles. Measurements of this species are provided in Appendix A, Table 4.7.

Remarks: *Alaskanella* sp. C occurs considerably higher in the section than *Alaskanella* sp. A (~74 m). Although there is a significant lithostratigraphic gap between the two forms, it is reasonable to conclude that the species are closely related. *Alaskanella* sp. A and *Alaskanella* sp. C share a similar test morphology but differ markedly in their finer details. *Alaskanella* sp. C is larger than *Alaskanella* sp. A and has a higher form ratio than the latter as well. Although it is larger, the spirotheca of *Alaskanella* sp. C tends to be thinner than that of *Alaskanella* sp. A. The septal pores and axial filling are more strongly pronounced in *Alaskanella* sp. C.

Alaskanella sp. C vaguely resembles the slightly older *Eoparafusulina linearis*, but the former has a lower form ratio, stronger chomata, and lacks cuniculi. Although the test morphology of *Alaskanella* sp. C is similar to *A. laudoni* Skinner and Wilde, 1966, the former has a much lower form ratio, stronger chomata, and fewer septal loops in its outer volutions. *Alaskanella* sp. C differs from *A. yukonensis* Skinner and Wilde, 1966 in its much greater size and lower form ratio.

Occurrence: 346.4 m above the base of the section (unit 64); level - upper part of the Wolfcampian Stage (lower part of the Artinskian Stage).

Genus ***Cuniculinella*** Skinner and Wilde 1965b

***Cuniculinella* sp. A** Skinner and Wilde 1965b

Plate 6, figures 4–6

Description: A robust species with an inflated fusiform test that attains six to seven volutions at maturity. Test lengths of mature specimens range from 8.30 to 11.06 mm (estimated from half length), averaging 9.31 mm. Test diameters range from 3.18 to 4.11 mm, averaging 3.76 mm. The average form ratio of mature specimens is 2.48. The axis of coiling is straight and is marked by a narrow, dense band of axial fillings. Lateral slopes are variable

but are typically gently convex. Poles are bluntly pointed. The innermost volutions are globular to elliptical and begin to take on the inflated fusiform shape of mature specimens by the third volution. Heights of the first through sixth volution average 0.097, 0.159, 0.233, 0.310, 0.350, and 0.417 mm. The proloculus is large and spherical to subspherical and slightly irregular. The outside diameters of proloculi among Riepe Spring Limestone specimens average 0.314 mm.

The spirotheca is thick and very coarsely alveolar. Wall thicknesses from the proloculus through the six volution average 0.024, 0.029, 0.048, 0.062, 0.090, 0.107, and 0.112 mm. Septal folding is intense and regular throughout the entire test. Septal folds are high, often reaching the top of the associated volution, and have steep sides with occasional flat tops similar to the septal folds observed in species of *Skinnerella*. Cuniculi are present in the outer volutions (Pl. 6, Fig. 4). Minute chomata are only present on the proloculus. Measurements of this species are provided in Appendix A, Table 4.8.

Remarks: *Cuniculinella* sp. A resembles several forms of the genus described by Skinner and Wilde (1965b) from the McCloud Limestone of northern California. *Cuniculinella* sp. A differs from *C. fusiformis* Skinner and Wilde, 1965b in its lower form ratio, slightly larger proloculus, and the presence of chomata on the proloculus. *C. calx* (Thompson and Wheeler, 1946) has a

slightly lower form ratio and thicker spirotheca. *C. munda* Skinner and Wilde, 1965b is smaller, has a smaller form ratio, and has more intensely fluted septa. *C. mira* Skinner and Wilde, 1965b has more sharply pointed poles, a slightly higher form ratio, and a larger average proloculus diameter. *C. rotunda* Skinner and Wilde, 1965b has a lower form ratio, thicker spirotheca, and a much larger proloculus.

Occurrence: 227.8 m above the base of the section (unit 48); level - middle to upper part of the Wolfcampian Stage (uppermost part of the Asselian(?) to lower part of the Sakmarian Stage).

***Cuniculinella*? sp. B**

Plate 7, figures 1, 2

Description: A large species with a slightly inflated, subcylindrical test that attains a length (estimated from half length in some cases) of 9.61 to 11.08 mm, averaging 10.29 mm. Test diameters range from 3.24 to 4.15 mm, averaging 3.67 mm, with an average form ratio of 2.81. The axis of coiling is straight and is strongly defined by the presence of very dense, lateral axial fillings that tend to thicken poleward. Lateral slopes are nearly straight to gently convex and the poles are broadly rounded. Heights of the first through sixth volution average 0.094, 0.159, 0.223, 0.308, 0.299, and 0.347 mm. The

proloculus is large and spherical, averaging 0.331 mm among the four measured specimens from the NSMR section.

The spirotheca is thick and coarsely alveolar. Wall thicknesses from the proloculus through the six volution average 0.026, 0.029, 0.051, 0.070, 0.090, 0.107, and 0.114 mm. The septa are numerous and strongly fluted throughout the length of the test and the septal folds are very high and narrow. Minute chomata are only present on the proloculus. Measurements of this species are provided in Appendix A, Table 4.9.

Remarks: The specimens in question bear a strong resemblance to the Leonardian *Schwagerina retusa* Knight, 1956 described from Moorman Ranch, Nevada. The forms regarded as *Cuniculinella* sp. A are much common than *Cuniculinella*? sp. B in unit 48 and only one axial specimen of the latter was recovered from the author's material (accompanied by four Smithsonian specimens), so critical tangential sections indicating the presence of outer cuniculi could not be observed. The generic assignment is made with reservation and is based on the overall similarity with *Cuniculinella* sp. A, in which the presence of cuniculi is confirmed.

Occurrence: 227.8 m above the base of the section (unit 48); level – middle to upper part of the Wolfcampian Stage (uppermost part of the Asselian(?) to lower part of the Sakmarian Stage).

Genus ***Dunbarinella*** Thompson 1942

Dunbarinella kauffmani Wilde 2006

Plate 3, figures 8–10

Dunbarinella sp. A ROSS and TYRRELL 1965, p. 628, pl. 77, figs. 24, 25.

Dunbarinella kauffmani WILDE 2006, p. 56, pl. 52, figs. 9-21.

Description: A species of *Dunbarinella* with a small, slightly inflated fusiform test that is subtly triangular in its axial profile. Riepe Spring Limestone specimens have six to seven (rarely eight) volutions and attain lengths ranging from 2.80 to 4.24 mm, averaging 3.32 mm. Test diameters range from 1.22 to 1.69 mm, averaging 1.41 mm with a form ratio of 2.33. The averages acquired for each of these characters are lower than the values provided in the descriptions of Wilde (2006), but this discrepancy is attributed to the inclusion of several potentially immature specimens of five and one-half or six volutions. Inner volutions are very tightly coiled. The axis of coiling is straight, and the lateral slopes are nearly straight to gently convex. Poles are bluntly to sharply pointed. The proloculus is small and spherical, averaging an outside diameter of 0.08 mm.

Spirotheca are thin and exhibit moderately developed keriotheca. Septal fluting is intense throughout much of the test. Dense secondary deposits are present along the axis, obscuring some septal folds. Small chomata are present in most volutions, but the tunnel is narrow and poorly-defined due to the dense axial filling. Measurements of this species are provided in Appendix A, Table 4.10.

Remarks: The NSMR specimens strongly resemble the types from Wilde's collections from New Well Peak and are only slightly more triangular. The two specimens of *Dunbarinella* sp. A illustrated by Ross and Tyrrell (1965) from the lower part of the Earp Formation are also extremely similar to *D. kauffmani*. The only difference between the two forms appears to be the slightly smaller proloculus of the former; therefore, it seems likely that Ross and Tyrrell's (1975) specimens belong to the same species as those of the present study and the Arizona specimens are synonymized herein. *Dunbarinella kauffmani* resembles *D. skinneri* Kauffman and Roth, 1966, but the former is less inflated, has fewer volutions, and has a narrower region of axial filling.

Occurrence: ~147 and 149.2 m above the base of the section (units 28, 30); level - middle part of the Virgilian Stage (lower to middle part of the Gzhelian Stage).

Genus ***Eoparafusulina*** Coogan 1960; emend. Skinner and Wilde 1965b

Eoparafusulina linearis (Dunbar and Skinner 1937)

Plate 11, figures 1–3

Schwagerina linearis DUNBAR and SKINNER 1937, p. 637, pl. 62, 12-15, pl. 63, figs. 1-7;

Parafusulina sp. THOMPSON and HAZZARD 1946, p. 50, pl. 13, fig. 11.

Parafusulina linearis (Dunbar and Skinner 1937). SLADE 1961, p. 89, pl. 15, fig. 1, pl. 16, 4-7.

Monodiexodina bispatulata WILLIAMS 1963, p. 33-35, pl. 1, figs. 1-5.

Monodiexodina linearis (Dunbar and Skinner 1937). ROSS 1962, p. 6-7, pl. 2, figs. 11-13; ROSS 1963, p. 160, pl. 14, figs. 1-7; PÉREZ RAMOS 1992, p. 28-29, pl. 6, figs. 1-4.

Eoparafusulina linearis (Dunbar and Skinner 1937). STEVENS and STONE 2007, p.42, pl.8, figs. 2, 3; STEVENS et al. 2014, figs. 6.2-6.5.

Description: A widespread and fairly long-ranging early Permian species with an extremely narrow, highly elongate subcylindrical test. Mature specimens attain a length of 11.14 to 14.11 mm, averaging 12.52 mm among the seven Riepe Spring Limestone specimens measured. Test diameters of measured

specimens range from 1.94 to 2.53 mm, averaging 2.27 mm. Mature tests of seven to eight volutions have an average form ratio of 5.61. The form ratio increases markedly and uniformly throughout the lifespan of *E. linearis*, with typical specimens having a much smaller form ratio between 2.5 and 3.0 in the first one to two volutions. The axis of coiling is often straight or nearly so, but occasional specimens may display a long axis which curves gently, gradually increasing in obliquity with growth of the test. Poles are broadly rounded and occasionally irregular in axial profile. Tests of *E. linearis* are often fractured along the mid-plane and through the proloculus, producing a minor offset of the two halves of the test and making accurate measurement of the proloculus difficult. The proloculus of the most intact measured specimen is somewhat small, with an outside diameter of 0.175 mm.

The spirotheca is moderately thick and finely keriothecal for a test of such size. The septa are tightly and regularly fluted along the base, producing low, small, dome-like septal loops throughout the test. Dense axial fillings are present across nearly the full length of the test and may be variable or irregular in their distribution (see *Remarks*). Small chomata are only present in the inner volutions, whereas pseudochomata (filled septal loops) may be present in outer volutions. Measurements of this species are provided in Appendix A, Table 4.11.

Remarks: *Eoparafusulina linearis* is a widespread North American fusulinid species that is known for its long and somewhat convoluted taxonomic history. The original assignment to *Schwagerina* was emended due to the presence of weakly-developed cuniculi in the outermost volutions. As a result, *E. linearis* was briefly regarded as a form of *Parafusulina*, but Coogan (1960) restricted the concept of *Parafusulina* to include only advanced, elongate forms with well-developed cuniculi present even in the early (inner) volutions, thus excluding *E. linearis* from *Parafusulina*.

Several authors (e.g., Ross, 1963; Williams, 1963; Yang and Yancey, 2000) have erroneously assigned *E. linearis* to the genus *Monodiexodina*, but helpful distinctions and clarification on this matter were provided by Stevens (1979) and Ueno (2006). *Monodiexodina*, according to Ueno (2006), is a distinctly Eurasian (i.e., Paleo-Tethyan) taxon with a questionable association to the North American forms of *Eoparafusulina*. Additionally, *M. bispatulata* (Williams, 1963), which undoubtedly belongs to *Eoparafusulina* as well, is herein considered to be a junior synonym of *E. linearis*.

Occurrence: ~281, ~293, 304.4 and 307.2 m above the base of the section (units 60, 61); level - upper part of the Wolfcampian Stage (upper part of the Sakmarian Stage).

Genus ***Pseudofusulina*** Dunbar and Skinner 1931; emend. Skinner and Wilde 1965a

Pseudofusulina mediotenebraeus Wilde 2006

Plate 6, figures 1–3

Pseudofusulina mediotenebraeus WILDE 2006, p. 70, pl. 78, figs. 1-7, 13, 14.

Description: A species of *Pseudofusulina* that is smaller than typical forms of the genus, with an evenly, somewhat elongate fusiform test. Mature tests of six to eight (most often seven) volutions attain lengths of 5.59 to 6.44 mm, averaging 6.09 mm. Diameters show less variation and range from 2.53 to 2.82 mm, averaging 2.67 mm and producing an average form ratio of 2.29. The axis of coiling is straight. Poles are bluntly rounded and the lateral slopes are nearly straight to very gently convex. The proloculus is small and shows little variation among the five specimens measured, averaging 0.119 mm in outside diameter.

The spirotheca shows the rugosity characteristic of the genus and is composed of a tectum and keriotheca with poorly developed alveoli. Septa are somewhat irregularly fluted across the test, producing broad, rounded septal loops of medial height. Sparse yet dense axial filings are present in the inner volutions. Chomata are present in the inner four to five volutions and border

a tunnel of moderate width. Equatorial sections demonstrate the presence of deep axial furrows along the test (Pl. 6, Fig. 2). Measurements of this species are provided in Appendix A, Table 4.12.

Remarks: The axial fillings surrounding the proloculus of *Pseudofusulina mediotenebraeus* are unique among other forms of the genus. The distinct secondary deposits paired with the smaller test size make identification of this form rather straightforward, although it has never been reported from Nevada. The only discernible difference between the Nevada specimens and those from Wilde's New Mexico collections is the slightly broader test (greater diameter) among the present specimens, producing a slightly lower average form ratio.

Occurrence: 215.8 m above the base of the section (unit 45); level - upper part of the Virgilian Stage (upper part of the Gzhelian Stage).

Family SCHWAGERINIDAE Dunbar and Henbest 1930

Genus ***Pseudoschwagerina*** Dunbar and Skinner 1936

Pseudoschwagerina* cf. *convexa Thompson 1954

Plate 12, figures 4, 5

Pseudoschwagerina convexa THOMPSON 1954, p.75, pl. 44, figs. 1-4, pl. 51, figs. 1-8; SLADE 1961, p. 76-77, pl. 12, figs. 7, 8; ROSS 1963, p. 147, pl. 28, figs. 2, 3; WILLIAMS 1963, p. 38-40, pl. 4, figs. 1-4; WILDE 2006, p. 83, pl. 93, figs. 1-5, pl. 97, figs. 6-11.

Stewartina convexa (Thompson 1954) MAGGINETTI et al. 1988, p. 21, pl. 4, figs. 3, 4; STEVENS and STONE 2007, p. 39, pl. 7, fig. 2.

Description: A species of *Pseudoschwagerina* with a large, highly inflated fusiform test that has six to seven volutions at maturity. Unfortunately, due to the extreme inflation of the test, Riepe Spring Limestone specimens belonging to *Pseudoschwagerina* are often crushed, making accurate measurements difficult or impossible. The Riepe Spring Limestone material has produced one nearly complete specimen, two poorly preserved specimens, and one obliterated and questionable specimen of *P.* cf. *convexa*. The most complete specimen of the present collection (Pl. 12, Fig. 5) closely resembles the holotype specimen illustrated by Thompson (1954) from the Hueco Mountains. The half length of the nearly complete specimen measures 3.50 mm at the sixth volution (of seven overall), and the test diameter is 4.27 mm. The axis of coiling is nearly straight or slightly irregular and the poles are broadly rounded. The juvenarium has well-developed tabular chomata, strongly fluted septa, and somewhat resembles a small, ventricose *Triticites*. Shell expands uniformly following the tightly coiled juvenarium. The

proloculus is very large and spherical, averaging 0.416 mm in outside diameter among NSMR specimens.

The spirotheca is thick for a *Pseudoschwagerina* and is coarsely alveolar. The spirotheca of the proloculus through seventh volution of the best-preserved specimen in the collections measures 0.025, 0.016, 0.033, 0.055, 0.076, 0.103, 0.115, and 0.153 mm in thickness. Septa are thick and strongly fluted in the polar regions. Broad, rounded septal loops are present throughout the equatorial region. Secondary axial fillings are not present. Chomata are often completely absent in the outermost volutions.

Remarks: *Pseudoschwagerina convexa* is easily distinguished from other forms of the genus by its sturdier, more elongate test and the presence of massive chomata in the inner volutions. These distinctions have led several authors to follow the suggestion of Wilde (1971) and regard the forms as *Stewartina convexa*. However, based on comparisons of *P. convexa* with other forms of *Pseudoschwagerina* and the broad concept of *Stewartina* provided by Wilde (including species of *Pseudoschwagerina*, *Schwagerina*, and *Pseudofusulina*), the authors do not see a need for amendment of the original description.

The Riepe Spring Limestone occurrence of this form is somewhat conspicuous as it appears to be somewhat lower than expected within the given faunal succession, occurring within the *Eoparafusulina linearis*

assemblage zone. The types of *Pseudoschwagerina convexa* were found in the upper Wolfcampian Alacran Mountain Formation and the species is characteristic of the LH-3 sequence (upper part of the Lenox Hills Formation) of Ross and Ross (2003). Stevens et al. (1979) assigned the *P. convexa* Zone of northeast Nevada and northwest Utah a position as the penultimate fusulinid zone of the Wolfcampian, followed by the questionable *Schwagerina aculeata*? Zone. Wilde (2006), however, described the occurrence of *P. convexa* from both the basal part of the "Lenoxian" at his Borrego section and the upper part of the "Lenoxian" at his Bugle Ridge section. It seems justifiable that *P. convexa* may range through much of the upper part of the Wolfcampian, but, based on the paucity of recovered specimens and the sub-par preservation, the assignment is made with some reservation.

Occurrence: 286.9 m above the base of the section (unit 60); level – upper part of the Wolfcampian (upper part of the Sakmarian).

Pseudoschwagerina robusta (Meek 1864)

Plate 10, figures 1, 2, 4

Fusulina robusta MEEK 1864, p. 3-4, pl. 2, fig. 3, 3a-c.

Schwagerina robusta (Meek) BEEDE and KNIKER 1924, p. 17-19, pl. 4, figs. 1-5, pl. 8, fig. 2.

Pseudoschwagerina uddeni (Beede and Kniker) DUNBAR and SKINNER 1936, p. 89, pl. 11, figs. 6-7.

Pseudoschwagerina robusta (Meek). THOMPSON and WHEELER 1946, p. 28, pl. 3, figs. 1-3, pl. 6, figs. 6-7; ROSS 1963, p. 149-150, pl. 24, figs. 1-3, pl. 25, fig. 3; SKINNER and WILDE 1965b, p. 71-72, pl. 32, fig. 14, pl. 33, figs. 1-6.

Description: A species with a large, globular to subglobular test that attains a length of 7.01 to 9.55 mm, averaging 8.40 mm in mature specimens of five to six volutions. Test diameter ranges from 4.58 to 5.98 mm with an average of 5.06 mm, with an average form ratio of 1.69. The juvenaria of specimens belonging to *Pseudoschwagerina robusta* typically have a slightly higher form ratio. The axis of coiling is nearly straight. Poles are very broadly rounded or occasionally slightly mammilate. Following the juvenarium (the innermost two volutions in this species), the shell begins to expand rapidly before decreasing in height in the final one to two volutions. The proloculus is very large, with an average outside diameter of 0.400 mm among the measured NSMR specimens.

The inner spirotheca is very thin and delicate for such a large form, making the test exceptionally fragile. Outer walls are noticeably thicker. Septa are thin and strongly fluted in the outer volutions. Secondary axial deposits are absent. Chomata are present and well-defined as small mounds

but are only observable within the juvenarium. Measurements of this species are provided in Appendix A, Table 4.13.

Remarks: Ross (1963) observed that *Pseudoschwagerina robusta* possibly represents an intermediate form between *P. uddeni* (Beede and Kniker, 1924) and *P. gerontica* Dunbar and Skinner, 1937. *Pseudoschwagerina robusta* is most easily confused with *P. uddeni*, but may be distinguished from the latter by its consistently larger proloculus and less mammilate polar regions. *Pseudoschwagerina gerontica* is more elongate in its outermost volutions and possesses strongly mammilate polar regions. One large specimen (not illustrated) somewhat resembles *P. gerontica*, but the defining features are not as pronounced as those of the type specimens Dunbar and Skinner (1937).

Occurrence: ~275, 282, 286.9, and ~292 m above the base of the section (beds 60, 61); level - upper part of the Wolfcampian Stage (upper part of the Sakmarian Stage).

Genus ***Schwagerina*** von Möller 1877

Schwagerina franklinensis Dunbar and Skinner 1937

Plate 14, figures 5–7

Schwagerina franklinensis DUNBAR and SKINNER 1937, p. 628, pl. 66, figs. 1-11; SLADE 1961, p. 88-89, pl. 16, figs. 2, 3; WILLIAMS 1963, p. 59-61, pl. 16, figs. 1-6; WILLIAMS 1966, p. 1146-1148, pl. 148, figs. 4-6.

Description: A species of *Schwagerina* with a highly elongate fusiform to slightly subcylindrical test that attains six to seven volutions at maturity. The seven measured specimens from the NSMR section range in length from 8.54 to 11.14 mm (estimated from half length), averaging 9.99 mm. Test diameters range from 2.43 to 2.74 mm, averaging 2.62. The average form ratio of mature specimens is 3.80. The innermost two to three volutions are very tightly coiled and may have irregular, lateral deposits of axial filling. The outer volutions of the test are more loosely coiled and the overall shape of the test remains rather uniform throughout growth. Poles are bluntly rounded and the lateral slopes are gently convex to nearly straight, although they appear somewhat irregular in several specimens. The proloculus is small to moderate in size and spherical, averaging 0.188 mm among Riepe Spring Limestone specimens.

The spirotheca is thin throughout the test and does not increase much in thickness until the third or fourth volution. Septal fluting is intense and somewhat irregular as the height and character of septal folds varies throughout a single test. Most folds are very high and narrow, often with sides that are parallel to one another. Septal folding tends to decrease

slightly in the equatorial region. Chomata are nearly imperceptible and are only present on the proloculus and in the first volution. Measurements of this species are provided in Appendix A, Table 4.14.

Remarks: *Schwagerina franklinensis* very closely resembles *S. crebrisepta* Ross, 1959 but is distinguished from the latter by its more even inflation, lower outer volutions, inconsistency of axial filling in the inner volutions, and lack of a juvenarium. Stratigraphically, the two forms seem to be nearly equivalent, with *S. franklinensis* having a slightly longer range, spanning the Wolfcampian-Leonardian boundary. Stevens et al. (1979) illustrated two forms of "*S.* cf. *crebrisepta*" in their fusulinid zonation of northeastern Nevada and northwestern Utah and the author suspects that these forms may belong to *S. franklinensis*, but this assignment remains to be verified.

Occurrence: ~343 and ~347 m above the base of the section (unit 64); level - upper part of the Wolfcampian Stage (lower part of the Artinskian Stage).

Schwagerina glassensis Ross and Ross 2003

Plate 12, figures 1–3

Schwagerina bellula ROSS 1963, p. 116, pl. 12, figs. 3, 5, 7, 8.

Description: A species of *Schwagerina* with a highly inflated, slightly obese fusiform test of moderate size. Ross (1963) referred to the form as "spindle-shaped". Mature Riepe Spring Limestone specimens attain seven or eight volutions and have lengths ranging from 6.08 to 7.83 mm, averaging 7.43 mm. Test diameters range from 2.56 to 3.40 mm, averaging 3.07 mm. The average form ratio among measured specimens is 2.40. The outer part of the shell is loosely coiled and expands uniformly, abruptly following a very tightly coiled juvenarium. The axis of coiling is slightly curved to straight and the lateral slopes are variable, even within a single specimen. Poles are bluntly pointed and occasionally "knobby" in appearance. The proloculus is thin-walled and quite small compared to the overall test size, averaging 0.108 mm among the measured specimens.

The spirotheca of the juvenarium is extremely thin but thickens considerably as the test begins to coil more loosely in the outer volutions. The septal fluting is regular throughout the test. Septal loops are high and evenly spaced, producing uniform arches. Thin, lateral deposits of axial filling are present in most specimens. Chomata are absent. Measurements of this species are provided in Appendix A, Table 4.15.

Remarks: Prior to the taxonomic revision of several West Texas schwagerinids by Ross and Ross (2003), the type specimens of *Schwagerina glassensis* were assigned to *S. bellula* Dunbar and Skinner, 1937. Forms

broadly and erroneously regarded as *S. bellula*, *S.* cf. *bellula*, or *S.* aff. *S. bellula* have been reported from the lower Wolfcampian to the lower Leonardian in the western and southwestern United States (Dunbar and Skinner, 1937; Slade, 1961; Douglass, 1974).

Schwagerina glassensis differs from *S. bellula* in having extremely narrow, thin-walled innermost volutions immediately followed by rapidly expanding, loosely coiled outer volutions. The stratigraphic ranges of the two forms differ as well. *Schwagerina bellula* is essentially mid-Wolfcampian, only occurring within the LH-1 sequence (lower part of the "Lenoxian") of the Glass Mountains, whereas *S. glassensis* is a slightly younger form, occurring within the upper Wolfcampian LH-2 sequence (middle part of the "Lenoxian" Substage).

Occurrence: 282, ~289, and ~292 m above the base of the section (units 60, 61); level - upper part of the Wolfcampian Stage (upper part of the Sakmarian Stage).

Schwagerina neolata Thompson 1954

Plate 8, figures 5–7

Schwagerina neolata THOMPSON 1954, p. 65, pl. 36, figs. 9-15; WILLIAMS 1963, p. 67, pl. 21, figs. 1-5.

Schwagerina diversiformis Dunbar and Skinner 1937. ROSS 1963 (part), p.123, pl. 12, figs. 1, 2; MAGGINETTI et al. 1988 (part), p. 16, pl. 2, fig. 10.

Description: A species of *Schwagerina* with a moderately sized, strongly fusiform test with an inflated medial region that possesses six to seven volutions at maturity. Test lengths among the seven measured specimens range from 7.94 to 10.78 mm (estimated from half length in some cases), averaging 9.13 mm. Diameters range from 2.98 to 3.40 mm, averaging 3.25 mm. Acquiring an accurate average form ratio was difficult because of the poor preservation of the outer volutions among most specimens. The first three or so volutions of the test are diagnostic as they are significantly more inflated than the following three to four outer volutions and are marked by very broad and dense axial fillings. The axis of coiling is nearly straight, and the lateral slopes are typically gently convex or straight, but may be slightly concave on the underside of the test. Poles are bluntly pointed. The proloculus is large and subspherical to spherical, averaging 0.285 mm in outside diameter.

The spirotheca is thick and dense, with well-developed alveolar keriotheca. Septal folds are numerous, narrow, high (commonly reaching the overlying volution), and tightly spaced throughout the length of the test. Phrenothecae may be present in the outermost volutions. Chomata are only

visible on the inner two volutions as very small hemispherical mounds. Measurements of this species are provided in Appendix A, Table 4.16.

Remarks: Although the specimens from the NSMR section strongly resemble several of the types illustrated by Thompson (1954) (particularly pl. 36, figs. 11, 12), *Schwagerina neolata* is seldom reported outside of the Hueco Mountains. Williams (1963) attributed what he observed as a very narrow geographic range to restrictive facies control imposed on the apparently highly environmentally sensitive species. Slade (1961) described forms he assigned to *S. neolata* from the Ferguson Mountain area, but only illustrated one specimen. The author is skeptical of Slade's assignment, as the average proloculus size among his measured specimens is much smaller than is typical of the species and the axial filling of the lone illustrated specimen is not nearly as broad or dense as the type material.

Occurrence: ~274 and ~275 m above the base of the section (unit 60); level – upper part of the Wolfcampian Stage (middle to upper part of the Sakmarian Stage).

Schwagerina wellsensis Thompson and Hansen 1954

Plate 9, figures 1, 2

Schwagerina wellsensis THOMPSON and HANSEN 1954, p. 64, pl. 32, figs. 1-6, 7-9, pl. 34, figs. 1-12; THOMPSON et al. 1958, p. 122-123, pl. 20, figs. 9-14; ROBINSON 1961, p. 112-113, pl. 17, fig. 6.

Description: A species of *Schwagerina* with a subtly inflated, elongate fusiform test of moderate to large size. Mature tests of six to seven volutions attain a length of 8.48 to 9.12 mm (estimated from half length in some cases), averaging 8.84 mm. Diameters range from 2.94 to an estimated 3.33 mm, averaging 3.12 mm. Of the six Riepe Spring Limestone specimens of *Schwagerina wellsensis* measured, four were preserved well enough to obtain an estimated average form ratio of 2.84. The axis of coiling is straight and is commonly accentuated by thin lateral deposits of axial filling. Lateral slopes are nearly straight or convexly tapered towards the polar regions. The poles are sharply to bluntly pointed. The test is loosely coiled and maintains a very consistent elongate fusiform shape throughout growth. The proloculus is large, thick-walled, and spherical with an average diameter of 0.27 mm among the measured Riepe Spring Limestone specimens.

The spirotheca, like most other inflated forms of *Schwagerina*, is thick and well-developed. Septa are strongly, narrowly, and evenly fluted across the length of the test. Chomata are extremely small and are typically only observable in the inner one or two volutions. Measurements of this species are provided in Appendix A, Table 4.17.

Remarks: *Schwagerina wellsensis* was originally described from upper Wolfcampian deposits exposed at a very nearby locality along the western edge of Low Mountain, approximately one mile southeast of Wells, Nevada. The types illustrated by Thompson (1954) are numerous and extremely variable in their overall size and the density of axial fillings but all specimens have consistently large proloculi. It seems reasonable to conclude that Thompson's types actually represent at least two different species of *Schwagerina*, but the forms presently illustrated compare closely to the "average" form among Thompson's original specimens. This group of morphotypes is regarded herein as the "*S. wellsensis* species complex." The size of the proloculus, lateral extent of axial filling, and elongate, evenly fusiform shape of the test serve as the primary criteria for the identification of *S. wellsensis*.

Occurrence: ~272, ~275, ~280, and ~289 m above the base of the section (units 60, 61); level - upper part of the Wolfcampian Stage (middle to upper part of the Sakmarian Stage).

***Schwagerina* sp. A**

Plate 7, figures 3–5

Description: A superficially "primitive" species of *Schwagerina* with a narrow, elongate fusiform test that attains five to six volutions at maturity. The measured specimens from the NSMR section range in length from 7.34 to 7.78 mm, averaging 7.61 mm. Test diameters range from 2.01 to 2.65 mm, averaging 2.26 mm. The average form ratio among measured specimens is 3.35. The test is loosely coiled throughout and seems to possess fewer volutions at maturity than most forms of the genus. Thicknesses of the first through fifth volutions of measured specimens average 0.051, 0.084, 0.175, 0.307, and 0.347 mm. Poles are bluntly pointed and the lateral slopes are nearly straight with minor undulations in the spirotheca. The proloculus is thin-walled and moderate in size, averaging 0.183 mm in outside diameter.

The spirotheca is thin and somewhat irregular but does not display the high rugosity characteristic of *Pseudofusulina*. Average wall thicknesses from the proloculus through the fifth volution are 0.019, 0.019, 0.024, 0.043, 0.073, and 0.078 mm. Septal fluting is strong but highly irregular throughout the test. Septal folds are typically high and narrow, often reaching the top of each volution, but occasionally appear short, broad, and flat-topped. The septal folds are widely spaced compared to contemporaneous *Schwagerina*. Sparse phrenothecae may be present in the outer volutions. Minute chomata are present on the proloculus and first to second volution. Measurements of this species are provided in Appendix A, Table 4.18.

Remarks: *Schwagerina* sp. A appears to be closely related to a group of smaller, irregular *Schwagerina* that originated in the latest Pennsylvanian and persisted through late Wolfcampian time. This group includes forms such as *S. campa* Thompson, 1954, *S. campensis* Thompson, 1954, *S. emaciata* (Beede, 1916), *S. providens* Thompson and Hazzard, 1946, *S. mccloudensis* Skinner and Wilde, 1965b, and *S. whartoni* Petocz, 1970.

Schwagerina sp. A differs from *S. campa* in its greater length, lower average form ratio, and larger proloculus. Although *Schwagerina* sp. A and *S. campensis* have approximately the same average proloculus size, the latter is larger, has a higher form ratio, and has more tightly spaced septal folds throughout the test. *Schwagerina* sp. A is larger than *S. emaciata* and has a larger proloculus. *S. providens* is nearly the same size as *Schwagerina* sp. A, but the former has more closely spaced septa and a larger proloculus. *S. mccloudensis* is slightly larger than *Schwagerina* sp. A and the walls are thicker. *Schwagerina* sp. A resembles several paratype specimens of *S. whartoni* of east-central Alaska, but the latter generally has a lower form ratio.

Occurrence: ~254 and ~258 m above the base of the section (units 56, 57); level - upper part of the Wolfcampian Stage (middle part of the Sakmarian Stage).

***Schwagerina* sp. B**

Plate 9, figures 3, 4

Description: A large species with an elongate, slightly inflated fusiform test of seven to eight volutions. Mature specimens are uniform in length, ranging between 10.11 to 11.42 mm (estimated from half length) and averaging 10.64 mm. Test diameters range from 2.94 to 3.83 mm, averaging 3.52 mm with an average form ratio of 3.06. The test has a small, tightly coiled juvenarium followed by much more loosely coiled outer volutions that increase dramatically in height between the third and fourth volutions. Thicknesses of the first through seventh volutions of measured specimens average 0.034, 0.046, 0.078, 0.194, 0.329, 0.411, and 0.411 mm. The axis of coiling often has a slight curvature in the outer volutions. Secondary deposits are present along the axis of coiling and sporadically thicken and thin throughout the length of the test. Poles are slightly mammilate and become more bluntly rounded throughout growth, as the poles are sharply rounded in the inner and middle volutions. The lateral slopes are variable and irregular but are often concave on at least one side of the test ("top" or "bottom"), giving axial sections a pinched profile. The proloculus is spherical, thin-walled, and relatively small, averaging 0.141 mm in outside diameter.

The spirotheca is very thin in the juvenarium but increases greatly in thickness and becomes coarsely alveolar between the third and fifth

volutions. Average wall thicknesses from the proloculus through the seventh volution are 0.014, 0.014, 0.02, 0.029, 0.05, 0.082, 0.102, and 0.106 mm. Septal fluting is intense and uniform throughout the test and the septal loops are high, regular, and evenly spaced. Unfortunately, the degree and nature of the septal fluting observed is not diagnostic of this morphotype because the septa are extremely similar amongst many schwagerinids of middle to late Wolfcampian age. Minute chomata are present on the proloculus and the first to second volution. Measurements of this species are provided in Appendix A, Table 4.19.

Remarks: At first glance, *Schwagerina* sp. B appears similar in overall test morphology to several other middle to late Wolfcampian forms of the genus, but the described species differs from previously described forms in the sum of its discrete characters. Although *Schwagerina* sp. B resembles *S. wellsensis*, the former has a much smaller proloculus, a thinner proloculus wall, and a distinct juvenarium. Both *Schwagerina* sp. B and *S. aculeata* Thompson and Hazzard, 1946 have reduced proloculi, but the outside diameter of the former is still smaller.

Occurrence: ~280, ~281, and 283.9 m above the base of the section (unit 60); level - upper part of the Wolfcampian Stage (middle to upper part of the Sakmarian Stage).

***Schwagerina* sp. C**

Plate 15, figures 1, 2

Description: A large, elongate species of *Schwagerina* with a subcylindrical test that attains six to eight volutions at maturity. Measured specimens range in length from 8.86 to 11.34 mm (estimated from half length), averaging 10.63 mm. Test diameters range from 1.84 to 2.34 mm (estimated from half width), averaging 2.06 mm with an estimated average form ratio of 5.23. The innermost volutions are very tightly coiled and the shell begins to loosely uncoil beyond the third volution. Heights of the first through sixth volutions of measured specimens average 0.054, 0.073, 0.103, 0.158, 0.235, and 0.235 mm. The axis of coiling curves slightly throughout growth and the lateral slopes are gently convex to wavy and irregular. Axial fillings are present but are mostly confined to the polar regions of the innermost volutions. Poles are bluntly to sharply pointed. The proloculus, which is often fractured, is spherical and of moderate size with an average outside diameter of 0.2 mm.

The spirotheca is moderately thin, keriothecal, and irregular, thickening and thinning laterally but lacking the intense rugosity characteristic of *Pseudofusulina*. Average wall thicknesses from the proloculus through the sixth volution are 0.021, 0.022, 0.028, 0.036, 0.045,

0.061, and 0.085 mm. Septal fluting is strong throughout the length of the test. Septal folds are high, often reaching the top of the associated volution, and may be steep-sided and regular to somewhat irregular. The height of the folds decreases near the equatorial portion of the test. Chomata are present only on the proloculus and are replaced by short septal loops filled with secondary deposits (pseudochomata). Although *Schwagerina* sp. C resembles primitive forms of *Parafusulina*, no fully developed cuniculi were observed in tangential sections. Measurements of this species are provided in Appendix A, Table 4.20.

Remarks: *Schwagerina* sp. C is likely related to a group of elongate, advanced *Schwagerina* which immediately precede the first appearance of early *Parafusulina* in the Leonardian. These forms of *Schwagerina* are not only characteristic of uppermost Wolfcampian deposits in North America but are also known from coeval Artinskian deposits of the Arctic and southern Urals. In addition to forms of *Schwagerina* like *S. jenkinsi* Thorsteinsson, 1960 (Canadian Arctic) and *S. mankomenensis* Petocz, 1970 (Alaska), the group also includes the approximately contemporaneous genera *Juresanella* Bensh and Kireeva in Bensh, 1987 and *Crenulosepta* Stevens and Stone, 2009.

Schwagerina sp. C most closely resembles the genus *Crenulosepta*, particularly *Crenulosepta inyoensis* Stevens and Stone, 2009 and *Crenulosepta wahlmani* Stevens and Stone, 2009, but differs primarily in the

more irregular nature of the septa in the former. The septal folds of *Schwagerina* sp. C are higher, steeper, and more irregular than those of *Crenulosepta*, which had also developed cuniculi in some, if not all, forms of the genus (Stevens and Stone, 2009).

Occurrence: ~347 and 392.5 m above the base of the section (unit 68); level - upper part of the Wolfcampian Stage (lower to middle part of the Artinskian Stage).

Family TRITICITIDAE Davydov 1986

Genus ***Triticites*** Girty 1904

Triticites bensonensis Ross and Tyrrell 1965

Plate 3, figures 14, 15

Triticites bensonensis ROSS and TYRRELL 1965, p. 629-630, pl. 77, figs. 26-31; MYERS 1988, pl. 6, figs. 9-11; STEVENS and STONE 2007, p. 24, pl.1, fig. 6.

Description: A small to moderately sized species of *Triticites* with a highly inflated fusiform test of six to seven volutions. Test lengths of Riepe Spring Limestone specimens range from 3.65 to 4.33 mm (estimated from half length

values in some cases), averaging 4.07 mm. Test diameters among mature specimens of *T. bensonensis* range from 1.89 to 2.35 mm, averaging 2.20 mm. The average form ratio of mature specimens is 1.86. The axis of coiling is straight and the lateral slopes are variable. Poles are bluntly pointed. The proloculus is spherical, small to moderate in size, and averages 0.118 in outside diameter.

The spirotheca is coarsely alveolar and is relatively thick for a smaller form of *Triticites*. The septal fluting is moderately developed throughout the test but is most intense along the axis and near the polar regions. Chomata are slightly overhanging to tabular and are approximately one-half of a volution in height. The tunnel is strong, relatively narrow, and straight throughout the test. Measurements of this species are provided in Appendix A, Table 4.21.

Remarks: *Triticites bensonensis* belongs to a North American species complex of small yet robust forms of *Triticites* that are common in lower to middle Gzhelian deposits. *Triticites bensonensis* most closely resembles *T. muddiensis* Cassity and Langenheim, 1966 from Arrow Canyon, Nevada, but differs from the latter in its more obese profile and gently concave distal lateral slopes. *Triticites bensonensis* differs from *T. hobblensis* Thompson, Verville, and Bissell, 1950 by having a consistently lower form ratio, a slightly smaller proloculus, and sharper poles.

Occurrence: 150.4 m above the base of the section (unit 30); level - middle part of the Virgilian Stage (lower to middle part of the Gzhelian Stage).

Triticites burgessae Burma 1942

Plate 1, figures 4–7

Triticites burgessae BURMA 1942, p. 744, pl. 118, figs. 2, 13; THOMPSON 1957, p. 316-318, pl. 28, figs. 1-6, 7; ROSS 1963, p. 99, pl. 4, figs. 1-6; ROSS, 1965, p. 1160, fig. 7; CASSITY and LANGENHEIM 1966, p. 946-947, pl. 112, figs. 12-16.

Description: One of the smallest known forms of *Triticites*, this species has a slightly elongate fusiform test that attains six to seven volutions at maturity. Test lengths range from 3.58 to an estimated 4.09 mm, averaging 3.81 mm. Test diameters range from 1.44 to 1.58 mm, averaging 1.51 mm. The average form ratio among Riepe Spring Limestone specimens is 2.53. The axis of coiling is straight and the lateral slopes are straight to gently convex. Axial fillings are absent. Poles are bluntly pointed. The proloculus is spherical and small, averaging 0.075 mm in outside diameter.

The spirotheca is extremely thin and very finely keriothecal, a trait observed in most very early species of *Triticites*. Septal fluting is weak to

moderate along the axial plane and is absent in the middle portion of the test. Chomata are massive, tabular, and quite large for such a miniscule test. Chomata may be lacking in the outermost volution. Measurements of this species are provided in Appendix A, Table 4.22.

Remarks: The authors' reservation in the assignment is due to the paucity of specimens in the collected material, as only three individuals were recovered from the lower informal member of the Riepe Spring Limestone. The uncommonly small size of the test and the tenuity of the spirotheca are the critical attributes in the diagnosis of the forms assigned herein to *Triticites* cf. *burgessae*. *Triticites burgessae* most closely resembles the related Missourian species *T. nebraskensis* Thompson, 1934 and *T. pygmaeus* Dunbar and Condra, 1927 but is easily distinguished from these forms. *T. burgessae* differs from *T. nebraskensis* in its smaller proloculus, shorter test, and much lower form ratio, and differs from *T. pygmaeus* in its smaller proloculus, thinner spirotheca, and typically higher form ratio.

Occurrence: 32.1 m above the base of the section (unit 6); level - lower part of the Missourian Stage (lower-middle part of the Kasimovian Stage).

Triticites* cf. *californicus Thompson and Hazzard 1946

Plate 5, figure 3

Triticites californicus THOMPSON and HAZZARD 1946, p. 42, pl. 10, figs. 10-14.

Description: An extremely large species of *Triticites* with an inflated fusiform test. The lone specimen of *T.* cf. *californicus* has seven volutions, a test length of 8.08 mm, and a diameter of 4.20 mm, producing a form ratio of 1.92. The form ratio increases gradually and uniformly throughout growth. The axis of coiling is straight and the lateral slopes are nearly straight. Poles are bluntly pointed. The proloculus is spherical and measures 0.318 mm in outside diameter.

The spirotheca is thick and coarse, increasing gradually in thickness throughout growth. Septa are moderately fluted along the axis of coiling and in the polar regions of the test. Chomata are wedge-shaped, tapering towards the poles, and border a straight tunnel of moderate width. Several chomata of the illustrated specimen are very slightly overhanging.

Remarks: The specimen designated as *Triticites* cf. *californicus* most closely resembles two closely related forms which also occur in the Riepe Spring Limestone at Spruce Mountain Ridge, *T. pinguis* and *T. cellamagnus*. *Triticites* cf. *californicus* differs from *T. pinguis* in its higher form ratio, thinner spirotheca, and slightly smaller proloculus. *Triticites cellamagnus*

has a similar form ratio, but also has thicker walls and the proloculus is larger as well.

Occurrence: 215.8 m above the base of the section (unit 45); level - upper part of the Virgilian Stage (upper part of the Gzhelian Stage).

Triticites* aff. *celebroides Ross 1965

Plate 1, figures 8–11

Description: A strongly elongate fusiform species of moderate size that attains six to seven volutions at maturity. Test lengths among the five measured specimens range from 5.59 to 6.99 mm (estimated from half lengths), averaging 6.26 mm. Test diameters range from 1.74 to 2.16 mm, averaging 2.01 mm with an estimated average form ratio of 3.13. The form ratio increases greatly following the second volution. The axis of coiling is nearly straight to slightly curved in the outer volutions and the nature of the lateral slopes varies accordingly. Poles are bluntly pointed. Axial fillings are absent. The proloculus is spherical and small, averaging 0.084 mm in outside diameter.

The spirotheca is thin and very weakly keriothecal. Septa are moderately fluted along the axis and in the polar regions. Sparse phrenothecae may be present. The chomata vary from small and mound-like

to larger and overhanging. Secondary deposits may be present on the chomata. The tunnel is nearly straight and expands rapidly throughout growth. Measurements of this species are provided in Appendix A, Table 4.23.

Remarks: *Triticites* aff. *celebroides* belongs to a geographically widespread group of elongate Missourian *Triticites*, several of which have often been associated with or mistaken for *T. ohioensis* Thompson, 1936 and *T. irregularis* (Staff, 1912). Discrepancy regarding *T. irregularis* was initially a result of Staff not providing sufficient details for his collection localities or measured specimens. Further ambiguity resulted from informal "typical varieties" (diagnostic forms) being described from multiple localities, including the Winterset Limestone of Iowa and the Brownwood Shale of Texas (Thompson et al., 1950). Additionally, White (1932) illustrated four varieties of *T. irregularis*, acknowledging that there were likely distinct species present within the group. Unfortunately, although White was explicit in his desire to avoid further complication of the interpretation of *T. irregularis*, the broad definition he provided seems to have had an impact on the initially dubious clarity and utility of the taxon.

Triticites aff. *celebroides* most closely resembles the types of *T. celebroides* from the lower Missourian part of the Gaptank Formation and the forms illustrated by Nestell (1989) from the Wynn Limestone Member of the

Palo Pinto Formation. The forms compare well in general test morphology and age, but *Triticites* aff. *celebroides* differs from true *T. celebroides* in its thinner spirotheca and lower average form ratio. *Triticites* aff. *celebroides* can be distinguished from *T. springvillensis* by its higher form ratio and smaller proloculus.

Occurrence: 32.1 m above the base of the section (unit 6); level - lower part of the Missourian Stage (lower-middle part of the Kasimovian Stage).

Triticites* cf. *cellamagnus Thompson and Bissell 1954

Plate 5, figure 4

Triticites cellamagnus THOMPSON and BISSELL 1954 (part), p. 43-44, pl. 11, figs. 1-11; THOMPSON et al. 1954, p. 121, pl. 19, figs. 13-15; BOSTWICK 1955, pl. 97, 4; SABINS and ROSS 1963 (part), p. 345-346, pl. 36, figs. 13, 14; WILDE 2006, p. 63, pl. 63, figs. 1-5, pl. 67, figs. 6-10; STEVENS and STONE 2007, p. 33, pl. 1, fig. 7.

Triticites cf. *cellamagnus* BOSTWICK 1955, pl. 97, figs. 6, 11, pl. 98, fig. 5; WILLIAMS 1963, p. 74-75, pl. 17, figs. 5-8.

Description: A species with a short, inflated fusiform test of medium to moderately large size. Only one poorly-preserved specimen was recovered

from the middle informal member of the Riepe Spring Limestone. The specimen has an estimated length of 6.02 mm (based on measured half length) and a width of 3.39 mm, with an average form ratio of 1.78. The first volution is nearly spherical, but the form ratio increases abruptly beyond the second volution. The axis of coiling is straight and the lateral slopes are straight to gently convex. External polar regions have been heavily corraded, but the interior poles are bluntly pointed. The proloculus is extremely faintly subspherical and large, measuring 0.419 mm in outside diameter.

The spirotheca is thick and well-developed, as is common amongst forms of *Triticites* Group IV (Wilde, 1976). Moderate fluting of the septa occurs along the axis of coiling and near the poles. The chomata are broad and overhanging, bordering a narrow and nearly straight tunnel.

Remarks: The form ratio for *Triticites cellamagnus* is typically between 2.0 and 2.4 (as per type specimens), but the lone specimen obtained from the Douglass-Henbest collection is corraded and missing part of the sixth volution, resulting in the lower form ratio. Several specimens of *T. pinguis* have a proloculus that nearly rival that of the illustrated specimen in diameter, but the form ratio of the latter is still larger. Although proloculus diameter alone is an inappropriate distinction among species, the proloculus in question is certainly impressive enough to strongly consider the given taxonomic assignment.

Occurrence: ~200 m above the base of the section (unit 42); level - upper part of the Virgilian Stage (upper part of the Gzhelian Stage).

Triticites creekensis Thompson 1954

Plate 4, figures 6, 7

Triticites creekensis THOMPSON 1954 (part), p. 42, pl. 9, figs. 22, 23, 25, pl. 10, figs. 1, 2, 6, 12; SLADE 1961, p. 73-74, pl. 10, fig. 4; CASSITY and LANGENHEIM 1966, p. 951, pl. 113, figs. 19, 20; STEINER and WILLIAMS 1968 (part), p. 56-57, pl. 11, figs. 3-5; WILDE 2006, p. 62-63, pl. 62, figs. 15-19.

Triticites cf. *creekensis* RICH 1961, pl. 145, figs. 17, 18.

Description: A species with a slightly elongate, inflated fusiform test of medium to moderately large size. Mature tests of six to eight loosely coiled volutions attain a length of 6.2 to 8.1 mm and a width of 2.8 to 4.0 mm, producing a form ratio of 2.0 to 2.7, although the typical form ratio is closer to 2.0 mm (Thompson, 1954). The two definitive specimens from the Riepe Spring Limestone have an average form ratio of 2.0. The axis of coiling is straight and the lateral slopes may be either concave or convex, occasionally demonstrating both contours in a single specimen (see Pl. 4, Fig. 6 and the

holotype specimen). Poles are sharply to bluntly pointed. The proloculus is spherical and large, averaging 0.281 mm in diameter.

The spirotheca is thickest in the equatorial portion of the test but thins noticeably towards the polar regions. Moderate fluting of the septa occurs along the axis of coiling and near the poles. Chomata vary from massive and tabular to low and mound-like. The tunnel is narrow and nearly straight along the equatorial plane.

Remarks: *Triticites creekensis* represents a medial form of *Triticites* Group IV (Wilde, 1976). The test of *T. creekensis* is more inflated than the shells of ancestral, advanced forms belonging to Wilde's (1976) *Triticites* Groups II and III. The proloculus of *T. creekensis* is also larger than most, if not all, early and middle Virgilian forms. However, the inflation of the test and the diameter of the proloculus seem insignificant when compared with slightly younger, advanced forms of *Triticites* Group IV such as *T. cellamagnus* and *T. pinguis*.

Occurrence: ~168 m above the base of the section (unit 34); level - upper part of the Virgilian Stage (upper part of the Gzhelian Stage).

Triticites cullomensis Dunbar and Condra 1927

Plate 4, figures 1, 2

Triticites cullomensis DUNBAR and CONDRA 1927, p. 93-95, pl. 5, figs. 5-10; DUNBAR and HENBEST 1942, p. 135-136, pl. 23, figs. 13-18; THOMPSON et al. 1950, p. 457-460, pl. 62, figs. 7-17, pl. 63, figs. 1-3; SABINS and ROSS 1963, p. 339, pl. 35, figs. 13-16.

Description: A species with an elongate, evenly fusiform to nearly elliptical test of moderate size. Among the Riepe Spring Limestone specimens studied, mature tests of six to seven volutions range in length from 5.46 to 6.14 mm, averaging 5.87 mm. Diameters range from 2.22 to 2.47 mm, averaging 2.35 mm with average form ratio of 2.5. The axis of coiling and the lateral slopes are straight, occasionally giving the test a slightly rhomboidal axial profile. Axial fillings are typically absent. Poles are bluntly pointed. The proloculus is spherical and of small to moderate size, averaging 0.121 mm in outside diameter.

The spirotheca is of moderate thickness but is well-developed. Septa are delicately fluted along the axis, whereas fluting may be nearly absent in the equatorial region. Chomata are inconspicuous, weakly developed mounds and may be missing from outer volutions. Measurements of this species are provided in Appendix A, Table 4.24.

Remarks: Like *Triticites creekensis*, morphotypes commonly attributed to *T. cullomensis* seem to be widely distributed in North America. The form is known to span much of the North American Virgilian (= uppermost part of the Kasimovian through Gzhelian). *Triticites cullomensis* most closely resembles *T. beedei* Dunbar and Condra, 1927, but differs from the latter in its less inflated, more elliptical profile. Although specimens of *T. cullomensis* may appear subtly rhomboidal, *T. beedei* is typically strongly rhomboidal and more inflated. Additionally, *T. beedei* commonly attains eight to nine volutions at maturity, compared to the six to seven of *T. cullomensis*.

Occurrence: 149.2 m above the base of the section (unit 30); level - middle part of the Virgilian Stage (lower to middle part of the Gzhelian Stage).

Triticites* cf. *inflatus White 1932

Plate 4, figure 3

Triticites ventricosus DUNBAR and CONDRA 1927 (part), p. 84-91, pl. 4, figs. 5, 6.

Triticites ventricosus (Meek) var. *inflatus* Galloway and Ryniker n. var. (ms.) WHITE 1932, p. 74-76, pl. 7, figs. 10-12.

Triticites inflatus WILDE 2006, p. 65, pl. 65, figs. 1-5; p. 241, pl. 70, figs. 6-15.

Description: A species with a highly inflated, obese fusiform test of moderately large size. Mature tests of seven to nine volutions attain a length of 7.3 to 8.3 mm and a width of 3.2 to 4.3 mm, with an average form ratio of 2.0 (White, 1932). The average form ratio of specimens from the Riepe Spring Limestone is 1.8. The axis of coiling is straight and the lateral slopes are moderately to strongly concave. Poles are mammilate to broadly pointed. The proloculus is typically large, varying from 0.240 to 0.280 mm (White, 1932).

The spirotheca is thick and well-developed. Septal fluting is concentrated along the axis of coiling. The chomata are high, narrow, and overhanging to massive and tabular. The tunnel is narrow and nearly straight along the equatorial plane.

Remarks: Specimens of *Triticites* cf. *inflatus* from the middle informal member of the Riepe Spring Limestone bear a strong resemblance to the specimens of *T. inflatus* from the Big Hatchet Mountains of New Mexico illustrated by Wilde (2006). Wilde noted that a group of specimens from his New Well Peak Section of the Big Hatchets have proloculi with a smaller diameter than most other specimens described and illustrated, although all other characters fit well with previous descriptions (compare Wilde, 2006, pl. 70, figs. 6-15). The few Riepe Spring Limestone specimens seem to fall within this group and possess slightly smaller proloculi, averaging 0.193 mm in diameter.

Occurrence: 178 m above the base of the section (unit 36); level- upper part of the Virgilian Stage (upper part of the Gzhelian Stage).

Triticites* cf. *jacksboroensis Kauffman and Roth 1966

Plate 3, figures 3, 4

Triticites jacksboroensis KAUFFMAN and ROTH 1966, p. 17-18, pl. 3, figs. 8-15; WILDE 2006, p. 53, pl. 50, figs. 14-18, 29-35, pl. 51, figs. 4-8.

Description: A species of *Triticites* with a slightly inflated, evenly fusiform test of moderate size. Riepe Spring Limestone specimens attain six to seven volutions at maturity. Test length ranges from 4.02 to 5.82 mm among measured specimens, averaging 4.68 mm. Test diameter ranges from 1.88 to 2.71 mm, averaging 2.22 mm with a form ratio of 2.16. Inner volutions have a lower form ratio than that of mature specimens and the test coils loosely and uniformly. The axis of coiling is straight and the lateral slopes are typically very gently convex. Axial fillings are completely absent. Poles are bluntly to broadly pointed. The proloculus is small to moderate in size, averaging 0.107 mm.

The spirotheca is moderately thick, distinctly yet delicately alveolar, and very characteristic of early Virgilian forms of *Triticites*. Septa are weakly

to moderately fluted across the axis of the test. Sparse phrenothecae may be present just poleward of the tunnel in the outer volutions. The chomata are massive and tabular with rounded to occasionally squared-off tops, reaching a maximum height of approximately one-half to two-thirds the height of the encompassing volution. The tunnel is straight and of moderate width. Measurements of this species are provided in Appendix A, Table 4.25.

Remarks: *Triticites* cf. *jacksboroensis* occurs at two levels over a 30 m interval in the lower informal member of the Riepe Spring Limestone. There is a notable difference in test size between the lone specimen from 70 m (Pl. 3, fig. 3; unit 16) and the more abundant forms recovered from 100.1 m above the base (Pl. 3, fig. 4; unit 21), but gross morphological similarities suggest that both forms may belong to the same species and are treated as such. Even with its greater size, the larger specimen from unit 16 still falls well within the original range provided for *T. jacksboroensis* by Kauffman and Roth (1966). Several specimens recovered from unit 21 were more similar in size to the lower specimen (NSMR 70-1), nearing six millimeters in length, but greater than 95% of the fusulinids from unit 21 were at least partially destroyed by physical compaction. Most of the larger specimens were unrecognizable beyond the keriothecal wall structure, making them unusable for study.

Occurrence: 70 and 100.1 m above the base of the section (units 16 and 21); level - lower part of the Virgilian Stage (lower part of the Gzhelian Stage).

Triticites pinguis Dunbar and Skinner 1937

Plate 5, figures 5–7

Triticites pinguis DUNBAR and SKINNER 1937, p. 620, pl. 47, figs. 12-19; BOSTWICK 1962, pl. 164, fig. 9, pl. 165, fig. 16, pl. 166, fig. 5; ROSS, 1963, p. 109, pl. 6, figs. 1, 3, 4; SABINS and ROSS 1963, p. 343-345, pl. 36, figs. 6-12; WILDE 2006, p.66, pl. 67, figs. 1-5, pl. 68, figs. 11-17, pl. 69, figs. 9-13. *Triticites californicus* Thompson and Hazzard 1946. STEVENS and STONE 2007, p. 33, pl. 1, fig. 9.

Description: A striking species of *Triticites* with an extremely ventricose fusiform (nearly subglobular) test. Mature specimens of six to seven volutions attain lengths ranging from 5.11 to 6.32 mm, with an average of 5.73 mm. Diameters range from 3.63 to 4.43 mm, averaging 4.00 mm. The average form ratio among mature Riepe Spring Limestone specimens is 1.44. Poles are broadly pointed to mammilate. The axis of coiling slopes gently toward the downturned poles, with steep upper slopes that are nearly straight to gently convex and lower slopes that may be slightly concave. The proloculus is spherical and extremely large, averaging 0.362 mm in outside diameter.

The spirotheca is thick and very coarse, with well-developed alveolar keriotheca. Septa are moderately fluted across the axis of the test, intensifying near the poles. Chomata are strong, tabular, and occasionally slightly overhanging. Dense secondary deposits may be associated with chomata, especially in medial volutions. The tunnel is fairly narrow and somewhat irregular in its path. Measurements of this species are provided in Appendix A, Table 4.26.

Remarks: The highly inflated test of *Triticites pinguis* is somewhat similar in shape to several species of *Pseudoschwagerina*, but there are several unmistakable traits that distinguish *T. pinguis* from this genus. First, *T. pinguis* exhibits massive, well-defined chomata in nearly each volution, the only exception being the final volution. Second, the shell is significantly more robust than *Pseudoschwagerina*, with much coarser alveolar keriotheca. Among other ventricose forms of *Triticites*, *T. pinguis* possesses one of the lowest average form ratios. Although *T. plummeri* Dunbar and Condra, 1927 is also highly inflated, it has a much smaller test and a smaller proloculus.

Occurrence: 215.8 m above the base of the section (unit 45); level - upper part of the Virgilian Stage (upper part of the Gzhelian Stage).

Triticites* cf. *primarius Merchant and Keroher 1939

Plate 2, figures 9–10

Triticites secalicus (Say) var. primarius MERCHANT and KEROHER 1939, p. 611-614, pl. 69, figs. 10-12.

Description: A distinct species of *Triticites* with an elongate fusiform test of moderately large size, attaining eight volutions at maturity. Although the test is highly elongate, it is not fully subcylindrical in shape and maintains a slightly inflated equatorial region. The lone specimen from the lower informal member of the Riepe Spring Limestone has a length of 7.75 mm. The test measures 2.15 mm in diameter and the form ratio is 3.61. The test coils uniformly, but the form ratio increases significantly throughout growth as the poles begin to elongate in the outer volutions. The axis of coiling is straight and the lateral slopes are nearly straight. Poles are bluntly pointed. Axial fillings are absent. The proloculus is spherical and small when compared to the overall size of the test, measuring 0.111 mm in outside diameter.

The spirotheca is relatively thin and weakly alveolar. Septa are thin and moderately fluted, closely resembling the septal fluting of *Triticites* sp. A. Fluting is most intense in the polar regions. Chomata are small and mound-like but may appear larger due to minor secondary deposits occurring

adjacent to the tunnel. The tunnel is straight to slightly skewed and widens considerably, though uniformly, throughout growth.

Remarks: The highly elongate fusiform shape of *Triticites* cf. *primarius* is reminiscent of a number of other middle to late Missourian triticitid taxa, but a side-by-side comparison of *T.* cf. *primarius* from the present study and the holotype of *T. primarius* from the Stanton Formation of Kansas demonstrates that the two specimens are nearly identical. Although more specimens would be ideal for accurate determination, the strong resemblance between the two specimens and the co-occurring fusulinid and conodont faunas of unit 14 are sufficient enough to support this tentative assignment.

Occurrence: 64.8 m above the base of the section (unit 14); level - upper part of the Missourian Stage (upper part of the Kasimovian Stage).

***Triticites* sp. A**

Plate 2, figures 7–10

Description: A small species with an elongate fusiform to slightly subcylindrical test of small to moderate size. Mature tests of six to seven volutions reach 3.84 to 5.66 mm in length (several estimated from half length), averaging 4.85 mm. Test diameters range from 1.59 to 2.05 mm,

averaging 1.90 with an average form ratio of 2.65. The axis of coiling is straight and the lateral slopes are nearly straight. Poles are bluntly pointed. The proloculus is spherical and relatively large compared to similar Missourian *Triticites*, averaging 0.138 mm among Riepe Spring Limestone specimens.

The spirotheca is thick for a smaller test but are still of the characteristically Missourian variety and weakly keriothecal. Septa are thin and regularly fluted along the axis, broadening near the poles. Septal fluting is minimal in the equatorial portion of the test. The chomata are moderately pronounced, varying from narrow and slightly overhanging to massive and tabular. Chomata are often present even in the outermost volutions. The tunnel is narrow and very straight. Measurements of this species are provided in Appendix A, Table 4.27.

Remarks: *Triticites* sp. A, along with *T.* aff. *celebroides*, belongs to a group of elongate Missourian *Triticites* often associated with or mistaken for *T. irregularis* (Staff, 1912). However, most specimens assigned to *T. irregularis* are notably different from those of *Triticites* sp. A illustrated in the present study. Regardless of problems in the taxonomy, comparisons of *Triticites* sp. A to White's (1932) forms demonstrate that specimens of *Triticites* sp. A are consistently smaller and slightly more inflated (= lower form ratio) with higher chambers, thicker spirotheca, and more robust chomata than *T.*

irregularis. *Triticites* sp. A also bears some resemblance to *T. springvillensis* Thompson, Verville, and Bissell, 1950, but differs primarily in its thicker, more developed spirotheca.

Occurrence: 64.8 m above the base of the section (unit 14); level- upper part of the Missourian Stage (upper part of the Kasimovian Stage).

***Triticites* sp. B**

Plate 3, figures 1, 2

Description: A species with an inflated, broadly elliptical test of small to moderate size. Mature specimens attain six to seven volutions. Specimens range in length from 4.00 to 4.39 mm, averaging 4.16 mm. Test diameters range from 1.71 to 1.96 mm, with an average of 1.89 mm. The average form ratio among the few Riepe Spring Limestone specimens is 2.21. The test is loosely and uniformly coiled throughout growth. The shape of the inner three or four volutions tends to be more fusiform than the strongly elliptical shape of the final one or two volutions. The axis of coiling is straight and the lateral slopes are markedly convex. The poles are very broadly rounded. Axial fillings are absent. Heights of the first through sixth volution average 0.041, 0.043, 0.089, 0.148, 0.222, and 0.231 mm. The proloculus is spherical and moderately small, with an average outside diameter of 0.104 mm.

Following the thin inner walls, the spirotheca of the outermost three or so volutions is moderately thick and coarse for a Missourian age form of *Triticites*. Wall thicknesses from the proloculus through the six volution average 0.012, 0.013, 0.016, 0.025, 0.049, 0.059, and 0.075 mm. Septal fluting is confined to the axis of coiling and polar regions. Fluting tends to become weaker towards the poles. Chomata are well-developed, rounded, nearly symmetrical mounds that border a straight tunnel. Measurements of this species are provided in Appendix A, Table 4.28.

Remarks: *Triticites* sp. B does not closely resemble any form of Missourian *Triticites* known to the authors. The new form is eye-catching among the more elongate and fusiform species with which it occurs. The shape of the test is vaguely reminiscent of the latest Missourian and early Virgilian forms *T. oryziformis* Newell, 1934 and *T. secalicus* (Say, 1823), but those taxa are larger, much more elongate, and have more intensely fluted septa. Based on the inferred correlation of unit 14 with the Stanton cyclothem of the Midcontinent region, *Triticites* sp. B may represent a Virgilian-like ancestral morphotype preceding *T. oryziformis*, which first occurs in the Iatan cyclothem of the Midcontinent.

Occurrence: 60.6 and 64.8 m above the base of the section (unit 14); level - upper part of the Missourian Stage (upper part of the Kasimovian Stage).

***Triticites* sp. C**

Plate 3, figures 6, 7

Description: A minute species with a short, inflated fusiform test that attains five to six volutions at maturity. Test lengths of mature specimens show little variance and range from 3.30 to 3.74 mm. Test diameters of mature specimens range from 1.69 to 2.01 mm. The average form ratio is 1.91. The axis of coiling is straight and the lateral slopes are nearly straight to gently convex. Poles are bluntly to sharply pointed. The proloculus is small and spherical, averaging 0.91 mm.

The spirotheca is very thin and nondescript in inner volutions but becomes quite thick (relative to test size) and coarsely alveolar, particularly in the outermost one to two volutions. The spirotheca tends to thin towards the poles. Septal fluting is moderate and is strongest in the polar regions of the test. Chomata are small and mound-like in the inner volutions but become more tabular throughout growth.

Remarks: The small size of *Triticites* sp. C is the diagnostic feature, as it appears seemingly out of place among larger *Triticites* Group II forms. *Triticites* sp. C bears some resemblance to the types of *T. bungerensis* Kauffman and Roth, 1966 from Bunger Limestone Member of the Graham

Formation in north-central Texas. Nearly all measured characters of *Triticites* sp. C compare well with Kauffman and Roth's (1966) types except for the average form ratio, which is slightly lower among the herein illustrated forms. *Triticites* sp. C bears an even stronger resemblance to forms assigned to *T. bungerensis* by Wilde (2006) from the Big Hatchet Mountains, which are shorter and more inflated than the type specimens. Wilde's inflated forms, which occur lower in the Virgilian than the types, may be closely related to the Riepe Spring Limestone forms rather than the Bunger Limestone forms, which seem to be slightly younger (based on Wilde's positioning).

Occurrence: 99.7 and 100.1 m above the base of the section (unit 21); level - lower part of the Virgilian Stage (lower part of the Gzhelian Stage).

Plate 1

All illustrated specimens are from the uppermost part of the Ely Limestone (figs. 1–3) and the lower informal member of the Riepe Spring Limestone (figs. 4-11), Spruce Mountain Ridge, Elko County, Nevada, U.S.A. Specimens beginning with "F24…" belong to the Douglass-Henbest collection. Scale bars = 1 mm.

1–3. *Eowaeringella* sp. A

1. NSMR 14.8-3, 14.8 m above the base of the section (unit 1), axial thin section

2. NSMR 14.8-4, 14.8 m above the base of the section (unit 1), axial thin section

3. NSMR 14.8-5, 14.8 m above the base of the section (unit 1), axial thin section

4–7. *Triticites burgessae* Burma, 1942

4. NSMR 32.1-1, 32.1 m above the base of the section (unit 6), axial thin section

5. NSMR 32.1-6, 32.1 m above the base of the section (unit 6), axial thin section

6. NSMR 32.1-14, 32.1 m above the base of the section (unit 6), axial thin section

7. NSMR 32.1-8, 32.1 m above the base of the section (unit 6), axial thin section

8–11. *Triticites* aff. *celebroides* Ross, 1965

8. NSMR 32.1-3, 32.1 m above the base of the section (unit 6), axial thin section

9. NSMR 32.1-10, 32.1 m above the base of the section (unit 6), axial thin section

10. NSMR 32.1-15, 32.1 m above the base of the section (unit 6), axial thin section

11. NSMR 32.1-9, 32.1 m above the base of the section (unit 6), axial thin section.

Plate 1

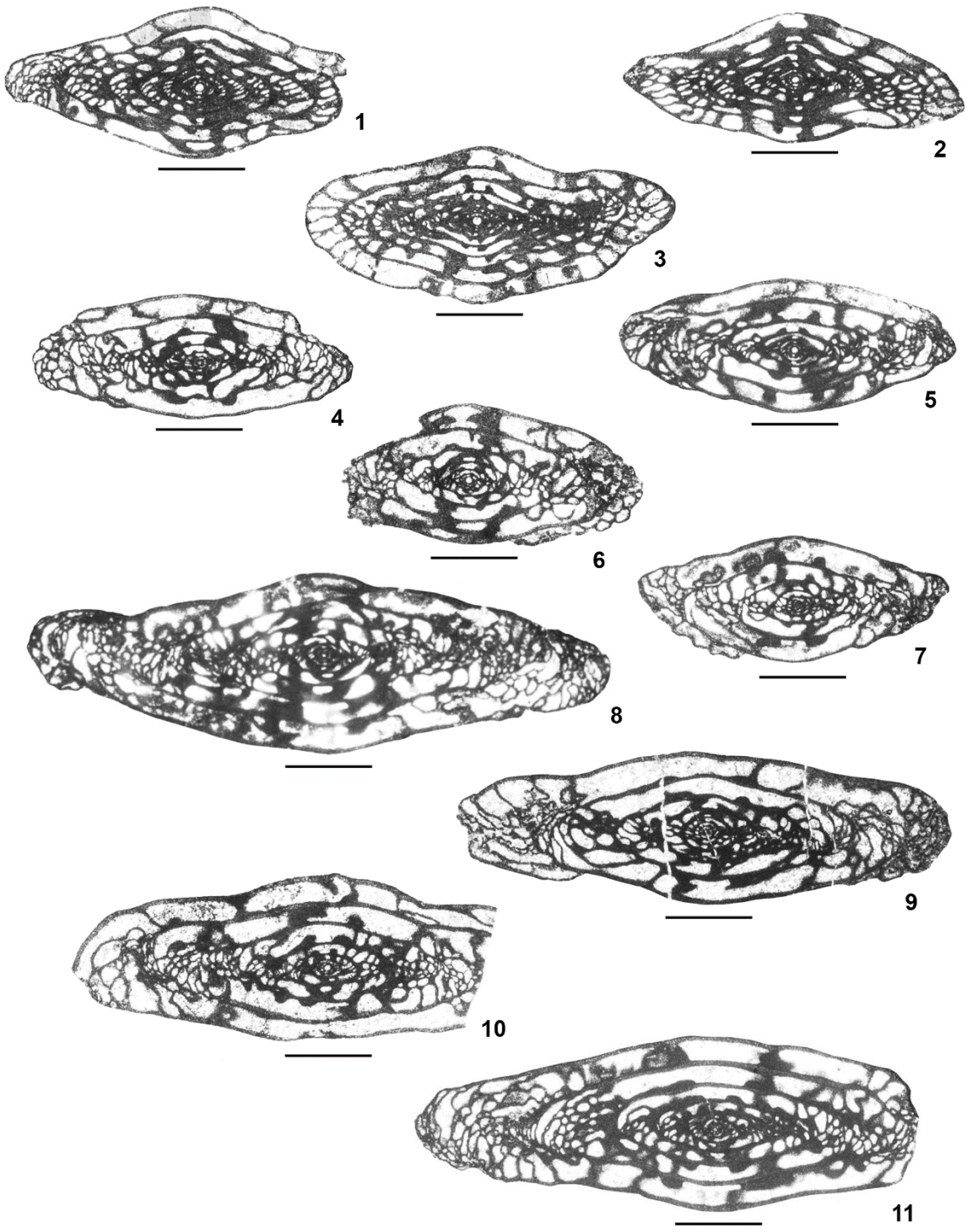

Plate 2

All illustrated specimens are from the lower informal member of the Riepe Spring Limestone, Spruce Mountain Ridge, Elko County, Nevada, U.S.A. Specimens beginning with "F24…" belong to the Douglass-Henbest collection. Scale bars = 1 mm.

1–6. *Eowaeringella* sp. B

1. NSMR 54.9-7, 54.9 m above the base of the section (unit 12), enlarged view of axial thin section to illustrate tripartite wall structure and planar septa

2. NSMR 54.9-7, 54.9 m above the base of the section (unit 12), enlarged view of axial thin section to illustrate tripartite wall structure and planar septa

3. NSMR 54.9-1, 54.9 m above the base of the section (unit 12), axial thin section

4. NSMR 54.9-2, 54.9 m above the base of the section (unit 12), axial thin section

5. NSMR 54.9-4, 54.9 m above the base of the section (unit 12), axial thin section

6. NSMR 54.9-5, 54.9 m above the base of the section (unit 12), axial thin section

7-9. *Triticites* sp. A

7. NSMR 64.8-14, 64.8 m above the base of the section (unit 14), axial thin section

8. NSMR 64.8-17, 64.8 m above the base of the section (unit 14), axial thin section

9. NSMR 64.8-18, 64.8 m above the base of the section (unit 14), axial thin section

10. *Triticites* sp. A?

10. NSMR 64.8-10, 64.8 m above the base of the section (unit 14), axial thin section

11. *Triticites* cf. *primarius* Merchant and Keroher, 1939

11. NSMR 64.8-9, 64.8 m above the base of the section (unit 14), axial thin section.

Plate 2

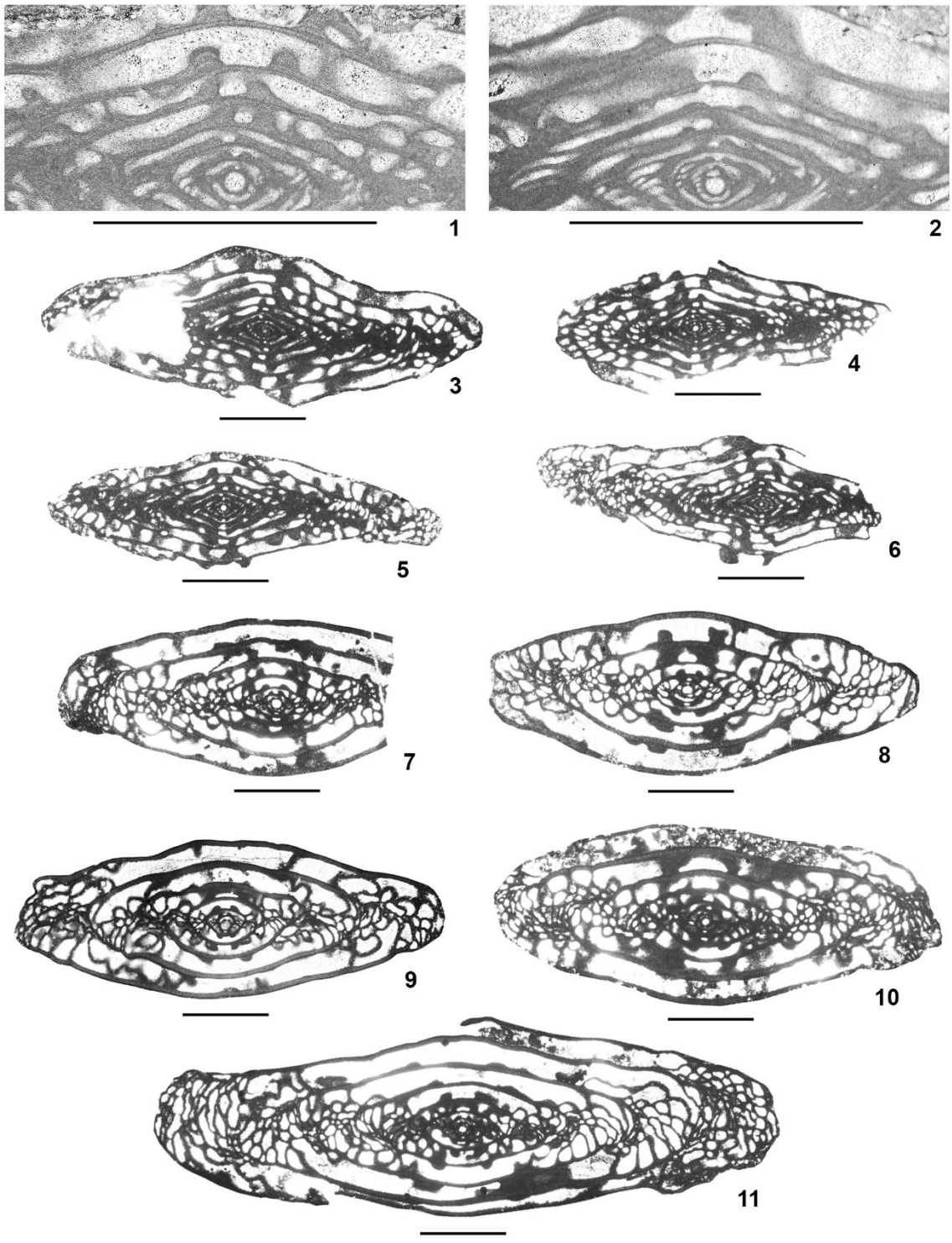

Plate 3

All illustrated specimens are from the lower (figs. 1-7) and middle (figs. 8-15) informal members of the Riepe Spring Limestone, Spruce Mountain Ridge, Elko County, Nevada, U.S.A. Specimens beginning with "F24…" belong to the Douglass-Henbest collection. Scale bars = 1 mm.

1, 2. *Triticites* sp. B

1. NSMR 60.6-5, 60.6 m above the base of the section (unit 14), axial thin section

2. NSMR 64.8-21, 64.8 m above the base of the section (unit 14), axial thin section

3, 4. *Triticites* cf. *jacksboroensis* Kauffman and Roth, 1966

3. NSMR 70-1, 70 m above the base of the section (unit 16), axial thin section

4. NSMR 100.1-8, 100.1 m above the base of the section (unit 21), axial thin section

5. *Pseudofusulinella* sp. A

5. NSMR 70-3, 70 m above the base of the section (unit 16), axial thin section

6, 7. *Triticites* sp. C

6. NSMR 100.1-6, 100.1 m above the base of the section (unit 21), axial thin section

7. NSMR 100.1-6, 100.1 m above the base of the section (unit 21), axial thin section

8–10. *Dunbarinella kauffmani* Wilde, 2006

8. NSMR 149.2-9, 149.2 m above the base of the section (unit 30), axial thin section

9. F24122-18, ~147 m above the base of the section (unit 30), axial thin section

10. NSMR 149.2-4, 149.2 m above the base of the section (unit 30), axial thin section

11–13. *Schubertella ciscoensis* Kauffman and Roth, 1966

11. NSMR 149.2-6, 149.2 m above the base of the section (unit 30), axial thin section

12. NSMR 150.4-5, 150.4 m above the base of the section (unit 30), axial thin section

13. F24123-9, ~150 m above the base of the section (unit 30), axial thin section

14, 15. *Triticites bensonensis* Ross and Tyrrell, 1965

14. F24123-11, ~150 m above the base of the section (unit 30), axial thin section

15. F24123-10, ~150 m above the base of the section (unit 30), axial thin section.

Plate 3

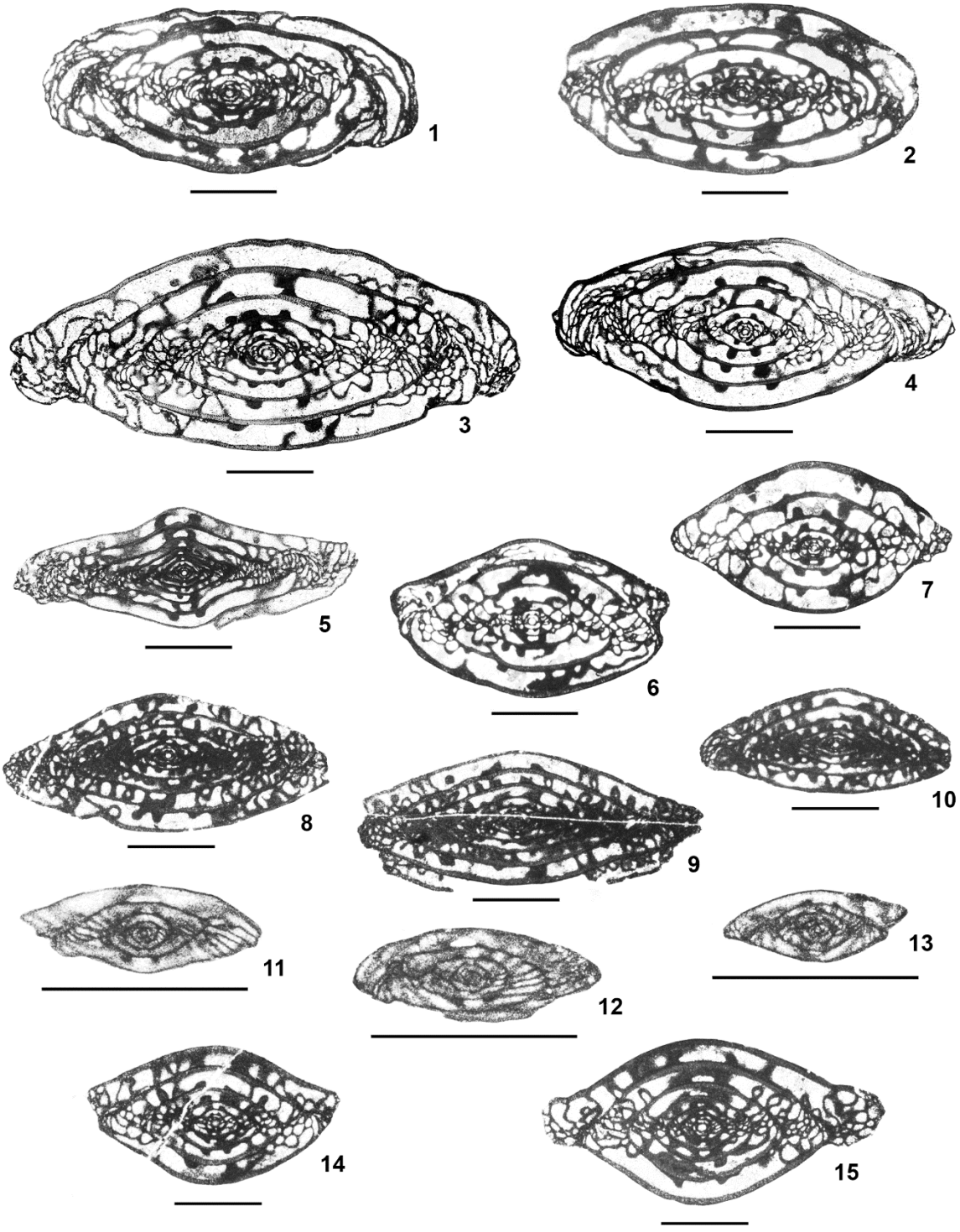

Plate 4

All illustrated specimens are from the middle informal member of the Riepe Spring Limestone, Spruce Mountain Ridge, Elko County, Nevada, U.S.A. Specimens beginning with "F24…" belong to the Douglass-Henbest collection. Scale bars = 1 mm.

1, 2. *Triticites cullomensis* Dunbar and Condra, 1927

1. USNM PAL 722043, 149.2 m above the base of the section (unit 30), axial thin section (immature specimen)

2. F24122-10, ~147 m above the base of the section (unit 30), axial thin section

3. *Triticites* cf. *inflatus* White, 1932

3. USNM PAL 722045, 178 m above the base of the section (unit 36), axial thin section

4. *Pseudofusulinella* cf. *nitida* Skinner and Wilde, 1965b

4. NSMR 178-4, 178 m above the base of the section (unit 36), axial thin section

5. *Triticites* aff. *creekensis* Thompson, 1954

5. F24124-31, ~168 m above the base of the section (unit 34), axial thin section; illustrated specimen bears a strong resemblance to Figure 6 but has a much smaller proloculus. All other characters are very similar

6, 7. *Triticites creekensis* Thompson, 1954

6. F24124-34, ~168 m above the base of the section (unit 34), axial thin section

7. F24124-37, ~168 m above the base of the section (unit 34), equatorial thin section

Plate 4

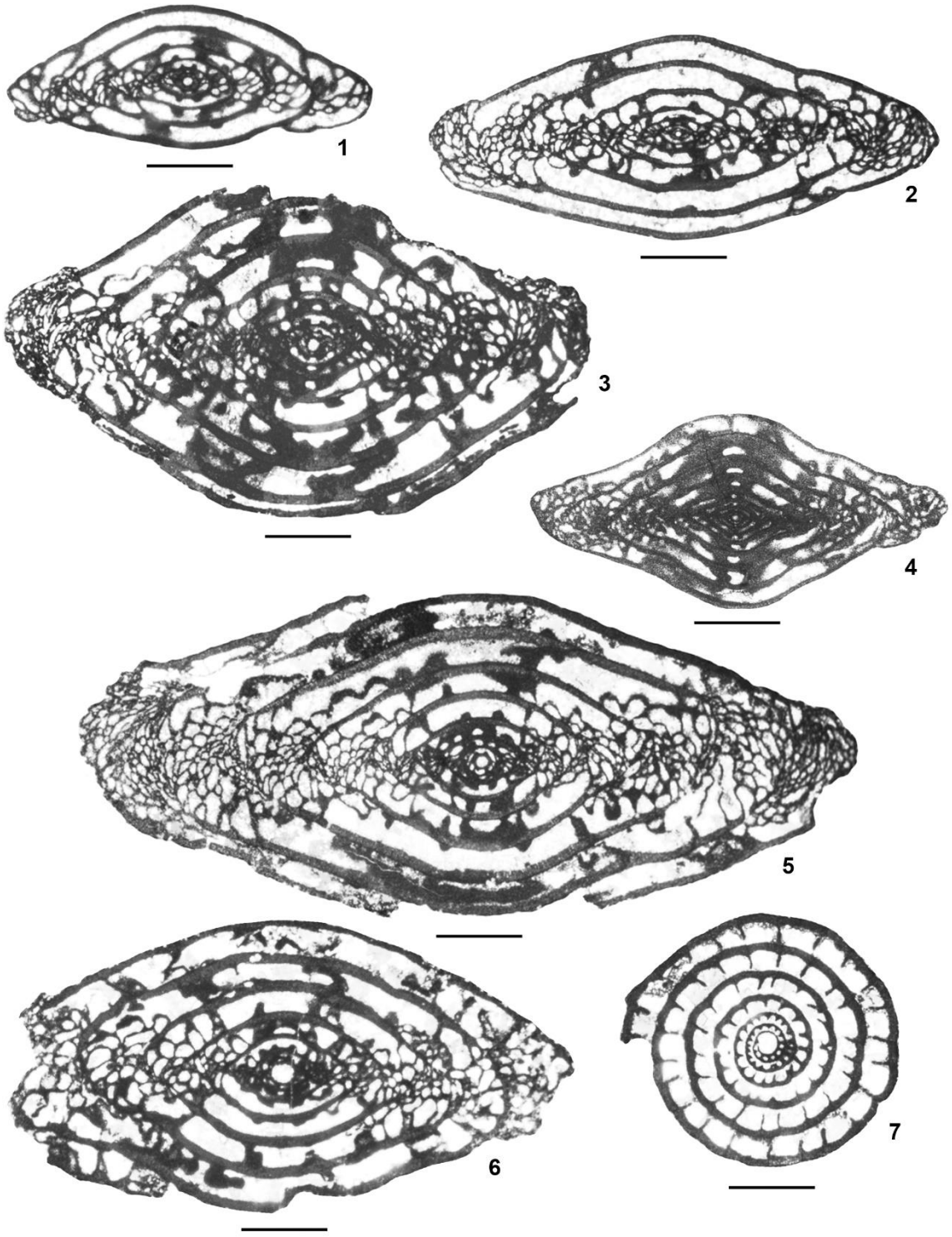

Plate 5

All illustrated specimens are from the middle informal member of the Riepe Spring Limestone, Spruce Mountain Ridge, Elko County, Nevada, U.S.A. Specimens beginning with "F24…" belong to the Douglass-Henbest collection. Scale bars = 1 mm.

1, 2. *Pseudofusulinella* sp. B

1. F24127-61, ~216 m above the base of the section (unit 45), axial thin section

2. F24127-64, ~216 m above the base of the section (unit 45), axial thin section

3. *Triticites* cf. *californicus* Thompson and Hazzard, 1946

3. NSMR 215.8-4, 215.8 m above the base of the section (unit 45), axial thin section

4. *Triticites* cf. *cellamagnus* Thompson and Bissell, 1954

4. F24126-26, ~199 m above the base of the section (unit 42), axial thin section

5–7. *Triticites pinguis* Dunbar and Skinner, 1937

5. F24127-25, ~216 m above the base of the section (unit 45), equatorial thin section

6. F24127-1, ~216 m above the base of the section (unit 45), axial thin section

7. F24127-9, ~216 m above the base of the section (unit 45), axial thin section.

Plate 5

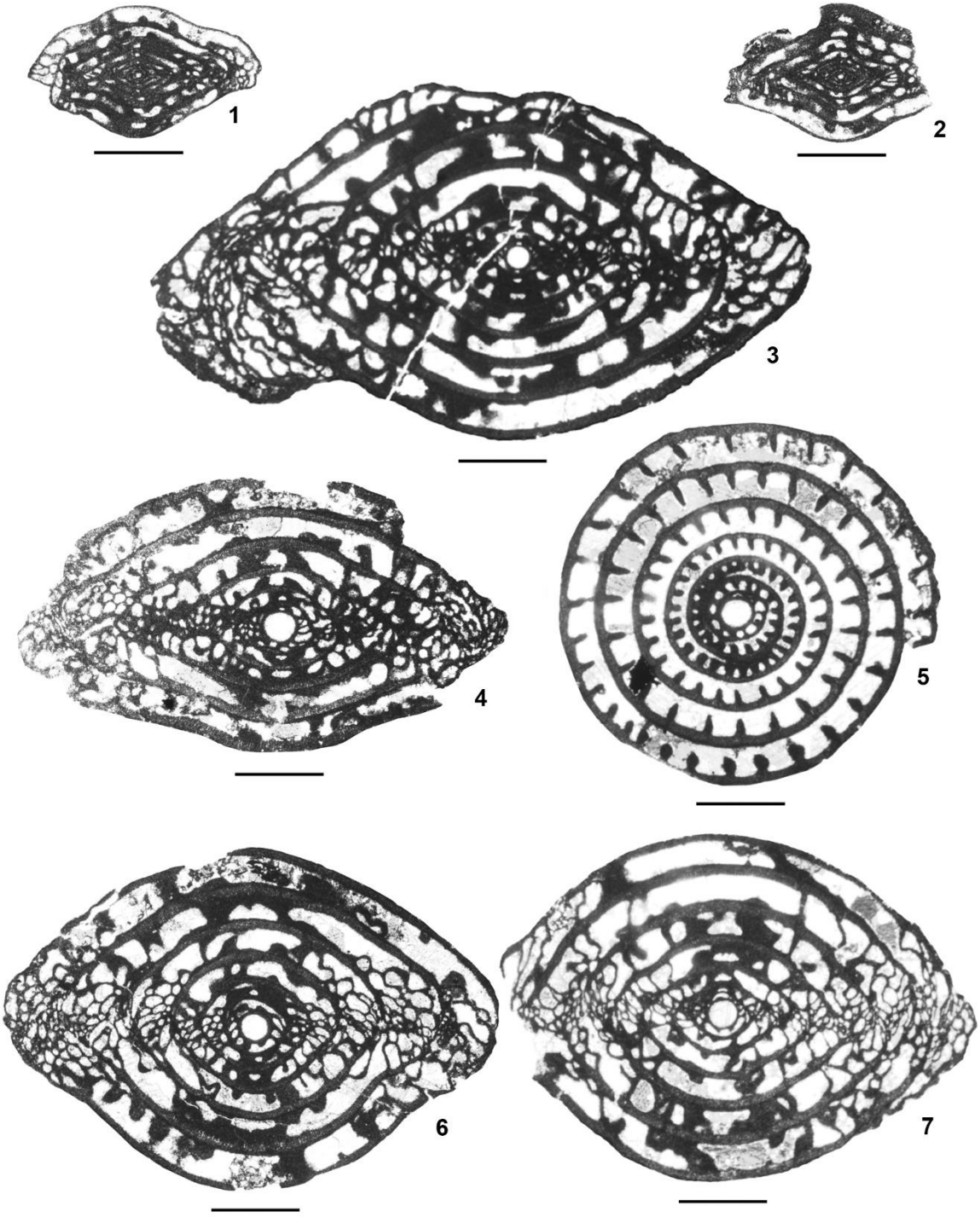

Plate 6

All illustrated specimens are from the middle informal member of the Riepe Spring Limestone, Spruce Mountain Ridge, Elko County, Nevada, U.S.A. Specimens beginning with "F24…" belong to the Douglass-Henbest collection. Scale bars = 1 mm.

1–3. *Pseudofusulina mediotenebraeus* Wilde, 2006

1. F24127-33, ~216 m above the base of the section (unit 45), axial thin section

2. F24127-48, ~216 m above the base of the section (unit 45), equatorial thin section

3. NSMR 215.8-7, 215.8 m above the base of the section (unit 45), axial thin section

4–6. *Cuniculinella* sp. A

4. NSMR 227.8-8, 227.8 m above the base of the section (unit 48), tangential thin section demonstrating the presence of cuniculi on the right side of the photomicrograph

5. F24128-6, ~228 m above the base of the section (unit 48), axial thin section

6. NSMR 227.8-7, 227.8 m above the base of the section (unit 48), axial thin section.

Plate 6

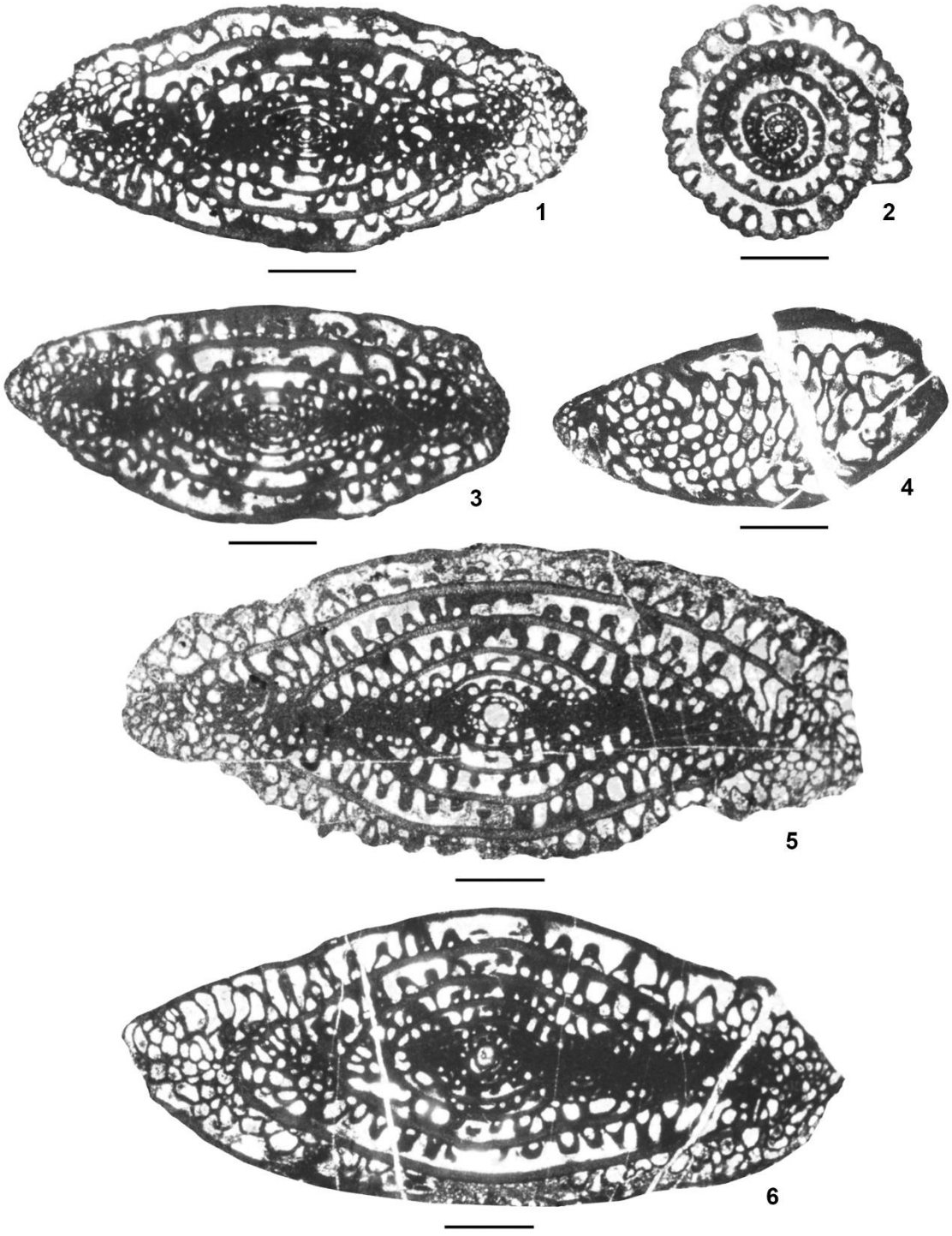

Plate 7

All illustrated specimens are from the upper informal member of the Riepe Spring Limestone, Spruce Mountain Ridge, Elko County, Nevada, U.S.A. Specimens beginning with "F24…" belong to the Douglass-Henbest collection. Scale bars = 1 mm.

1, 2. *Cuniculinella*? sp. B

1. F24128-11, ~228 m above the base of the section (unit 48), axial thin section

2. F24128-16, ~228 m above the base of the section (unit 48), axial thin section

3–5. *Schwagerina* sp. A

3. F24130-1, ~254 m above the base of the section (unit 56), axial thin section

4. F24130-2, ~254 m above the base of the section (unit 56), axial thin section

5. F24130-5, ~254 m above the base of the section (unit 56), axial thin section.

Plate 7

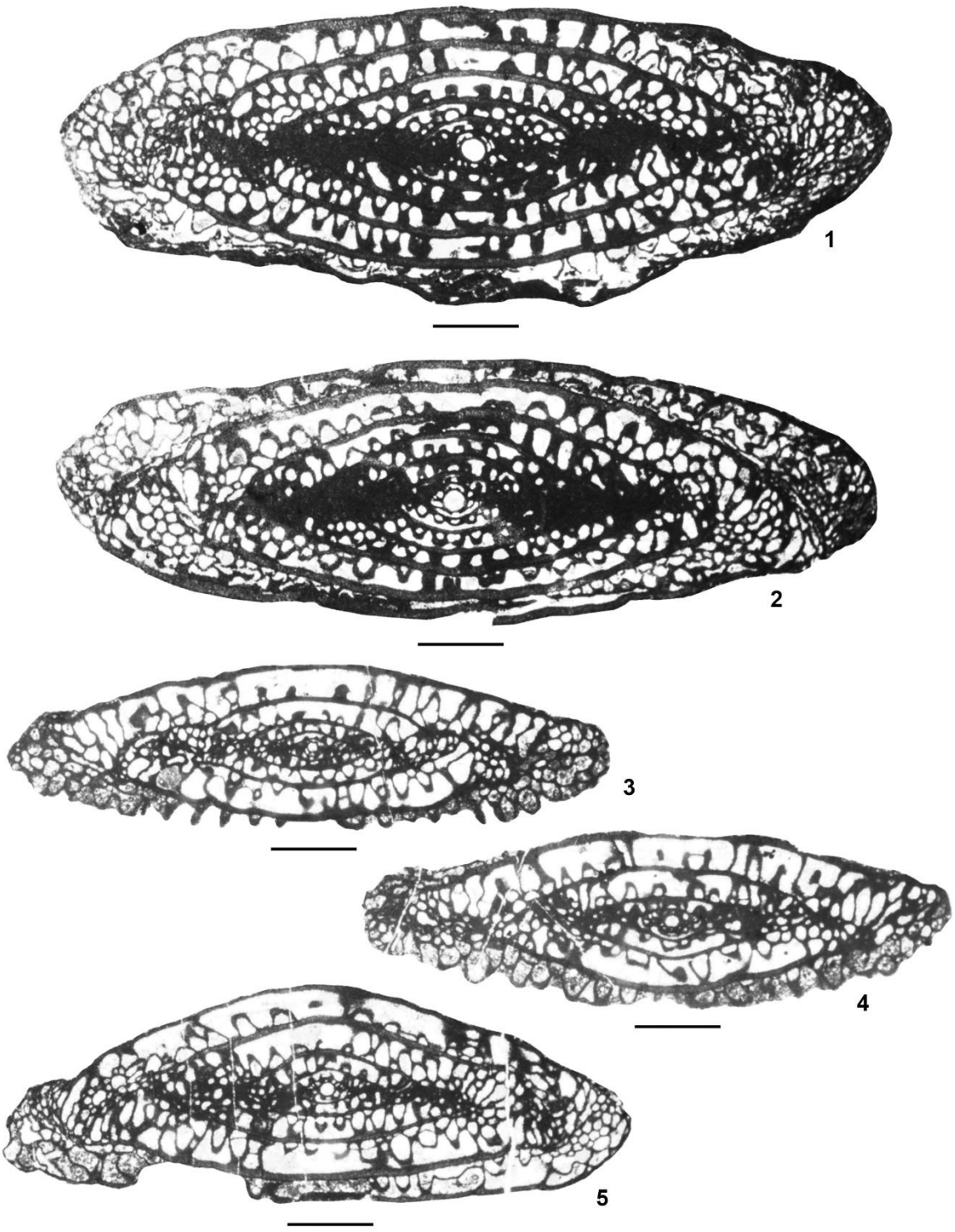

Plate 8

All illustrated specimens are from the upper informal member of the Riepe Spring Limestone, Spruce Mountain Ridge, Elko County, Nevada, U.S.A. Specimens beginning with "F24…" belong to the Douglass-Henbest collection. Scale bars = 1 mm.

1–4. *Alaskanella* sp. A

1. F24133-1, ~272 m above the base of the section (unit 60), axial thin section

2. F24133-14, ~272 m above the base of the section (unit 60), axial thin section

3. F24133-6, ~272m above the base of the section (unit 60), axial thin section

4. NSMR 272.3-4, 272.3 m above the base of the section (unit 60), axial thin section

5–7. *Schwagerina neolata* Thompson, 1954

5. F24134-2, ~274 m above the base of the section (unit 60), axial thin section

6. F24134-5, ~274 m above the base of the section (unit 60), axial thin section

7. F24134-4, ~274 m above the base of the section (unit 60), axial thin section.

Plate 8

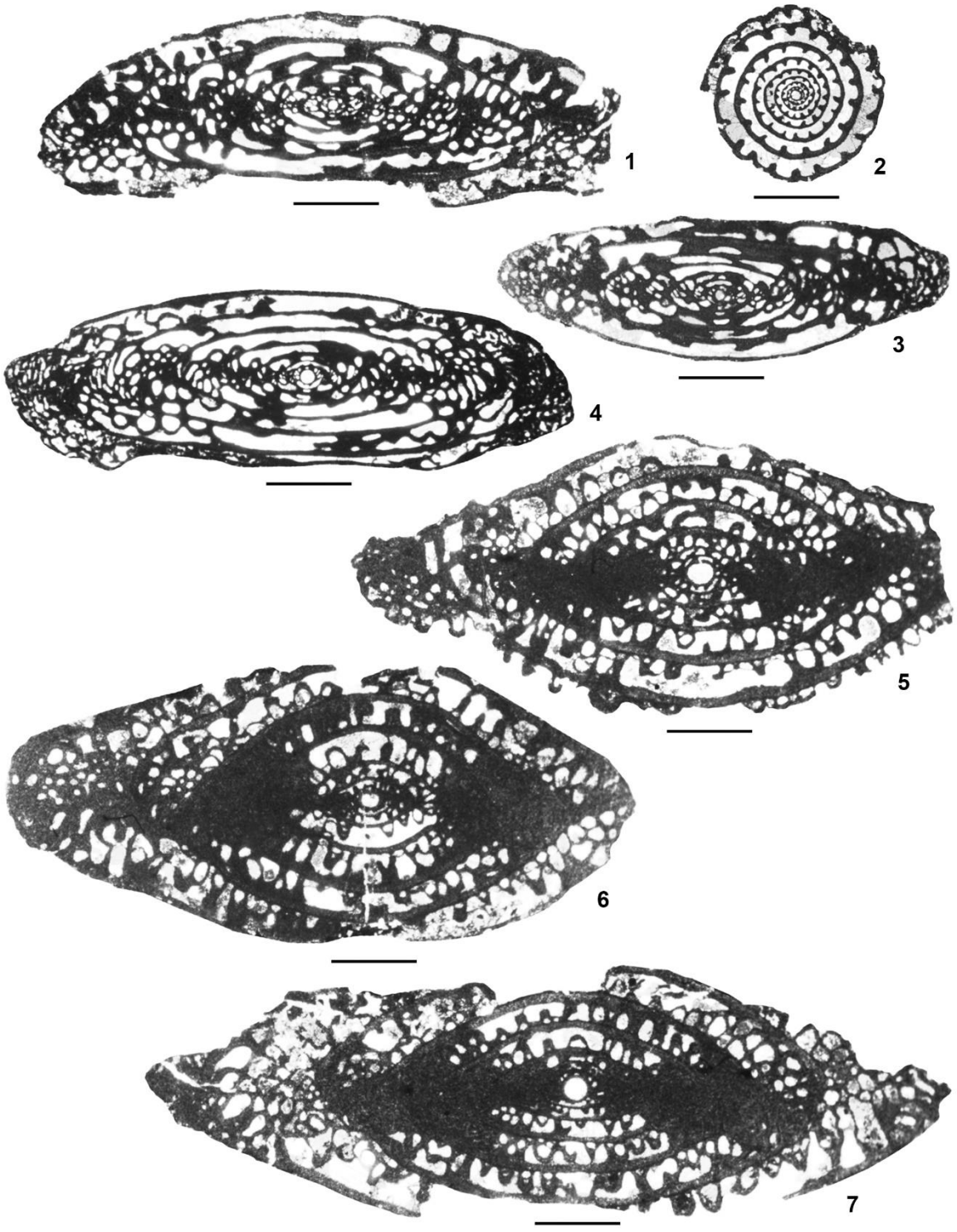

Plate 9

All illustrated specimens are from the upper informal member of the Riepe Spring Limestone, Spruce Mountain Ridge, Elko County, Nevada, U.S.A. Specimens beginning with "F24…" belong to the Douglass-Henbest collection. Scale bars = 1 mm.

1, 2. *Schwagerina wellsensis* Thompson, 1954

1. F24136-3, ~280 m above the base of the section (unit 60), axial thin section

2. F24141-8, ~289 m above the base of the section (unit 60), axial thin section

3, 4. *Schwagerina* sp. B

3. F24136-2, ~280 m above the base of the section (unit 60), axial thin section

4. F24138-1, ~281 m above the base of the section (unit 60), axial thin section.

Plate 9

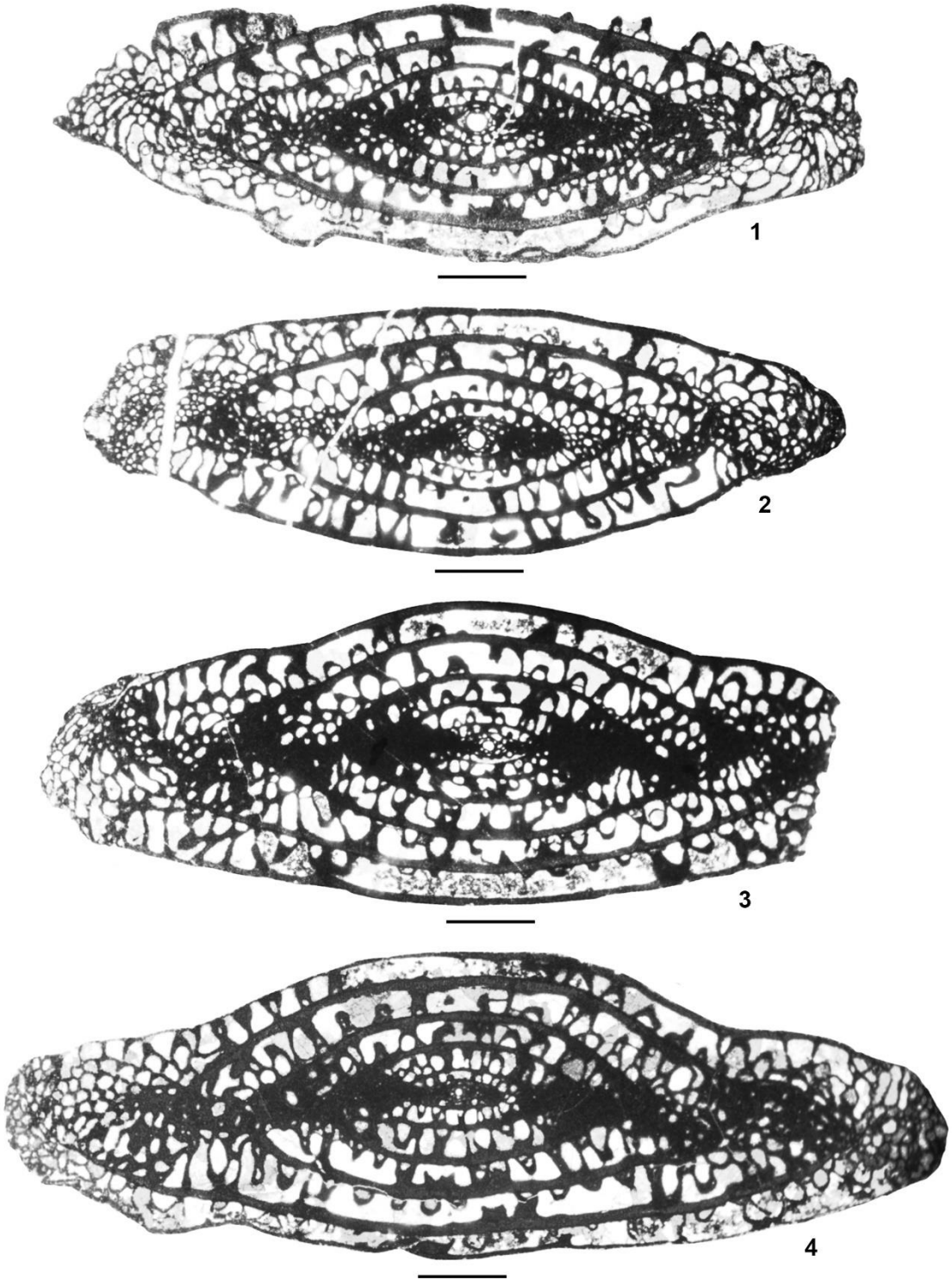

Plate 10

All illustrated specimens are from the upper informal member of the Riepe Spring Limestone, Spruce Mountain Ridge, Elko County, Nevada, U.S.A. Specimens beginning with "F24…" belong to the Douglass-Henbest collection. Scale bars = 1 mm.

1, 2, 4. *Pseudoschwagerina robusta* (Meek, 1864)

1. F24143-3, ~292 m above the base of the section (unit 61), axial thin section

2. F24143-6, ~292 m above the base of the section (unit 61), equatorial thin section

4. NSMR 286.9-3, 286.9 m above the base of the section (unit 60), axial thin section

3. *Alaskanella* sp. B

3. F24146-24, ~295 m above the base of the section (unit 61), axial thin section.

Plate 10

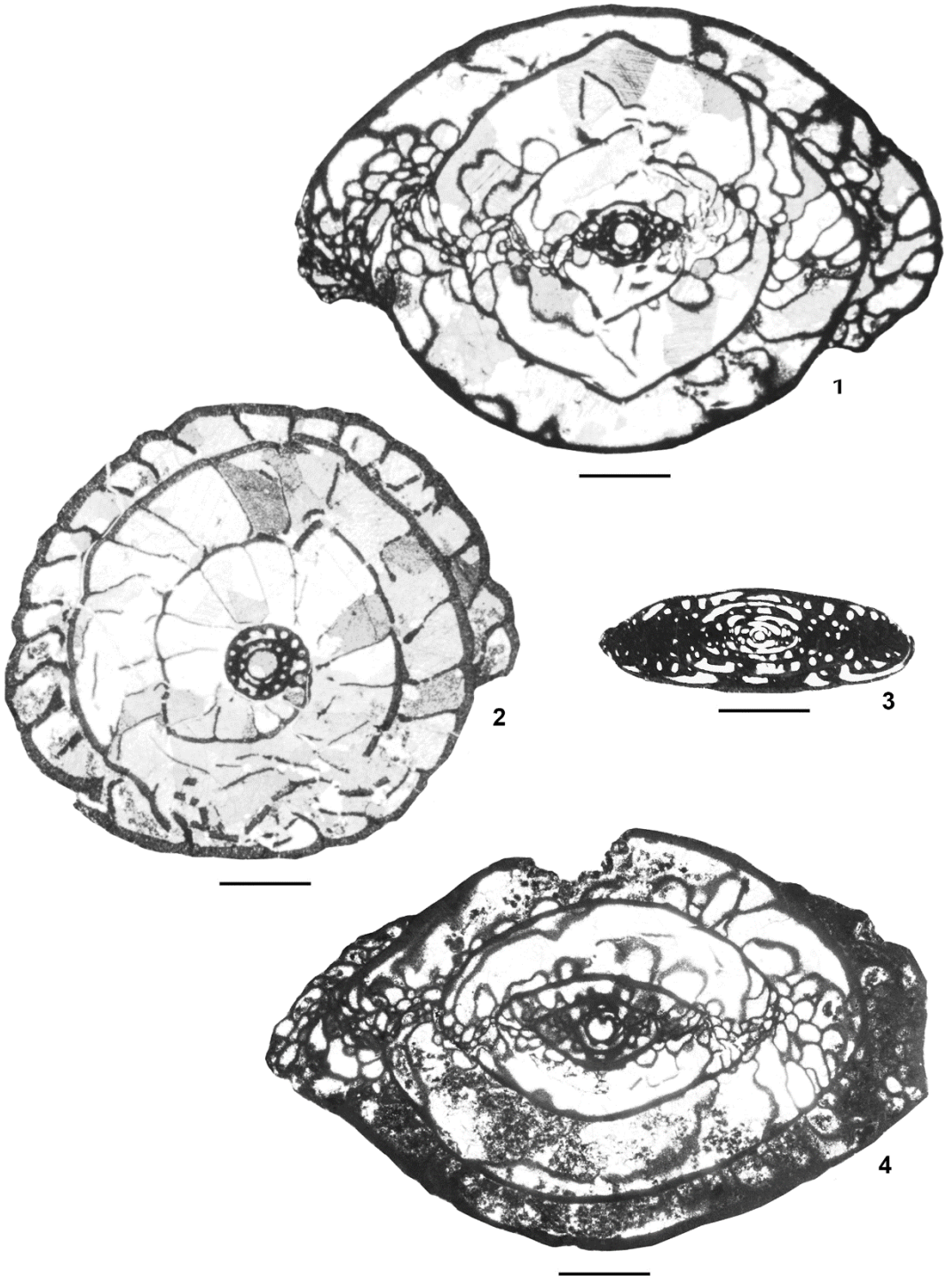

Plate 11

All illustrated specimens are from the upper informal member of the Riepe Spring Limestone, Spruce Mountain Ridge, Elko County, Nevada, U.S.A. Specimens beginning with "F24…" belong to the Douglass-Henbest collection. Scale bars = 1 mm.

1–4. *Eoparafusulina linearis* (Dunbar and Skinner, 1937)

1. NSMR 304.4-2, 304.4 m above the base of the section (unit 61), axial thin section

2. F24138-8, ~281 m above the base of the section (unit 60), axial thin section

3. NSMR 304.4-1, 304.4 m above the base of the section (unit 61), axial thin section.

Plate 11

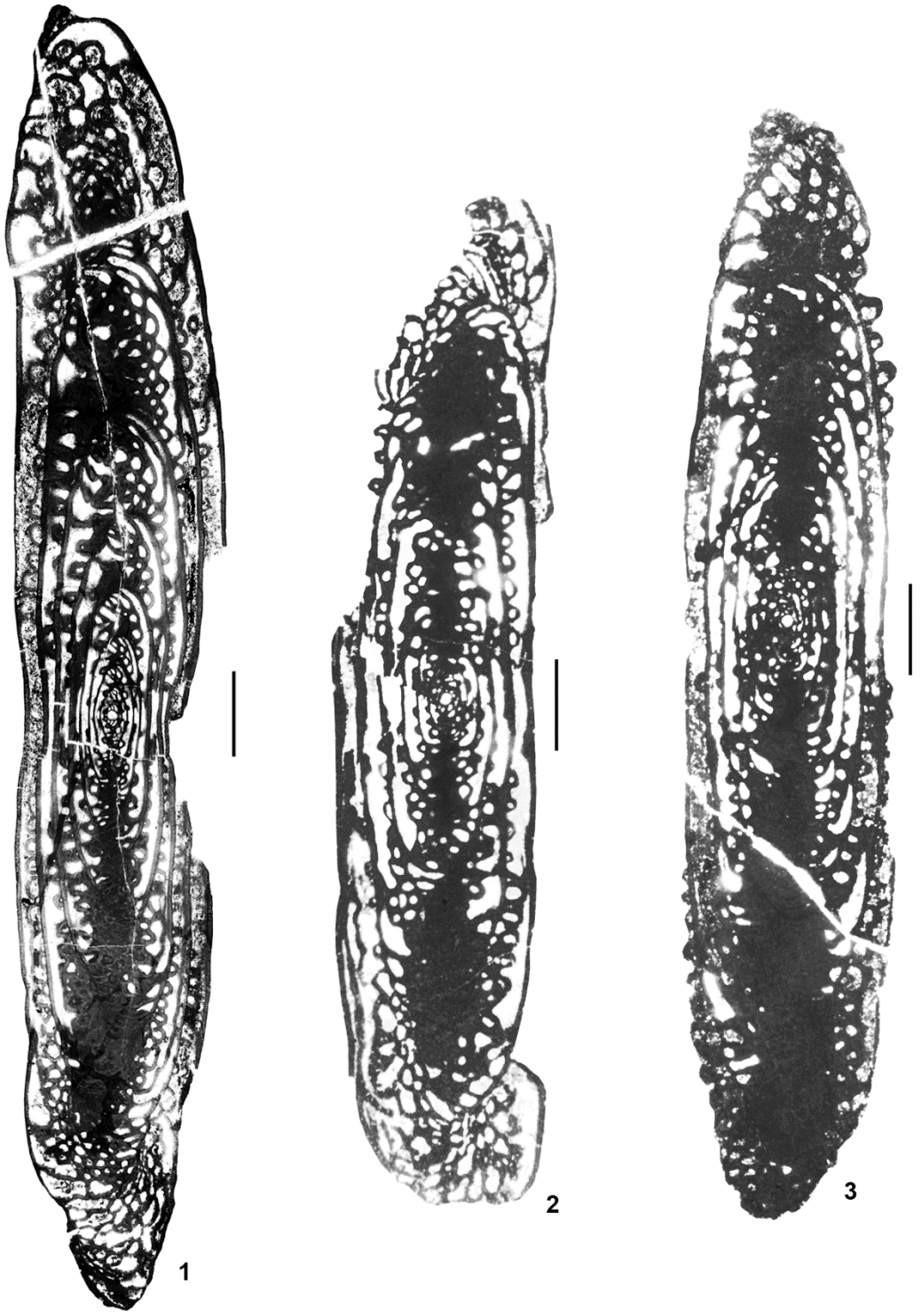

Plate 12

All illustrated specimens are from the upper informal member of the Riepe Spring Limestone, Spruce Mountain Ridge, Elko County, Nevada, U.S.A. Specimens beginning with "F24…" belong to the Douglass-Henbest collection. Scale bars = 1 mm.

1–3. *Schwagerina glassensis* Ross and Ross, 2003

1. F24143-11, ~292 m above the base of the section (unit 61), axial thin section

2. F24143-37, ~292 m above the base of the section (unit 61), equatorial thin section

3. F24143-16, ~292 m above the base of the section (unit 61), axial thin section

4, 5. *Pseudoschwagerina* cf. *convexa* Thompson, 1954

4. NSMR 286.9-1, 286.9 m above the base of the section (unit 60), axial thin section

5. NSMR 286.9-2, 286.9 m above the base of the section (unit 60), axial thin section.

Plate 12

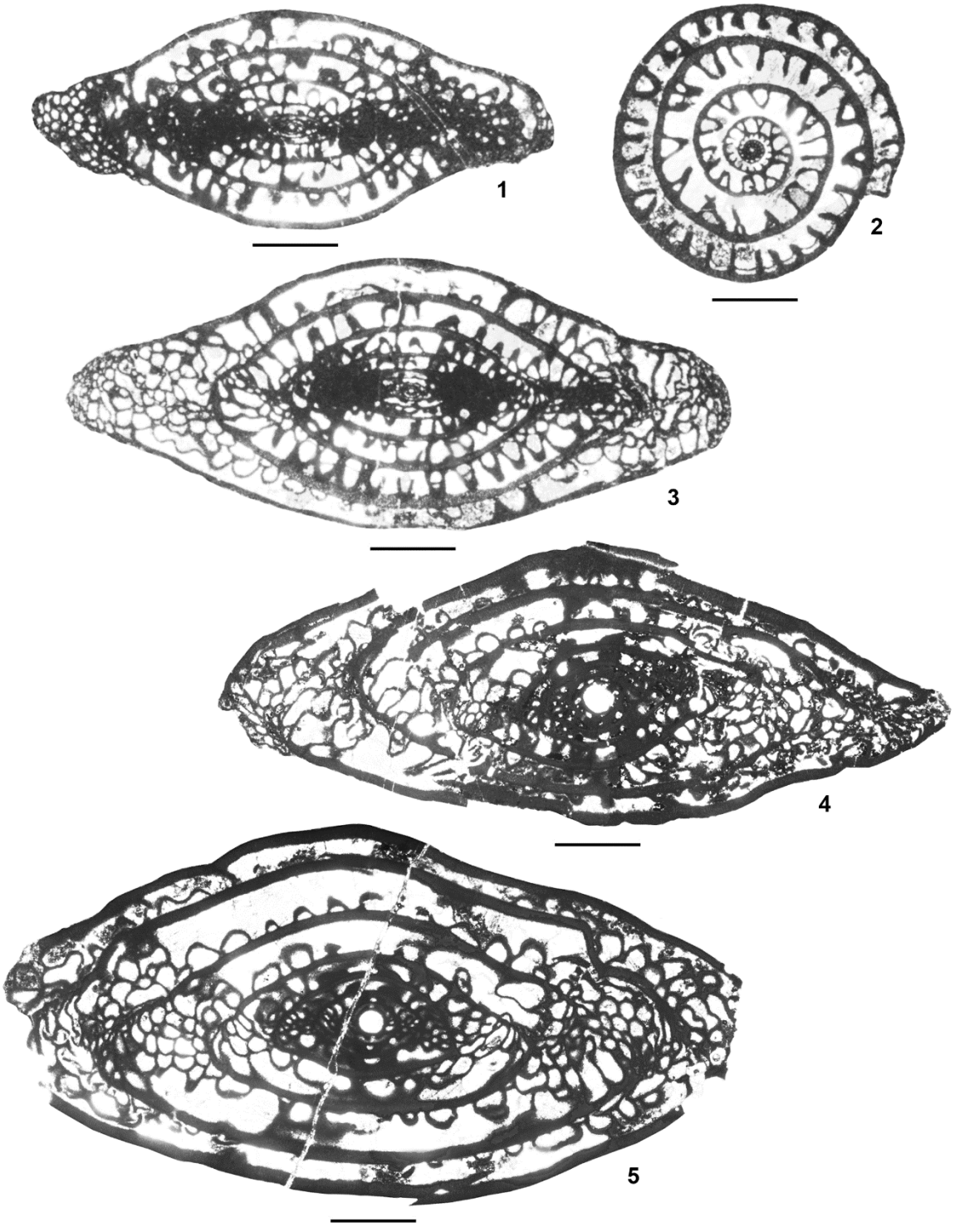

Plate 13

All illustrated specimens are from the upper informal member of the Riepe Spring Limestone, Spruce Mountain Ridge, Elko County, Nevada, U.S.A. Specimens beginning with "F24…" belong to the Douglass-Henbest collection. Scale bars = 1 mm.

1-6. *Schwagerina* sp.

1. F24152-16, level of recovery excluded from field notes of R.C. Douglass, axial thin section

2. F24152-14, level of recovery excluded from field notes of R.C. Douglass, axial thin section

3. F24152-1, level of recovery excluded from field notes of R.C. Douglass, axial thin section

4. F24151-25, level of recovery excluded from field notes of R.C. Douglass, equatorial thin section

5. NSMR 346.4-4, 346.4 m above the base of the section (unit 64), tangential thin section illustrating incipient cuniculi

6. F24152-2, level of recovery excluded from field notes of R.C. Douglass, axial thin section

7. *Schwagerina* sp. C

7. F24181-10**,** level of recovery excluded from field notes of R.C. Douglass, tangential thin section illustrating incipient cuniculi.

Plate 13

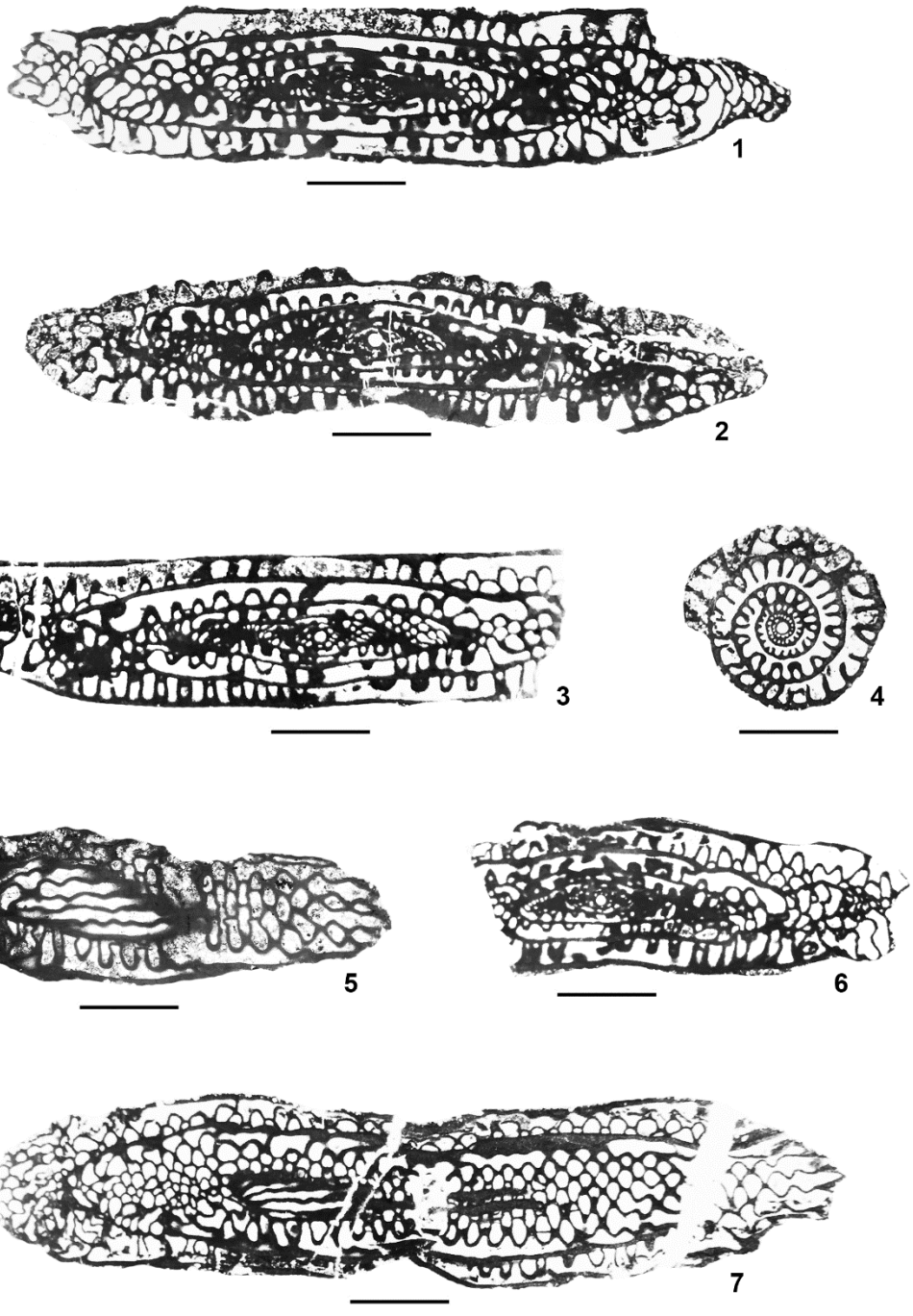

Plate 14

All illustrated specimens are from the upper informal member of the Riepe Spring Limestone, Spruce Mountain Ridge, Elko County, Nevada, U.S.A. Specimens beginning with "F24…" belong to the Douglass-Henbest collection. Scale bars = 1 mm.

1–4. Gen. n. A sp. A

1. F24181-12, level of recovery excluded from field notes of R.C. Douglass, axial thin section

2. F24178-22, ~343 m above the base of the section (unit 64), axial thin section

3. F24178-25, ~343 m above the base of the section (unit 64), axial thin section

4. F24178-23, ~343 m above the base of the section (unit 64), axial thin section

5–7. *Schwagerina franklinensis* Dunbar and Skinner, 1937

5. F24178-11, ~343 m above the base of the section (unit 64), equatorial thin section

6. F24180-1, ~347 m above the base of the section (unit 64), axial thin section

7. F24178-3, ~343 m above the base of the section (unit 64), axial thin section.

Plate 14

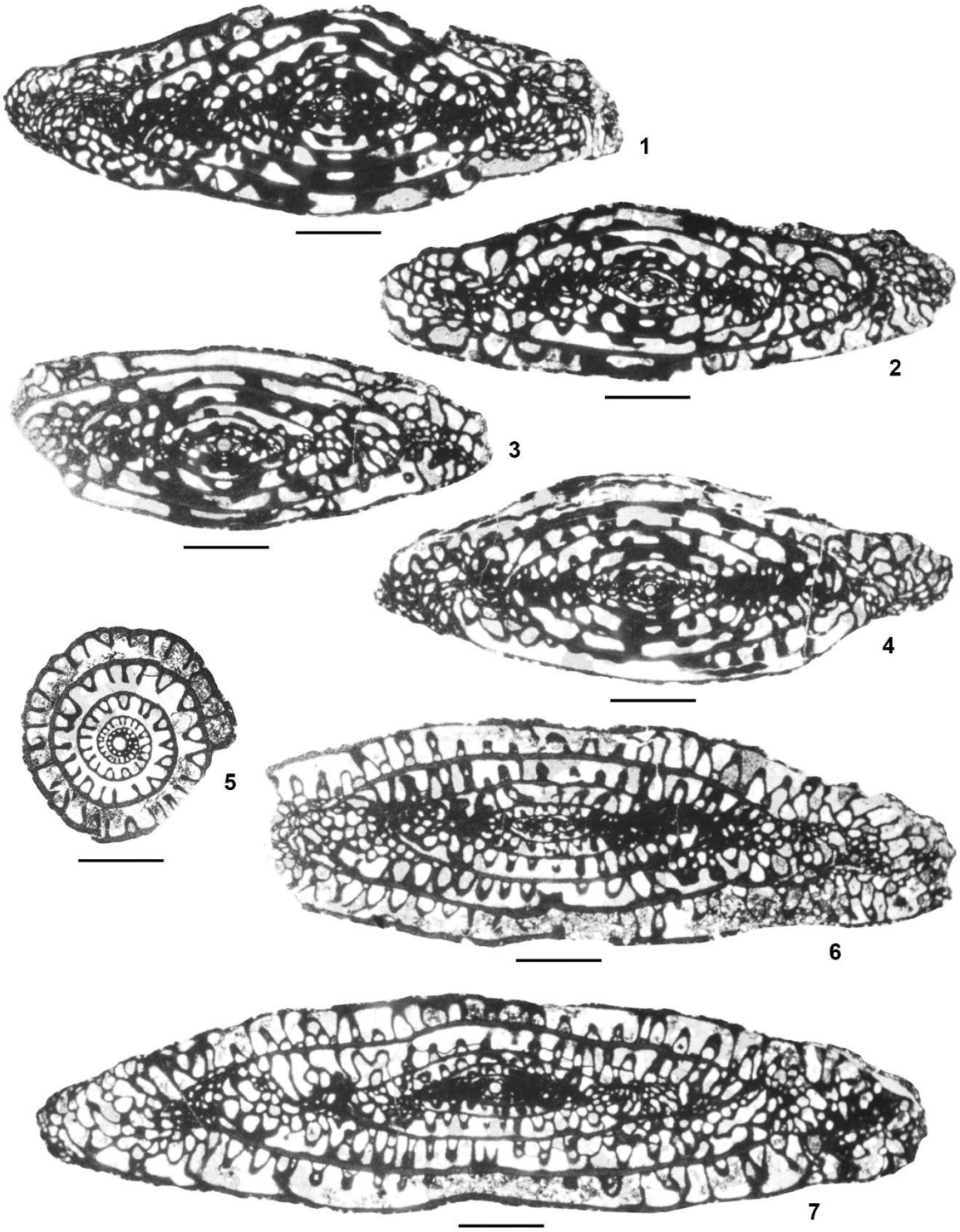

Plate 15

All illustrated specimens are from the upper informal member of the Riepe Spring Limestone, Spruce Mountain Ridge, Elko County, Nevada, U.S.A. Specimens beginning with "F24…" belong to the Douglass-Henbest collection. Scale bars = 1 mm.

1, 2. Schwagerina sp. C

1. F24180-22, ~347 m above the base of the section (unit 64), axial thin section

2. NSMR 392.5-4, 392.5 m above the base of the section (unit 68), axial thin section

3–6. Alaskanella sp. C

3. NSMR 346.4-1, 346.4 m above the base of the section (unit 64), axial thin section

4. F24179-18, ~346 m above the base of the section (unit 64), equatorial thin section

5. F24179-2, ~346 m above the base of the section (unit 64), axial thin section

6. F24179-3, ~346 m above the base of the section (unit 64), axial thin section.

Plate 15

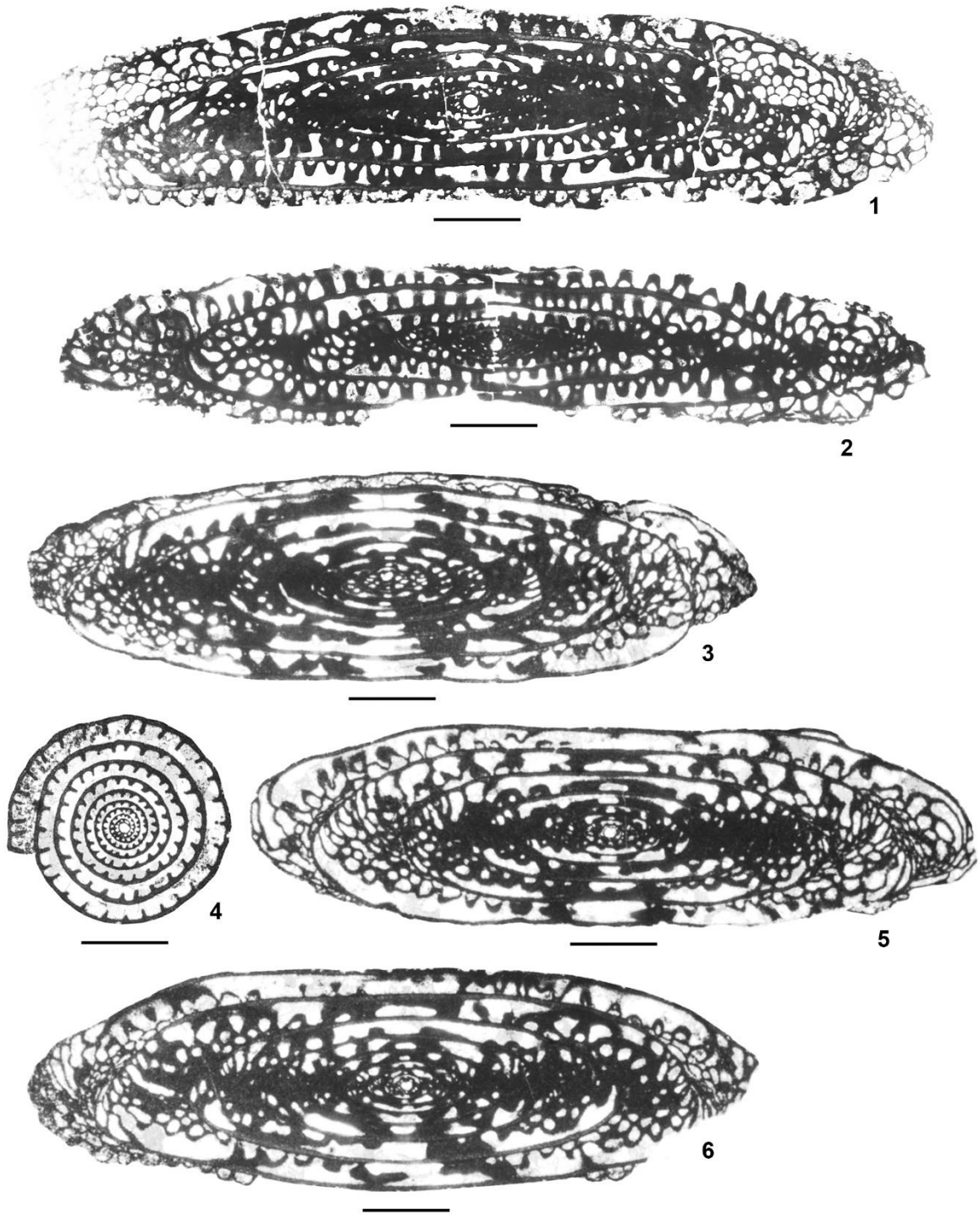

CHAPTER 5 – INTRODUCTORY REMARKS

The monotypic genus *Douglassites* Read and Nestell, 2018 was described from unpublished fusulinid material on loan from the Smithsonian's Douglass-Henbest collection. Raymond Douglass preliminarily assigned the specimens to an informal new genus which he called "*Rugotriticites*," but the observed ontogenesis and wall structure indicate that the forms belong to the Schubertellidae rather than the Triticitidae.

All specimens of *Douglassites sprucensis* Read and Nestell, 2018 were recovered from unit 34 in the middle informal member of the Riepe Spring Limestone. Figure 5.0 illustrates the relative stratigraphic position of the interval discussed in this chapter (outlined in red) within the NSMR section.

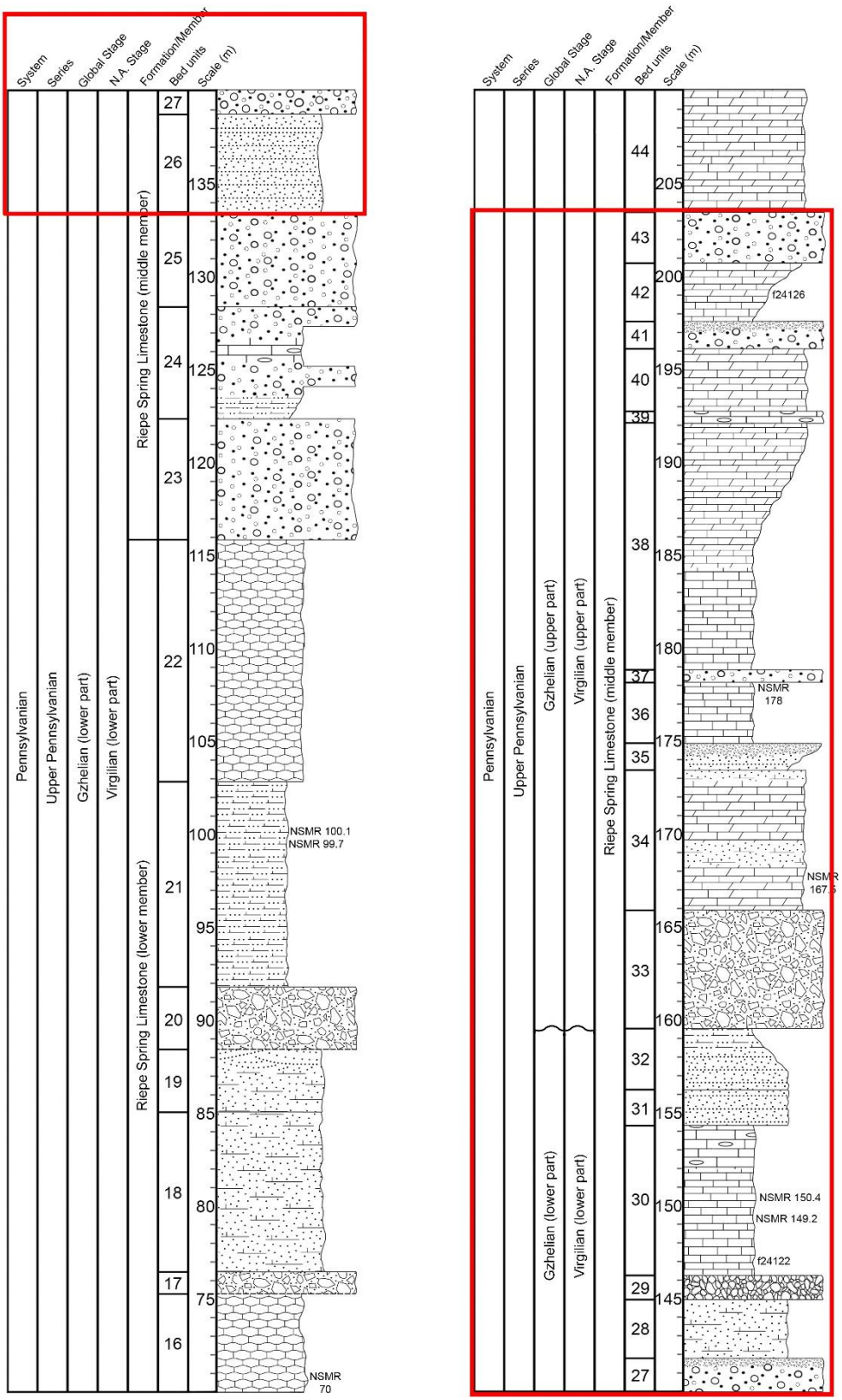

Fig. 5.0 – Stratigraphic column illustrating the portion of the NSMR section discussed in the following chapter (outlined in red).

The Micropaleontology Project, Inc.

Queens College/Rosenthal Lib 4th Floor
65-30 Kissena Blvd
Flushing, NY 11367-1575
PH: 718-570-0505
Fax: 718-570-0506
Nov. 12, 2018

Michael T. Read
Earth & Environmental Sciences, UT Arlington
Geosciences Building, Office 208

Dear Mr. Read,

I am writing to inform you that permission is formally granted for you to include in your dissertation your manuscript jointly authored with Merlynd Nestell, published in Micropaleontology vol. 64 (4), entitled: Douglassites, a new genus of schubertellid fusulinid from the Virgilian (Upper Pennsylvanian) of Elko County, Nevada, U.S.A."

Please do not hesitate to contact me if you need any other information in support of your request.

Sincerely yours,

Prof. Michael A. Kaminski
Editor-in-Chief, *Micropaleontology*

CHAPTER 5: *DOUGLASSITES*, A NEW GENUS OF SCHUBERTELLID FUSULINID FROM THE VIRGILIAN (UPPER PENNSYLVANIAN) OF ELKO COUNTY, NEVADA, U.S.A.

Michael T. Read and Merlynd K. Nestell

Read, M.T., and Nestell, M.K., 2018, *Douglassites*, a new genus of schubertellid fusulinid from the Virgilian (Upper Pennsylvanian) of Elko County, Nevada, U.S.A.: Micropaleontology, v. 64, no. 4, p. 317–327.

Abstract: A new genus of large schubertellid fusulinid, *Douglassites* n. gen., is described from the upper Virgilian (Upper Pennsylvanian) part of the Riepe Spring Limestone of Spruce Mountain Ridge, Elko County, Nevada, where it occurs with forms belonging to *Triticites* Group IV. The new monotypic genus was identified from thin sections acquired on loan from the Douglass-Henbest collection of the Smithsonian National Museum of Natural History. *Douglassites sprucensis* n. gen. n. sp. is among the largest known Carboniferous species of Schubertellidae and exhibits a spirothecal development that parallels forms of the predominantly Paleo-Tethyan and Peri-Gondwanan Biwaellinae subfamily (i.e., *Biwaella* and *Dutkevichites*). The occurrence of such a large and advanced form of schubertellid in Upper Pennsylvanian deposits of western North America is unique, as the appearance of *D. sprucensis* n. gen. n. sp. considerably predates the major radiation and dispersal events of the Cisuralian (Early Permian) and Guadalupian (Middle Permian) age Schubertellidae.

Introduction

A new genus of Late Pennsylvanian schubertellid fusulinid, *Douglassites* n. gen., is described from the middle member of the Riepe Spring Limestone of North Spruce Mountain Ridge (NSMR), Elko County, Nevada. Several peculiarities of the new taxon along with its potential, yet not fully understood phylogenetic affinities, are discussed. *Douglassites*

sprucensis n. gen. n. sp. is an unusual fusulinid that, although assigned to the Schubertellidae, has several characters resembling features of primitive forms of North American Triticites and several small Paleo-Tethyan schwagerinids (e.g., *Schwageriniformis* Bensh in Rauser-Chernousova et al. 1996). *Douglassites sprucensis* n. gen. n. sp. is only known to occur in one thick limestone unit of the upper Virgilian part of the Riepe Spring Limestone (unit 9), where it has been recovered with *Triticites creekensis* Thompson 1954. This large and inflated species of *Triticites* is well known from similar aged strata in the Midcontinent and western parts of the United States and provides valuable biostratigraphic control. To date, no distinct intermediate ancestral forms preceding the first appearance of *D. sprucensis* have been identified, but the Virgilian age *Schubertella ciscoensis* Kauffman and Roth 1966 occurs below *D. sprucensis* n. gen. n. sp. in the section.

Geologic Setting

The onset of Variscan-Alleghenian-Ouachita orogenesis during Devonian time and the subsequent Carboniferous closure of the Rheic Ocean resulted in the termination of a major tropical-subtropical marine migratory corridor separating Laurasia and Gondwanaland and the pronounced physiographic isolation of Pennsylvanian benthos (Ross 1967; Groves et al. 2007; Nance et al. 2010). The low diversity Late Pennsylvanian schubertellid stock of the Midcontinent-Andean faunal province originated from migrant

Paleo-Tethyan forms of *Eoschubertella* Thompson 1937 or *Schubertina* Marshall 1969, which appeared along the coast of western Pangea by the late Bashkirian (Early Pennsylvanian), and experienced little diversification through the Middle and Late Pennsylvanian (Groves et al. 2007; Davydov 2014). In addition to the herein erected monotypic genus *Douglassites* n. gen., Late Pennsylvanian forms of elongate (e.g., fusiform, subcylindrical, cylindrical) schubertellids from western and southwestern North America only include one prominent genus (i.e., *Schubertella* Staff and Wedekind 1910), whereas Gzhelian (Late Pennsylvanian) age schubertellids from Paleo-Tethyan and Peri-Gondwanan faunal provinces experienced a minor radiation, giving rise to the Biwaellinae (i.e., *Biwaella* Morikawa and Isomi 1960 and *Dutkevichites* Davydov 1984) (Davydov 2011).

The Upper Pennsylvanian to Cisuralian mixed carbonate-siliciclastic strata of the Riepe Spring Limestone outcrop in upper Paleozoic strata of ranges throughout eastern Nevada and western Utah. The type section of the Riepe Spring Limestone as defined by Steele (1960) is located near the northern end of Ward Mountain, southeast of Moorman Ranch, in White Pine County, Nevada (39°10'33.75"N, 114°55'59.80"W). Steele (1960) also assigned outcrops in the Carbon Ridge area of Eureka County and the Ruth mining district to the Riepe Spring Limestone. The exposure of Riepe Spring Limestone discussed herein is located within Section 1 of Hope (1972) in the Spruce Mountain Quadrangle (USGS Map GQ-942), where it is nearly 400 m

thick and is characterized by numerous medium to very thick quartzose conglomerate beds interstratified with the dominant beds of limestone and calcareous sandstone. Spruce Mountain Ridge extends directly north of Spruce Mountain and approximately 15 km east of the junction of US Route 93 (Great Basin Highway) and Route 229 (Fig. 5.1). The Riepe Spring Limestone of Spruce Mountain Ridge is assigned a lower Missourian through upper Wolfcampian age range based on conodont occurrences (Fig. 5.2) (Read and Nestell, in press). Nearly equivalent Upper Pennsylvanian and Cisuralian regional units in the area include parts of the Strathearn Formation, Buckskin Mountain Formation, Carbon Ridge Formation, Ferguson Mountain Formation, and the Garden Valley Formation (Douglass 1974; Marcantel 1975; Wardlaw et al. 2015).

The Riepe Spring Limestone of Spruce Mountain Ridge is readily differentiated into three informal "lower, middle, and upper" members. Distinctions among the various lithostratigraphic units of the formation have never been discussed, but Section 1 of Hope (1972) provides a marginal to open marine succession with two recognizable primary lithofacies transitions. The lithostratigraphy and integrated biostratigraphy of the full exposure of the Riepe Spring Limestone succession are topics included in ongoing projects.

The lower member of the Riepe Spring Limestone is composed of silty to sandy, occasionally cherty limestone that is nearly indistinguishable from

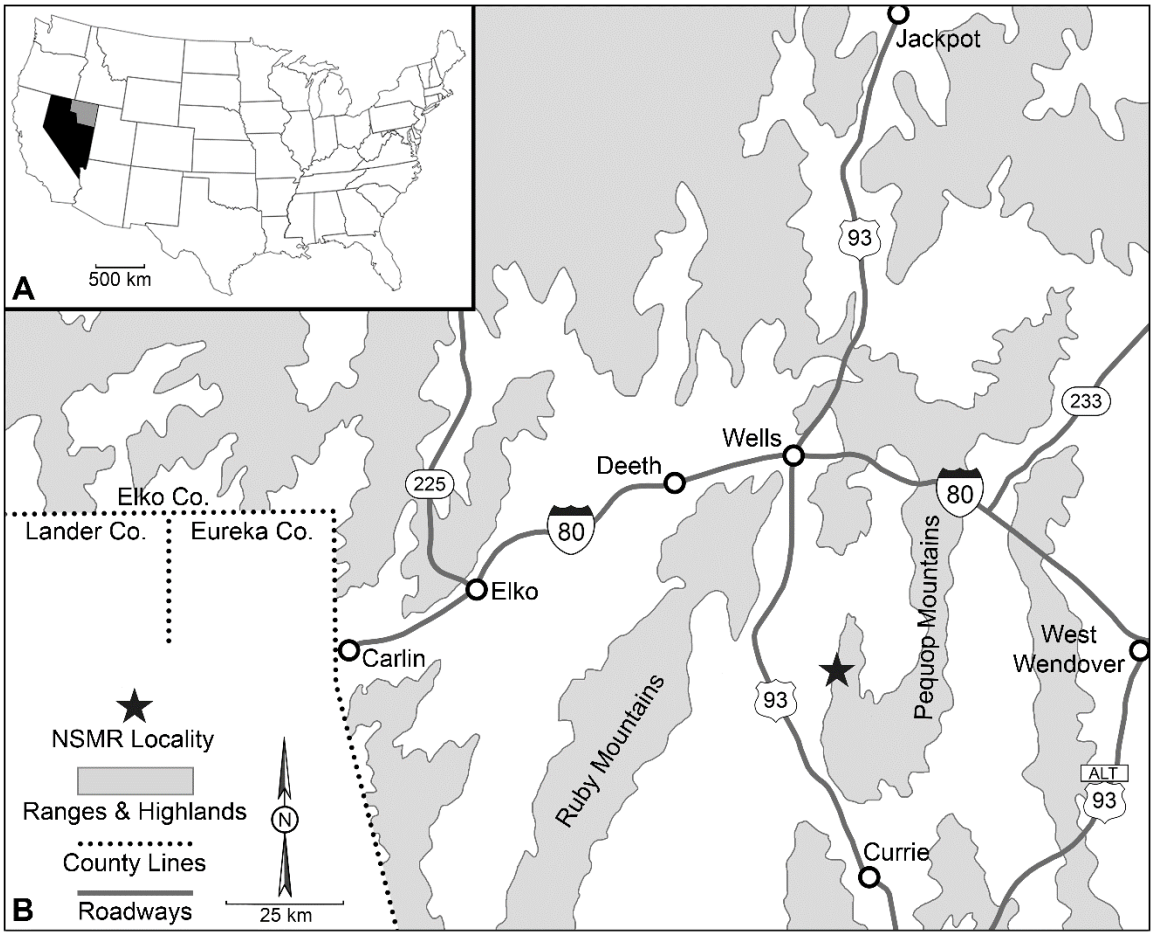

Figure 5.1 – A) Location of Elko County (gray), Nevada (black), U.S.A.; **B)** Map of Elko County, Nevada, illustrating the location of the Pennsylvanian-Permian North Spruce Mountain Ridge (NSMR) section (from Read and Nestell, 2018).

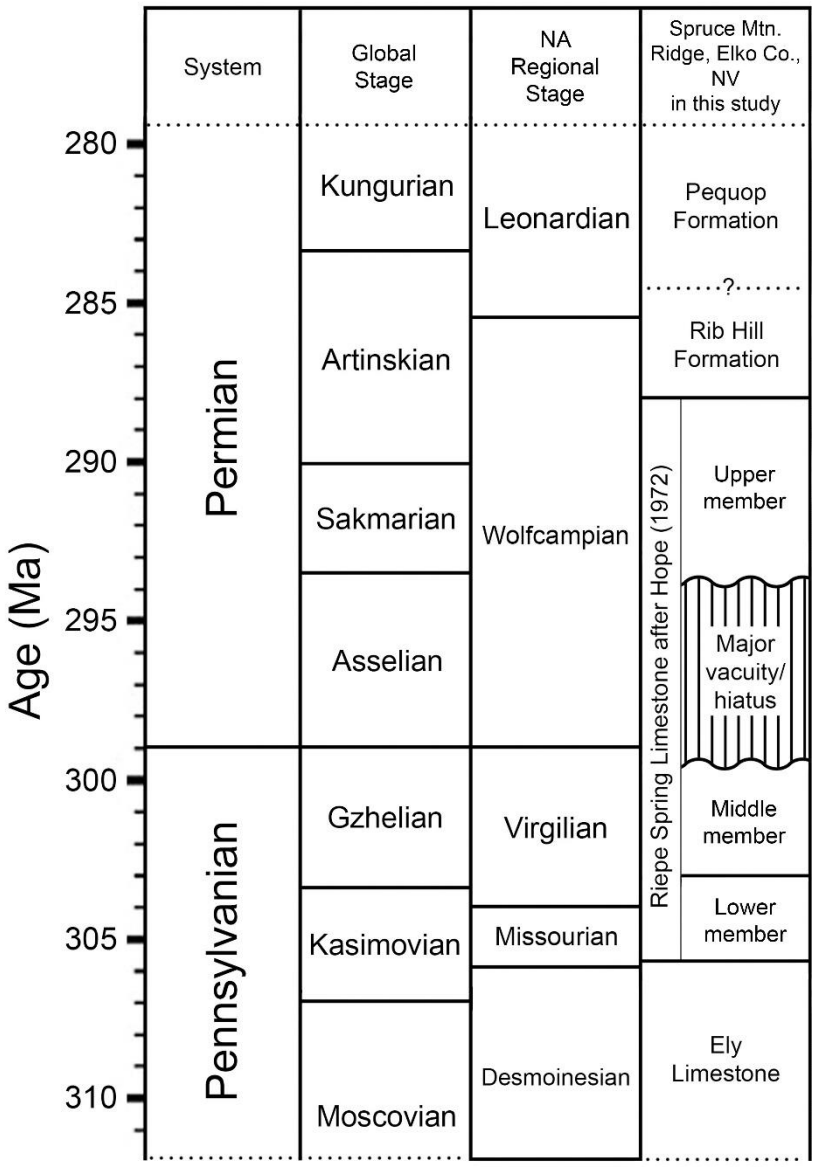

Figure 5.2 – Stratigraphic position of the Riepe Spring Limestone in the Spruce Mountain Ridge area (from Read and Nestell, 2018).

the uppermost part of the underlying Ely Limestone. The Ely Limestone and the Riepe Spring Limestone are differentiated by the presence of the sporadic beds of quartzose conglomerate with granules, pebbles, and cobbles of chert, quartzite, and silicified limestone throughout the latter. The present study is based on a measured section from the middle member of the Riepe Spring Limestone, which is separated from the lower member of the formation by a distinct reddish-brown sandstone and an overlying graded, granule and pebble orthoconglomerate that forms a false peak on the west side of the hill (Fig. 5.3). The only recovered specimens of *Douglassites sprucensis* n. gen. n. sp. were obtained from this middle member of the Riepe Spring Limestone, in a limestone bed approximately 21 meters above the conglomerate of the false peak (unit 9; 40°40'45.40"N, 114°49'37.34"W) (Fig. 5.4). The middle member of the Riepe Spring Limestone is composed of both limestone and quartzose limestone and has the highest volume of interbedded conglomerate in the unit. Many of the limestone beds have been partially to significantly dolomitized. Based on integrated fusulinid-conodont biostratigraphy, the middle member of the Riepe Spring Limestone of the NSMR section ranges from lower to upper Virgilian in age. A distinct faunal change in the *Triticites* fauna between units 5 and 9 suggests a brief mid-Virgilian hiatus, and a 6.3 m thick conglomerate (unit 8) within this interval is likely associated with the disconformity (Fig. 5.4). The upper member of the Riepe Spring Limestone, as discussed by Read and Nestell (in press), is composed of

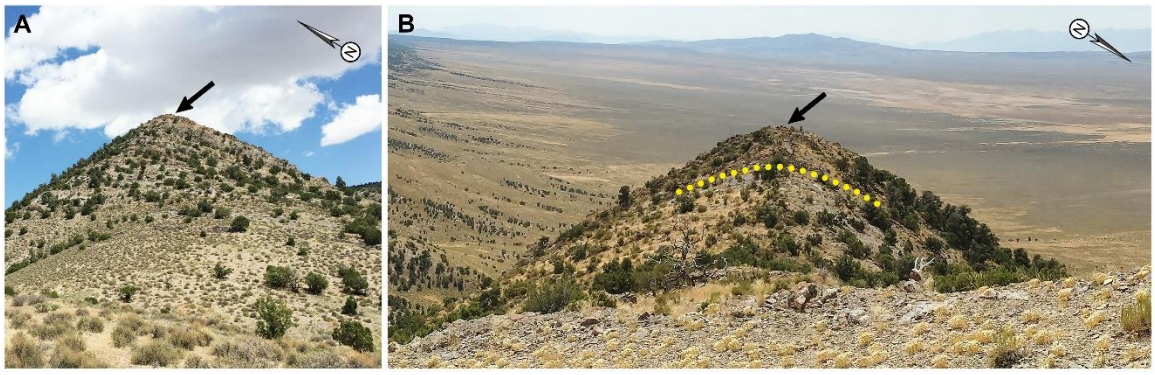

Figure 5.3 – A) Northeastward view of the lower part of the North Spruce Mountain Ridge section(upper most part of the Ely Limestone and lower member of the Riepe Spring Limestone) (photo: 40°40'30.30"N, 114°49'55.86"W); arrow denotes conglomeratic false peak separating the lower and middle members of the Riepe Spring Limestone; **B)** Southwestward view of the upper and middle member of the Riepe Spring Limestone (photo: 40°40'49.46"N, 114°49'32.68"W); arrow denotes same position in both images; dotted line denotes horizon of *Douglassites sprucensis* n. gen. n. sp. (from Read and Nestell, 2018).

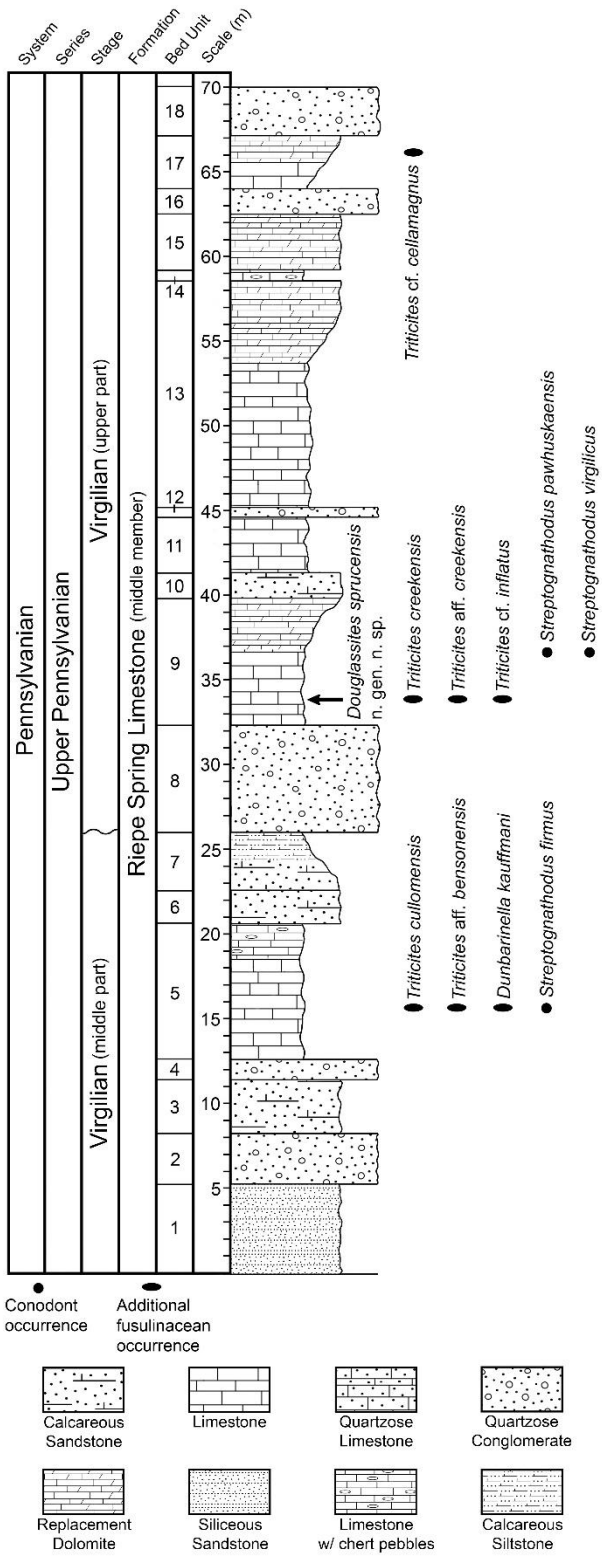

Figure 5.4 – Columnar section of the Virgilian (Upper Pennsylvanian) interval of interest and accompanying fusulinid/conodont occurrences from the middle member of the Riepe Spring Limestone at the NSMR measured section (from Read and Nestell, 2018).

darker, muddy to coarsely quartzose limestone and calcareous sandstone, with several thin conglomeratic beds in the lower portion.

Materials and Method

Much of the sample material for this study was acquired via specimen loan of thin sections from the Department of Paleobiology at the Smithsonian National Museum of Natural History (Douglass-Henbest collection). The specimens borrowed were in a suite of 1,279 thin sections made from the original material collected by Raymond Douglass and Merlynd Nestell in 1969 from a long section that included the Riepe Spring Limestone and closely followed Section 1 of Hope (1972). Specimens of *Douglassites sprucensis* n. gen. n. sp. include 17 axial and nine equatorial thin sections. Six Douglass-Henbest specimens of *Triticites* and one *Dunbarinella* are illustrated (Pl. 2). Additional illustrated specimens of middle and late Virgilian *Triticites* and *Dunbarinella* were obtained from material collected from the same interval by Mike Read, Merlynd Nestell, and Bruce Wardlaw (Fig. 5.4). Specimens of *Douglassites* n. gen. n. sp. are also present in the new material collected but are not illustrated.

Conodont P_1 elements belonging to *Streptognathodus virgilicus* Ritter 1995 and *Streptognathodus pawhuskaensis* (Harris and Hollingsworth 1933) were also recovered from just above the occurrence of *D. sprucensis* n. gen. n. sp. *Streptognathodus firmus* Kozitskaya 1978 occurs below *D. sprucensis* in

unit 5 (Fig. 5.4). Conodont elements were collected from limestone samples processed by acid digestion in a ~10% formic acid solution and the insoluble residues separated with tetrabromoethane ("carbon tetrabromide") to isolate the high-density mineral fraction containing conodont elements.

Systematic Paleontology

Order **SCHUBERTELLIDA** Skinner 1931

Family **SCHUBERTELLIDAE** Skinner 1931

Douglassites Read and Nestell n. gen.

Type species: *Douglassites sprucensis* n. gen. n. sp. from the upper Virgilian (Upper Pennsylvanian) of the middle member of the Riepe Spring Limestone, Spruce Mountain Ridge, Elko County, Nevada, by monotypy.

Etymology: For Dr. Raymond C. Douglass (deceased), formerly of the U.S. Geological Survey, in the style of *Dutkevichites*.

Remarks: R.C. Douglass is credited with originally recognizing the significance of the studied specimens possibly belonging to a new genus, which he tentatively and informally regarded as "*Rugotriticites*" because of the high degree of rugosity in the spirotheca, but a description of the new

taxon never followed because the collection was never formally studied. Closer inspection of the coiling of the innermost volutions in well-oriented specimens, minute chomata, predominantly planar septa, and nature of the outer wall structure suggest that the specimens described herein are not related to *Triticites* (family Triticitidae Davydov in Chuvashov et al. 1986), but belong to the family Schubertellidae.

Douglassites sprucensis Read and Nestell n. gen. n. sp.

Plate 1, figures 1-4, 6-9

Holotype: F24124-7 (Pl. 1, figs. 4a-4c), from the upper Virgilian (Upper Pennsylvanian) of the middle member of the Riepe Spring Limestone, Spruce Mountain Ridge, Elko County, Nevada, U.S.A.

Diagnosis: Mature test is exceptionally large for a schubertellid. Juvenarium exhibits "endothyroid" or skewed initial growth stages characteristic of the Schubertellidae. Axis of coiling rotates to become typically fusiform beyond the first two volutions. Differs from *Schubertella* Staff and Wedekind 1910 and *Biwaella* Morikawa and Isomi 1960 in its large size for a schubertellid, greater number of volutions, and fluted septa. Resembles the near-contemporaneous Paleo-Tethyan genus *Dutkevichites* Davydov 1984, but also differs in its larger size, more fusiform shape, greater number of volutions,

more uniform coiling, more intensely fluted septa, and higher degree of rugosity in the spirotheca. The juvenaria of some specimens resemble mature *Fusiella schubertellinoides* Suleimanov 1949. Closely resembles *Schwageriniformis* in general test morphology, but species of *Schwageriniformis* have a "schwagerinid" spirotheca and lack the skewed initial chambers of schubertellids.

Occurrence: Middle member of the Riepe Spring Limestone, bed 9 (text-figs. 3, 4); upper part of the Virgilian Stage.

Description: A large schubertellid species with an elongate fusiform to subcylindrical test of six to eight volutions. The majority of the 26 specimens studied have seven volutions. The initially, variably skewed axis of coiling straightens beyond the first one to two volutions. Coiling of the following volutions is fusiform planispiral. Mature tests with lengths of 3.50 to 5.25 mm (averaging 4.13 mm) and widths of 1.06 to 1.96 mm (averaging 1.42 mm) have an average form ratio of 2.94. Individual measurements are provided in Table 8.1. Poles range from broadly rounded to irregularly pointed and scalloped. Some of the perceived variability is likely a product of the orientation of individual specimens. The proloculus is spherical and minute, with an average outside diameter of 0.068 mm. The test expands significantly beyond the third volution, and the outer volutions are loosely coiled. Heights

of the first through seventh volutions average 0.028, 0.033, 0.046, 0.082, 0.141, 0.197, and 0.239 mm. The walls of the proloculus and inner three volutions are very thin, but the spirotheca significantly thickens beyond the third volution. Wall thicknesses for the initial chamber through the seventh volution average 0.008, 0.009, 0.010, 0.014, 0.020, 0.034, 0.055, and 0.064 mm. The thin inner spirotheca, as in forms of the Biwaellinae, has a simple, poorly defined structure of tectum and lower tectorium. The coarse wall structure of the outer volutions, interpreted as keriothecal by Douglass, is similar to the Biwaellinae-type of mature spirotheca illustrated by Davydov (2011) or early schwagerinids, in which the outer volutions are perforated by parallel "mural pores" in the former or very weak keriotheca in the latter (Pl. 16, Fig. 4c). Septa are subtly to moderately fluted along the axis of coiling, narrowly at first before expanding and intensifying towards the poles. Chomata are extremely low, indistinct, often irregular in the inner volutions, and appear characteristically schubertellid. Measured tunnel widths are highly variable. Equatorial sections have heavily scalloped volutions, indicating that the test was externally ribbed by deep septal furrows like some forms of *Dutkevichites* (see *Dutkevichites* sp. B in Kobayashi and Altiner 2008, pl. 1, fig. 25).

Etymology: For Spruce Mountain Ridge, from which the only known specimens of the genus have been recovered.

Materials: Twenty-six total specimens from Elko County, Nevada, U.S.A.; 17 axially oriented specimens and nine equatorially oriented specimens; axial sections: F24124-1-F24124-17; equatorial (sagittal) sections: F24124- 18-F24124-26.

Remarks: Measured specimens of *Douglassites sprucensis* n. gen. n. sp. demonstrate a bimodal form ratio distribution with groups clustered around means of 2.56 and 3.37. Although such a distribution may suggest that there are two distinct species present, there is insufficient evidence among the other measured characters to support separation of the new taxon. Further argument for a monotypic classification is supported by the pointed nature of the poles in some axial specimens, particularly in the well-oriented holotype specimen. Any deviation from a precise pole-to-pole axial orientation of a specimen would cause the polar regions to appear blunted. Therefore, form ratios seem to be strongly influenced by minute variances in the angle of orientation. Additionally, several specimens do not have a strongly pronounced "endothyroid" initial axis of coiling, indicating that the skewed angle may not be as large as that observed in other schubertellids, and that this feature is also highly sensitive to specimen orientation. A similar observation was discussed by Kobayashi (2005) regarding specimens of the Japanese type species of *Biwaella*, *B. omiensis* Morikawa and Isomi 1960.

A distinct ancestry for *Douglassites sprucensis* n. gen. n. sp. is not clear in the fusulinid assemblage collected from the Riepe Spring Limestone of the NSMR section. Although *D. sprucensis* n. gen. n. sp. has a wall structure that is similar to that of the Biwaellinae, no species of *Biwaella* or *Dutkevichites* are known from Upper Pennsylvanian deposits of western and southwestern North America. The earliest appearance of any Biwaellinae migrant in North America is the middle Cisuralian age *Biwaella americana* Skinner and Wilde 1965a, which was originally described as part of a well-documented fusulinid assemblage from the Big Hatchet Mountains of southwest New Mexico (Skinner and Wilde 1965a). *Biwaella americana* is also known from the Riepe Spring Limestone of Spruce Mountain Ridge, but this form occurs in the upper member of the formation and is Cisuralian in age as well (Read and Nestell, in press). To date, no forms of *Dutkevichites* have been recovered from western or southwestern North America. The apparent absence of all Biwaellinae taxa from the region during the Pennsylvanian suggests that neither *Biwaella* nor *Dutkevichites* gave rise to *D. sprucensis* n. gen. n. sp. Having never been previously reported or described elsewhere, it is also unlikely that *D. sprucensis* n. gen. n. sp. itself is a migrant taxon, and it is probable that the genus was endemic to the shallow, coastal region of what is now northeast Nevada. Similar endemism has been reported from the Cisuralian age sweetognathid conodont fauna from higher in the NSMR

section in the upper member of the Riepe Spring Limestone (Read and Nestell, in press).

Although there is significant morphological disparity between the diminutive *Schubertella ciscoensis* and the more advanced *D. sprucensis* n. gen. n. sp., the former is the only schubertellid known to occur within close, albeit disconformable stratigraphic proximity to the occurrence of the new genus. Inspection and comparison of *Schubertella* (both *S. ciscoensis* and its descendent, *S. kingi* Dunbar and Skinner 1937) and *D. sprucensis* n. gen. n. sp. reveal that the dimensions of the juvenaria in specimens of *D. sprucensis* n. gen. n. sp. are similar to the dimensions in mature specimens of *Schubertella*. One particularly useful thin section from the Douglass-Henbest collection (F24124-6) includes a specimen of *D. sprucensis* next to a smaller, subaxially (tangentially) oriented schubertellid (Fig. 5.5). In a note on the margin of the thin section, R. C. Douglass preliminarily assigned the smaller form to *Schubertella*. If the smaller specimen does indeed belong to *Schubertella*, the overall similarity between the juvenaria of specimens of *D. sprucensis* and mature *Schubertella* is evident in the photomicrograph. Alternatively, the smaller form may represent an immature specimen of *D. sprucensis* n. gen. n. sp. that had not yet constructed its outer, perforate volutions.

The lack of any apparent ancestral or transitional forms preceding *D. sprucensis* n. gen. n. sp. makes it difficult to unequivocally dismiss a potential

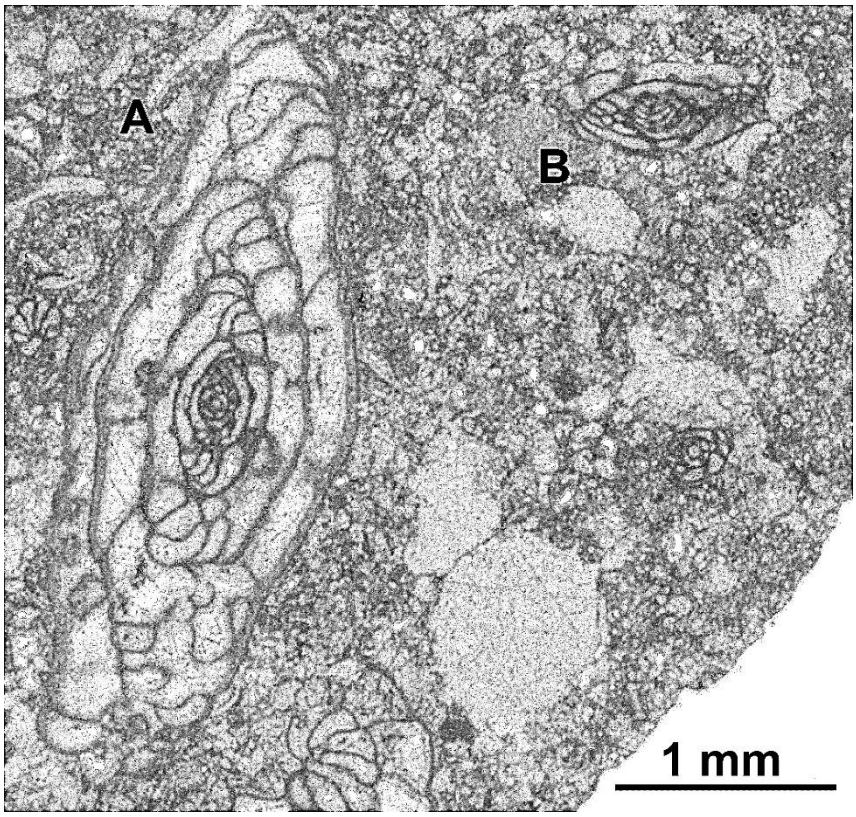

Figure 5.5 – Thin section of an obliquely oriented specimen of *Douglassites sprucensis* n. gen. n. sp. (A; F24124-6) alongside a subaxially (tangentially) oriented specimen questionably assigned to *Schubertella* (B). Photomicrograph emphasizes the morphological similarity between the juvenarium of *D. sprucensis* n. gen. n. sp. and mature forms of *Schubertella* (from Read and Nestell, 2018).

schwagerinid affinity, particularly with similar ambiguity surrounding the origins of *Biwaella* among fusulinid taxonomists. This degree of uncertainty is acknowledged, but a comprehensive evaluation of the following evidence suggests that a schubertellid ancestry is more likely. A comparison of *D. sprucensis* n. gen. n. sp. to the co-occurring forms of *Triticites* is significant in this regard. Although the wall structure of *D. sprucensis* n. gen. n. sp. does resemble that of very early *Triticites*, these forms predate *D. sprucensis* n. gen. n. sp. by at least four million years, developing during the early and middle Kasimovian. The keriothecal wall structure of late Virgilian forms of *Triticites* is extremely coarse and well-developed, consisting of an upper and lower alveolar keriotheca which do not easily recrystallize like the spirotheca of *D. sprucensis* n. gen. n. sp. Specimens of *D. sprucensis* n. gen. n. sp. and *Triticites* from bed 9 show notable disparity in the level of spirothecal preservation under identical, nondolomitic diagenetic conditions. It is important to point out that pore-like structures are known to have developed independently in test walls several times throughout the Carboniferous, as evidenced by genera such as *Protriticites* Putrya 1948, *Anulofusulinella* Wilde 2006, and the endothyroid *Bradyina* Möller 1878. Finally, the chomata are significantly underdeveloped, often nearly imperceptible beyond the juvenarium, and the septa are very weakly fluted.

Table 5.1 – Measurements (in millimeters) for *Douglassites sprucensis* n. gen. n. sp. 5

Specimen no.	Length (mm)	Half Length (mm)	Width (mm)	Half Width (mm)	Form Ratio	No. of Volutions	Diameter of Proloculus (mm)	Thickness of Spirotheca (mm)								
								0	1	2	3	4	5	6	7	8
F24124-1	4.78	—	1.96	—	2.45	8	0.066	0.008	0.010	0.011	0.012	0.022	0.029	0.060	0.065	0.096
F24124-2	—	2.24	1.36	—	3.30	6	0.071	0.008	0.011	0.011	0.013	0.022	0.045	0.064		
F24124-3	—	1.81	1.06	—	3.44	6	0.060	0.007	0.009	0.012	0.011	0.016	0.040	0.059		
F24124-4	—	—	1.43	—	—	7	0.063	0.009	0.011	0.008	0.010	0.012	0.028	0.052	0.064	
F24124-5	—	2.01	1.55	—	2.60	7	0.069	0.007	0.008	0.009	0.018	0.019	0.035	0.051	0.087	
F24124-6	3.50		1.34	—	2.62	6	0.057	0.008	0.008	0.010	0.014	0.025	0.033	0.062		
F24124-7	4.43		1.30	—	3.40	7	0.052	0.007	0.007	0.009	0.014	0.024	0.026	0.045	0.075	
F24124-8	—	2.18	1.30	—	3.35	6	0.062	0.007	0.008	0.010	0.014	0.021	0.036	0.060		
F24124-9	—	1.94	1.09	—	3.57	7	0.083	0.010	0.008	0.011	0.013	0.018	0.040	0.042	0.057	
F24124-10	3.97		1.33	—	2.98	7	0.053	0.010	0.010	0.011	0.012	0.023	0.028	0.056	0.061	
F24124-11	3.89		1.54	—	2.52	7	0.072	0.006	0.007	0.009	0.015	0.017	0.033	0.050	0.065	
F24124-12	3.80		1.44	—	2.65	6	0.086	0.008	0.011	0.012	0.016	0.020	0.042	0.063		
F24124-13	4.21		1.55	—	2.72	7	0.076	0.008	0.009	0.010	0.020	0.024	0.036	0.043	0.066	
F24124-14	4.87		1.55	—	3.14	7.5	0.068	0.007	0.007	0.009	0.010	0.012	0.024	0.038	0.045	—
F24124-15	—	1.99	1.50	—	2.67	7	0.076	0.007	0.006	0.009	0.012	0.014	0.028	0.060	—	
F24124-16	—	1.52	1.37	—	2.22	6	0.080	0.009	0.013	0.012	0.019	0.033	0.042	0.061		
F24124-17	—	2.62	1.55	—	3.38	7	—	—	0.008	0.013	0.014	0.023	0.033	0.067	0.054	

	Height of Volutions (mm)								Tunnel Angle (degrees)							
	1	2	3	4	5	6	7	8	1	2	3	4	5	6	7	8
F24124-1	0.024	0.035	0.047	0.075	0.107	0.183	0.268	0.258	13	19	30	25	31	37	37	—
F24124-2	0.033	0.043	0.047	0.115	0.160	0.186			—	17	36	62	56	76		
F24124-3	0.032	0.027	0.032	0.080	0.158	0.161			—	13	22	53	54	65		
F24124-4	0.029	0.030	0.048	0.065	0.124	0.215	0.284		—	—	24	40	53	67	—	
F24124-5	0.033	0.030	0.041	0.076	0.117	0.186	0.224		—	25	32	54	53	61	55	
F24124-6	0.028	0.036	0.064	0.080	0.185	0.216			—	34	31	37	46	72		
F24124-7	0.024	0.026	0.037	0.066	0.114	0.168	0.182		—	—	21	41	56	65	65	
F24124-8	0.023	0.031	0.040	0.060	0.117	0.233			—	—	24	31	33	50		
F24124-9	0.027	0.034	0.040	0.071	0.100	0.112	—		13	23	30	40	49	56	—	
F24124-10	0.030	0.032	0.044	0.060	0.121	0.205	0.188		14	16	21	31	56	55	—	
F24124-11	0.025	0.033	0.051	0.082	0.130	0.187	0.252		—	13	27	55	52	71	—	
F24124-12	0.024	0.037	0.053	0.124	0.189	0.233			15	20	27	57	69	61		
F24124-13	0.029	0.031	0.049	0.107	0.177	0.180	0.204		—	16	23	31	39	54	62	
F24124-14	0.021	0.029	0.035	0.049	0.104	0.193	0.367	—	—	28	34	23	42	47	56	—
F24124-15	0.032	0.030	0.041	0.067	0.146	0.218	—		—	13	23	44	52	64	50	
F24124-16	0.030	0.041	0.061	0.122	0.207	0.257			—	39	38	58	63	—		
F24124-17	0.029	0.043	0.056	0.092	0.145	0.212	0.209		—	19	34	43	58	65	—	

Discussion

The newly described, monotypic genus *Douglassites* n. gen. from the middle member of the Riepe Spring Limestone of North Spruce Mountain Ridge (NSMR), Nevada, is among the largest known Carboniferous forms of the family Schubertellidae. *Douglassites sprucensis* n. gen. n. sp. has an elongate fusiform to subcylindrical test that measures two and one-half to three times larger than that of *Schubertella ciscoensis*. The conspicuous and apparently short-lived new genus has only been recovered from a single thick limestone bed within the NSMR section where it is associated with robust and diagnostic forms of the genus *Triticites*, including *T. creekensis* Thompson 1954 and *T.* cf. *inflatus* (White 1932). Such forms of *Triticites* are common and widely distributed in the western, southwestern, and Midcontinent regions of North America and have well-constrained stratigraphic and temporal ranges. Pairing these characteristically late Virgilian forms of *Triticites* with the sparse conodont fauna of the middle member of the Riepe Spring Limestone has provided precise biostratigraphic control for *D. sprucensis* n. gen. n. sp. and allowed for placement of the new genus within the *Triticites* Group IV Zone (fusulinid zone) of Wilde (1976; 2006) and the *Streptognathodus virgilicus* [*sensu stricto*] Zone (conodont zone) of Barrick et al. (2013b).

In addition to being much larger than its familial contemporaries, *Douglassites sprucensis* n. gen. n. sp. exhibits several puzzling characters

that are unique to the Pennsylvanian schubertellids of North America. The most apparent feature is the general resemblance of the test of *D. sprucensis* n. gen. n. sp. to small forms of *Triticites* and *Schwageriniformis*, both of which belong to the family Triticitidae. *D. sprucensis* n. gen. n. sp. most closely bears an axial resemblance to the late Kasimovian (Late Pennsylvanian) *Schwageriniformis asiaticus* (Bensh 1962), but only superficially. The fundamental differences between *D. sprucensis* n. gen n. sp. and the schwagerinid genera are apparent in the more discrete morphological features of the spirotheca and juvenaria of the former.

Well-oriented axial specimens of *Douglassites sprucensis* n. gen. n. sp. demonstrate that the innermost volutions have an axis of coiling that is skewed to the outer, more loosely coiled volutions. The so-called endothyroid growth stage in the initial one to two volutions succeeding the proloculus is a characteristic feature of most genera of Schubertellidae (excluding *Grovesella* Davydov and Arefifard 2007). Therefore, although the test of *D. sprucensis* n. gen. n. sp. is comparatively large, with fluted septa, and at first glance resembles forms of the *Triticitidae*, the early ontogeny of *D. sprucensis* n. gen. n. sp. demonstrates that the new genus belongs to the Schubertellidae.

Close inspection of the spirotheca also provides further evidence for distinction of *Douglassites sprucensis* n. gen. n. sp. from the Triticitidae and reveals the presence of an uncommon wall structure. The test of *D. sprucensis* n. gen. n. sp. is characterized by a differential growth succession composed of

two separate spirothecal compositions. The inner volutions of *D. sprucensis* n. gen. n. sp. exhibit a very thin, nondescript wall structure composed of a dark tectum and lighter lower tectorium, whereas the much thicker outer volutions are perforated by narrow mural pores that resemble simple, weakly developed keriotheca. The spirothecal development observed in *D. sprucensis* n. gen. n. sp. is like that of the schubertellid genus *Biwaella* (Pl. 16, Fig. 5). A similar wall structure progression was illustrated and described for *Biwaella* by Davydov (2011, fig. 3A, 3B and *Biwaella* "Remarks" subheading). Intriguingly, although there exists an unmistakable similarity between the test walls of the two genera, it is unlikely that a form of *Biwaella* gave rise to *Douglassites* n. gen. n. sp. The former first appeared in tropical to subtropical Paleo-Tethyan provinces during the early Gzhelian as a descendant of *Schubertella* and did not disperse to the west coast of Pangea until the Cisuralian (Davydov 2011; 2014). Due to the absence of *Biwaella* in western Pangea during the Virgilian, the similarities between *D. sprucensis* n. gen. n. sp. and the Biwaellinae are likely attributed to parallel evolution of the spirotheca in the two disparate schubertellid groups. As such, a North American form of *Schubertella* serves as the most likely evolutionary predecessor to *D. sprucensis* n. gen. n. sp., which, based upon ontogenetic similarities between the two genera, could have developed its greater size via peramorphosis and the addition of three to four significantly larger chambers in mature tests.

Plate 16

1–4, 6–9. Oriented specimens of *Douglassites sprucensis* Read and Nestell, n. gen. n. sp. from the middle member of the Riepe Spring Limestone (Virgilian), Elko County, Nevada, U.S.A.

1. *Douglassites sprucensis* Read and Nestell, n. gen. n. sp., F24124-10, axial section

2. *Douglassites sprucensis* Read and Nestell, n. gen. n. sp., F24124-12, axial section

3. *Douglassites sprucensis* Read and Nestell, n. gen. n. sp., F24124-14, axial section

4a. *Douglassites sprucensis* Read and Nestell, n. gen. n. sp., F24124-7, axial section of holotype

4b. *Douglassites sprucensis* Read and Nestell, n. gen. n. sp., F24124-7, close-up of the juvenarium of holotype specimen

4c. *Douglassites sprucensis* Read and Nestell, n. gen. n. sp., F24124-7, close-up of the porous outer wall structure of holotype specimen, arrows denote presence of mural pores (MP)

6. *Douglassites sprucensis* Read and Nestell, n. gen. n. sp., F24124-26, equatorial (sagittal) section

7. *Douglassites sprucensis* Read and Nestell, n. gen. n. sp., F24124-19, equatorial (sagittal) section

8. *Douglassites sprucensis* Read and Nestell, n. gen. n. sp., F24124-25, equatorial (sagittal) section

9. *Douglassites sprucensis* Read and Nestell, n. gen. n. sp., F24124-24, equatorial (sagittal) section

5. *Biwaella americana* Skinner and Wilde 1965a, F24128-15, close-up of outer wall structure for comparison

10. *Biwaella poletaevi* Davydov 2011, SUI 114239, axial section of paratype, from Davydov (2011, fig. 4.B), specimen illustrating similarities in the inner volutions and septa of *Douglassites* n. gen. n. sp. and Gzhelian (Late Pennsylvanian) age forms of *Biwaella*

11. *Biwaella zhikalyaki* Davydov 2011, SUI 114234, axial section of paratype, from Davydov (2011, fig. 3.G), additional specimen illustrating similarities in the inner volutions and septa of *Douglassites* n. gen. n. sp. and Gzhelian (Late Pennsylvanian) age forms of *Biwaella*.

Plate 16

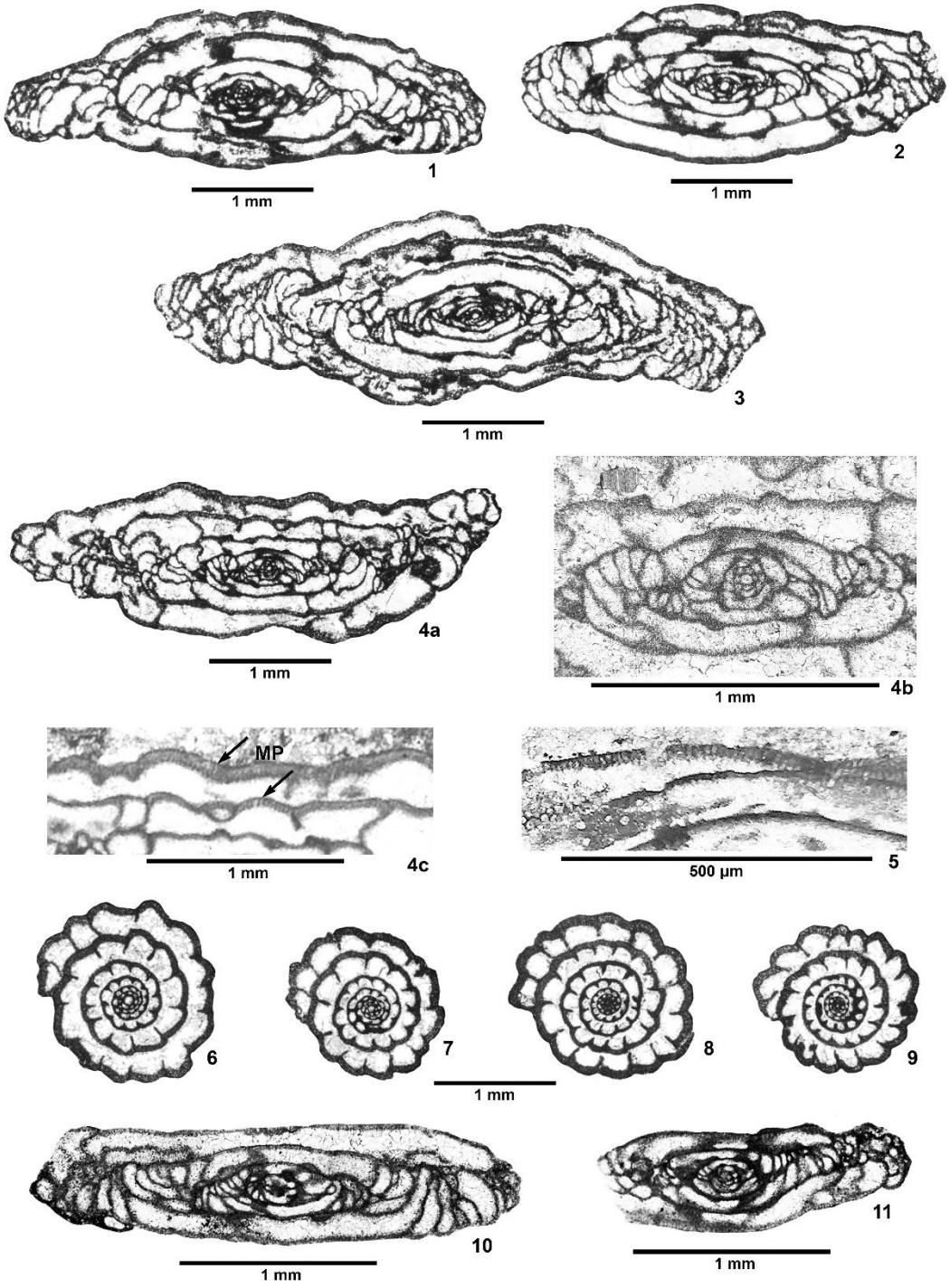
1
1 mm
2
1 mm
3
1 mm
4a
1 mm
4b
1 mm
MP
1 mm
4c
500 µm
5
6
7
8
9
1 mm
10
1 mm
11
1 mm

Plate 17

Illustrated forms of Virgilian age *Triticites* and *Dunbarinella* recovered in association with *Douglassites sprucensis* n. gen. n. sp.

1. *Triticites* aff. *bensonensis* Ross and Tyrrell 1965, USNM PAL 722042, axial section
2. *Triticites* aff. *bensonensis* Ross and Tyrrell 1965, F24123-11, axial section
3. *Triticites cullomensis* Dunbar and Condra 1927, USNM PAL 722043, axial section of immature specimen
4. *Triticites cullomensis* Dunbar and Condra 1927, F24122-10, axial section
5. *Dunbarinella kauffmani* Wilde 2006, F24122-18, axial section
6. *Dunbarinella kauffmani* Wilde 2006, USNM PAL 722044, axial section
7. *Triticites* aff. *creekensis* Thompson 1954, F24124-31, axial section
8. *Triticites* cf. *inflatus* (White 1932), USNM PAL 722045, axial section
9. *Triticites creekensis* Thompson 1954, F24124-34, axial section
10. *Triticites creekensis* Thompson 1954, F24124-37, equatorial section
11. *Triticites* cf. *cellamagnus* Thompson and Bissell 1954, F24126-26, axial section.

Plate 17

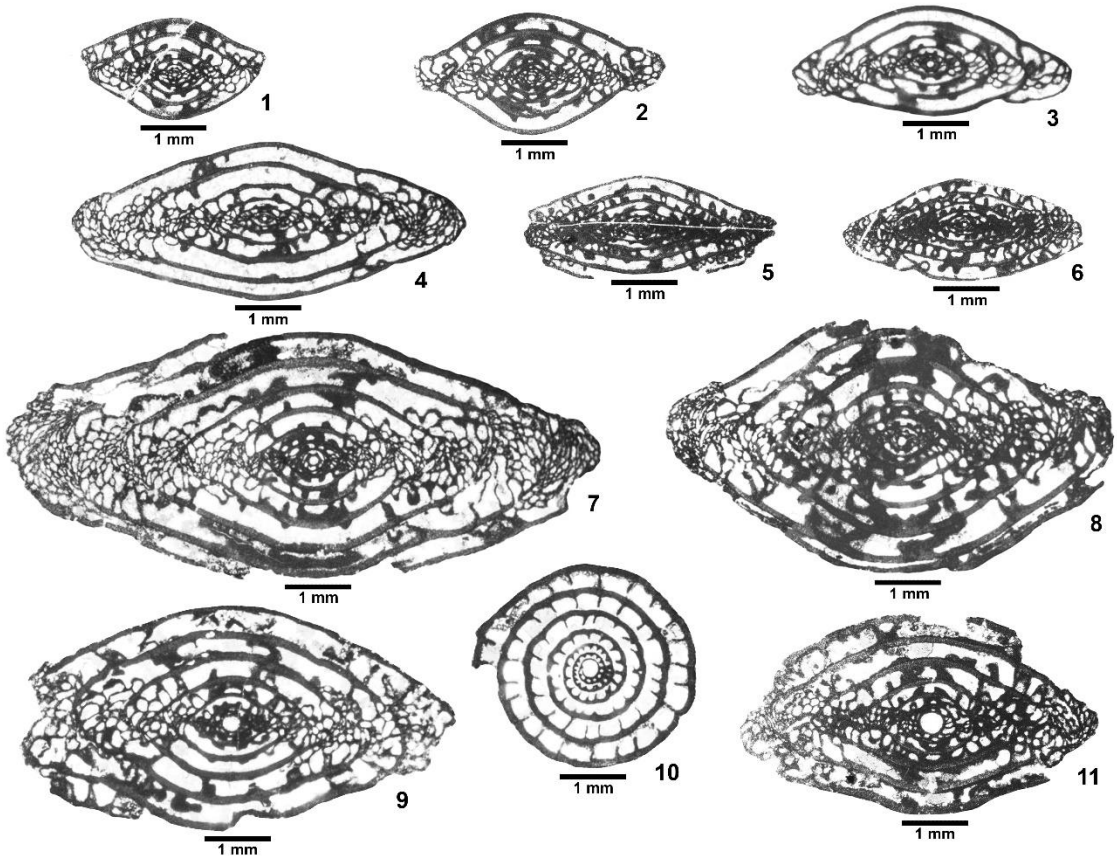

CHAPTER 6 – INTRODUCTORY REMARKS

The occurrence of the fusulinid genus *Biwaella* is uncommon in Upper Pennsylvanian-Cisuralian marine deposits of western Pangea. Consequently, many American workers have little knowledge of this predominantly Paleo-Tethyan genus. However, the discovery of a single well-preserved specimen of *B. americana* Skinner and Wilde, 1965a from the Smithsonian led to the finding of several other specimens in recently collected material from the same bedding unit of the NSMR section (unit 48). R.C. Douglass' personal notes indicated that one thin section from the Douglass-Henbest collection contained a small specimen which Douglass referred to as "*Biwaella*?" (F24128-15), prompting the consideration of the implications of the occurrence of this surprising taxon. Several specimens are illustrated from the Riepe Spring Limestone, each of which was recovered from unit 48 in the lower part of the upper member (Fig. 6.0). No conodonts were obtained from this horizon, but the specimens of *B. americana* are associated with two forms of the early Cisuralian fusulinid genus *Cuniculinella*.

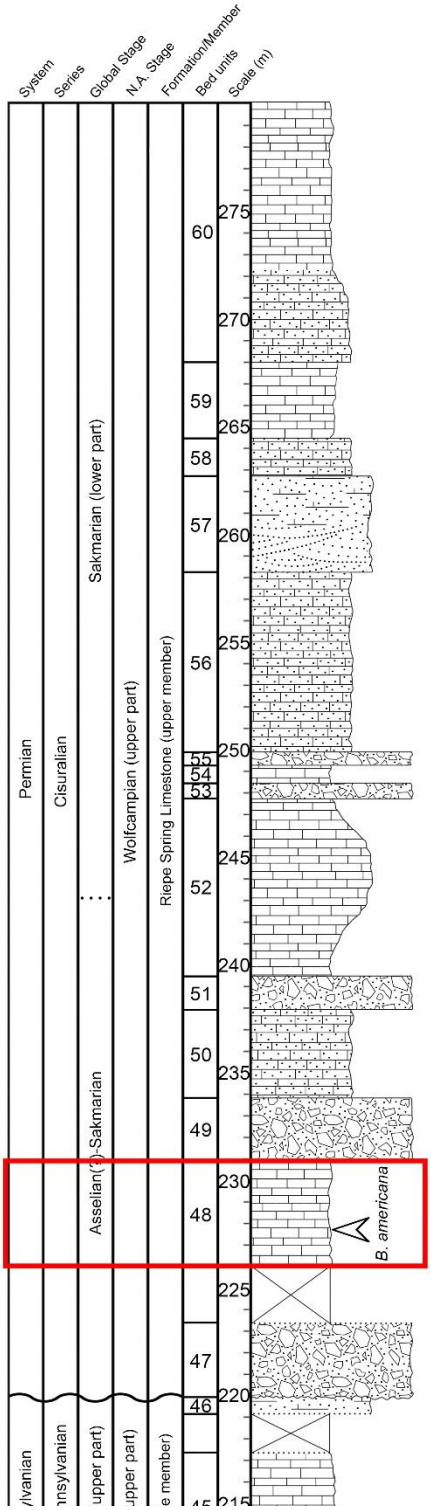

Fig. 6.0.1 – Stratigraphic column illustrating the position of *Biwaella americana* in the NSMR section (outlined in red).

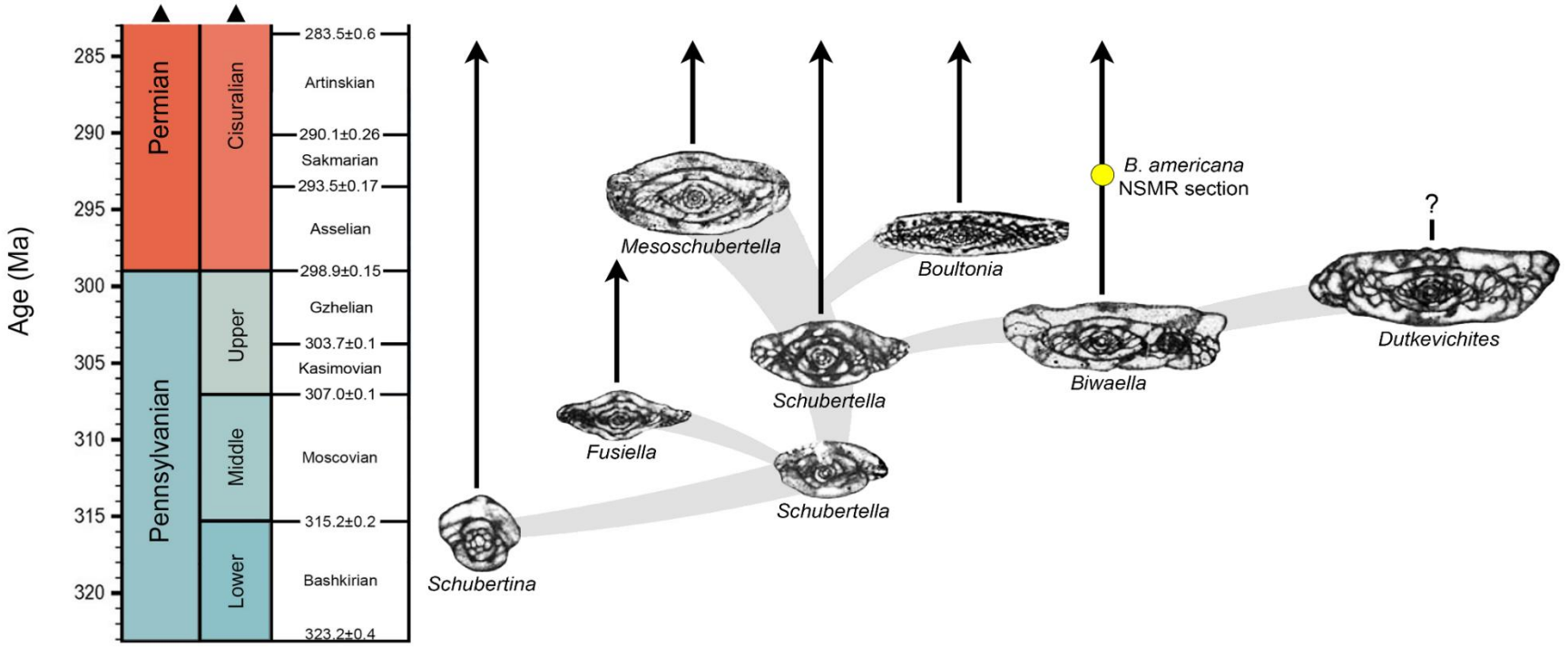

Figure 6.0.2 – Inferred phylogeny of the early Schubertellidae and the level of *Biwaella americana* from the NSMR section (yellow) (redrawn from Davydov, 2011).

CHAPTER 6: GLOBAL DISTRIBUTION OF THE FUSULINACEAN GENUS *BIWAELLA*

"ГЛОБАЛЬНОЕ РАСПРОСТРАНЕНИЕ РОДА *BIWAELLA* (FUSULINOIDA)"

Michael T. Read and Merlynd K. Nestell

Accepted and soon to be published; Global distribution of the fusulinacean genus *Biwaella*, Paleontological Journal, v. 53, no. 8, Pleiades Publishing.

The Late Pennsylvanian-Cisuralian fusulinacean genus *Biwaella* Morikawa et Isomi, 1960 has been described from a number of tropical to subtropical Tethyan and Peri-Gondwanan localities along with sparse occurrences from the Boreal and Midcontinent-Andean faunal provinces. The present study provides a synthesis of the known global distribution and migratory timescales of *Biwaella* and describes the first occurrence of *B. americana* Skinner et Wilde, 1965a from Nevada, U.S.A.

An integrated study of recently collected fusulinacean material and specimens on loan from the Smithsonian National Museum of Natural History (Douglass-Henbest collection) has provided a new occurrence of the uncommon genus *Biwaella* Morikawa et Isomi, 1960 from the western United States. Rare specimens of *Biwaella americana* Skinner et Wilde, 1965a were recovered from a single, thick limestone bed in the upper informal member of the Riepe Spring Limestone (Cisuralian, Lower Permian) at North Spruce Mountain Ridge (NSMR), Elko County, Nevada, U.S.A. Prior to the discovery of the herein illustrated NSMR forms, the only description of *Biwaella* from the American west or southwest was that of the type specimens illustrated by Skinner and Wilde (1965a) and re-illustrated by Wilde (2006), which were obtained from the Artinskian part of the Horquilla Formation at New Well Peak, Hidalgo County, New Mexico, U.S.A. The type species of *Biwaella*, *B. omiensis* Morikawa et Isomi, 1960, was described from nearly coeval Cisuralian deposits of the Samegai Formation near Lake Biwa, Shiga

Prefecture, Japan. *Biwaella* is one of the larger and more evolved genera of the Schubertellidae Skinner, 1931 possessing a loosely coiled, often irregular test and a perforate outermost wall structure that is atypical among genera of the family. Although the nature of the outer spirotheca has been previously interpreted as schwagerinid by several foraminiferal workers (e.g., Rauser-Chernousova et al., 1996; Forke, 2002; Kobayashi, 2005), the coarse wall structure is composed of simple, parallel pores that do not branch like true, lachrymiform alveolar keriotheca (Pl. 18, Fig. 1B, 1C) (Davydov, 2011). Additional support of a schubertellid affinity is provided by the distinct lack of septal fluting. The tests of *Biwaella* are often erratic and highly plastic, particularly in the polar regions of mature specimens, leading to difficulties in adequately orienting thin sections and resulting in a wide variety of axial profiles among illustrated specimens. Due to such inconsistencies in the shape of the test, the diagnostic wall structure of the Biwaellinae Davydov (e.g., *Biwaella* Davydov and *Dutkevichites* Davydov in Davydov, 1984) is a critical character in identification.

Biwaella likely arose from an ancestral, subtropical stock of western Tethyan *Schubertella* Staff et Wedekind, 1910 during the earliest Gzhelian (Late Pennsylvanian) (Davydov, 2011). Several questionably transitional forms potentially linking *Schubertella* to *Biwaella* have been previously described from the Darvaz and Japan (e.g., *Biwaella*? *tshelamtshiensis* Davydov, 1984, *B.* sp. in Kobayashi, 1993, and an unnamed species of

Biwaella reported by Leven and Davydov, 2001), but there are uncertainties regarding the true affinities of these taxa. The earliest unequivocal species of the genus, *B. poletaevi* Davydov, 2011 and *B. zhikalyaki* Davydov, 2011, were described from the western part of the Donets Basin, Ukraine, in association with the lower Gzhelian *Schagonella proimplexa* Zone (Davydov, 2011). Following the restricted initial appearance of the genus in the early Gzhelian, the distributional extent of *Biwaella* is poorly understood until its proliferation during the late Asselian and Sakmarian (early Cisuralian). Despite this apparent discontinuity within the lineage, a comparison between the older Ukrainian specimens illustrated by Davydov (2011) and Cisuralian taxa demonstrates that little change occurred within the genus during the Carboniferous-Permian transition.

By the early Cisuralian (Asselian-Sakmarian), species of *Biwaella* had dispersed throughout the tropical and subtropical continental platforms and shelves of the Tethyan, Peri-Gondwanan, and Boreal faunal provinces (Davydov, 2014). Descriptions of Cisuralian forms of *Biwaella* from Tethyan and Peri-Gondwanan realms include occurrences in Japan (Morikawa, Isomi, 1960; Kobayashi, 1993, 2005), Afghanistan (Leven, 1997), Iran (Zandkarimi et al., 2014), the Carnic Alps (Forke, 2002), Slovenia (Kochansky-Devidé, 1970), Croatia (Kochansky-Devidé, 1959), and Montenegro (Kochansky-Devidé, 1962) (Fig. 6.1). A thorough summary of Cisuralian occurrences and potential synonyms of *Biwaella* from North and South China is provided by

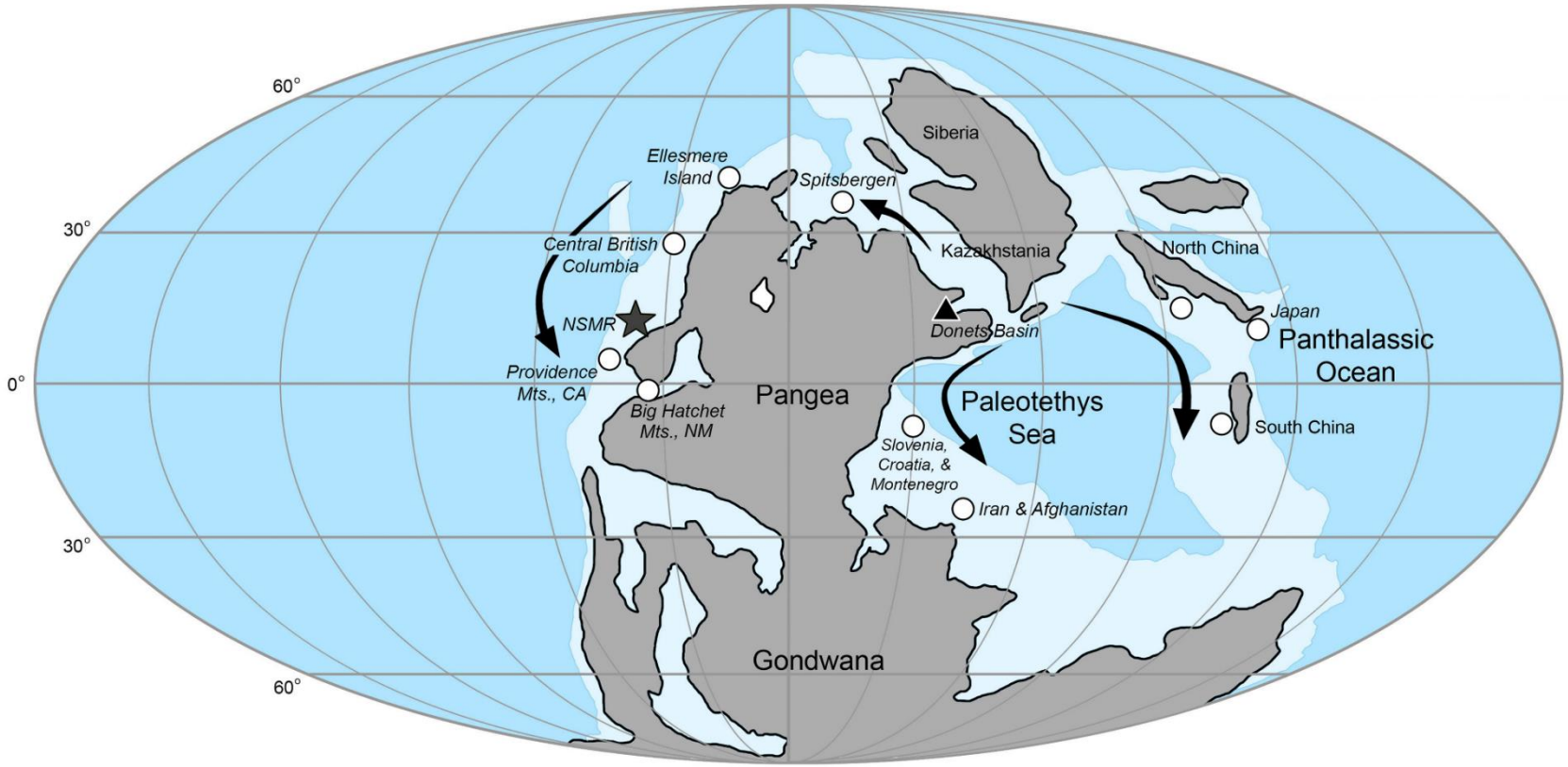

Figure 6.1 – Sakmarian (early Cisuralian) paleogeographic map depicting major occurrences and migratory pathways (arrows) of the fusulinacean genus *Biwaella*. Proposed origination of *Biwaella* in the Donets Basin region is based on the current earliest, definitive occurrences of the genus. *Medium gray* – deep ocean; *light gray* – shelf/platform; *dark gray* – continents; *triangle* – Gzhelian (Late Pennsylvanian) occurrence; *circle* – Cisuralian occurrence; *star* – North Spruce Mountain Ridge, Elko County, Nevada, U.S.A. (modified from Scotese, 2014).

Kobayashi (2005). Although temperate occurrences of *Biwaella* are less common than in tropical and subtropical latitudes, forms recovered from upper Asselian Boreal deposits are contemporaneous with Tethyan and Peri-Gondwanan occurrences, indicating that there was no lag in the timing of northward migration. The few Boreal localities include Spitsbergen of the Svalbard archipelago (Davydov, 2014) and Ellesmere Island of the Canadian Arctic (González, 2016).

Having arisen from a Tethyan schubertellid stock that was previously isolated from Midcontinent-Andean fusulinacean faunas by the closure of the Rheic Ocean, *Biwaella* is regarded as a migrant taxon in western Pangea. Only two previously described occurrences of *Biwaella* are known from western North America, both of which are regarded as Artinskian in age. Orchard et al. (2001) described *B.* ex gr. *B. provecta* (Wang et Sun, 1973) from the *Chalaroschwagerina vulgaris* Zone of the Cache Creek Terrane of central British Columbia, Nechako region, and Skinner and Wilde (1965a) reported the aforementioned occurrence of *B. americana* from New Mexico, U.S.A. The recent discovery of *B. americana* from the Riepe Spring Limestone in northeast Nevada provides additional information regarding the poorly understood migratory timing of the genus along the west coast of Pangea. The NSMR specimens of *B. americana* are significant in that they were recovered from moderately older Cisuralian strata of the upper Asselian-lower Sakmarian. The lower occurrence within the upper informal member of

the Riepe Spring Limestone of the NSMR section demonstrates that species of *Biwaella* had dispersed into the tropics of western Pangea earlier than the middle or late Artinskian as suggested by Davydov (2014).

Order **Schubertellida** Skinner, 1931

Family **Schubertellidae** Skinner, 1931

Genus ***Biwaella*** Morikawa et Isomi, 1960

Biwaella americana Skinner et Wilde, 1965a

Pl. 18, Figs. 1-8

Biwaella americana Skinner et Wilde, 1965a, p. 99, pl. 13, figs. 7–16.

A species with a small, irregularly subcylindrical to cylindrical test that commonly possesses five (rarely six) volutions at maturity. North Spruce Mountain Ridge specimens attain lengths (estimated from half lengths) ranging from 1.88 to 2.72 mm, averaging 2.22 mm. Diameters of mature specimens range from 0.46 to 0.66 mm, averaging 0.56 mm and producing an average form ratio of 3.80. Poles are broadly rounded to nearly amorphous in some instances. Lateral slopes may be highly irregular but are often nearly horizontal for much of the length of the test. The proloculus is minute, averaging 0.058 mm in outside diameter, although one specimen (F24128-15)

has an unusually large proloculus measuring 0.077 mm. The test begins to expand rapidly following the first two volutions. Heights of the first through fifth volutions among the NSMR specimens average 0.022, 0.028, 0.040, 0.058, 0.082 mm. The inner spirotheca is thin and nondescript, composed of a tectum and a lighter, poorly defined lower tectorium, whereas the outer spirotheca is much thicker and distinctly punctuated by evenly spaced mural pores. Septa are planar throughout much of the test but are typically curved in the far polar regions. Secondary axial fillings are absent. Chomata are very low, indistinct, and often absent in the outer volutions. Overall, the averages of measured characters among NSMR specimens fit well within the ranges provided by Skinner and Wilde (1965a). No conodont elements were collected from the *Biwaella* horizon, but several forms of *Cuniculinella* Skinner et Wilde, 1965b, a fusulinacean genus known from upper Wolfcampian (Sakmarian-Artinskian) deposits of the McCloud Limestone of northern California, were recovered in abundance alongside the sparse *B. americana*.

***Biwaella*? sp.**

Pl. 18, Fig. 9

Schubertella kingi? Thompson et Hazzard, 1946, p. 40–41, pl. 10, figs. 9.

Thompson and Hazzard (1946) illustrated several specimens of the prolific late Gzhelian-early Cisuralian species *Schubertella kingi* Dunbar et Skinner, 1937 from the Providence Mountains of southern California, U.S.A. One particularly large, tangentially oriented form was described by the original authors as potentially representing a "giant" specimen of *S. kingi*. The authors of the present study are skeptical of this assignment and suggest that the specimen may be a species of *Biwaella*. A comparison of the size and shape with NSMR specimens and types of *B. americana* is presented on Plate 18. The specimen was described as measuring at least 2.30 mm long and 0.70 mm in diameter. The septa are plane near the center of the test and curve in the polar regions. The original authors' estimated values, although slightly larger than the presently illustrated forms of *B. americana*, are close to the maxima provided by Skinner and Wilde (1965a). Unfortunately, the original photomicrograph does not clearly illustrate fine details of the test, so the nature of the thick, outer spirotheca and the true taxonomic assignment remain unknown. The questionable form was collected from an upper Asselian or lower Sakmarian interval which was placed within fusulinid zone 3 of Stevens and Stone (2007), indicating that it is nearly equivalent in age to the NSMR specimens.

Plate 18

Illustrated specimens of *Biwaella americana* Skinner et Wilde, 1965a from northeast Nevada, southwest New Mexico, and southern California.

1.A. No. F24128-15 (USNM), lower Sakmarian, upper part of the Riepe Spring Limestone, Elko County, Nevada, U.S.A.

1.B. No. F24128-15 (USNM), enlarged image of the perforate wall structure observed in the outer spirotheca; arrow designates mural pores

1.C. No. 24128-15 (USNM), additional enlarged image of the perforate wall structure observed in the outer spirotheca; arrow designates mural pores

2. No. UTA/NSMR 227.8-6, lower Sakmarian, upper part of the Riepe Spring Limestone, Elko County, Nevada, U.S.A.

3. No. UTA/NSMR 227.8-7, lower Sakmarian, upper part of the Riepe Spring Limestone, Elko County, Nevada, U.S.A.

4. No. UTA/NSMR 227.8-8, lower Sakmarian, upper part of the Riepe Spring Limestone, Elko County, Nevada, U.S.A.

5. No. UTA/NSMR 227.8-9, lower Sakmarian, upper part of the Riepe Spring Limestone, Elko County, Nevada, U.S.A.

6. No. P-52833, from Coll. NM-158, Skinner and Wilde, 1965a, axial section of paratype, Artinskian, upper part of the Horquilla Formation, Hidalgo County, New Mexico, U.S.A.

7. No. P-52831, from Coll. NM-158, Skinner and Wilde, 1965a, equatorial (sagittal) section of paratype, Artinskian, upper part of the Horquilla Formation, Hidalgo County, New Mexico, U.S.A.

8. No. P-52826, from Coll. NM-158, Skinner and Wilde, 1965a, axial section of holotype, Artinskian, upper part of the Horquilla Formation, Hidalgo County, New Mexico, U.S.A.

9. "*Schubertella kingi*" Thompson et Hazzard, 1946 (Stanford University Paleontological Type Collection, no. 7681) illustrated by Thompson and Hazzard (1946), tangential section, lower Cisuralian (upper Asselian-lower Sakmarian), Bird Spring Formation, San Bernardino County, California; originally described as a "giant" specimen of *Schubertella kingi*, the authors suspect it may be an erroneously identified form of *Biwaella*.

Plate 18

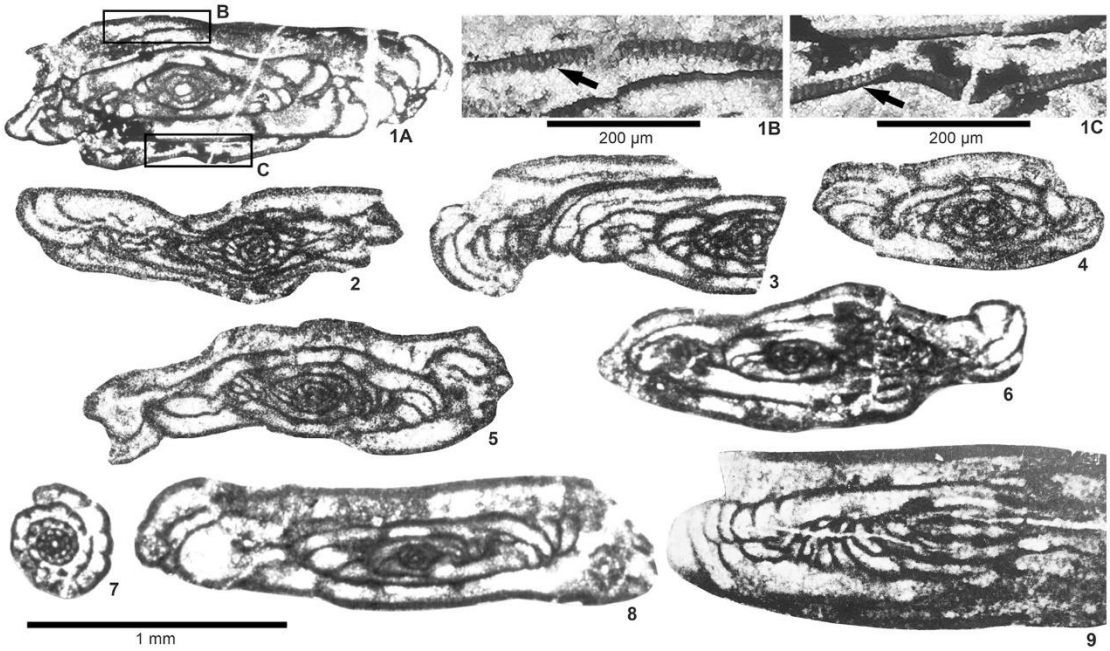

CHAPTER 7 – INTRODUCTORY REMARKS

This article discusses the Kasimovian-Gzhelian (Late Pennsylvanian) conodont succession from the uppermost part of the Ely Limestone and the lower and middle informal members of the Riepe Spring Limestone at Spruce Mountain Ridge, Elko County, Nevada. The stratigraphic section presented herein coincides with the lower ~238 m of the full columnar section illustrated in Chapter 3 (Figs. 7.0.1, 7.0.2).

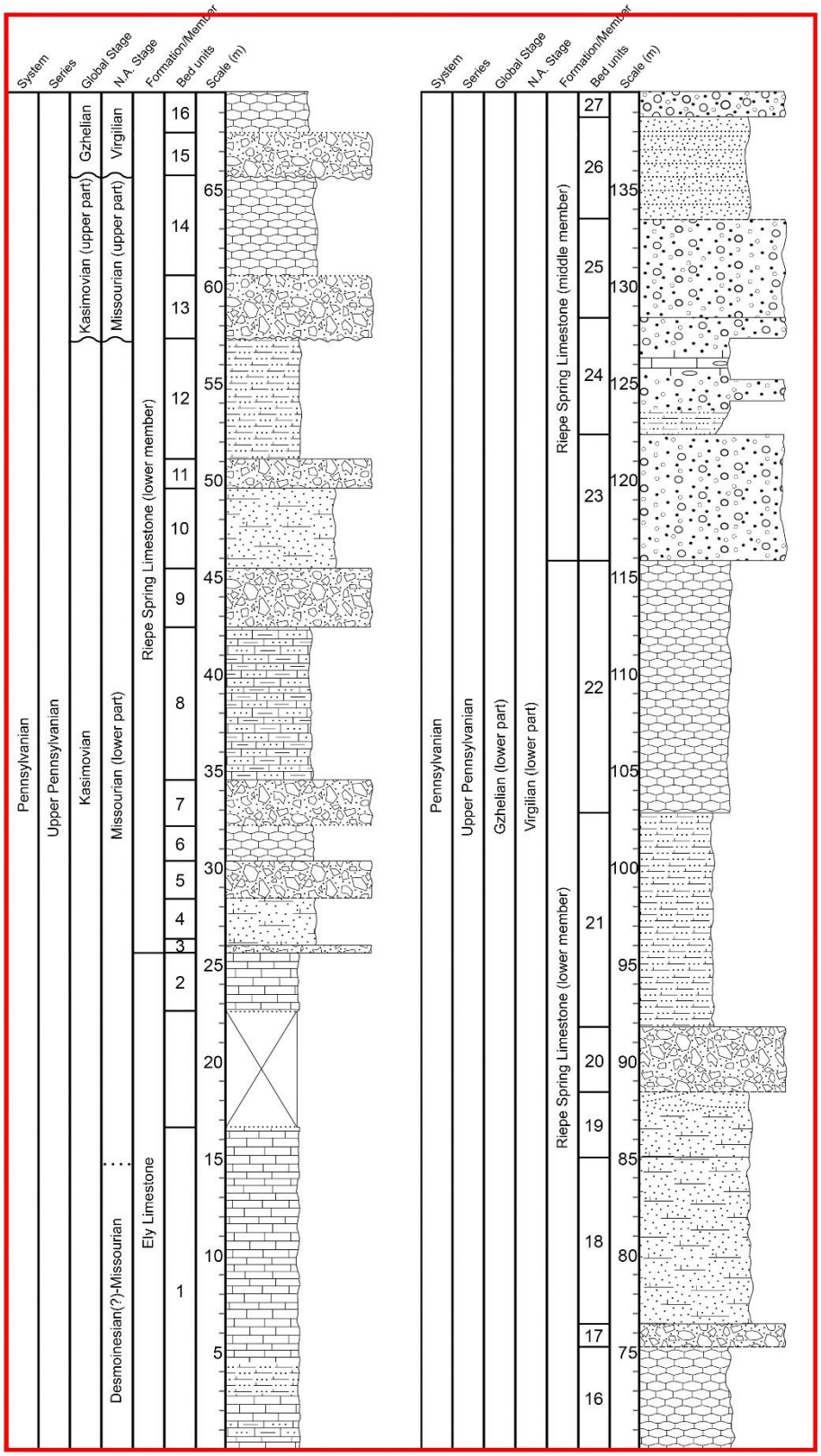

Fig. 7.0.1 – Stratigraphic column illustrating the portion of the NSMR section discussed in the following chapter (outlined in red).

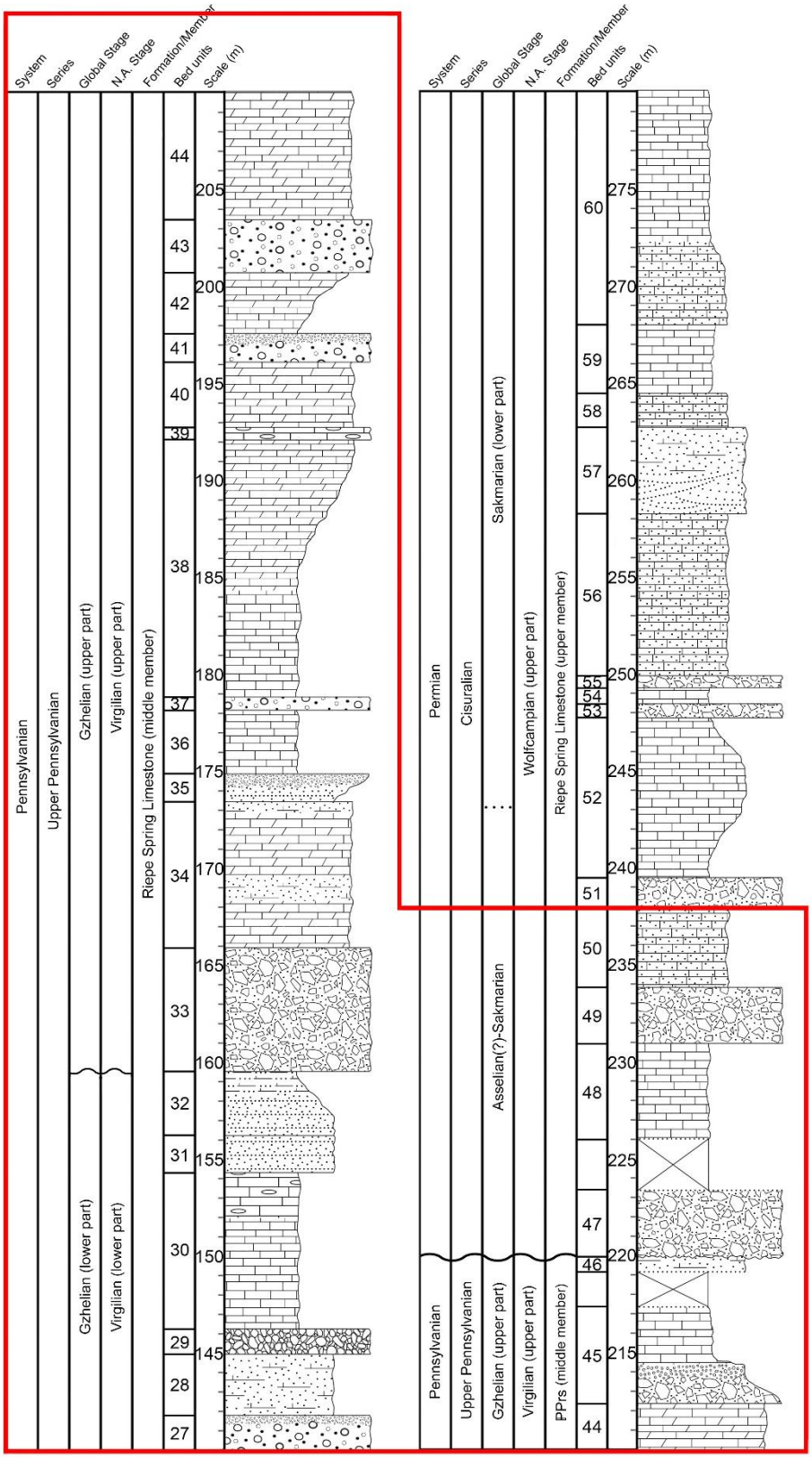

Fig. 7.0.2 – Conitnued stratigraphic column illustrating the portion of the NSMR section discussed in the following chapter (outlined in red).

CHAPTER 7: KASIMOVIAN–GZHELIAN (LATE PENNSYLVANIAN) CONODONTS FROM THE LOWER AND MIDDLE PARTS OF THE RIEPE SPRING LIMESTONE, SPRUCE MOUNTAIN RIDGE, ELKO COUNTY, NEVADA

Abstract: A sparse Late Pennsylvanian conodont succession is present in the mixed carbonate-siliciclastic strata of the uppermost part of the Ely Limestone and the lower and middle informal members of the Riepe Spring Limestone at Spruce Mountain Ridge, Elko County, Nevada. The Upper Pennsylvanian strata of the North Spruce Mountain Ridge (NSMR) section measure approximately 220 m thick and are composed of alternating deposits of quartzose carbonate rocks, calcareous sandstone, and quartzose conglomerate. The recovered conodont assemblage primarily consists of *Idiognathodus* and *Streptognathodus* morphotypes ranging from early-middle Kasimovian to late Gzhelian in age. *Adetognathus lautus* and sparse morphotypes of *Hindeodus* occur in the underlying uppermost part of the Ely Limestone, but do not provide adequate age control. Eight previously described idiognathodid species occur in the collections from the lower and middle informal members of the Riepe Spring Limestone. Kasimovian species include *Idiognathodus cancellosus*, *I.* aff. *confragus*, *Streptognathodus elegantulus*, and *S.* aff. *firmus*. Gzhelian species include *I. lateralis*, *S. pawhuskaensis*, *S. virgilicus*, and *S. bellus*. Integration of the accompanying Late Pennsylvanian fusulinid succession provides additional age constraint throughout the lower and middle informal members of the Riepe Spring Limestone.

Introduction

This article describes the occurrences and distribution of Late Pennsylvanian conodonts from the uppermost part of the Ely Limestone and the lower and middle informal members of the Riepe Spring Limestone at Spruce Mountain Ridge, Elko County, northeast Nevada. The stratigraphic section illustrated in Figure 7.1 corresponds to the lower 237.9 m of the complete North Spruce Mountain Ridge (NSMR) section discussed in Chapters 3 and 4. The portion of the section discussed herein includes the uppermost 25.7 m of the Ely Limestone, the lower and middle informal members of the Riepe Spring Limestone, and the lowest 18 m of the upper informal member of the Riepe Spring Limestone in order to align the upper limit of this stratigraphic section with the base of the section presented in Chapter 8. A lithostratigraphic overview for the complete NSMR section is presented in Chapter 3.

Little work has been published on the conodont faunas of the Riepe Spring Limestone outside of the type area near Ely, Nevada. The Kasimovian (Upper Pennsylvanian)-Artinskian (upper-middle Cisuralian) section at Spruce Mountain Ridge is uncommon for the Riepe Spring Limestone, as most documented exposures of the formation are strictly Permian deposits disconformably overlying Middle or Upper Pennsylvanian strata. As a result, the few previous accounts of the conodont succession from the Riepe Spring Limestone described early to middle Cisuralian faunas consisting primarily

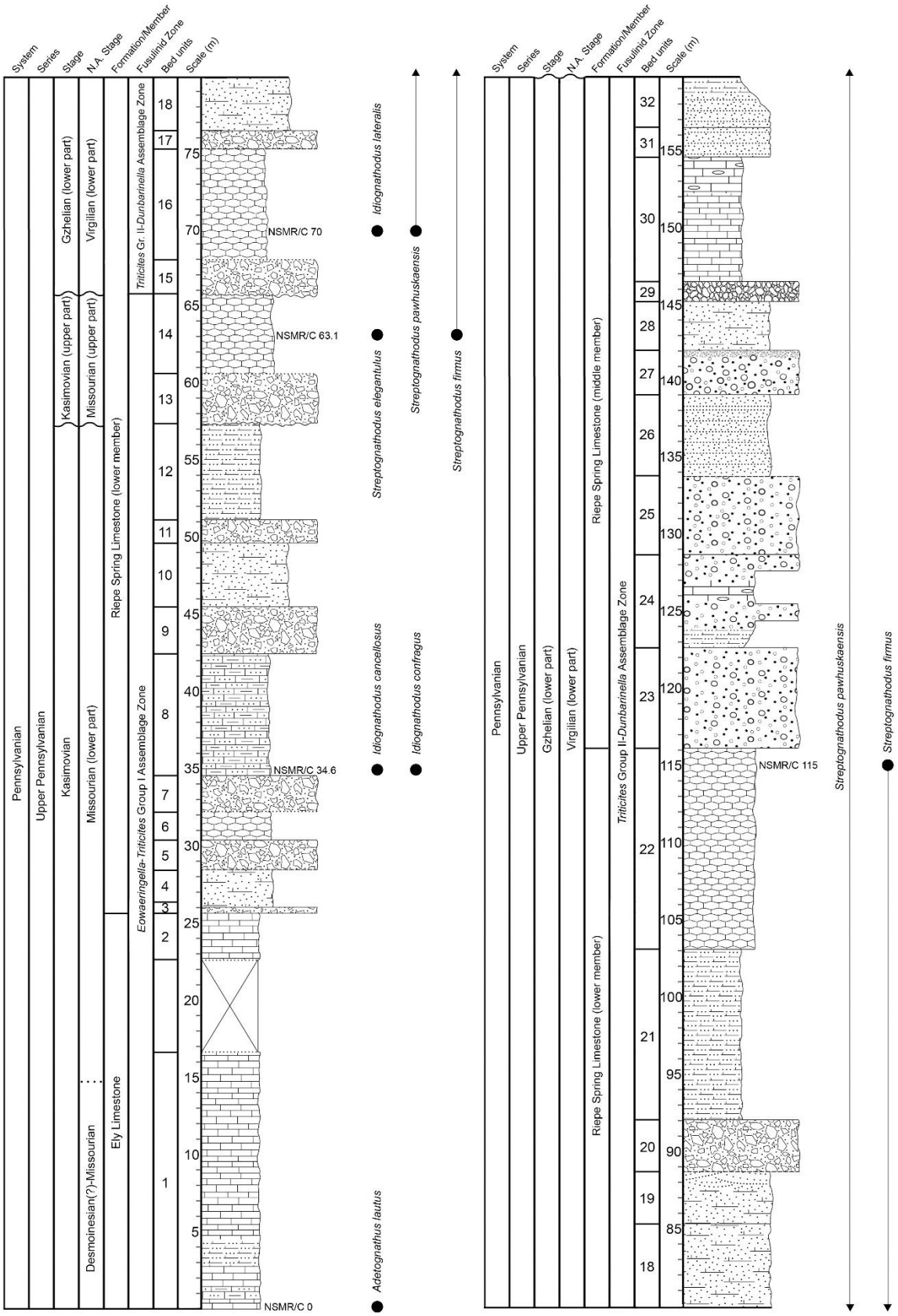
System
Series
Stage
N.A. Stage
Formation/Member
Fusulinid Zone
Bed units
Scale (m)
Pennsylvanian
Upper Pennsylvanian
Kasimovian
Gzhelian (lower part)
Kasimovian (upper part)
Desmoinesian(?)-Missourian
Missourian
Virgilian (lower part)
Missourian (upper part)
Ely Limestone
Riepe Spring Limestone (lower member)
Eowaeringella-Triticites Group I Assemblage Zone
Triticites Gr. II-Dunbarinella Assemblage Zone
Riepe Spring Limestone (middle member)
NSMR/C 0
NSMR/C 34.6
NSMR/C 63.1
NSMR/C 70
NSMR/C 115
Adetognathus lautus
Idiognathodus cancellosus
Idiognathodus confragus
Streptognathodus elegantulus
Idiognathodus lateralis
Streptognathodus pawhuskaensis
Streptognathodus firmus

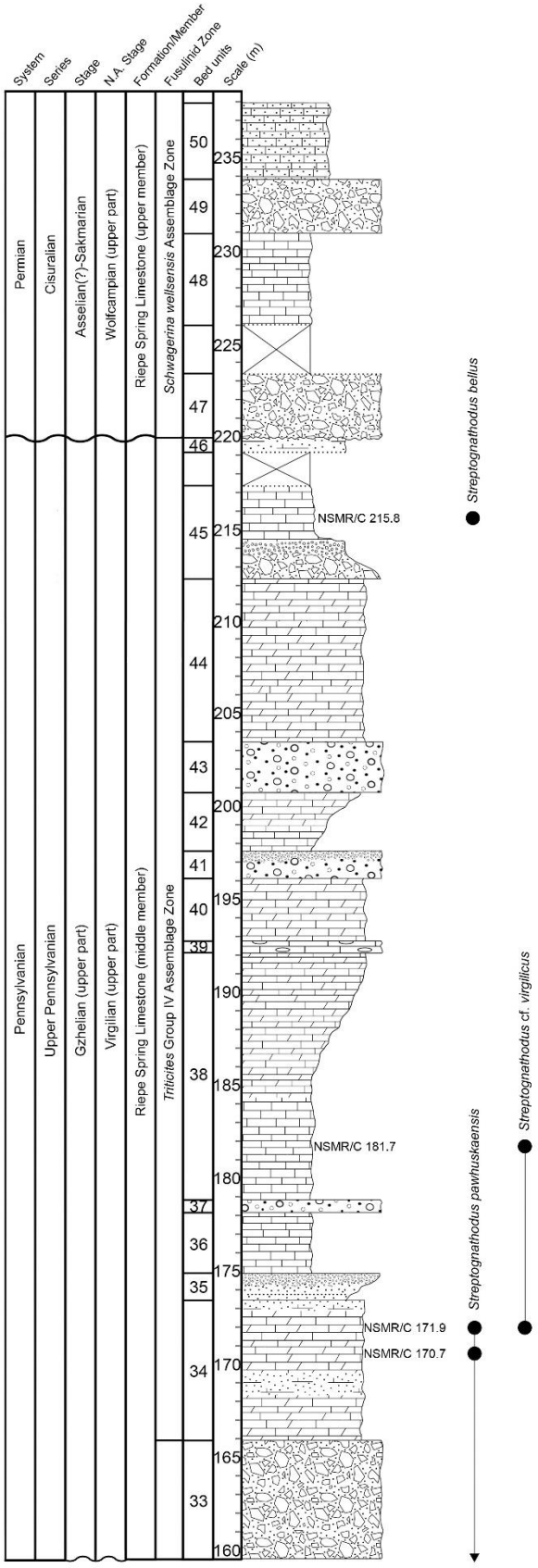
System
Series
Stage
N.A. Stage
Formation/Member
Fusulinid Zone
Bed units
Scale (m)
Permian
Pennsylvanian
Cisuralian
Upper Pennsylvanian
Asselian(?)-Sakmarian
Gzhelian (upper part)
Wolfcampian (upper part)
Virgilian (upper part)
Riepe Spring Limestone (upper member)
Riepe Spring Limestone (middle member)
Schwagerina wellsensis Assemblage Zone
Triticites Group IV Assemblage Zone
50
49
48
47
46
45
44
43
42
41
40
39
38
37
36
35
34
33
235
230
225
220
215
210
205
200
195
190
185
180
175
170
165
160
NSMR/C 215.8
NSMR/C 181.7
NSMR/C 171.9
NSMR/C 170.7
Streptognathodus bellus
Streptognathodus pawhuskaensis
Streptognathodus cf. virgilicus

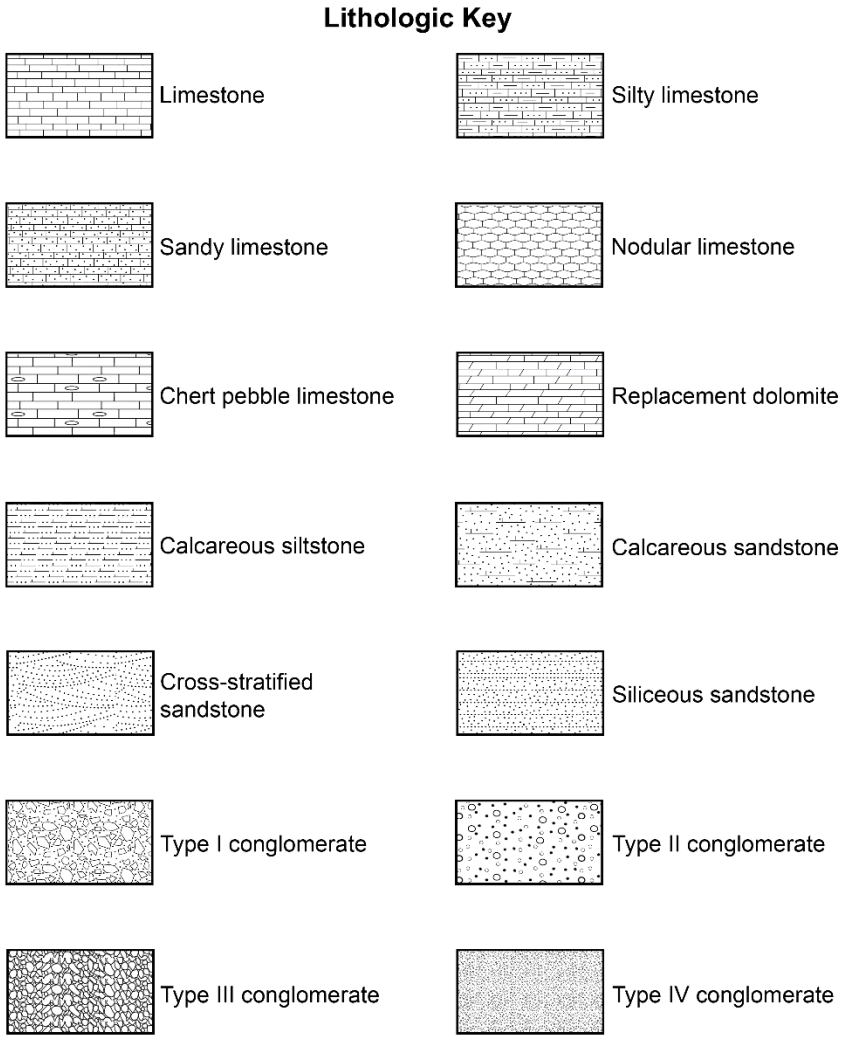

← **Figure 7.1** – Multiple page figure includes a lithologic key and stratigraphic columns of the NSMR measured section with conodont occurrences. NSMR numbers along the right side of the columns correspond with collection numbers of samples.

of sweetognathid conodonts (e.g., *Sweetognathus*, *Neostreptognathodus*) (see Ritter, 1986, 1987). The Upper Pennsylvanian portion of the NSMR section preserves idiognathodid conodonts never reported from the Riepe Spring Limestone, including nominate species of two biozones of the Kasimovian and Gzhelian (i.e., *Streptognathodus virgilicus* and *S. bellus*). The integration of Late Pennsylvanian conodont and fusulinid assemblages shows that at least four significant erosional disconformities occur throughout the lower and middle informal members of the Riepe Spring Limestone, including a vacuity spanning the Kasimovian-Gzhelian boundary. Consequently, large portions of major conodont interval zones are not preserved within the measured section and zonal assignments may be inferred from occurrences in single bedding units. Fusulinid zonation provides an additional framework allowing for more precise age control where conodont data are insufficient or lacking. The fusulinid zones illustrated in Figure 7.1 are those defined in Chapter 4.

Location, Materials, and Methods

Spruce Mountain Ridge extends north of Spruce Mountain (10,262 ft/ 3,127 m) approximately 24 km and is bordered by Clover Valley to the west and Independence Valley to the east. The measured section, herein regarded as the North Spruce Mountain Ridge (NSMR) section, is located 16 km north of Spruce Mountain and 15 km east northeast of the junction of U.S. Route 93 (Great Basin Highway) and Spruce Mountain Road (Fig. 7.2). The base of the

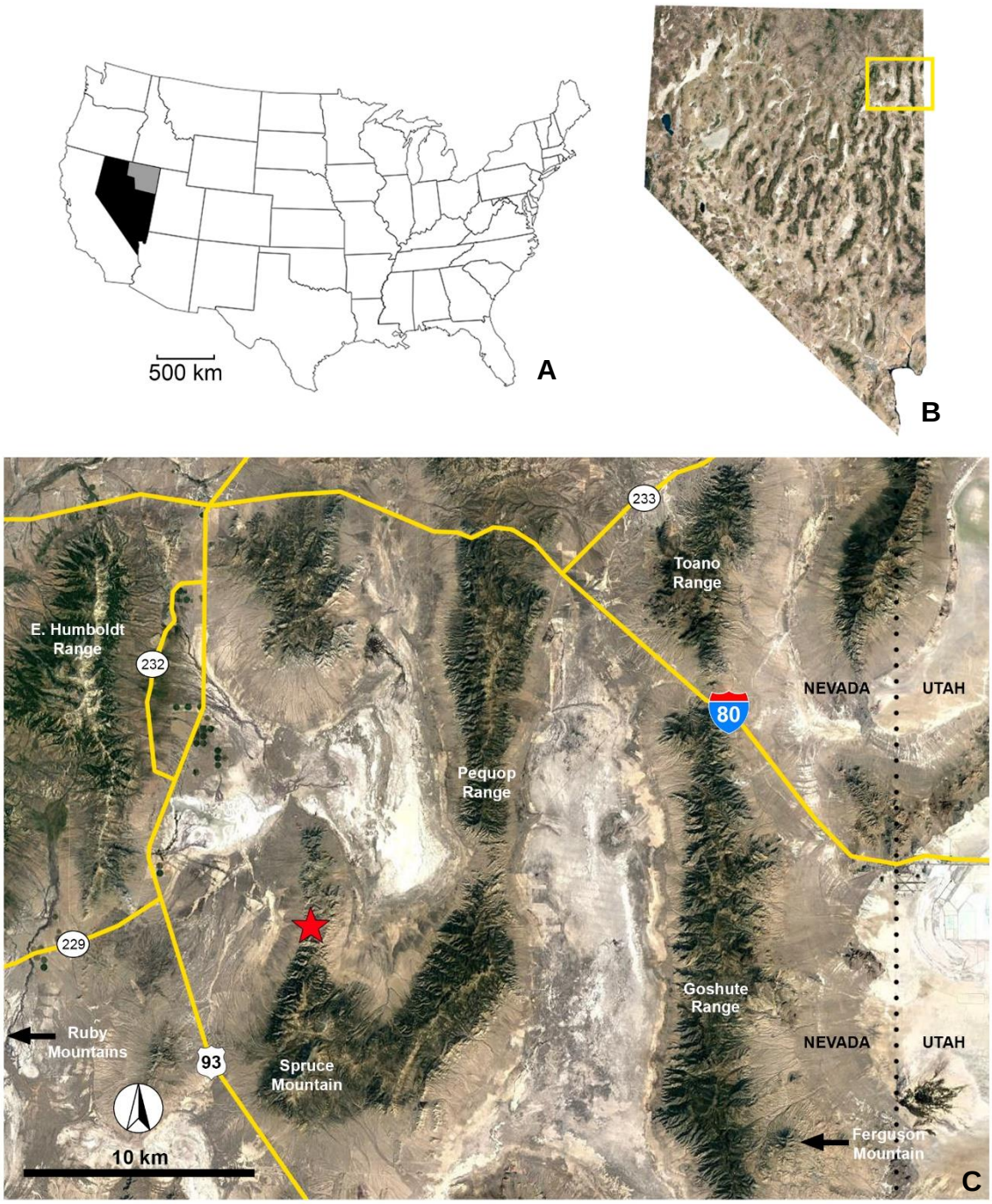

Figure 7.2 – **A)** Elko County (gray), Nevada (black), U.S.A.; **B)** Satellite map of Nevada, U.S.A. Yellow enclosed region shows the Spruce Mountain area; **C)** Enlarged image of the yellow enclosed region in Fig. 7.2B. Red star = North Spruce Mountain Ridge section (NSMR) (modified from Google Earth, 2014).

measured section is on the far west side of the north-south ridge (40º 40' 47.08" N, 114º 49' 35.04" W), nearly 500 m above where the alluvium of Clover Valley obscures the upper part of the Ely Limestone.

All Late Pennsylvanian conodonts were collected from the uppermost part of the Ely Limestone and the overlying lower and middle informal members of the Riepe Spring Limestone at Spruce Mountain Ridge. The NSMR section coincides with Section 1 of Hope (1972) and USGS Map GQ-942 (map). Samples were taken at 1.5 m intervals where fossiliferous limestone outcrops were available.

Samples were broken into small pieces (two to six centimeters in diameter) with a hammer, rinsed thoroughly to remove carbonate dust, and chemically digested using a buffered 8-10% formic acid solution. The formic acid solution was changed every 1.5 days and the digestion process was repeated until nearly all soluble material was dissolved. Insoluble residues were gently sieved between 16 and 120 meshes and were collected with each change of the buffered acid solution. Complete digestion of a three to five-kilogram carbonate sample typically required seven to 10 days of continuous processing.

Insoluble residues were dried in an oven at 60º C after the sample material was completely digested. All recovered conodont elements were assigned a CAI (Conodont Color Alteration Index) value of 3.5 to 4, thereby eliminating any concern of further thermal alteration at the moderately low

drying temperature. The heavy mineral fraction of the insoluble reside was then separated from quartz sand and dolomite grains using separation funnels and a solution of tetrabromoethane ("carbon tetrabromide") with acetone measured to a density of 2.81 to 2.84 g/ml, depending on the volume of dolomite in a given sample. Separation funnels were covered and stirred twice daily for two to three days. Once captured, the heavy fraction was rinsed with acetone and left to dry under a fume hood for several days. Samples were left under the hood until completely odorless and were then picked for conodont elements.

The preservation of most specimens is quite poor, and many specimens show signs of hydrothermal alteration (i.e., apatite recrystallization). Most elements were at least partially broken as well, likely as a result of the pervasive microfracturing of many limestone units within the NSMR section. In addition to the poor preservation, conodont yields from the lower and middle informal members of the Riepe Spring Limestone were unexpectedly low. Most carbonate rock samples weighing approximately three to five kilograms produced between zero and three moderately preserved, mature specimens (P_1 elements). Low yields are attributed herein to terrigenous sediment dilution and unfavorably shallow paleoenvironments. Many of the recovered faunules are composed predominantly or entirely of extremely small and delicate P_1 elements and could represent juvenile populations inhabiting nearshore "nursery" grounds. The 14 specimens illustrated herein

are the best-preserved conodont material collected from the Upper Pennsylvanian part of the NSMR section.

Systematic Paleontology

Systematic descriptions prepared in the style of *Bulletins of American Paleontology*.

Class **CONODONTA** Pander, 1856

Subclass **CONODONTI** Branson, 1938

Order **OZARKODINIDA** Dzik, 1976

Family **CAVUSGNATHIDAE** Austin and Rhodes, 1981

Genus ***ADETOGNATHUS*** Lane, 1967

Type species.—*Cavusgnathus lautus* Gunnell, 1933.

Remarks.—A long-ranging, Serpukhovian (Late Mississippian) to early Cisuralian taxon with Class III symmetry and a carminiscaphate P_1 element characterized by a deep medial sulcus and short but pronounced transverse ridges (Lane, 1968). As with other cavusgnathid conodonts, the blade of *Adetognathus* attaches directly to the margin of the platform ("parapet") rather than continuing as a medial carina.

Adetognathus shares a common P_1 element morphology with other genera of the *Cavusgnathidae*, including *Clydagnathus* Rhodes, Austin, and Druce, 1969, *Cavusgnathus* Harris and Hollingsworth, 1933, and *Cloghergnathus* Austin in Austin and Mitchell, 1975. Of these genera, *Adetognathus* most closely resembles *Cavusgnathus*, but differs in its diminished to absent fixed blade and longer free blade (Sweet, 1988).

Adetognathus lautus (Gunnell, 1933)

Pl. 19, Fig. 1

Adetognathus lautus (Gunnell, 1933) Lane and Straka, 1974, p. 64-65, figs. 36.17, 36.21, 36.22, 36.25-36.31, figs. 38.1-38.4, 38.6-38.8, 38.10-38.15, 38.20, figs. 39.1-39.3, 39.7-39.14 [see Lane and Straka, 1974 for main synonymy].

Diagnosis.—A species of *Adetognathus* in which the platform of the large, tapered P_1 element is characterized by a deep medial sulcus and steep, peripheral transverse ridges.

Description.—The P_1 element of *Adetognathus lautus* has a blade of short to moderate length bearing six to nine denticles, the largest and dorsal-most of which is high and wide, occupying the position of the blade-platform junction. The P_1 element has a high dorso-ventral to rostro-caudal ratio and lacks

accessory features (i.e., nodes, lobes, carina). The blade attaches directly to the parapet of the dorsal process. Regardless of the chirality of a given P_1 element, the blade attaches to the right-hand side parapet (in oral view), indicating that the blade is positioned rostrally in dextral elements and caudally in sinistral elements. The unattached, left-hand side parapet extends slightly beyond the deflected blade-platform junction and terminates abruptly and steeply towards the aboral surface. The platform is lanceolate in in oral view and may exhibit a pinched shape with a pronounced caudal crimp. The platform lacks ornamentation except for two marginal rows of steeply-dipping transverse ridges that are completely interrupted by a deep medial sulcus. The basal cavity occupies the entire aboral length of the platform and is typically narrow but may be flared ventrally.

Occurrence.—Base of the NSMR section (~0 m, unit 1); level - lower-middle part of the Kasimovian Stage (lower part of the Missourian Stage). Occurs with *Hindeodus* sp. (not illustrated).

Remarks.—The cavusgnathid conodonts are best known for their strong intergeneric morphological similarities. The resulting difficulty faced by biostratigraphers in recognizing forms of *Clydagnathus* Rhodes et al., 1969, *Cavusgnathus* Harris and Hollingsworth, 1933, and *Adetognathus* was summarized by Sweet (1988), in which he admitted to often finding it difficult

to distinguish species of one genus from the next. Although *Adetognathus* is typically considered a biostratigraphically ineffective taxon, the genus does serve as a useful paleoenvironmental indicator as it is considered euryhaline and is often associated with extremely shallow or even marginal marine deposits (Sweet, 1988; Orchard et al., 2001).

Family **IDIOGNATHODONTIDAE** Harris and Hollingsworth, 1933

Genus ***IDIOGNATHODUS*** Gunnell, 1931

Type species.—*Idiognathodus claviformis* Gunnell, 1931.

Remarks.—A Bashkirian (Early Pennsylvanian) through early Gzhelian (Late Pennsylvanian) idiognathodid taxon characterized by a robust, carminiscaphate P_1 element with accessory lobes and rows of transverse ridges ornamenting the dorsal process. The free blade attaches to the platform in a medial position where it is confluent with a short carina composed of indistinct, fused denticles.

P_1 elements of *Idiognathodus* differ from those of *Streptognathodus* in the lack of a well-developed medial trough bifurcating the parallel to subparallel transverse ridges of the platform. The medial carina of *Idiognathodus* is typically shorter and more irregular than the moderately long, straight carina characteristic of many forms of *Streptognathodus*.

Idiognathodus cancellosus (Gunnell, 1933)

Pl. 19, Fig. 2

Streptognathodus cancellosus Gunnell, 1933, p. 270, pl. 31, fig. 10; Kozitskaya et al., 1978, pl. XXVI, figs. 11-14, pl. XXVII, figs. 8, 10; Barrick and Boardman, 1989, pl. 1, figs. 11, 18; Stevens et al., 2001, fig. 13.10; Ritter et al., 2002 (part), p. 513-514, fig. 8.13; Goreva and Alekseev, 2010, pl. 1, fig. 6.

Idiognathodus cancellosus (Gunnell, 1933). Heckel et al., 2011, p. 264, pl. 1, figs. 15, 17, 18, 20, 27; Barrick et al., 2013a, pl. 3, fig. 10 (re-illustration of holotype); Rosscoe and Barrick, 2013, p. 361, figs. 5g, 5h, 5m, 5q-5s; Lucas et al., 2016, fig. 41.20, 41.21.

Diagnosis.— A species of *Idiognathodus* bearing a P_1 element with reduced accessory lobes and a short medial carina followed by one to two rows of small nodes extending toward the dorsal termination of the platform.

Description.—The single recovered P_1 element of *Idiognathodus cancellosus* lacks the free blade and blade-platform junction. Typically, the free blade of *I. cancellosus* is long, robust, and slightly arcuate. The blade meets the platform in a medial position, transitioning to a medial carina. The carina

extends approximately one-quarter to one-third the length of the platform, terminating ventral to the dorsal extent of the reduced caudal lobe. Caudal lobe extends approximately two-fifths the length of the platform and the rostral lobe terminates just ventral of the former, approximately one-third the length of the platform. The small caudal lobe of the lone Riepe Spring Limestone specimen is partially damaged and bears two fused nodes, whereas the rostral lobe is fully intact and bears three smaller, less strongly fused nodes. The platform is widest just dorsal to the extent of the accessory lobes and tapers evenly toward the dorsal terminus. P_1 elements of *I. cancellosus* have a high dorso-ventral to rostro-caudal ratio due to the significant reduction of the accessory lobes. The adcarinal ridges of the illustrated specimen are poorly preserved, particularly the caudal ridge, but the rostral ridge is short, moderately ornamented with fused nodes, and clearly separates the main platform from the rostral lobe. The margins of the platform appear slightly elevated due to the presence of short, parallel transverse ridges that are interrupted medially by a shallow groove. The dorsal termination of the platform is bluntly pointed. Although much of the basal cup is missing from the illustrated specimen, the basal cavity is deep and wide, as in most idiognathodids.

Occurrence.—34.6 m above the base of the section (unit 8); level - lower-middle part of the Kasimovian Stage (lower part of the Missourian Stage). Occurs with *Idiognathodus* aff. *confragus*.

Remarks.—*Idiognathodus cancellosus* was originally described by Ellison (1941) as a species of *Streptognathodus* due to the interruption of the dorsal transverse ridges by a medial groove. However, the groove is distinctly less pronounced than the medial trough that is now characteristic of *Streptognathodus*. *Idiognathodus cancellosus* is considered the ancestral form to *I. confragus*, from which the former differs by having a more developed medial groove and nodes dorsal to the carina.

Idiognathodus cancellosus bears some resemblance to other early Missourian forms of the genus with a medial groove and slightly raised platform margins, including *I. biliratus* Gunnell, 1933 and *I. pseudocarinatus* Rosscoe and Barrick, 2013. *Idiognathodus cancellosus* differs from the *I. biliratus* by bearing both caudal and rostral lobes and having a shorter medial carina. *Idiognathodus pseudocarinatus* also has a longer medial carina than *I. cancellosus* and bears short, isolated transverse ridges dorsal of the carina rather than discrete, hemispherical nodes. The dorsal termination of the platform in *I. pseudocarinatus* is also more sharply pointed than that of *I. cancellosus*.

Idiognathodus* aff. *confragus Gunnell, 1933

Pl. 19, Fig. 3

Diagnosis.—A species of *Idiognathodus* bearing a narrow P_1 element with a short medial carina, reduced to absent rostral lobe and a reduced, ventrally shifted caudal lobe ornamented with one to several small nodes.

Description.—The P_1 element of *Idiognathodus* aff. *confragus* has a long, slightly arcuate free blade which transitions dorsally into a short, unornamented medial carina extending slightly less than one-third the length of the platform. The caudal lobe is reduced in size and is located on the ventral third of the platform, terminating just dorsal of the medial carina. The herein illustrated specimen (Pl. 19, Fig. 3) bears three discrete, hemispherical nodes along the caudal lobe. The rostral lobe is also ventrally shifted, but is smaller in size and bears fewer nodes, and the accessory lobes are bordered by lightly ornamented caudal and rostral adcarinal ridges terminating adjacent to their respective accessory lobes. The caudal adcarinal ridge is longer and very slightly caudally deflected, producing a small gap between the parapet and the carina. The rostral adcarinal ridge is nearly straight and approximately two-thirds the length of the caudal ridge. Beyond the adcarinal ridges, the caudal margin of the platform is slightly concave, whereas the rostral margin is convex. Dorsal two-thirds portion of the

platform is ornamented with subparallel transverse ridges extending the remaining length of the platform. The dorsal termination of the platform is triangular and sharp. The basal cup is slightly flared ventrally, and the basal cavity is deep and wide.

Occurrence.—34.6 m above the base of the section (unit 8); level - lower-middle part of the Kasimovian Stage (lower part of the Missourian Stage). Occurs with *Idiognathodus cancellosus*.

Remarks.— *Idiognathodus* aff. *confragus* differs from *I. confragus* in its shorter medial carina, which only reaches just over one-half the length of the caudal lobe in the illustrated specimen. *Idiognathodus* aff. *confragus* differs from *I. cancellosus*, with which it co-occurs, in the ventrally shifted accessory lobes and lack of medial nodosity following the carina. Ritter et al. (2002) noted that the similarity between these two forms is more pronounced in smaller specimens of *I. cancellosus*, but this is unsurprising given the remarkable similarities among most juvenile idiognathodids.

Idiognathodus lateralis Hogancamp, Barrick, and Strauss, 2016

Pl. 19, Fig. 9

Idiognathodus lateralis Hogancamp, Barrick, and Strauss, 2016, p. 495, 497, figs. 15A-15M [see Hogancamp, Barrick, and Strauss, 2016 for main synonymy].

Diagnosis.—A species of *Idiognathodus* bearing asymmetrical P_1 elements with a weakly-developed caudal lobe and a caudally positioned eccentric groove partially to fully disrupting the transverse ridges of the dorsal process.

Description.—The P_1 elements of *Idiognathodus lateralis* form an asymmetrical pair in which the sinistral and dextral elements differ in overall size, platform shape, lobe size/placement, and the nature of the caudal eccentric groove. However, due to the absence of sinistral specimens from the present collection, a description of only the dextral P_1 element follows. For a comprehensive description of the sinistral P_1 element of *I. lateralis* see the type description provided by Hogancamp et al. (2016).

The blade of the dextral P_1 element attaches in a medial position and transitions into a short, subtly denticulate carina. The medial carina of the one specimen recovered from the lower informal member of the Riepe Spring Limestone extends approximately one-third the length of the platform and is deflected ventrally toward the rostral adcarinal ridge. The rostral adcarinal ridge consists of one to two discrete nodes directly above the ventral-most transverse ridge and is nearly straight. The longer caudal adcarinal ridge of

the illustrated specimen is deflected away from the carina at an angle of approximately 42º (measured with ImageJ). Both rostral and caudal adcarinal ridges terminate ventral to the termination of the carina. P_1 elements (both sinistral and dextral) of *I. lateralis* characteristically lack a rostral accessory lobe and have a moderately well-developed caudal lobe bearing one to five or more discrete to partially fused nodes. The caudal lobe of the illustrated specimen is narrow and bears two partially fused nodes. Slightly undulating, subparallel transverse ridges occupy the dorsal two-thirds of the platform and are partially interrupted by an incipient, caudally shifted eccentric groove. This placement and weak degree of development in the eccentric groove are consistent with the description of dextral elements provided by Hogancamp et al. (2016). The dorsal termination of the platform is triangular, slightly caudally deflected, and sharp.

Occurrence.—70 m above the base of the section (unit 16); level - basal part of the Gzhelian Stage (lower part of the Virgilian Stage). Occurs with *Streptognathodus pawhuskaensis*.

Remarks.—A single dextral P_1 element of *Idiognathodus lateralis* was recovered from the nodular limestone of unit 16 in association with more abundant *Streptognathodus pawhuskaensis*. Despite the poor preservation of the lone specimen, the strongly deflected caudal adcarinal ridge, reduced

caudal lobe, and lack of a rostral lobe clearly indicate that the specimen is the dextral P_1 element of *I. lateralis*.

Idiognathodus lateralis belongs to the basal Gzhelian *I. simulator* group, consisting of idiognathodids bearing asymmetrical P_1 element pairs, caudal eccentric grooves, and short adcarinal ridges. This group includes I. simulator (Ellison, 1941), *I. auritus* (Chernykh, 2005), *I. praenuntius* (Chernykh, 2005), *I. lateralis*, and *I. luganicus* (Kozitskaya, 1978) (Hogancamp et al., 2016). Of these closely related forms, *I. lateralis* most closely resembles *I. praenuntius*, from which it is differs by exhibiting a higher dorso-ventral to rostro-caudal ratio.

Genus ***STREPTOGNATHODUS*** Stauffer and Plummer, 1932

Type species.—*Streptognathodus excelsus* Stauffer and Plummer, 1932.

Remarks.—A genus of idiognathodid which arose from *Idiognathodus* during middle Kasimovian (early-middle Missourian) time and became the dominant conodont genus through the remainder of the Late Pennsylvanian. *Streptognathodus* differs from other idiognathodids by having a P_1 element with a distinct medial trough along the oral surface of the platform and having reduced accessory lobes or lacking them altogether. The major faunal transition nearly coinciding with the Carboniferous-Permian boundary

records the beginnings of the ecological replacement of *Streptognathodus* with *Sweetognathus* during the early Cisuralian.

Streptognathodus bellus Chernykh and Ritter, 1997

Pl. 19, Fig. 14

Streptognathodus bellus Chernykh and Ritter, 1997 (part), p. 464, figs. 4.1-4.6; Forke, 2002, p. 259, pl. 44, figs. 1-3; Chernykh, 2005, p. 131-132, pl. 7, figs. 13-16; Boardman et al., 2009 (part), p. 124-125, pl. 2, fig. 11, pl. 3, fig. 9.

Diagnosis.—A species of *Streptognathodus* characterized by numerous long, pronounced transverse ridges and a shallow, rostrally shifted trough.

Description.—The P_1 element of *Streptognathodus bellus* typically has a nearly straight free blade of moderate length, but the single, dextral Riepe Spring Limestone specimen is lacking the blade. The blade transitions into a medial carina of moderate length, approximately one-third the length of the platform in the illustrated specimen. One to three nodes commonly occur dorsal to the termination of the carina. The herein illustrated form bears one partially fused node followed by one discrete node. A shallow, rostrally deflected trough follows the carinal terminus. The platform is asymmetrical with a nearly straight ventral one-third and a dorsal two-thirds that deflects

caudally. This deflection coincides with a slight crimp in the caudal margin of the platform adjacent to the termination of the carina. The illustrated specimen lacks both caudal and rostral accessory lobes, but incipient lobes bearing a single node may occasionally be present in larger, potentially gerontic specimens. The nodose caudal adcarinal ridge forms a nearly straight parapet close to the carina with a slight rostral deflection of the dorsal half of the ridge. The rostral adcarinal ridge is nearly straight as well, but the full ventral extent of the parapet is obscured by a foreign grain adhering to the illustrated specimen. The dorsal two-thirds portion of the platform is ornamented with straight to slightly bent transverse ridges. The longest transverse ridges are located immediately dorsal to the crimp along the caudal margin and are entirely uninterrupted by the shallow trough, whereas the shorter, dorsal-most ridges are bifurcated by the trough. Opposing dorsal-most transverse ridges are at a slight angle to one another, causing them to be slightly offset. The dorsal termination of the platform is sharp. The basal cavity is deep and moderately wide, and the basal cup is medially flared.

Occurrence.—215.8 m above the base of the section (unit 45); level - uppermost part of the Gzhelian Stage (uppermost part of the Virgilian Stage). *Streptognathodus bellus* occurs with the fusulinids *Triticites pinguis* Dunbar and Skinner, 1937 and *Pseudofusulina mediotenebraeus* Wilde, 2006.

Remarks.—In the Midcontinent, the *Streptognathodus bellus* Zone succeeds the long-ranging *S. virgilicus* (*s.s.*) Zone and is defined by the first appearance of the former in the Brownville Limestone Member of the Wood Siding Formation (Boardman et al., 2009; Barrick et al., 2013a). Boardman et al. (2009) considered *S. bellus* the ancestral form to each of the three late Gzhelian through Asselian *Streptognathodus* lineages described therein. These Midcontinent lineages include a "robust lineage," a "nodular lineage," and an "elongate lineage." In South China and the southern Urals, the *S. bellus* Zone is considered the penultimate conodont biozone of the Gzhelian and is followed by the uppermost Gzhelian *S. wabaunsensis* Zone (Wang et al., 2018).

Streptognathodus bellus bears a close resemblance to several other latest Gzhelian to early Cisuralian forms of slender, unornamented (i.e., lobe-less) forms of *Streptognathodus*. *Streptognathodus bellus* is distinguished from *S. brownvillensis* by its more robust P_1 element and the greater continuity of its transverse ridges. *Streptognathodus longus* Chernykh, 2005 is narrower, has a slightly deeper trough, and a shorter medial carina. *Streptognathodus elongatus* Gunnell, 1933 is also narrower and has a deeper trough with a longer carina.

Streptognathodus elegantulus Stauffer and Plummer, 1932

Pl. 19, Figs. 7, 8

Streptognathodus elegantulus Stauffer and Plummer, 1932, p. 197, pl. 4, figs. 6, 7, 22, 27; Ellison, 1941 (part), p. 127-128, pl. 22, figs. 2, 3, 5; Lane et al., 1971, p. 401, pl. 1, fig. 28; Kozitskaya et al., 1978, pl. 28, figs. 5, 8–11; Barrick and Boardman, 1989, p. 1987, pl. 2, figs. 7, 13; Ritter, 1995, p. 1146, fig. 9.9; Barrick et al., 2013a; p. 249, fig. 9.24, 9.28; Lucas et al., 2016, fig. 41.11.

Streptognathodus aff. *elegantulus* Stauffer and Plummer, 1932. Forke and Samankassou, 2000, p. 201, pl. 37, figs. 15, 16.

Streptognathodus excelsus Stauffer and Plummer, 1932. Lucas et al., 2017b, pl. 2, figs. 3, 4.

Streptognathodus spatulatus Gunnell, 1933, p. 281, pl. 32, fig. 14.

Diagnosis.—A species of *Streptognathodus* bearing an elongate-lanceolate (broad) carminiscaphate P_1 element with a strongly flared caudal adcarinal ridge and no accessory lobes.

Description.—The P_1 element of *Streptognathodus elegantulus* has a long, slightly curved, rostrally deflected free blade commonly with 10-15 partially fused denticles. Stauffer and Plummer (1932) reported that the number of denticles may occasionally exceed 25; however, to the author's knowledge,

this high number is unsubstantiated. The free blade meets the platform in a medial position as the denticles reduce in height and begin to strongly fuse. The carina is typically around one-third the length of the platform and may be followed by one or two small nodes. The caudal adcarinal ridge is much larger than the rostral and extends the caudal margin of the platform upwards to the level of the blade-platform junction. The larger caudal adcarinal ridge is distinctively flared following a minor crimp in the caudal margin of the platform. The crimp typically occupies a position adjacent to the termination of the carina. The shorter rostral adcarinal ridge terminates just dorsally of the blade-platform junction. The margins of the platform are ornamented with a row of transverse ridges on either side (rostral and caudal). A shallow medial trough of moderate width separates the transverse ridges. The shortest, dorsal-most ridges may be uninterrupted. The basal cavity is deep and of moderate width.

Occurrence.—63.1 m above the base of the section (unit 14); level - upper part of the Kasimovian Stage (upper part of the Missourian Stage). Occurs with *Streptognathodus* aff. *firmus*.

Remarks.—*Streptognathodus elegantulus* belongs to the middle Kasimovian *S. gracilis* complex along with *S. gracilis* Stauffer and Plummer, 1932, *S. corrugatus* Gunnell, 1933, and *S. excelsus* Stauffer and Plummer, 1932

(Barrick and Boardman, 1989; Ritter et al., 2002). The constituents of the group appear to have coincident ranges and the *S. gracilis* conodont zone of the Midcontinent comprises two major and four minor cyclothems (Barrick et al., 2013a).

Of the four related species, the P_1 element of *Streptognathodus elegantulus* most closely resembles S. *gracilis* but differs in its larger, flared caudal lobe and by typically being more robust overall. *Streptognathodus elegantulus* differs from both *S. corrugatus* and *S. excelsus* by lacking a rostral lobe.

Streptognathodus* aff. *firmus Kozitskaya, 1978

Pl. 19, Figs. 4-6

"Transitional forms between *Streptognathodus isakovae* Goreva and Alekseev, 2006 and *S. firmus*," Barrick et al., 2013a, figs. 9.1, 9.3, 9.4.

Diagnosis.—A species of *Streptognathodus* characterized by a carminiscaphate P_1 element with a long carina, deep medial trough, and a lack of caudal or rostral lobes.

Description.—The P_1 element of *Streptognathodus* aff. *firmus* has a moderately long free blade with partially fused denticles that transition into

a well-defined medial carina. The carina is highly elongated and bisects more than two-thirds of the platform. The diagnostic carina is positioned medially within a deep trough and may be either continuous and followed by several dorsal, discrete nodes or subtly denticulate for most of its length. The elongate-lanceolate platform is narrow, and the gently biconvex margins are ornamented with transverse ridges which extend nearly to the carina and are straight to dorsally curved with a slight caudal deflection. The adcarinal ridges are nearly subequal in length, terminating adjacent to the blade-platform junction, but the caudal ridge is typically slightly longer and extends just beyond (ventrally) the blade-platform junction. The dorsal termination of the platform may be bluntly or sharply pointed. The basal cavity is deep and narrow, but may flare slightly near the midpoint of the platform.

Occurrence.—63.1 and 115 m above the base of the section (units 14, 22); level - upper part of the Kasimovian Stage to the middle part of the Gzhelian Stage (upper part of the Missourian Stage to middle part of the Virgilian Stage). Occurs with *Streptognathodus elegantulus*.

Remarks.—The forms herein regarded as *Streptognathodus* aff. *firmus* are considered synonymous with the transitional forms between *S. isakovae* and *S. firmus* illustrated by Barrick et al. (2013a) from the upper Kasimovian

Tinajas Member of the Atrasado Formation in central New Mexico. Although the carina of *S.* aff. *firmus* is long, younger forms of *S. firmus* have a carina that spans the entire length of the platform. *Streptognathodus* aff. *firmus* resembles *S. ruzhencevi* but the latter has a more symmetrical platform (Barrick and Boardman, 1989). *Streptognathodus* aff. *firmus* bears a general resemblance to *S. brownvillensis* but differs from the latter in its straighter platform and weaker adcarinal ridges (Boardman et al., 2009).

Streptognathodus pawhuskaensis (Harris and Hollingsworth, 1933)

Pl. 19, Figs. 10-12

Polygnathus pawhuskaensis Harris and Hollingsworth, 1933, p. 199-200, pl. 1, figs. 12a, 12b.

Streptognathodus alekseevi Barskov et al., 1981, pl. 1, figs. 11-14; Barskov et al., 1987, pl. 21, figs. 10-12; Barrick and Boardman, 1989, pl. 3, figs. 3, 6, 19, 22, 24.

Streptognathodus pawhuskaensis (Harris and Hollingsworth, 1933). Ritter, 1994, fig. 5.1; Ritter, 1995, p. 1150, fig. 9.21; Ritter et al., 2002, p. 515, figs. 9.1, 9.5-9.7; Heckel et al., 2011, p. 266, pl. 2, figs. 1, 2, 3, 5; Barrick et al., 2013a, pl. 4, figs. 16, 17; Lucas et al., 2016, figs. 41.5-41.7; Lucas et al., 2017b, pl. 3, figs. 25-27, 29, 30.

Diagnosis.—A species of *Streptognathodus* bearing a P_1 element characterized by a lack of accessory lobes and a deep, broad medial trough with a u-shaped dorsal termination.

Description.—The P_1 element of *Streptognathodus pawhuskaensis* has a long, straight to slightly curved free blade, typically with 10-12 partially fused denticles. The medial carina is smooth to subtly nodose and bisects one-half or more of the platform. One to two accessory nodes may be present dorsal to the termination of the carina. The medial trough is broad and deep throughout its length. The platform is subtly asymmetrical, with a slight caudal deflection of the dorsal half of the platform immediately following the carina. The platform is widest adjacent to the termination of the carina. Caudal and rostral accessory lobes are completely absent. The adcarinal ridges are ornamented with short transverse ridges, are nearly parallel to one another, and are typically subequal in length. The parapets transition seamlessly into the more dorsal margins of the platform which are lined with steep transverse ridges. The dorsal termination of the platform varies from sharply pointed to broadly rounded. The basal cavity is deep and moderately wide. The cup is short and medially flared, typically extending from the blade-platform junction to approximately two-thirds to three-quarters the length of the platform and terminating ventral to the dorsal extent of the medial trough.

Occurrence.—70, 170.7, and 171.9 m above the base of the section (units 16, 34); level - basal to upper part of the Gzhelian Stage (lower to upper part of the Virgilian Stage). Occurs with *Idiognathodus lateralis* and *Streptognathodus virgilicus* (independently).

Remarks.—*Streptognathodus pawhuskaensis* is one of the most recognizable species of *Streptognathodus* and is easily distinguished by the broad, u-shaped medial trough. Despite the distinctiveness, *S. pawhuskaensis* is one of two Missourian holdover species of *Streptognathodus* persisting into the middle Virgilian. Consequently, *S. pawhuskaensis* lacks the utility of most other idiognathodids.

Streptognathodus* cf. *virgilicus Ritter, 1994

Pl. 19, Fig. 13

Streptognathodus elegantulus Stauffer and Plummer, 1932. Ellison, 1941 (part), pl. 22, fig. 10.

Streptognathodus elongatus Gunnell, 1933. Chernykh and Reshetkova, 1987, pl. 4, figs. 4, 5; Barskov et al., 1987, pl. 22, figs. 10, 11.

Streptognathodus virgilicus Ritter, 1994, p. 1150-1151, figs. 10.11-10.14; Goreva and Alekseev, 2010, pl. 1, fig. 14.

Streptognathodus ex gr. *virgilicus* Ritter, 1994. Chernykh et al., 2006, pl. 2, figs. 19, 20.

Diagnosis.—A species of *Streptognathodus* bearing a straight, unornamented P_1 element characterized by steep transverse ridges interrupted by a deep medial trough.

Description.—The P_1 element of *Streptognathodus virgilicus* bears a medial carina extending one-third to two-fifths the length of the platform. The medial carina is followed dorsally by two to three discrete, hemispherical nodes. The v-shaped medial trough is deep and moderately wide, decreasing in width dorsally. The platform is nearly symmetrical with subtly biconvex margins bearing steep, evenly spaced transverse ridges. Nearly all transverse ridges, except for the dorsal-most one to two, are completed interrupted by the medial trough. The platform is widest adjacent to the medial nodes and tapers evenly toward the dorsal terminus. Caudal and rostral accessory lobes are absent. The symmetry of the caudal and rostral adcarinal ridges is difficult to ascertain because all collected specimens lack the ventral-most portion of the platform, but both parapets are ornamented with transverse ridges similar to those of the dorsal portion of the platform. The dorsal termination of the platform is sharply rounded and may have a slight caudal curve. The basal cavity is deep and moderately wide.

Occurrence.—171.9 and 181.7 m above the base of the section (units 34 and 38); level - upper part of the Gzhelian Stage (upper part of the Virgilian Stage). Occurs with *Streptognathodus pawhuskaensis* (unit 34).

Remarks.—*Streptognathodus virgilicus* bears a general resemblance to other unornamented middle to late Virgilian forms of *Streptognathodus*, but is differentiated by the length of the carina and the nature of the medial trough. *Streptognathodus pawhuskaensis* has a broader trough and shorter transverse ridges ornamenting the platform margins. *Streptognathodus vitali* and *S. ruzhencevi* each have a longer row of discrete nodes following the termination the carina, commonly extending to two-thirds or more of the platform length. *Streptognathodus holtensis* Ritter, 1994 has a broader trough and a much lower dorso-ventral to rostro-caudal ratio.

Upper Pennsylvanian Conodont Biostratigraphy and Correlation

Kasimovian Stage

The uppermost part of the Ely Limestone is considered lower-middle Kasimovian (= lower Missourian) based on the occurrence of the fusulinid genus *Eowaeringella*. No diagnostic conodonts were collected from the upper part of the Ely Limestone. The lowest recovered NSMR conodonts include *Adetognathus* and sparse *Hindeodus*, two genera which show little variability

throughout much of the Pennsylvanian. The lowest recovered idiognathodid P_1 elements from the lower informal member of the overlying Riepe Spring Limestone belong to *Idiognathodus cancellosus* (Gunnell, 1933) and *I.* aff. *confragus* Gunnell, 1933. These two forms co-occur 34.6 m above the base of the section in a thin limestone interbedded within the calcareous siltstone of unit 8. *Idiognathodus cancellosus* and *I. confragus* are concurrent in the lower-middle Kasimovian Dennis major cyclothem of the North American Midcontinent (Barrick et al., 2013b). The Dennis cycle is assigned to the *I. confragus* Zone, which spans from the first appearance of the nominate species to the first appearance of *Streptognathodus gracilis* Stauffer and Plummer, 1932 in the base of the Hogshooter minor cyclothem (Barrick et al., 2013b). In the Conemaugh marine units of the northern Appalachian Basin (i.e., Ohio) the stratigraphic ranges of *I. cancellosus* and *I. confragus* narrowly overlap in the lower part of the Upper Brush Creek Limestone of the Glenshaw Formation (Heckel et al., 2011; Klasen, 2007 unpublished thesis). In the Illinois Basin this interval is correlative with the Shoal Creek marine unit (Heckel and Weibel, 1991). The co-occurrence of these two forms in north-central Texas has yet to be observed, with *I. cancellosus* occurring in the upper part of the Salesville Formation and *I. confragus* first appearing near the base of the Wynn Limestone (Barrick and Boardman, 1989).

The next 28.5 m of section are devoid of diagnostic P_1 elements, but the presence of *Eowaeringella* sp. B 54.9 m above the base of the section (unit 12)

indicates that the stratigraphic interval between units 8 and 12 is no lower than the lower-middle Kasimovian (= lower Missourian). Directly above unit 12, the scoured base of the overlying conglomerate (unit 13) is associated with a mid-Kasimovian erosional disconformity separating lower-middle and upper Kasimovian units. The erosional vacuity spans the full length of the *Streptognathodus gracilis* Zone, encompassing a time interval equivalent to the Hogshooter through the Plattsburg minor cyclothems in the Midcontinent region. The duration of the vacuity is inferred from the next lowest occurring conodonts. *Streptognathodus elegantulus* Stauffer and Plummer, 1932 occurs with *S.* aff. *firmus* Kozitskaya, 1978 63.1 m above the base of the section in the shallow-water nodular limestone of unit 14. These two forms are only known to co-occur within the span of one upper Kasimovian (= upper Missourian) cycle in the Midcontinent (i.e., Stanton Limestone) and north-central Texas (i.e., upper Winchell Limestone). The occurrence of the fusulinid *Triticites* cf. *primarius* Merchant and Keroher, 1939 at 64.8 m provides further evidence supporting the inferred correlation, as this species is characteristic of both the Stanton Limestone and Winchell Limestone as well.

The Stanton/Winchell-equivalent unit 14 is erosionally truncated by a 2.2 m thick conglomerate at 65.8 m (unit 15). The observed fauna of unit 16 indicates that the disconformity at the base of the underlying conglomerate juxtaposes upper Kasimovian and lower Gzhelian strata. In total, the

abbreviated upper Kasimovian part of the Riepe Spring Limestone is composed of just two units (units 13, 14) and measures only 8.5 m thick.

Gzhelian Stage

The lowest recovered Gzhelian fauna occurs 4.2 m above the Kasimovian-Gzhelian disconformity at 70 m above the base of the section (unit 16) and includes *Streptognathodus pawhuskaensis* (Harris and Hollingsworth, 1933) and *Idiognathodus lateralis* Hogancamp, Barrick, and Strauss, 2016, a species belonging to the *S. simulator* group (Hogancamp and Barrick, in press). *Streptognathodus pawhuskaensis* is a long-ranging Kasimovian holdover taxon offering little age control, but the occurrence of *I. lateralis* is critically important for constraint of the Kasimovian-Gzhelian erosional vacuity. *Idiognathodus lateralis* first appears in the Heebner Shale Member of the Oread Formation in Kansas and is known from *S. simulator* Zone equivalents in the Donets Basin, the southern Urals, Novaya Zemlya (Russian Arctic archipelago), the Moscow Basin, and South China (Hogancamp et al., 2016). In the Cerros de Amado region of south-central New Mexico *I. lateralis* occurs with *S. ruzhencevi* (Kozur, 1976) in the slightly younger Burrego Member of the Atrasado Formation, which Barrick et al. (2013b) interpreted as correlative with the Lecompton major cyclothem and the *S. vitali* Zone. However, *Streptognathodus vitali* Chernykh, 2002 was not found in association with *I. lateralis* and *S. pawhuskaensis* at Spruce

Mountain Ridge. Therefore, unit 16 is herein assigned to the basal Gzhelian *S. simulator* Zone.

Conodont occurrences throughout the remaining 40.4 m of the lower informal member (units 17-22) and the entirety of the middle informal member (units 23-46) of the Riepe Spring Limestone are exceptionally low and poor in quality. Many of the P_1 elements collected are unidentifiable juvenile specimens and the larger specimens often lack diagnostic parts of the platform. The highest occurring conodonts from the lower informal member of the Riepe Spring Limestone were recovered from 115 m above the base of the section, 0.9 m below the top of unit 22 and the contact between the lower and middle informal members of the Riepe Spring Limestone. The faunule includes 20 juvenile P_1 elements and two small fragments of free blades from larger specimens. Unfortunately none of the complete specimens were mature enough for confident species-level identification.

The lowest identifiable conodonts from the middle informal member of the Riepe Spring Limestone occur 170.7 and 171.9 m above the base of the section and are assigned to *Streptognathodus pawhuskaensis* and *S. virgilicus* Ritter, 1994. These forms occur together ~11 m above a mid-Gzhelian erosional disconformity (base of unit 33) and denote the highest occurrence of *S. pawhuskaensis* in the NSMR section. *Streptognathodus virgilicus* occurs again slightly higher at 181.7 m above the base of the section (unit 38). Due to the long range of these taxa, the occurrence of

Triticites creekensis Thompson, 1954 at 167.5 m provides more precise age control regarding the upper limit of the erosional vacuity and indicates that unit 34 is upper Gzhelian and equivalent to the lower part of Wilde's (1990) PW-1 Zone of the Permian Basin and the Big Hatchet Mountains. *Streptognathodus pawhuskaensis* and *T. creekensis* both occur in the lower "Newwellian" interval of the Sheridan Canyon Member of the Horquilla Formation at New Well Peak in the Big Hatchets, but the New Mexican occurrence of the former is interpreted as younger than the highest occurrence of *S. pawhuskaensis* in the Midcontinent based on fusulinid occurrences (Wilde, 2006; Lucas et al., 2017b).

Much of the remaining middle informal member of the Riepe Spring Limestone failed to yield mature or adequately preserved conodont elements, if any were recovered at all. A number of small, immature P_1 elements resembling *Streptognathodus virgilicus* were recovered from 198.8 and 209.5 m, but the associated fusulinid fauna of advanced Group IV *Triticites* suggests that this interval is younger than the upper range limit of *S. virgilicus*. *Streptognathodus bellus* Chernykh and Ritter, 1997 is the youngest Late Pennsylvanian conodont found in the Riepe Spring Limestone and occurs 215.8 m above the base of the section, four meters below a major Gzhelian-Sakmarian(?) erosional disconformity. In the Midcontinent the *S. bellus* Zone immediately follows the *S. virgilicus* (s.s.) Zone and is defined by the first appearance of *S. bellus* in the Brownville cyclothem where it occurs

with *S. brownvillensis* Ritter, 1994, and extends up to the first appearance of *S. flexuosus* Chernykh and Ritter, 1997 in the Five Point cyclothem. *Streptognathodus bellus* is considered the progenitor of several late Gzhelian lineages and is characteristic of the upper Gzhelian in the southern Urals at Aidaralash Creek (below the Asselian GSSP) and the "Newwellian" part of the Horquilla Formation as well (Chernykh and Ritter, 1997; Boardman et al., 2009; Lucas et al., 2017b).

Conclusions

The lower and middle informal members of the Riepe Spring Limestone at Spruce Mountain Ridge, Elko County, Nevada, preserve a Kasimovian-Gzhelian conodont succession composed of widely distributed and well-constrained idiognathodid species. Unfortunately, the Upper Pennsylvanian strata of the North Spruce Mountain Ridge (NSMR) section are interrupted by at least four significant erosional disconformities, allowing for the recognition of only partial faunal zones. The lowest recognized conodont zone (in part) in the NSMR section is the *Idiognathodus confragus* Zone, to which the lowest 31.6 m of the Riepe Spring Limestone are tentatively assigned based on the occurrence of *I.* aff. *confragus* (units 3-12). The upper limit of the *I. confragus* zone at Spruce Mountain Ridge is placed at the top of Unit 12, where the calcareous siltstone is channelized by the quartzose conglomerate of unit 13. Based on conodont and fusulinid

occurrences in the overlying nodular limestone of unit 14, the erosional vacuity is equivalent to the time interval separating the deposition of the Dennis and Stanton cyclothems in the Midcontinent region. Unit 14 preserves the approximately Stanton (Kansas)/Winchell (north-central Texas) Limestone-equivalent faunal transition from the mid-Kasimovian *S. gracilis* Zone to the upper Kasimovian *I. eudoraensis* Zone. Neither of the nominate species were recovered from the Riepe Spring Limestone, but the rare co-occurrence of *S. elegantulus* and *S.* aff. *firmus* supports this correlation.

Units 13 and 14 preserve the only stratigraphic record of the upper part of the Kasimovian Stage in the lower informal member of the Riepe Spring Limestone, as another significant erosional surface occurs at the base of unit 15, juxtaposing upper Kasimovian and lower Gzhelian strata. The faunule of unit 16 is composed of the diagnostic early Gzhelian species *Idiognathodus lateralis* and the long-ranging Kasimovian holdover species *Streptognathodus pawhuskaensis*, both of which occur in the basal Gzhelian *S. simulator* Zone. Much of the remaining 150 m of the Upper Pennsylvanian portion of the Riepe Spring Limestone are assigned to the *S. virgilicus* Zone, although very few well-preserved specimens of the nominate taxon were found. In addition to the paucity of decent specimens, many of the recovered P_1 elements from the middle informal member of the Riepe Spring Limestone are juvenile or immature specimens, making species-level assignments nearly impossible in most instances. The stratigraphically highest

Pennsylvanian conodont occurrence, and thus the highest recognized Gzhelian conodont biozone, is that of *S. bellus*, occurring just below a major disconformity spanning the Pennsylvanian-Permian boundary and separating the middle and upper informal members of the Riepe Spring Limestone.

Plate 19

All illustrated specimens were collected from the upper part of the Ely Limestone and the lower and middle informal members of the Riepe Spring Limestone, Spruce Mountain Ridge, Elko County, Nevada, U.S.A.

1. *Adetognathus lautus* (Gunnell, 1933); NSMR/C 0-1, base of the NSMR section; upper part of the Ely Limestone (0 m; unit 1). Oral view of P_1 element.

2. *Idiognathodus cancellosus* (Gunnell, 1933); NSMR/C 34.6-1, 34.6 m above the base of the NSMR section; lower informal member of the Riepe Spring Limestone (unit 8). Oral view of broken P_1 element.

3. *Idiognathodus* aff. *confragus* Gunnell, 1933; NSMR/C 34.6-2, 34.6 m above the base of the NSMR section; lower informal member of the Riepe Spring Limestone (unit 8). Oral view of broken P_1 element.

4-6. *Streptognathodus* aff. *firmus* Kozitskaya, 1978

4. NSMR/C 63.1-1, 63.1 m above the base of the NSMR section; lower informal member of the Riepe Spring Limestone (unit 14). Oral view of broken P_1 element

5. NSMR/C 63.1-2, 63.1 m above the base of the NSMR section; lower informal member of the Riepe Spring Limestone (unit 14). Oral view of broken P_1 element

6. NSMR/C 63.1-3, 63.1 m above the base of the NSMR section; lower informal member of the Riepe Spring Limestone (unit 14). Oral view of broken P_1 element

7, 8. *Streptognathodus elegantulus* Stauffer and Plummer, 1932

7. NSMR/C 63.1-4, 63.1 m above the base of the NSMR section; lower informal member of the Riepe Spring Limestone (unit 14). Oral view of P_1 element.

8. UTA/NSMR/C 63.1-5, 63.1 m above the base of the NSMR section; lower informal member of the Riepe Spring Limestone (unit 14). Oral view of broken P_1 element

9. *Idiognathodus lateralis* Hogancamp, Barrick, and Strauss, 2016; NSMR/C 70-1, 70 m above the base of the NSMR section; lower informal member of the Riepe Spring Limestone (unit 16). Oral view of broken P_1 element

10-12. *Streptognathodus pawhuskaensis* (Harris and Hollingsworth, 1933)

10. NSMR/C 70-2, 70 m above the base of the NSMR section; lower informal member of the Riepe Spring Limestone (unit 16). Oral view of P_1 element

11. NSMR/C 70-3, 70 m above the base of the NSMR section; lower informal member of the Riepe Spring Limestone (unit 16). Oral view of broken P_1 element

12. NSMR/C 171.9-1, 171.9 m above the base of the NSMR section; middle informal member of the Riepe Spring Limestone (unit 34). Oral view of P_1 element

13. *Streptognathodus* cf. *virgilicus* Ritter, 1994; NSMR/C 181.7-1, 181.7 m above the base of the NSMR section; middle informal member of the Riepe Spring Limestone (unit 38). Oral view of broken P_1 element

14. *Streptognathodus bellus* Chernykh and Ritter, 1997; NSMR/C 215.8-1, 215.8 m above the base of the NSMR section; middle informal member of the Riepe Spring Limestone (unit 45). Oral view of broken P_1 element.

Plate 19

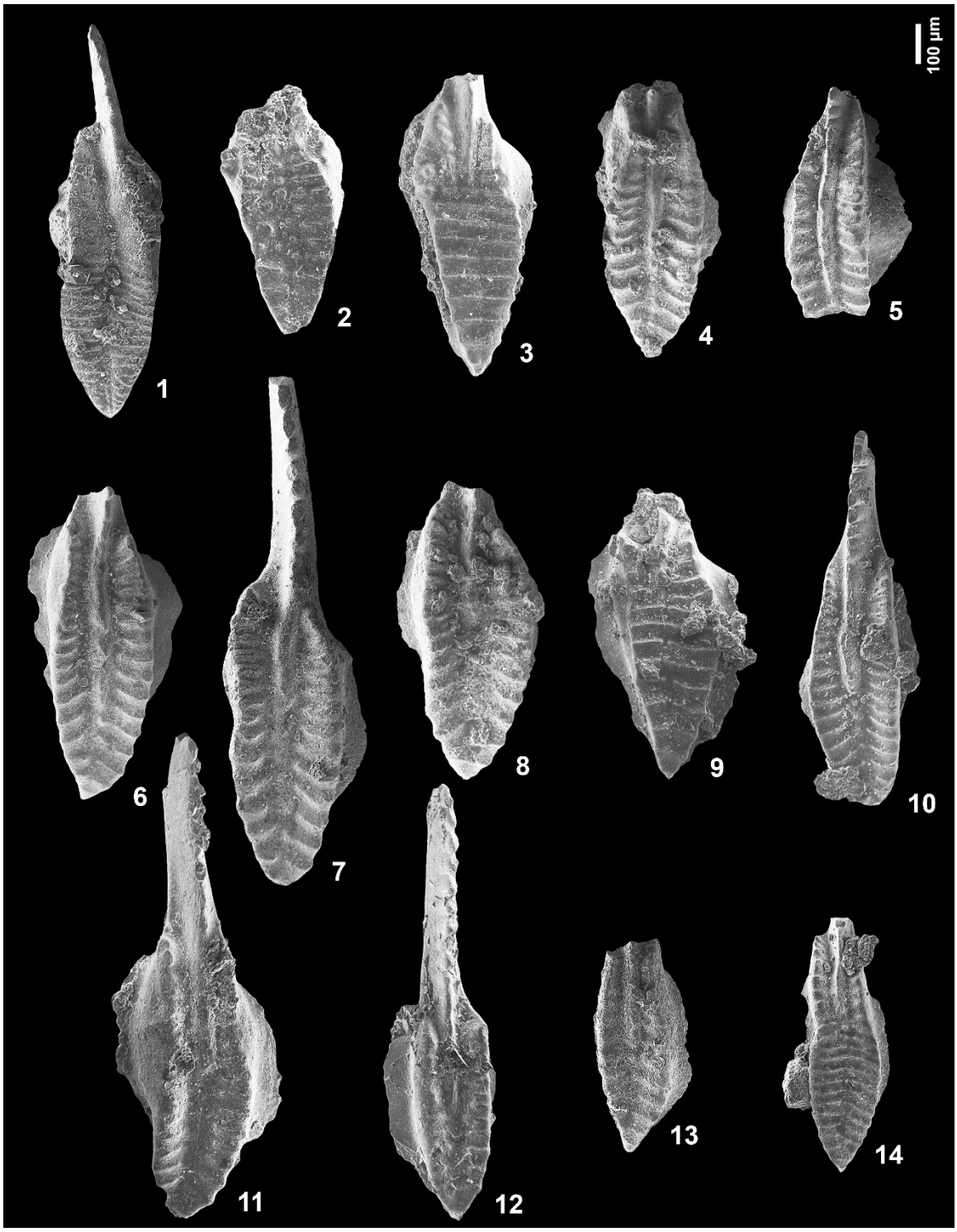

CHAPTER 8 – INTRODUCTORY REMARKS

This article discusses the Sakmarian-Artinskian (early to middle Cisuralian) conodont succession from the upper informal member of the Riepe Spring Limestone at Spruce Mountain Ridge, Elko County, Nevada. The informal upper member is referred to as the upper "part" of the Riepe Spring Limestone in this chapter. The stratigraphic section presented herein coincides with the upper 180 m of the full columnar section illustrated in Chapter 3 (Fig. 8.0).

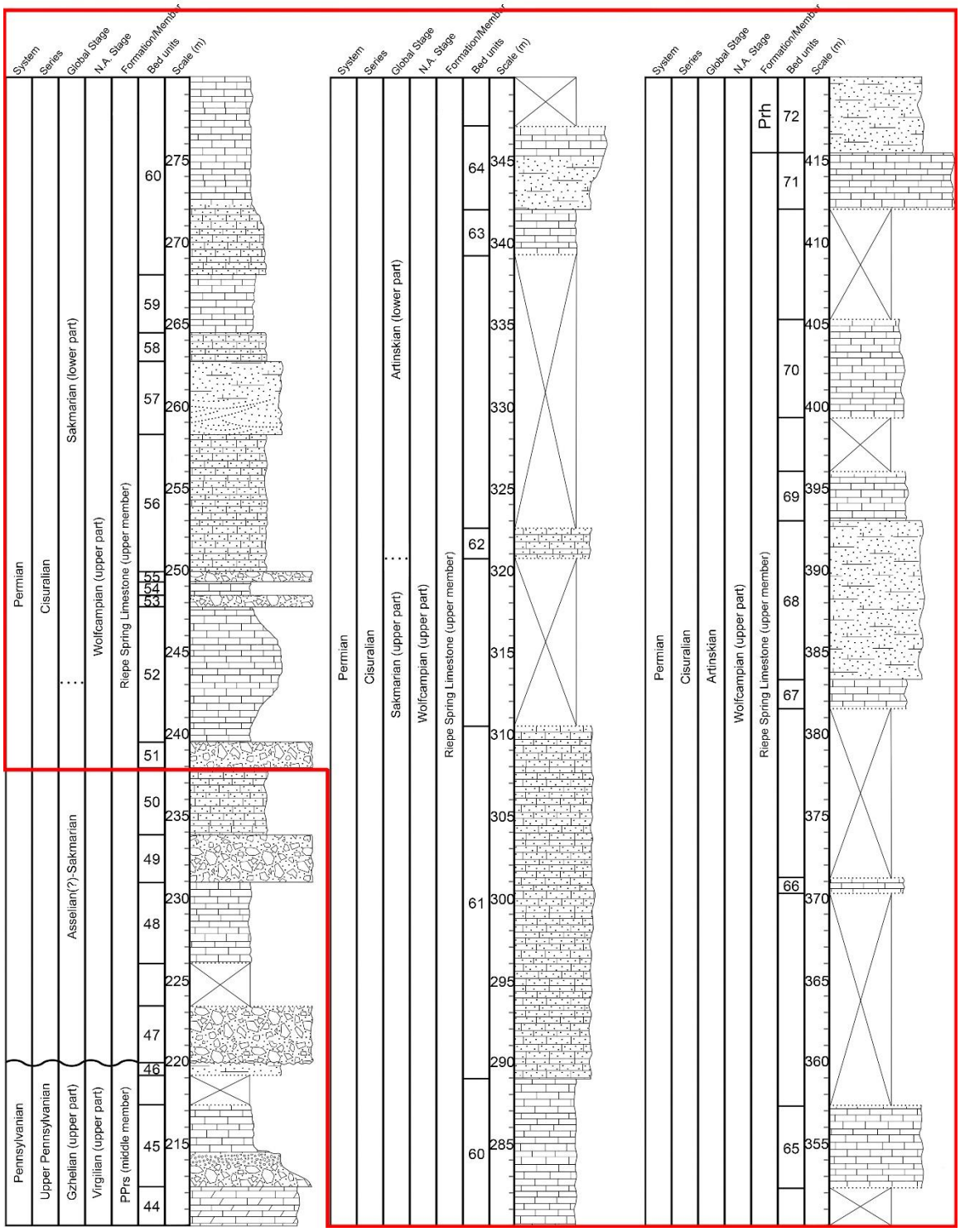

Fig. 8.0 – Stratigraphic column illustrating the portion of the NSMR section discussed in the following chapter (outlined in red).

PALEONTOLOGICAL
RESEARCH INSTITUTION

Jonathan R. Hendricks
Director of Publications
1259 Trumansburg Road
Ithaca, NY 14850
607.273.6623 x20
jrh42@cornell.edu
priweb.org

October 11, 2018

Michael T. Read
Earth & Environmental Sciences, UT Arlington
Geosciences Building, Office 208

Dear Mr. Read,

On behalf of the Paleontological Research Institution, I am writing to inform you that permission is formally granted for you to include in your dissertation your forthcoming accepted manuscript for the *Bulletins of American* Paleontology (no. 395-396), titled "Cisuralian (Early Permian) sweetognathid conodonts from the upper part of the Riepe Spring Limestone, North Spruce Mountain Ridge, Elko County, Nevada."

Please do not hesitate to let me know if I can provide any other information in support of your request.

Sincerely,

Jonathan Hendricks

CHAPTER 8: CISURALIAN (EARLY PERMIAN) SWEETOGNATHID CONODONTS FROM THE UPPER PART OF THE RIEPE SPRING LIMESTONE, NORTH SPRUCE MOUNTAIN RIDGE, ELKO COUNTY, NEVADA

Michael T. Read and Merlynd K. Nestell

Citation: Read, M.T., and Nestell, M.K., in press, Cisuralian (Early Permian) sweetognathid conodonts from the upper part of the Riepe Spring Limestone, North Spruce Mountain Ridge, Elko County, Nevada: Bulletins of Paleontology, no. 395–396, p. 89–113.

Abstract: The upper part of the Riepe Spring Limestone at North Spruce Mountain Ridge, south of Wells, Nevada, records considerable fluctuations in sedimentation trends and base level along the northern Ferguson Trough in the post-Antler foreland. A thick, mixed carbonate-siliciclastic succession follows an unconformity that spans the Carboniferous-Permian boundary and preserves a shallow-water, Sakmarian through Artinskian age (early to middle Cisuralian) conodont fauna. The low-diversity assemblage is largely composed of cosmopolitan species of the ozarkodinid genus *Sweetognathus*, dominated by *Sweetognathus expansus*, *S.* '*merrilli*', *S. binodosus*, and *S.* '*whitei*'. The recovered conodonts are accompanied by a fusulinid fauna similar to that observed in Cisuralian deposits of the Bird Spring Formation of southeastern California and southern Nevada. The faunal turnover during which ornamented Cisuralian species of *Streptognathodus* were replaced by *Sweetognathus* species is not preserved within the section, as this transition appears to coincide with the hiatus. Descriptions are presented for a previously undocumented sweetognathid carinal configuration (Type V group), which exhibits features of both nodose and sulcus-bearing forms. Two new Type V species, *S. wardlawi* n. sp. and *S. duplex* n. sp., are described, and the occurrence of Sakmarian age P_1 elements that bear a strong resemblance to *Neostreptognathodus pequopensis* is discussed.

Introduction

The Riepe Spring Limestone comprises nearly 13,000 square km (approximately 8,000 square mi) of exposed Pennsylvanian and Permian strata across eastern Nevada and adjacent western Utah (Steele, 1960). A recently measured stratigraphic section of the upper part of the Riepe Spring Limestone at North Spruce Mountain Ridge, Elko County, Nevada, is 180 m thick and composed of a variety of lithofacies, representing both marginal and shallow marine environments. The measured section is located 15 km east northeast of the junction of Highway 93 and Spruce Mountain Road, approximately 57 km south of Wells, Nevada (Fig. 8.1). The measured section closely follows Section 1 of Hope (1972), which was previously sampled for fusulinids by Raymond Douglass of the U.S. Geological Survey and Merlynd Nestell in 1969 and 1970. Although nearly 1,300 axially and equatorially oriented thin sections were produced from the collected material, no formal taxonomic identifications or further investigation of the section and formation followed. A number of thin sections from the Smithsonian's Douglass Collection, along with recently collected and prepared fusulinid specimens from North Spruce Mountain Ridge, have been identified in this study to accompany the conodont biostratigraphy. The pairing of these two critical biostratigraphic indices allows for much-needed, expanded age control of this section.

The assemblage recovered from the lower to middle Cisuralian

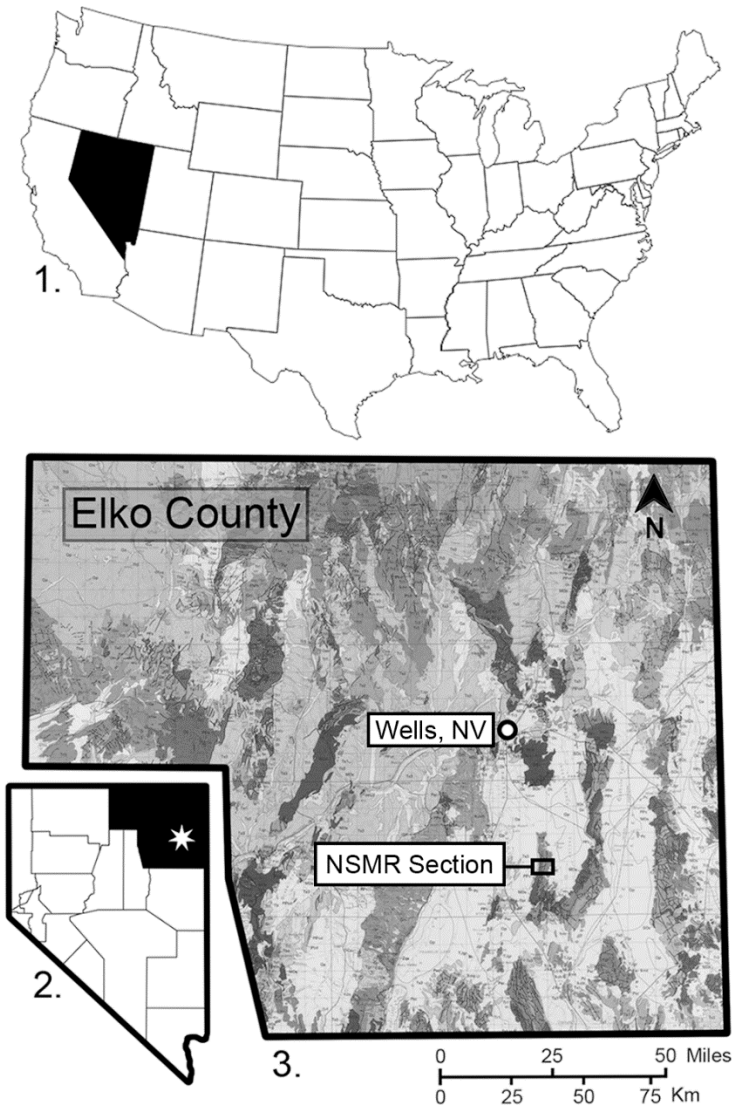
1.
Elko County
N
Wells, NV
NSMR Section
2.
3.
0 25 50 Miles
0 25 50 75 Km
4.
683
684
682
N
Peu
PPrs
Prh
Ppu
Ppl
4505
Quaternary alluvial fan deposits
Ppl
Ppu
Prh
PPrs
4504
Peu
Pel
Quaternary alluvial fan deposits

(Wolfcampian) part of the Riepe Spring Limestone has aided in the identification of an approximate Sakmarian- Artinskian boundary within the section, and has provided new information regarding the iterative evolutionary trends observed within sweetognathid conodont lineages. Previous published investigations of Wolfcampian conodont faunas from the Riepe Spring Limestone have primarily focused on localities near Moorman Ranch, Nevada (Clark and Behnken, 1971; Clark, 1974; Behnken, 1975; Ritter, 1986, 1987) and western Utah (Ritter, 1987; Ritter and Robinson, 2009). Since the work of Ritter (1987), only preliminary conodont work has been conducted on nearby sections of the Riepe Spring Limestone in the Pequop Mountains (Wardlaw et al., 1998; Tierney, 2010).

Regional Geologic Setting

During Sakmarian to late Artinskian (middle to late Wolfcampian) time, the Ferguson and Dry Mountain troughs occupied much of northeast and north-central Nevada within the post-Antler foreland (Wardlaw et al., 1995).

← **Figure 8.1** – 1. United States; Nevada identified in black. 2. Nevada, United States; Elko County identified in black; star indicates North Spruce Mountain Ridge (NSMR) section. 3. Detail of Elko County with the location of the NSMR section enclosed (modified from Stewart & Carlson, 1978). 4. Enlarged area of the NSMR section illustrating the succession of upper Paleozoic strata; el, lower part of the Ely Limestone; eu, upper part of the Ely Limestone; rs, Riepe Spring Limestone; rh, Rib Hill Formation; pl, lower part of the Pequop Formation; pu, upper part of the Pequop Formation; star indicates location of measured section within the upper part of the Riepe Spring Limestone (after Hope, 1972). Projection and 1,000 m grid: UTM, Zone 11T (from Read and Nestell, in press).

The Ferguson and Dry Mountain troughs (Fig. 8.2), as well as the preceding Butte Basin (referred to as the Ely Shelf by Stevens and Stone, 2007), were parts of a tectonically controlled and physiographically partitioned trough and shelf complex that may have represented the northern extension of the Bird Spring Platform, better known from exposures in southeastern California and southern Nevada (Stevens and Stone, 2007). The Butte Basin refers to regional marine deposits of Gzhelian (latest Pennsylvanian) and Asselian (earliest Permian) age and is used to avoid potential confusion with the underlying Ely Basin and Ely Platform of Early to Middle Pennsylvanian age (Larson and Langenheim, 1979; Wardlaw et al., 1995). The nearly equatorial paleogeographic setting (approximately 12°- 15° N latitude) was confined by remnants of the Devonian to Mississippian Antler orogenic belt to the west, the Oquirrh- Uinta Uplift to the northeast, and the Deep Creek-Tintic Uplift to the south (Fig. 8.2) (Stevens, 1979; Scotese, 2014). The succession of shallow to marginal marine strata comprising the upper part of the Riepe Spring Limestone at North Spruce Mountain Ridge was deposited on the northernmost shelf of the Ferguson Trough, or Ferguson- Uinta Basin, portion of the complex between the bounding highlands to the north and south (Fig. 8.2) (Stevens, 1979; Miller et al., 1992).

The architecture and depositional patterns of the Ferguson Trough were dictated by episodes of local to regional uplift and subsidence paired with global

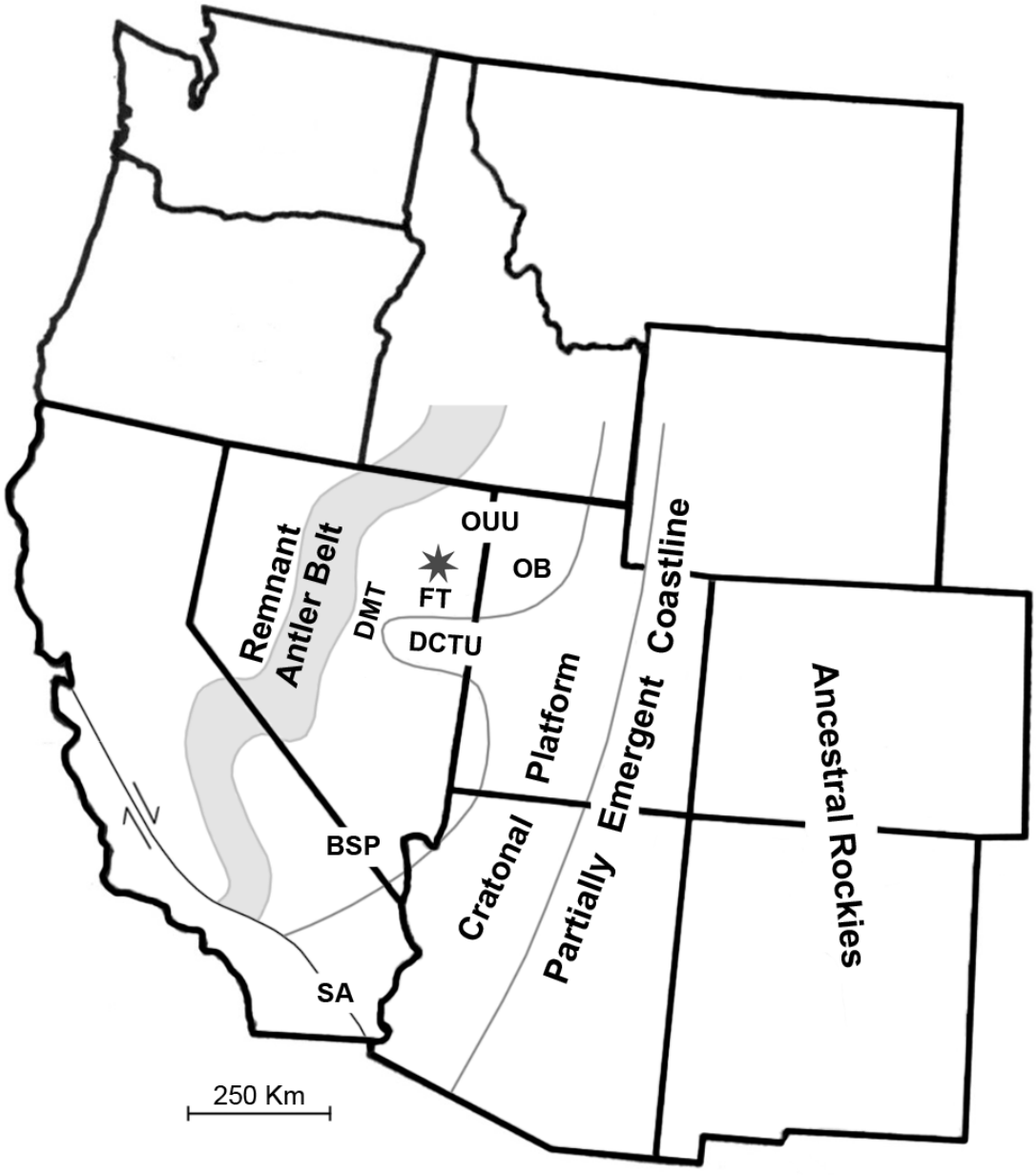

Figure 8.2 – Paleogeographic map of western North America during the Sakmarian and early Artinskian stages of the Cisuralian (Early Permian). Abbreviations: BSP, Bird Spring Platform; DCTU, Deep Creek-Tintic Uplift; DMT, Dry Mountain Trough; FT, Ferguson Trough; OB, Oquirrh Basin; OUU, Oquirrh-Uinta Uplift; SA, San Andreas Fault (Cenozoic); star, North Spruce Mountain Ridge Section (modified from Wardlaw et al., 1995; Stevens & Stone, 2007).

sea-level fluctuations attributed to peak Gondwanan glaciation and the ensuing waning stages of the late Paleozoic ice age. Nearly contemporaneous unconformities across the Great Basin region demonstrate the profound, synchronous effects of tectonostratigraphic and glacioeustatic variability on the shallow platforms and marginal basins along the west coast of Pangea. Evidence for localized Pennsylvanian through Permian deformation (post-Antler and pre-Sonoma) has been reported from the nearby Pequop Mountains directly to the east (Marcantel, 1975; Sweet and Snyder, 2003), Carlin Canyon to the west (Dott, 1955; Trexler et al., 2004), east-central Nevada (Snyder et al., 1991; Gallegos et al., 1991), southwest Nevada (Schiappa et al., 1999), southern Idaho (Mahoney et al., 1991; Geslin, 1998), and southeast California (Stevens et al., 1997; Stevens and Stone, 2007). Investigations of glacioeustasy from Midcontinent cyclothems have proposed that the third and final glacial interval of the late Paleozoic ice age produced a base level drop of 60 to 120 m, which led to widespread coastal emergence, and the subsequent erosion and incision of exposed Upper Pennsylvanian and Cisuralian marine strata (Rygel et al., 2008). The 60 m range in the approximation of the maximum extent of base level change is ascribed to uncertainties regarding total glacial aerial coverage and the number of independent ice sheets (Isbell et al., 2003). A period of pronounced Gondwanan deglaciation began during the Asselian and persisted intermittently throughout the Cisuralian, with a collapse of continental ice

sheets in southwest Gondwana occurring near the Sakmarian- Artinskian boundary (Montañez and Poulsen, 2013).

Stratigraphy

Steele (1960) initially described the Riepe Spring Limestone as a predominantly massive, coralline, fusulinid-bearing limestone unit. The type section is located on the north side of Ward Mountain, White Pine County, Nevada (39°10'33.75"N, 114°55'59.80"W). Prior to the formal description, the strata of the Riepe Spring Limestone were considered to be within the upper part of the underlying Ely Limestone (Spencer, 1917; Pennebaker, 1932). The Riepe Spring Limestone of the Spruce Mountain Quadrangle provides a discontinuous Carboniferous-Permian boundary section, unlike the conventional stratigraphic interpretation of Steele (1960) in which the Cisuralian Riepe Spring Limestone disconformably overlies the nearly lithologically indistinguishable Pennsylvanian Ely Limestone. Such strictly Permian sections of the Riepe Spring Limestone have been described from Burbank Hills, Utah, Moorman Ranch, Nevada, and the Ruth mining district near Rib Hill, Nevada (Steele, 1960; Ritter, 1987). The stratigraphic discrepancy is partially attributed to the southward thinning of the conglomeratic intervals within the Riepe Spring Limestone of Spruce Mountain Ridge and the southern Pequop Mountains (Marcantel, 1975). Further inconsistencies in the regional stratigraphic interpretation of the

Riepe Spring Limestone may be attributed to differing definitions of the formation (*e.g.*, Steele, 1960 and Hope, 1972). The USGS geologic map of the Spruce Mountain Quadrangle (Map GQ-942) of Hope (1972) described the Riepe Spring Limestone as the Pennsylvanian-Permian succession of mixed carbonate- siliciclastic strata above the thinner bedded limestone of the Ely Limestone and below the fine, calcareous sandstone of the Rib Hill Formation. The same strata were referred to as the "Riepe Spring Formation" by Marcantel (1975), who suggested that the unit may be genetically related to the Strathearn Formation of the Carlin Canyon, Nevada area. The Pennsylvanian-Permian concept of the Riepe Spring Limestone described by Hope (1972) is used herein because of the priority of USGS Map GQ-942 to the measured section. A forthcoming discussion of the stratigraphy of Section 1 from Hope (1972) is being prepared by the authors.

The base of the measured section within the upper part of the Riepe Spring Limestone at North Spruce Mountain Ridge (40°40'47.08"N, 114°49'35.04"W) is distinguished by a chert-cobble paraconglomerate (one meter thick), a lithofacies interpreted as nearshore clastic-wedge deposits that were shed during the discrete episodes of regional uplift to the north (Yochelson and Fraser, 1973; Marcantel, 1975). The top of the conglomerate quickly grades upward into a silty limestone in less than ten centimeters. The limestone transitions to a foraminiferal wackestone and grainstone, overlain by two more thin, quartzose paraconglomerate beds at approximately

ten meters above the base of the section. A thick quartzose limestone overlies the conglomerate beds, and gradually transitions into a calcareous quartz arenite just above 20 m into the section. The nearly five meter thick arenaceous unit contains small-scale hummocks (two to five centimeters) and laminations that have been interpreted as thin tempestite deposits. Highly abraded fusulinid specimens, many of which are missing outer volutions, are present as well. The remaining strata composing the western face of the ridge up to the crest (approximately 25 m higher) are fairly continuous limestone exposures with slightly varying percentages of fine sand- sized terrigenous material. Just beyond the crest of the ridge, at approximately 52 m, the terrigenous component of the limestone increases, and exposure becomes very poor.

Quartzose, sparsely crinoidal limestone composes the majority of the exposed eastern dip-slope of the ridge, where thick intervals are completely obscured by talus (Fig. 8.3.2). The base of the ridge flattens into a saddle where the covered intervals and sporadic limestone beds are interbedded with resistant, platy, yellowish orange-brown sandstone. The adjacent limestone outcrops are darker in color, more crinoidal, and muddier than the coarser, clastic limestone observed between 52 and 85 m above the base of the section. Above the highest, easternmost carbonate bed of the Riepe Spring Limestone lays the Rib Hill Formation (Fig. 8.3.2). The Rib Hill Formation beyond the measured section is similarly poorly exposed and is composed of platy

Figure 8.3 – 1. Lower portion of the North Spruce Mountain Ridge section. The southeastward facing photograph was taken from the crest of the ridge (approximately 52 m above the base of the section; 40°40'49.84"N, 114°49'32.55"W). Bruce Wardlaw can be seen looking for a snack at lower right; the star indicates the base of the measured section. 2. Upper portion of the North Spruce Mountain Ridge section. The eastward facing photograph was also taken from the crest of the ridge and demonstrates the poor exposure along the dip-slope and saddle to the east of the crest; the star indicates the contact between the Riepe Spring Limestone and the overlying Rib Hill Formation.

calcareous sandstone talus broken from thin beds approximately one to two centimeters thick.

Systematic Paleontology

Repository.—All illustrated specimens are reposited in the Paleontology Repository at the University of Iowa (SUI numbers).

Class **CONODONTA** Pander, 1856

Subclass **CONODONTI** Branson, 1938

Order **OZARKODINIDA** Dzik, 1976

Family **SWEETOGNATHIDAE** Ritter, 1986

Genus ***NEOSTREPTOGNATHODUS*** Clark, 1972

Type species.—*Streptognathodus sulcoplicatus* (Youngquist et al., 1951).

Remarks.—*Neostreptognathodus* represents the dominant ozarkodinid genus of the late Artinskian and Kungurian Stages of the Permian. The genus shows a strong morphological resemblance to the bifurcated or laterally elongated forms of *Sweetognathus*, the inferred ancestors of *Neostreptognathodus*. Members of *Neostreptognathodus* display a partially to fully developed dorsoventral sulcus or trough. Carinal margins are occupied by discrete nodes, transverse ridges, or dorsoventral (longitudinal) parapets. Basal

representatives of the genus maintain the pustulose microornamentation characteristic of *Sweetognathus*.

Neostreptognathodus* aff. *pequopensis Behnken, 1975

Pl. 21, Figs. 9–11; Pl. 22, Figs. 1–3

Diagnosis.—A species of *Neostreptognathodus* bearing a carminiscaphate P_1 element with two rows of discrete, irregularly hemispherical carinal denticles separated by a shallow sulcus.

Description.—The P_1 element of *Neostreptognathodus* aff. *pequopensis* has a free blade of short to moderate length, bearing four to six partially fused ventral denticles. The carina bears five to eight pairs of discrete, pustulose, hemispherical denticles that are separated by a fully developed dorsoventral sulcus. Beyond the paired nodes, a papillary denticle is situated at the dorsal termination of the dorsal process, bringing the sulcus to a close and extending beyond the border of the basal cavity. *Neostreptognathodus* aff. *pequopensis* is classified as a Type IV sweetognathid.

Occurrence.—9.7 m, 30.8 m, 34 m, 36.2 m, 39.7 m, 43.1 m, 51.7 m, 60.5 m, and 65.5 m above the base of the section; level - Sakmarian Stage.

Remarks.—*Neostreptognathodus* aff. *pequopensis* closely resembles *N. pequopensis* in nearly its full suite of morphological characters. The denticles of specimens collected from North Spruce Mountain Ridge differ slightly from typical specimens of *Neostreptognathodus pequopensis*. Those of *N.* aff. *pequopensis* are generally lower than the denticles of *N. pequopensis*, and the lateral margins of the former slope more gently toward the basal cup. It should be noted that the orientation of the free blade attachment shows variability in the specimens collected. Some specimens display the typical median attachment at the blade-carina junction (Pl. 21, Figs. 9, 10; Pl. 22, Fig. 2), whereas others have a single auxiliary, lateral denticle positioned at the junction (Pl. 22, Figs. 1, 3). The nature of the free blade attachment is generally not considered a species-level distinction, nor does the presence of the auxiliary node seem indicative of chirality, or "handedness," in P_1 elements. All four of the specimens imaged represent dextral elements, and both morphotypic variants are observed. The forms described herein are regarded as *N.* aff. *pequopensis* rather than *N. pequopensis* primarily on the basis of apparent diachroneity rather than morphological differences.

Genus ***PSEUDOHINDEODUS*** Gullo and Kozur, 1992

Type species.—*Pseudohindeodus ramovsi* Gullo and Kozur, 1992.

Remarks.—An early to middle Permian sweetognathid conodont genus

having a carminiscaphate P_1 element with a free blade separated from the narrow carina by a distinctive notch. In most cases the free blade and carina are subequal in length. The carina may be subtly denticulate or adenticulate with faint microornamentation and the dorsal termination is abrupt, dropping steeply to the base of the dorsal process. The basal cavity is broad and deep, occupying more than half of the length of the element, and has a characteristic crimp that runs continuously along the outer margin of the cup.

Pseudohindeodus stevensi (Clark and Carr, 1982)

Pl. 22, Fig. 6

Diplognathodus stevensi Clark and Carr, 1982, p. 132, pl. 1, figs. 1, 3, 8, 9–13; Ritter, 1986, p. 147, pl. 3, figs. 3, 5; Chernykh, 2006, p. 97, pl. 12, figs. 1a, 1b, 2a, 2b; Wardlaw et al., 2015, pp. 375, 376, pl. 2, figs. 1–12.
Pseudohindeodus stevensi Gullo and Kozur, 1992, p. 222.

Diagnosis.—A species of *Pseudohindeodus* having a small P_1 element distinguished by a rhomboidal, broadly flared platform and a narrow carina with a dorsoventral row of faint microornamentation.

Description.—The P_1 element of *Pseudohindeodus stevensi* has a free blade

bearing three to five partially fused denticles, often with three smaller accessory denticles located ventrally to the main cusp. Two reduced denticles occupy the notch of the junction between the free blade and the carina. The carina is short, narrow, and displays a single dorsoventral row of fine, chevron-shaped notches. The platform is often slightly asymmetrical and rhomboidal in oral and aboral orientations. The outer one-third of the basal cup is lower than the inner portion following a distinctive crimp.

Occurrence.—177.3 m above the base of the section; level - Artinskian Stage.

Genus ***SWEETOGNATHUS*** Clark, 1972

Type species.—*Spathognathodus whitei* Rhodes, 1963.

Remarks.—Carminiscaphate P_1 elements may be assigned to one of four carinal configurations (Types I, II, III, and IV) previously described by Ritter (1986), or a new Type V. Sweetognathids with a Type V configuration have a either a median sulcus or "dimples" along the ventral half of the carina, and discrete nodes on the dorsal half. The dorsal processes of *Sweetognathus* P_1 elements, regardless of specific denticulation (or lack thereof), are distinctly ornamented with secondary pustules.

Sweetognathus anceps Chernykh, 2005

Pl. 22, Figs. 4, 5

Sweetognathus behnkeni Kozur. Irwin et al., 1983, p. 1034, fig. 2n.

Sweetognathus inornatus Ritter, 1986. Ding and Wan, 1990, p. 151, pl. 2, fig. 16, 17.

Sweetognathus anceps Chernykh, 2005, p. 204, pl. 21, fig. 13.

Sweetognathus whitei (Rhodes, 1963). Boardman et al., 2009, p. 118, pl. 30, fig. 9; Wardlaw et al., 2015, 379, pl. 1, fig. 15.

Diagnosis.—A species of *Sweetognathus* in which the P_1 element is characterized by transversely elongated, dumbbell-shaped carinal denticles with pustulose microornamentation.

Description.—A sweetognathid with a P_1 element having a short to moderate free blade bearing four to five partially fused, laterally compressed denticles. The free blade meets the dorsal process in a median position, and the junction is occupied by the first small, pustulose denticles. The carina is laterally expanded and bears six to eight nodose, dumbbell-shaped denticles, which may display asymmetrical irregularities. The lateral margins of the carina drop steeply to the oral surface of the basal cup. Beyond the midpoint, the spacing between individual denticles increases dorsally, and the carina narrows to a single node at the dorsal terminus. *Sweetognathus anceps* is

classified as a Type III sweetognathid.

Occurrence.—51.7 m and 59.3 m above the base of the section; level - upper part of the Sakmarian Stage.

Remarks.—Although there is a strong morphological resemblance in many regards between *Sweetognathus anceps* and its immediate descendent, *S.* '*whitei*', the former lacks the dorsoventral ridge characteristic of the dorsal process of the latter (Chernykh, 2005).

Sweetognathus behnkeni Kozur, 1975

Pl. 22, Fig. 13

Spathognathodus whitei Rhodes, 1963. Clark and Behnken, 1971, p. 430, pl. 1, figs. 2, 5.

Sweetognathus whitei (Rhodes, 1963). Clark, 1974, p. 716, pl. 2, figs. 15, 17; Riglos Suarez et al., 1987, p. 331, pl. 19.3, figs. 13, 16; Wardlaw et al., 2015, p. 379, pl. 1, figs. 18, 19.

Sweetognathus behnkeni Kozur. Bando et al., 1980, 43, pl. 4, fig.4; Ritter, 1986, p. 161, pl. 2, figs. 11–15; Riglos Suarez et al., 1987, p. 331, pl. 19.3, figs. 17, 19, 20, 22.

Diagnosis.—A species of *Sweetognathus* bearing a broad P_1 element in which the carina is ornamented with narrow, teardrop-shaped transverse ridges. The ventral and dorsal-most carinal ridges are obliquely deflected toward their respective ends of the dorsal process.

Description.—A sweetognathid species that, like *Sweetognathus anceps*, bears a general resemblance to *S.* '*whitei*'. The long free blade of *S. behnkeni* has six to eight partially fused to fused denticles meeting the carina in a median position. The oral surface of the dorsal process is wide, up to nearly one-half the length of the carina, and displays a highly inflated lenticular shape. A sharply raised dorsoventral ridge traverses nearly the entire length of the carina, with peaks occurring in correspondence to the positions of the pustulose lateral denticles. The transversely elongated denticles are perpendicular (or nearly so) to the dorsoventral ridge at the widest portion (midpoint) of the carina but bow ventrally and dorsally as the carina tapers to its longitudinal margins. The ventral-most ridges may split into two small, bulbous nodes at the marginal extent of the narrow, arcuate denticles. *Sweetognathus behnkeni* is classified as a Type III sweetognathid.

Occurrence.—177.3 m above the base of the section; level - Artinskian Stage.

Remarks.—Although several authors (Igo, 1981; Mei et al., 2002) have

previously designated *Sweetognathus behnkeni* a junior synonym of *S.* '*whitei*' and used the name to describe large, gerontic specimens of the latter species, *S. behnkeni* is herein regarded as a valid species. *Sweetognathus behnkeni* is notably absent from the lower range of *S.* '*whitei*' at both North Spruce Mountain Ridge and Moorman Ranch, Nevada, suggesting that the form is indeed distinct (Kozur, 1975; Ritter, 1986). The occurrence of *S. behnkeni* at North Spruce Mountain Ridge is 84.5 m higher than the first occurrence of *S.* '*whitei*' and the approximate base of the Artinskian Stage. Ritter (1986) presented a sound ontogenetic argument for the morphological similarities between *S. behnkeni* and *S.* '*whitei*', stating that it is likely that a number of specimens of *S. behnkeni* must have passed through a juvenile phase that may be hard to distinguish from *S.* '*whitei*', whereas others exhibit discernible characteristics of *S. behnkeni* at an immature or subadult level.

Sweetognathus binodosus Chernykh, 2005

Pl. 20, Fig. 14; Pl. 21, Figs. 1–3

Sweetognathus inornatus Ritter, 1986, p. 163, pl. 3, figs. 12, 14.

Sweetognathus aff. *whitei* (Rhodes, 1963). Orchard, 1984, p. 211, pl. 23.1, fig. 1.

Sweetognathus whitei (Rhodes). Ding and Wan, 1990, p. 151, pl. 2, figs. 5, 9, 11, 15; Holterhoff et al., 2013, p. 116, fig. 4.12.

Sweetognathus merrilli Kozur, 1975. Kozur, 1995, p. 197, pl. 2, figs. 4, 6; Stevens et al., 2001, p. 126, fig. 17.2, 17.5, 17.6.

Sweetognathus anceps Chernykh, 2005, p. 205, pl. 21, figs. 14, 15.

Sweetognathus binodosus Chernykh, 2005, p. 203, pl. 20, figs. 5–8.

Diagnosis.—A species of *Sweetognathus* in which the carina of the P_1 element consists of a variable series of hemi-oblate, low cross-oval, or depressed dumbbell-shaped pustular nodes.

Description.—The free blade of *Sweetognathus binodosus* is straight to slightly arcuate (in rare instances) and bears three to six laterally compressed, partially fused denticles that increase in height ventrally. The carina is composed of four to eight nodular, subtly elongated denticles with pustulose microornamentation along the oral surface. The ventral-most and dorsal-most denticles of the carina are often small, laterally depressed, discrete nodes and are more hemispherical, closely resembling those of *S.* '*merrilli*'. The broadly flared basal cup is smooth in oral view and may be ventrally flared, tapering to the dorsal termination of the carina. Two morphotypes of *S. binodosus*, "Type A" and "Type B," are recognized in the assemblage from the upper part of the Riepe Spring Limestone. The carinal denticles of "Type A" display subtle transverse elongation and may have a faint, weakly-developed dorsoventral ridge, resembling forms exemplified by

the holotype specimen of Chernykh (2005) and those illustrated by Dehari (2016, unpublished thesis). The denticles of "Type B" specimens are more bulbous and distinctly bilobate. *Sweetognathus binodosus* is classified as a Type III sweetognathid.

Occurrence.—5.3 m, 26.8 m, 51.7 m, and 59.3 m above the base of the section; level - lower part of the Sakmarian to the Artinskian Stage.

Remarks.—The "Type A" morphotypic variant of *S. binodosus* is best represented by the holotype specimen of Chernykh (2005), specimens illustrated by Dehari (2016, unpublished thesis), and by two of the North Spruce Mountain Ridge specimens collected from 51.7 m above the base of the section (Pl. 21, Figs. 1, 2) in association with *S. anceps*. "Type B" specimens have carinal denticles that are slightly more laterally depressed than those of "Type A" forms (Pl. 21, Fig. 3). Two "Type B" specimens were collected from 5.3 m above the base of the measured section.

***Sweetognathus duplex* n. sp.**

Pl. 20, Figs. 7–13

Holotype.—Pl. 20, Fig. 10, SUI 145779.

Type locality and horizon.—Upper part of the Riepe Spring Limestone, Spruce Mountain Ridge, Elko County, Nevada; beds 2 and 9.

Etymology.—Duplex (Lat.) - double; two-faced. The name *Sweetognathus duplex* n. sp. is derived from the juxtaposition of two distinct carinal morphologies along a single dorsal process.

Diagnosis.—A species of *Sweetognathus* with both a well-developed median sulcus and discrete bulbous nodes, one following the other (dorsoventrally), along the carina.

Description.—The free blade of the P_1 element of *Sweetognathus duplex* n. sp. is slightly arcuate in oral view, approximately one-third of the overall length, and bears five to six laterally compressed denticles becoming more strongly fused dorsally. A sharp, continuous transition from the fused denticles of the blade to the v-shaped, ventral portion of a median sulcus occupies the junction of the free blade and the dorsal process. The sulcus is narrow and dorsoventrally oriented, much like the sulci observed in members of *Neostreptognathodus*. Both the lateral parapets and the trough of the sulcus are ornamented with secondary pustules. The parapets of the sulcus in transitional forms may exhibit an undulating profile, with indentations in correspondence to remnants of ancestral denticles. The sulcus extends to the

midpoint of the carina and is abruptly supplanted by nodose denticles resembling those of the "Type B" morphotype of *S. binodosus*. Three to four sets of bifurcated nodes comprise the dorsal half of the carina, uniformly decreasing and tapering in width dorsally. The maximum width of the nodose denticles is scarcely wider than the maximum width of the preceding sulcus. A single small node occupies the dorsal termination of the carina. The basal cup is ventrally flared and tapers tightly to the dorsal terminus. *Sweetognathus duplex* n. sp. is classified herein as a Type V sweetognathid.

Occurrence.—5.3 and 26.8 m above the base of the section; type level - Sakmarian Stage.

Remarks.—The ventral sulcus of *Sweetognathus duplex* n. sp. most closely resembles that of *Neostreptognathodus pnevi* Kozur and Movshovitsch in Movshovitsch et al., 1979. However, the sulcus of *N. pnevi* is narrower, steeper, and not as intensely pustulose. The junction of the free blade and dorsal process is often discontinuous or asymmetrical in *N. pnevi* as well.

Sweetognathus expansus (Perlmutter, 1975)

Pl. 20, Figs. 1–3

Ozarkadina expansa Perlmutter, 1975, pp. 98, 99, pl. 3, figs. 1–27.

Sweetognathus adenticulus Ritter, 1986, p. 165, pl. 4, figs. 9, 18, 19, 21.

Sweetognathus expansus von Bitter and Merrill, 1990, p. 107, pl. 3, figs. A–O; Ritter, 1995, pp. 1148, 1149, fig. 10.7; Mei et al., 2002, p. 84, fig. 10.27; Chernykh, 2005, pl. 20, figs. 1, 9, 10; Boardman et al., 2009, p. 140, pl. 17, fig. 7; pl. 20, fig. 13; pl. 24, figs. 5, 6; pl. 25, figs. 16–19; pl. 26, figs. 1–12, 14–18; pl. 27, figs. 9, 13, 14; pl. 29, figs. 1–11; Wardlaw et al., 2015, p. 376, pl. 1, fig. 1.

Wardlawella expansus Kozur, 1995, p. 168.

Diplognathodus expansus Chernykh, 2006, pp. 66–68, pl. 2, fig. 28.

Diagnosis.—A comparatively small species of *Sweetognathus* in which the P_1 element is characterized by a short free blade and a pustulose, adenticulate to subtly nodose carina.

Description.—The P_1 element has a short free blade consisting of three to five fused denticles subequal in height. The junction of the free blade and carina occurs just beyond the ventral margin of the broadly expanded platform and is marked by a transition from short, fused free blade denticles to a pustulose carina. The dorsal process occupies two-thirds to four-fifths of the length. A straight, dorsoventral furrow bisects the aboral side of the basal cavity. Two morphotypes of *S. expansus* are recognized: an adenticulate form and a subtly denticulate form. Boardman et al. (2009) proposed that the two morphotypes

likely demonstrate ecophenotypic variability, whereas others have considered the nodular forms transitional morphotypes (Chernykh et al., 2013). The nodose form generally has partially fused to undulating, low pustulose denticles either along the entire oral surface of the carina or the dorsal one-third. The carina gradually decreases in height dorsally in both morphotypes. *Sweetognathus expansus* is classified as a Type I sweetognathid.

Occurrence.—4 m, 5.3 m, 15.3 m, and 26.8 m above the base of the section; level - Asselian to the upper part of the Sakmarian Stage.

Sweetognathus 'merrilli' Kozur, 1975

Pl. 20, Figs. 4–6

Sweetognathus whitei (Rhodes, 1963). Merrill, 1973, p. 310, pl. 3, fig. 9.

Sweetognathus inornatus Ritter, 1986, p. 163, pl. 3, figs. 13, 15; 165, pl. 4, fig. 13; Holterhoff et al., 2013, p. 116, fig. 4.10.

Sweetognathus merrilli Kozur, 1975. Chernykh, 2005, p. 203, pl. 20, figs. 2, 11.

Diagnosis.—A species of *Sweetognathus* having a P_1 element characterized by a nodose carina bearing a single row of low, hemispherical denticles with pustulose microornamentation.

Description.—The free blade of *Sweetognathus* '*merrilli*' is of short to moderate length, with three to six partially to strongly fused, laterally compressed denticles increasing in height ventrally. The blade attaches to the dorsal process in a median position. The low, dorsal-most denticles of the free blade transition smoothly into the knot-like denticles of the carina, and the junction is occupied by the first small, pustulose node. The dorsal process is composed of four to eight discrete, nodose denticles reaching a maximum diameter between one-half and two-thirds length (dorsally) along the carina. Carinal denticles of *S.* '*merrilli*' typically reach a maximum diameter of one-fifth to one-seventh the length of the carina itself. Beyond the broadest denticles, the dorsal-most nodes decrease slightly in diameter, but the carina very rarely displays a papillary termination like those observed in more derived forms of *Sweetognathus*. In some cases, the carina may exhibit a dorsal curvature or minor torsion. The basal cavity is wide and spans approximately two-thirds the length of the P_1 element. *Sweetognathus* '*merrilli*' is classified as a Type II sweetognathid.

Occurrence.—4 m, 5.3 m, 26.8 m, and 36.2 m above the base of the section; level - upper part of the Asselian to the lower part of the Artinskian Stage.

Remarks.—Discrepancies regarding *Sweetognathus merrilli* and *S.* aff. *merrilli* (herein referred to as *S.* '*merrilli*') arose from the discovery of Bolivian forms of the genus that were isotopically dated as middle Asselian in age, but strongly resembled Sakmarian forms known from the Urals (Chernykh, 2005, 2006; Henderson et al., 2009). The older *S. merrilli* is also known from the North American Midcontinent (Boardman et al., 2009) and bears highly irregular pustulose nodes, whereas the younger *S.* '*merrilli*' has more orderly, hemispherical carinal nodes (Chernykh et al., 2013; Henderson, personal communication, 2016). Both the regular nature of the denticles of the dorsal process and the co-occurrence with *S. binodosus* serve as the rationale for the taxonomic assignment of the forms illustrated from North Spruce Mountain Ridge.

Sweetognathus* cf. *obliquidentatus (Chernykh in Chuvashov et al., 1990)

Pl. 22, Figs. 7, 8

Diagnosis.—A species of *Sweetognathus* in which the P_1 element bears a partially developed dorsoventral sulcus and sinuous, pustulose transverse ridges along the carina.

Description.—Only one partial specimen of *Sweetognathus* cf. *obliquidentatus* was recovered from the Riepe Spring Limestone of North Spruce Mountain

Ridge. A complete discussion of the specimen is not possible because it lacks the free blade and the ventral portion of the dorsal process. The median and dorsal portions of the carina display a narrow sulcus and thin, raised transverse denticles, respectively. The sulcus is bordered by low transverse ridges that fully connect to close the sulcus. The ridges are irregular and are composed of single rows of pustules. Spacing between the ridges is widest beyond the midpoint of the carina (dorsally). Both the carina and the basal cup taper to a papillary dorsal termination of the platform. *Sweetognathus* cf. *obliquidentatus* has characteristics of both Types III and IV, but does not meet the criteria of Type V.

Occurrence.—82.8 m above the base of the section; level - upper part of the Sakmarian to the Artinskian Stage.

Sweetognathus sulcatus Ritter, 1986

Pl. 21, Fig. 5

Sweetognathus sulcatus Ritter, 1986, p. 165, pl. 4, figs. 8, 12.

Diagnosis.—A species of *Sweetognathus* with a median platform sulcus that is laterally bounded by partially to fully nodose irregular parapets on either side.

Description.—The nature of the free blade of *Sweetognathus sulcatus* (as described by Ritter, 1986) is not known from the available specimens imaged. The carina is dominated by a dorsoventral sulcus that runs nearly the full length of the oral surface of the dorsal process. Nodose ridges on each side of the sulcus outline the lateral margins of the carina, tapering to close the sulcus both ventrally and dorsally. Pustulose microornamentation is present along the entire carina. The dorsal termination of the carina displays a large, u-shaped denticle that wraps around the end of the sulcus. The oral surface of the basal cup is broadly flared and unornamented. *Sweetognathus sulcatus* is classified as a Type IV sweetognathid.

Occurrence.—26.8 m above the base of the section; level - middle to upper part of the Sakmarian Stage.

Remarks.—It may be inferred from the specimens shown by Ritter (1986) that the free blade attaches to the dorsal process in a median position. Ritter (1986) noted that the free blade spans approximately one-fifth of the overall length, but there was no accompanying image. The supplemental specimen of *Sweetognathus sulcatus* illustrated alongside the holotype by Ritter (1986) is similar to *N. labialis* (Chernykh, 2012), known from Kungurian age strata of

the southern Ural Mountains near Mechetlino (Chernykh, 2012). A single specimen recovered from North Spruce Mountain Ridge has an auxiliary carinal denticle beyond the initial U-shaped dorsal termination. The smaller, dorsal-most denticle maintains a shape similar to the immediately preceding denticle.

***Sweetognathus wardlawi* n. sp.**

Pl. 21, Figs. 4, 6–8

Holotype.—Pl. 21, Fig. 6, SUI 145787.

Type locality and horizon.—Upper part of the Riepe Spring Limestone, Spruce Mountain Ridge, Elko County, Nevada; bed 2.

Etymology.—For Dr. Bruce Wardlaw (deceased, 1947–2016).

Diagnosis.—A species of *Sweetognathus* that has a P_1 element displaying large, partially fused, hemispherical to hemi-oblate pustulose denticles that transition from concave to convex nodes along the oral surface near the midpoint of the carina.

Description.—The P_1 element bears four to six laterally depressed, fused denticles decreasing in size dorsally. The lower, dorsal denticles are more strongly fused. The dorsal process is composed of a nodose carina with six to seven inflated, hemispherical to hemi-oblate denticles, the oral profiles of which invert between the midpoint and two-thirds length of the carina. The three to five ventral-most denticles are strongly fused and exhibit a concave, dish-like interior with pustulose microornamentation. The concave denticles may be partially connected by a shallow sulcus. Beyond the transitional point, the two to four dorsal denticles are discrete to partially fused, hemi-oblate nodes that decrease in size dorsally. The longitudinal trough does not extend beyond the transitional point of the carina. The cup of the P_1 element is caudoventrally flared with a steeply tapered dorsal region, whereas the rostral margin has a shallower, symmetrically flared base. *Sweetognathus wardlawi* n. sp. is classified herein as a Type V sweetognathid.

Occurrence.—5.3 m above the base of the section; type level - Sakmarian Stage.

Remarks.—*Sweetognathus wardlawi* n. sp. most closely resembles *S. binodosus*, its inferred evolutionary predecessor, but differs with the presence of depressed dimples in the center of the strongly fused ventral denticles of

the carina. Unlike *S. duplex* n. sp., the depressed portion of the carina in *S. wardlawi* n. sp. is not fully and uniformly connected by a median sulcus.

Sweetognathus 'whitei' (Rhodes, 1963)

Pl. 22, Figs. 9–12

Sweetognathus whitei (Rhodes). Igo, 1981, p. 72, pl. 7, figs. 2, 4, 5, 6; Orchard, 1984, p. 211, pl. 23.1, figs. 3–5; Henderson and McGugan, 1986, p. 229, figs. 7.4–7.7; Ritter, 1986, p. 63, pl. 3, figs. 17, 20, 21; Wang et al., 1987, p. 1052, figs. 6.17, 6.18; Riglos Suárez et al., 1987, p. 329, pl. 19.2, figs. 9–11, 13; p. 331, pl. 19.3, figs. 12, 14, 15; Mei et al., 2002, p. 72, fig. 10.25; Chernykh, 2005, p. 211, pl. 24, figs. 6, 7, 11; Wardlaw et al., 2015, p. 379, pl. 1, figs. 11–14, 16, 17.

Sweetognathus aff. *clarki* (Kozur in Kozur and Mostler, 1976). Chernykh, 2005, p. 205, pl. 21, fig. 12.

Sweetognathus aff. *whitei* (Rhodes). Chernykh, 2005, p. 211, pl. 24, fig. 8; Chernykh, 2006, p. 103, pl. 15, figs. 1, 8; Henderson, 2014, p. 15, figs. 2.5-2.7.

Diagnosis.—A species of *Sweetognathus* bearing a P_1 element characterized by a nodose carina with well-developed dumbbell to lightly subcrescentric denticles. The carina has a thin, raised dorsoventral ridge typically accented with a single row of pustules.

Description.—The P_1 elements of *Sweetognathus* '*whitei*' have a free blade of moderate length with as many as seven partially fused, laterally compressed denticles. The dorsal process is flat to lightly arcuate in lateral view with the largest carinal denticles often located at the highest point. When compared with other members of the genus, the carinal surface of *S.* '*whitei*' appears laterally expanded in oral view. The carina is ornamented with seven to nine transverse dumbbell or bow tie-shaped denticles, where the median region of the node is thinner than the marginal extent. The oral surface dips steeply between carinal denticles, forming narrow lateral grooves between the transverse nodes. The dorsoventral ridge serves as the only ornamentation of the depressed lateral grooves. The dorsal-most denticles of the carina abruptly narrow to a papillary termination, occasionally accompanied by a single node. *Sweetognathus* '*whitei*' is classified as a Type III sweetognathid.

Occurrence.—82.8 m, 114.5 m, 132.4 m, 161.5 m, 173.9 m, and 177.3 m above the base of the section; level - Artinskian Stage.

Remarks.—Topotype specimens of *Sweetognathus whitei* from the uppermost part of the Tensleep Sandstone of Wyoming have yielded isotopic values that fit those of late Asselian time (Chuvashov et al., 2013). For this reason, the form that serves as the index for the base of the Artinskian Stage has been

designated *S.* '*whitei*', or *S.* aff. *whitei*. The motivation supporting the distinction has been discussed by Dr. Charles Henderson (pers. comm. 2017) and in Permophiles (Henderson, 2014) and the two forms are readily distinguished from one another. The dumbbell-shaped denticles of the Asselian age *S. whitei* are somewhat irregular and the margins of the denticles gently taper to the lower platform, whereas the margins of the much more regular denticles of *S.* '*whitei*' (*S.* aff. *whitei*) drop steeply toward the platform (Henderson, 2014).

Biostratigraphy

Conodont yields throughout the Cisuralian part of the Riepe Spring Limestone at North Spruce Mountain Ridge are low, with 20 of 40 samples bearing few taxonomically identifiable P_1 elements (Table 1). Productive limestone beds yielded an average of fewer than six P_1 elements per five kg of digested sample material. The paucity of conodont elements, high volume of terrigenous clastic material within nearly all of the limestone present, and the thin intervals of fusulinid wackestone and packstone indicate the presence of a significant dilution factor related to high sedimentation rates associated with regional tectonism and the close proximity of the Ferguson trough to the fluctuating coastline.

Six genera of conodonts were recovered from the Sakmarian-Artinskian measured section, including *Sweetognathus*, *Hindeodus*,

Sweetina, *Mesogondolella*, *Pseudohindeodus*, and *Neostreptognathodus*. Several rounded fragments of *Streptognathodus* P_1 elements were collected at 5.3 m and 20 m above the base of the section, but the extreme degree of abrasion to which the elements have been subjected suggests that the grains have undergone significant reworking and these are excluded from the faunal distribution. The lowest Cisuralian conodont specimens recovered from the section include *S. expansus* (Perlmutter, 1975) and *S.* '*merrilli*' Kozur, 1975. The suite of conodonts recovered from the second lowest conodont-producing Permian-age limestone bed at 5.3 m above the base of the section is composed primarily of sweetognathids (e.g., *Sweetognathus* and *Neostreptognathodus*) and includes *S. expansus*, *S.* '*merrilli*', *S. binodosus* Chernykh, 2005, *S. wardlawi* n. sp., and *S. duplex* n. sp. A GSSP proposal by the Subcommission on Permian Stratigraphy has tentatively assigned *S. binodosus* the status of co-index species for the base of the Sakmarian Stage alongside *Mesogondolella monstra* Chernykh, 2005, the primary biostratigraphic signal (voting in progress) (Chernykh et al., 2016). The *S. binodosus* Zone (partial range lineage biozone) spans from the base of the Sakmarian to the first occurrence of *S. anceps* in the late Sakmarian (Henderson, 2016).

Sweetognathus duplex n. sp. has been recovered from two levels within the measured section, at 5.3 m and 26.8 m, allotting the new species a narrow range within the Sakmarian *S. binodosus* Zone. Although there is a co-occurrence of *S. duplex* n. sp. and *S. wardlawi* n. sp. at 5.3 m above the base

of the section, this bed has proven to be the only point of the section to yield *S. wardlawi* n. sp. A single specimen of *S. sulcatus* Ritter, 1986 was also recovered from 26.8 m above the base of the section. *Sweetognathus sulcatus* has been previously reported from Sakmarian deposits of the Cerro Alto Formation in the Franklin Mountains of west Texas (Ritter, 1986) and the Kurort Formation of the Dal'ny Tulkas section in Russia (Davydov et al., 2005). Fusulinid associations within the *S. binodosus* Zone of the Riepe Spring Limestone include *Schwagerina neolata* Thompson, 1954, *Schwagerina wellsensis* Thompson, 1954, and *Eoparafusulina linearis* (Dunbar and Skinner, 1937) (Fig. 8.4). *Sweetognathus anceps* Chernykh, 2005, the evolutionary predecessor of *S.* '*whitei*', occurs along with *S. binodosus* at 51.7 m, denoting the base of the *S. anceps* Zone (late Sakmarian; partial range lineage zone) (Henderson, 2016). Beyond the first occurrence of *S. anceps*, the dip-slope and thick accumulations of talus make the recovery of adequate sample material more difficult, but a partial, immature specimen of *S. anceps* was also recovered from 59.3 m above the base of the section.

The approximate base of the Artinskian Stage, denoted by the first occurrence of *Sweetognathus* '*whitei*', is estimated to be 82.8 m above the base of the section, 31.1 m above the lowest recovered specimens of *S. anceps* (Fig. 8.4). The lowest specimens of *S.* '*whitei*' occur in association with highly irregular and poorly preserved specimens of *S.* cf. *obliquidentatus* (Chernykh

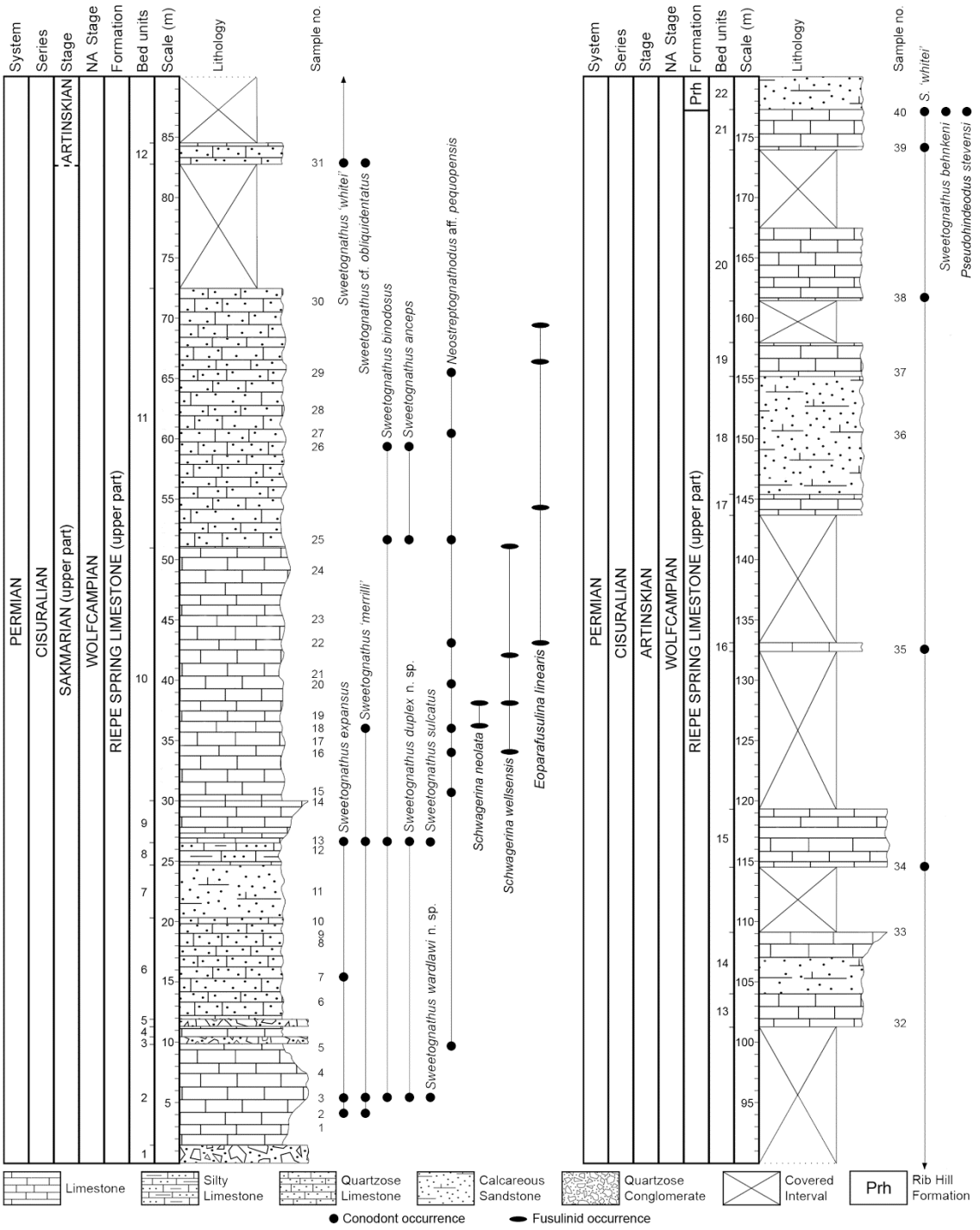

Figure 8.4 – Detailed lithologic column of the Cisuralian portion of the upper part of the Riepe Spring Limestone at North Spruce Mountain Ridge with accompanying conodont (circles) and fusulinid (ovals) distributions. Sample numbers are provided for the conodont material collected. The chronostratigraphic scale includes international standards and the corresponding North American stage.

in Chuvashov et al., 1990), which has been previously reported from Sakmarian and Artinskian age strata of the Urals (Chuvashov and Chernykh, 1998; Chuvashov et al., 2013) and, most recently, Carlin Canyon, Nevada (Dehari, 2016, unpublished thesis). *Pseudohindeodus stevensi* (Clark and Carr, 1982), *S. behnkeni* (Kozur, 1975), and a large, transitional form of *S.* '*whitei*' (to *S. behnkeni*) were collected at 177.3 m along with the continued occurrence of *S.* '*whitei*' within the Artinskian age uppermost part of the Riepe Spring Limestone.

Cisuralian Conodont Fauna

Type V Sweetognathids: A Novel Carinal Configuration

P_1 elements of *Sweetognathus* are known for their high degree of intraspecific morphological plasticity and are characterized by dense pustulose microornamentation along the oral surface of the dorsal process (Behnken, 1975; Wang et al., 1987; Vuolo et al., 2014; Henderson, 2016). Sweetognathid P_1 elements display either adenticulate (Type I), discretely nodose (Type II), transversely ridged (Type III), or dorsoventrally troughed (Type IV) carinal morphologies (Ritter, 1986; Wang et al., 1987). Type I remained the singular carinal configuration of the family until the differentiation of the carina in *S. merrilli* (Type II) occurred during the middle part of the Asselian (Chernykh et al., 2013). The discretely denticulate sweetognathid forms of the Asselian (*S. merrilli* and *S.* '*merrilli*')

provided opportunities for further carinal modification during the early part of the Sakmarian when *S. binodosus* arose from *S.* '*merrilli*' and introduced the Type III morphological group (Chuvashov et al., 2013). The Type III carinal configuration was initially produced by the lateral development of hemispherical nodes and gradually became more pronounced into the Artinskian Stage. Type IV sweetognathids include the members of *Neostreptognathodus* and a few earlier, sulcus-bearing forms of *Sweetognathus*, such as *S. sulcatus*, *S. obliquidentatus*, and *S. clarki* (Kozur in Kozur and Mostler, 1976) (Ritter, 1986; Wang et al., 1987). In addition to these previously described sweetognathid classifications, a new group, herein regarded as Type V, has been demonstrated by the recently discovered forms *S. wardlawi* n. sp. and *S. duplex* n. sp. recovered from the upper part of the Riepe Spring Limestone. Sweetognathids exhibiting a Type V configuration have a carina resembling a composite of the Type III and Type IV groups, in which the ventral half of the carina is predominantly centrally concave along the oral surface, but the dorsal portion is composed of subtly elongated, nodose (convex) denticles, much like those of *S. binodosus* (Read and Nestell, 2017a). The half-and-half arrangement observed in the Type V group is most similar to the transition near the midpoint of the carina in some specimens of *N. pnevi* Kozur and Movshovitsch in Movshovitsch et al., 1979 (those designated *N. lectulus* Chernykh, 2012), in which the parapets are adenticulate (or nearly so) along the ventral portion of the carina and

strongly transversely ridged dorsally, and *N.* sp. 4 Chernykh, 2005. Neither *S. wardlawi* n. sp. nor *S. duplex* n. sp. have been reported from any nearby, approximately coeval marine deposits.

The strongly fused, vaguely molariform, ventral carinal denticles of *Sweetognathus wardlawi* n. sp. have dish-like fossae, herein regarded as "dimples," which are connected by a very faint, shallow median groove that partially interrupts the outer rim of the denticles. The concave nature of the denticles is not a product of surface damage or occlusal microwear over time, as close inspection has revealed that the surface texture on the interior of the dimples remains highly pustulose (see Pl. 21, Fig. 8). Type V dimples may represent a lineal feature that preceded the somewhat irregular and nodular sulci observed in specimens of *S. sulcatus*. The faint groove bisecting the ventral denticles of *S. wardlawi* n. sp. and a pronounced rim separating the dorsal-most denticles of *S. sulcatus* (Pl. 21, Fig. 5) demonstrate potential transitional features between the two species. Samples collected just beneath the limestone bed that produced the only specimens of *S. wardlawi* n. sp. failed to provide any identifiable conodont elements, and the truncation of Cisuralian strata by the underlying disconformity renders the study of any potential lower range of the species impossible at this locality.

Sweetognathus duplex n. sp. may represent the next phyletic step in the "depressed" or sulcus-bearing lineage of *Sweetognathus*. The denticles along the dorsal half of the carina in specimens of *S. duplex* n. sp. resemble

those of *S. binodosus* (see Pl. 20, Figs. 9, 12), but the latter species shows no sign of sulcus development. The oldest recovered specimen of *S. duplex* n. sp., which was acquired from the same bed as all specimens of *S. wardlawi* n. sp., retains marginal relict denticles along the sulcus. The sulcus feature of *S. duplex* n. sp., like the dimples of *S. wardlawi* n. sp., maintains pustules within the central depression that extend upward to the lateral margins of the carina. *Sweetognathus duplex* n. sp. does not bear resemblance to either *S. obliquidentatus* or *S. clarki* and was not recovered higher than the *S. binodosus* Zone within the section. Therefore, the species does not seem to have extended the sulcus-bearing lineage of *Sweetognathus* beyond the end of the Sakmarian Stage.

Déjà Vu: Sweetognathus *and* Neostreptognathodus

Instances of morphological innovation resulting in near homeomorphism between members of *Sweetognathus* (Type IV) and *Neostreptognathodus* have been previously reported from Cisuralian conodont faunas in China, Iran, Russia, and the western United States (Ritter, 1986; Wang et al., 1987; Mei et al., 2002; Davydov et al., 2005). The Type V sweetognathids described herein represent a similar expression of this sulcus-based platform morphology. In each instance, members of *Sweetognathus* developed depressions, or a partial to complete sulcus along the carina, a trait that was later reproduced with greater degrees of success

and proliferated by various species of *Neostreptognathodus* (e.g., *N. ruzhencevi* Kozur in Kozur and Mostler, 1976 and *N. pnevi*) during the late Artinskian and Kungurian (late Cisuralian).

Similarly, repetitive manifestations of platform depressions in ozarkodinid P_1 elements through late Paleozoic time are well-known from troughed and untroughed members of the Idiognathodontidae. During the Middle and Late Pennsylvanian, troughed platforms evolved, disappeared, and subsequently reappeared several times throughout the complex and interwoven lineages of the genera *Idiognathodus*, *Streptognathodus*, and *Swadelina* (Lambert et al., 2003; Rosscoe and Barrick, 2009, 2013; Hogancamp et al., this volume). The successive development of a dorsal trough in *Swadelina* and *Streptognathodus* has been attributed to neoteny (paedomorphosis) in species of *Idiognathodus*, which lack a trough in adult forms (Sweet, 1988; Lambert et al., 2003). However, in Cisuralian Type IV and Type V representatives of *Sweetognathus*, the unique forms appear to have evolved particularly rapidly from a stock that bore no ancestral sulci. Furthermore, juvenile specimens of most sweetognathids are often difficult to distinguish at the species level, and typically display a Type I or Type II configuration with no early signs of carinal differentiation, and, therefore, sulcus development through paedomorphosis may be ruled out. Perhaps the timing of this early Cisuralian experimentation, which coincides with the departure of troughed and/or nodular Carboniferous holdovers, such as

Adetognathus and *Streptognathodus*, left morphospace vacancies that were quickly filled by *Sweetognathus*, the next available, innovative shallow-water taxon.

P_1 elements bearing a striking resemblance to *Neostreptognathodus pequopensis* Behnken, 1975 were recovered from 5.7 m above the lowest occurrence of *Sweetognathus*, and continue to occur intermittently over the next 55.8 m. The occurrence of these forms, herein regarded as *Neostreptognathodus* aff. *pequopensis*, within the Sakmarian stratigraphic interval of the upper part of the Riepe Spring Limestone at a level significantly below the first occurrence of *S.* '*whitei*' (Rhodes, 1963) is noteworthy and seemingly anomalous. *Neostreptognathodus pequopensis* is regarded as the progenitor of the genus and a cosmopolitan species denoting the latest part of the Artinskian (early part of the North American Leonardian) (Behnken, 1975). If *N.* aff. *pequopensis* is indeed *N. pequopensis*, these specimens would represent the earliest known occurrence of the species, predating the base of the recognized *N. pequopensis* Zone (partial range lineage biozone) by five to seven million years (Henderson, 2016). Although *N.* aff. *pequopensis* was one of the most commonly recovered forms within the lower portion of the section (along with *S. expansus*, *S.* '*merrilli*', and *S. binodosus*), there is no observed co-occurrence with *S.* '*whitei*' at any level within the North Spruce Mountain Ridge section. Presently no data support a more sustained temporal range and a definitive claim of earliest

occurrence. The high degree of diachroneity between these forms, potential for homeomorphy among conodonts, and lack of continuous recovery has prompted the tentative assignment herein of the older specimens to *N.* aff. *pequopensis*. Interestingly, the original early Leonardian age type specimens described by Behnken (1975) were collected from the Pequop Formation in the Pequop Mountains, mere miles to the northeast of the North Spruce Mountain Ridge locality. The lower and upper parts of the Pequop Formation comprise the entire eastern half of North Spruce Mountain Ridge at the given locality, but this interval is separated from the Riepe Spring Limestone by a thick sequence of the predominantly unfossiliferous Rib Hill Formation (Fig. 8.1). Of all other closely related conodont studies from the Pequop Range, Nevada (Wardlaw et al., 1998; Henderson et al., 2012), Carlin Canyon, Nevada (Dehari, 2016, unpublished thesis), Ferguson Mountain, Nevada (Clark, 1974; Behnken, 1975), and Moorman Ranch, Nevada (Clark, 1974; Behnken, 1975; Ritter, 1986), none have demonstrated a Sakmarian age occurrence of any form so closely resembling *N. pequopensis* (or *N.* aff. *pequopensis*). The specimens of *Sweetognathus obliquidentatus* illustrated by Chernykh (2005, 2006) from the southern Ural Mountains bear a general resemblance, but the denticles are more transversely elongated. Further sampling of coeval regional strata is necessary before a detailed discussion of potential phylogenetic implications for *Sweetognathus* and *Neostreptognathodus* is issued.

Table 8.1 – Distribution of sweetognathid conodonts from the Cisuralian portion of the Riepe Spring Limestone at North Spruce Mountain Ridge, Elko County, Nevada.

	upper part of the Riepe Spring Limestone																				
Sample no.	2	3	5	7	13	15	16	18	20	22	25	26	27	29	31	34	35	38	39	40
Meters above base	4	5.3	9.7	15.3	26.8	30.8	34	36.2	39.7	43.1	51.7	59.3	60.5	65.5	82.8	114.5	132.4	161.5	173.9	177.3
Sweetognathus expansus	2	10		1	1															
S. 'merrilli'	1	2			2			1												
S. binodosus		6			1						3	1								
***S. duplex* n. sp.**		3			2															
***S. wardlawi* n. sp.**		6																		
S. sulcatus					1															
S. anceps											1	1								
S.* cf. *obliquidentatus															2					
S. 'whitei'															1	1	3	6	17	19
S. behnkeni																				1
Neostreptognathodus* aff. *pequopensis			4			3	2	1	2	1	1		1	3						
Pseudohindeodus stevensi																				1

Conclusions

The Cisuralian part of the Riepe Spring Limestone at North Spruce Mountain Ridge, Elko County, Nevada, preserves a sparse and distinctive Sakmarian to Artinskian conodont fauna that is dominated by species of the ozarkodinid genus *Sweetognathus*. The measured section, which was included in the upper part of Section 1 from Hope (1972), records 180 m of nearshore and open shelf deposition along the northern Ferguson Trough in the post-Antler foreland. Two new, rare Sakmarian age forms of the genus *Sweetognathus*, *S. duplex* n. sp. and *S. wardlawi* n. sp., were recovered from the upper part of the Riepe Spring Limestone in association with the *S. binodosus* Zone (partial range lineage biozone; lower to middle Sakmarian). Each of the new species demonstrates a partially depressed and nodose carinal morphology, categorized herein as the Type V sweetognathid configuration. The Type V carinal configuration resembles an amalgamation of the Type II and Type IV sweetognathid groups described by Ritter (1986). In addition to the newly described species of *Sweetognathus*, peculiar forms representing an apparent early occurrence of the genus *Neostreptognathodus* were recovered from multiple levels within a 55.8 m thick (9.7 m to 65.5 m) Sakmarian age interval of the measured section. The anomalous forms, herein regarded as *N.* aff. *pequopensis*, may call into question some aspects of the accepted phylogeny of *Sweetognathus* and *Neostreptognathodus*, but more regional sampling must be done before these relationships are well

understood. Beyond the last occurrence of *N.* aff. *pequopensis* at 65.5 m, an estimated base of the Artinskian has been identified in association with the first occurrence of *S.* '*whitei*' at 82.8 m above the base of the section.

Plate 20

All illustrated specimens were collected from the upper part of the Riepe Spring Limestone, North Spruce Mountain Ridge, Elko County, Nevada, U.S.A. SUI 145772–145803. Scale bar at lower left corresponds with Figs. 8 and 9. Scale bar at lower right corresponds with Figs. 11 and 12.

1-3. *Sweetognathus expansus* (Perlmutter, 1975)

1. SUI 145772, 5.3 m above the base of the section (sample no. 3). Oral view of broken P_1 element.
2. SUI 145773, 5.3 m above the base of the section (sample no. 3). Oral view of P_1 element.
3. SUI 145774, 5.3 m above the base of the section (sample no. 3). Oral view of P_1 element.

4-6. *Sweetognathus* '*merrilli*' Kozur, 1975

4. SUI 145775, 5.3 m above the base of the section (sample no. 3). Oral view of broken P_1 element.
5. SUI 145776, 5.3 m above the base of the section (sample no. 3). Slightly oblique oral view of broken P_1 element.
6. SUI 145777, 34 m above the base of the section (sample no. 16). Oral view of P_1 element.

7-13. *Sweetognathus duplex* Read and Nestell, in press

7. Paratype, SUI 145778, 26.8 m above the base of the section (sample no.

13). Oral view of broken P_1 element.

8. Paratype, SUI 145778, 26.8 m above the base of the section (sample no. 13). Detail of ventral median sulcus.

9. Paratype, SUI 145778, 26.8 m above the base of the section (sample no. 13). Detail of dorsal denticles.

10. Holotype, SUI 145779, 26.8 m above the base of the section (sample no. 13). Oral view of P_1 element.

11. Holotype, SUI 145779, 26.8 m above the base of the section (sample no. 13). Detail of ventral median sulcus.

12. Holotype, SUI 145779, 26.8 m above the base of the section (sample no. 13). Detail of dorsal denticles.

13. Paratype, SUI 145780, 5.3 m above the base of the section (sample no. 3). Oral view of broken P_1 element.

14. *Sweetognathus binodosus* Chernykh, 2005; SUI 145781, 5.3 m above the base of the section (sample no. 3). Oral view of broken P_1 element.

Plate 20

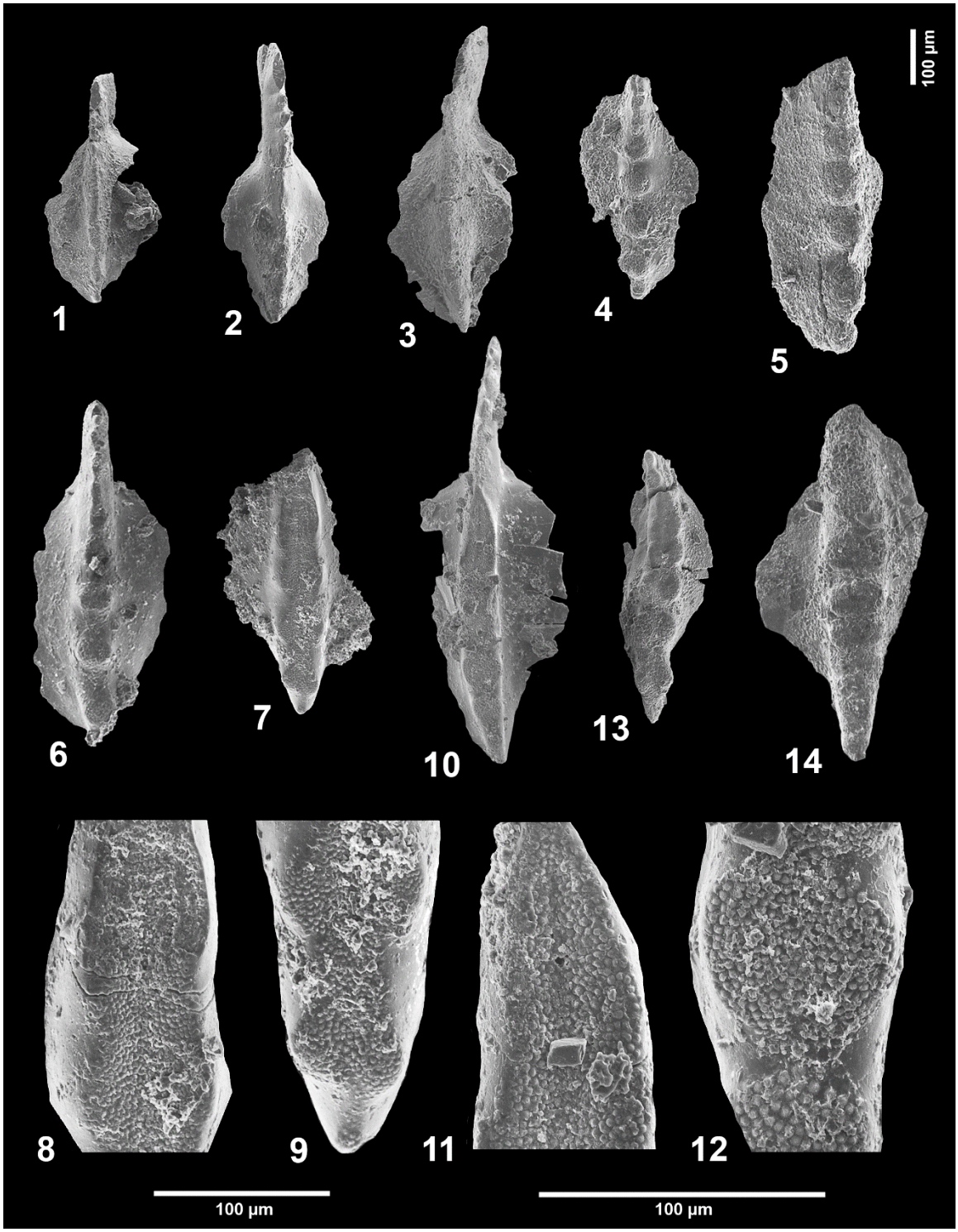

Plate 21

All illustrated specimens were collected from the upper part of the Riepe Spring Limestone, North Spruce Mountain Ridge, Elko County, Nevada, U.S.A.

1-3. *Sweetognathus binodosus* Chernykh, 2005

1. SUI 145782, 51.7 m above the base of the section (sample no. 25). Oral view of P_1 element.
2. SUI 145783, 51.7 m above the base of the section (sample no. 25). Oral view of broken P_1 element.
3. SUI 145784, 5.3 m above the base of the section (sample no. 3). Oral view of broken P_1 element.

4, 6-8. *Sweetognathus wardlawi* Read and Nestell, in press

4. Paratype, SUI 145785, 5.3 m above the base of the section (sample no. 3). Slightly oblique oral view of P_1 element.
6. Paratype, SUI 145787, 5.3 m above the base of the section (sample no. 3). Oral view of broken P_1 element.
7. Holotype, SUI 145788, 5.3 m above the base of the section (sample no. 3). Oral view of P_1 element.
8. Holotype, SUI 145788, 5.3 m above the base of the section (sample no. 3). Detail of a carinal denticle illustrating the pustules along the interior of a "dimple" amidst heavy recrystallization.

5. *Sweetognathus sulcatus* Ritter, 1986; SUI 145786, 26.8 m above the base of the section (sample no. 13). Oral view of broken P_1 element.

9-11. *Neostreptognathodus* aff. *pequopensis* Behnken, 1975

9. SUI 145789, 65.5 m above the base of the section (sample no. 29). Oral view of P1 element. Immature specimen.

10. SUI 145790, 9.7 m above the base of the section (sample no. 5). Oral view of P_1 element.

11. SUI 145791, 30.8 m above the base of the section (sample no. 15). Detail of carinal denticles of broken P_1 element.

Plate 21

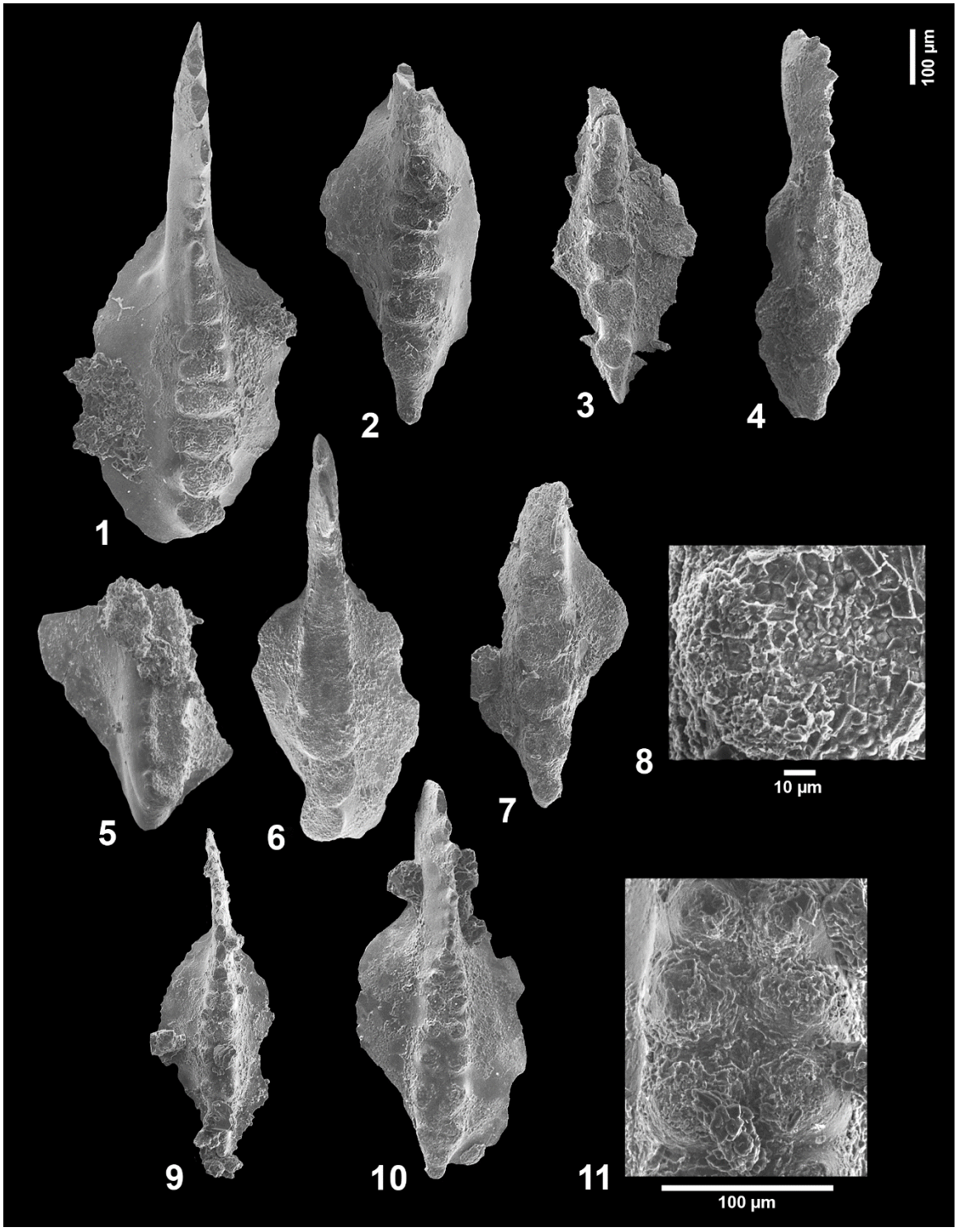

Plate 22

All illustrated specimens were collected from the upper part of the Riepe Spring Limestone, North Spruce Mountain Ridge, Elko County, Nevada, U.S.A.

1-3. *Neostreptognathodus* aff. *pequopensis* Behnken, 1975

1. SUI 145792, 30.8 m above the base of the section (sample no. 15). Oral view of P_1 element.
2. SUI 145793, 34 m above the base of the section (sample no. 16). Oblique oral view of P_1 element.
3. SUI 145794, 30.8 m above the base of the section (sample no. 15). Oral view of P_1 element.

4, 5. *Sweetognathus anceps* Chernykh, 2005

4. SUI 145795, 51.7 m above the base of the section (sample no. 25). Oral view of broken P_1 element.
5. SUI 145796, 59.3 m above the base of the section (sample no. 26). Oral view of broken P_1 element. Immature specimen.

6. *Pseudohindeodus stevensi* (Clark and Carr, 1982); SUI 145797, 177.3 m above the base of the section (sample no. 40). Oral view of P_1 element.

7, 8. *Sweetognathus* cf. *obliquidentatus* (Chernykh in Chuvashov et al., 1990)

7. SUI 145798, 82.8 m above the base of the section (sample no. 31). Oral view of broken P_1 element.

8. SUI 145798, 82.8 m above the base of the section (sample no. 31). Detail of dorsal denticles.

9-12. *Sweetognathus* '*whitei*' (Rhodes, 1963)

9. SUI 145799, 114.5 m above the base of the section (sample no. 34). Oblique view of broken P_1 element.

10. SUI 145800, 132.4 m above the base of the section (sample no. 35). Oral view of broken P_1 element.

11. SUI 145801, 173.9 m above the base of the section (sample no. 39). Oral view of P1 element.

12. SUI 145802, 177.3 m above the base of the section (sample no. 40). Oral view of broken P_1 element. Transitional specimen to *S. behnkeni*.

13. *Sweetognathus behnkeni* Kozur, 1975; SUI 145803, 177.3 m above the base of the section (sample no. 40). Oral view of broken P_1 element.

Plate 22

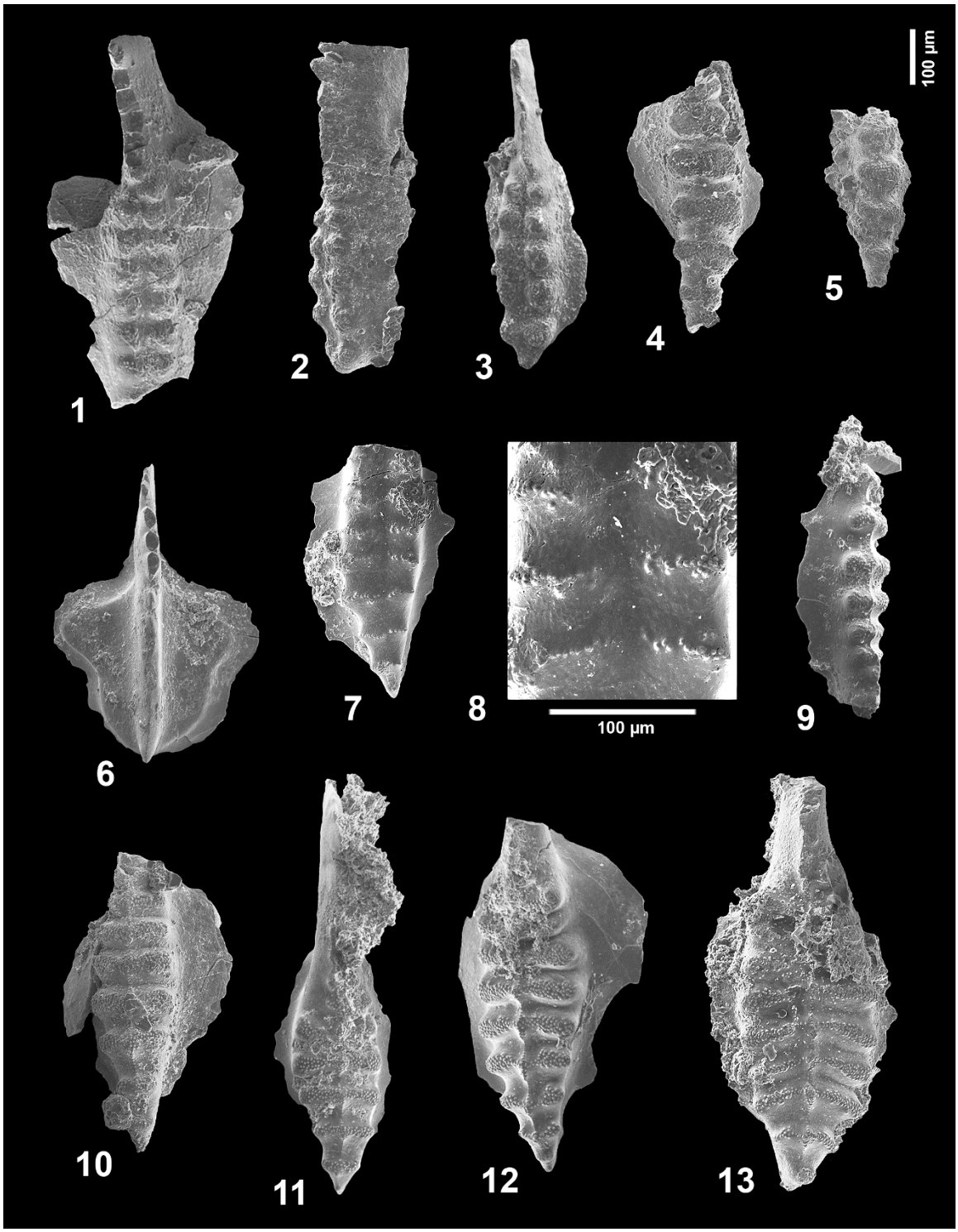

CHAPTER 9: CONCLUSIONS

This study is concerned with the marine microfaunal succession of the Riepe Spring Limestone at Spruce Mountain Ridge, Elko County, northeast Nevada. The principal objective of this study is the integration of Kasimovian (Upper Pennsylvanian) through Artinskian (mid-Cisuralian) fusulinid and conodont assemblages, thereby providing high-resolution age control of a critically understudied North American Pennsylvanian-Permian boundary section. The following is a summary of the conclusions previously discussed in Chapters 3-8.

I. The deposition of the Riepe Spring Limestone at Spruce Mountain Ridge occurred during the third and final glacial stage of the late Paleozoic ice age. As a result, the mixed carbonate-siliciclastic strata of the Riepe Spring Limestone record evidence of rapid glacioeustatic fluctuations and subsequent coastal emergence along the margins of the Ferguson Trough.

II. Four types of chert pebble conglomerate macrofacies and 10 primary carbonate and siliciclastic microfacies are identified from the uppermost part of the Ely Limestone, the Riepe Spring Limestone, and the Rib Hill Formation. The variety of lithofacies reflects considerable changes in the depositional settings of the Ferguson Trough throughout the Late Pennsylvanian and Cisuralian. Inferred

paleoenvironments include backshore, marginal marine, shoreface, mid-shelf, and outer shelf or potentially slope-related settings.

III. Six lower Missourian through upper Wolfcampian fusulinid assemblage zones are recognized in the uppermost part of the Ely Limestone and the Riepe Spring Limestone at Spruce Mountain Ridge, including: *Eowaeringella-Triticites* Group I assemblage (lower to upper Missourian); *Triticites* Group II-*Dunbarinella* assemblage zone (lower to middle Virgilian); *Triticites* Group IV assemblage zone (upper Virgilian); *Schwagerina wellsensis* assemblage zone (upper Wolfcampian); *Eoparafusulina linearis* assemblage zone (upper Wolfcampian); "advanced" *Schwagerina* assemblage zone (upper Wolfcampian).

IV. At least four significant erosional disconformities are present in the Kasimovian-Artinskian strata of the Riepe Spring Limestone, including mid-Kasimovian (mid-Missourian), upper Kasimovian to lower Gzhelian (upper Missourian to lower Virgilian), mid-Gzhelian (mid-Virgilian), and upper Gzhelian to upper Asselian(?)/lower Sakmarian (upper Virgilian to mid-Wolfcampian) erosional vacuities. Fusulinid and conodont assemblages provide the age control for the upper and lower limits of the disconformities.

V. The recently described fusulinid *Douglassites sprucensis* from the middle informal member of the Riepe Spring Limestone is among the

largest known Pennsylvanian species of Schubertellidae, commonly reaching more than four millimeters in length and averaging seven volutions at maturity. *Douglassites sprucensis* exhibits a finely porous wall structure that is characteristic of the subfamily Biwaellinae and resembles the nearly coeval Paleo-Tethyan genus *Dutkevichites*, with which it shares a common schubertellid ancestor, but the latter has never been reported from North America.

VI. *Biwaella americana* is reported from Nevada for the first time. *Biwaella* is considered a Paleo-Tethyan schubertellid genus of which very few forms migrated to western Pangea during the Cisuralian. To date, *B. americana* is the only species of *Biwaella* to be described from the United States and was previously only known from the Artinskian(?) type specimens of Skinner and Wilde (1965a) from the Big Hatchet Mountains, New Mexico. The herein described Nevadan forms of *B. americana* were recovered from slightly older (upper Asselian(?)-lower Sakmarian) deposits, indicating that migrant forms of *Biwaella* had reached the tropics of western Pangea earlier than previously suggested.

VII. Five Upper Pennsylvanian conodont zones discussed by Barrick et al. (2013b) are recognized (in part) from the sparse Kasimovian-Gzhelian conodont succession from the lower and middle informal members of the Riepe Spring Limestone at Spruce Mountain Ridge, including:

Idiognathodus confragus Zone (lower-middle Kasimovian); *Idiognathodus eudoraensis* Zone (upper Kasimovian); *Idiognathodus simulator* Zone (lower Gzhelian); *Streptognathodus virgilicus* [*s.s.*] Zone (middle Gzhelian); *Streptognathodus bellus* Zone (upper Gzhelian).

VIII. Twelve species belonging to three genera of sweetognathid conodonts, including two new species, are described from the upper informal member of the Riepe Spring Limestone. The two new species, *Sweetognathus duplex* and *Sw. wardlawi*, each exhibit a previously unidentified carinal configuration in which the P_1 element bears both discrete nodes and a medial sulcus. These forms further demonstrate the high degree of morphological plasticity and innovation often observed in the early Cisuralian sweetognathids.

IX. The occurrence of *Neostreptognathodus* aff. *pequopensis* below the FO of *Sweetognathus* '*whitei*' in the upper informal member of the Riepe Spring Limestone may represent an instance of remarkable homeomorphism within closely related sweetognathid conodonts or potentially the earliest known occurrence of *Neostreptognathodus*, predating the upper Artinskian (upper-middle Cisuralian; lower Leonardian) *N. pequopensis* Zone by five to seven million years.

LITERATURE CITED

Adams, J.E., Cheney, M.G., DeFored, R.K., Dickey, R.I., Dunbar, C.O., Hills, J.M., King, R.E., Miller, A.K., and Needham, C.E., 1939, Standard Permian section of North America: AAPG Bulletin, v. 23, p. 1673–1681.

Akmetshina, L.Z., 1990, Konodonti pogranichnykh otlozheniy karbona i permi vostochnoy okraini Prikaspiyskoy vpadini [Conodonts of Carboniferous-Permian boundary deposits of the eastern margin of the Caspian depression]: Byulleten Moskovskogo Obshchestva Ispytateley Prirody, Otdeleniye geologicheskoye, v. 65, no. 1, p. 80–88. [in Russian]

Alekseev, A.S., and Goreva, N.V., 2006, Kasimovian and Gzhelian (Upper Pennsylvanian) conodont zonation in Russia: Newsletter on Carboniferous Stratigraphy, v. 24, p. 40–43.

Asquith, G.B., and Drake, J.F., 1985, Depositional history and reservoir development of a Permian *Fistulipora–Tubiphytes* bank complex, Blalock Lake East Field, West Texas, *in* Roehl, P.O., and Choquette, P.W., eds., Carbonate Petroleum Reservoirs: Berlin-Heidelberg, Springer-Verlag, p. 311–316.

Austin, R.L., and Mitchell, M., 1975, Middle Dinantian platform conodonts from County Fernanagh and County Tyrone, Northern Ireland: Bulletin of the Geological Survey of Great Britain, v. 55, p. 43–54.

Austin, R.L., and Rhodes, F.H.T., 1981, Cavusgnathidae, *in* Robinson, R.A., ed., Treatise on Invertebrate Paleontology, Pt. W, Miscellanea, Supp. 2, Conodonta: University of Kansas Press, Lawrence, KS, p. 158–160.

Baars, D.L., Ross, C.A., Ritter, S.M., and Maples, C.G., 1994a, Proposed repositioning of the Pennsylvanian-Permian boundary in Kansas, *in* Baars, D.L., ed., Revision of stratigraphic nomenclature in Kansas: Kansas Geological Survey Bulletin 230, p. 5–10.

Baars, D.L., Ritter, S.M., Maples, C.G., and Ross, C.A., 1994b, Redefinition of the Upper Pennsylvanian Virgilian Series in Kansas, *in* Baars, D.L., ed., Revision of stratigraphic nomenclature in Kansas: Kansas Geological Survey Bulletin 230, p. 11–16.

Baesemann, J.F., 1973, Missourian (Upper Pennsylvanian) conodonts of northeastern Kansas: Journal of Paleontology, v. 47, no. 4, p. 689–710.

Bando, Y., Bhatt, D.K., Gupta, V.J., Hayashi, S., Kozur, H., Nakazawa, K., and Wang, Z.H., 1980, Some remarks on the conodont zonation and

stratigraphy of the Permian: Recent Researches in Geology, v. 8, p. 1–53.

Barosh, P.J., 1964, Lower Permian stratigraphy of east-central Nevada and adjacent Utah: U.S. Geological Survey Open-File Report 64-10, 144 p.

Barrick, J.E., 2012, Microscopic marvels of the Paleozoic: Conodonts: http://barricklab.org/twiki/pub/Lab/LinkList/Barrick_Conodonts.pdf

Barrick, J.E., and Boardman, D.R., 1989, Stratigraphic distribution of morphotypes of *Idiognathodus* and *Streptognathodus* in Missourian-lower Virgilian strata, north-central Texas: Texas Tech University Studies in Geology, v. 2, p. 167–189.

Barrick, J.E., and Heckel, P.H., 2000, A provisional conodont zonation for Late Pennsylvanian (late Late Carboniferous) strata in the Midcontinent region of North America: Newsletter on Carboniferous Stratigraphy, v. 18, p. 5–22.

Barrick, J.E., Heckel, P.H., and Boardman, D.R., 2008, Revision of the conodont *Idiognathodus simulator* (Ellison 1941), the marker species for the base of the Late Pennsylvanian global Gzhelian Stage: Micropaleontology, v. 54, no. 2, p. 125–138.

Barrick, J.E., Lucas, S.G., and Krainer, K., 2013a, Conodonts of the Atrasado Formation (uppermost Middle to Upper Pennsylvanian), Cerros de Amado Region, central New Mexico, U.S.A.: Carboniferous-Permian transition in New Mexico, New Mexico Museum of Natural History and Science Bulletin, v. 59, p. 239–252.

Barrick, J.E., Lambert, L.L., Heckel, P.H., Rosscoe, S.J., and Boardman, D.R., 2013b, Midcontinent Pennsylvanian conodont zonation: Stratigraphy, v. 10, no. 1–2, p. 55–72.

Barskov, I.S., and Alekseev, A.S., 1975, Middle and Upper Carboniferous conodonts of the Moscow region: Izvestiya Akademii Nauk SSSR, Seriya Geologicheskaya, no. 6, p. 84–99. [in Russian]

Barskov, I.S., Isakova, T.N., and Shchastlivceva, N.P., 1981, Conodonts of the Gzhelian and Asselian boundary beds, southern Urals: Izvestiya Akademii Nauk SSSR, Seriya Geologicheskaya, v. 5, p. 78–87. [in Russian]

Barskov, I.S., Alekseev, A.S., Goreva, N.V., Kononova, L.I., and Migdisova, A.V., 1984, Zonal'naya shkala karbona Vostochno-Yevropeiskoi platformy po konodontam [Carboniferous conodont zonation of the East-European Platform], *in* Menner, V.V., ed., Paleontologicheskaya kharakteristika stratotipicheskikh i opornykh razrezov karbona

Moskovskoi sineklizy [Palaeontological characteristics of the Carboniferous stratotypes and key sections of the Moscow Syncline]: University Publishing House, Moscow, p. 143–147. [In Russian]

Barskov, I.S., Alekseev, A.S., Kononova, L.I., and Migdisova, A.V., 1987, Atlas of Devonian and Carboniferous conodonts: Moscow University Press, Moscow, 141 p. [in Russian]

Beauchamp, B., and Henderson, C.M., 1994, The Lower Permian Raanes Great Bear Cape and Trappers Cove Formations, Sverdrup Basin, Canadian Arctic: Stratigraphy and conodont zonation: Bulletin of Canadian Petroleum Geology, v. 42, no. 4, p. 562–597.

Beede, J.W., and Kniker, H.T., 1924, Species of the genus *Schwagerina* and their stratigraphic significance: University of Texas Bulletin, v. 2433, 100 p.

Behnken, F.H., 1975a, Conodonts as Permian biostratigraphic indices, *in* Cys, J.M., and Toomey, D.F., eds., Permian Exploration, Boundaries and Stratigraphy: West Texas Geological Society and SEPM Permian Basin Section, v. 75–65: p. 84–90.

Behnken, F.H., 1975b, Leonardian and Guadalupian (Permian) conodont biostratigraphy in western and southwestern United States: Journal of Paleontology, v. 49, no. 2, p. 284–315.

Bengston, P., 1988, Open nomenclature: Palaeontology, v. 31, no. 1, p. 223–227.

Bengtson, S., 1976, The structure of some Middle Cambrian conodonts, and the early evolution of conodont structure and function: Lethaia, v. 9, no. 2, p. 185–206.

Bengtson, S., 1983, The early history of the Conodonta: Fossils and strata, no. 15, p. 5–19.

Bensh, F.R., 1962. Pozdnekamennougol'nye i rannepermskie fuzulinidy Severnoi Fergany [Late Carboniferous and early Permian fusulinids of Northem Fergana], *in* Verkhov, V. I., ed., Stratigraphy and paleontology of Uzbekistan and surrounding areas, Tashkent: Academy of Sciences of Uzbekistan, no. 1, p. 186-252. [in Russian]

Berge, J.S., 1960, Stratigraphy of the Ferguson Mountain area, Elko County, Nevada: Brigham Young University Geology Studies, v. 7, no. 5, 63 p.

Bissell, H.J., Permian rocks of parts of Nevada, Utah, and Idaho: GSA Bulletin, v. 73, p. 1083–1110.

Bitter, P.H. von, 1972, Environmental control of conodont distribution in the Shawnee Group (Upper Pennsylvanian) of eastern Kansas: The University of Kansas Paleontological Contributions, art. 59, 105 p.

Bitter, P.H. von, and Merrill, G.K., 1990, Effects of variation on the speciation and phylogeny of *Diplognathodus*: Courier Forschungsinstitut Senckenberg, v. 118, p. 105–129.

Boardman, D.R., and Heckel, P.H., 1989, Glacial-eustatic sea-level curve for early Upper Pennsylvanian sequence in north-central Texas and biostratigraphic correlation with curve for Midcontinent North America: Texas Tech University Studies in Geology, v. 2, pp. 63–73.

Boardman, D.R., Wardlaw, B.R., and Nestell, M.K., 2009, Stratigraphy and conodont biostratigraphy of the uppermost Carboniferous and Lower Permian from the North American Midcontinent: Kansas Geological Society Bulletin, v. 255, 146 p.

Bostwick, D.A., 1955, Stratigraphy of the Wood River Formation, south-central Idaho: Journal of Paleontology, v. 29, no. 6, p. 113–125.

Bostwick, D.A., 1962, Fusulinid stratigraphy of beds near the Gaptank-Wolfcamp boundary, Glass Mountains, Texas: Journal of Paleontology, v. 36, no. 6, p. 1189–1200.

Brady, H.B., *in* Etheridge, R., 1873, Notes on certain genera and species mentioned in the foregoing lists: Scotland Geological Survey Memoir, explanation sheet 23, app. 2, p. 93–107.

Branson, E.B., 1938, Stratigraphy and paleontology of the Lower Mississippian of Missouri: Part 1: University of Missouri Studies, v. 13, no. 3, 208 p.

Burchfiel, B.C., and Davis, G.A., 1972, Structural framework and evolution of the southern part of the Cordilleran orogen, western United States: American Journal of Science, v. 272, p. 97–118.

Burma, B.H., 1942, Missourian *Triticites* of the northern Mid-Continent: Journal of Paleontology, v. 16, no. 6, p. 739–755.

Burrett, C., Udchachon, M., Thassanapak, H., and Chitnarin, A., 2015, Conodonts, radiolarians and ostracodes in the Permian E-Lert Formation, Loei Fold Belt, Indochina Terrane, Thailand: Geological Magazine, v. 152, no. 1, p. 106–142.

Cashman, P.H., Villa, D.E., Taylor, J.W., Davydov, V.I., and Trexler, J.H., 2011, Late Paleozoic contractional and extensional deformation at Edna Mountain, Nevada: GSA Bulletin, v. 123, no. 3–4, p. 651–668.

Cassity, P.E., and Langenheim, R.L., 1966, Pennsylvanian and Permian fusulinids of the Bird Spring Group from Arrow Canyon, Clark County, Nevada: Journal of Paleontology, v. 40, no. 4, p. 931–968.

Cheng-Yuan, W., Ritter, S.M., and Clark, D.L., 1987, The *Sweetognathus* Complex in the Permian of China: Implications for evolution and homeomorphy: Journal of Paleontology, v. 61, no. 5, p. 1047–1057.

Chernykh, V.V., 2005, Zonal methods in biostratigraphy. A zonal scale of the Lower Permian of the Urals by conodonts: Ekaterinburg: Russian Academy of Science, Ural Division, A. N. Zavaritskiy Institute of Geology and Geochemistry, 215 p. [in Russian]

Chernykh, V.V., 2006, Lower Permian conodonts of the Urals: Ekaterinburg: Russian Academy of Sciences, Ural Division, A. N. Zavaritskiy Institute of Geology and Geochemistry, 130 p. [in Russian]

Chernykh, V.V., 2012, Conodont biochronotype of the lower boundary of the Kungurian Stage in the Urals: Ezhegodnik-2011, Institute of Geology and Geochemistry of Urals Branch of Russian Academy Sciences, v. 159, p. 27–32. [in Russian]

Chernykh, V.V., 2015, Usolka section: Upper Carboniferous (Gzhelian) deposits: XVIII International Congress on the Carboniferous and Permian, Guidebook, p. 56–71.

Chernykh, V.V., and Reshetkova, N.P., 1987, Biostratigraphy and conodonts of the Carboniferous-Permian boundary beds from the western slope of the southern and central Urals: Ekaterinburg: Uralian Science Center, Academy of Science, USSR, 50 p. [in Russian]

Chernykh, V.V., and Reshetkova, N.P., 1988, Zonalnoye raschleneniye pogranichnikh otlozheniy karbona i permi zapadnogo sklona srednogo i yuzhnogo Urala po konodontam [Conodont zonal subdivision of the Carboniferous-Permian boundary deposits on the Western slope of mid- and south Urals], *in* Chuvashov, B.I., ed., Biostratigrafiya i litologiya verkhnego paleozoya Urala [Upper Paleozoic biostratigraphy and lithology of the Urals], Collection of Scientific Papers, Sverdlovsk, p. 62–78. [in Russian]

Chernykh, V.V., and Ritter, S.M., 1997, *Streptognathodus* (Conodonta) succession at the proposed Carboniferous-Permian boundary stratotype section, Aidaralash Creek, northern Kazakhstan: Journal of Paleontology, v. 71, no. 3, p. 459–474.

Chernykh, V.V., Ritter, S.M., and Wardlaw, B.R., 1997, *Streptognathodus isolatus* new species (Conodonta): Proposed index for the

Carboniferous-Permian boundary: Journal of Paleontology, v. 71, no. 1, p. 162–164.

Chernykh, V.V., Chuvashov, B.I., and Davydov, V.I., 2006, Paleontological characteristics of Late Pennsylvanian in Usolka section: Geologija, v. 49, p. 205–217.

Chernykh, V.V. Chuvashov, B.I., Shen, S.Z., and Henderson, C.M., 2013, Proposal for the Global Stratotype Section and Point (GSSP) for the base-Sakmarian Stage (Lower Permian): Permophiles, v. 58, p. 16–26.

Chernykh, V.V., Chuvashov, B.I., Shen, S.Z., and Henderson, C.M., 2016, Proposal for the Global Stratotype Section and Point (GSSP) for the base-Sakmarian Stage (Lower Permian): Permophiles, v. 63, p. 4–18.

Choquette, P.W., and James, N.P., 1987, Limestone diagenesis: The deep-burial environment: Geoscience Canada, v. 14, p. 3–35.

Chuvashov, B.I., Leven, E.Y., and Davydov, V.I., 1986, Boundary deposits of Carboniferous and Permian in Urals, Pre-Urals, and middle Tien Shan: Nauka, Moscow, 151 p. [in Russian]

Chuvashov, B.I., and Chernykh, V.V., 1998, Interzonation of Artinskian fusulinids and conodonts (Western Urals, Russia): Permophiles, v. 31, p. 21–25.

Chuvashov, B.I., and Chernykh, V.V., 2011, Mechetlino section (south Urals)-potential stratotype of the lower boundary of the Kungurian Stage: Doklady Rossiiskoii Akademii Nauk, v. 441, no. 5, p. 657–660. [in Russian]

Chuvashov, B.I., Chernykh, V.V., Shen, S.Z., and Henderson, C.M., 2013, Proposal for the Global Stratotype Section and Point (GSSP) for the base-Artinskian Stage (Lower Permian): Permophiles, v. 58, p. 26–34.

Clark, D.L., 1972, Early Permian Crisis and its bearing on Permo-Triassic conodont taxonomy: Geologica et Palaeontologica, v. 1, p. 147–158.

Clark, D.L., 1974, Factors of Early Permian conodont paleoecology in Nevada: Journal of Paleontology, v. 48, no. 4, p. 710–720.

Clark, D.L., 1983, Extinction of conodonts: Journal of Paleontology, v. 57, no. 4, p. 652–661.

Clark, D.L., and Behnken, F.H., 1971, Conodonts and biostratigraphy of the Permian, *in* Sweet, W.C., and Bergstrom, S.M., eds., Symposium on Conodont Biostratigraphy: GSA Memoir 127, p. 415–439.

Clark, D.L., Carr, T.R., Behnken, F.H., Wardlaw, B.R., and Collinson, J.W., 1979, Permian conodont biostratigraphy in the Great Basin, *in*

Sandberg, C.A., and Clark, D.L., eds., Conodont biostratigraphy of the Great Basin and Rocky Mountains, Brigham Young University Geological Studies, v. 26, no. 3, p. 143–147.

Clark, D.L., and Carr, T.R., 1982, Permian *Hindeodus* and *Diplognathodus*: Implications for late Paleozoic conodont multielement taxonomy: Geologica et Palaeontologica, v. 15, p. 125–138.

Cohen, K.M., Harper, D.A.T., Gibbard, P.L., and Fan, J.X., 2013 (updated), The ICS International Chronostratigraphic Chart, Episodes v. 36, 199–204.

Coogan, A.H., 1960, Stratigraphy and paleontology of the Permian Nosoni and Dekkas Formations (Bollibokka Group): University of California Publications in Geological Sciences, v. 36, no. 5, p. 243–316.

Crowell, J.C., 1974, Origin of late Cenozoic basins in southern California, *in* Dickinson, W.R., ed., Tectonics and sedimentation: SEPM Special Publication 22, p. 190–204.

Cushman, J.A., 1921, Foraminifera of the Philippine and adjacent seas: U.S. National Museum Bulletin, v. 100, p. 1–608.

Cushman, J.A., 1933, The foraminifera of the tropical Pacific collections of the "Albatross," 1899-1900: U.S. National Museum Bulletin, v. 161, pt. 2, Lagenidae to Alveolinellidae, p. 1–79.

Davydov, V.I., 1984, On the origin of *Schwagerina*: Paleontological Journal, v. 4, p. 3–16.

Davydov, V.I., 1986, Fusulinids of Carboniferous-Permian boundary beds of Darvaz, *in* Chuvashov, B.I., Leven, E.Y., and Davydov, V.I., eds., Carboniferous-Permian Boundary beds of the Urals, Pre-Urals and Central Asia: Nauka, Moscow, p. 103-125. [In Russian]

Davydov, V.I., 2011, Taxonomy, nomenclature, and evolution of the early schubertellid fusulinids: Acta Palaeontologica Polonica, v. 56, no. 1, p. 181–194.

Davydov, V.I., 2014, Warm water benthic foraminifera document the Pennsylvanian-Permian warming and cooling events – The record from the Western Pangea tropical shelves: Palaeogeography, Palaeoclimatology, Palaeoecology, v. 414, p. 284–295.

Davydov, V.I., Glenister, B.F., Spinosa, C., Ritter, S.M., Chernykh, V.V., Wardlaw, B.R., and Snyder, W.S., 1998, Proposal of Aidaralash as Global Stratotype Section and Point (GSSP) for the base of the Permian System: Episodes, v. 21, p. 11–18.

Davydov, V.I., Bowring, S., Chernykh, V.V., Chuvashov, B.I., Ramezani, J., Schmitz, M.J., Snyder, W.S., and Wardlaw, B.R., 2004, Precise radiometric calibration of the Late Paleozoic time scale – New opportunity in development: Proceedings of the International Geological Congress, Florence, Italy, v. 1, 612 p.

Davydov, V.I.., Schmitz, M.D., Snyder, W.S., and Wardlaw, B.R., 2005, Progress toward development of the Cisuralian (Lower Permian) timescale (biostratigraphy, chronostratigraphy, radiometric calibration): The Nonmarine Permian, New Mexico Museum of Natural History and Science Bulletin, v. 30, p. 48–55.

Davydov, V.I., and Arefifard, S, 2007, Permian fusulinid fauna of Gondwanan affinity from Kalmard Region, east-central Iran and its significance for the tectonics and paleogeography: Paleontologia Electronica, v. 10, no. 2, 40 p.

Davydov, V.I., Korn, D., and Schmitz, M.D., 2012, The Carboniferous Period, *in* Gradstein, F., Ogg, J., Schmitz, M., and Ogg, G., eds., The Geologic Timescale 2012: Elsevier, p. 603–625.

Dehari, E., 2016, Upper Pennsylvanian-Lower Permian carbonate sedimentology and conodont biostratigraphy of the Strathearn and Buckskin Mountain Formations, Carlin Canyon, Nevada [MS Thesis]: University of Calgary, 237 p.

Dickinson, W.R., 1977, Paleozoic plate tectonics and the evolution of the Cordilleran continental margin, *in* Stewart, J.H., Stevens, C.H., and Fritsche, A.E., eds., Paleozoic paleogeography of the western United States: SEPM, Pacific Section, Pacific Coast Paleogeography Symposium 1, p. 137–155.

Dickinson, W.R., 2002, The Basin and Range province as a composite extensional domain: International Geology Review, v. 44, p. 1–38.

Dickinson, W.R., 2006, Geotectonic evolution of the Great Basin: Geosphere, v. 2, no. 7, p. 353–368.

Ding, H., and Wan, S., 1990, The Carboniferous-Permian conodont event-stratigraphy in the south of the North China Platform: Courier Forschungsinstitut Senckenberg, v. 118, p. 131–155.

Dott, R.H., 1955, Pennsylvanian stratigraphy of Elko and northern Diamond Ranges, northeastern Nevada: AAPG Bulletin, v. 39, p. 2211–2305.

Douglass, R.C., 1966, Restudy of *Triticites secalicus* (Say), the type species of *Triticites*: Micropaleontology, v. 12, no. 1, p. 71–78.

Douglass, R.C., 1974, Fusulinids in the Basin and Range province in California, Nevada, and Utah: Journal of Paleontology, v. 48, no. 4, p. 846–853.

Douglass, R.C., 1977, The development of fusulinid biostratigraphy, *in* Kauffman, E.G., and Hazel, J.E., eds., Concepts and Methods of Biostratigraphy: Dowden, Hutchinson, and Ross, Inc., p. 463–481.

Dunbar, C.O., and Condra, G.E., 1927, The Fusulinidae of the Pennsylvanian System in Nebraska: Nebraska Geological Survey Bulletin, v. 2, 135 p.

Dunbar, C.O., and Henbest, L.G., 1930, The fusulinid genera *Fusulina*, *Fusulinella* and *Wedekindella*: American Journal of Science, v. 20, p. 357–364.

Dunbar, C.O., and Skinner, J.W., 1931, New fusulinid genera from the Permian of West Texas: American Journal of Science, v. 22, 252–268.

Dunbar, C.O., and Skinner, J.W., 1936, *Schwagerina* versus *Pseudoschwagerina* and *Paraschwagerina*: Journal of Paleontology, v. 10, no. 8, p. 83–98.

Dunbar, C.O., and Skinner, J.W., 1937, Permian Fusulinidae of Texas, *in* The Geology of Texas: The University of Texas Bulletin, v. 3, no. 3701, p. 517–825.

Dunbar, C.O., and Henbest, L.G., 1942, Pennsylvanian Fusulinidae of Illinois: Illinois State Geological Survey Bulletin, no. 67, 218 p.

Dunham, R.J., 1962, Classification of carbonate rocks according to depositional texture, *in* Ham, W.E., ed., Classification of Carbonate Rocks: AAPG Memoir, v. 1, p. 108–121.

Dutkevich, G.A., 1934, Onekotorykh novykh vidakh fuzulinid iz verkhnego i srednego karbona Verkhne-Chusovskikh Gorodknov na reke Chusovoy (zapadnyi sklon Srednego Urala) [Some new species of Fusulinidae from the Upper and Middle Carboniferous of Verkhne-Chussovskye Gorodki on the Chussovaya River (western slope of the Middle Urals)]: Trudy Neftyanogo Geologo-razvedochnogo Instituta, Seriya A, v. 36, 3–98. [in Russian]

Dvořák, J., 1972, Shallow-water character of nodular limestones and their paleogeographic interpretation: Neues Jahrbuch für Geologie und Paläontologie, Monatshefte, 1972, p. 509–511.

Dzik, J., 1976, Remarks on the evolution of Ordovician conodonts: Acta Palaeontologica Polonica, v. 21, p. 395–455.

Ehrenberg, C.G., 1854, Mikrogeologie: L. Voss, Leipzig, 374 p.

Einsele, G., 2000, Sedimentary Basins: Evolution, Facies, and Sediment Budget, Second Edition: Berlin-Heidelberg, Springer-Verlag, 792 p.

Ellison, S., 1941, Revision of the Pennsylvanian conodonts: Journal of Paleontology, v. 15, no. 2, p. 107–143.

Epshteyn, O.G., Terekhova, T.P., and Solovieva, M.N., 1985, Paleozoi Koryakskogo Nagorya (fauna foraminifer, biostratigrafiya) [Paleozoic of the Koryak Highland (foraminifera fauna, biostratigraphy)]: Voprosy Mikropaleontologii, v. 27, p. 47–77. [in Russian]

Evans, J.G., and Theodore, T.G., 1978, Deformation of the Roberts Mountains allochthon in north-central Nevada: USGS Professional Paper 1060, 38 p.

Fairbridge, R.W., 1957, The dolomite question, *in* Regional aspects of carbonate deposition: SEPM Special Publication 5, p. 125–178.

Fedorowski, J., Bamber, E.W., and Stevens, C.H., 2007, Lower Permian colonial rugose corals, western and northwestern Pangaea: Taxonomy and distribution: NRC Research Press, Ottawa, Canada, 231 p.

Flügel, E., 2010, Microfacies of carbonate Rocks: Analysis, interpretation and application, 2nd edition, Springer-Verlag, Berlin, 1006 p.

Folk, R.L., 1959, Practical petrographic classification of limestones: AAPG Bulletin, v. 43, p. 1–38.

Folk, R.L., 1962, Spectral subdivision of limestone types, *in* Ham, W.E., ed., Classification of Carbonate Rocks: AAPG Memoir, v. 1, p. 62–84.

Forke, H.C., 2002, Biostratigraphic subdivision and correlation of uppermost Carboniferous/Lower Permian sediments in the southern Alps: fusulinoidean and conodont faunas from the Carnic Alps (Austria/Italy), Karavanke Mountains (Slovenia), and southern Urals (Russia): Facies, v. 47, p. 201–275.

Forke, H.C., and Samankassou, E., 2000, Biostratigraphical correlation of late Carboniferous sections in the Carnic Alps (Austria/Italy): Integrated paleontological data, facies, and discussion: Facies, v. 42, p. 177–210.

Fursenko, A.V.,1958, Osnovnye etapy razvitiya faun foraminifer v geologicheskom proshlom [Fundamental stages of the development of foraminiferal faunas in the geological past]: Trudy Instituta Geologicheskikh Nauk, Akademiia Nauk Belorusskoi SSR, Minsk, v. 1, p. 10–29. [in Russian]

Gallagher, S.J., and Somerville, I.D., 2003, Lower Carboniferous (late Visean) platform development and cyclicity in southern Ireland: Foraminiferal

biofacies and lithofacies evidence: Rivista Italiana di Paleontologia e Stratigrafia, v. 109, no. 2, p. 159–171.

Gallegos, D.M., Snyder, W.S., and Spinosa, C., 1991, Tectonic implications of facies patterns, Lower Permian Dry Mountain trough, east-central Nevada, *in* Cooper, J.D., and Stevens, C.H., eds., Paleozoic paleogeography of the western United States, Volume II: SEPM Pacific Section, p. 343–356.

Geslin, J.K., 1998, Distal Ancestral Rocky Mountains tectonism: Evolution of the Pennsylvanian-Permian Oquirrh-Wood River Basin, southern Idaho: GSA Bulletin, v. 110, no. 5, p. 644–663.

Gingras, M.K., Pemberton, S.G., Muelenbachs, K., and Machel, H., 2004, Conceptual models for burrow-related, selective dolomitization with textural and isotopic evidence from the Tyndall Stone, Canada: Geobiology, v. 2, no. 1, p. 21–30.

Girty, G.H., 1904, *Triticites*, a new genus of Carboniferous foraminifera: American Journal of Science, v. 17, p. 234–240.

González, D.C., 2016, Late Pennsylvanian-Early Permian stratigraphy, sedimentology and paleoceanography of the Sverdrup Basin, NW Ellesmere Island, Arctic Canada [MS Thesis]: University of Calgary, 440 p.

Google Earth, 2013, Spruce Mountain, Elko County, Nevada, USA: 40° 31’53.43” N, 114° 50’03.30” W.

Google Earth, 2014, Spruce Mountain, Elko County, Nevada, USA: 40° 31’53.43” N, 114° 50’03.30” W.

Goreva, N.V., and Alekseev, A.S., 2010, Upper Carboniferous conodont zones of Russia and their global correlation: Stratigraphy and Geological Correlation, v. 18, no. 6, p. 593–606.

Groves, J.R., Kulagina, E.I., and Villa, E., 2007, Diachronous appearances of the Pennsylvanian fusulinid *Profusulinella* in Eurasia and North America: Journal of Paleontology, v. 81, no. 2, p. 227–237.

Gullo, M., and Kozur, H.W., 1992, Conodonts from the pelagic deep-water Permian of central Western Sicily (Italy): Neues Jahrbuch für Geologie und Paläontologie. Abhandlungen, v. 184, no. 2, p. 203–234.

Gunnell, F.H., 1931, Conodonts from the Fort Scott Limestone of Missouri: Journal of Paleontology, v. 5, no. 3, p. 244–252.

Gunnell, F.H., 1933, Conodonts and fish remains from the Cherokee, Kansas City, and Wabaunsee Groups of Missouri and Kansas: Journal of Paleontology, v. 7, no. 3, p. 261–297.

Harris, R.W., and Hollingsworth, R.V., 1933, New Pennsylvanian conodonts from Oklahoma: American Journal of Science, series 5, v. 25, p. 193–204.

Heckel, P.H., and Cocke, J.M., 1969, Phylloid algal-mound complexes in outcropping Upper Pennsylvanian rocks of Mid-Continent: AAPG Bulletin, v. 53, p. 1058–1074.

Heckel, P.H., and Weibel, C.P., 1991, Current status of conodont-based biostratigraphic correlation of Upper Pennsylvanian succession between Illinois and Midcontinent, *in* Weibel, C.P., ed., Sequence stratigraphy in mixed clastic-carbonate strata, Upper Pennsylvanian, east-central Illinois: Illinois State Geological Survey, SEPM Great Lakes section, 21st Annual Field Conference, p. 60–69.

Heckel, P.H., Boardman, D.R., and Barrick, J.E., 2002, Desmoinesian-Missourian regional stage boundary reference position for North America, *in* Hills, L.V., Henderson, C.M., and Bamber, E.W., eds., The Carboniferous and Permian of the world: Canadian Society of Petroleum Geologists Memoir, v. 19, p. 710–724.

Heckel, P.H., Alekseev, A.S., Barrick, J.E., Boardman, D.R., Goreva, N.V., Isakova, T.N., Nemyrovska, T.I., Ueno, K., Villa, E., and Work, D.M., 2006, Choice of conodont *Idiognathodus simulator* (*sensu stricto*) as the event marker for the base of the global Gzhelian Stage (Upper Pennsylvanian Series, Carboniferous System): Episodes, v. 31, no. 3, p. 319–325.

Heckel, P.H., Barrick, J.E., and Rosscoe, S.J., 2011, Conodont-based correlation of marine units in lower Conemaugh Group (Late Pennsylvanian) in Northern Appalachian Basin: Stratigraphy, v. 8, no. 4, p. 253–269.

Henderson, C.M., 1989, Conodont paleontology and biostratigraphy of the Upper Carboniferous to Lower Permian Canyon Fiord, Belcher Channel, Nansen, an unnamed, and Van Hauen Formations, Canadian Arctic Archipelago [PhD Dissertation]: University of Calgary, 228 p.

Henderson, C.M., 2014, Response and comments by C.M. Henderson: The GSSP Process and the GSSPs proposed for base-Sakmarian and base-Artinskian stages: Permophiles, v. 59, p. 13–17.

Henderson, C.M., 2016, Permian conodont biostratigraphy, *in* Lucas, S.L., and Shen, S.Z., eds., The Permian Timescale: Geological Society, London, Special Publications, v. 450, p. 119–142.

Henderson, C.M., and McGugan, A., 1986, Permian conodont biostratigraphy of the Ishbel Group, southwestern Alberta and southeastern British Columbia: Contributions to Geology, University of Wyoming, v. 24, p. 219–235.

Henderson, C.M., Schmitz, M., Crowley, J., and Davydov, V.I., 2009, Evolution and geochronology of the *Sweetognathus* lineage from Bolivia and the Urals of Russia; biostratigraphic problems and implications for Global Stratotype Section and Point (GSSP) definition: Permophiles, v. 53, no.1, p. 20–21.

Henderson, C.M., Wardlaw, B.R., Davydov, V.I., Schmitz, M.D., Schiappa, T.A., Tierney, K.E., and Shen, S.Z., 2012, Proposal for base-Kungurian GSSP: Permophiles, v. 56, p. 8–21.

Hoare, R.D., Permian fusulinids from the Sunflower Reservoir area of norther Nevada: Journal of Paleontology, v. 37, no. 6, p. 1143–1149.

Hogancamp, N.J., Barrick, J.E., and Strauss, R.E., 2016, Geometric morphometric analysis and taxonomic revision of the Gzhelian (Late Pennsylvanian) conodont *Idiognathodus simulator* from North America: Acta Palaeontologica Polonica, v. 61, no. 3, p. 477–502.

Hogancamp, N.J., and Barrick, J.E., in press, Morphometric analysis and taxonomic revision of North American species of the *Idiognathodus eudoraensis* Barrick, Heckel, and Boardman, 2008 group (Missourian, Upper Pennsylvanian conodonts): Bulletins of American Paleontology, no. 395–396.

Holterhoff, P.F., Walsh, T.R., and Barrick, J.E., 2013, Artinskian (Early Permian) conodonts from the Elm Creek Limestone, a heterozoan carbonate sequence on the eastern shelf of the Midland Basin, West Texas: New Mexico Museum of Natural History and Science Bulletin, v. 60, p. 109–119.

Hope, R.A., 1972, Geologic map of the Spruce Mountain Quadrangle, Elko County, Nevada: Geologic Quadrangle Maps of the United States, U.S. Geological Survey, to accompany Map GQ-942, 3 p.

Igawa, T.F., 2003, Microbial contribution to deposition of upper Carboniferous and lower Permian seamount-top carbonates, Akiyoshi, Japan: Facies, v. 48, p. 61–78.

Igo, H., 1981, Permian conodont biostratigraphy of Japan: Palaeontological Society of Japan Special Papers, v. 24, p. 1–51.

Irwin, W.P., Wardlaw, B.R., and Kaplan, T.A., 1983, Conodonts of the western Paleozoic and Triassic Belt, Klamath Mountains, California and Oregon: Journal of Paleontology, v. 57, no. 5, p. 1030–1039.

Isakova, T.N., 1989, Konodonty asselskogo i sakmarskogo jarusov Juzhnogo Urala [Conodonts of the Asselian and Sakmarian Stages in the southern Urals]: Voprosy Mikropaleontologii, v. 30, 58–65. [in Russian]

Isakova, T.N., 1998, Review of the conodonts of the Sakmarian stratotype section (south Urals), *in* Szaniawski, H., ed., Proceedings of the Sixth European Conodont Symposium (ECOS IV), Palaeontologia Polonica, v. 58, p. 261–271.

Isbell, J.L., Miller, M.F., Wolfe, K.L., and Lenaker, P.A., 2003, Timing of late Paleozoic glaciation in Gondwana: Was glaciation responsible for the development of northern hemisphere cyclothems?: GSA Special Paper, v. 370, p. 5–24.

James, E., 1832, Winter cantonment near Council Bluff, *in,* James, E., ed., Account of an expedition from Pittsburg to the Rocky Mountains, ch. 8, p. 146–166.

James, N.P., and Jones, B., 2016, Origin of carbonate sedimentary rocks: American Geophysical Union, Wiley Publishing, West Sussex, UK, 446 p.

Jansma, P.E., and Speed, R.C., 1995, Kinematics of underthrusting in the Paleozoic Antler foreland basin: The Journal of Geology, v. 103, no. 5, p. 559–575.

Johnson, R.A., and Loy, K.L., 1992, Seismic reflection evidence for seismogenic low-angle faulting in southwestern Arizona: Geology, v. 20, p. 597–600.

Jordan, C.F., 1971, Lower Permian stratigraphy of southern New Mexico and West Texas [PhD Dissertation]: Rice University, 140 p.

Kasatkina, A.P., and Buryi, G.I., 1996a, On the relation of chaetognaths and conodonts: Albertiana, v. 18, p. 21–23.

Kasatkina, A.P., and Buryi, G.I., 1996b, About the relationship of the Chaetognatha with conodonts, *in* Dzik, J., ed., Sixth European Conodont Symposium (ECOS XI): Abstracts with Programs, p. 27.

Kasatkina, A.P., and Buryi, G.I., 1997, Chaetodonta, a new animal superphylum and its position in animal systematics: Doklady Biological Sciences, v. 356, p. 503–505.

Kasatkina, A.P., and Buryi, G.I., 1999, The position of the phyla Chaetognatha and Euconodontophylea in the classification of Metazoa: Zoosystematica Rossica, v. 8, no. 1, p. 21–26.

Katvala, E.C., and Henderson, C.M., Conodont sequence biostratigraphy and paleogeography of the Pennsylvanian-Permian Mount Mark and Fourth Lake Formations, southern Vancouver Island: Canadian Society of Petroleum Geologists Memoir, v. 19, p. 461–478.

Kauffman, A.E., and Roth, R.I., 1966, Upper Pennsylvanian and Lower Permian fusulinids from North-Central Texas: Cushman Foundation for Foraminiferal Research Special Publication, no. 8, 49 p.

Ketner, K.B., 2012, An alternative hypothesis for the mid-Paleozoic Antler orogeny in Nevada: USGS Professional Paper 1790, 11 p.

Ketner, K.B., 2013, Stratigraphy of lower to middle Paleozoic rocks of northern Nevada and the Antler orogeny: USGS Professional Paper 1799, 23 p.

Klasen, R.L., 2007, Sequence stratigraphic analysis of the lower and upper Brush Creek interval (Late Pennsylvanian), southeastern Ohio [MS Thesis]: Ohio University, 89 p.

Knight, R.L., 1956, Permian fusulines from Nevada: Journal of Paleontology, v. 30, p. 773–792.

Kobayashi, F., 1993, Fusulinaceans contained in pebbles of the intraformational conglomerate of the Kanyo Formation, north of Itsukaichi, southern Kwanto Mountains, Japan: Humans and Nature, v. 2, p. 125–137.

Kobayashi, F., 2005, Early Permian fusulinaceans in the Hangiri-Shimokuzu area, eastern part of the Kanto Mountains, Japan: Nature and Human Activities, v. 9, p. 11–31.

Kobayashi, F. and Altiner, D., 2008, Fusulinoidean faunas from the Upper Carboniferous and Lower Permian Platform Limestone in the Hadim area, central Taurides, Turkey, Rivista Italiana di Paleontologia e Stratigrafia, v. 114, no. 2, p. 191–232.

Kochansky-Devidé, V., 1959, Karbonske i Permske fuzulinidne foraminifere Velebita i Like: Palaeontologia Jugoslavica, v. 3, 60 p.

Kochansky-Devidé, V., 1962, Milanović M. Donjopermske fuzulinide i vapnenačke alge područja Tare u Crnoj Gori: Geološki Vjesnik, v. 15, no. 1, p. 195–227.

Kochansky-Devidé, V., 1970, Permski mikrofosili zahodnih Karavank: Geologija-Razprave in Porčila, v. 13, p. 175–256.

Kossovaya, O., Vachard, D., and Izart, A., 2013, Climatic impact on the reef biota in the Cisuralian and Guadalupian (Permian), East European Platform, *in* Gąsiewicz, A., and Słowakiewicz, M., eds., Paleozoic Climate Cycles: Their Evolutionary and Sedimentological Impact: Geological Society, London, Special Publication 376, p. 343–366.

Kozitskaya, R.I., Kossenko, Z.A., Lipnyagov, O.M., and Nemyrovskaya, T.I., 1978, Konodonty karbona Donetskogo bassejna [Carboniferous conodonts of the Donets Basin]: Naukova Dumka, Akademiâ Nauk Ukrainskoj SSR, Kiev, 136 p. [in Russian]

Kozur, H., 1975, Beiträge zur conodontenfauna des Perm: Geologisch-palaontologische Mitteilungen Innsbruck, v. 5, no. 4, 41 p. [in German]

Kozur, H., 1989, The taxonomy of the gondolellid conodonts in the Permian and Triassic: Courier Forschungsinstitut Senckenberg, v. 117, p. 409–469.

Kozur, H., 1995, Permian conodont zonation and its importance for the Permian stratigraphic standard scale: Geologische-Paläontologische Mitteilungen Innsbruck, v. 20, p. 165–205.

Kozur, H., and Mostler, H., 1976, Neue conodonten aus dem Jungpalaozoikum und der Trias: Geologisch-palaontologische Mitteilungen Innsbruck, v. 6, no. 2, p. 1–40. [in German]

Lambert, L.L., Heckel, P.H., and Barrick, J.E., 2003, *Swadelina* new genus (Pennsylvanian Conodonta), a taxon with potential chronostratigraphic significance: Micropaleontology, v. 49, no. 2, p. 151–158.

Lane, H.R., 1967, Uppermost Mississippian and Lower Pennsylvanian conodonts from the type Morrowan region, Arkansas: Journal of Paleontology, v. 41, no. 4, p. 920–942.

Lane, H.R., 1968, Symmetry in conodont element-pars: Journal of Paleontology, v. 42, no. 5, p. 1258–1263.

Lane, H.R., Merrill, G.K., Straka, J.J., and Webster, G.D., 1971, North American Pennsylvanian conodont biostratigraphy, *in* Sweet, W.C., and Bergstrom, S.M., eds., Symposium on conodont biostratigraphy: GSA Memoir 127, p. 395–414.

Lane, H.R., and Straka, J.J., 1974, Late Mississippian and Early Pennsylvanian conodonts Arkansas and Oklahoma: GSA Special Paper 152, 143 p.

Langenheim, R.L., Nelson, W.J., Grove, K.A., and McGovney, J.E., 1977, Fusulinids in carbonate microfacies of Bird Spring Group, Arrow

Canyon Quadrangle, Clark County, Nevada: Journal of Paleontology, v. 51, no. 5, p. 1016–1022.

Larson, E.R., and Langenheim, R.L., Jr., 1979, The Mississippian and Pennsylvanian (Carboniferous) systems in the United States – Nevada: United States Geological Survey Professional Paper, v. 1110-BB, BB1-BB19.

Lawson, A.C., 1906, The copper deposits of the Robinson Mining District, Nevada: University of California Publications, Bulletin of the Department of Geology, v. 4, no. 14, p. 287–357.

Leven, E.Y., 1997, Permian stratigraphy and Fusulinida of Afghanistan with their paleogeographic and paleotectonic implications: GSA Special Paper, v. 316, 134 p.

Leven, E.Y., and Davydov, V.I., 2001, Stratigraphy and fusulinids of the Kasimovian and lower Gzhelian (Upper Carboniferous) in the southwestern Darvaz (Pamir): Rivista Italiana di Paleontologia e Stratigrafia, v. 107, no. 1, p. 3–46.

Levy, M., and Christie-Blick, N., 1989, Pre-Mesozoic Palinspastic reconstruction of the eastern Great Basin (western United States): Science, v. 245, p. 1454–1462.

Lucas, S.G., Wilde, G.L., Robbins, S., and Estep, J.W., 2000, Lithostratigraphy and fusulinaceans of the type section of the Bursum Formation, Upper Carboniferous of south-central New Mexico: New Mexico Museum of Natural History and Science Bulletin, v. 16, p. 1–13.

Lucas, S.G., Krainer, K., Barrick, J.E., and Vachard, D., 2016, The Pennsylvanian System of the Mud Springs Mountains, Sierra County, New Mexico, USA: New Mexico Museum of Natural History and Science Bulletin, v. 69, 58 p.

Lucas, S.G., Krainer, K., and Vachard, D., 2017a, The Newwellian Substage of the Wolfcampian Stage in the southwestern United States: Permophiles, v. 64, p. 13–19.

Lucas, S.G., Krainer, K., Barrick, J.E., Vachard, D., and Ritter, S.M., 2017b, Lithostratigraphy and microfossil biostratigraphy of the Pennsylvanian-lower Permian Horquilla Formation at New Well Peak, Big Hatchet Mountains, New Mexico, USA: Stratigraphy, v. 14, nos. 1–4, p. 223–246.

Mack, G.H., Giles, K.A., and Durr, C.W., 2013, Sequence Stratigraphy of the lower-middle Hueco transition interval (lower Permian, Wolfcampian),

Robledo Mountains, New Mexico: New Mexico Geology, v. 35, no. 2, p. 27–37.

Magaritz, M., and Peryt, T.M., 1994, Mixed evaporative and meteoric water dolomitization: isotope study of the Zechstein Limestone (upper Permian), southwestern Poland: Sedimentary Geology, v. 92, p. 257–272.

Magginetti, R.T., Stevens, C.H., and Stone, P., 1988, Early Permian fusulinids from the Owens Valley Group, east-central California: GSA Special Paper 217, 61 p.

Mahoney, J.B., Link, P.K., Burton, B.R., Geslin, J.K., and O'Brien, J.P., 1991, Pennsylvanian and Permian Sun Valley Group, Wood River Basin, south-central Idaho, *in* Cooper, J.D., and Stevens, C.H., eds., Paleozoic paleogeography of the western United States, Volume II: SEPM Pacific Section, p. 551–579.

Mamet, B., and Pinard, S., 1992, Note sur la taxonomie des petits foraminifères du Paléozoïque supérieur [A taxonomic note on upper Paleozoic smaller foraminifera]: Bulletin de la Société belge de Géologie, v. 99, p. 373–398. [in French]

Marcantel, J.B., 1973, Upper Pennsylvanian and lower Permian sedimentation in northeast Nevada [PhD Dissertation]: Ohio State University, 112 p.

Marcantel, J.B., 1975, Late Pennsylvanian and Early Permian sedimentation in northeast Nevada: AAPG Bulletin, v. 59, no. 11, p. 2079–2098.

Marshall, F.C., 1969, Lower and Middle Pennsylvanian fusulinids from the Bird Spring Formation near Mountain Springs Pass, Clark County, Nevada: Brigham Young University Geology Studies, v. 16, p. 97–154.

Maslov, V.P., 1956, Fossil calcareous algae of the USSR: Trudy Instituta Geologičeskih Nauk, Geologičeskaâ Seriâ, v. 160, 301 p. [in Russian]

McCutcheon, V.A., and Wilson, E.C., 1963, *Kleopatrina*, new name for *Ptolemaia*, McCutcheon and Wilson: Journal of Paleontology, v. 37, no. 1, p. 299.

McLaughlin, K.P., 1952, Microfauna of the Pennsylvanian Glen Eyrie Formation, Colorado: Journal of Paleontology, v. 26, no. 4, p. 613–621.

Meek, F.B., 1864, Description of the Carboniferous fossils: California Geological Survey, Paleontology of California, v. 1, p. 1–16.

Meek, F.B., and Hayden, F.V., 1858, Descriptions of new organic remains collected in Nebraska Territory in the year 1857, by. F.V. Hayden, Geologist to the Exploring Expedition under the command of Lieut.

G.K. Warren, Top. Engr. U.S. Army, together with some remarks on the geology of the Black Hills and portions of the surrounding country: Proceedings of the Academy of Natural Sciences of Philadelphia, p. 41–59.

Meek, F.B., and Hayden, F.V., 1858, Remarks on the Lower Cretaceous beds of Kansas and Nebraska, together with descriptions of some new species of Carboniferous fossils from the valley of Kansas River: Proceedings of the Academy of Natural Sciences of Philadelphia, vol. 10, p. 256–264.

Meek, F.B., and Hayden, F.V., 1865, Paleontology of the Upper Missouri: Smithsonian Contributions to Knowledge, v. 14, p. 1–136.

Mei, S., and Henderson, C.M., 2001, Evolution of Permian conodont provincialism and its significance in global correlation and paleoclimate implication: Palaeogeography, Palaeoclimatology, Palaeoecology, v. 170, p. 237–260.

Mei, S., Henderson, C.M., and Wardlaw, B.R., 2002, Evolution and distribution of the conodonts *Sweetognathus* and *Iranognathus* and related genera during the Permian, and their implications for climate change: Palaeogeography, Palaeoclimatology, Palaeoecology, v. 180, p. 57–91.

Merchant, F.E., and Keroher, R.P., 1939, Some fusulinids from the Missouri Series of Kansas: Journal of Paleontology, v. 13, no. 6, p. 594–614.

Merriam, C.W., and Anderson, C.A., 1942, Reconnaissance survey of the Roberts Mountains, Nevada: GSA Bulletin, v. 53, p. 1675–1728.

Merrill, G.K., 1973, Pennsylvanian nonplatform conodont genera I: *Spathognathodus*: Journal of Paleontology, v. 47, no. 2, p. 289–314.

Merrill, G.K., and Powell, R.J., 1980, Paleobiology of juvenile (nepionic?) conodonts from the Drum Limestone (Pennsylvanian, Missourian-Kansas City area) and its bearing on apparatus ontogeny: Journal of Paleontology, v. 54, no. 5, p. 1058–1074.

Miklukho-Maclay, A.D., Rauser-Chernousova, D.M., and Rosovskaya, S.E., 1959, Fusulinida order, *in* Rauser-Chernousova, D.M., and Fursenko, A.V., eds., Osnovy Paleontologii, Prosteishie 1, p. 201–215. [in Russian]

Miller, E.L., Miller, M.M., Stevens, C.H, Wright, J.E., and Madrid, R., 1992, Late Paleozoic paleogeographic and tectonic evolution of the western U.S. Cordillera, *in* Burchfiel, B.C., Lipman, P.W., and Zoback, M.L., eds., The Cordilleran Orogen: Conterminous U.S.: Geological Society of America, Boulder, CO, p. 57-106.

Möller, V. von, 1878, Die spiral-gewunden Foraminiferen des russischen Kohlenkalkes [The coiled foraminifera of Russian coal lime]: Mémoires de l'Académie Impériale des Sciences de St.-Pétersbourg, v. 7, no. 25, 147 p.

Möller, V. von, 1879, Die foraminiferan des russischen Kohlenkalkes [The foraminifera of Russian coal lime]: Mémoires de l'Académie Impériale des Sciences de St. Pétersbourg, v. 27, no. 5, 131 p.

Montañez, I.P., and Poulsen, C.J., 2013, The late Paleozoic ice age: An evolving paradigm: Annual Review of Earth and Planetary Sciences, v. 41, p. 629–656.

Morikawa, R., and Isomi, H., 1960, A new genus, *Biwaella*, *Schwagerina*-like *Schubertella*: Science Reports of the Saitama University, Series B: Biology and Earth Sciences, v. 3, 301–305.

Movshovitsch, E.V., Kozur, H., Pavlov, A.M., Pnev, V.P., Polozova, A.N., Chuvashov, B.I., and Bogoslovskaya, M.F., 1979, Conodont complexes of the Lower Permian of the Pre-Urals region and problems of correlations of Lower Permian deposits, *in* Papulov, G.N., and Puchkov, V.N., eds., Conodonts of the Urals and their Stratigraphic Significance: Academy of Science, Urals Science Center, Sverdlovsk, USSR, p. 94–131.

Müller, K.J., and Nogami, Y., 1971, Über die feinbau der conodonten [About the construction of conodonts]: Memoirs of the faculty of science, Kyoto University, Series of Geology and Mineralogy, v. 38, p. 1–87.

Müller, K.J., and Nogami, Y., 1972, Growth and function of conodonts, *in* Proceedings of the 24th International Geological Congress, Montreal, p. 20–27.

Murdock, D.J.E., Dong, X., Repetski, J.E., Marone, F., Stampanoni, M., and Donoghue, P.C.J., 2013, The origin of conodonts and of vertebrate mineralized skeletons: Nature, v. 502, p. 546–553.

Murphy, M.A., Power, J.D., and Johnson, J.G., 1984, Evidence for Late Devonian movement within the Roberts Mountains allochthon, Roberts Mountains, Nevada: Geology, v. 12, p. 20–23.

Myers, D.A., 1988, Stratigraphic distribution of fusulinid foraminifera from the Manzano Mountains, New Mexico: U.S. Geological Survey Professional Paper, no. 1446-A, B, 65 p.

Nail, R.S., 1991, Fusulinacean biostratigraphy across the Missourian-Virgilian (Upper Pennsylvanian) boundary in the Brazos River Valley, north-central Texas [MS Thesis]: University of Texas at Arlington, 287 p.

Nail, R.S., 1996, Middle-Late Pennsylvanian fusulinid faunas from Midcontinent North America and the Paradox Basin, Utah and Colorado [PhD Dissertation]: Texas Tech University, 354 p.

Nance, R.D., Gutiérrez-Alonso, G., Keppie, J.D., Linnemann, U., Murphy, J.B., Quesada, C., Strachan, R.A., and Woodcock, N.H., 2010, Evolution of the Rheic Ocean: Gondwana Research, v. 17, p. 194–222.

Needham, C.E., 1937, Some New Mexico Fusulinidae: New Mexico School of Mines Bulletin, v. 14, 88 p.

Nestell, M.K., 1989, The Desmoinesian-early Missourian fusulinacean succession in the Brazos River Valley, north-central Texas: Texas Tech University Studies in Geology, v. 2, p. 95–112.

Nestell, M.K., and Blome, C.D., 2015, Some contrasting biostratigraphic links between the Baker and Olds Ferry Terranes, eastern Oregon: Micropaleontology, v. 61, no. 4–5, p. 389–417.

Orchard, M.J., 1984, Early Permian conodonts from the Harper Ranch beds, Kamloops area, southern British Columbia: Geological Survey of Canada, Current Research, Part B, 84-1B, p. 207–215.

Orchard, M.J., Cordey, F., Rui, L., Bamber, E.W., Mamet, B., Struik, L.C., Sano, H., and Taylor, H.J., 2001, Biostratigraphic and biogeographic constraints on the Carboniferous to Jurassic Cache Creek Terrane in central British Columbia: Canadian Journal of Earth Sciences, v. 38, p. 551–578.

Pander, C.H., 1856, Monographie der fossilen Fische des silurischen Systems der russisch-baltischen Gouvernements: Königlich Akademie der Wissenschaften, St. Petersburg, 91 p. [in German]

Parsons, T., 1995, Chapter 7: The Basin and Range province, *in* Olsen, K.H., ed., Continental Rifts: Evolution, structure, tectonics, vol. 25: Elsevier Science, Amsterdam, Netherlands, p. 277–326.

Pennebaker, E.N., 1932, Geology of the Robinson (Ely) mining district in Nevada: Mining and Metallurgy, v. 13, p. 163–168.

Perez Ramos, O., 1992, Permian biostratigraphy and correlation between southeast Arizona and Sonora: Boletín de Departamento de Geología, Universidad de Sonora, v. 9, no. 2, p. 1–74.

Perlmutter, B., 1975, Conodonts from the uppermost Wabaunsee Group (Pennsylvanian) and the Admire and Council Grove Groups (Permian) in Kansas: Geologica et Palaeontologica, v. 9, p. 95–115.

Petocz, R.G., 1970, Biostratigraphy and lower Permian Fusulinidae of the Upper Delta River area, east-central Alaska Range: GSA Special Paper, no. 130, 94 p.

Purnell, M.A., and Donoghue, P.C.J., 1998, Skeletal architecture, homologies and taphonomy of ozarkodinid conodonts: Paleontology, v. 41, no. 1, p. 57–102.

Purnell, M.A., Donoghue, P.C.J., and Aldridge, R.J., 2000, Orientation and anatomical notation in conodonts: Journal of Paleontology, v. 74, no. 1, p. 113–122.

Purser, B.H., Tucker, M.E., and Zenger, D.H., 1994, Problems, progress and future research concerning dolomites and dolomitization, *in* Purser, B.H., Tucker, M.E., and Zenger, D.H., eds., Dolomites: A Volume in Honour of Dolomieu: Special Publication of the International Association of Sedimentologists, no. 21, Oxford, UK, Blackwell, 451 p.

Putrya, F.S., 1948, *Protriticites*, a new fusulinid genus: Trudy Lvovskovo Geologischeskovo Obshchestva pri Gosudarstvenem Universitete Ivana Franko Paleontologicheskaya Seria 9, v. 1, p. 89–96.

Ramezani, J., and Bowring, S.A., 2017, Advances in numerical calibration of the Permian timescale based on radioisotopic geochronology, *in* Lucas, S.G., and Shen, S.Z., eds., The Permian Timescale: Geological Society, London, v. 450, p. 51–60.

Rauser-Chernousova, D.M., Bensh, F.S., Vdovenko, M.V., Gibshman, N.B., Leven, E.Y., Lipina, O.A., Reitlinger, E.A., Solov'eva, M.N., and Chediya, I.O., 1996, Guidebook on the systematics of Paleozoic foraminifers: Nauka, Moscow, 207 p. [in Russian]

Read, M.T., and Nestell, M.K., 2017a, Sakmarian (Early Permian) sulcus-bearing sweetognathid conodonts from Nevada: Early experimentation and novel carinal configurations: Geological Society of America, Abstracts with Programs, 49, no. 46-3.

Read, M.T., and Nestell, M.K., 2017b, Biostratigraphy of the Pennsylvanian-Permian boundary interval of the Riepe Spring Limestone, North Spruce Mountain Ridge, Nevada: Further evidence for Late Paleozoic glacio-eustatic fluctuations: SEPM, North American Micropaleontology Section, Geologic Problem Solving with Microfossils IV, Abstracts with Programs, p. 159–160.

Read, M.T., and Nestell, M.K., 2018, *Douglassites*, a new genus of schubertellid fusulinid from the Virgilian (Upper Pennsylvanian) of Elko County, Nevada, U.S.A.: Micropaleontology, v. 64, no. 4, p. 317–327.

Read, M.T., and Nestell, M.K., in press, Global distribution of the fusulinacean genus *Biwaella*: Paleontological Journal, v. 53, no. 8.

Read, M.T., and Nestell, M.K., in press, Cisuralian (Early Permian) sweetognathid conodonts from the upper part of the Riepe Spring Limestone, North Spruce Mountain Ridge, Elko County, Nevada: Bulletins of American Paleontology, no. 395-396, p. 89–113.

Reshetkova, N.P., and Chernykh, V.V., 1986, New conodonts from Asselian deposits on the west slope of the Urals: Paleontological Journal, v. 4, 99–104.

Rhodes, F.H.T., 1952, A classification of Pennsylvanian conodont assemblages: Journal of Paleontology, v. 26, no. 6, p. 886–901.

Rhodes, F.H.T., 1963, Conodonts from the topmost Tensleep Sandstone of the eastern Big Horn Mountains, Wyoming: Journal of Paleontology, v. 37, no. 2, p. 401–408.

Rhodes, F.H.T., Austin R.L., and Druce, E.C., 1969, British Avonian (Carboniferous) conodont faunas, and their value in local and intercontinental correlation: Bulletin of the British Museum of Natural History, supp. 5, 316 p.

Rich, M., 1961, Stratigraphic section and fusulinids of the Bird Spring Formation near Lee Canyon, Clark County, Nevada: Journal of Paleontology, v. 35, no. 6, p. 1159–1180.

Riding, R., and Guo, L., 1992, Affinity of *Tubiphytes*: Paleontology, v. 35, no. 1, p. 37–49.

Riglos Suárez, M., Hünicken, M.A., and Merino, D., 1987, Conodont biostratigraphy of the Upper Carboniferous-Lower Permian rocks of Bolivia, *in* Austin, R.L., ed., Conodonts: investigative techniques and applications: British Micropalaeontological Society, Ellis Horwood Publishers, London, p. 317–325.

Ritter, S.M., 1986, Taxonomic revision and phylogeny of post-Early Permian crisis *bisselli-whitei* Zone conodonts with comments on late Paleozoic diversity: Geologica et Palaeontologica, v. 20, p. 139–165.

Ritter, S.M., 1987, Biofacies-based refinement of Early Permian conodont biostratigraphy, in central and western USA: Conodont Investigation Techniques and Applications, p. 382–403.

Ritter, S.M., 1994, New species and subspecies of *Streptognathodus* (Conodonta) from the Virgilian (Late Carboniferous) of Kansas: Journal of Paleontology, v. 68, no. 4, p. 870–878.

Ritter, S.M., 1995, Upper Missourian-lower Wolfcampian (upper Kasimovian-lower Asselian) conodont biostratigraphy of the Midcontinent, U.S.A.: Journal of Paleontology, v. 69, no. 6, p. 1139–1154.

Ritter, S.M., Barrick, J.E., and Skinner, M.R., 2002, Conodont sequence biostratigraphy of the Hermosa Group (Pennsylvanian) at Honaker Trail, Paradox Basin, Utah: Journal of Paleontology, v. 76, no. 3, p. 495–517.

Ritter, S.M., and Robinson, T.S., 2009, Sequence stratigraphy and biostratigraphy of Carboniferous-Permian boundary strata in western Utah, *in* Geology and Geological Resources and Issues of Western Utah: UGA Publication 38, p. 27–42.

Roberts, T.G., 1949, Part III: Fusulinidae, *in* Newell, N.D., Chronic, J., and Roberts, T.G., eds., Upper Paleozoic of Peru: Columbia University Science Bureau, New York, NY, p. 174–241.

Roberts, R.J., Hotz, P.E., Gilluly, J., and Ferguson, H.G., 1958, Paleozoic rocks in north-central Nevada: AAPG Bulletin, v. 42, no. 12, p. 2813–2857.

Robinson, G.B., 1961, Stratigraphy and Leonardian fusulinid paleontology in central Pequop Mountains, Elko County, Nevada: Brigham Young University Geology Studies, v. 8, p. 93–146.

Ross, C.A., 1959, The Wolfcamp Series (Permian) and new species of fusulinids, Glass Mountains, Texas: Journal of the Washington Academy of Sciences, v. 49, p. 299–316.

Ross, C.A., 1962, Fusulinids from the Leonard Formation (Permian), western Glass Mountains, Texas: Contributions from the Cushman Foundation for Foraminiferal Research, v. 13, no. 1, p. 1–21.

Ross, C.A., 1963, Standard Wolfcampian Series (Permian), Glass Mountains, Texas: GSA Memoir, v. 88, 205 p.

Ross, C.A., 1965, Late Pennsylvanian Fusulinidae from the Gaptank Formation, West Texas: Journal of Paleontology, v. 39, no. 6, p. 1151–1176.

Ross, C.A., 1967, *Eoparafusulina* from the Neal Ranch Formation (Lower Permian), West Texas: Journal of Paleontology, v. 41, no. 4, p. 943–946.

Ross, C.A., 1969, Middle and Upper Pennsylvanian fusulinaceans, Gila Mountains, Arizona: Journal of Paleontology, v. 43, no. 6, p. 1405–1422.

Ross, C.A., and Tyrrell, W.W., 1965, Pennsylvanian and Permian fusulinids from the Whetstone Mountains, southeast Arizona: Journal of Paleontology, v. 39, no. 4, p. 615–635.

Ross, C.A., and Ross, J.R.P, 1987a, Late Paleozoic sea levels and depositional sequences, *in* Ross, C.A., and Haman, D., eds., Timing and depositional history of eustatic sequences: Constraints on seismic stratigraphy: Cushman Foundation for Foraminiferal Research Special Publication 24, p. 137–149.

Ross, C.A., and Ross, J.R.P, 1987b, Biostratigraphic zonation of Late Paleozoic depositional sequences, *in* Ross, C.A., and Haman, D., eds., Timing and depositional history of eustatic sequences: Constraints on seismic stratigraphy: Cushman Foundation for Foraminiferal Research Special Publication 24, p. 151–168.

Ross, C.A., and Ross, J.R.P., 1994, The need for a Bursumian Stage, uppermost Carboniferous, North America: Permophiles, v. 24, p. 3–6.

Ross, C.A., and Ross, J.R.P., 2003, Sequence evolution and sequence extinction: Fusulinid biostratigraphy and species-level recognition of depositional sequences, Lower Permian, Glass Mountains, West Texas, U.S.A.: Micropaleontologic Proxies for Sea-level Change and Stratigraphic Discontinuities, SEPM Special Publication no. 75, p. 317–359.

Ross, C.A., and Ross, J.R.P., 2009, Paleontology, a tool to resolve late Paleozoic structural and depositional histories: Geologic Problem Solving with Microfossils: A Volume in Honor of Garry D. Jones, SEPM Special Publication no. 93, p. 95–109.

Rosscoe, S.J., and Barrick, J.E., 2009, Revision of *Idiognathodus* species from the Desmoinesian-Missourian (~Moscovian-Kasimovian) boundary interval in the Midcontinent Basin, North America: Palaeontographica Americana, v. 62, p. 115–147.

Rosscoe, S.J., and Barrick, J.E., 2013, North American species of the conodont genus *Idiognathodus* from the Moscovian-Kasimovian boundary composite sequence and correlation of the Moscovian-Kasimovian Stage boundary: New Mexico Museum of Natural History and Science Bulletin, v. 60, p. 354–371.

Rui, L., and Nassichuk, W.W., 1994, Fusulinaceans at the Middle/Upper Pennsylvanian (Desmoinesian/Missourian) boundary in the Canadian Arctic Archipelago: Pangea: Global environments and resources, Canadian Society of Petroleum Geologists Memoir 17, p. 907–926.

Rygel, M.C., Fielding, C.R., Frank, T.D., and Birgenheier, L.P., 2008, The magnitude of late Paleozoic glacioeustatic fluctuations: A synthesis, Journal of Sedimentary Research, v. 78, p. 500–511.

Sabins, F.F., and Ross, C.A., 1963, Late Pennsylvanian-Early Permian fusulinids from southeast Arizona: Journal of Paleontology, v. 37, no. 2, p. 323–365.

Sabolev, N.N., and Nakrem, H.A., 1996, Middle Carboniferous-Lower Permian conodonts of Novaya Zemlya: Norsk Polarinstitutt Skrifter, no. 199, 128 p.

Sanderson, G.A., Verville, G.J., Groves, J.R., and Wahlman, G.P., 2001, Fusulinacean biostratigraphy of the Virgilian Stage (Upper Pennsylvanian) in Kansas: Journal of Paleontology, v. 75, no. 4, p. 883–887.

Say, T., 1823, *in* James, E., Account of an expedition from Pittsburgh to the Rocky Mountains: Philadelphia, PA, Carey and Lea, v. 1, p. 146–152.

Schellwien, E., 1908, Monographie der fusulinen, Teil 1, Die fusulinen des Russisch-Arctischen Meeresgebietes [Monograph of the fusulinids, Part 1, The fusulinids of the Russian-Arctic marine area]: Palaontographica, v. 55, p. 145–194. [in German]

Schiappa, T.A., Snyder, W.S., and Trexler, J.H., Jr., 1999, Tectonic signatures within the Pennsylvanian-Early Permian Tippipah Limestone, Nevada Test Site: Geological Society of America, Abstracts with Programs, 31, A-54.

Scotese, C.R., 2014, Atlas of Permo-Carboniferous paleogeographic maps (Mollweide Projection), Maps 53-64, 4, The late Paleozoic, PALEOMAP Atlas for ArcGIS, PALEOMAP Project, Evanston, IL.

Seilacher, A., 1982, Distinctive features of sandy tempestites, *in* Einsele G., and Seilacher, A., eds., Cyclic and Event Stratification: Berlin-Heidelberg, Springer-Verlag, p. 333-349.

Shchegolev, A.K., and Kozitskaya, R.I., 1984, Paleontological substantiation of the Upper Carboniferous preliminary scale for Europe and Central Asia, *in* Menner, V.V., and Grigorjeva, A.D., eds., Verkhnii karbon SSSR. Mezhvedomstvennyi stratigraficheskii komitet SSSR, Trudy, T. 13 [Upper Carboniferous of the USSR. Interdepartmental Stratigraphic Committee of the USSR, Proceedings, vol. 13]: Moscow, Nauka, p. 107–113. [in Russian]

Silberling, N.J., and Roberts, R.J., 1962, Pre-Tertiary stratigraphy and structure of northwestern Nevada: GSA Special Paper 72, 58 p.

Skinner, J.W., 1931, Primitive fusulinids of the Mid-Continent Region: Journal of Paleontology, v. 5, no. 3, p. 253–259.

Skinner, J.W., and Wilde, G.L., 1965a, Lower Permian (Wolfcampian) fusulinids from the Big Hatchet Mountains, southwestern New Mexico: Contributions from the Cushman Foundation for Foraminiferal Research, v. 16, no. 3, p. 95–104.

Skinner, J.W., and Wilde, G.L., 1965b, Permian biostratigraphy and fusulinid faunas of the Shasta Lake area, northern California: The University of Kansas Paleontological Contributions, Protozoa, art. 6, 98 p.

Skinner, J.W., and Wilde, G.L., 1966, Permian fusulinids from Pacific Northwest and Alaska, pt. 8: *Alaskanella*, new Permian fusulinid genus: The University of Kansas Paleontological Contributions, paper 4, p. 55–58.

Skinner, J.W., and Wilde, G.L., 1967, *Eowaeringella*, a new generic designation for fusulinids of the group of *Wedekindellina ultimata*: Journal of Paleontology, v. 41, no. 4, p. 1004–1005.

Slade, M.L., 1961, Pennsylvanian and Permian fusulinids of the Ferguson Mountain area Elko County, Nevada: Brigham Young University Geology Studies, v. 8, p. 55–94.

Snyder, W.S., Spinosa, C., and Gallegos, D.M., 1991, Pennsylvanian-Permian tectonism on the western U.S. continental margin, *in* Raines, G.L., Lisle, R.E., Schafer, R.W., and Wilkinson, W.H., eds., Geology and Ore Deposits of the Great Basin: Geological Society of Nevada, Reno, NV, p. 5–20.

Speed, R.C., and Sleep, N.H., 1982, Antler orogeny and foreland basin: A model: GSA Bulletin, v. 93, p. 815–828.

Spencer, A.C., 1917, Geology and ore deposits of Ely, Nevada: United States Geological Survey Professional Paper 96, 189 p.

Staff, H.V., 1912, Monographie der Fusulinen, Teil III, Die Fusulinen (Schellwienien) Nordamerikas [Monograph of the fusulinids, Part 3, The fusulinids of North America]: Palaeontographica, v. 59, p. 157–192. [in German]

Staff, H.V., and Wedekind, R., 1910, Der Oberkarbon Foraminiferensapropelit Spitzbergens: Bulletin of the Geological Institution of the University of Uppsala, v. 10, p. 81–123. [in German]

Stauffer, C.R., and Plummer, H.J., 1932, Texas Pennsylvanian conodonts and their stratigraphic relations: University of Texas Bulletin, v. 3201, p. 13–50.

Steele, G., 1960, Pennsylvanian-Permian stratigraphy of east-central Nevada and adjacent Utah, Guidebook to the Geology of East Central Nevada: Intermountain Association of Petroleum Geologists, Eleventh Annual Field Conference, p. 91–133.

Steiner, M.B., and Williams, T.E., 1968, Fusulinidae of the Laborcita Formation (Lower Permian), Sacramento Mountains, New Mexico: Journal of Paleontology, v. 42, no. 1, p. 51–60.

Stevens, C.H., 1965, Pre-Kaibab Permian stratigraphy and history of Butte Basin, Nevada and Utah: AAPG Bulletin, v. 49, p. 139–156.

Stevens, C.H., 1971, Distribution and diversity of Pennsylvanian marine faunas relative to water depth and distance from shore: Lethaia, v. 4, no. 4, p. 403–412.

Stevens, C.H., 1979, Lower Permian of the central Cordilleran Miogeosyncline: GSA Bulletin, Part II, v. 90, p. 381–455.

Stevens, C.H., 2008, Fasciculate rugose corals from Gzhelian and lower Permian strata, Pequop Mountains, northeast Nevada: Journal of Paleontology, v. 82, no. 6, p. 1190–1200.

Stevens, C.H., Wagner, D.B., and Sumsion, R.S., 1979, Permian fusulinid biostratigraphy, central Cordilleran Miogeosyncline: Journal of Paleontology, v. 53, no. 1, p. 29–36.

Stevens, C.H., Stone, P., Dunne, G.C., Greene, D.C., Walker, J.D., and Swanson, B.J., 1997, Paleozoic and Mesozoic evolution of east-central California: International Geology Review, v. 39, p. 788–829.

Stevens, C.H., Stone, P., and Ritter, S.M., 2001, Conodont and fusulinid biostratigraphy and history of the Pennsylvanian to Lower Permian Keeler Basin, east-central California: Brigham Young University Geology Studies, v. 46, p. 99–142.

Stevens, C.H., and Stone, P., 2007, The Pennsylvanian-Early Permian Bird Spring Carbonate Shelf, southeastern California: Fusulinid biostratigraphy, paleogeographic evolution, and tectonic implications: GSA Special Paper, no. 429, 82 p.

Stevens, C.H., and Stone, P., 2009a, New Permian fusulinids from Conglomerate Mesa, southeastern Inyo Mountains, east-central California: Journal of Paleontology, v. 83, no. 1, p. 9–29.

Stevens, C.H., and Stone, P., 2009b, New fusulinids from Lower Permian turbidites at Conglomerate Mesa, southeastern Inyo Mountains, east-central California: Journal of Paleontology, v. 83, no. 3, p. 399–404.

Stevens, C.H., Poole, F.G., and Amaya-Martínez, R., 2014, Late Paleozoic fusulinids from Sonora Mexico: Importance for interpretation of depositional settings, biogeography, and paleotectonics: Revista Mexicana de Ciencias Geológicas, v. 31, no. 1, p. 14–27.

Stewart, J.H., 1980, Geology of Nevada: Nevada Bureau of Mines and Geology Special Publication 4, 136 p.

Stewart, J.H., and Poole, F.G., 1974, Lower Paleozoic and uppermost Precambrian Cordilleran miogeocline, Great Basin, western United States, *in* Dickinson, W.R., ed., Tectonics and sedimentation: SEPM Special Publication 22, p. 28–57.

Stewart, J.H., and Carlson, J.E., 1978, Geologic map of Nevada, U.S. Geological Survey and Nevada Bureau of Mines and Geology, Scale 1:500,000.

Suleimanov, I.S., 1949, New fusulinid species of subfamily Schubertellinae Skinner from Carboniferous and lower Permian deposits of Bashkirian pre-Urals: Trudy Instituta Geologičeskih Nauk, Geologičeskaâ Seriâ, v. 105, no. 35, p. 22–43. [in Russian]

Sweet, W.C., 1985, Conodonts: Those fascinating little whatzits: Journal of Paleontology, v. 59, no. 3, p. 485–494.

Sweet, W.C., 1988, The Conodonta: morphology, taxonomy, paleoecology, and evolutionary history of a long-extinct animal phylum: Oxford Monographs on Geology and Geophysics, v. 10, 212 p.

Sweet, D., and Donoghue, P.C.J., 2001, Conodonts: Past, Present, Future: Journal of Paleontology, v. 75, no. 6, p. 1174–1184.

Sweet, D., Snyder, W.S., Trexler, J.H., Groves, J., and Davydov, V.I., 2001, Two previously unrecognized upper Paleozoic tectonic unconformities in the central Pequop Mountains, Nevada: Geological Society of America, Abstracts with Programs, v. 33, no. 5, p. A-47.

Sweet, D., and Snyder, W.S., 2003, Middle Pennsylvanian through Early Permian tectonically controlled basins: Evidence from the central Pequop Mountains, northeast Nevada: AAPG Search and Discovery Article #90012, 4 p.

Szaniawski, H., 1980, Fused clusters of paraconodonts, *in* Schonlaub, H.P., ed., Guidebook and abstracts, second European Conodont Symposium (ECOS II): Abhandlungen der Geologischen Bundesanstalt, v. 35, p. 211.

Szaniawski, H., 1982, Chaetognath grasping spines recognized among Cambrian protoconodonts: Journal of Paleontology, v. 56, no. 3, p. 806–810.

Szaniawski, H., 1987, Preliminary structural comparisons of protoconodont, paraconodont and euconodont elements, *in* Aldridge, R.J., ed., Paleobiology of conodonts: Ellis Horwood, Chichester, p. 35–47.

Szaniawski, H., 2002, New evidence for the protoconodont origin of chaetognaths: Acta Palaeontologica Polonica, v. 47, no. 3, p. 405–419.

Szaniawski, H., and Bengtson, S., 1993, Origin of euconodont elements: Journal of Paleontology, v. 67, no. 4, p. 640–654.

Terrill, D.F., Henderson, C.M., and Anderson, J.S., 2018, New applications of spectroscopy techniques reveal phylogenetically significant soft tissue residue in Paleozoic conodonts: Journal of Analytical Atomic Spectrometry, v. 33, p. 992–1002.

Thatcher, W., Foulger, G.R., Julian, B.R., Svarc, J., Quilty, E., and Bawden, G.W., 1999, Present-day deformation across the Basin and Range province, western United States: Science, v. 283, no. 5408, p. 1714–1718.

Thompson, M.L., 1936, Pennsylvanian fusulinids from Ohio: Journal of Paleontology, v. 10, no. 8, p. 673–683.

Thompson, M.L., 1937, Fusulinids of the Subfamily Schubertellinae: Journal of Paleontology, v. 11, no. 2, p. 118–125.

Thompson, M.L., 1942, New genera of Pennsylvanian fusulinids: America Journal of Science, v. 240, no. 6, p. 403–420.

Thompson, M.L., 1948, Studies of American fusulinids: University of Kansas Paleontological Contributions, Protozoa, art. 1, 184 p.

Thompson, M.L., 1951, New genera of fusulinid foraminifera: Contributions from the Cushman Foundation for Foraminiferal Research, v. 2, no. 4, p. 115–119.

Thompson, M.L., 1954, American Wolfcampian fusulinids: The University of Kansas Paleontological Contributions, Protozoa, art. 5, 226 p.

Thompson, M.L., 1957, Northern Midcontinent Missourian fusulinids: Journal of Paleontology, v. 31, no. 2, p. 289–328.

Thompson, M.L., 1965, Pennsylvanian and Early Permian fusulinids from Fort St. James area, British Columbia, Canada: Journal of Paleontology, v. 39: 224–234.

Thompson, M.L., and Wheeler, H.E., 1946, Permian fusulinids of northern California, *in* Thompson, M.L., Wheeler, H.E., and Hazzard, J.C., eds., Permian Fusulinids of California: GSA Memoir, v. 17, p. 21–36.

Thompson, M.L., and Hazzard, J.C., 1946, Permian fusulinids of southern California, *in* Thompson, M.L., Wheeler, H.E., and Hazzard, J.C., eds., Permian Fusulinids of California: GSA Memoir, v. 17, p. 37–53.

Thompson, M.L., Verville, G.J., and Bissell, H.J., 1950, Pennsylvanian fusulinids of the south-central Wasatch Mountains, Utah: Journal of Paleontology, v. 24, no. 4, pp. 430–465.

Thompson, M.L., Dodge, H.W., and Youngquist, W., 1958, Fusulinids from the Sublett Range, Idaho: Journal of Paleontology, v. 32, no. 1, p. 113–125.

Thompson, G.A., and Burke, D.B., 1973, Rate and direction of spreading in Dixie Valley, Basin and Range province, Nevada: GSA Bulletin, v. 84, p. 627–632.

Thorsteinsson, R., 1960, Permian rocks and faunas of Grinnell Peninsula, Arctic Archipelago: Geological Survey of Canada Memoir, v. 309, p. 1–89.

Tierney, K.E., 2010, Carbon and strontium isotope stratigraphy of the Permian from Nevada and China: Implications from an icehouse to greenhouse transition [PhD Dissertation]: Ohio State University, 106 p.

Trexler, J.H., Snyder, W.S., Cashman, P.H., Gallegos, D.M., and Spinosa, C., 1991, Mississippian through Permian orogenesis in eastern Nevada: Post-Antler, pre-Sonoma tectonics of the western Cordillera, *in* Cooper, J.D., and Stevens, C.H., eds., Paleozoic paleogeography of the western United States, Volume II: SEPM, Pacific Section, p. 317–329.

Trexler, J.H., Cashman, P.H., Cole, J.C., Snyder, W.S., Tosdal, R.M., and Davydov, V.I., 2003, Widespread effects of middle Mississippian deformation in the Great Basin of western North America: GSA Bulletin, v. 115, no. 10, p. 1278–1288.

Trexler, J.H., Cashman, P.H., Snyder, W.S., and Davydov, V.I., 2004, Late Paleozoic tectonism in Nevada: Timing, kinematics, and tectonic significance: GSA Bulletin, v. 116, no. 5–6, p. 525–538.

Turner, S., Burrow, C.J., Schultze, H.P., Blieck, A., Reif, W.E., Rexroad, C.B., Bultynck, P., and Nowlan, G.S., 2010, False Teeth: Conodont-vertebrate phylogenetic relationships revisited: Geodiversitas, v. 32, no. 4, p. 545–594.

Ueno, K., Mizuno, Y., Wang, X., and Mei, S., 2002, Artinskian conodonts from the Dingjiazhai Formation of the Baoshan block, West Yunnan, Southwest China: Journal of Paleontology, v. 76, no. 4, p. 741–750.

Ueno, K., 2006, The Permian antitropical fusulinoidean genus *Monodiexodina*: Distribution, taxonomy, paleobiogeography and paleoecology: Journal of Asian Earth Science, v. 26, p. 380–404.

Valentine, J.W., 2004, On the Origin of Phyla: University of Chicago Press, Chicago, IL, 614 p.

Verville, G.J., 1957, Wolfcampian fusulinids from the Tensleep Sandstone in the Big Horn Mountains, Wyoming: Journal of Paleontology, v. 31, no. 2, p. 349–352.

Verville, G.J., Thompson, M.L., and Lokke, D.H., 1956, Pennsylvanian fusulinids of Eastern Nevada: Journal of Paleontology, v. 30, no. 6, p. 1277–1287.

Vuolo, I., Henderson, C.M., Nicora, A., Shen, S.Z., Angiolini, L., and Balini, M., 2014, Co-occurrence of *Sweetognathus whitei* Rhodes, 1963 with early Sakmarian conodonts in SE Pamir: Permophiles, v. 60, p. 8–10.

Wahlman, G.P., 2013, Pennsylvanian to Lower Permian (Desmoinesian-Wolfcampian) fusulinid biostratigraphy of Midcontinent North America: Stratigraphy, v. 10, no. 1–2, p. 73–104.

Wahlman, G.P., and Tasker, D.R., 2013, Lower Permian (Wolfcampian) carbonate shelf-margin and slope facies, central basin platform and Hueco Mountains, Permian Basin, West Texas, USA: Deposits, Architecture and Controls of Carbonate Margin, Slope, and Basinal Settings, SEPM Special Publication 105, p. 305–333.

Wang, K.L., and Sun, X.F., 1973, Carboniferous and Permian foraminifera of the Chinling Range and its geologic significance: Acta Geologica Sinica, v. 2, p. 137–171.

Wang, Z.H., and Qi, Y.P., 2002, Report on the Upper Pennsylvanian conodont zonation from the Nashui section of Loudian, Guizhou, China: Newsletter on Carboniferous Stratigraphy, v. 20, p. 29–32.

Wang, Z.H., and Qi, Y.P., 2003, Report of upper Visean-Serpukhovian conodont zonation in South China: Newsletter on Carboniferous Stratigraphy, v. 21, p. 22–24.

Wang, Q., Wang, Y., Qi, Y., Wang, X., Choh, S.J., Lee, D.C., and Lee, D.J., 2018, Revised conodont and fusuline biostratigraphy of the Bamchi Formation (Pyongan Supergroup) at the Bamchi section, Yeongwol and

the Carboniferous-Permian boundary in South Korea: Alcheringa, v. 42, no. 2, p. 244–257.

Wanless, H.R., 1979, Limestone response to stress: Pressure solution and dolomitization: Journal of Sedimentary Petrology, v. 49, p. 437–462.

Wardlaw, B.R., and Collinson, J.W., 1979, Youngest Permian conodont faunas from the Great Basin and Rocky Mountain region, *in* Sandberg, C.A., and Clark, D.L., eds., Conodont biostratigraphy of the Great Basin and Rocky Mountains, Brigham Young University Geological Studies, v. 26, no. 3, p. 151–164.

Wardlaw, B.R., and Collinson, J.W., 1986, Paleontology and deposition of the Phosphoria Formation: University of Wyoming Contributions to Geology, v. 24, no. 2, p. 107–142.

Wardlaw, B.R., Snyder, W.S., Spinosa, C., and Gallegos, D.M., 1995, Permian of the Western United States, *in* Scholle, P.A., Peryt, T.M., and Ulmer-Scholle, D.S., eds., The Permian of Northern Pangea 2: Sedimentary Basins and Economic Resources: Berlin-Heidelberg, Springer-Verlag, p. 23–40.

Wardlaw, B.R., Davydov, V.I, Mei, S., and Henderson, C.M., 1998, New reference sections for the Upper Carboniferous and Lower Permian in northeast Nevada: Permophiles, v. 31, p. 5–8.

Wardlaw, B.R., and Nestell, M.K., 2014, The first appearance of *Streptognathodus isolatus* in the Permian of Texas: Permophiles, v. 59, p. 17–20.

Wardlaw, B.R., Gallegos, D.M., Chernykh, V.V., and Snyder, W.S., 2015, Early Permian conodont fauna of the Garden Valley Formation, Eureka County, Nevada: Micropaleontology, v. 61, nos. 4–5, p. 369–387.

White, M.P., 1932, Some Texas Fusulinidae: The University of Texas Bulletin, no. 3211, 106 p.

Wind, F.H., 1973, Stratigraphic zonation and paleoecology of conodonts of the Chase Group, Lower Permian, Kansas [MS Thesis]: Florida State University, 224 p.

Wilde, G.L., 1962, Lower Permian biostratigraphic relationships and sedimentation: Permian Basin Section SEPM Guidebook no. 62-7, Leonardian Facies of the Sierra Diablo Region, West Texas, p. 68–90.

Wilde, G.L., 1971, Phylogeny of *Pseudofusulinella* and its bearing on Early Permian stratigraphy: Paleozoic Perspectives: A Paleontological

Tribute to G. Arthur Cooper, Smithsonian Contributions to Paleobiology, v. 3, p. 363–379.

Wilde, G.L., 1976, Fusulinid evidence for the Pennsylvanian-Permian boundary: The Age of the Dunkard: Proceedings of the first I.C. White Memorial Symposium, p. 123–141.

Wilde, G.L., 1990, Practical fusulinid zonation: the species concept; with Permian Basin emphasis: West Texas Geological Society Bulletin, v. 29, no. 7, p. 5–34.

Wilde, G.L., 2002, The Newwellian Substage: Rejection of the Bursumian Stage: Permophiles, v. 41, p. 53–62.

Wilde, G.L., 2006, Pennsylvanian-Permian fusulinaceans of the Big Hatchet Mountains, New Mexico: New Mexico Museum of Natural History and Science Bulletin, v. 38, 331 p.

Williams, T.E., 1963, Fusulinidae of the Hueco Group (Lower Permian), Hueco Mountains, Texas: Yale University Peabody Museum of Natural History Bulletin 18, 122 p.

Williams, T.E., 1966, Permian Fusulinidae of the Franklin Mountains, New Mexico-Texas: Journal of Paleontology, v. 40, no. 5, p. 1142–1156.

Yancey, T.E., and Stevens, C.H., 1981, Early Permian fossil communities in northeastern Nevada and northwestern Utah, *in* Gray, J., Boucot, A.J., and Berry, W.B.N., eds., Communities of the past: Ross Publishing, Stroudsburg, PA, p. 243–269.

Yang, Z., and Yancey, T.E., 2000, Fusulinid biostratigraphy and paleontology of the Middle Permian (Guadalupian) strata of the Glass Mountains and Del Norte Mountains, West Texas, *in* Wardlaw, B.R., Grant, R.E., and Rohr, D.M., eds., The Guadalupian Symposium: Smithsonian Contributions to the Earth Sciences, v. 32, 415 p.

Yochelson, E.L., and Fraser, G.D., 1973, Interpretation of depositional environment in the Plympton Formation (Permian), southern Pequop Mountains, Nevada, from physical stratigraphy and a faunule: Journal of Research of the U.S. Geological Survey, v. 1, no. 1, p. 19–32.

Youngquist, W., Hawley, R.W., and Miller, A.K., 1951, Phosphoria conodonts from southeastern Idaho: Journal of Paleontology, v. 25, no. 3, p. 356–364.

Zandkarimi, K., Najafian, B., Bahrammanesh, M., and Vachard, D., 2014, Permian foraminiferal biozonation in the Alborz Mountains at Valiabad section (Iran): Permophiles, v. 60, p. 10–16.

Zeller, R.A., 1958, The geology of the Big Hatchet Peak quadrangle, Hidalgo County, New Mexico [PhD Dissertation]: University of California, 260 p.

APPENDIX A

FUSULINID MEASUREMENTS

(CHAPTER 4)

Table 4.1 – Measurements of *Eowaeringella* sp. A

Specimen no.	Length (mm)	Half length (mm)	Width (mm)	Half width (mm)	Form ratio	Number of volutions	Diameter of proloculus (mm)
NSMR 14.8-2	—	1.92	—	0.74	2.59	8	0.089
NSMR 14.8-3	—	2.24	1.76	—	2.54	7	0.129
NSMR 14.8-4	—	1.99	—	0.79	2.52	8	0.102
NSMR 14.8-5	—	2.28	1.82	—	2.52	8	0.126
NSMR 14.8-6	4.50	—	—	0.93	2.41	8	0.114

Specimen no.	Height of volutions (mm)							
	1	2	3	4	5	6	7	8
NSMR 14.8-2	0.034	0.050	0.086	0.107	0.127	0.167	0.180	—
NSMR 14.8-3	0.044	0.051	0.082	0.110	0.145	0.158	0.197	
NSMR 14.8-4	0.041	0.048	0.088	0.106	0.123	0.165	0.173	—
NSMR 14.8-5	0.027	0.055	0.069	0.094	0.119	0.145	0.171	0.225
NSMR 14.8-6	0.034	0.043	0.062	0.070	0.109	0.144	0.169	0.241

Specimen no.	Thickness of spirotheca (mm)								
	0	1	2	3	4	5	6	7	8
NSMR 14.8-2	0.010	0.017	0.024	0.033	0.031	0.041	0.043	0.039	—
NSMR 14.8-3	0.010	0.012	0.019	0.031	0.034	0.035	0.033	0.042	
NSMR 14.8-4	0.012	0.014	0.019	0.020	0.028	0.024	0.042	0.031	—
NSMR 14.8-5	0.012	0.013	0.018	0.021	0.018	0.018	0.034	0.032	0.028
NSMR 14.8-6	0.010	0.010	0.017	0.019	0.021	0.025	0.030	0.032	0.030

Specimen no.	Tunnel angle (degrees)							
	1	2	3	4	5	6	7	8
NSMR 14.8-2	—	12	13	16	13	15	22	—
NSMR 14.8-3	—	11	15	16	18	23	—	
NSMR 14.8-4	21	11	11	17	15	22	23	—
NSMR 14.8-5	19	11	14	15	19	25	25	—
NSMR 14.8-6	23	18	17	21	21	24	31	—

Table 4.2 – Measurements of *Eowaeringella* sp. B

Specimen no.	Length (mm)	Half length (mm)	Width (mm)	Half width (mm)	Form ratio	Number of volutions	Diameter of proloculus (mm)
NSMR 54.9-1	5.61	2.81	1.84	0.92	3.05	8	0.093
NSMR 54.9-2	—	—	—	—	—	8.5	0.109
NSMR 54.9-4	5.13	2.57	—	—	—	8	0.099
NSMR 54.9-5	6.00	3.00	1.86	0.93	3.23	9	0.095

Specimen no.	Height of volutions (mm)								
	1	2	3	4	5	6	7	8	9
NSMR 54.9-1	0.042	0.048	0.088	0.086	0.116	0.158	0.144	0.211	
NSMR 54.9-2	0.031	0.038	0.067	0.078	0.090	0.135	0.152	—	—
NSMR 54.9-4	0.036	0.041	0.069	0.081	0.099	0.109	0.172	—	
NSMR 54.9-5	0.033	0.041	0.061	0.083	0.098	0.110	0.174	0.188	—

Specimen no.	Thickness of spirotheca (mm)									
	0	1	2	3	4	5	6	7	8	9
NSMR 54.9-1	0.012	0.010	0.015	0.014	0.018	0.022	0.027	0.032	—	
NSMR 54.9-2	0.012	0.008	0.013	0.015	0.020	0.025	0.023	0.022	—	—
NSMR 54.9-4	0.013	0.007	0.015	0.013	0.017	0.023	0.024	0.027	—	
NSMR 54.9-5	0.012	0.009	0.016	0.015	0.021	0.019	0.028	0.033	0.042	—

Specimen no.	Tunnel angle (degrees)								
	1	2	3	4	5	6	7	8	9
NSMR 54.9-1	19	16	14	13	16	18	25	21	
NSMR 54.9-2	19	20	12	11	14	13	16	22	—
NSMR 54.9-4	15	13	14	13	14	17	17	19	
NSMR 54.9-5	16	12	15	11	13	19	23	29	—

Table 4.3 – Measurements of *Pseudofusulinella* sp. A

Specimen no.	Length (mm)	Half length (mm)	Width (mm)	Half width (mm)	Form ratio	Number of volutions	Diameter of proloculus (mm)
F24127-61	—	1.42	1.51	—	1.88	7	0.086
F24127-64	—	1.35	1.58	—	1.71	7.5	0.094
NSMR 215.8-10	—	1.79	—	0.93	1.93	9	0.108
NSMR 215.8-14	3.67	—	—	0.75	2.44	7	—

Specimen no.	Height of volutions (mm)								
	1	2	3	4	5	6	7	8	9
F24127-61	0.042	0.046	0.061	0.106	0.135	0.156	0.203		
F24127-64	0.029	0.031	0.056	0.062	0.105	0.138	0.167	0.211	
NSMR 215.8-10	0.024	0.029	0.040	0.085	0.087	0.100	0.157	0.144	0.220
NSMR 215.8-14	—	—	0.082	0.104	0.131	0.143	0.175		

Specimen no.	Thickness of spirotheca (mm)									
	0	1	2	3	4	5	6	7	8	9
F24127-61	0.009	0.011	0.013	0.023	0.028	0.033	0.032	0.033		
F24127-64	0.010	0.009	0.100	0.015	0.021	0.031	0.038	—	—	
NSMR 215.8-10	0.009	0.010	0.011	0.015	0.030	0.031	0.037	—	0.050	0.049
NSMR 215.8-14	—	—	—	0.019	0.030	0.032	0.031	0.033		

Specimen no.	Tunnel angle (degrees)								
	1	2	3	4	5	6	7	8	9
F24127-61	12	10	9	9	12	16	20	—	—
F24127-64	—	14	9	7	14	16	21	13	—
NSMR 215.8-10	—	12	9	11	10	11	10	17	21
NSMR 215.8-14	—	—	15	17	19	18	26		

Table 4.4 – Measurements of *Schubertella ciscoensis* Kauffman and Roth, 1966

Specimen no.	Length (mm)	Half length (mm)	Width (mm)	Half width (mm)	Form ratio	Number of volutions	Diameter of proloculus (mm)
F24122-7	0.82	—	0.37	—	2.22	4	0.032
F24122-18	0.96	—	0.35	—	2.74	4	0.028
F24122-22	1.26	—	0.47	—	2.68	5	0.034
F24123-9	0.92	—	0.36	—	2.59	4	0.038
NSMR 149.2-6	1.18	—	0.43	—	2.73	4	0.038
NSMR 149.2-8	0.59	—	0.29	—	2.07	4	0.026
NSMR 149.2-11	0.93	—	—	—	—	4	0.036

Specimen no.	Height of volutions (mm)				
	1	2	3	4	5
F24122-7	0.022	0.026	0.050	0.084	
F24122-18	0.019	0.027	0.045	0.075	
F24122-22	0.021	0.027	0.028	0.046	0.073
F24123-9	0.024	0.038	0.041	0.060	
NSMR 149.2-6	0.025	0.033	0.039	0.078	
NSMR 149.2-8	0.023	0.026	0.028	0.036	
NSMR 149.2-11	0.024	0.040	0.048	—	

Specimen no.	Thickness of spirotheca (mm)					
	0	1	2	3	4	5
F24122-7	0.005	0.007	0.006	0.008	0.009	
F24122-18	—	0.007	0.008	0.012	0.011	
F24122-22	0.005	0.007	0.008	0.009	0.010	0.013
F24123-9	0.006	0.007	0.011	0.011	0.010	
NSMR 149.2-6	0.005	0.005	0.007	0.008	0.007	
NSMR 149.2-8	—	0.007	0.007	0.011	0.009	
NSMR 149.2-11	0.007	0.006	0.007	0.008	—	

Table 4.5 – Measurements of Genus n. A sp. A

Specimen no.	Length (mm)	Half length (mm)	Width (mm)	Half width (mm)	Form ratio	Number of volutions	Diameter of proloculus (mm)
F24178-22	6.73	—	2.21	—	3.04	7	0.176
F24178-23	6.80	—	2.51	—	2.71	7.5	0.162
F24178-25	—	3.05	2.16	—	2.82	7	0.214
F24178-26	—	3.20	2.39	—	2.68	6.5	0.200
F24178-30	—	3.09	—	1.40	2.21	7	0.161
F24181-12	7.17	—	—	1.33	2.70	8	0.144

Specimen no.	Height of volutions (mm)							
	1	2	3	4	5	6	7	8
F24178-22	0.040	0.042	0.059	0.127	0.176	0.183	0.284	
F24178-23	0.036	0.061	0.066	0.131	0.174	0.222	0.279	0.302
F24178-25	0.039	0.069	0.101	0.122	0.173	0.201	0.198	
F24178-26	0.032	0.075	0.129	0.194	0.241	0.320	0.191	
F24178-30	0.043	0.063	0.089	0.156	0.204	0.259	0.282	
F24181-12	0.034	0.053	0.062	0.163	0.189	0.213	0.276	0.262

Specimen no.	Thickness of spirotheca (mm)								
	0	1	2	3	4	5	6	7	8
F24178-22	0.012	0.011	0.017	0.021	0.032	0.034	0.046	0.056	
F24178-23	0.018	0.015	0.023	0.025	0.027	0.045	0.055	0.056	0.065
F24178-25	0.021	0.020	0.027	0.036	0.031	0.052	0.061	0.078	
F24178-26	0.020	0.018	0.021	0.041	0.050	0.066	0.061	0.073	
F24178-30	0.019	0.016	0.026	0.027	0.045	0.058	0.054	0.057	
F24181-12	0.017	0.013	0.018	0.020	0.029	0.036	0.058	0.076	0.067

Specimen no.	Tunnel angle (degrees)							
	1	2	3	4	5	6	7	8
F24178-22	11	20	24	22	34	33	—	
F24178-23	16	10	10	20	21	28	21	33
F24178-25	18	18	25	27	21	34	—	
F24178-26	8	13	15	21	25	30	—	
F24178-30	18	16	18	18	16	31	26	
F24181-12	10	18	13	18	14	22	26	—

Table 4.6 – Measurements of *Alaskanella* sp. A

Specimen no.	Length (mm)	Half length (mm)	Width (mm)	Half width (mm)	Form ratio	Number of volutions	Diameter of proloculus (mm)
F24133-1	—	3.93	—	1.08	3.64	7	0.153
F24133-2	—	3.07	—	—	—	7	0.151
F24133-3	5.03	—	—	—	—	7	0.260
F24133-4	8.79	—	—	—	—	7	0.195
F24133-5a	—	—	2.21	—	—	8	0.233
F24133-5b	—	1.57	1.10	—	2.86	6	0.149
F24133-6	5.52	—	1.74	—	3.18	7	0.161
NSMR 272.3-2A	—	2.86	—	0.95	3.01	7	0.138
NSMR 272.3-3	—	3.88	—	—	—	7	0.149

Specimen no.	Height of volutions (mm)							
	1	2	3	4	5	6	7	8
F24133-1	0.048	0.063	0.099	0.152	0.148	0.241	0.252	
F24133-2	0.050	0.075	0.091	0.149	0.152	—	—	
F24133-3	0.049	0.065	0.058	0.119	0.116	0.131	—	
F24133-4	0.055	0.080	0.109	0.132	0.186	0.180	—	
F24133-5a	0.065	0.081	0.089	0.106	0.139	0.204	0.160	0.227
F24133-5b	0.042	0.068	0.101	0.128	0.123	0.111		
F24133-6	0.045	0.067	0.083	0.115	0.121	0.193	0.197	
NSMR 272.3-2A	0.033	0.046	0.064	0.099	0.132	0.223	0.285	
NSMR 272.3-3	0.052	0.070	0.100	0.122	0.177	0.178	—	

Specimen no.	Thickness of spirotheca (mm)								
	0	1	2	3	4	5	6	7	8
F24133-1	0.019	0.015	0.018	0.038	0.046	0.065	0.073	0.072	
F24133-2	0.017	0.018	0.026	0.042	0.049	0.064	0.066	—	
F24133-3	0.026	0.021	0.023	0.025	0.040	0.057	0.055	—	
F24133-4	0.018	0.020	0.023	0.031	0.043	0.064	0.084	—	
F24133-5a	0.022	0.020	0.026	0.033	0.041	0.057	0.066	0.074	0.079
F24133-5b	0.016	0.014	0.017	0.018	0.037	0.043	0.067		
F24133-6	0.019	0.021	0.022	0.023	0.027	0.044	0.071	0.085	
NSMR 272.3-2A	0.120	0.019	0.028	0.038	—	0.060	0.076		
NSMR 272.3-3	0.014	0.026	0.028	0.053	0.045	0.067	—		

Specimen no.	Tunnel angle (degrees)							
	1	2	3	4	5	6	7	8
F24133-1	15	23	27	32	25	32	—	
F24133-2	20	18	20	29	24	28	—	
F24133-3	16	23	24	33	36	36	—	
F24133-4	14	15	23	24	38	52	48	
F24133-5a	17	18	23	35	44	35	51	—
F24133-5b	10	21	25	28	31	50		
F24133-6	11	19	21	32	37	40	44	
NSMR 272.3-2A	17	27	28	40	38	41	61	
NSMR 272.3-3	14	14	16	26	33	38	29	

Table 4.7 – Measurements of *Alaskanella* sp. C

Specimen no.	Length (mm)	Half length (mm)	Width (mm)	Half width (mm)	Form ratio	Number of volutions	Diameter of proloculus (mm)
F24179-1	9.59	—	2.44	—	3.94	7	0.211
F24179-2	8.88	—	2.42	—	3.67	7	0.161
F24179-3	—	4.56	2.70	—	3.38	8	0.162
F24179-4	8.05	—	2.47	—	3.26	9	0.116
F24179-5	—	5.34	2.65	—	4.03	8	0.176
F24179-7	9.86	—	2.79	—	3.54	9	0.157
F24179-8	9.12	—	2.18	—	4.18	8.5	0.117

Specimen no.	Height of volutions (mm)								
	1	2	3	4	5	6	7	8	9
F24179-1	0.062	0.087	0.103	0.159	0.210	0.281	0.343		
F24179-2	0.048	0.070	0.101	0.125	0.194	0.225	0.323		
F24179-3	0.038	0.064	0.075	0.099	0.148	0.199	0.272	0.317	
F24179-4	0.025	0.045	0.054	0.085	0.121	0.176	0.228	0.246	0.239
F24179-5	0.046	0.057	0.081	0.101	0.165	0.206	0.252	0.324	
F24179-7	0.051	0.072	0.085	0.116	0.171	0.184	0.245	0.312	0.279
F24179-8	0.029	0.041	0.057	0.085	0.112	0.157	0.172	0.175	0.229

Specimen no.	Thickness of spirotheca (mm)									
	0	1	2	3	4	5	6	7	8	9
F24179-1	0.020	0.009	0.017	0.019	0.044	0.064	0.056	0.068		
F24179-2	0.013	0.014	0.023	0.020	0.044	0.045	0.067	0.063		
F24179-3	0.013	0.015	0.018	0.021	0.027	0.045	0.061	0.051	0.059	
F24179-4	0.014	0.013	0.013	0.019	0.029	0.030	0.043	0.061	0.058	0.049
F24179-5	0.011	0.014	0.019	0.021	0.025	0.037	0.047	0.062	0.055	
F24179-7	0.015	0.017	0.017	0.023	0.036	0.059	0.045	0.064	0.059	0.055
F24179-8	0.012	0.013	0.015	0.021	0.031	0.027	0.048	0.064	0.066	0.063

Specimen no.	Tunnel angle (degrees)								
	1	2	3	4	5	6	7	8	9
F24179-1	18	19	20	32	38	57	—		
F24179-2	18	24	23	22	32	32	48		
F24179-3	15	28	18	23	26	28	40	51	
F24179-4	—	15	19	27	28	29	43	54	—
F24179-5	19	19	25	28	40	46	62	—	
F24179-7	—	9	16	24	27	34	45	—	—
F24179-8	21	15	27	20	31	50	49	64	—

Table 4.8 – Measurements of *Cuniculinella* sp. A

Specimen no.	Length (mm)	Half length (mm)	Width (mm)	Half width (mm)	Form ratio	Number of volutions	Diameter of proloculus (mm)
F24128-3	5.79	—	2.77	—	2.09	5	0.299
F24128-5	6.48	—	2.81	—	2.31	5.5	0.318
F24128-6	—	4.29	—	2.00	2.15	6	0.345
F24128-8	4.66	—	2.20	—	2.12	4.5	0.279
NSMR 227.8-6	—	5.53	—	2.06	2.69	6.5	0.349
NSMR 227.8-7	—	4.15	3.18	—	2.61	6	0.292

Specimen no.	Height of volutions (mm)						
	1	2	3	4	5	6	7
F24128-3	0.108	0.165	0.277	0.393	0.356		
F24128-5	0.054	0.141	0.205	0.241	0.339	0.349	
F24128-6	0.139	0.218	0.270	0.373	0.379	0.473	
F24128-8	0.044	0.108	0.191	0.263	0.299		
NSMR 227.8-6	0.113	0.154	0.240	0.319	0.361	0.431	0.418
NSMR 227.8-7	0.125	0.166	0.217	0.268	0.365	0.415	

Specimen no.	Thickness of spirotheca (mm)							
	0	1	2	3	4	5	6	7
F24128-3	0.022	0.037	0.055	0.065	0.105	0.119		
F24128-5	0.023	0.022	0.040	0.065	0.074	0.099	0.108	
F24128-6	0.025	0.039	0.064	0.069	0.110	0.126	—	
F24128-8	0.020	0.015	0.035	0.056	0.086	0.092		
NSMR 227.8-6	0.024	0.028	0.036	0.042	0.075	0.094	0.124	0.113
NSMR 227.8-7	0.030	0.035	0.058	0.072	0.089	0.112	0.104	

Table 4.9 – Measurements of *Cuniculinella*? sp. B

Specimen no.	Length (mm)	Half length (mm)	Width (mm)	Half width (mm)	Form ratio	Number of volutions	Diameter of proloculus (mm)
F24128-7	9.61	—	3.63	—	2.65	7	0.208
F24128-11a	9.88	—	3.63	—	2.72	7	0.351
F24128-11b	—	5.43	—	1.85	2.93	7	0.334
F24128-16	10.00	—	3.24	—	3.08	7	0.302
NSMR 227.8-1	—	5.54	—	2.08	2.67	6.5	0.337

Specimen no.	Height of volutions (mm)						
	1	2	3	4	5	6	7
F24128-7	0.076	0.101	0.194	0.265	0.374	0.364	0.410
F24128-11a	0.096	0.170	0.234	0.317	0.373	0.326	—
F24128-11b	0.094	0.244	0.281	0.325	0.320	—	—
F24128-16	0.086	0.132	0.201	0.297	0.282	0.291	0.289
NSMR 227.8-1	0.117	0.149	0.203	0.292	0.385	0.417	0.422

Specimen no.	Thickness of spirotheca (mm)							
	0	1	2	3	4	5	6	7
F24128-7	0.028	0.027	0.038	0.059	0.065	0.103	0.101	0.100
F24128-11a	0.031	0.040	0.075	0.077	0.088	0.105	0.122	—
F24128-11b	0.024	0.029	0.057	0.080	0.114	0.121	—	—
F24128-16	0.022	0.024	0.041	0.083	0.090	0.103	0.098	0.107
NSMR 227.8-1	0.028	0.027	0.044	0.050	0.093	0.102	0.136	0.128

Table 4.10 – Measurements of *Dunbarinella kauffmani* Wilde, 2006

Specimen no.	Length (mm)	Half length (mm)	Width (mm)	Half width (mm)	Form ratio	Number of volutions	Diameter of proloculus (mm)
F24122-18	4.24	—	—	0.85	2.50	8	0.074
F24122-19	3.02	—	1.29	—	2.33	7	0.061
F24122-21	—	—	1.29	—	—	7	0.079
NSMR 149.2-1	2.80	—	1.47	—	1.91	6	0.088
NSMR 149.2-4	2.94	—	1.23	—	2.40	6.5	0.090
NSMR 149.2-9	—	1.96	1.66	—	2.36	7	0.079
NSMR 149.2-10	3.00	—	1.22	—	2.46	5.5	0.088

Specimen no.	Height of volutions (mm)							
	1	2	3	4	5	6	7	8
F24122-18	0.032	0.041	0.048	0.063	0.101	0.149	0.176	0.216
F24122-19	0.022	0.027	0.047	0.078	0.105	0.148	0.209	
F24122-21	0.027	0.030	0.049	0.074	0.132	0.155	0.158	
NSMR 149.2-1	0.033	0.064	0.103	0.123	0.202	0.249		
NSMR 149.2-4	0.022	0.036	0.052	0.088	0.120	0.212	—	
NSMR 149.2-9	0.027	0.035	0.050	0.081	0.133	0.166	0.214	
NSMR 149.2-10	0.023	0.029	0.050	0.101	0.152	0.258		

Specimen no.	Thickness of spirotheca (mm)								
	0	1	2	3	4	5	6	7	8
F24122-18	0.008	0.011	0.011	0.013	0.022	0.025	0.038	0.060	0.057
F24122-19	0.007	0.008	0.010	0.015	0.020	0.035	0.053	0.074	
F24122-21	0.008	0.007	0.013	0.015	0.025	0.029	0.040	0.057	
NSMR 149.2-1	0.012	0.012	0.015	0.027	0.035	0.045	0.700		
NSMR 149.2-4	0.009	0.010	0.012	0.017	0.021	0.025	0.043	0.056	
NSMR 149.2-9	0.008	0.009	0.008	0.012	0.022	0.036	0.040	0.064	
NSMR 149.2-10	0.008	0.008	0.009	0.018	0.026	0.042	0.059		

Specimen no.	Tunnel angle (degrees)							
	1	2	3	4	5	6	7	8
F24122-18	—	19	16	1	22	21	28	—
F24122-19	—	21	16	26	24	23	21	
F24122-21	17	10	21	29	21	21	—	
NSMR 149.2-1	26	22	21	27	27	27		
NSMR 149.2-4	25	15	21	23	19	23	19	
NSMR 149.2-9	—	12	21	24	20	26	31	
NSMR 149.2-10	—	15	21	25	29	31		

Table 4.11 – Measurements of *Eoparafusulina linearis* (Dunbar and Skinner, 1937)

Specimen no.	Length (mm)	Half length (mm)	Width (mm)	Half width (mm)	Form ratio	Number of volutions	Diameter of proloculus (mm)
F24138-8	11.14	—	2.18	—	5.12	7	0.160
F24138-17	11.79	—	1.94	—	6.07	7	—
F24138-20	11.63	—	—	—	—	7.5	—
F24144-27	—	6.54	2.53	—	5.16	8	—
NSMR 304.4-1	14.11	—	—	1.26	5.60	9	0.145
NSMR 304.4-2	13.33	—	—	1.07	6.23	8	0.233
NSMR 304.4-3	12.54	—	2.29		5.48	9	0.161

Specimen no.	Height of volutions (mm)								
	1	2	3	4	5	6	7	8	9
F24138-8	0.047	0.051	0.075	0.134	0.153	0.211	0.203		
F24138-17	0.060	0.068	0.100	1.340	—	0.181	0.171		
F24138-20	0.029	0.062	0.095	0.135	0.178	0.148	0.166	—	
F24144-27	0.064	0.079	0.094	0.156	0.188	0.232	0.246	—	
NSMR 304.4-1	0.043	0.053	0.086	0.063	0.114	0.124	0.203	0.119	0.227
NSMR 304.4-2	0.053	0.067	0.087	0.121	0.135	0.148	0.191	—	
NSMR 304.4-3	0.039	0.052	0.079	0.094	0.131	0.148	0.147	0.164	0.227

Specimen no.	Thickness of spirotheca (mm)									
	0	1	2	3	4	5	6	7	8	9
F24138-8	0.016	0.015	0.023	0.023	0.031	0.046	0.088	0.096		
F24138-17	0.028	0.029	0.028	0.038	0.048	0.065	0.073	0.069		
F24138-20	0.016	0.024	0.029	0.035	0.038	0.072	0.063	0.060	—	
F24144-27	0.022	0.028	0.026	0.041	0.051	0.059	0.077	0.083	0.083	
NSMR 304.4-1	0.014	0.015	0.015	0.022	0.019	0.026	0.056	0.071	0.068	0.073
NSMR 304.4-2	0.015	0.015	0.024	0.029	0.054	0.059	0.081	0.086	—	
NSMR 304.4-3	0.012	0.013	0.014	0.022	0.043	0.046	0.052	0.054	0.066	0.059

Table 4.12 – Measurements of *Pseudofusulina mediotenebraeus* Wilde, 2006

Specimen no.	Length (mm)	Half length (mm)	Width (mm)	Half width (mm)	Form ratio	Number of volutions	Diameter of proloculus (mm)
F24127-33	6.43	—	2.82	—	2.28	7.5	0.122
F24127-35	5.59	—	2.58	—	2.17	7	0.135
NSMR 215.8-6	5.30	—	2.26	—	2.34	6	0.115
NSMR 215.8-7	5.88	—	2.53	—	2.33	7	0.109
NSMR 215.8-12	6.44	—	2.74	—	2.35	7	0.114

Specimen no.	Height of volutions (mm)							
	1	2	3	4	5	6	7	8
F24127-33	0.033	0.049	0.094	0.140	0.168	0.246	0.337	0.338
F24127-35	0.043	0.069	0.097	0.148	0.192	0.386	0.360	
NSMR 215.8-6	0.062	0.088	0.132	0.237	0.278	0.358		
NSMR 215.8-7	0.039	0.068	0.108	0.169	0.233	0.318	0.373	
NSMR 215.8-12	0.051	0.088	0.145	0.201	0.260	0.359	—	

Specimen no.	Thickness of spirotheca (mm)								
	0	1	2	3	4	5	6	7	8
F24127-33	0.012	0.012	0.015	0.023	0.034	0.074	0.089	0.119	0.121
F24127-35	0.015	0.018	0.017	0.036	0.049	0.094	0.111	0.126	
NSMR 215.8-6	0.012	0.015	0.018	0.040	0.063	0.074	0.078		
NSMR 215.8-7	0.011	0.013	0.025	0.032	0.056	0.067	0.107	0.081	
NSMR 215.8-12	0.015	0.020	0.035	0.046	0.059	0.082	0.114	0.126	

Table 4.13 – Measurements of *Pseudoschwagerina robusta* (Meek, 1864)

Specimen no.	Length (mm)	Half length (mm)	Width (mm)	Half width (mm)	Form ratio	Number of volutions	Diameter of proloculus (mm)
F24135-26	9.55	—	5.98	—	1.60	5	0.431
F24139-49	7.99	—	—	—	—	6	0.481
F24143-3	7.01	—	4.91	—	1.43	5	0.310
F24143-4	8.73	4.37	4.78	2.39	1.83	6	0.419
F24143-5	8.71	—	4.58	—	1.90	5.5	0.357

Specimen no.	Height of volutions (mm)					
	1	2	3	4	5	6
F24135-26	0.142	0.261	0.862	0.958	0.699	
F24139-49	0.160	0.025	—	—	—	—
F24143-3	0.095	0.139	—	—	—	
F24143-4	0.103	0.146	0.202	0.397	0.939	0.410
F24143-5	0.036	0.122	0.238	0.643	0.531	0.717

Specimen no.	Thickness of spirotheca (mm)						
	0	1	2	3	4	5	6
F24135-26	0.038	0.046	0.069	0.051	0.104	0.112	
F24139-49	0.036	0.047	0.055	0.077	0.127	0.108	—
F24143-3	0.020	0.025	0.040	0.041	0.068	0.109	
F24143-4	0.040	0.047	0.062	0.071	0.114	0.117	0.132
F24143-5	0.025	0.014	0.035	0.071	0.076	0.093	0.145

Table 4.14 – Measurements of *Schwagerina franklinensis* Dunbar and Skinner, 1937

Specimen no.	Length (mm)	Half length (mm)	Width (mm)	Half width (mm)	Form ratio	Number of volutions	Diameter of proloculus (mm)
F24178-2	—	5.52	2.67	—	4.13	7	0.181
F24178-3	—	5.42	—	1.35	4.01	6	0.180
F24178-8	—	4.85	2.51	—	3.86	6	0.243
F24180-1	—	4.68	2.61	—	3.59	6	0.163
F24180-3	9.33	—	2.70	—	3.46	6	0.192
F24180-4	—	4.27	2.43	—	3.51	6	0.171
F24180-5		5.57	2.74	—	4.07	7	0.183

Specimen no.	Height of volutions (mm)						
	1	2	3	4	5	6	7
F24178-2	0.051	0.060	0.113	0.195	0.263	0.347	0.299
F24178-3	0.055	0.086	0.136	0.270	0.368	0.346	
F24178-8	0.062	0.111	0.171	0.249	0.330	0.258	
F24180-1	0.044	0.078	0.185	0.286	0.315	0.346	
F24180-3	0.045	0.107	0.174	0.349	0.376	0.403	
F24180-4	0.057	0.081	0.161	0.249	0.310	0.318	
F24180-5	0.044	0.089	0.140	0.169	0.254	0.325	0.357

Specimen no.	Thickness of spirotheca (mm)							
	0	1	2	3	4	5	6	7
F24178-2	0.026	0.015	0.023	0.022	0.045	0.067	0.081	0.054
F24178-3	0.018	0.017	0.027	0.029	0.057	0.085	0.080	
F24178-8	0.027	0.026	0.045	0.035	0.074	0.082	0.064	
F24180-1	0.020	0.024	0.026	0.044	0.057	0.098	0.072	
F24180-3	0.026	0.019	0.033	0.045	0.062	0.091	0.104	
F24180-4	0.021	0.022	0.026	0.046	0.062	0.073	0.084	
F24180-5	0.023	0.019	0.025	0.033	0.049	0.085	0.086	0.084

Table 4.15 – Measurements of *Schwagerina glassensis* Ross and Ross, 2003

Specimen no.	Length (mm)	Half length (mm)	Width (mm)	Half width (mm)	Form ratio	Number of volutions	Diameter of proloculus (mm)
F24141-13	—	3.91	—	—	—	7.5	0.098
F24143-12	7.47	—	3.09	—	2.42	7	0.138
F24143-13	—	3.92	2.95	—	2.65	7	0.105
F24143-14	6.08	—	2.56	—	2.38	7	0.076
F24143-16	7.77	—	3.17	—	2.45	8	0.074
F24143-24	7.65	—	3.26	—	2.35	8	0.135
NSMR 282-5	—	4.29	—	1.95	2.20	8	0.119

Specimen no.	Height of volutions (mm)							
	1	2	3	4	5	6	7	8
F24141-13	0.033	0.036	0.058	0.108	0.228	—	—	—
F24143-12	0.030	0.054	0.093	0.207	0.341	0.393	0.388	
F24143-13	0.043	0.044	0.086	0.190	0.361	0.413	0.424	
F24143-14	0.028	0.033	0.061	0.129	0.280	0.352	0.445	
F24143-16	0.027	0.038	0.061	0.094	0.195	0.316	0.390	0.385
F24143-24	0.034	0.044	0.091	0.189	0.264	0.335	0.433	0.325
NSMR 282-5	0.038	0.040	0.081	0.128	0.245	0.409	0.447	0.387

Specimen no.	Thickness of spirotheca (mm)								
	0	1	2	3	4	5	6	7	8
F24141-13	0.009	0.010	0.014	0.021	0.037	0.057	0.082	0.112	—
F24143-12	0.013	0.014	0.015	0.027	0.048	0.083	0.104	0.084	
F24143-13	0.010	0.010	0.012	0.024	0.066	0.096	0.106	0.096	
F24143-14	0.009	0.010	0.010	0.023	0.030	0.050	0.089	0.097	
F24143-16	0.009	0.009	0.014	0.018	0.032	0.061	0.076	0.102	0.095
F24143-24	0.012	0.010	0.018	0.027	0.049	0.072	0.093	0.118	0.070
NSMR 282-5	0.013	0.013	0.015	0.021	0.034	0.055	0.061	0.114	0.082

Table 4.16 – Measurements of *Schwagerina neolata* Thompson, 1954

Specimen no.	Length (mm)	Half length (mm)	Width (mm)	Half width (mm)	Form ratio	Number of volutions	Diameter of proloculus (mm)
F24134-2	—	4.19	3.39	1.69	2.47	6	0.376
F24134-3	—	—	3.40	1.70	—	6	0.263
F24134-4	10.78	5.39	—	—	—	7	0.339
F24134-5	—	—	3.23	—	—	7	0.289
F24134-7	9.45	—	—	—	—	7	0.264
F24135-5	7.94	—	3.24	1.62	2.45	6	0.236

Specimen no.	Height of volutions (mm)						
	1	2	3	4	5	6	7
F24134-2	0.106	0.162	0.273	0.403	0.517	—	
F24134-3	0.085	0.134	0.286	0.357	0.342	—	
F24134-4	0.077	0.097	0.155	0.326	0.342	—	—
F24134-5	0.080	0.089	0.212	0.431	0.406	—	—
F24134-7	0.067	0.081	0.184	0.212	0.396	0.299	—
F24135-5	0.073	0.094	0.221	0.320	0.384	0.413	

Specimen no.	Thickness of spirotheca (mm)							
	0	1	2	3	4	5	6	7
F24134-2	0.029	0.030	0.046	0.069	0.126	0.131	—	
F24134-3	0.027	0.024	0.038	0.061	0.100	0.101	—	
F24134-4	0.029	0.033	0.035	0.066	0.083	0.121	—	—
F24134-5	0.022	0.017	0.027	0.050	0.069	0.103	0.130	—
F24134-7	0.026	0.028	0.027	0.058	0.067	0.119	—	—
F24135-5	0.025	0.027	0.034	0.052	0.093	0.111	0.141	

Table 4.17 – Measurements of *Schwagerina wellsensis* Thompson and Hansen, 1954

Specimen no.	Length (mm)	Half length (mm)	Width (mm)	Half width (mm)	Form ratio	Number of volutions	Diameter of proloculus (mm)
F24133-22	—	—	—	—	—	6	0.312
F24135-1	9.09	4.55	3.29	—	2.77	6	0.259
F24135-3	—	—	—	—	—	5	0.276
F24136-3	9.12	4.56	3.33	1.66	2.74	6	0.281
F24141-8	8.48	—	2.93	—	2.89	6	0.258

Specimen no.	Height of volutions (mm)					
	1	2	3	4	5	6
F24133-22	0.081	0.15	0.252	0.269	—	—
F24135-1	0.084	0.148	0.213	0.35	0.447	—
F24135-3	0.08	0.148	0.223	0.339	—	
F24136-3	0.081	0.139	0.234	0.263	0.279	0.416
F24141-8	0.057	0.121	0.238	0.325	0.393	—

Specimen no.	Thickness of spirotheca (mm)						
	0	1	2	3	4	5	6
F24133-22	0.033	0.022	0.043	0.077	0.12	0.099	—
F24135-1	0.025	0.028	0.044	0.067	0.121	0.122	—
F24135-3	0.024	0.021	0.038	0.06	0.072	—	
F24136-3	0.025	0.023	0.046	0.073	0.091	0.097	0.123
F24141-8	0.027	0.028	0.037	0.067	0.094	0.157	—

Table 4.18 – Measurements of *Schwagerina* sp. A

Specimen no.	Length (mm)	Half length (mm)	Width (mm)	Half width (mm)	Form ratio	Number of volutions	Diameter of proloculus (mm)
F24130-1	—	3.89	—	1.04	3.74	4.5	0.220
F24130-2	7.34	—	—	1.00	3.65	5	0.145
F24130-3	—	3.83	—	1.23	3.12	6	0.141
F24130-5	7.67	—	2.65	—	2.89	5	0.197
F24131-7	—	—	—	1.06	—	5	0.211

Specimen no.	Height of volutions (mm)					
	1	2	3	4	5	6
F24130-1	0.064	0.104	0.220	0.394	—	
F24130-2	0.051	0.059	0.112	0.209	0.397	
F24130-3	0.041	0.059	0.122	0.219	0.310	0.411
F24130-5	0.054	0.112	0.236	0.401	0.375	
F24131-7	0.047	0.084	0.186	0.312	0.305	

Specimen no.	Thickness of spirotheca (mm)						
	0	1	2	3	4	5	6
F24130-1	0.028	0.027	0.027	0.041	0.087	—	
F24130-2	0.017	0.012	0.021	0.039	0.063	0.084	
F24130-3	0.016	0.015	0.016	0.029	0.056	0.066	0.069
F24130-5	0.017	0.025	0.026	0.057	0.087	0.067	
F24131-7	0.018	0.015	0.028	0.049	0.072	0.095	

Table 4.19 – Measurements of *Schwagerina* sp. B

Specimen no.	Length (mm)	Half length (mm)	Width (mm)	Half width (mm)	Form ratio	Number of volutions	Diameter of proloculus (mm)
F24136-1	—	5.33	3.59	1.80	2.97	7.5	0.155
F24136-2	—	5.26	3.63	—	2.90	7.5	0.162
F24136-5	—	5.21	—	—	—	8	0.113
F24136-8	—	5.34	2.94	—	3.63	7	0.162
F24136-12	—	5.06	3.83	—	2.64	8	0.138
F24138-1	—	5.71	3.61	—	3.16	8	0.117

Specimen no.	Height of volutions (mm)							
	1	2	3	4	5	6	7	8
F24136-1	0.034	0.051	0.087	0.225	0.346	0.439	0.441	—
F24136-2	0.029	0.044	0.081	0.159	0.311	0.437	0.393	0.416
F24136-5	0.029	0.038	0.059	0.131	0.239	0.391	—	—
F24136-8	0.042	0.054	0.092	0.220	0.363	0.369	0.370	
F24136-12	0.030	0.045	0.070	0.195	0.304	0.437	0.428	0.302
F24138-1	0.038	0.043	0.077	0.236	0.411	0.390	0.423	—

Specimen no.	Thickness of spirotheca (mm)								
	0	1	2	3	4	5	6	7	8
F24136-1	0.013	0.012	0.015	0.039	0.061	0.093	0.098	0.121	—
F24136-2	0.012	0.013	0.020	0.017	0.052	0.081	0.128	0.111	0.125
F24136-5	0.011	0.012	0.014	0.023	0.037	0.073	0.102	0.118	—
F24136-8	0.019	0.013	0.024	0.036	0.065	0.086	0.105	0.121	
F24136-12	0.015	0.012	0.016	0.024	0.048	0.088	0.116	0.103	0.071
F24138-1	0.016	0.024	0.029	0.035	0.038	0.072	0.063	0.060	—

Table 4.20 – Measurements of *Schwagerina* sp. C

Specimen no.	Length (mm)	Half length (mm)	Width (mm)	Half width (mm)	Form ratio	Number of volutions	Diameter of proloculus (mm)
NSMR 392.5-1	8.86	—	—	0.95	4.66	7	0.163
NSMR 392.5-2	—	6.05	—	1.08	5.58	7	—
NSMR 392.5-3	—	5.08	—	—	—	6	0.218
NSMR 392.5-4	—	5.35	—	0.92	5.82	6	—

Specimen no.	Height of volutions (mm)						
	1	2	3	4	5	6	7
NSMR 392.5-1	0.044	0.067	0.092	0.144	0.201	0.196	—
NSMR 392.5-2	0.063	0.080	0.097	0.163	0.256	0.180	0.259
NSMR 392.5-3	0.046	0.077	0.102	0.183	0.214	—	
NSMR 392.5-4	0.044	0.064	0.108	0.137	0.235	0.247	

Specimen no.	Thickness of spirotheca (mm)							
	0	1	2	3	4	5	6	7
NSMR 392.5-1	0.020	0.022	0.025	0.026	0.043	0.041	0.083	—
NSMR 392.5-2	0.016	0.023	0.030	0.047	0.050	0.073	0.084	—
NSMR 392.5-3	0.019	0.018	0.024	0.030	0.041	0.061	0.078	
NSMR 392.5-4	0.021	0.021	0.034	0.043	0.046	0.059	0.077	

Table 4.21 – Measurements of *Triticites bensonensis* Ross and Tyrrell, 1965

Specimen no.	Length (mm)	Half length (mm)	Width (mm)	Half width (mm)	Form ratio	Number of volutions	Diameter of proloculus (mm)
F24123-1	—	2.17	2.24	—	1.94	7	0.112
F24123-9	—	2.02	2.32	—	1.74	6	0.145
F24123-10	4.24	—	—	1.17	1.81	8	0.097
F24123-11	—	1.82	1.89	—	1.93	7	0.119
NSMR 150.4-1	—	1.52	1.63	—	1.86	5	0.081
NSMR 150.4-4	2.75	—	1.54	—	1.81	6	0.112

Specimen no.	Height of volutions (mm)							
	1	2	3	4	5	6	7	8
F24123-1	0.048	0.068	0.103	0.126	0.203	0.284	0.299	
F24123-9	0.060	0.068	0.108	0.167	0.242	0.359		
F24123-10	0.038	0.046	0.083	0.109	0.189	0.238	0.282	—
F24123-11	0.049	0.052	0.092	0.128	0.137	0.246	0.254	
NSMR 150.4-1	0.041	0.074	0.112	0.195	0.276			
NSMR 150.4-4	0.046	0.056	0.093	0.139	0.244	0.229		

Specimen no.	Thickness of spirotheca (mm)								
	0	1	2	3	4	5	6	7	8
F24123-1	0.008	0.010	0.016	0.025	0.051	0.075	0.081	0.082	
F24123-9	0.014	0.013	0.031	0.032	0.073	0.091	0.118		
F24123-10	0.012	0.015	0.016	0.022	0.050	0.061	0.084	0.098	—
F24123-11	0.011	0.014	0.021	0.034	0.054	0.061	0.091	0.076	
NSMR 150.4-1	0.009	0.016	0.017	0.023	0.049	0.089			
NSMR 150.4-4	—	0.011	0.016	0.028	0.042	0.065	0.086		

Specimen no.	Tunnel angle (degrees)							
	1	2	3	4	5	6	7	8
F24123-1	13	16	18	15	22	34	23	
F24123-9	21	18	21	17	22	31		
F24123-10	12	16	13	19	17	29	26	31
F24123-11	16	18	14	15	28	23	35	
NSMR 150.4-1	27	24	25	20	30			
NSMR 150.4-4	9	13	17	21	30	—		

Table 4.22 – Measurements of *Triticites burgessae* Burma, 1942

Specimen no.	Length (mm)	Half length (mm)	Width (mm)	Half width (mm)	Form ratio	Number of volutions	Diameter of proloculus (mm)
NSMR 32.1-1	3.77		1.44	—	2.62	6	0.077
NSMR 32.1-6	—	2.05	1.58	—	2.59	6	0.098
NSMR 32.1-14	—	2.03	1.66	—	2.45	6	0.094

Specimen no.	Height of volutions (mm)					
	1	2	3	4	5	6
NSMR 32.1-1	0.033	0.051	0.089	0.140	0.194	0.229
NSMR 32.1-6	0.037	0.053	0.082	0.151	0.241	0.228
NSMR 32.1-14	0.039	0.054	0.087	0.152	0.238	0.297

Specimen no.	Thickness of spirotheca (mm)						
	0	1	2	3	4	5	6
NSMR 32.1-1	0.008	0.011	0.013	0.017	0.026	0.037	0.038
NSMR 32.1-6	0.009	0.009	0.020	0.015	0.033	0.052	0.051
NSMR 32.1-14	0.009	0.012	0.012	0.021	0.032	0.030	0.057

Specimen no.	Tunnel angle (degrees)					
	1	2	3	4	5	6
NSMR 32.1-1	—	17	31	26	32	38
NSMR 32.1-6	23	17	20	22	28	39
NSMR 32.1-14	18	32	34	30	28	32

Table 4.23 – Measurements of *Triticites* aff. *celebroides* Ross, 1965

Specimen no.	Length (mm)	Half length (mm)	Width (mm)	Half width (mm)	Form ratio	Number of volutions	Diameter of proloculus (mm)
NSMR 32.1-3	6.81	—	2.11	—	3.23	7	0.096
NSMR 32.1-9	6.99	3.49	2.04	—	3.42	8	0.063
NSMR 32.1-10	5.59	2.79	1.74	—	3.22	7	0.080
NSMR 32.1-12	5.79	—	2.16	—	2.68	7	0.082
NSMR 32.1-15	6.12	3.06	1.99	—	3.08	6.5	0.101

Specimen no.	Height of volutions (mm)							
	1	2	3	4	5	6	7	8
NSMR 32.1-3	0.042	0.058	0.105	0.145	0.212	0.251	0.312	
NSMR 32.1-9	0.023	0.035	0.055	0.076	0.139	0.191	0.262	0.276
NSMR 32.1-10	0.040	0.042	0.056	0.098	0.149	0.226	0.260	
NSMR 32.1-12	0.041	0.050	0.094	0.123	0.194	0.314	0.267	
NSMR 32.1-15	0.019	0.040	0.071	0.133	0.252	0.235	0.337	

Specimen no.	Thickness of spirotheca (mm)								
	0	1	2	3	4	5	6	7	8
NSMR 32.1-3	0.007	0.011	0.016	0.021	0.031	0.045	0.053	0.052	
NSMR 32.1-9	0.007	0.007	0.009	0.013	0.026	0.032	0.051	0.052	0.054
NSMR 32.1-10	0.010	0.012	0.011	0.013	0.029	0.039	0.042	0.054	
NSMR 32.1-12	0.009	0.009	0.017	0.018	0.034	0.059	0.051	0.041	
NSMR 32.1-15	0.010	0.008	0.009	0.015	0.024	0.034	0.056	0.063	

Specimen no.	Tunnel angle (degrees)							
	1	2	3	4	5	6	7	8
NSMR 32.1-3	25	18	20	24	28	46	49	
NSMR 32.1-9	—	—	26	19	27	36	55	51
NSMR 32.1-10	—	26	18	24	30	55	44	
NSMR 32.1-12	15	25	16	19	27	41	—	
NSMR 32.1-15	—	20	32	31	41	55	—	

Table 4.24 – Measurements of *Triticites cullomensis* Dunbar and Condra, 1927

Specimen no.	Length (mm)	Half length (mm)	Width (mm)	Half width (mm)	Form ratio	Number of volutions	Diameter of proloculus (mm)
F24122-10	6.14	—	2.47	—	2.49	7	0.090
NSMR 149.2-3	4.35	—	1.73	—	2.51	6	0.145
NSMR 149.2-7	6.01	—	—	1.11	2.70	6	0.139
NSMR 150.4-2a	—	2.73	2.36	—	2.32	7	0.111

Specimen no.	Height of volutions (mm)						
	1	2	3	4	5	6	7
F24122-10	0.033	0.057	0.104	0.174	0.275	0.317	0.268
NSMR 149.2-3	0.038	0.063	0.107	0.161	0.232	0.240	
NSMR 149.2-7	0.050	0.084	0.161	0.270	0.295	0.204	
NSMR 150.4-2a	0.036	0.065	0.109	0.178	0.247	0.291	0.309

Specimen no.	Thickness of spirotheca (mm)							
	0	1	2	3	4	5	6	7
F24122-10	0.010	0.012	0.017	0.035	0.045	0.082	0.077	0.091
NSMR 149.2-3	0.012	0.015	0.017	0.023	0.039	0.067	0.083	
NSMR 149.2-7	0.015	0.012	0.020	0.036	0.072	0.099	0.075	
NSMR 150.4-2a	0.008	0.008	0.014	0.047	0.061	0.067	0.074	0.083

Specimen no.	Tunnel angle (degrees)						
	1	2	3	4	5	6	7
F24122-10	19	—	25	31	31	46	—
NSMR 149.2-3	12	15	22	32	32	44	
NSMR 149.2-7	17	15	29	33	33	39	
NSMR 150.4-2a	—	15	17	14	21	30	32

Table 4.25 – Measurements of *Triticites* cf. *jacksboroensis* Kauffman and Roth, 1966

Specimen no.	Length (mm)	Half length (mm)	Width (mm)	Half width (mm)	Form ratio	Number of volutions	Diameter of proloculus (mm)
NSMR 70-1	5.82	—	2.52	—	2.31	7	0.136
NSMR 100.1-6	4.88	—	2.33	—	2.09	6	0.131
NSMR 100.1-7	5.26	—	2.71	—	1.94	7	0.091
NSMR 100.1-8	4.37	—	1.91	—	2.29	7	0.083
NSMR 100.1-9a	—	2.15	1.88	—	2.29	6	—
NSMR 100.1-9b	—	2.07	—	—	—	7	0.084
NSMR 100.1-10	4.02	—	1.98	—	2.03	7	0.115

Specimen no.	Height of volutions (mm)						
	1	2	3	4	5	6	7
NSMR 70-1	0.042	0.068	0.116	0.163	0.242	0.328	0.313
NSMR 100.1-6	0.065	0.096	0.161	0.231	0.247	0.281	
NSMR 100.1-7	0.039	0.063	0.096	0.177	0.213	0.363	0.459
NSMR 100.1-8	0.028	0.039	0.067	0.125	0.226	0.265	0.248
NSMR 100.1-9a	—	0.086	0.125	0.148	0.238	0.237	
NSMR 100.1-9b	0.031	0.041	0.088	0.125	0.196	0.294	—
NSMR 100.1-10	0.022	0.053	0.081	0.167	0.261	0.266	—

Specimen no.	Thickness of spirotheca (mm)							
	0	1	2	3	4	5	6	7
NSMR 70-1	0.011	0.016	0.018	0.025	0.049	0.051	0.079	0.081
NSMR 100.1-6	0.013	0.014	0.017	0.032	0.085	0.064	0.095	
NSMR 100.1-7	0.012	0.011	0.019	0.022	0.049	0.058	0.065	0.084
NSMR 100.1-8	0.010	0.009	0.011	0.017	0.029	0.048	0.071	0.059
NSMR 100.1-9a	—	0.011	0.026	0.029	0.039	0.049	0.067	
NSMR 100.1-9b	0.010	0.009	0.012	0.021	0.039	0.046	0.086	0.068
NSMR 100.1-10	0.011	0.012	0.014	0.017	0.036	0.053	0.069	—

Specimen no.	Tunnel angle (degrees)						
	1	2	3	4	5	6	7
NSMR 70-1	27	24	21	23	35	38	—
NSMR 100.1-6	25	39	34	46	70	—	
NSMR 100.1-7	25	25	34	19	35	61	
NSMR 100.1-8	—	24	22	33	35	33	57
NSMR 100.1-9a	—	22	27	31	31	36	
NSMR 100.1-9b	23	30	28	28	29	38	—
NSMR 100.1-10	24	28	33	28	26	—	—

Table 4.26 – Measurements of *Triticites pinguis* Dunbar and Skinner, 1937

Specimen no.	Length (mm)	Half length (mm)	Width (mm)	Half width (mm)	Form ratio	Number of volutions	Diameter of proloculus (mm)
F24127-1	5.81	—	3.98	—	1.46	6	0.370
F24127-2	5.11	—	3.74	—	1.37	7	0.364
F24127-9	6.18	—	4.12	—	1.50	6.5	0.389
F24127-11	6.32	—	4.43	—	1.43	6.5	0.402
NSMR 215.8-5	5.20	—	—	2.04	1.27	7	0.283
NSMR 215.8-7b	5.78	—	3.63	—	1.59	6	0.362

Specimen no.	Height of volutions (mm)						
	1	2	3	4	5	6	7
F24127-1	0.130	0.190	0.228	0.332	0.412	0.400	
F24127-2	0.093	0.119	0.230	0.268	0.324	0.433	—
F24127-9	0.090	0.123	0.229	0.319	0.405	0.420	0.380
F24127-11	0.116	0.138	0.353	0.329	0.411	0.429	0.305
NSMR 215.8-5	0.138	0.173	0.243	0.317	0.384	0.391	—
NSMR 215.8-7b	0.132	0.142	0.262	0.336	0.338	0.378	

Specimen no.	Thickness of spirotheca (mm)							
	0	1	2	3	4	5	6	7
F24127-1	0.029	0.033	0.067	0.075	0.083	0.154	0.111	
F24127-2	0.026	0.031	0.043	0.059	0.101	0.123	0.125	—
F24127-9	0.028	0.023	0.055	0.080	0.101	0.118	0.116	0.096
F24127-11	0.026	0.036	0.044	0.080	0.100	0.125	0.130	0.105
NSMR 215.8-5	0.045	0.046	0.055	0.072	0.089	0.107	0.096	—
NSMR 215.8-7b	0.021	0.045	0.049	0.082	0.125	0.122	0.141	

Specimen no.	Tunnel angle (degrees)						
	1	2	3	4	5	6	7
F24127-1	20	13	12	17	21	28	
F24127-2	22	16	15	18	29	23	—
F24127-9	26	25	22	25	24	29	—
F24127-11	26	20	17	17	22	24	—
NSMR 215.8-5	30	13	11	19	26	30	—
NSMR 215.8-7b	25	18	18	17	24	31	

Table 4.27 – Measurements of *Triticites* sp. A

Specimen no.	Length (mm)	Half length (mm)	Width (mm)	Half width (mm)	Form ratio	Number of volutions	Diameter of proloculus (mm)
NSMR 64.8-2	5.66	—	1.92	—	2.95	6	0.132
NSMR 64.8-10	5.12	—	—	0.99	2.58	7	0.109
NSMR 64.8-14	—	2.51	1.84	—	2.73	6	0.141
NSMR 64.8-15	—	1.95	1.68	—	2.32	6	0.131
NSMR 64.8-17	—	2.69	—	1.01	2.66	6	0.145
NSMR 64.8-18	5.15	—	1.94	—	2.60	6	0.146

Specimen no.	Height of volutions (mm)						
	1	2	3	4	5	6	7
NSMR 64.8-2	0.055	0.104	0.172	0.216	0.270	0.240	
NSMR 64.8-10	0.039	0.064	0.101	0.152	0.198	0.263	—
NSMR 64.8-14	0.051	0.090	0.136	0.201	0.203	0.236	
NSMR 64.8-15	0.040	0.056	0.111	0.153	0.201	0.285	
NSMR 64.8-17	0.047	0.082	0.141	0.248	0.344	—	
NSMR 64.8-18	0.053	0.083	0.141	0.181	0.254	0.253	

Specimen no.	Thickness of spirotheca (mm)							
	0	1	2	3	4	5	6	7
NSMR 64.8-2	0.012	0.016	0.025	0.048	0.055	0.068	0.075	
NSMR 64.8-10	0.008	.0.016	0.026	0.036	0.061	0.070	0.077	—
NSMR 64.8-14	0.012	0.014	0.020	0.037	0.055	0.065	0.072	
NSMR 64.8-15	0.007	0.010	0.013	0.028	0.042	0.066	0.077	
NSMR 64.8-17	0.009	0.009	0.022	0.032	0.069	0.067	0.087	
NSMR 64.8-18	0.011	0.011	0.015	0.028	0.068	0.074	0.073	

Specimen no.	Tunnel angle (degrees)						
	1	2	3	4	5	6	7
NSMR 64.8-2	32	28	36	36	57	54	
NSMR 64.8-10	24	28	27	24	34	48	—
NSMR 64.8-14	28	21	30	33	50	44	
NSMR 64.8-15	24	31	28	43	39	50	
NSMR 64.8-17	—	28	29	29	37	44	
NSMR 64.8-18	26	34	32	35	62	—	

Table 4.28 – Measurements of *Triticites* sp. B

Specimen no.	Length (mm)	Half length (mm)	Width (mm)	Half width (mm)	Form ratio	Number of volutions	Diameter of proloculus (mm)
NSMR 60.6-5	4.39	—	1.96	—	2.24	6.5	0.129
NSMR 64.8-4	4.00	—	1.71	—	2.35	6	0.109
NSMR 64.8-20	4.09	—	1.96	—	2.09	6	0.081
NSMR 64.8-21	4.16	—	1.92	—	2.16	7	0.098

Specimen no.	Height of volutions (mm)						
	1	2	3	4	5	6	7
NSMR 60.6-5	0.055	0.005	0.081	0.139	0.222	0.235	0.174
NSMR 64.8-4	0.030	0.049	0.082	0.129	0.198	0.219	
NSMR 64.8-20	0.040	0.070	0.106	0.179	0.260	0.254	
NSMR 64.8-21	0.040	0.049	0.086	0.146	0.207	0.215	0.269

Specimen no.	Thickness of spirotheca (mm)							
	0	1	2	3	4	5	6	7
NSMR 60.6-5	0.017	0.019	0.021	0.024	0.055	0.057	0.078	0.060
NSMR 64.8-4	0.011	0.009	0.015	0.023	0.045	0.055	0.074	
NSMR 64.8-20	0.010	0.009	0.012	0.026	0.046	0.058	0.065	
NSMR 64.8-21	0.011	0.013	0.015	0.027	0.049	0.065	0.081	0.078

Specimen no.	Tunnel angle (degrees)						
	1	2	3	4	5	6	7
NSMR 60.6-5	14	22	34	29	30	45	—
NSMR 64.8-4	21	28	29	39	37	32	
NSMR 64.8-20	25	27	31	42	52	53	
NSMR 64.8-21	14	20	28	35	40	47	51

APPENDIX B

INTEGRATED FUSULINID AND CONODONT DISTRIBUTIONS

(CHAPTERS 4, 7, and 8)

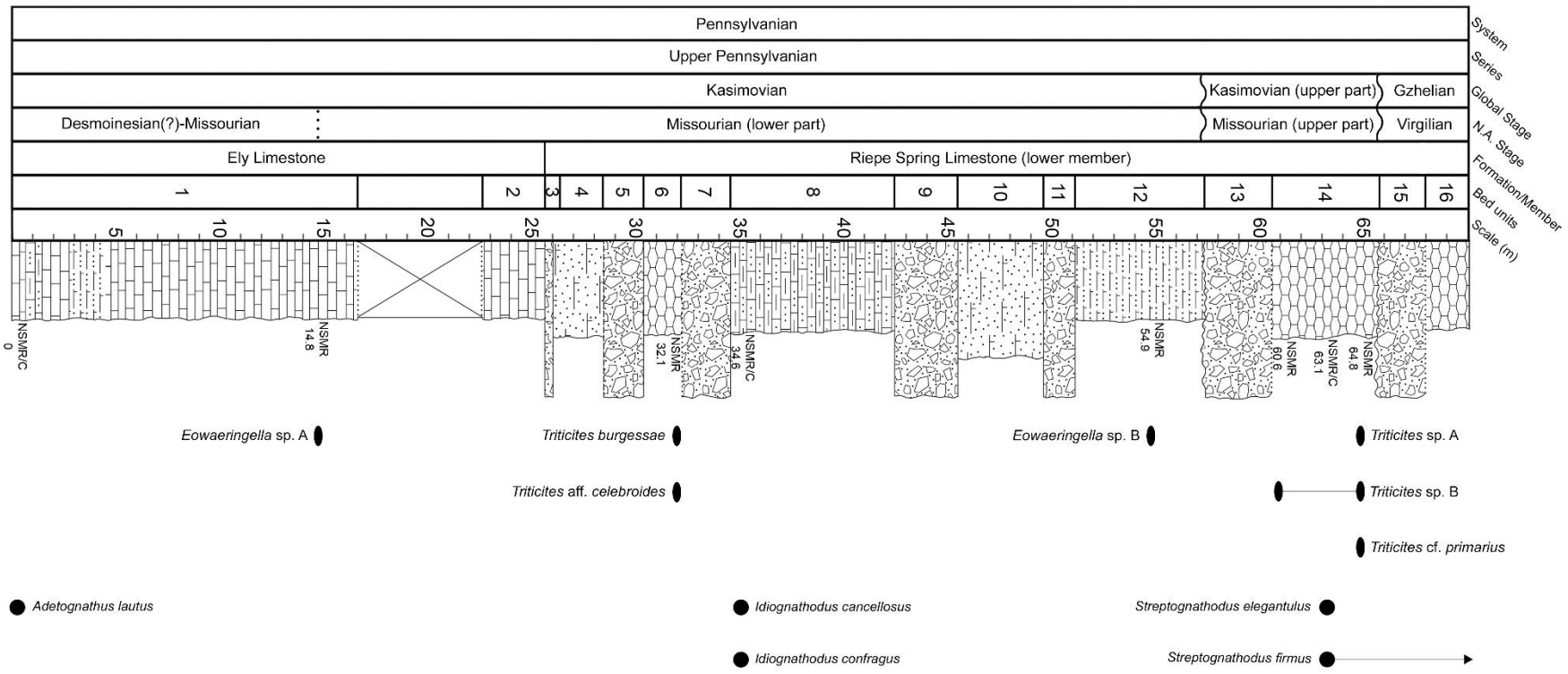
Pennsylvanian
Upper Pennsylvanian
Kasimovian
Kasimovian (upper part)
Gzhelian
Desmoinesian(?)-Missourian
Missourian (lower part)
Missourian (upper part)
Virgilian
Ely Limestone
Riepe Spring Limestone (lower member)
System
Series
Global Stage
N.A. Stage
Formation/Member
Bed units
Scale (m)
NSMR/C 0
NSMR 14.8
NSMR 32.1
NSMR/C 34.6
NSMR 54.9
NSMR 60.6
NSMR/C 63.1
NSMR 64.8
Eowaeringella sp. A
Triticites burgessae
Eowaeringella sp. B
Triticites sp. A
Triticites aff. celebroides
Triticites sp. B
Triticites cf. primarius
Adetognathus lautus
Idiognathodus cancellosus
Streptognathodus elegantulus
Idiognathodus confragus
Streptognathodus firmus

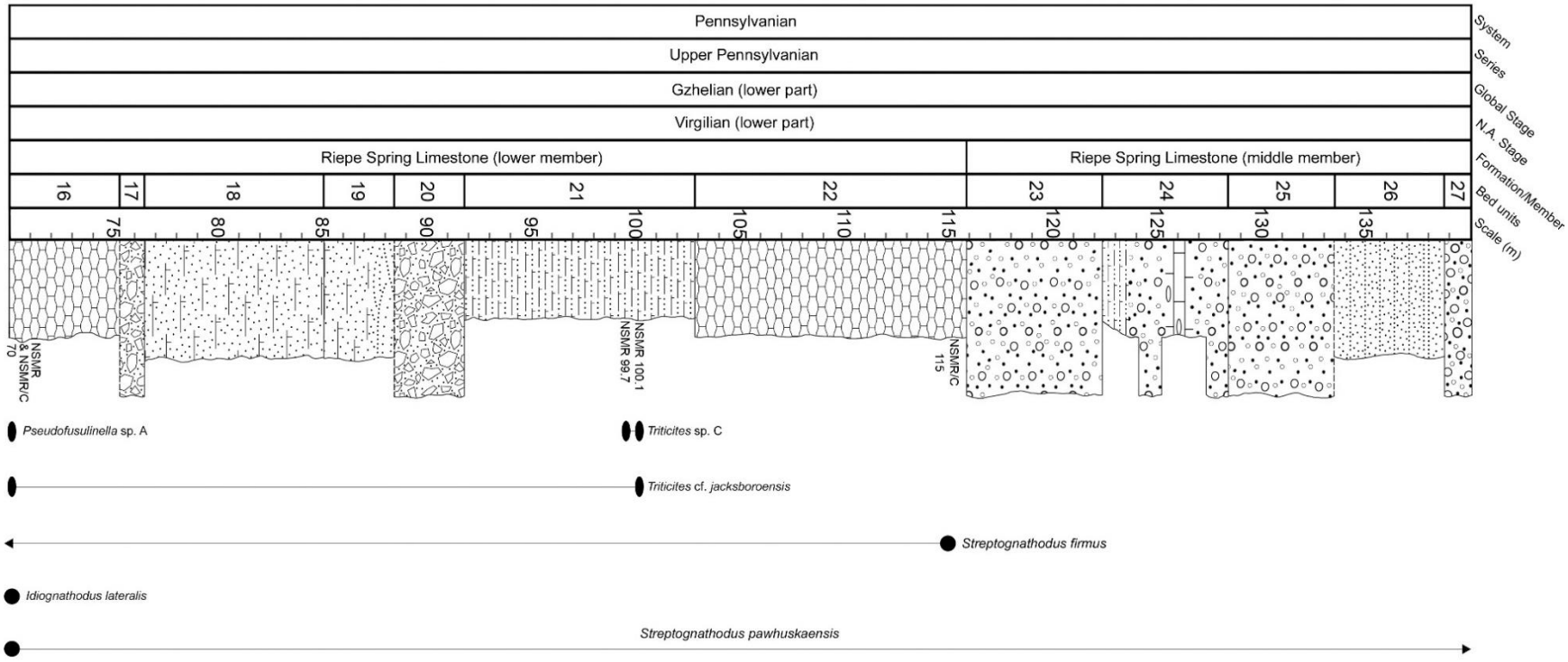
Pennsylvanian
Upper Pennsylvanian
Gzhelian (lower part)
Virgilian (lower part)
Riepe Spring Limestone (lower member)
Riepe Spring Limestone (middle member)
16
17
18
19
20
21
22
23
24
25
26
27
75
80
85
90
95
100
105
110
115
120
125
130
135
System
Series
Global Stage
N.A. Stage
Formation/Member
Bed units
Scale (m)
NSMR 70 & NSMR/C
NSMR 100.1 NSMR 99.7
NSMR/C 115
Pseudofusulinella sp. A
Triticites sp. C
Triticites cf. jacksboroensis
Streptognathodus firmus
Idiognathodus lateralis
Streptognathodus pawhuskaensis

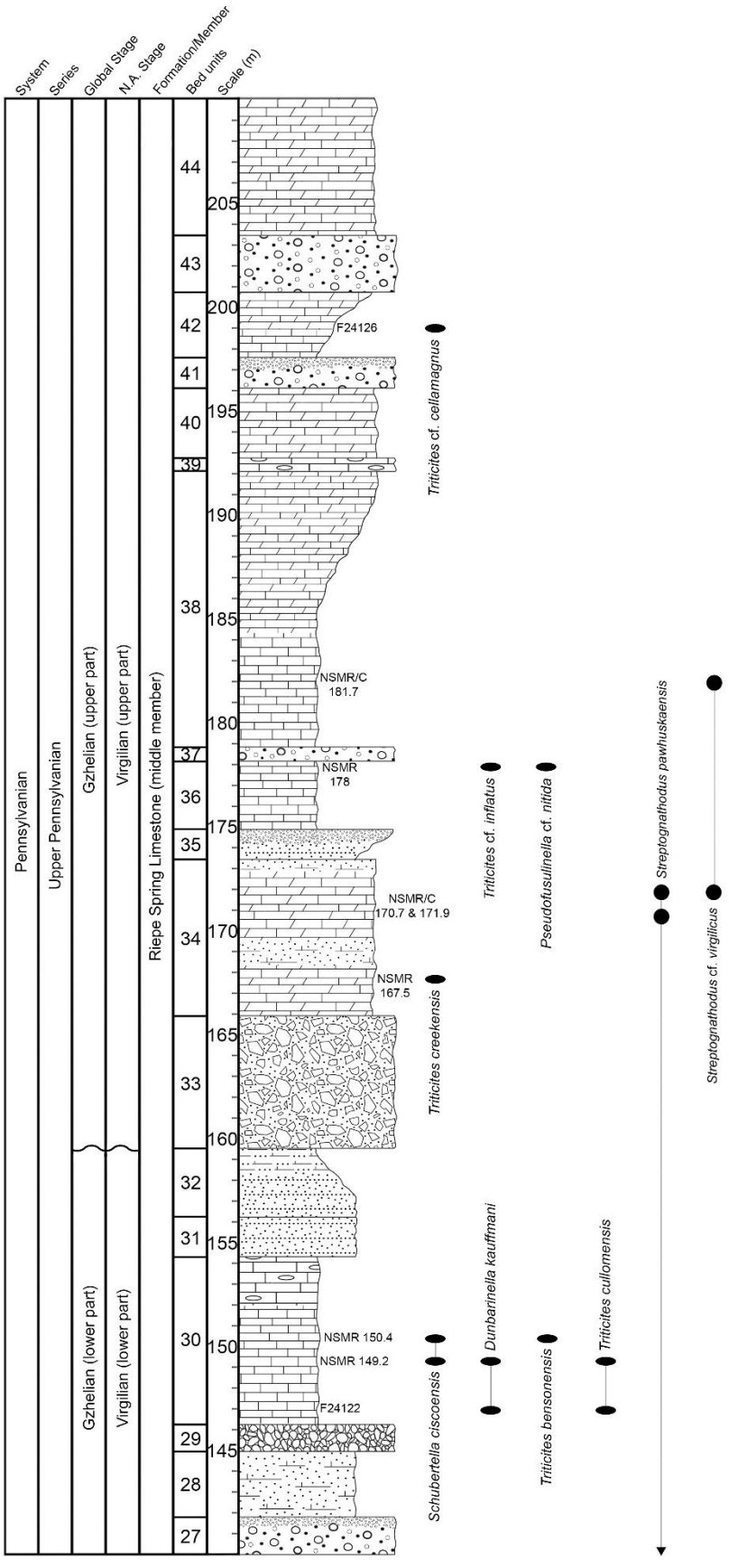
System
Series
Global Stage
N.A. Stage
Formation/Member
Bed units
Scale (m)
Pennsylvanian
Upper Pennsylvanian
Gzhelian (upper part)
Virgilian (upper part)
Riepe Spring Limestone (middle member)
Gzhelian (lower part)
Virgilian (lower part)
44
43
42
41
40
39
38
37
36
35
34
33
32
31
30
29
28
27
205
200
195
190
185
180
175
170
165
160
155
150
145
F24126
NSMR/C 181.7
NSMR 178
NSMR/C 170.7 & 171.9
NSMR 167.5
NSMR 150.4
NSMR 149.2
F24122
Triticites cf. cellamagnus
Triticites cf. inflatus
Pseudofusulinella cf. nitida
Triticites creekensis
Dunbarinella kaufftmani
Triticites bensonensis
Triticites cullomensis
Schubertella ciscoensis
Streptognathodus pawhuskaensis
Streptognathodus cf. virgilicus

System
Series
Global Stage
N.A. Stage
Formation/Member
Bed units
Scale (m)
Pennsylvanian
Permian
Upper Pennsylvanian
Cisuralian
Gzhelian (upper part)
Asselian(?)-Sakmarian
Sakmarian (lower part)
Virgilian (upper part)
Wolfcampian (upper part)
PPrs (middle member)
Riepe Spring Limestone (upper member)
44
45
46
47
48
49
50
51
52
53
54
55
56
57
58
59
60
215
220
225
230
235
240
245
250
255
260
265
270
275
F24136
NSMR/C 277.6
F24135
NSMR/C 274.1
F24134
F24133
NSMR/C 271.9
NSMR/C 268.7
NSMR/C 264.7
F24131
F24130
NSMR/C 253.2
NSMR/C 247.6
NSMR/C 243.2
NSMR/C 241.9
NSMR 227.8
NSMR 215.8, 215.8/C
Triticites pinguis
Triticites cf. californicus
Pseudofusulinella sp. B
Pseudofusulina mediotenebraseus
Streptognathodus bellus
Biwaella americana
Cuniculinella sp. A
Cuniculinella sp. A
Schwagerina sp. A
Pseudoschwagerina robusta
Alaskanella sp. A
Schwagerina wellsensis
Schwagerina neolata
Schwagerina sp. B
Sweetognathus expansus
Sweetognathus 'merrilli'
Sweetognathus binodosus
Sweetognathus duplex
Sweetognathus wardlawi
Sweetognathus sulcatus
Neostreptognathodus aff. pequopensis

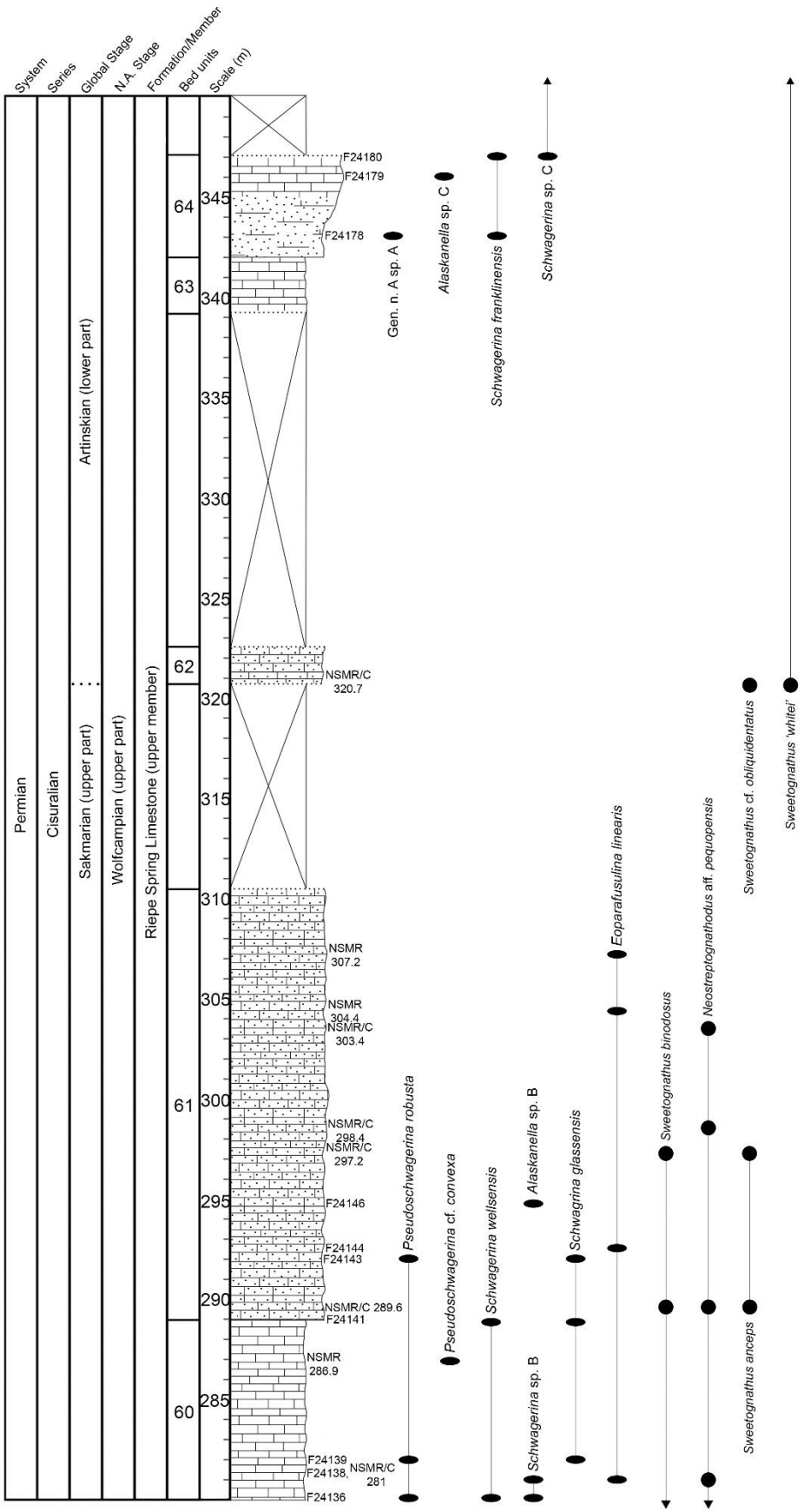
System
Series
Global Stage
N.A. Stage
Formation/Member
Bed units
Scale (m)
Permian
Cisuralian
Artinskian (lower part)
Sakmarian (upper part)
Wolfcampian (upper part)
Riepe Spring Limestone (upper member)
64
63
62
61
60
345
340
335
330
325
320
315
310
305
300
295
290
285
F24180
F24179
F24178
NSMR/C 320.7
NSMR 307.2
NSMR 304.4
NSMR/C 303.4
NSMR/C 298.4
NSMR/C 297.2
F24146
F24144
F24143
NSMR/C 289.6
F24141
NSMR 286.9
F24139
F24138,
NSMR/C 281
F24136
Gen. n. A sp. A
Alaskanella sp. C
Schwagerina franklinensis
Schwagerina sp. C
Pseudoschwagerina robusta
Pseudoschwagerina cf. convexa
Schwagerina wellsensis
Alaskanella sp. B
Schwagerina sp. B
Schwagrina glassensis
Eoparafusulina linearis
Sweetognathus binodosus
Neostreptognathodus aff. pequopensis
Sweetognathus cf. obliquidentatus
Sweetognathus anceps
Sweetognathus 'whitei'

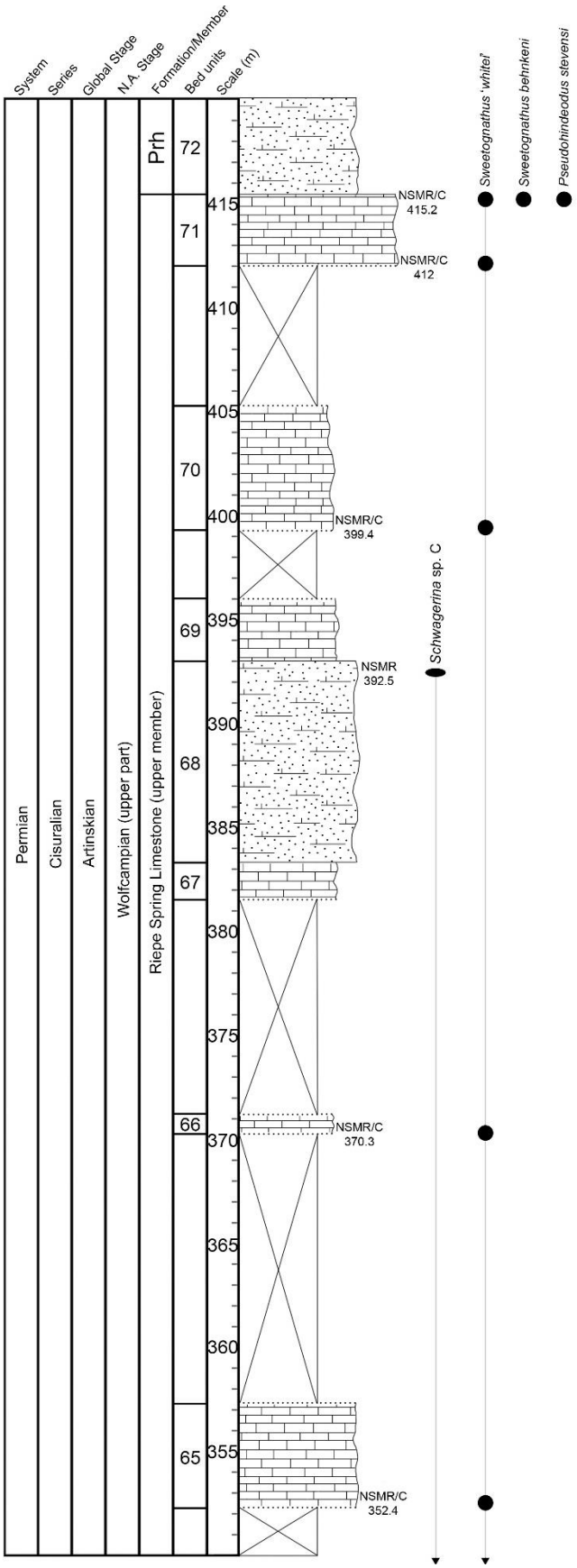
System
Series
Global Stage
N.A. Stage
Formation/Member
Bed units
Scale (m)
Permian
Cisuralian
Artinskian
Wolfcampian (upper part)
Riepe Spring Limestone (upper member)
Prh
72
71
70
69
68
67
66
65
415
410
405
400
395
390
385
380
375
370
365
360
355
NSMR/C 415.2
NSMR/C 412
NSMR/C 399.4
NSMR 392.5
NSMR/C 370.3
NSMR/C 352.4
Schwagerina sp. C
Sweetognathus 'whitei'
Sweetognathus behnkeni
Pseudohindeodus stevensi